Conference organised by:

DMBIUBIH

CMBEBiH 2015

http://www.cmbebih2015.dmbiubih.org

1st Conference on Medical and Biological Engineering in Bosnia and Herzegovina

Expand your horizons through biomedical engineering

PROCEEDINGS

March 13-15, 2015
Sarajevo, Bosnia and Herzegovina

1st Conference on Medical and Biological Engineering in Bosnia and Herzegovina

Expand your horizons through biomedical engineering

CMBEBiH 2015

PROCEEDINGS

March 13-15, 2015

Sarajevo, Bosnia and Herzegovina

WELCOME

It is my great pleasure to welcome you at the 1st Conference on Medical and Biological Engineering in Bosnia and Herzegovina (CMBEBIH 2015) held in Sarajevo from 13th to 15th of March 2015. It is a true joy to share with you this very special event, as CMBEBIH is the first Conference of Biomedical Engineering in our country and hopefully it will become a tradition for all of us.

Sarajevo is a special place. Sarajevo, the host city of the CMBEBiH2015, is the meetingpoint of four world's largest religions, the unique connection of east and west. It is the leading political, social and cultural center of Bosnia and Herzegovina and one of the most interesting tourist destinations in Europe. Many come for the first time, and are enchanted by the soul of this place. And they keep returning.

The general theme of CMBEBIH 2015 is: „Expand your horizonst hrough biomedical engineering". The Conference program consists of Plenary/Keynote lectures, oral and poster sessions, workshops, special sessions, round table discussions and student workshops.

Members of the Bosnia and Herzegovina Medical and Biological Engineering Society are very proud that they were the initiators and organizers of the 1st Conference in our country. Also, special thanks to our collaborators, the International Federation for Medical and Biological Engineering, Academy of Science and Arts of Bosnia and Herzegovina, University of Sarajevo, University of Tuzla, International Burch University, University of Bihac and University of Zenica for their continuous support through this process.

I would like to thank all the members of the CMBEBIH 2015 Conference Committee, Honorary Chairs, Scientific Committee, Sponsors, Partners and Organising Committee for their help before and during the Conference. I also thank all reviewers for their time spent on reviewing the papers and all their comments aimed at helping authors improving their papers. I am particularly grateful to all Keynote Speakers. Finnally, I thank all authors for submitting papers and for their patience through the process.

I feel confident that you will enjoy CMBEBIH 2015 both scientifically and socialy. We will make every effort to make CMBEBIH 2015 an unforgettable event, and an event you will want to attend again next year. This is also the place where you will meet your old friends and make new ones.

Together we will continue on the journey expend horizons through biomedical engineering and we will face new challenges and opportunities that will make us a stronger, more innovative, and most importantly, a more cohesive scientific community.

We look forward to meeting you all in Sarajevo. And we look forward to welcome you back in the future, because, believe me, you will want to come back!

Almir Badnjević
Conference Chair
President of Bosnia and Herzegovina Medical
and Biological Engineering Society

COMMITTEES

Conference Chair

Badnjević Almir, Bosnia and Herzegovina Medical and Biological Engineering Society, Verlab, Verification Laboratory, Sarajevo, Bosnia and Herzegovina

Conference Co-chairs

Omerhodžić Ibrahim, Bosnia and Herzegovina Medical and Biological Engineering Society, Clinical Centre University of Sarajevo
Dedić Mirza, Bosnia and Herzegovina Medical and Biological Engineering Society, University of Sarajevo, Faculty of Pharmacy

Honorary Chairs

Magjarević Ratko, President of Internation Federation of Medical and Biological Engineering (IFMBE)
Avdispahić Muharem, Rector of University of Sarajevo
Antunović Ranko, University of East Sarajevo, Faculty of Mechanical Engineering
Behlilović Narcis, University of Sarajevo, Faculty of Electrical Engineering
Bodonyi Claire, Embassy of France in Bosnia and Herzegovina
Džaferović Ejub, University of Sarajevo, Faculty of Mechanical Engineering
Hadžović-Džuvo Almira, University of Sarajevo, Faculty of Medicine
Hodžić Atif, University of Bihać, Faculty of Technical Engineering
Kunosić Suad, University of Tuzla, Faculty of Science
Ljuca Farid, Pro rector for scientific research of University of Tuzla
Mujagić Zlata, University of Tuzla, Faculty of Pharmacy
Pjanić Edin, University of Tuzla, Faculty of Electrical Engineering
Šahinović Refik, Rector of University of Bihać
Škrijelj Rifat, University of Sarajevo, Faculty of Science
Uzunoglu Mehmet, International Burch University
Završnik Davorka, University of Sarajevo, Faculty of Pharmacy
Zečić Dževad, Rector of University of Zenica

Scientific Committee

President of Scientific Committee: Mujčić Aljo, University of Tuzla, Faculty of Electrical Engineering
Aganović Damir, Clinical Center University of Sarajevo
Avdagić Zikrija, University of Sarajevo, Faculty of Electrical Engineering
Avdaković Samir, University of Sarajevo, Faculty of Electrical Engineering
Babić Zdenka, University of Banja Luka, Faculty of Electrical Engineering
Beganović Adnan, Clinical Centre University of Sarajevo
Begić Zijo, Clinical Centre University of Sarajevo
Biščević Mirza, Clinical Centre University of Sarajevo, Faculty of Medicine
Bečić Fahir, University of Sarajevo, Faculty of Pharmacy
Bošković Dušanka, University of Sarajevo, Faculty of Electrical Engineering
Busuladžić Mustafa, University of Sarajevo, Faculty of Medicine
Božić Milorad, University of Banja Luka, Faculty of Electrical Engineering
Čorić Jozo, University of Zenica, Faculty of Health Studies Zenica
Džudžević-Čančar Hurija, University of Sarajevo, Faculty of Pharmacy

Hasić Sabaheta, University of Sarajevo, Faculty of Medicine
Hukić Mirsada, Academy of sciences and arts of Bosnia and Herzegovina
Huseinagić Haris, University Clinical Center Tuzla, Faculty of Medicine Tuzla
Jadrić Radivoj, University of Sarajevo, Faculty of Medicine
Kiseljaković Emina, University of Sarajevo, Faculty of Medicine
Kovačević Peđa, Univesity of Banja Luka, Faculty of Medicine
Kozarić Amina, International Burch University Sarajevo
Lacković Igor, University of Zagreb, Faculty of Electrical Engineering and Computing Zagreb
Marjanović Damir, International Burch University Sarajevo
Nurkić Midhat, University of Tuzla, Faculty of Medicine, University Clinical Center Tuzla
Mašić Izet, University of Sarajevo, Faculty of Medicine
Mešić Elmedin, University of Sarajevo, Faculty of Mechanical Engineering
Omanović Mikličanin Enisa, University of Sarajevo, Faculty of agricultural and food science
Omerbašić Ago, University of Sarajevo, Faculty of Medicine
Pilav Ilijaz, Clinical Center University of Sarajevo, Faculty of Medicine
Rotim Krešimir, President of Southeast Europe Neurosurgical Society
Sapčanin Aida, University of Sarajevo, Faculty of Pharmacy
Stojanović Radovan, University of Montenegro, Faculty of Electrical Engineering
Solakovic Nedim, University of Bihac
Subasi Abdulhamit, International Burch University
Suljanović Nermin, University of Tuzla , Faculty of Electrical Engineering
Turan Yusuf, International Burch University Sarajevo
Velija Zelija Ašimi, Clinical Center University of Sarajevo
Vehabović Midhat, Bosnalijek Sarajevo
Vranić Edina, University of Sarajevo, Faculty of Pharmacy
Zajc Matej, University of Ljubljana, Faculty of Electrical Engineering
Zubčević Smail, Clinical Center University of Sarajevo, Faculty of Medicine

Organising Commitee

Begić Edin
Binakaj Zahida
Čatić Tarik
Dedić Adi
Drljević Harun
Gurbeta Lejla
Hadžić Mirsad
Herenda Safija
Hrvat Emina
Huskić Vildana
Insanić Jusufović Fatima
Kadić Ajdin
Kadić Azra
Kadić Nedžad
Klepo Lejla
Kulović Edin
Maleškić Emina
Ostojić Jelena
Rovčanin Bekir
Škrijelj Venesa
Tahto Ema
Trogrlić Darko

PARTNERS

Organised by:

Co-Organiser

Endorsed by:

Partners:

Exclusive media partners:

Conference Friend:

Tourist partner:

Media partners:

SPONSORS:

Golden sponsor:

Silver sponsor:

Sponsors:

KEYNOTE SPEAKERS

Ratko Magjarevic, Ph.D.
The President of International Federation for Medical and Biological Engineering (IFMBE)
Full Professor of Electronic Instrumentation and Biomedical Engineering
University of Zagreb
Title:Challenges of Biomedical Engineering – Research, Industrialization, Sustainability

Leandro Pecchia, Ph.D.
Treasurer of the Health Technology Assessment Division of the International Federation of
Medical and Biomedical Engineering (IFMBE)
Assistant Professor of Biomedical Engineering
University of Warwick
Title:Applied Biomedical Signal Processing and Intelligent eHealth for falls prediction in the elderly

Dejan Milosevic, Ph.D.
Academician, Professor of Physics, University of Sarajevo, Faculty of Science
Title:Attoscience

Werner Mäntele, Ph.D.
Institut für Biophysik der Johann Wolfgang Goethe-Universität
Title:Spectroscopists do it with Light: Development of Optical Sensors for Medical Applications

Hervé Liebgott, Ph.D.
InstitutUniversitaire de France &Creatis, Lyon, France Title:Ultrasound advanced imaging: beyond anatomy

Mustafa Kahramanyol, Ph.D.
Professor emeritus from Gülhane Military Medical Academy, presently Consultant at Kent ENT
Medical Centre, Ankara, Türkiye Title:The GülhaneMastoidectomy

Atilla Aydinli, Ph.D.
Bilkent University, Department of Physics, Turkey
Title:Advances in Plasmonic Detection: Plexcitonic Crystals

Dragan Primorac, Ph.D.
University professor, pediatric medical doctor, forensic expert and geneticist
Title:Personalised medicine: myth or reality

Yves Lemoigne, Ph.D.
IFMP Ambilly France & CERN, Geneva, Switzerland
Title:17 years of high-level education in Medical Physics for Eastern Europe

Mark Bale, Ph.D.
Chair of Bioethics committee of the Council of Europe
Title:Emerging technologies and human rights: what are the challenges?

Mario Medvedec, Ph.D.
Clinical Biomedical Engineer
Professor of Biomedicine and Health; Clinical Medical Sciences; Nuclear Medicine
University Hospital Centre Zagreb, Department of Nuclear Medicine and Radiation Protection
Title:Vision and Provision of Clinical Engineering Division - CED/IFMBE

Damir Marjanovic, Ph.D.
Head of Genetics and Bioengineering Department, International Burch University
Title:Automation of the Forensic DNA Analysis Procedures: Advantages and Challenges

Zijad Dzemic, M.S.
Member of Board of Directors of European Association of National Metrology Institutes
(EURAMET), Institute of Metrology of Bosnia
Title:National metrology institute for Quality of life

GENERAL INFORMATION

Organizer: Bosnia and Herzegovina Medical and Biological Engineering Society
Co-organizers: International Burch University and Faculty of Medicine University of Sarajevo
Endorsed by: International Federation for Medical and Biological Engineering (IFMBE), Academy Of Sciences and Arts of Bosnia and Herzegovina, IEEE Section of Bosnia and Herzegovina, University of Sarajevo, University of Tuzla, University of Zenica, University of Bihać.
Sponsors:
Golden sponsorship: Verlab doo
Silver sponsorship: Medtronic
Regular sponsorship: DevLogic, Bosnalijek, Bor Banka, Prevent, Pobjeda-RudetddGoražde, Hotel Europe Sarajevo, Print Design doo
Partners: Faculty of Electrical Engineering (University of Sarajevo), Faculty of Pharmacy (University of Sarajevo), Faculty of Pharmacy (University of Tuzla), University Clinical Center of Sarajevo, Faculty of Mechanical Engineering (University of Sarajevo), Faculty of Mechanical
Engineering (University of East Sarajevo), Faculty of Science (University of Sarajevo)
Conference Friend: Embassy of France with her Excellenay Claire Bodonyi
Partner Associations: Pharmaceutical Chamber of Federation of Bosnia and Herzegovina, Southeast European Neurosurgical Society (SENS), STELEX, BoHeMSA, Pharmaceutical Society of Bosnia and Herzegovina, Association of Students of Medical Faculty, UNUBIH, Federal Medical Chamber of Bosnia and Herzegovina.
Exclusive TV partner: N1 TV
Exclusive Radio partner: RSG radio
Exclusive web media: eKapija portal
Media partners: BH-index, Valetudo, Krajina u srcu.net, krajina.ba, ekskluziva.ba, krupljani.ba, Studomat, biscani.net, FENA
Event partner: IEEE MECO 2015
Tourist partner: Kompas Sarajevo

CONFERENCE VENUE
INTERNATIONAL BURCH UNIVERSITY
Francuske revolucije bb, Ilidza
71000 Sarajevo,
Bosnia and Herzegovina http://www.ibu.edu.ba/

STUDENT WORKSHOP VENUE
MEDICAL FACULTY, UNIVERSITY OF SARAJEVO
Cekaluša 90, 71000 Sarajevo, Bosna i Hercegovina
Tel: +387 33 226 478 http://mf.unsa.ba//

CONFERENCE THEMES

1. BIOMEDICAL SIGNAL PROCESSING
Physiological systems modeling
Time-frequency and time scale analysis
Nonlinear dynamic analysis
Adaptive and parametric filtering and estimation
Pattern recognition and soft computing techniques
Data mining and processing

2. BIOMEDICAL IMAGING AND IMAGE PROCESSING
Magnetic resonance imaging / Computed tomography / Mammography
Ultrasound imaging / Optical imaging and microscopy
PET and SPECT
Electrical and magnetic source imaging / Impedance imaging
Multimodality imaging / Novel imaging modalities
Image processing, analysis and classification

3. BIOSENSORS AND BIOINSTRUMENTATION
Physical sensors and sensor systems
Bioelectric, biological and chemical sensors and sensor systems
Physiological monitoring / Instrumentation / Integrated systems
Implantable technologies, sensors and systems
Wearable sensors / Body area and wireless sensor networks / Telemetric systems

4. BIO-MICRO/NANO TECHNOLOGIES
Internal, implanted and portable miniaturized systems
BioMEM / NEMS
Microfluidics / Lab-on-a-chip devices
Nano-biotechnology

5. BIOMATERIALS
Biomaterials for sensing and actuation
Biomimetics, bioinspired and patterned biomaterials
Biomaterials in cellular and tissue engineering

6. BIOMECHANICS, ROBOTICS AND MINIMALLY INVASIVE SURGERY
Musculoskeletal models and human movement analysis
Orthotic, prosthetic and rehabilitation robotics and biomechanics
Cardiovascular and respiratory fluid mechanics and biomechanics
Human-robot interaction / Robot-aided surgery
Biologically inspired robotics / Micro-biorobotics Minimally invasive surgery

7. CARDIOVASCULAR, RESPIRATORY AND ENDOCRINE SYSTEMS ENGINEERING
Cardiac and respiratory function and modeling
Cardiovascular and respiratory signal processing and modeling
Cardiovascular electrophysiology and regulation
Respiratory disease / Sleep disorder / Respiratory engineering
Endocrine systems, function, modeling and control

8. NEURAL AND REHABILITATION ENGINEERING
Brain physiology and modeling
Neural signal processing
Neural interfaces and regeneration
Motor and sensory neuroprostheses/ Brain-machine interface
Rehabilitation and wearable technologies
Brain functional imaging / Neurological disorders

9. MOLECULAR, CELLULAR AND TISSUE ENGINEERING
Biomaterial-cell interactions
Cellular force transduction
Embryonic and stem cells in regenerative medicine
Electrical fields at the cell and protein scale
Electroporation
Tissue engineering / Scaffolds in tissue engineering

10. BIOINFORMATICS AND COMPUTATIONAL BIOLOGY
Bioinformatics and computational modeling of complex omic data
Systems biology / Systems medicine
Translational biomedical informatics for clinical applications
Modeling of molecular, cellular and organ pathways

11. CLINICAL ENGINEERING AND HEALTH TECHNOLOGY ASSESSMENT
Clinical engineering / Health technology management
Health technology policy, economics and ethics / Health technology assessment
Technology development, commercialization, assessment and management
Safety and human factors engineering for medical devices and systems
IT in medicine / Equipment interconnectivity and integration
Clinical engineering and disaster preparadness

12. HEALTH INFORMATICS, E-HEALTH AND TELEMEDICINE
Personal, pervasive, preventive, and participatory health systems
Ambient assisted living / Smart homes Body area networks / Wireless technologies
mHealth/ eHealth / Telemedicine
Health information management / Electronic health records
Decision support methods and systems

13. BIOMEDICAL ENGINEERING EDUCATION
Biomedical engineering education and curriculum development
Biomedical undergraduate and graduate student research projects
Career development in biomedical engineering

14. PHARMACEUTICAL ENGINEERING
Pharmaceutical Development in Industry
Bio-/Pharmaceutical Manufacturing
Pharmaceutical Devices
Pharmacokinetics

PROCEEDINGS

Attoscience

D.B. Milošević[1, 2]

[1] Faculty of Science, University of Sarajevo, Sarajevo, Bosnia and Herzegovina
[2] Academy of Sciences and Arts of Bosnia and Herzegovina, Sarajevo, Bosnia and Herzegovina

Abstract— **Lasers, as sources of strong electromagnetic field, have enabled the investigation of nonlinear light-matter interaction. Thirty years ago ultrafast lasers have reached a fundamental limit – the duration of the laser pulses in visible and near infrared range was limited to few optical cycles and was measured in femtoseconds (1 fs = 10^{-15} s). The route to generate and measure even shorter attosecond (1 as = 10^{-18} s) pulses is based on extreme nonlinear optics and on the technology of laser carrier-envelope phase stabilization. In the 21st century researchers have broken the femtosecond barrier and new area of science – attoscience – has emerged. We discuss these revolutionary attosecond tools and their application to myriad problems in science.**

Keywords— **Physics, Attoscience, Atomic and Molecular Physics, Optics, Lasers.**

I. Introduction: Historical Development of the Measurement of Time and Lasers

In the history of humankind the measurement of time is among the earliest endeavors that maybe classified as science. An example is the development of calendars in ancient civilizations. For the daytime measurement in hours the Egyptians have developed the sun-clocks or sundials (for night time, the water-clocks were invented). In the 14th century the mechanical clocks were developed in Europe. Galileo has studied the pendulum motions using his heartbeats so that, at the end of the 16th century, the time precision was measured in seconds. The sub-second time resolution has become possible with the development of fast photography. The famous is the Muybridge's photo series (1878) which proved that horse's hooves do leave the ground at a running pace. The time resolution better than millisecond was achieved in mid-1900ies using stroboscopy (example is the Edgerton's photograph of a bullet passing through an apple).

The time scale of chemical reactions is the period of oscillations of atoms in molecule which is 10-100 fs (1 fs = 10^{-15} s). Therefore, it is not surprising that the chemists were those who paved the way for a further improvement of the time resolution [1]. Norrish, Porter and Eigen in 1967 have been awarded by the Nobel prize in chemistry for reaching the millisecond to nanosecond scale. They used the flash photolysis method in 1950s. This was before the realization of the first laser by Maiman in 1960.

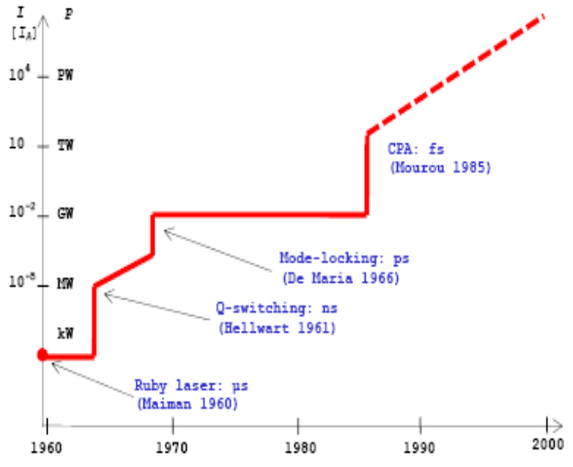

Fig. 1. Timeline of the laser intensity and the pulse length evolution from the free-running laser (Maiman) to the chirped pulse amplification (CPA) laser (Mourou).

A historical development of the lasers is presented in Fig. 1. The time in years is denoted on the abscissa, while on the ordinate the maximum power P in watts, achieved by such lasers, is shown. The corresponding peak intensity I, obtained by focusing of such laser pulses on an area of 10 μm, is also depicted on the ordinate. It is expressed in atomic units of intensity $I_A = 3.51 \times 10^{16}$ W/cm^2 (this intensity corresponds to the electric field which electron feels in the hydrogen atom). In 1960s the development of the laser technique was very fast. The nanosecond giant pulses have become possible by Q-switching (Hellwart 1961), while the picosecond pulses were realized by mode-locking [2]. The sub-picosecond pulses were achieved using dye lasers in 1970s (Shank and Ippen 1974 [3]; in 1986 the pulses of duration of 6 fs were achieved [4]). As concerns the maximum power of the laser pulses, for almost 20 years, it was limited to the gigawatt pulses which were achieved by mode locking. The discovery of the chirped pulse amplification (CPA) technique by Mourou and co-workers in 1985 has introduced a qualitative improvement in the size and performance of the laser systems: the solid state Ti:Sapphire femtosecond lasers, which operate at 800 nm and enable terawatt powers, have rapidly replaced the dye lasers and are now a standard laboratory tool. Furthermore, the fo-

cused laser pulse intensity has become comparable to the corresponding atomic unit, so that the influence of the laser field on the atomic processes cannot be treated as a perturbation. It has become evident that new, nonperturbative, theoretical approaches for treatment of atomic processes in such strong fields should be developed. For a review see [5,6].

II. FEMTOCHEMISTRY

In the context of application of short laser pulses, two more Nobel prizes in chemistry should be mentioned. The first one was awarded to Herschbach, Lee and Polanyi in 1986 for their contributions concerning the dynamics of chemical elementary processes. Their crossed molecular beam-laser studies have probed the molecular dynamics with nanosecond to picosecond resolution. Second, in 1999 the Nobel prize was acknowledged to Ahmed Zewail for his studies of the transition states of chemical reactions using femtosecond spectroscopy. In fact, he has shown that it is possible with ultrafast laser technique to see how atoms in a molecule move during a chemical reaction. As we have mentioned, these processes develop on the time scale of the period of oscillation of atoms in molecule which is 10-100 fs, so that this area of science was named the femtochemistry. In analogy, the term femtobiology was introduced. An example of recent achievements in this area is presented in [7]. Combining high spatial and temporal resolution, the molecular dynamics can be explored with the so called 4D (three spatial dimensions and time) microscopy [8].

III. ATTOPHYSICS

The length of one optical cycle of 800 nm Ti:Sapphire laser is 2.7 fs, which sets a lower limit on the laser pulse duration. This is the so-called femtosecond barrier (see the review article by DiMauro and Agostini [9]). Namely, a pulse of light should be at least one cycle long (pulse length of two cycles was realized in [10]). Therefore, the pulses shorter than 1 fs = 10^{-15} s can be achieved only using the shorter wavelengths, i.e. using higher carrier frequencies. New area of physics which explores the processes shorter than 1 fs is called attophysics (1 as = 10^{-18} s). According to Wikipedia, the attophysics is a branch of physics wherein attosecond duration pulses of electrons or photons are used to probe dynamic processes in matter with unprecedented time resolution. This branch of physics which involves studying some of the fastest physical events is also known as attoscience. The term attochemistry is also in use. Today, attophysicists mostly study molecular phenomena, such as how a particular protein breaks down under X-ray bombardment. One of the primary goals of attosecond science is to provide more insights into the dynamics of atomic electrons. Femtochemistry explores the dynamics of atoms in a molecule. For the electrons this time scale is too slow. Namely, the atomic unit of time is 24.2 as. If one supposes that the Bohr model of atom (old quantum theory) is valid then the electron in the hydrogen atom needs 152 as to make a full circle around the nucleus. How „short“ is an attosecond? One attosecond is to 1 second as one second is to the age of the universe. Imagine how different our universe is compared to the universe when it was born. The world of attoseconds is equally different from our world.

The first proposal how to generate attosecond pulses was based on Fourier synthesis, i.e. on mimicking the operation of a mode-locked laser. In principle, one has to produce a comb of equidistant frequencies in the spectral domain with controlled relative phases. In 1990 Hänsch [11] has proposed using sum and frequency mixing for this purpose, while in 1992 Farkas and Toth [12] have recognized that high-order harmonic generation (HHG) could easily produce a broad spectral domain in a series of lines separated by twice the fundamental frequency (see the next section). In 1994 Kaplan [13] has suggested another physical effect for obtaining a broad series of equidistant frequencies: cascaded stimulated Raman scattering (see also papers [14,15] by Harris and Sokolov). Both the harmonic and Raman methods have now been realized, and in the case of HHG pulses as short as 130 as were synthesized [16]. The phase-locking of a periodic spectrum of equidistant frequencies results in a periodic intensity profile in the time domain, i.e. using this method a comb or train of attosecond pulses was realized. For producing a single attosecond pulse two methods were proposed and realized [9]. The first one is based on the high sensitivity of HHG on laser polarization. High harmonics are efficiently emitted only if the laser field is linearly polarized. Using special field configurations it becomes possible to have a linearly polarized field during a very short interval of time and thus to extract a single pulse from the pulse train. The second method was based on HHG by few-cycle pulses. This will be discussed in section V. Therefore, the attosecond pulses were realized and this has opened a possibility for various applications of attoscience [9].

IV. HIGH-ORDER HARMONIC GENERATION AND THE ATTOSECOND PULSE TRAIN

We will now discuss the three-step model of HHG [6] which offers a semiclassical explanation of this process. In the first step, the electron tunnels out through the potential barrier formed by the atomic potential (ionization potential

denoted by I_P) and the laser field potential (potential energy $-zF(t_0)$, where $F(t_0)$ is the electric field at the ionization time t_0). In the second step, the electron is accelerated by the laser field which has maximum at t_0. After a half of the optical cycle, the field is again maximal but in the opposite direction so that the electron moves toward the nucleus. It is back at the origin at the time t, $z(t) = z(t_0)$, and has accumulated the kinetic energy E_K on its way through the laser field. Finally, in the third step, the electron recombines with the parent ion, releasing this kinetic energy plus ionization potential in the form of a high harmonic whose energy is $n\hbar\omega = I_P + E_K$. The energy E_K is proportional to I/ω^2 so that, for a strong laser field, the harmonic order n can be few hundreds. At the time of recombination the laser field is close to zero. The harmonic emission time is only a fraction of the optical cycle $T = 2\pi/\omega$ ($T = 2.7$ fs for 800 nm), so that the duration of the harmonic pulse is in the attosecond region. By mode-locking of several neighbor harmonics one can obtain a train of attosecond pulses which are shorter than 100 as [17].

V. Few-Cycle Pulses and Above-Threshold Ionization

We have mentioned that with dye lasers, having a centre wavelength around 600 nm, the pulses as short as 6 fs were reported already in 1987 [4]. These ultrashort pulses were 2 cycles long. However, the technical limitations of dye laser technology have prevented further progress and applications. The breakthrough came 10 years latter and is based on Ti:Sapphire mode-locked laser. Amplified pulses of duration less than 30 fs are fed into a hollow fibre filled with dilute noble gas and the self-phase modulation broadens the spectrum to a bandwidth of several hundreds nanometers. After compensation of dispersion, pulses of 5 fs were achieved [18]. These pulses have superior performances and they are powerful enough to drive strong-field processes.

For characterization of a linearly polarized few-cycle laser pulse, besides the electric field vector amplitude and the carrier frequency ω, a new parameter has to be introduced. This is the carrier-envelope phase (CEP) or the so-called absolute phase ϕ. By definition, this is the relative phase between the carrier wave and the envelope. If the carrier wave and the envelope are in phase ($\phi = 0$) the field has one strong positive peak and two lower negative peaks. The consequence is that for strong-field ionization (the so-called above-threshold ionization (ATI) [5,6,19]), due to a high nonlinearity of this process, most electrons are emitted in the directions determined by the laser field direction which corresponds to this strong peak. For $\phi = \pi$ this peak is in the opposite direction. This led Paulus et al. [20] to an idea to use the so-called stereo-ATI experiment in order to determine the absolute phase. First experimental evidence of absolute phase effects was realized with a circularly polarized laser field. This experiment was successfully simulated in [21,22]. In the above-mentioned experiment by Paulus et al. [20] the phase ϕ changes from one laser shot to the other. For a further development of attoscience it was necessary to stabilize this phase. A half of the Nobel prize in physics in 2005 has been awarded to Hall and Hänsch for their contributions to the development of laser-based precision spectroscopy, including the optical frequency comb technique [23]. They invented self referencing or f-to-$2f$ technique for stabilizing a femtosecond laser's frequency comb. This has enabled in 2003 to stabilize the CEP in a femtosecond pulse amplifier and to apply it to HHG [24]. The value of CEP can be determined via its effect on the spectrum of high-energy ATI electrons as predicted by [25] and experimentally observed in [26].

At the end of this section, we mention an interesting attosecond double-slit experiment [27]. For some values of the absolute phase, the electrons which go to the left are emitted at one moment only, while the electrons which go to the right are emitted in two instants of time. Therefore, on the right detector clear interference fringes are observed. This is a realization of the famous double-slit or which-way experiment, well known in quantum physics. However, the slits are not in space but in time. More precisely, we have two windows in time during which the probability of ATI is large.

VI. Molecular Orbital Tomography and Laser-Induced Electron Diffraction

One of the applications of attophysics is the so-called molecular orbital tomography [28] using which we can "see" the amplitude and phase of an electron in a molecule. This can be achieved by rotating molecule and recording the high-harmonic spectrum. From the obtained experimental data we calculate the molecular ground state wave function (see Fig. 2).

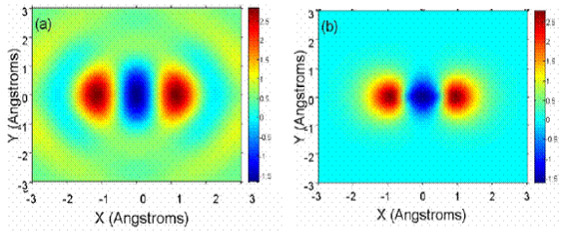

Fig. 2. Reconstruction of the ground state wave function of N_2 molecule. Molecular orbital $3\sigma_g$: (a) calculated using experimental data, (b) calculated using molecular quantum mechanics.

There is a close association between the molecular tomography method and the more familiar application of tomographic imaging in medicine. When a patient goes to the hospital for a tomographic scan, a series of two-dimensional X-ray images are taken, with the X-rays passing at different angles through the patient's body. In the molecular tomography, the patient is replaced by a molecule, and the X-rays by recombining electrons.

It has recently been shown that it is possible combining short laser pulses with electron diffraction method to rapidly map the molecular structure in three dimensions (3D) [29]. This is a step toward 3D molecular movie. It was demonstrated in trifluoroiodomethane (CF_3I molecule). Improving the method of Ref. [29] the molecular movie of the retinal, a visual-system molecule that rapidly changes shape when it absorbs light, may be possible. A better method that can be used for such 3D movies is the laser-induced electron diffraction (LIED) – a technique that uses the elastically scattered photoelectrons to construct diffraction images of the parent molecule [30,31].

VII. CONCLUDING REMARKS

We have briefly reviewed the history of the time measurement from the ancient civilizations to the end of the 20th century. This period has finished with the development of femtochemistry using which it was possible to track the motion of atoms in molecules. The beginning of the 21st century was characterized with the rapid development of a new area of science – attoscience. After short introduction to the attoscience, we have devoted our attention to two processes which are important for attophysics: high-order harmonic generation and above-threshold ionization by few-cycle laser pulses. At the end of this paper, we mention some recent achievements of attophysics and give references for further reading. In several recent experiments it was shown that attosecond electron motion can be controlled by strong short pulses and that it can be used to directly measure the electric field of the laser pulse (see the review articles [32,33,34,35]). It was also demonstrated how is possible to image molecular structures (orbitals) and dynamics using the highly nonlinear interaction between light and molecules [28]. This has opened a possibility for application of attophysics in molecular physics and quantum chemistry. The dream of following electronic and structural changes inside a molecule during a chemical reaction, i.e., the attochemistry [36], is becoming a reality. More recent reviews related to attoscience can be found in the book [37] which should be published in 2015.

REFERENCES

1. A.H. Zewail, Femtochemistry: Atomic-scale dynamics of the chemical bond using ultrafast lasers (Nobel lecture), *Angew. Chem., Int. Ed. Engl.* **39**, 2586-2631 (2000).
2. A.J. DeMaria, D.A. Stetser, H. Heynau, Self mode-locking of lasers with saturable absorbers, *Appl. Phys. Lett.* **8**, 174-176 (1966).
3. C.V. Shank, E.P. Ippen, Subpicosecond kilowatt pulses from a mode-locked cw dye laser, *Appl. Phys. Lett.* **24**, 373-375 (1974).
4. R.L. Fork, C.H. Brito Cruz, P.C. Becker, C.V. Shank, Compression of optical pulses to six femtoseconds by using cubic phase compensation, *Opt. Lett.* **12,** 483-485 (1987).
5. W. Becker, F. Grasbon, R. Kopold, D.B. Milošević, G.G. Paulus, H. Walther, Above-threshold ionization: From classical features to quantum effects, *Adv. At. Mol. Opt. Phys.* **48**, 35-98 (2002).
6. D.B. Milošević, F. Ehlotzky, Scattering and reaction processes in powerful laser fields, *Adv. At. Mol. Opt. Phys.* **49**, 373-532 (2003).
7. M.M. Lin, L. Meinhold, D. Shorokhov, A.H. Zewail, Unfolding and melting of DNA (RNA) hairpins: the concept of structure-specific 2D dynamic landscapes, *Chem. Phys. Phys. Chem.* **10,** 4227-4239 (2008).
8. B. Barwick, H.S. Park, O.-H. Kwon, J.S. Baskin, A.H. Zewail, 4D Imaging of Transient Structures and Morphologies in Ultrafast Electron Microscopy, *Science* **322,** 1227-1231 (2008).
9. P. Agostini, L.F. DiMauro, The physics of attosecond light pulses, *Rep. Prog. Phys.* **67,** 813-856 (2004).
10. G. Steinmeyer, D.H. Sutter, L. Gallmann, N. Matuschek, U. Keller, Frontiers in ultrashort pulse generation: Pushing the limits in linear and nonlinear optics, *Science* **286,** 1507-1512 (1999).
11. T.W. Hänsch, A proposed sub-femtosecond pulse synthesizer using separate phase-locked laser oscillators, *Opt. Commun.* **80**, 70-75 (1990).
12. G. Farkash, C. Toth, Proposal for attosecond light pulse generation using laser induced multiple-harmonic conversion processes in rare gases, *Phys. Lett.* A **168**, 447-450 (1992).
13. A.E. Kaplan, Subfemtosecond pulses in mode-locked 2π solitons of the sascade stimulated Raman scattering, *Phys. Rev. Lett.* **73**, 1243-1246 (1994).
14. S.E. Harris, A.V. Sokolov, Broadband spectral generation with refractive index control, *Phys. Rev.* A **55**, R4019-R4022 (1997).
15. S.E. Harris, A.V. Sokolov, Subfemtosecond Pulse Generation by Molecular Modulation, *Phys. Rev. Lett.* **81**, 2894-2897 (1998).
16. Y. Mairesse, A. de Bohan, L.J. Frasinski, H. Merdji, L.C. Dinu, P. Monchicourt, P. Breger, M. Kovačev, R. Taïeb, B. Carré, H.G. Muller, P. Agostini, P. Salières, Attosecond synchronization of high-harmonic soft X-rays. *Science* **302**, 1540-1543 (2003).
17. D.B. Milošević, W. Becker, Attosecond pulse trains with unusual nonlinear polarization, *Phys. Rev.* A **62**, 011403(R) (2000).
18. M. Nisoli, S. De Silvestri, O. Svelto, R. Szipöcs, K. Ferencz, Ch. Spielmann, S. Sartania, F. Krausz, Compression of high-energy laser pulses below 5 fs, *Opt. Lett.* **22**, 522-524 (1997).
19. D.B. Milošević, G.G. Paulus, D. Bauer, W. Becker, Above-threshold ionization by few-cycle pulses, *J. Phys. B: At. Mol. Opt. Phys.* **39**, R203-R262 (2006).
20. G.G. Paulus, F. Grasbon, H. Walther, P. Villoresi, M. Nisoli, S. Stagira, E. Priori, S. De Silvestri, Absolute-phase phenomena in photoionization with few-cycle laser pulses, *Nature* **414**, 182-184 (2001).

21. D.B. Milošević, G.G. Paulus, W. Becker, Phase-dependent effects of a few-cycle laser pulse, *Phys. Rev. Lett.* **89**, 153001 (2002).
22. D.B. Milošević, G.G. Paulus, W. Becker, Above-threshold ionization with few-cycle laser pulses and the relevance of the absolute phase, *Laser Phys.* **13**, 948-958 (2003).
23. T.W. Hänsch, Nobel Lecture: Passion for precision, *Rev. Mod. Phys.* **78**, 1297-1309 (2006).
24. A. Baltuška, Th. Udem, M. Uiberacker, M. Hentschel, E. Goulielmakis, Ch. Gohle, R. Holzwarth, V.S. Yakovlev, A. Scrinzi, T.W. Hänsch, F. Krausz, Attosecond control of electronic processes by intense light fields, *Nature* **412**, 611-615 (2003).
25. D.B. Milošević, G.G. Paulus, W. Becker, High-order above-threshold ionization with few-cycle pulse: a meter of the absolute phase, *Opt. Exp.* **11**, 1418-1429 (2003).
26. G.G. Paulus, F. Lindner, H. Walther, A. Baltuška, E. Goulielmakis, M. Lezius, F. Krausz, Measurement of the phase of few-cycle laser pulses, *Phys. Rev. Lett.* **91**, 253004 (2003).
27. F. Lindner, M.G. Schätzel, H. Walther, A. Baltuška, E. Goulielmakis, F. Krausz, D.B. Milošević, D. Bauer, W. Becker, G.G. Paulus, Attosecond double-slit experiment, *Phys. Rev. Lett.* **95**, 040401 (2005).
28. J. Itatani, J. Levesque, D. Zeidler, H. Niikura, H. Pépin, J.C. Kieffer, P.B. Corkum, D.M. Villeneuve, Tomographic imaging of molecular orbitals, *Nature* **432**, 867-871 (2004).
29. C.J. Hensley, J. Yang, M. Centurion, Imaging of isolated molecules with ultrafast electron pulses, *Phys. Rev. Lett.* **109**, 133202 (2012).
30. C.I. Blaga, J. Xu, A.D. DiChiara, E. Sistrunk, K. Zhang, P. Agostini, T. A. Miller, L.F. DiMauro, and C.D. Lin, Imaging ultrafast molecular dynamics with laser-induced electron diffraction, *Nature* **483**, 194-197 (2012).
31. E. Hasović, D.B. Milošević, Strong-field approximation for above-threshold ionization of polyatomic molecules. II. The role of electron rescattering off the molecular centers, *Phys. Rev. A* **89**, 053401 (2014).
32. A. Scrinzi, M.Yu. Ivanov, R. Kienberger, D.M. Villeneuve, Attosecond physics, *J. Phys. B: At. Mol. Opt. Phys.* **39**, R1-R37 (2006).
33. K. Midorikawa, Y. Nabekawa, A. Suda, XUV multiphoton processes with intense high-order harmonics, *Prog. Quantum Electron.* **32**, 43-88 (2008).
34. M. Nisoli, G. Sansone, New frontiers in attosecond science, *Prog. Quantum Electron.* **33**, 17-59 (2009).
35. F. Krausz, M. Ivanov, Attosecond physics, *Rev. Mod. Phys.* **81**, 163-234 (2009).
36. P. Salières, A. Maquet, S. Haessler, J. Caillat, R. Taïeb, Imaging orbitals with attosecond and Ångström resolutions: toward attochemistry? *Reports on Progress in Physics* **75**, 062401 (2012).
37. D.B. Milošević, Few-cycle-laser-pulse induced and assisted processes in atoms, molecules, and nanostructures, in *Ultrafast ionization dynamics induced and probed by laser pulses, attosecond XUV/soft-X-ray pulses, and (intense) XUV/X-ray pulses from FELs: From atoms, molecules and clusters to nano-objects and solids*, edited by Markus Kitzler and Stefanie Gräfe, Springer, 2015. (to be published)

Dejan B. Milošević is with the Faculty of Science, University of Sarajevo, Zmaja od Bosne 35, 71 000 Sarajevo, BiH (phone: 387-33-610-157; e-mail: milo@bih.net.ba).

Advances in Plasmonic Detection: Plexcitonic Crystals

Ertugrul Karademir[1], Atilla Aydinli[1]

[1]Deparment of Physics, Bilkent University, 06800 Ankara, Turkey

Abstract— **Optical detection at the nanometer scale is based on light matter interaction. Surface plasmons offer a method to localize light into subwavelength dimensions. In this work, a new platform for investigation of plasmon-exciton coupling called plexcitonic crystals is presented. These crystals demonstrate reversible plasmon-exciton coupling control with azimuthal rotation.**

Keywords— **Light-matter interaction, plexcitonic crystals**

Many approaches abound in the field of chemical and biological detection with varying degrees of sensitivity, robustness and cost. The physical mechanisms responsible for the detection vary greatly. Optical detection is one of the most common approaches due to its speed, flexibility and low cost. Mass production of detection platforms require smaller sizes. The basis for any detection lies in the interaction at the nanoscale and biological detection is no exception. At the heart of the Surface Plasmon Resonance (SPR) detection of biological entities lays the interaction of surface plasmons with biological species through modification of the plasmon environment. Research into light matter interaction promises improvements in detection. In cases of biological entities emitting light involves excitons which are bound electron-hole pairs. The strong electrical fields of plasmons can be used to enhance and amplify excitonic emission through plasmon exciton coupling. Strongly coupled plasmon-exciton modes are called plexcitons [1] which can be used for detection. We propose a new platform for next generation of plasmonic detectors consisting of one and two dimensional corrugated surface patterns coated with a thin metal film and a dye solution. This system shows a controlled coupling action based on the excitation direction of SPP modes. In this work, we explain the physical basis of this scheme based on the control of wavelengths of the forbidden surface plasmon modes.

Periodic corrugation on the metallic surface establishes a band gap region in the dispersion spectrum of surface plasmons when excited with Kretschmann configuration, while direction of plasmon excitation changes the effective periodicity of the corrugation. Three kinds of such patterns have been tested; a one dimensional uniform, a triangular, and a square lattice type crystals. These crystals are fabricated with laser interference lithography. Photoresist coated glass substrates are exposed under deep UV light. With one exposure we obtain one dimensional lattice. Performing another exposure after rotating the sample gives us two dimensional lattice structures. Rotation of the sample for the second exposure determines the rotational symmetry of the lattice. For triangular lattice we rotate the sample 60° in azimuthal direction where as for the square lattice case the azimuthal rotation is 90°.

Resulting lattice structures are defined on photo sensitive polymer after development. Following the development, we coat the samples with Ag film in a thermal evaporation chamber. Ag film thickness determines the ohmic loss that propagating surface plasmons suffer [2].

For all three cases, we identify the directionality of the bandgap. In 1D uniform crystal band gap wavelength approaches to zero, as the propagation direction is shifted from groove perpendicular to groove parallel cases. For triangular and square lattice cases, band gap center oscillates between two finite values for every 60° and 90°s, respectively. We utilized this behavior to control surface plasmon and J-aggregate coupling.

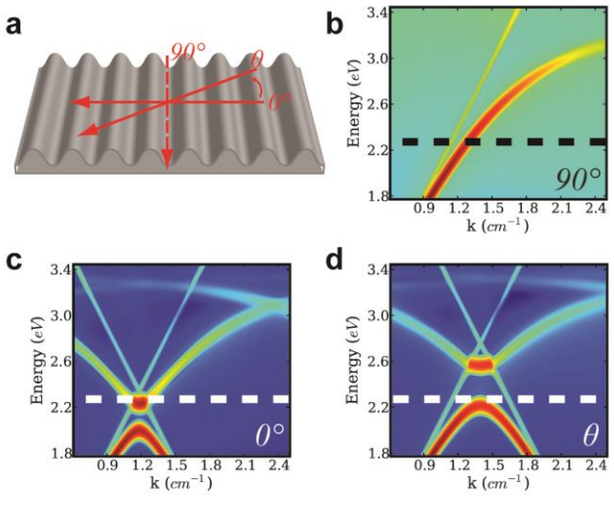

Fig. 1 1D Plexcitonic crystals.

As the J-aggregate we use a cyanine based dye, TDBC, dissolved in poly vinyl alcohol (PVA) matrix in 0.75 mM concentrations. TDBC inside the PVA matrix forms long chains. Resulting excitonic film has a very sharp absorption peak at 590 nm wavelength. Hence, combined with the surface plasmon mode distribution on the metallic surface,

J-aggregate dye offers a reversible tenability with azimuthal rotation. Resulting coupled plasmon-exciton pairs manifest anti-crossing in the dispersion spectra. Anti-crossing or Rabi splitting shows the strength of plasmon-exciton coupling.

Square lattice gives the ability to tune a larger band gap, whereas triangular lattice gives higher number of symmetry points. On square lattice plexcitonic crystals we shift the plasmonic band gap center from 610 nm to 560 nm wavelength passing through the absorption peak of J-aggregate dye matrix. On this crystal when the plasmonic bad-gap is far from the absorption line, Rabi splitting energy is around 60 meV. As the crystal is rotated in the azimuthal direction,splitting energy drops down to 30 meV. When absorption line is totally inside the band gap, we don't see any distinct feature on the dispersion curve indicating strong coupling between plasmons ans excitons. Hence SPPs and excitons becomes uncoupled. The process is reversible. Thus further azimuthal rotation recovers the strong coupling. This diminishing and recovering behavior is repeated at every 90° azimuthal rotation.

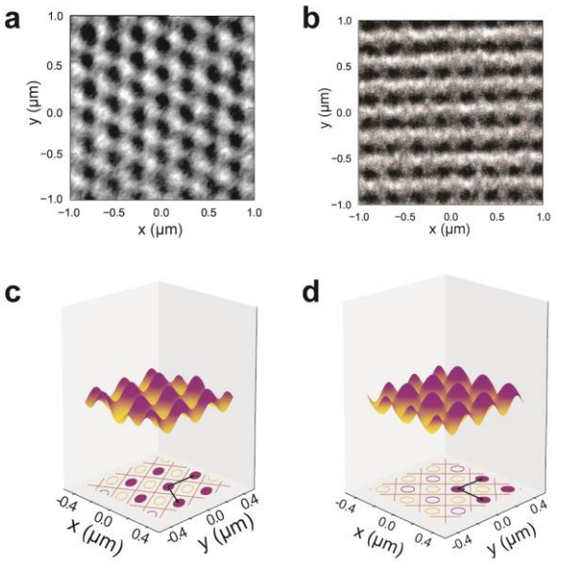

Fig. 2 2D Plexcitonic Crystals

Band gap width can be adjusted with groove depth. Simulations show that, deep triangular lattice can result in omnidirectional decoupling of plexcitons. In simulating the triangular lattice plexcitonic crystal, we choose a groove depth of 80 nm and pitch of the grating is chosen as the plasmonic band gap contains absorption line of the TDBC dye matrix at 0° azimuthal rotation. With 80 nm groove depth, simulations show absorption line of J-aggregate matrix always stays inside the band gap thus forms a omnidirectionally decoupled plexcitonic crystal.

Crystals are periodic structures that exhibit certain symmetries under translation and rotation operations. Periodic nature of such structures yields interesting phenomena in photonic, plasmonics, and biological sensors. For instance, photonic crystals block propagation of photons for a band of energies and allows propagation of others [3,4]. In the case of plasmonic crystals, periodic metallic structures have been shown to display forbidden and allowed bands for propagating plasmons in all crystal directions [5]. We have present a new platform that exploits the geometric dependence of SPP propagation to tune the coupling strength of the SPP-exciton pair. This leads to formation of plexcitons. Directional dependence of plexciton formation in 1D and 2D plexcitonic crystals is demonstrated. Plexcitonic crystals show bare excitonic regions where exciton line intersects the edges of the band gap. In 2D case, this is extended further with the rotational symmetry of the crystal. These crystals show both a tunable energy range of band gap centre for a broad range of wavelengths in the visible, and allow control of interaction strength of plasmon-exciton pairs. This platform is a promising approach for use in surface plasmon based biological sensors.

1. N. T. Fofang, T.-H. Park, O. Neumann, N. A. Mirin, P. Nordlander, and N. J. Halas, "Plexcitonic Nanoparticles: Plasmon− Exciton Coupling in Nanoshell− J-Aggregate Complexes," Nano Lett. **8**, 3481–3487 (2008).
2. S. Balci, C. Kocabas, S. Ates, E. Karademir, O. Salihoglu, and A. Aydinli, "Tuning surface plasmon-exciton coupling via thickness dependent plasmon damping," Phys Rev B **86**, 235402 (2012).
3. S. John, "Strong localization of photons in certain disordered dielectric superlattices," Phys Rev Lett **58**, 2486–2489 (1987).
4. J. O. Vasseur, P. A. Deymier, B. Chenni, B. Djafari-Rouhani, L. Dobrzynski, and D. Prevost, "Experimental and Theoretical Evidence for the Existence of Absolute Acoustic Band Gaps in Two-Dimensional Solid Phononic Crystals," Phys Rev Lett **86**, 3012–3015 (2001).
5. S. C. Kitson, W. L. Barnes, and J. R. Sambles, "Full Photonic Band Gap for Surface Modes in the Visible," Phys Rev Lett **77**, 2670–2673 (1996).

Vision and Provision of Clinical Engineering Division - CED/IFMBE

M. Medvedec

University Hospital Centre Zagreb/Department of Nuclear Medicine and Radiation Protection, Zagreb, Croatia

Abstract— **Clinical engineering is the branch of biomedical engineering dealing with all aspects of medical equipment and technologies used in hospitals and other clinical settings. Clinical Engineering Division is a special division of the International Federation for Medical and Biological Engineering (CED/IFMBE).**

The CED/IFMBE vision is to be a primary international thriving professional, scientific and educational forum for developing, establishing and promoting clinical engineering. The CED/IFMBE mission is to advance worldwide research, development, learning, knowledge, skills and competences on healthcare technology management, to promote global communication and networking, to advance and disseminate worldwide safety tools and effective decision-making processes within the healthcare technology management system, to define and promote quality standards and to encourage excellence in clinical engineering practices and processes worldwide, to stimulate innovation and efficient use of technology-related resources in healthcare worldwide, and to internationally represent and advocate the interests of clinical engineering profession and their global exchange.

In recent years, the CED/IFMBE has been making efforts to provide revised division's charter, multilingual translations of the six volumes from the Ziken 'How to manage' book series for healthcare technology, a comprehensive publication on human factors engineering, an open-access international journal of clinical engineering and healthcare technology assessment, its dedicated web-site and e-conferencing tool, an on-line directory of clinical engineering teaching units and professional associations, clinical engineering awards, international program for certification in clinical engineering, global center for healthcare technology managers on disaster preparedness training, as well as other benefits.

The IFMBE is the only international professional organization that has the CED focusing specifically on all aspects of life cycle management of healthcare technologies. Taking into account the recent activities and the outcomes of its completed and running projects during the last two terms of the CED/IFMBE Board, the latter time seems to be probably one of the most fruitful periods in its history, to the benefit of clinical engineers and healthcare systems, but primarily for the benefit of all patients worldwide.

Keywords— **biomedical engineering, clinical engineering, International Federation for Medical and Biological Engineering, Clinical Engineering Division**

I. Introduction

Biomedical engineering integrates physical, mathematical and life sciences with engineering principles and design concepts applicable in biology and medicine, for the purpose of improving health and quality of life. It creates knowledge from the molecular to system levels, develops and evaluates materials, methods, devices, technologies, information, etc. for the prevention, diagnosis, treatment and palliation of a disease, for optimal health care delivery and patient care and rehabilitation. Clinical engineering is the branch of biomedical engineering dealing with all aspects of medical equipment and technologies used in hospitals or other clinical settings.[1,2]

History of the International Federation for Medical and Biological Engineering (IFMBE) dates back in 1959 when a group of medical engineers, physicists and doctors met in Paris and founded an organization entitled International Federation for Medical Electronics and Biological Engineering. In the mid-1960s, the name of that organization was shortened to International Federation for Medical and Biological Engineering. The IFMBE is primarily a federation of national and transnational organizations and has an estimated 140,000 members in more than 60 affiliated organizations representing their interests in biomedical engineering. High extrapolated membership number is also due to the fact that biomedical engineers are recently among the fastest growing professions, showing strong demands because an aging population is likely to need more medical care and because of increased public awareness of biomedical engineering advances and their benefits. The IFMBE and the International Organization for Medical Physicists (IOMP) are two constituent member organizations of a union called the International Union for Physical and Engineering Sciences in Medicine (IUPESM), thus further contributing to the advancement of physical and engineering sciences in medicine for the benefit and well being of humanity. The objectives of the IFMBE are scientific, technological, literary, and educational. Within the field of biomedical engineering IFMBE's aims are to encourage research and the application of knowledge, and to disseminate information and promote collaboration. As the IFMBE grew, its constituency and objectives changed, while clinical engineering became a viable sub-discipline with an

increasing number of members busy in the health care sector. The IFMBE today represents those engaged in research and development, as well as in clinical engineering. The latter category of clinical engineering now amounts to approximately half of the total membership.[1,3,4]

Since the IFMBE may establish special divisions within the fields of interests to facilitate the growth and development of a branch of the subject and holding of meetings and seminars on special topics, a part of the organizational structure of the IFMBE are currently two divisions: Clinical Engineering Division (CED/IFMBE) and Health Technology Assessment Division (HTAD/IFMBE). Originally established as a working group in 1979, CED/IFMBE attained official division status in 1985. At the present time, CED/IFMBE Board consists of 7 elected members, 2 co-opted members and 7 collaborators.[1,5]

The objective of this paper is to present activities and the achievements of the CED/IFMBE, particularly during the latest two 3-year terms of the CED/IFMBE Board (2009-2015).

II. Role and Activities of CED/IFMBE

A. Vision

The CED/IFMBE vision is to be a primary international thriving professional, scientific and educational forum for developing, establishing and promoting clinical engineering and clinical engineering profession, and for all those who undertake and use clinical engineering principles in healthcare, industry, academia, government, non-governmental organizations, consumer organizations, consultancies and other stakeholders, with the purpose of improving healthcare delivery through the advancement of safe and effective innovation, deployment and management of healthcare technology.[1,6]

B. Mission

The CED/IFMBE mission is to advance worldwide learning, knowledge, research, development and communication of healthcare technology management in the clinical engineering community and other professional communities, and its understanding by other stake holders; to promote global communication, networking and understanding of challenges related to healthcare technology management; to define and promote an international body of knowledge, skills and competences on which the profession of clinical engineering can be practiced in various clinical setting; to advance and disseminate worldwide safety tools and effective decision-making processes within the healthcare technology management system; to define and promote quality standards in clinical engineering practices worldwide; to stimulate innovation and efficient use of technology-related resources in healthcare worldwide; to internationally represent and advocate the interests of clinical engineering professionals and their global exchange; to encourage, through education and training, excellence in clinical engineering practices and processes, and professional exposure worldwide. [1,6]

C. Objectives and tasks

The objectives of the IFMBE specialized division shall be to stimulate research, creation, knowledge and application of new developments within a fields of medical and biological engineering; to develop and improve co-operation and exchange of information among interested and competent individuals working in different countries; to promote collaboration between specialists and subspecialists, including those belonging to other scientific societies and, in particular, to medical societies; to work on other objectives as approved by the IFMBE Administrative Council for each specialized division.[1]

In addition to these general specialized division's objectives and in support of its vision and mission, the CED/IFMBE is particularly focusing on a number of specific objectives and tasks in order to stimulate knowledge creation and sharing through research and application of new methodologies and practices within the field of clinical engineering; to support and improve co-operation and exchange of ideas, information and expertise through meetings, publications and other services for clinical engineers working in different countries, aiming the development of competent clinical engineers and their interaction with experienced clinical engineering leaders; to survey globally for the current state of the clinical engineering profession, both for individuals and institutions, and make global clinical engineering directory; to create, adapt, promote and translate technical and professional guidelines and manuscripts for the activities within the clinical engineering field; to promote collaboration between individual clinical engineers, groups, institutions and clinical engineering societies; to support exchange visits with regional or national societies to engage them closer with the CED/IFMBE and its international benchmarking; to promote sharing of exchange and mentoring programs - student/faculty/practitioner; to examine and update training programs and workshops contents including special train the trainers programs and the usage of existing course models; to promote the CED/IFMBE mission by building strategic relationships with appropriate agencies, and interested public and private sector organizations; to facilitate continuing professional development and to promote improvements in the capacity and quality of healthcare delivery; to collaborate with global, regional,

national and local organizations interested in health technology management to improve the science and increase the outcomes from health technology policy around the world; to examine and update global clinical engineering competencies, body of knowledge, certification programs, study curricula, benchmarking support services and clinical engineering recognitions and awards, as well as present capacity and future needs for manpower and competencies in clinical engineering; to develop dedicated website and other means of communication, including e-conferencing, to ensure that the CED/IFMBE and its work and deliverables are archived, conveyed to and understood by its members and all healthcare technology stakeholders; to investigate the convergence of clinical engineering and information technology (IT) and its education, practice and leadership impact; to conduct periodical international meetings that address the interests and needs of members from all disciplines and backgrounds with an interest in healthcare technology and reflect the CED/IFMBE's international nature; to enhance the potential of the CED/IFMBE working groups to serve as a means of building consensus on issues involving CED/IFMBE, related to policy matters of importance to the public and private sectors and to facilitate interaction with the professionals practicing in any related area within the wide spectrum of IFMBE membership; to support the initiatives and the development of clinical engineering methodologies in those countries whose stakeholders request such support, including developing countries; to increase individual and organizational membership from all the above groups throughout the world to generate sponsorship and networking opportunities for clinical engineering field and its members; to develop and manage systems for the governance and administration of the CED/IFMBE that are responsive, transparent, professional, and accountable to its members and, in particular, to create, adopt and revise the CED/IFMBE charter; to work with publishers to support the publication and diffusion of a peer-reviewed international journal on clinical engineering that meets the interests and needs of the CED/IFMBE scope.[1,5,6]

In recent years, there have been three CED/IFMBE working groups dealing with Professional Practice and Education, Standards and Guidelines, and Strategic Development and Communications, respectively. These groups have been selectively focused on the topics, objectives and tasks just listed above.[1,6]

III. Results and discussion

From a strategic point of view, one of the most significant achievements during the recent years has been, perhaps, the refreshing and rewriting of the CED/IFMBE Charter. The new Charter further adds and strengthens the grounds for recognizing and securing more hands to help constantly and reliably working with(in) CED/IFMBE Board, thus fostering and empowering the potential of its constitutive individuals - chairman, vice-chairman, secretary, treasurer, elected, co-opted and collaborating members, as well as groups - committees and working groups. The basis for that are updated rules and requirements on their engagements during the terms of offices, and towards the smooth realization of the CED/IFMBE objectives, specific activities, governance and meetings.[1]

Since educational and training materials in the developing world can prove difficult and expensive to access, CED/IFMBE has been collaborating with different institutions and individuals to make certain texts available in a few languages of the developing world. Six volumes from the Ziken International 'How to manage' book series for healthcare technology (Guide 1: How to Organize a System of Healthcare Technology Management; Guide 2: How to Plan and Budget for your Healthcare Technology; Guide 3: How to Procure and Commission your Healthcare Technology; Guide 4: How to Operate your Healthcare Technology Effectively and Safely; Guide 5: How to Organize the Maintenance of your Healthcare Technology; Guide 6: How to Manage the Finances of your Healthcare Technology Management Teams) were translated into Spanish by the efforts of the Biomedical Engineering faculty and students at Tec de Monterrey Medical School in Monterrey, Mexico. The translation project included about 1,750 standard author's pages in English. The volumes are currently available for free download from the 'CED Global, Clinical Engineering Division' group among Yahoo!Groups at https://groups.yahoo.com/neo/groups/CEDGlobal/files/Training%20Resources/ (English) and at https://groups.yahoo.com/neo/groups/CEDGlobal/files/Training%20Resources/Ziken%20in%20Spanish/ (Spanish). A Chinese version of that book series has been recently completed, and discussions are under way for a French or Arabic translation. [1,5,6]

Canadian group of authors have just completed writing a comprehensive publication on Human Factors Engineering and the volume is currently undergoing external review, all as an approved CED/IFMBE funded project. This publication will help clinical engineers and others in using human factor engineering tools at their facilities to deal with the application of information on physical and psychological characteristics to the design of devices and systems for human use, i.e. with the collection of data and principles about human characteristics, capabilities, and limitations, in relation to machines, machine systems, work methods, jobs and environments and taking into account the safety, comfort, and productiveness of human users and operators. Like

the books from Ziken International Book Series and their translations, this volume will be available for free download on the CED website too. There is already interest to perform translations into other languages.[1,5]

Initial steps have been accomplished for the establishment of the 'International Journal of Clinical Engineering and Healthcare Technology Assessment' - IJCEHTA (formation of the International Board of Associate Editors/Reviewers, creation of the Call for Papers and a flowchart of the peer-review process, definition of the reviewers' topics of expertise and key-words), a collaboration between the two respective Divisions of the IFMBE (CED and HTAD). The IJCEHTA is expected to start its publication with a first issue in 2015. This open-access IJCEHTA aims to encourage knowledge and experience exchange in Clinical Engineering and promote the role and the involvement of Biomedical Engineers in Health Technology Assessment. The main objective of the IJCEHTA is to cover state-of-the-art advancements in clinical engineering practice and health technology assessment with the main focus on medical devices. The scope of the IJCEHTA includes all aspects of the state-of-the-art advancements in clinical engineering practices, new standards and health technology assessment reports from the biomedical engineer point of view. The IJCEHTA will serve as a forum for the wide range of clinical and biomedical engineers, health policy makers and professionals interested in the economic, ethical, medical and public health implications of health technology. It covers the development, evaluation, diffusion and use of health technology, as well as its impact on healthcare technology management.[1,5]

Securing donations from the largest healthcare provider system in the USA to establish and host initial web-space for the CED/IFMBE, the latter could be finally found at https://groups.yahoo.com/neo/groups/CEDGlobal/. This accomplishment has allowed CED/IFMBE products to be timely posted, shared and to begin engaging clinical engineering community around the world. It facilitated the sharing of items such as CED/IFMBE meeting agendas and minutes, pending projects, news, call for volunteers and other documents and information pertinent to this community. Currently, there are about 200 registered members of that group, with more than 750 postings to date. In addition, established on-line capabilities, such as Cisco WebEx Meetings allowed CED/IFMBE to conduct virtual meeting at the required and agreed periodicity. The very first such a meeting combining face-to-face and on-line communication was organized during the World Congress of Medical Physics and Biomedical Engineering in Munich, Germany, in 2009, while the current pace is monthly to quarterly organized virtual meetings. Currently, the new CED/IFMBE web-site is under development. The structure of the web-site is ready. This CED/IFMBE project budget was used to hire specialists, who developed the site based on suggestions made by that project leader who is an IT expert. The tools used for development allows different types of inclusion and exclusions without the need of an IT expert. A person responsible for the site, probably CED/IFMBE secretary in the near future, will help as moderator and add or retrieve material sent by clinical engineers worldwide. The next step will be to populate the site, which is a kind of a problem for CED/IFMBE members since it requires a lot of dedicated time. Thus, that will be done as a result of authorized collaboration with the external group of American experts. It is expected that by the end of 2015, the site will be fully functioning and in use for all activities related of the CED/IFMBE.[1,5,6,7]

The possibility to find contact data of and to establish correspondence with colleagues in order to begin professional exchange, mandate the need to access to biomedical/clinical teaching units, associations and practitioners worldwide. Thus, the Directory of teaching units and professional associations has been updated and posted at http://who.ceb.unicamp.br/, as a result of the CED/IFMBE project supported by the World Health Organization (WHO). Further project completed in 2011 in collaboration with the WHO was the compilation of the glossary of medical devices terms, that are specifically used in health technology management by clinical engineers.[1,5]

Recent outcome of the CED/IFMBE project on Clinical Engineering Awards is the production of all the documentation necessary to start new awards program during the forthcoming IUPESM2015 World Congress of Medical Physics and Biomedical Engineering in Toronto, Canada. Award program would offer 3 awards: 1) the CED/IFMBE Award to individual who has distinguished him/her-self for outstanding international or regional contributions to the field of Clinical Engineering - to be given triennially, 2) the Clinical Engineering Teamwork Award to individual(s) who fostered and facilitated cooperation between healthcare technology managers to achieve outstanding impact on the clinical engineering field - to be given annually, and 3) the Best Clinical Engineering Article Award to individual(s) who published an outstanding clinical engineering article in the IFMBE Conferences Proceedings and Journals, demonstrating innovation and making a contribution to research, to achieve progress in Clinical Engineering - to be given annually. The Award Program documents that were developed are: Award Scoring Criteria to be used by the CED/IFMBE Award Committee to classify the selected candidates; Clinical Engineering Outstanding Teamwork Award Application Evaluation Form to be used by the CED/IFBME Award Committee to evaluate the proposals; Clinical Engineering Outstanding Teamwork Award Appli-

cation to be used by the applicants or indications; Award letter to individuals to be sent to clinical engineering societies, making them aware of the award program;, and CED/IFMBE award rules and prizes. The function of the CED/IFMBE award committee has been also discussed and defined, as to divulge the awards and rules to the clinical engineering community, receive, evaluate and select the nominations requests, and send the selected nominations to the IFMBE Award Committee.[1]

Guidelines for professional development and regulation, together with the role of the International Certification in Clinical Engineering have been studied within the corresponding important CED/IFMBE project. The intention of the project is to further understand the corresponding potentials for the global strategy, and finally to create the international umbrella program for certification, either to certify or to certify the certifiers, as a way to mark the achievements of clinical biomedical engineers who have fulfilled mutually agreed requirements in education and training. A global survey on national and international programs for certification in clinical engineering has been done and ongoing, special sessions and roundtables have been organized during scientific and professional meetings, thematic texts for books and guides are being written (ex. WHO book 'Human resources for medical devices' and Elsevier book 'Clinical Systems Engineering), and the contacts/cooperation with the Healthcare Technology Certification Commission and the American College of Clinical Engineering (USA) on possible modalities of support for international certification programs in clinical engineering has been established and ongoing.[1,6,8]

The CED/IFMBE project on Global Center for Healthcare Technology Managers on Disaster Preparedness Training deals with the need for a global center in case of disasters events of various types, causing loss of lives, property destruction and affecting populations all over the world. The outcome of this project is building the capacity of healthcare technology managers in hospitals around the world to be better prepared to continue the delivery of critical healthcare services during and after such disasters. In particular, this project has been designed to collect information and develop resources on how health technology management can be better prepared to face and function before, during and after disaster. Since the initiation of the project, an interdisciplinary thematic workshops and sessions have been organized during global meetings, contacts/collaboration were established with the IUPESM/Health Technology Task Group - HTTG, WHO and, in particular, Pan-American Health Organization - PAHO. Furthermore, the process of collecting content for populating an appropriate global website for information and resources on disaster preparedness for hospital-based technology managers has been initiated.

IV. Conclusion

The IFMBE is the only international professional organization that has the CED focusing specifically on all aspects of life cycle management of healthcare technologies, while embracing all those who professionally practice in relation to clinical engineering field, whether in health care facilities, industry, academic institutions, government, business, voluntary sector, and so on. Taking into account the recent CED/IFMBE activities and the outcomes of its completed and running projects during the last two terms of the CED/IFMBE Board, the latter time seems to be probably one of the most fruitful periods in its history, to the benefit of clinical engineers, other related professionals and healthcare systems, but primarily for the benefit of all patients worldwide.

Acknowledgment

The author is very grateful to all those internal and external individuals who have been contributing by any means to the activities and the achievements of the CED/IFMBE, as described in this paper.

References

1. IFMBE at http://www.ifmbe.org
2. Biomedical Engineering at http://en.wikipedia.org/wiki/Biomedical_engineering
3. IFMBE at http://en.wikipedia.org/wiki/International_Federation_of_Medical_and_Biological_Engineering
4. IUPESM at http://www.iupesm.org/
5. IFMBE Clinical Engineering Division at http://responsive.24x7mag.com/2014/09/ifmbe-clinical-engineering-division/
6. CED Global, Clinical Engineering Division! at https://groups.yahoo.com/neo/groups/CEDGlobal/info
7. Kaiser Permanente at https://healthy.kaiserpermanente.org/html/kaiser/index.shtml
8. American College of Clinical Engineering at http://accenet.org/Pages/Default.aspx

M. Medvedec is with the University of Zagreb School of Medicine, University Hospital Centre Zagreb, Department of Nuclear Medicine and Radiation Protection, Kispaticeva 12, HR-10000 Zagreb, Croatia (phone: +385-1-2388-664; e-mail: mario.medvedec@kbc-zagreb.hr), currently serving as elected member of the Clinical Engineering Division Board of the International Federation for Medical and Biological Engineering

Applied Biomedical Signal Processing and Intelligent eHealth for falls prediction in the elderly

Leandro Pecchia

[1] Applied Biomedical Signal Processing and Intelligent eHealth Lab, School of Engineering, University of Warwick, Coventry, UK

Abstract— **Falls are a major problem of later life. Several multifactorial intervention have been proposed to prevent falls. Healthcare technologies to support falls prediction have been proposed too, in order to: assess the risk of falling, detect falls, and predict fall impact. This paper will present the preliminary results of two studies using physiological monitoring to predict falls in medium term (months) and short term (few minutes before. The preliminary results here described suggests that physiological monitoring can support fall prevention, by informing prevention strategies (i.e. helping priorities subjects at higher risk of falling) or by generating warning to patients and nurses in case an elevated risk of falling in the next few minutes is forecasted.**

Keywords— **falls in elderly, accidental falls prediction, physiological monitoring, HRV.**

I. Introduction

Falls are a major problem of later life. About 30% of the citizen over 65 years old is expected to fall each year, losing quality of life and independency[1], of the whole family. The British National Institute for Health and Care Excellence (NICE) estimated that falls costs £2.3 billion per year to the UK National Health Service (NHS) [2].

Falls are caused by complex and dynamic interaction of intrinsic (subject specific) and extrinsic (circumstance dependent) risk factors. However, many studies investigated specific circumstances in which the probability of falling is much higher, especially in-door. For instance, recent studies proved that the 30% of indoor falls happen while rising from a bed or chairs and that there are peaks of risk of falling in specific hours of the day[3].

Therefore, multifactorial interventions seem to be most effective approaches to prevent falls. These comprised a mix of interventions including exercises, training, multifactorial home assessments, home safety interventions (i.e. elimination of specific risks) and vitamin D supplementation [4]. Several technologies have been proposed to support these interventions. Many focused on fall detections using: wearable accelerometers; unobtrusive technologies as cameras, Kinect, microphones; ambient sensors either monitoring directly the subject using infrared and pulse-Doppler radar systems, or monitoring the ambient response to falls measuring floor vibrations. Fewer studies aimed to detect falls while happening in order to predict the impact (pre-impact fall prediction) and eventually reduce harms (i.e. inflating airbags). Some studies proposed technologies for the risk of falling assessment, using body-worn kinematic sensors or heel and toe clearance.

Tis paper will present the preliminary results of a study investigating how physiological monitoring and biomedical signal processing can enhance those technologies assessing the risk of falling in the middle term (few weeks) and predicting falls due to specific circumstances (i.e. rising from bed or chair) in the short term (few minutes before).

In particular, two case studies will be presented in which Heart Rate Variability (HRV) was used to predict falls or to assess the risk of falling, proving that:

1) HRV resulted systematically depressed in fallers (compared to an homogeneous control group of non-fallers);
2) Subject with a depressed HRV showed a significantly increased relative risk of falling in the next months.
3) It is possible to predict orthostatic hypotension, which is the main cause of falls happening while rising, monitoring the HRV in the 5 minutes before standing-up.

HRV was chosen as it is considered a reliable estimator of Autonomous Nervous System (ANS), which is responsible for many mechanisms that control human equilibrium.

II. Methods

A. 24 hours HRV to assess the risk of falling in the next few months

The first study was a cross-sectional studies study that analyzed clinical 24h ECG Holter recordings of 168 hypertensive patients (72±8years, 60 female), of which 47 subjects experienced a fall within the 3 months from the registration. The database was collected in the framework of the Smart Health and Artificial intelligence for Risk Estimation

(SHARE) project and details about the database can be found elsewhere [5]. The undelaying hypothesis was that a depressed HRV was associated with an increased risk of falling. According to conventions used for cross-sectional studies, the following was assumed: a depressed HRV (lower variation at the high frequency and a less chaotic behavior) was the "risk factor" under investigation; fallers were considered as "cases" and non-fallers as "controls"; patients with a depressed HRV for at least the 10% of the day (nominally 24 hours) where considered "exposed" to the risk factor under investigation. Details about the HRV processing can be find in [6].

B. Short term HRV to assess the risk of falling due to standing hypotension in the next few minutes

Ten healthy subjects were enrolled with the following inclusion criteria: no pathological cardiovascular conditions, neurological or psychiatric disorders or other severe diseases; not taking any medication at the moment of the study; not professional athletes or high-level sport participants; no caffeine or alcohol intake in the 12 hours prior to the measurements. The volunteers were invited to seat in a comfortable position for a baseline recording of the systolic blood pressure (BP) and ECG. Then volunteers were invited to lay down in supine position for 10 minutes. During the last 5 minutes, ECG was recorded continuously using commercial wearable devices and systolic BPs was recorded 4 times (once each 60 seconds). Finally, volunteers were invited to stand up actively, following standardized movements. Once standing, systolic BPs during the second minute after standing was recorded, as according to literature this is when the huger drop-down in blood pressure is measured. Further details on the signal processing and the model training and testing can be seen in [7].

III. RESULTS

The first study demonstrated that HRV measures changed significantly ($p<0.01$) in fallers and depressed HRV patterns were consistently observed in fallers. Moreover, subjects showing these depressed patterns presented a relatively higher risk of falling in the next few months. Particularly, the odds ratio (OR) of falling being positive to this pattern was significant: OR=5.12 (CI 95% 1.42-18.41; $p<0.01$) [6].

The second study proved that it is possible to predict drop down due to standing hypotension with 82.5% accuracy, with a false positive rate of 10% and a false negative 7.5%) [7]. Also in this study, a depressed HRV was significantly associated with an increased risk of severe blood pressure dropdowns, which are responsible for up to the 30% of in-door falls.

These results suggested that the HRV can be used to indirectly monitor the status of ANS, which is responsible of controlling several physiological mechanisms that are essential to maintain balance in humans.

IV. CONCLUSIONS

These two preliminary studies proved for the first time an association between a depressed HRV and the risk of falling. The first study used 24 hours HRV to assess the risk of falling in the next 3 months. These results, if confirmed by more robust prospective trials, can help choosing the target populations informing clinical interventions aiming to prevent falls. Moreover, the second case study suggested that the monitoring of short term HRV can help predicting some falls, happening in specific circumstances and due to specific risk factors. However, this subgroup of falls represent a significant part of in-doors falls.

REFERENCES

1. Katz R, Shah P. *The patient who falls: challenges for families, clinicians, and communities*. JAMA. 2010;303(3):273-4. doi:303/3/273 [pii] 10.1001/jama.2009.2016.
2. guidelines NIfCEN. *Falls: assessment and prevention of falls in older people*. 2013. http://guidance.nice.org.uk/CG161.
3. Healey F, Scobie S, Oliver D, Pryce A, Thomson R, Glampson B. *Falls in English and Welsh hospitals: a national observational study based on retrospective analysis of 12 months of patient safety incident reports*. Quality and Safety in Health Care. 2008;17(6):424-30.
4. Gillespie LD, Robertson MC, Gillespie WJ, Lamb SE, Gates S, Cumming RG et al. *Interventions for preventing falls in older people living in the community*. The Cochrane Library. 2009.
5. Melillo P, Izzo R, Luca N, Pecchia L. *Heart rate variability and target organ damage in hypertensive patients*. BMC cardiovascular disorders. 2012;12(1):105. doi:1471-2261-12-105 [pii] 10.1186/1471-2261-12-105.
6. Melillo P, Jovic A, De Luca N, Morgan SP, Pecchia L. *Automatic prediction of falls via Heart Rate Variability and data mining in hypertensive patients: the SHARE project experience*. 6th European Conference of the International Federation for Medical and Biological Engineering. Springer International Publishing; 2015. p. 42-5.
7. Sannino G, Melillo P, De Pietro G, Stranges S, Pecchia L. *To What Extent It Is Possible to Predict Falls due to Standing Hypotension by Using HRV and Wearable Devices? Study Design and Preliminary Results from a Proof-of-Concept Study*. Ambient Assisted Living and Daily Activities. Springer; 2014. p. 167-70.

Corresponding author: Leandro Pecchia is with the School of Engineering of the University of Warwick. Library Road, Coventry, CV4 7AL, UK (email: l.pecchia@warwick.ac.uk). Dr Pecchia is the responsible of the Applied Biomedical Signal Processing and Intelligent eHealth lab: http://www2.warwick.ac.uk/fac/sci/eng/research/systems/abspie/

The Gülhane Mastoidectomy

Mustafa Kahramanyol*

Abstract:

This study is being presented in order to acquaint the audience with the outcomes of a previously described technique of chronic otitis media surgery: which consists of improved radical mastoidectomy, inferiorly based fascioperiosteal flap and large meatoconchoplasty [7,9]. The technique is named as the Gülhane Mastoidectomy. In this technique, autologous bones and soft tissues have been used as a reparative material.

255 patients have been operated on and treated utilizing the technique mentioned above during a period of 22 consecutive years. Despite extensive otologic destruction and the concomitant severe complications, the technique rendered impressive outcomes: the surgical cavities of the destructed mastoid bones became smaller by the time and remained healthy, providing a good life quality for the patients. Fourteen patients experienced immediate postoperative complications. Cholesteatoma recurrence was observed in but one patient.
The outcomes confirm the value and usefulness of the technique. The value of use of autologous bone and soft tissue as a reparative material is unchallengeable.

Key words: Chronic otitis media, Radical mastoidectomy, Saucerization, Meatoconchoplasty, Surgical flaps, Gülhane mastoidectomy, Gülhane flap

Introduction

Despite rapid advancement in medicine of our age and tremendous perfection in surgical techniques, certain patients with chronic otitis media still suffer major otologic complications and no conservative surgical technique is adequate to thoroughly treat their diseases. Most of the hitherto known surgical techniques have serious drawbacks: dependence on constant medical care, disfiguration of the surgically created structures, recurrence, obligation to further surgical interventions, high rate of complications, psychological problems, high costs etc. [1,12,15,17,22,24].

In 1992, Kahramanyol described a particular technique for surgical treatment of chronic otitis media with cholesteatoma and related complications [7]. The technique consisted of improved radical mastoidectomy, inferiorly based fascioperiosteal flap and large meatoconchoplasty. The technique has been named as “The Gülhane Mastoidectomy” and the flap utilized in the technique “The Gülhane Flap”.

Materials and methods

319 patients have been operated on during the period between the years 1982 and 2004, applying the method described by Kahramanyol [7,9]. All of the patients, without exception, had severe otologic destructions and some of them concomitant major complications such as postauricular fistula, subcortical abscess, spontaneous mastoidal excavation, Bezold’s abscess, parapharyngeal abscess, facial paresis or paralysis, total hearing loss, vertigo, spontaneous nystagmus, meningitis, brain abscess, hemiplegia and coma. Therefore, they were classified as to be not good candidates for conservative surgery.

---

*Mustafa Kahramanyol, MD, Professor of Otorhinloryngology, Kent ENT Medical Center, Tandoğan, Ankara, Türkiye.
mkahramanyol@yahoo.com, Ph.:905424523133

During surgery, postoperative care and follow-up terms, the criteria described by Kahramanyol have strictly been observed [7,9]. Therefore, the principles and the details of the technique shall not be described herein. Yet, some of these patients have also received reconstruction of the tympanum which is beyond the scope of this report.

Surgery revealed presence of cholesteatoma in all of the cases, though at varying degrees. In addition, some had granulation tissue formation, osteitis, labyrinthitis, destruction of dural or sigmoid sinus plates, erosion of the facial canal at various levels and degrees, erosion of the semicircular canals, perisinusal abscess, intracranial abscesses and petrous bone cholesteatoma. The ossicular chains were largely destroyed or fused in all of the cases. To be exact, 227 of the patients had no Stapedial suprastructure, whatsoever.

The patients were invited for follow-up at various periods and the records have been kept properly. Essentially, the periods varied from one month to three years, but any patient was welcomed at any time and close ties were constantly kept alive. Nevertheless, it was possible to obtain proper follow-ups and recordings only of 255 of patients (202 males and 53 females, aged 9 to 71 years). The full length of the follow-up period varies between one to twenty one years. Contacts with the remaining 64 patients were lost. Therefore they were not included in the study.

Results

Fourteen patients experienced immediate postoperative complications: three patients had inadequate meatoconchoplasties, one patient had displacement of the flap, one patient had perichonditis, three patients had spontaneous nystagmus, two patients had transient facial paresis, three patients developed total sensoryneural hearing loss and one patient developed necrosis of the flap.

One month postoperatively, in all of the patients, epithelisation of the mastoid cavity was still in progress but completed in two months. At 1 to 21 years postoperatively, all of the patients displayed healthy cavities and sufficiently large meatoconchoplasties The postauricular areas were smooth and taut; no anterior displacement of the pinna have been encountered. There was no recurrence of osteitis. Most of the patients had healthy mastoid and tympanic cavities during the entire period of the follow-up. Only twenty six of them were found to have slightly wet mastoid cavities. All of the patients had strong flap constitution and good epithelisation over the flap. In one of the patients, due to the necrosis of the flap, mastoid cavity had to be left denuded, as it had been the custom in classic radical mastoidectomy.

The volume of the cavities, one month postoperatively, depending on the patient, varied from 2.5cc to 11cc. On the first year postoperatively, the mean cavity volume of the regular group had decreased by 30% and subsequently on the third year postoperatively by 37,5%, comparing the volume measured one month postoperatively.

X-rays obtained in Schüller's position and/or CT scans and MRI , performed on the seventh day and on the fourth year postoperatively reveal increased osseous densities over the sigmoid sinus. [7,9] Even after more than twenty years, CT scans showed healthy mastoid bone and flap. [Fig.6].CT scans also provided an opportunity to objectively measure the changes in bone density of the concerned areas. Within three years, the density increased from about 70 to about 250 Hounsfield Units (HU).

Discussion

The management of chronic otitis media and the preference of its surgical approaches have been a source of controversy ever since.

It is said that in the presence of otitis media with cholesteatoma and/or related complications, classic radical mastoidectomy with open cavity is still the most common

technique applied in its treatment [13,18,22,24]. Unfortunately, its cavity health has always been a problem [1,12,16]. To overcome the problems inherited by the classical radical mastoidectomy, many techniques have been developed, but came out that every one of them harbored problems. In particular, flaps developed for that purpose did not produce expected outcomes [2,10,11,17,25]. Further scientific studies brought many authors to the concept of saucerization of the cavity walls, large meatoconchoplasty and microsurgical perfection in radical mastoidectomy [4,13,14,20,23,24].

Kahramanyol added the fascioperiosteal flap concept to the abovementioned achievements. He stated that the technique, which he has described in 1992, provided a small and trouble free mastoid cavity relieving the patient of dependence on the physician and securing a healthy life further on [7,9]. He argued that "the rationale behind this method, which is not an obliteration method, is to facilitate new bone formation underneath and epithelisation over the surface of the fascioperiosteal flap". Thus, our study aimed to examine the validity of that statement and expected outcomes.

There were some complications during the surgery, but the authors are tempted to conclude that they have not arisen specifically because this particular method had been utilized; believing that under the similar circumstances, these complications may occur no matter which technique is used.

The cavity volume measurements confirm constant decrease over the time. The authors are of the opinion that this is due to the neoosteogenic activity which takes place at the surface of contact by the periosteal layer and the mastoid bone. As a matter of fact, this activity has been documented by Kahramanyol [7,9]. Besides, the bone density measurements show increase, which also support the postulate of neoosteogenic activity.

Physical examination of the cavities, revealed healthy grounds; epithelisation was excellent in all of the patients. Only twenty six patients had slightly wet cavities which were easy to cure instantly. This must be the outcome of a strong flap which is both nurtured by the postauricular artery and supported by the periosteum. This strong flap provides excellent grounds for epithelisation, which does not exfoliate uncontrollably. In some of the patients, only dry and small earwax collections were to be seen.

Here one ought to note that, some of the patients experienced disturbances in equilibrium and sometimes pain while being exposed to high or low temperature, while swimming or while being examined by the otologist. This, despite the effort to shield the vestibule against the environment by a blanket provided by the flap and the neoosteogenic bone, must be a side effect of an open cavity and in particular exposed oval and round windows, which are unavoidable elements of the technique.

Conclusions

In this study, a surgical technique, consisting of improved radical mastoidectomy, inferiorly based fascioperiosteal flap, perfected microsurgical techniques and large meatoconchoplasty has been applied on 255 patients who had chronic otitis media with cholesteatoma and related complications. Here its long term results, alongside with the scientific research findings, are presented. In brief, the mastoid cavities of the patients became smaller by the time and remained healthy; Despite preoperative severe otologic destructions and life threatening concomitant complications, all of the patients had healthy flaps and great majority of them had dry cavities even 21 years postoperatively. For the patients, in particular for those of the rural or poor origins, this means, to be relived of dependence of lifelong and costly medical care. The value of use of the autologous bone and soft tissue as a reparative material is unchallengeable.

References

1. Babighian G (2002) Posterior and attic osteoplasty: hearing results and recurrence in cholesteatoma. Otology & Neurotology 23:14-17
2. Black B (1998) Mastoidectomy elimination (Obliterate, Reconstruct or Ablate?). The American Journal of Otology 19:551-557
3. Brown JS (1982) A ten year stasistical follow-up of 1142 consecutive cases of cholesteatoma : The closed vs the open technique. Laryngoscope 92: 390-396
4. Fish U (1980) Surgical treatment of acquired cholesteatoma. In: Tympanoplasty and Stapedectomy, Georg Thieme Verlag, Stuttgart, New York, pp 40-55
5. Glasscock ME III, Shambaugh GE Jr. (1990) Indications for modified radical mastoidectomy. In: Surgery of the Ear, WB Saunders Company, Philadelphia, London,Toronto,Montreal, Sydney, Tokyo, pp 231-232
6. Hilger JA, Hohmann A (1962) The pedicle graft in tympanomastoid surgery. Laryngoscope 72: 1121-1124
7. Kahramanyol M (1992) Fascioperiosteal flap and neoosteogenesis in radical mastoidectomy. Ear, Nose & Throat Journal 71:70-77
8. Kahramanyol M, Muş N, Özkaptan Y, Aktaş D, Özünlü A (1993) Fascioperiosteal flap and neoosteogenesis in radical mastoidectomy. In: Proceedings of the XVth World Congress of Otorhinolaryngology-Head and Neck Surgery, Istanbul. Multiscience Publishing, Essex,U.K, pp 137-138
9. Kahramanyol M, Özünlü A, Pabuşçu Y (2000) Fascioperiosteal flap and neo-osteogenesis in radical mastoidectomy: long term results. Ear, Nose & Throat Journal 79:524-526
10. Linthicum F H Jr. (2002) The fate of mastoid obliteration tissue: a histopathological study. Laryngoscope 112:1777-1781
11. Ojala K, Sorri M**,** Sipila P, Palva A (1982) Late changes in ear canal volumes after mastoid obliteration. Arch. Otolaryngol. 108:208-209
12. Palva T, Palva A, Salmivalli A (1968) Radical mastoidectomy with cavity obliteration. Arch. Otolaryng. 88:119-123
13. Paparella M M, Kim C S (1977) Mastoidectomy update. Laryngoscope 87:1977-1988
14. Portmann M (1979) Ear surgery for inflammation and infection alone. In: The Ear and Temporal Bone, Masson Publishing USA Inc., New York, Paris, pp: 43-84
15. Ragheb SM, Gantz BJ, McCabe BF (1987) Hearing results after cholesteatoma surgery. Laryngoscope 97: 1254-1263
16. Robertson J B, Mason T P, Stidham K R (2003) Mastoid obliteration: autogenous cranial bone pÂte reconstruction. Otology & Neurotology 24:132-140
17. Sadé J (1982) Treatment of retraction pockets and cholesteatoma. The Journal of Laryngology and Otology 96:685-704
18. Sadé J, Weinberger J, Berco E, Brown M, Halevy A (1982) The marsupialized (radical) mastoid. The Journal of Laryngology and Otology 96:869-875
19. Satar B, Yetişer S, Özkaptan Y (2002) Evolving acoustic characteristics of the canal wall down cavities due to neo-osteogenesis by periosteal flap. Otology & Nuerotology 23:845-849
20. Sheehy J L (1988) Cholesteatoma surgery: canal wall down procedures. Ann Otol Rhinol Laryngol 97:30-35
21. Siim C, Tos M (1987) Partial and total reconstruction of old radical cavities. Arch Otolaryngol Head Neck Surg 113:635-643
22. Smyth GDL (1982) Practical suggestions on the surgical management of the cholesteatoma ear. Laryngoscope 92: 452-457
23. Smyth GDL (1992) Toynbee memorial lecture 1992: facts and fantasies in modern otology: the ear doctor's dilemma. The Journal of Laryngology and Otology 106:591-596

24. Tos M (1995) The open cavity. In: Manual of Middle Ear Surgery, Volume II. Georg Thieme Verlag, Stuttgart, New York. pp 294-321
25. Turner JL (1966) Obliteration of mastoid cavities in surgery for chronic ear. Arch Otolaryngol 75: 885-896
26. Van Hasselt C A (1994) Toynbee memorial lecture 1994: mastoid surgery and the Hong Kong Flap. The Journal of Laryngology and Otology 108: 825-833

Remote Pacemaker Programming – 15 Years After

Božidar Ferek-Petrić

Medtronic Academia Central&Eastern Europe, Principal Medical Affairs Specialist, Zagreb, Croatia

Abstract—**We demonstrated 15 years ago the remote programming of cardiac pacemakers utilizing the Internet infrastructure. Our system comprised client and server whereby TCP/IP protocol was deployed as a link provider. An old programmer was connected to server. Server controlled the programmer and pacing parameters. Patient's ECG signal was led into the same computer. Remote computer, running the client software displayed the graphic user interface comprising patient's ECG waveform in real time and programming control pull-down menu. 9 patients having implanted Siemens-Elema Prolog pacemakers underwent the remote follow-up sessions whereby server was at the patient's site, while the client was in the pacemaker center.**

Remote follow-up sessions were regularly done until the battery end-of-life. We successfully performed: magnet rate measurement for battery voltage test, Vario™ threshold test and patient's intrinsic rhythm test. ECG waveform quality was sufficient and there was no arrhythmia observed. We didn't experience problems with the link between client and server. Patients accepted the new method of follow-up, being confident about its safety and reliability.

Our acute human experiments demonstrated feasibility of the remote patient follow-up. Therefore, development of new systems for patient follow-up have been initiated worldwide. Nevertheless, there is still today no commercial system available for remote programming of implantable devices. There are various systems for remote interrogation of diagnostic memory that can reveal patient's arrhythmia and status of an implantable device. More than million users in US and 350 000 in Europe of the Medtronic CareLink system avoid travel discomfort and expenses whereby increasing the patient's safety. Latest wireless telemetry devices have continuous connection to the patient's home unit that transmits the interrogated data via mobile network. Any impeding failure of the therapy delivers an alarm to the physicians having access to the system. The alarm is even sent to the personal smartphone. Though significantly improving the principles of follow-up, patients still have to refer to the pacemaker center if any changes of the therapy parameters are needed. Regarding safety and reliability, the technology for implementing of our teleprogramming system in the latest devices is completely mature. Nevertheless, legislative obstacles prevent rapid development and practical application.

Keywords— **pacemakers. ICD, telemedicine, follow-up, CareLink**

I. Introduction

Cardiac implantable devices, such as cardiac pacemakers and cardioverters-defibrillators are used for treatment of arrhythmia and prevention of sudden cardiac death. Once implanted, communication with an already implanted medical device requires the use of a programmer. Programmer is an external device which permits the downlink from the programmer to the medical device as well as the receipt of a subsequent uplink from the medical device to the programmer. Download of data collected by the medical device, reprogramming or interrogation of the medical device, enables physicians to precisely tailor the therapy to the patient's needs and to ensure proper operation. Programmer is usually placed within the hospital or physician's office so that physician is directly next to the patient while communicating with the implanted device. Therefore patients have to travel to the hospital or doctor's office to do the follow-up procedure. Regular follow-up is needed according to the prescribed individual schedule to either diagnose or likely to prevent the hazardous events. The hazard can occur from an impending system failure, a cardiac electrotherapy malfunction and disturbance, or a cardiac arrhythmia.[1] Many complications occur transiently, therefore being hardly detected. Accordingly, a problem can remain to be undetected if the follow-up schedule is rare. Patients may live in a variety of locations being remote from the physician's office, including such locations as islands, mountainous areas or other areas where travel is difficult. Accordingly, travel expenses incur significant cost to the patient follow-up. A system that permits remote communication with a medical device would significantly improve the patent's safety and decrease the cost of the therapy. Such a system should enable remote programming and interrogation such that one or more physicians may utilize the communication and provide guidance for the subsequent interpretation and programming of the device.

II. Methods

Our system for remote follow-up was built of custom developed hardware and software.[2,3] It was designed around the client/server paradigm, whereby server was at the patient's location and the client at the physician's location, as

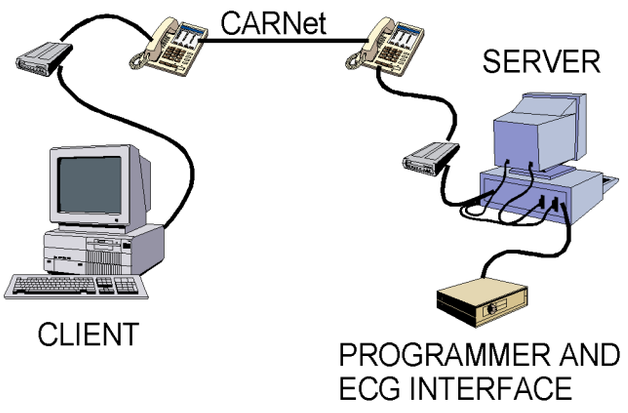

Figure 1

illustrated in figure 1. At that time, the most convenient computer language for implementation of the teleprogramming was Java™ (Sun Microsystems, Inc., San Jose, CA), a high-level object-oriented interpreted programming

language being architecture-neutral and portable.[4] The Java platform has two components: the Java Virtual Machine (Java VM)[5] and the Java Application Programming Inteface (Java API). The Java API is a large collection of ready-made software components that provide many useful capabilities, such as graphical user interface (GUI) widgets. Probably the most well-known Java programs are Java applets. An applet is a Java program that adheres to certain conventions that allow it to run within a Java-enabled browser. Common type of Java programs are also applications, where a Java application is a standalone program that runs directly on the Java platform. Therefore the software was written in Java language, so it is usable without extra effort on many popular hardware platforms and operating systems. Furthermore, the software has some additional inherent robustness and it has sufficient performance on commonly available hardware.

The server is the most complex component in our system, which provides real-time data about the patient's state, accepts and executes the operator's commands, monitors the system's overall performance and reliability, resolves all dubious situations and acts in emergency situations. The server was designed to take all this responsibility because it is nearest to the patient, and failure of any of the components between it and the patient are least likely.

The client shows to an operator a graphic user interface that visually and functionally mimics existing follow-up equipment. It displays the ECG waveform of the patient, and comprises the controls of the ECG recording and display as well as the pacemaker programming hardware on the server side. We deployed the standard TCP/IP network protocol as the link provider. The two main issues that could impede the deployment of TCP/IP – security and quality of service – are addressed by using private temporary links. Internet Protocol (IP) is a protocol by which data is sent from one computer to another on the Internet. Each computer on the Internet has at least one address that uniquely identifies it from all other computers on the Internet. When data is transmitted, it is divided into a number of packets that can arrive in a different order than the order they were sent in the network. The Internet Protocol just delivers them. It's up to another protocol, the Transmission Control Protocol (TCP) to put them back in the right order. UDP is an alternative to TCP/IP that doesn't provide sequencing of the packets that the data arrives in. The server consists of a computer, a modem, a standard pacemaker programmer and a digital ECG. We used a Sun SparcStation 4 computer to run the server software and connect all the other components. However, it is possible to use any other hardware platform and OS that has a Java runtime environment. As we used an old model of the pacemaker programmer (Siemens-Elema model 600, Solna, Sweden) that was normally operated using switches, we developed a special hardware interface that connects the programmer to the computer through a standard printer parallel port and simulates the closed switches. Accordingly, server software had the full control of the programmer's operation and state. Digital ECG device is an OEM board produced by Medlab GmbH (Karlsruhe, Germany). Its bandwidth was adjusted between 0.1 and 25 Hz with the sampling rate of 50 Hz. It was connected to the computer by a standard RS232 serial port.

The software server's main tasks are to handle the client's requests, dispatch the patient's ECG waveform to clients in real time and to take care of the patient's security. Every

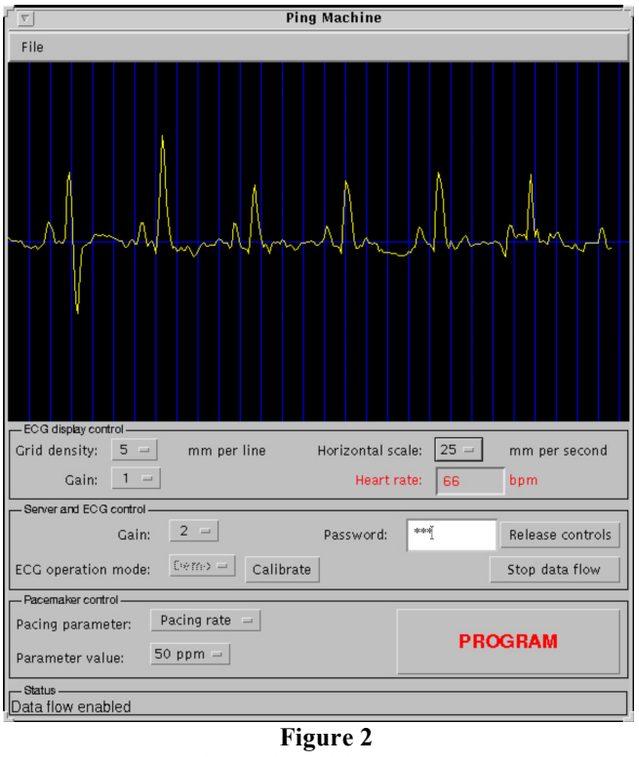

Figure 2

one of these tasks is conducted in a separate thread, so the abnormal termination of any of them could be detected and the operator alarmed. The software server is designed to be easily expandable for new features and hardware components by using carefully designed class interfaces. The client side consists of a computer with no special hardware attached. It has two main tasks: to display the incoming ECG waveform in real time and to communicate the operator's commands to the server. It also monitors the state of the network link for unexpected behavior, but as it has little power over the situation, its actions are limited to alarming the operator. Figure 2 shows the graphic user interface of the client.

To resolve the two most important shortcomings of the TCP/IP protocol, privacy and quality of service, we decided to use a Croatian Academic Research Network – CARNet infrastructure. The network traffic flows in two separate streams. We use one TCP connection for transferring control messages and state updates between the server and the client, and one connectionless UDP stream for transferring real-time waveform data.

Figure 3 illustrates the data flow. The TCP connection is reliable and warrants either delivery or failure notification, therefore being used for data such as commands to the server and messages to clients designating the server changes. It is also used to send the calculated heart beat rate to the clients after each beat. As this message is sent periodically and rather often, it serves as a periodical probe to measure the connection's reliability.

The other data stream consists of only two bytes per message – one data point of the ECG waveform and its ordinal number. Since digitized waveforms have an inherent redundancy, UDP packets are satisfactory for this purpose because it is not crucially important that every packet arrives. However, this should not normally happen on our dedicated network link, so we use such events as an additional measure of the link reliability. A 19.2kbps throughput

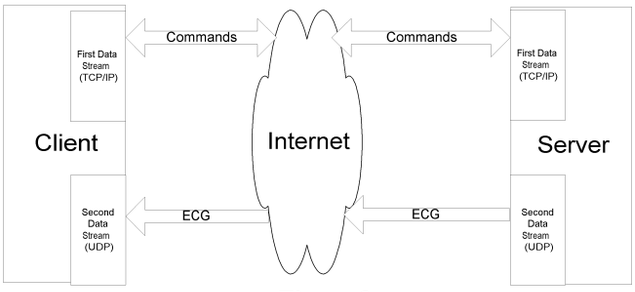

Figure 3

rate was sufficient for normal operation.

UDP can be also used for transmission of the marker channels as well as of the various biochemical sensors signals. Missing data packets, however, should not normally happen on dedicated network link and therefore this event may be used as an additional test of the network link. The amount of missing data packets may be used as a parameter to indicate to the users the fidelity of the link.

We selected a group of 9 patients having Siemens-Elema Prolog pacemaker not totally dependent on cardiac pacing that were programmable utilizing our system. Video conference was available on the both sides. The video image of the server side (6 km distant) was displayed on the screen and it was possible to communicate with physicians and the patient.

III. RESULTS

First teleprogramming session was done on June 15th 1999 whereby more than 40 cardiologists and reporters witnessed this first acute human experiment. We successfully demonstrated: pacing rate programming for spontaneous intrinsic rhythm evaluation, threshold test and magnet test rate and programming of output voltage.

Further sessions were repeated every six months during the period of five years until battery elective replacement time occurred in each patient. All together 72 teleprogram-

ming sessions were performed. All patients underwent the pacemaker replacement procedure due to the end-of-life battery status detected.

IV. DISCUSSION

Our system could never become a commercial service because it was functional only on a limited group of patients having the pacemakers being at that time already outdated. Nevertheless, the presentation[6] of our system significantly influenced the further development of telemedicine in cardiac electrotherapy.

Several commercial systems have been developed . Contemporary remote systems for implantable cardiac devices provide a broad range of data about the patient and the implanted device. Telemedicine includes remote monitoring as well as remote follow-up. Remote monitoring is the continual interrogation of the device to detect patient- or device-related adverse events earlier than with standard follow-up visits. Remote follow-up aims to replace scheduled and unscheduled face-to-face follow-up visits due to the interrogation of the automatic pacemaker functions. Currently available remote systems, such as Home Monitoring, CareLink, Merlin.net, and Latitude, have in common that they interrogate the device, send these data to a server, and provide the data to the physician on a secured web site.[7] Large, long-term, randomized trials are comparing remote and conventional approaches with the aim of demonstrating the benefits of telemedicine in this patient group.

According to Eucomed data, about 550,000 devices are implanted each year in Europe. That means that 2 million existing cardiac device patients will need 2.6 million in-office follow-up visits potentially needed. When utilizing the remote monitoring, quality patient care and cost-effectiveness come together. may give faster time to clinical action.[8] They have significant implications for the device clinic workflow. Automatic transmissions are rapidly processed, allowing clinicians to focus on clinically important findings.[9] They also better preserve patient retention and adherence to scheduled follow-up compared with in-person evaluations.[10] Systems for remote monitoring provide a means for performing constant surveillance, with the ability to identify salient problems rapidly. Remote home monitoring reduces the volume of device clinic visits and provides early detection of patient and/or system problems.[11] These systems effectively demonstrated their cost-benefit. This is mainly accomplished by reducing the number of battery charges and inappropriate shocks, resulting in fewer device replacements, and by reducing the number of in-clinic follow-up visits.[12]

Global connectivity and ease of use may improve patient compliance. The systems are easy to use whereby LCD screen with visual feedback provides step-by-step instructions and confirmation when information has been sent.

However, all these studies have proven the feasibility of systems without capability for teleprogramming which includes remote change of therapy parameters.

Regarding safety and reliability, the technology for implementing of the teleprogramming system in the latest generation of devices is completely mature. Furthermore, concern about the patients' safety is completely unjustified, especially in regard to the possibility of hacking the system and doing the criminal act by provocation of intentional harm to the patient. Long-term experience in various services via Internet such as online banking and money transfer via Internet demonstrated the very high safety standards. Nevertheless, only legislative obstacles prevent rapid development and practical application. We can only assume further benefits for the healthcare if teleprogramming would be included in contemporary remote follow-up systems.

V. CONCLUSIONS

Modern communication and computer technology opens new possibilities for patient management. In order to efficiently utilize the features of modern cardiac electrotherapy devices, being diagnostic as well as therapeutic devices, remote follow-up procedure became a standard. It very much increased the safety of the patients from various possible hazards and decrease the incidence of sudden death. It also decreases the cost of the therapy and increase the comfort of the patients. Internet is certainly an infrastructure that will be used for this purpose with the prerequisite that safety standards are maintained. Unfortunately, 15 years after our acute human experiment, there is no system available for the remote programming of the device.

REFERENCES

1. W. Irnich: "Pacemaker-Related Patient Mortality", *PACE* 1999; 22:1279-83.
2. K. Tonković K, B. Ferek-Petrić. "Utilizing the Internet in Pacemaker Follow-up", *Proceedings of the 8th International IMEKO Conference on Measurement In Clinical Medicine.* Dubrovnik, 1998, pp. 11/5 - 11/8.
3. B. Ferek-Petrić: "*System For Remote Communication With An Implantable Medical Device"*, European Patent Number EP1196082B1, EPO Bulletin 2010/10, München, 10.03.2010.
4. J.Gosling, B.Joy, and G.Steele: "*The Java™ Language Specification*", Mountain View CA, Sun Microsystems Inc. 1996.6. Hunt C. TCP/IP Network Administration. Sebastopol CA, O'Reilly & Associates Inc. 1992.
5. T. Lindholm, F. Yellin: "*The Java™ Virtual Machine Specification"*, Mountain View CA, Sun Microsystems Inc. 1997..

6. B. Ferek Petrić, V. Goldner, D. Kosi, M. Lovrić Benčić, B. Buljević, K. Tonković, I. Čikeš: *"Pacemaker Programming via Internet"*, PACE 2002; 25 (No 4, part II): 598.
7. A. Schuchert: *"Telemedicine in pacemaker therapy and follow-up"*, Herzschrittmacherther Elektrophysiol. 2009 Dec;20(4):164-72. doi: 10.1007/s00399-009-0058-1.
8. G.H.1. Crossley, A. Boyle, H. Vitense, Y. Chang, R.H. Mead; CONNECT Investigators: *"The CONNECT (Clinical Evaluation of Remote Notification to Reduce Time to Clinical Decision) trial: the value of wireless remote monitoring with automatic clinician alerts",* J Am Coll Cardiol. 2011 Mar 8;57(10):1181-9. doi: 10.1016/j.jacc.2010.12.012. Epub 2011 Jan 20.
9. E.M.1. Cronin, E.A. Ching, N. Varma, D.O. Martin, B.L. Wilkoff, B.D. Lindsay: *"Remote monitoring of cardiovascular devices: a time and activity analysis",* Heart Rhythm. 2012 Dec;9(12):1947-51. doi: 10.1016/j.hrthm.2012.08.002. Epub 2012 Aug 3.
10. N. Varma, J. Michalski, B. Stambler, B.B. Pavri; TRUST Investigators: *"Superiority of automatic remote monitoring compared with in-person evaluation for scheduled ICD follow-up in the TRUST trial - testing execution of the recommendations"*, Eur Heart J. 2014 May 21;35(20):1345-52. doi: 10.1093/eurheartj/ehu066. Epub 2014 Mar 3.
11. N. Varma, R.P. Ricci*: "Telemedicine and cardiac implants: what is the benefit?"*, Eur Heart J. 2013 Jul;34(25):1885-95. doi: 10.1093/eurheartj/ehs388. Epub 2012 Dec 4.
12. H. Burri, C. Sticherling, D. Wright, K. Makino, A. Smala, D. Tilden: "*Cost-consequence analysis of daily continuous remote monitoring of implantable cardiac defibrillator and resynchronization devices in the UK*", Europace. 2013 Nov;15(11):1601-8. doi: 10.1093/europace/eut070. Epub 2013 Apr 18.

Data mining, procesiranje i web-bazirani prikaz EKG signala

Emir Žunić[1], Bahira Žunić[2]

[1] Info Studio d.o.o. Sarajevo, Sarajevo, Bosna i Hercegovina
[2] Goethe-Institut Sarajevo, Sarajevo, Bosna i Hercegovina

Sažetak **— Cilj rada je da promovira primjenu računarskih znanosti i vještina u projektiranju web-baziranog sistema za analiziranje, procesiranje i prikaz EKG signala. Primjena računara u snimanju, obradi i analizi EKG signala predstavlja jednu od najranijih primjena računarske tehnike u medicinske svrhe. Od primarnog interesa za primjenu računarskih sistema u obradi EKG signala je pravilno tumačenje i detektovanje različitih valova i intervala električnih aktivnosti srca. U radu će na nekoliko konkretnih primjera biti prikazano efikasno korištenje Data mining metoda kao nove discipline koja ima za cilj da filtrira podatke u bazama podataka, da ih sumira i pronalazi obrazce prilikom obrade stvarnih EKG signala. Nad profiltriranim podacima je testirano i analizirano mnoštvo algoritama za detekciju QRS kompleksa, te je izvršena implementacija onog algoritma koji je pokazao najbolje rezultate u svrhu HRV analize.**

Ključne riječi **— Data mining, EKG signal, procesiranje, web-bazirana aplikacija.**

I. Uvod

Postavljanje teze o postojanju bioelektriciteta, od strane italijanskog anatoma Luigi Galvanija davne 1786. godine, imati će mnogo veći uticaj u medicini nego što se tada smatralo [1]. Elektrokardiogram (EKG) ustvari predstavlja snimanje električnih aktivnosti srca postavljanjem elektroda na površini tijela. Godine 1903. holandski liječnik Einthoven [2] javnosti je predočio poboljšanu tehnologiju snimanja EKG-a primjenom niza galvanometara kao uređaja za snimanje, te korištenjem mnogih ljudskih subjekata sa različitim srčanim abnormalnostima. Time je uveo osnove u elektrokardiografiju koje su i danas široko prisutne.

Razvoj nauke o snimanju električnih aktivnosti srca (EKG) odvija se u posljednjih 30-tak godina, kada je F. N. Wilson objavio naučni rad na temu unipolarnog snimanja ovog signala [3].

Primjena računara u snimanju, obradi i analizi EKG signala predstavlja jednu od najranijih primjena računarske tehnike u medicinske svrhe [4]. Od primarnog interesa za primjenu računarskih sistema u obradi EKG signala bilo je pravilno tumačenje i detektovanje različitih valova i intervala električnih aktivnosti srca.

U srcu postoji poseban sistem koji služi za stvaranje ritmičkih impulsa (akcionih potencijala) i njihovo sprovođenje kroz čitavo srce izazivajući pri tome ritmičko kontrahovanje srčanog mišića. Vremenski promjenljiva električna aktivnost srca, odnosno akcioni potencijali koji se prenose kroz srce, mogu da se mjere pomoću površinskih elektroda, pri čemu se dobiva zapis poznat pod nazivom elektrokardiogram. EKG je signal sa karakterističnom morfologijom u kojoj je moguće uočiti nekoliko pojava, koje se nazivaju talasi, a svaki od njih karakterističan je za određenu fazu u provođenju akcionih potencijala kroz srce. Signal ima karakterističnu morfologiju koju čine P-QRS-T-U kompleks [5].

Iz svega navedenog jasno se nametnula potreba za realiziranjem sistema za analiziranje i procesiranje EKG signala. Neizostavan dio jednog ovako implementiranog web-baziranog sistema je svakako "rudarenje" podataka, prikaz i obrada EKG signala na nekoliko različitih načina, čime se prikazuje što jasnija slika o zdravstvenom stanju pacijenta.

Rudarenje podataka ili podatkovno rudarenje (engl. *Data mining*) je sortiranje, organiziranje ili grupisanje velikog broja podataka i izvlačenje relevantnih informacija. Data mining [6] je nova disciplina koja ima za cilj da filtrira podatke u bazama podataka, da ih sumira i pronalazi obrasce. Data mining ne treba posmatrati kao jednostavnu-vremensku vježbu. Kako vrijeme odmiče nove vrste objekata i dezena mogu privući pažnju, i mogu biti vrijedni u traženju potrebnih podataka.

Data mining je, zbog dobrih razloga, nedavno privukao veliku pažnju: to je nova tehnologija, rješava nove proleme, sa velikim potencijalom za komercijalna i naučna otkrića. Međutim, ne treba očekivati da pruži odgovore na sva ptanja. Kao i sva otkrića procesa, uspješan Data mining je sposobnost sretnog slučajnog otkrića. Dok pronalaženje podataka obezbjeđuje korisne alate, to ne znači da će neizbježno dovesti do važnih, interesantnih ili vrijednih rezultata.

U ovom radu je prikazano da se na vrlo elegantan način mogu objediniti Data mining i procesiranje nad stvarnim EKG signalima, te isti u realnom vremenu prikazivati putem web-baziranih aplikacija. Dati procesirani signali su time putem web pretraživača dostupni osobama koje iste analiziraju (doktorima npr.), ili pak i samim pacijentima. Iskorak u ovom radu predstavlja i računarski urađena HRV analiza, koja se pokazala kao izuzetno snažan alat za sve vrste dijagnostike rada ljudskog srca.

II. DATA MINING

Pojam Data mining bi se mogao objasniti kao proces pronalaženja korisnog znanja ili informacija, odnosno otkrivanje znanja iz velike količine podataka. Rudarenjem poboljšava proces donošenja odluka na strateško-poslovnoj razini pružajući uvid u "skrivene" podatke *business intelligence* (BI) metodologijom. Rudarenjem se također otkrivaju odnosi, logičnost, pravilnost, te općenito bilo kakve strukture među podacima. Rudarenje podrazumijeva organiziranje baza čišćenjem podataka kako bi se pristupilo znanju i sticanju istog na temelju postojećih podataka u bazama. Razvoj tehnologije, računara, interneta bitno doprinosi lakšem organiziranju podataka, no da bi oni postali korisni, potrebno je njihovo pretvaranje u informacije i znanje.

Data mining predstavlja tehniku pretraživanja podataka u cilju identifikacije traženih uzoraka i njihovih međusobnih relacija. Jednostavno rečeno, Data mining je postupak izdvajanja interesantnih, novih i potencijalno korisnih informacija ili uzoraka, sadržanih u velikim bazama podataka (slika 1).

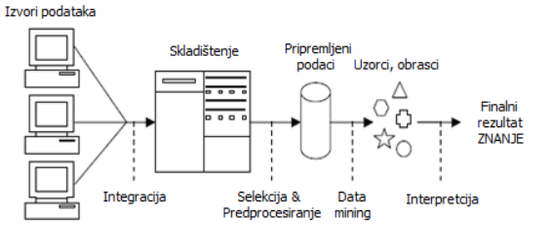

Slika 1 Procesiranje podataka i Data mining

Osnovni cilj Data mining-a jeste otkrivanje do sada nepoznatih odnosa, relacija, formi ponašanja između podataka. Prilikom same pretrage podataka Data mining pomaže analitičaru da riješi neke od sljedećih problema [7]:

- *Klasifikacija* – analiziraju se skupovi podataka, otkrivaju skrivene veze i utvrđuju elementi (funkcije) za njihovo grupisanje u jednu od nekoliko klasa,
- *Asocijacija podataka* – utvrđuju se osobine koje se javljaju zajedno kod više uzoraka, odnosno veze među proizvoljnim atributima,
- *Grupisanje* – proces određivanja grupa podataka koji su međusobno slični, ali različiti od ostalih grupa podataka. Pri tome se indentifikuju i promjenljive po kojima se vrši najbolje grupisanje i
- *Predviđanje* – otkriva se ponašanje objekta na osnovu posmatranja tokom vremena i vrše se predviđanja. Utvrđuju se pravilnosti iz primjera i na osnovu toga određuju očekivane numeričke vrednosti.

U narednom poglavlju ovog rada će ukratko biti opisani koraci koji se koriste u Data mining tehnikama, a koji su primjenjivani i tokom pripreme podataka realnih EKG signala koji su korišteni za web-bazirani prikaz i analizu.

III. FAZE U PROCESU DATA MINING-A

Data mining se može primijeniti u svim onim oblastima gdje se raspolaže velikim količinama podataka čijom analizom se žele otkriti određena pravila, zakonitosti i veze.

Životni ciklus jednog Data mining projekta, pa i onog korištenog u ovom radu, se satroji iz 8 koraka [8]:

1. Sakupljanje podataka
2. Filtriranje podataka i transformacija
3. Kreiranje i izbor modela
4. Procjena kvaliteta modela
5. Kreiranje izvještaja
6. Ocjenjivanje modela
7. Integracija Data mining modela u aplikaciju
8. Upravljanje modelom

Sakupljanje podataka je obično prvi korak u Data mining projektu. Poslovni podaci su uskladišteni u brojnim sistemima, internetu, bazama podataka kompanija, i prvi korak obično predstavlja prenos relevantnih podataka u bazu podataka gdje se podaci analiziraju. Nakon što se sakupe, podaci se mogu semplovati da bi se smanjila veličina trening skupa podataka. U mnogim slučajevima, obrasci koji su pronađeni na skupu od 50 000 uzoraka su isti kao i oni pronađeni na trening skupu od 1 000 000 uzoraka.

Filtriranje podataka i transformacija je najintenzivniji korak u Data mining projektu kada su resursi u pitanju. Cilj filtriranja podataka je odstranjivanje irelevantnih i suvišnih informacija iz skupa podataka. To podrazumijeva uklanjanje duplih i nepotpunih podataka, njihovu tranformaciju u jedinstven sistem podataka, izabiranje podgrupa podataka, određivanje broja promjenljivih sa kojima je moguće raditi. Cilj transformacije podataka je promjena izvornog podatka u drugačiji format tipa podataka. Postoje različite tehnike koje se mogu primijeniti za korak filtriranja i transformaciju podataka, a najčešće korišćene su; transformacija tipova podataka, neprekidna transformacija kolona, grupisanje, rad sa vrijednošću koja nedostaje, brisanje abnormalnih slučajeva, itd.

Kreiranje i izbor modela je treći korak koji se primjenjuje nakon filtriranja i transformacije podataka. Tek kada se podaci filtriraju i kada se promjenljive transformišu u pogodne tipove podataka, može se započeti sa kreiranjem

modela. Prije kreiranja modela treba se razumiti cilj Data mining projekta i vrsta Data mining zadatka koji će se koristiti. Za svaki Data mining problem postoji nekoliko odgovarajućih algoritama. Preciznost algoritma zavisi od prirode podataka kao što su: broj stanja atributa koji se koriste za predviđanje, prenos vrijednosti svakog atributa, veza između atributa, itd.

Procjena kvaliteta modela – U dijelu kreiranja modela kreira se skup modela koristeći algoritme i tehnike Data mining-a, ali nakon kreiranja neophodno je izvršiti i evaluaciju tog modela. Postoji nekoliko popularnih alata za evaluaciju kvaliteta modela koji mogu biti od pomoći u ovoj fazi procesa.

Kreiranje izvještaja – Nakon kreiranja modela i evaluacije kvaliteta tog modela vrši se kreiranje izvještaja koji se eventualno dostavljaju menadžerima na uvid. Većina Data mining alata ima osobinu kreiranja izveštaja koji omogućavaju korisnicima da generišu prethodno definisan izveštaj sa tekstualnim i grafičkim detaljima Data mining modela.

Ocjenjivanje modela – U većini Data mining projekata pronalaženje obrazaca i modela je samo pola posla; konačni cilj je upotreba tog modela za predviđanje (*scoring*). Da bi se dobile predviđene vrijednosti neophodno je postojanje već istreniranog modela i skupa novih podataka.

Integracija Data mining modela u aplikaciju – Integrisanje Data mining modela u poslovne aplikacije predstavlja ponovnu primjenu poslovne inteligencije na poslovni sistem. Sve više aplikacija uključuje i Data mining komponentu, a prednosti Data mining-a su velike. Data mining se uveliko koristi i u aplikacijama za medicinske svrhe. Jedna zdravstvena institucija može čuvati podatke o historijama bolesti svih pacijenata u proteklih pet ili više godina, ali kako će ona predvidjeti ishod bolesti ili liječenja pojedinog pacijenta? Upravo Data mining može poslužiti da bi se npr. predvidio ishod raznih bolesti ili ishod liječenja pojedinog pacijenta.

Upravljanje modelom – Svaki Data mining model ima svoj životni ciklus. U nekim oblastima primjene obrasci su relativno stabilni i modeli ne zahtjevaju učestalo ponovno treniranje modela. Međutim, u mnogim oblastima obrasci se mijenjaju često i iz tog razloga bi se nove verzije modela morale praviti poprilično često.

Postoji jako mnogo alata koji omogućavaju upotrebu Data mining tehnika i mašinskog učenja nad podacima. Za naučna istraživanja, pa samim time i za ovaj rad, od posebnogg interesa su alati čije je korištenje besplatno. Poslužitelji za anlizu podataka (DMS od engl. *Data Mining Server*) javno su dostupni mrežni servisi. Za potrebe ovog rada korišten je DMS server pod nazivom Statsoft [9] koji je vrlo jednostavan za korištenje i predstavlja jedan od vodećih svjetskih besplatnih Data mining softvera.

IV. OPIS EKG SISTEMA

EKG signal je specifična prezentacija električne aktivnosti srca [10]. Ovaj fiziološki signal daje informacije o stanju i aktivnostima srčanog mišića. Električna aktivnost srca mjerena na površini tijela – koži predstavlja EKG signal. To je fiziološki višekanalni signal koji se snima sistemom biopotencijalnih elektroda strateški raspoređenih na površini tijela, na grudnom košu i ekstremitetima.

Srce je mišić veličine pesnice. Prosječno je težine oko 500 g, dugo je oko 15 cm u najdužem pravcu, i orijentisano je na dole u grudnoj šupljini ka srednjoj liniji tijela sa lijeve strane. Shematski se srce može podijeliti na četiri dijela: dvije pretkomore (*atriji*) koje su smještene na gornjem dijelu srca i dvije komore (*ventrikule*) na donjem dijelu srca. Anatomija ljudskog srca [11] prikazana je na slici 2.

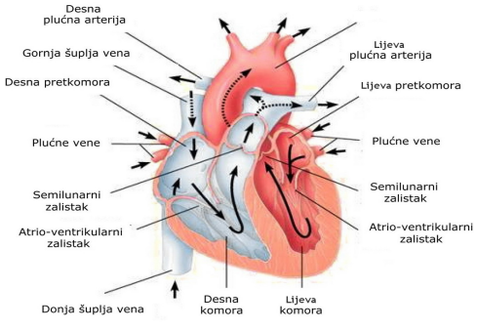

Slika 2 Anatomija srca

Tradicionalni EKG uređaji električne promjene srca registruju pomoću užarene niti – pera koja ostavlja trag na termički osjetljivom papiru koji se kreće standardnom brzinom. Kretanje papira predstavlja proticanje vremena, a kretanje pera je određeno upravo veličinom napona na elektrodama koje su vezane na odvode na tijelu pacijenta. Pero se kreće ka gore kada je napon pozitivan, a ka dole kada je negativan, ocrtavajući promjene napona u vremenu na pokretnoj traci papira [11], kako je ilustrovano na slici 3.

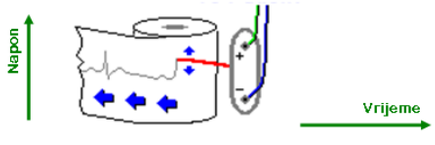

Slika 3 Princip rada elektrokardiografa

Tradicionalni EKG uređaji su kalibrirani za papir koji se pomjera brzinom od 25 mm/s i pojačanjem elektro-signala takvim da amplituda od 10 mm na papiru odgovara promjeni potencijala u iznosu od 1 mV.

Zapis EKG signala vrši se na milimetarskom papiru. Vrijeme je predstavljeno na x-osi, tj. u horizontalnom smjeru se prikazuje protok vremena. Zato vertikalne linije olakšavaju očitanje protoka vremena. Pošto se papir standardno kreće brzinom od 25 mm u sekundi, svaki razmak od 1 mm predstavlja 0.04 sekunde. Svaka peta linija je "pojačana" da bi olakšala brojanje, tako da vrijeme između podebljanih linija iznosi 0.2 sekunde, a jedna sekunda je predstavljena sa 5 velikih kocki. Vertikalna, y-osa, predstavlja amplitudu tj. izmjereni električni napon u milivoltima. Svaki vertikalni milimetar – tj. razmak između dvije horizontalne linije predstavlja 0.1 milivolt. Deset vertikalnih kockica predstavljaju 1 mV. Srčani ritam se može odrediti ako se broj 60.000 podijeli sa vremenom koje je proteklo između dva susjedna R talasa, izraženo u milisekundama. Kod elektronskih EKG uređaja moguće je sresti i brzine različite od 25 mm/s, a to je najviše u situacijama kada je srčani ritam brži ili znatno sporiji od prosječnog [11].

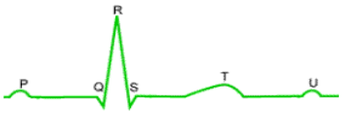

Slika 4 Jedan period EKG zapisa

Svaki vrh EKG krive se označava slovom počevši od slova P do U, redom po engleskom alfabetu. Svaki vrh odgovara određenoj električnoj aktivnosti srca (slika 4).

EKG signal koji je već univerzalno prepoznatljiv, odlikuje se uočljivim P talasom iza kojeg slijedi QRS kompleks sa izraženim R talasom. Visoki R talas je kod tradicionalnog rada, a i kod računarski baziranih uređaja, odrednica koja služi za računanje srčanog ritma i praćenje ispravnog rada srca.

Nad korištenim EKG signalima su putem besplatnog DMS softvera primijenjene Data mining tehnike opisane u prethodnom poglavlju, te je nad tako pripremljenim i donekle profiltriranim podacima izvršena implementacija algoritama za detekciju QRS kompleksa, što će detaljno biti opisano u narednom poglavlju.

V. Opis korištenih algoritama

Mogućnost detekcije QRS kompleksa u EKG signalima je važan dio u području medicinske instrumentacije. Implementirani su mnogi sistemi i analitičke metode koje zahtijevaju tačnu automatsku detekciju QRS kompleksa u prisustvu različitih šumova i smetnji, u čiju je svrhu kreiran veliki broj različitih algoritama. Međutim, savremeni elektrokardiogrami snimaju EKG signal onečišćen različitim signalima smetnji. Ti signali uključuju neizbježne smetnje gradske mreže, smetnje usljed kontrakcije mišića, disanja, itd. Programi za analizu EKG-a zahtijevaju podatke bez šumova, pa se u tu svrhu implementiraju različiti filteri, bilo digitalni, bilo analogni, koji eliminiraju te izvore šuma.

Neki izvori šuma, poput onog uzrokovanog gradskom mrežom, mogu biti lako uklonjeni prije snimanja, no ostale treba ukloniti nakon što je signal snimljen. Zbog toga je potrebno realizirati učinkovite algoritme za distinkciju EKG signala od različitih izvora šuma.

Signali koji su korišteni da bi se izvršio prikaz i analiza EKG-a preuzeti su sa standarnih baza podataka anotiranih EKG signala, a jedna od njih je i MIT-BIH baza [12]. Oblik jednog od korištenih signala prikazan je na slici 5.

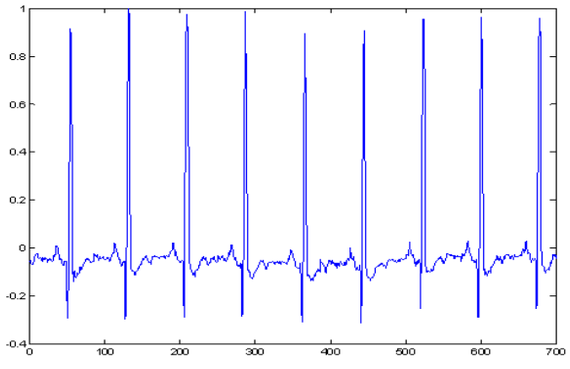

Slika 5 Analizirani EKG signal

EKG signal može biti ometan raznim smetnjama. Neke od najčešćih će biti objašnjene u nastavku.

Smetnja gradske mreže – sastoji se od smetnje frekvencije 50 Hz i njenih harmonika, a za određeno mjerenje je nepromjenljiva; može se simulirati kombinacijama sinusoida amplitude polovine vrijednosti od vrha do vrha EKG signala.

Kontaktni šum elektroda – pojavljuje se pri gubitku kontakta elektrode s kožom; uzrokuje potpuni gubitak signala na određeno vrijeme, daje kratkotrajni signal maksimalne amplitude mjernog instrumenta nakon čega eksponencijalno pada do bazne razine, te traje oko 1 s.

Smetnja usljed pokreta – prelazne pojave uzrokovane promjenom impedance između elektrode i kože, pomakom elektrode mijenja se impedanca naponskog djelitelja koga čine koža i pojačalo, čime se mijenja ulazni napon pojačala; traje 100 do 500 ms, amplitude 500% vrijednosti od vrha do vrha EKG signala.

Kontrakcija mišića (EMG) – može se aproksimirati frekventno ograničenim (do 10 kHz) Gaussovim bijelim šumom srednje vrijednosti 0, varijanse oko 10% vrijednosti od vrha do vrha EKG signala

Smetnja usljed disanja – može se predstaviti sinusnim signalom amplitude 15% vrijednosti od vrha do vrha EKG signala frekvencije disanja (0.15 do 0.3 Hz). Amplituda EKG signala također varira s disanjem za oko 15%, varijacije se mogu reprezentirati amplitudnom modulacijom sinusnim signalom.

Smetnja gradske mreže simulirana je dodavanjem sinusoide od 50 Hz. Smetnja usljed slučajne kontrakcije mišića, reda veličine 1 mV (elektromiografska smetnja) dobivena je dodavanjem vektora slučajnih brojeva koji poprimaju vrijednosti iz intervala [-0.5, 0.5]. Kao treći izvor smetnje korištena je smetnja usljed disanja koja predstavlja niskofrekventni pomak uzrokovan ritmičkim udisanjem i izdisanjem. Ta smetnja realizirana je dodavanjem sinusoide frekvencije 0.333 Hz osnovnom signalu. Izgled signala nakon djelovanja smetnji prikazan je na slikama 6 – 8.

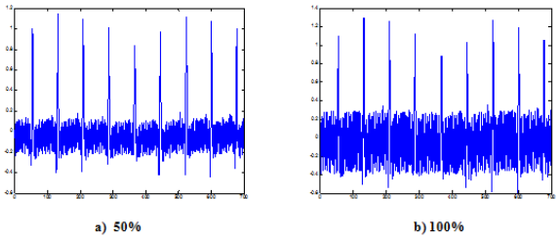

Slika 6 Smetnja gradske mreže (50 Hz)

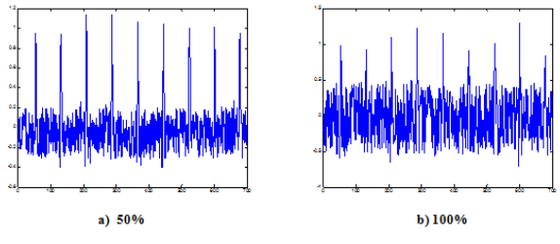

Slika 7 Smetnja usljed mišićne kontrakcije

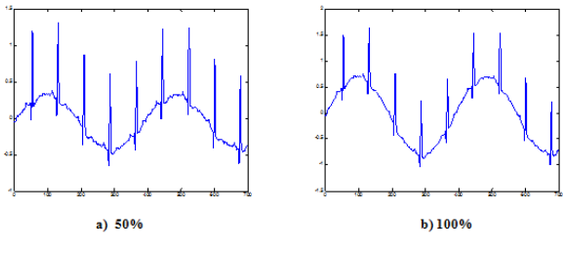

Slika 8 Smetnja usljed disanja

Četiri su osnovna algoritma korištena za detekciju QRS kompleksa [11]:

1. AF – algoritmi bazirani na amplitudi i I derivaciji
2. FD – algoritmi bazirani samo na I derivaciji
3. FS – algoritmi bazirani na I i na II derivaciji
4. DF – algoritmi koji se odnose na digitalne QRS propusne filtere

Algoritmi AF1 i FD1 su analizirani i testirani na različite vrste smetnji uz različite postupke zašumljenosti. Na slici 9 prikazan je broj detektovanih nepostojećih QRS kompleksa za ovako zašumljene signale, dok je na slici 10 prikazan broj procentualnih vrijednosti ispravno detektovanih QRS kompleksa. Bitno je napomenuti da je testiranje provedeno nad nekoliko realnih EKG signala iz MIT-BIH baze signala, te su na slikama prikazani prosječni rezultati istih.

	AF1	FD1
Gradska mreža 50%	0	0
Gradska mreža 100%	0	0
EMG 50%	0	0
EMG 100%	6	0
Disanje 50%	0	0
Disanje 100%	0	0

Slika 9 Broj detektovanih nepostojećih QRS kompleksa

	AF1	FD1
Gradska mreža 50%	93.75 %	100 %
Gradska mreža 100%	81.25 %	93.75 %
EMG 50%	100 %	100 %
EMG 100%	75 %	37.5 %
Disanje 50%	100 %	100 %
Disanje 100%	81.25 %	100 %

Slika 10 Procentualni prikaz ispravno detektovanih QRS kompleksa

Nakon izvšenih testiranja algoritama, FD1 se pokazao općenito superiornijim algoritmu AF1, iako treba napomenuti da u slučaju 100% EMG smetnje navedeni algoritam pokazuje znatno lošije rezultate. Vremensko kašnjenje koje se javlja u analiziranom signalu kao razlika vremenskog indeksa vršne vrijednosti QRS kompleksa i indeksa filterom detektovanih kompleksa, a koje je posljedica primjene digitalnog filtera, pokazalo se relativno malo kod testiranja navedena dva algoritma. Stoga su ovi algoritmi prikladni i za primjene u kritičnim područjima medicine.

Na osnovu predočenih zaključaka i rezultata izvršena je implementacija FD1 algoritma i prikaz takvih signala putem web aplikacije (slika 11). Data aplikacija predstavlja kompaktan web-bazirani sistem za obuku iz domena EKG sistema. Implementacija iste je u potpunosti zasnovana na ORACLE tehnologijama i Javi EE, počevši od razvojnih alata do izvršnog okruženja. Korišteni podaci su pohranjeni u Oracle Database 11g bazu podataka. Kao aplikativni server korišten je Oracle WebLogic Server. Radne stanice mogu imati instaliran bilo koji Web pretraživač za korištenje implementirane aplikacije. Razvojno okruženje u kojem je realizirana aplikacija je Oracle JDeveloper 11g.

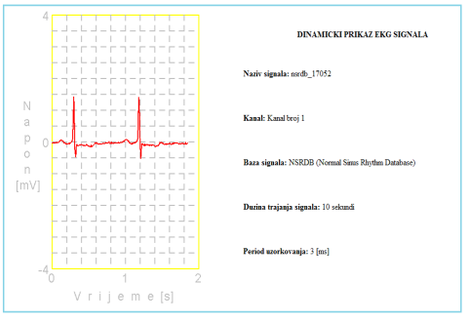

Slika 11 Web-bazirani prikaz EKG signala

Osim prikaza EKG signala, realizirana web aplikacija podržava i njegovu obradu (slika 12), kao što su prikaz R-R intervala, te analiza promjene srčanog ritma (HRV). Analiza promjene srčanog ritma je jedna od glavnih metoda predviđanja i otkrivanja raznih vrsta oboljenja.

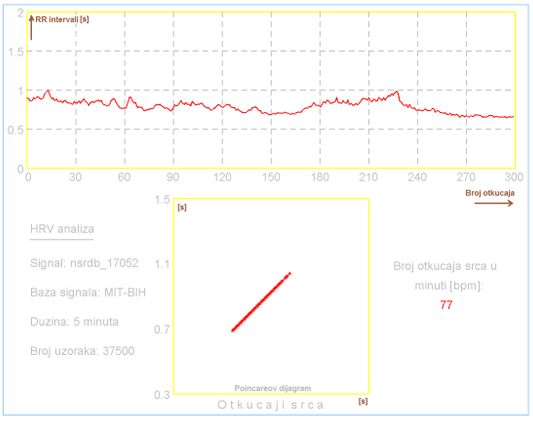

Slika 12 Web-bazirana HRV analiza EKG signala

Predočena HRV analiza je pokazala izuzetno dobre rezultate učinkovitosti za mnoštvo korištenih EKG signala. Na prikazanoj web stranici je osim analize predočen i broj otkucaja srca koji je na datim uzorcima signala imao 100% tačnost.

VI. ZAKLJUČAK

Većina aktivnosti koje se obavljaju u okviru savremenih sistema zdravstvene zaštite, prevencije i tretmana bolesti, te rehabilitacije pacijenata uključuje probleme čije uspješno rješavanje zahtijeva primjenu inžinjerskog pristupa.

Posljednjih godina nagli razvoj tehnologije u oblasti telekomunikacija i računarstva, uz istovremeno značajno pojeftinjenje hardvera, omogućio je razvoj novih oblika komunikacija među ljekarima, skladištenje i veliku brzinu pretraživanja uskladištenih podataka kako za pojedince tako i grupe pacijenata, analizu podataka novim metodama i na taj način savremenu i bržu zdravstvenu zaštitu.

Dva analizirana i implementirana algoritma (AF1 i FD1) testirana su na različite vrste smetnji, pri čemu su signalima dodati različiti oblici zašumljenosti (smetnja gradske mreže, smetnja usljed mišićne kontrakcije, te usljed disanja). Nakon izvršenih testiranja algoritama, FD1 se pokazao općenito superiorniji algoritmu AF1. Izbor algoritma koji će se primjenjivati u praksi ovisi o uvjetima u kojima će implementirani algoritam raditi, odnosno o tipu smetnje koja je u radnom okruženju najviše zastupljena. Potrebno je izabrati onaj algoritam koji je "najotporniji" na određenu vrstu pogreške, odnosno najtačnije detektuje QRS komplekse.

Signali su nakon obrade putem predloženih Data mining metoda prikazani na posebno dizajniranoj web aplikaciji. Osim samog prikaza izvršena je i detaljna HRV analiza svakog signala. Na osnovu dobivenih rezultata mišljenja sam da će HRV analiza u skoroj budućnosti postati jedno od glavnih "oružja" medicinskog osoblja u predviđanju i propisivanju prevencija od različitih vrsta oboljenja.

LITERATURA

1. A. D. Waller, “One of the electromotive changes connected with the beat of the mammalian heart, and the human heart in particular”, Phil Trans B 180:169, 1889.
2. W. Einthoven, “Die galvanometrische Registrirung des menschlichen ECGs, zugleich eine Beurtheilung der Anwendung des Capillar-Elecktrometers in der Physiologie ”, Pflugers Arch Ges Physiol 99:472, 1903.
3. F. N. Wilson, F. S. Johnson, I. G. W. Hill, “The interpretation of the falvanometric curves obtained when one electrode is distant from the heart and the other near or in contact with the ventricular surface”, Am Heart J 10:176, 1934.
4. J. M. Jenkins, “Computerized electrocardiography”, CRC Crit Rev Bioeng 6:307, 1981.
5. T. A. Pryor, E. Drazen, M. Laks, “Computer Systems for the Processing of diagnostic electrocardiograms”, Los Alamitos, Calif, IEEE Computer Society Press, 1980.
6. P. N. Tan, M. Steinbach, V. Kumar, “Introduction to Data Mining”, ISBN 0-321-20448-4
7. J. Graham, J. S. S. Williams, “Data Mining - Theory, Methodology, Techniques,and Applications”, Springer-Verlag Berlin Heidelberg, 2006.
8. W. R. Zbigniew, S. Tsumoto, D. Zighed, “Mining Complex Data”, Third International Workshop, Springer-Verlag Berlin Heidelberg, 2008.
9. http://www.statsoft.com
10. D. Bošković, “Integracija objektno orijentisanih tehnika u implementaciji algoritma sistema realnog vremena”, magistarski rad, Elektrotehnički fakultet Sarajevo, mart 2004.
11. E. Žunić, “Web-bazirani sistem za obuku iz domena EKG sistema”, Master rad, Elektrotehnički fakultet Sarajevo, septembar 2010.
12. http://www.physionet.org/cgi-bin/ATM

USER VERIFICATION FOR HEMOGLOBIN A1c ON COBAS 501 ROCHE ANALYZER

E. Kučukalić, J. Ćorić, J. Mujić, L. Ćurović and A. Bodulović

Department of Clinical Chemistry, Clinical Center of Sarajevo University, Sarajevo, Bosnia and Herzegovina

Abstracts: **Glycated hemoglobin (HbA1c) is formed by non-enzymatic binding of glucose to the free amino group of the N-terminal end of the ß-chain of hemoglobin A. HbA1c is representative of the mean blood glucose level over three months. The aim of the study was to evaluate new method in laboratory by defining precision and trueness for determination of HbA1c at the Cobas 501 Roche analyzer, by immunoturbidimetric method. We determined the concentrations of total hemoglobin and HbA1c. HbA1c is measured in a latex agglutination inhibition test. The presence of HbA1c in the sample results in reduced levels of agglutination. The increase in absorption is inversely proportional to the concentration of HbA1c in the sample. Venous blood samples from diabetic patients are collected into K_3EDTA containing vacutainer tubes. Commercial controls PreciControl HbA1cN (PCA1N) and PreciControl HbA1cP (PCA1P) at two levels were used for quality control. Analytical validation of HbA1c included: within-run imprecision, between-day imprecision, inaccuracy and comparation determination on the human samples on 2 systems: Dimension XPanda and Cobas 501 Roche analyzers. Within-run imprecision on the commercially controls for PCA1N is 4,6% and PCA1P is 3,6%; between-day imprecision on commercially controls is 7,5% PCA1N for and 8,2% for PCA1P respectively; inaccuracy on commercially controls for PCA1N is 1,8% and PCA1P is 4,8% . Method comparasion on human samples show in the range of method linearity correlation coefficient from 0,99. The presented results of the analytical evaluation methods for the determination of Cobas 501 Roche analyzer showed an acceptable accuracy and precision.**

Keywords: **glycated hemoglobin HbA1c, diabetes, Cobas 501 Roche analyzer**

INTRODUCTION

Glycated hemoglobin (HbA1c) is representative of the mean blood glucose level over three months. HbA1c referes to the product of a non-enzymatic reaction between glucose and hemoglobin A1(1). The human erythrocyte is freely permeable to glucose, which can non-enzymatic combine with hemoglobin to form HBA1c. This non-enzymatic reaction between the alpha-amino group of the N-terminal valine of the hemoglobine beta-chain and glucose takes place to form an unstable aldimine of Schiff base intermediate. This reaction is slow and occurs at a rate that is proportional to the glucose concentration in the blood (2, 3).

The first arbitrary criteria for diagnosis of diabetes mellitus appeared in 1980. These criteria were based on blood glucose in non-pregnant adults (OGTT) (4). In 1997, these criteria were supplemented with the value of fasting plasma glucose (FPG) more central to the diagnosis. Twelve years later, in 2009, the International Expert Committee for Diagnosis and Management of Diabetes recommended that HbA1c be used as the preferred test for diagnosing type 2 diabetes (T2D) (5). The diagnosis of diabetes should be made solely on the basis of an HbA1c value $\geq$ 6.5 % (48 mmol/mol) (6).

MATERIALS AND METHODS

The Cobas 501 Roche assay measures both HbA1c and total hemoglobin. The HbA1c measurement is based on a turbidimetric inhibition immunoassay principle, and the measurement of the total hemoglobin is based on a modification of the alkalne hematin reaction. Using the values obtained for each of these two analytes, the relative proportion of the total hemoglobin that is glycated is calculated and reported. Pre-treatment to remove the labile

fraction is not necessary as only the rearranged form of HbA1c is detected. All hemoglobin variants that are glycated at the beta-chain N-terminus and have epitopes identical to that of HbA1c are measured by this assay. The increase in absorption is inversely proportional to the concentration of HbA1c in the sample. Venous blood samples from diabetic patients are collected into K_3EDTA containing vacutainer tubes. Commercial controls PreciControl HbA1cN (PCA1N) and PreciControl HbA1cP (PCA1P) at two levels were used for quality control. Analytical validation of HbA1c included: within-run imprecision on the commercially controls (N=20); between-day imprecision commercially controls (N=25); inaccuracy on commercially controls (N=15) and comparation determination on the human samples (N=20) on 2 systems: Dimension XPanda and Cobas 501 Roche analyzers.

The results were analyzed by standard statistical methods and expressed as means $\pm SD$. Statistical test were performed by the statistical package Statistic for Windows. The correlation was analyzed by the Passing-Bablok linear regression test.

RESULTS

Inaccuracy of the HbA1c in series was determined in 15 measurements on commercially controls PCA1N and PCA1P. The Cobas 501 Roche assay inaccuracy results were presented in Table 1.

Table 1 Inaccuracy of HbA1c assay

Sample	Expeced value (%)	Observed value (%)	Inaccuracy Bias (%)
PCA1N	5,40	5,31	1,8
PCA1P	10,80	10,30	4,8

Inaccuracy on commercially controls for PCA1N is 1,8% and PCA1P is 4,8%.

Within-run precision of HbA1c was evaluated by analyzing a total 20 times during same day. A day-after-day precision measurement was carried out in the period of 10 days. The results of the Cobas 501 Roche assay precision within-run and between-run analyses are showed in Table 2.

Table 2 Precision of HbA1c assay

Sample	Mean value (%)	SD	CV(%)
Within-run			
PCA1N	5,3	0,24	4,6
PCA1P	10,1	0,36	3,6
Between-run			
PCA1N	5,2	0,39	7,5
PCA1P	9,8	0,80	8,2

The coefficient of variation (CV%) values for the within-run precision were 3,6-4,6% , with those for the between-run ranging 7,5-8,2%.

The Cobas 501 Roche HBA1c assay was compared to the Dimension XPanda (Siemens) assay. Data from the study were analyzed using Passing-Bablok regression and are summarized in the figure 1.

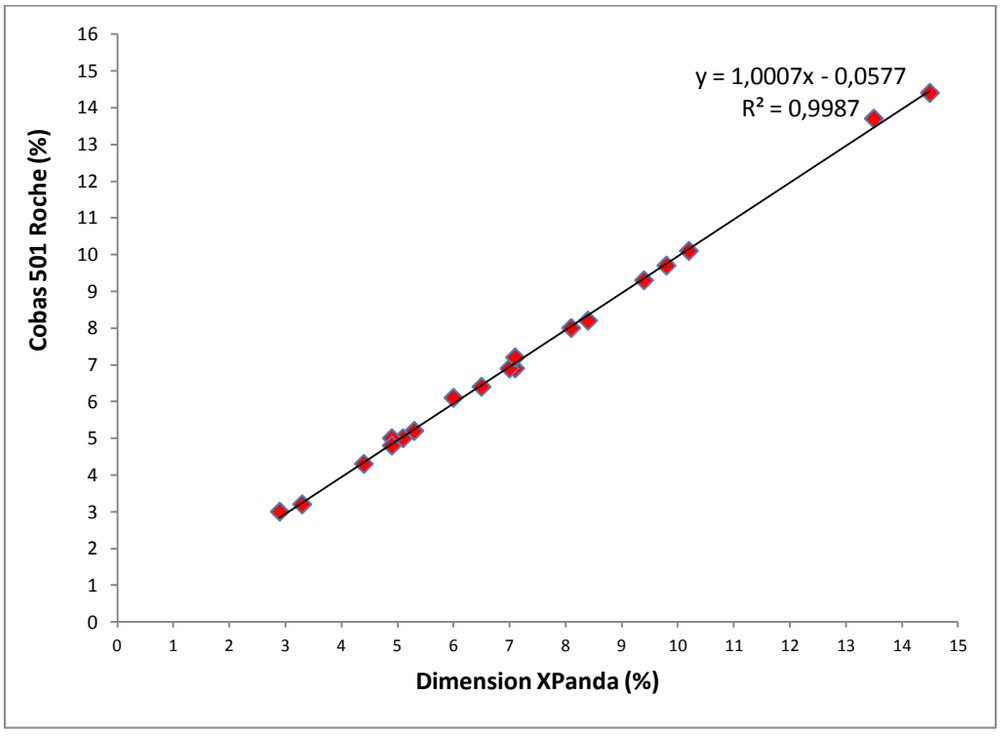

Figure 1 Correlation between the results of HBA1c whole blood using Dimension XPanda and Cobas 501 Roche analyzers

On the whole range of measure, the two methods showed a good correlation ($R^2 = 0,998$).

DISCUSSION

Hemoglobin A1c is an indirect measure of the mean blood glucose level over the previous 2-3 months. The HbA1c assay provides a reliable measure of chronic glycemia. Randomized controlled trials and observational studies have shown that HbA1c is a good predictor of microvascular complications including retinopathy, microalbuminuria and peripheral neuropathy. It is also suggested that the HbA1c assay helps to predict the likelihood of developing diabetes in the future (7,8).

Assays for HbA1c have developed over years from assays with large uncertainties, to the current tests with a high degree of precision and trueness. The HbA1c results are now also used for the diagnosis of diabetes. The external quality control material must be as commutable as possible and should have a target value achived with a reference method procedure. For tests used for the monitoring of diseases, the precision of the tests are often more important than the trueness. Long time stability of the internal QC HbA1c material is therefore of prime importance. Lyophilized materials are often used because they meet the requirements of stability. Due to lack of commutability

of lyophilized materials, method dependent target values and acceptance limits have to be assigned to the materials. Sometimes locally defined target values and acceptance limits have to be applied (9).

The overall performance of the Roche HbA1c assay was evaluated by determining precision, inaccuracy and comparasion. The HbA1c assay showed good results in all parameters evaluated in these studies. The Cobas 501 Roche assay showed good precision. The obtained CV% values for the within-run were 3,6-4,6%,witch was in accordance with the manufacturers recommendation. Between-day precision on commercially controls is 7,5-8,2 respectively. Inaccuracy on commercially controls for PCA1N is 1,8 % and PCA1P is 4,8 %. Comparasion on human samples show in the range of method linearity correlation coefficient from 0,99.

CONCLUSION

Long time has passed since the discovery of HbA1c and its introduction in the laboratory practice related to the management of diabetes mellitus. Great improvements have been achived on the analytical side. The presented results of the analytical evaluation methods for the determination of HbA1c on the Roche-Cobas 501 analyzer showed an acceptable accuracy and precision.

REFERENCES

1. D.E.Golstein, R.R Little, H.M. Wiedmeyer, J.D. England, E.M. Mc-Kenzie, *Glycated Hemoglobin: methodologies and clinical applications*, Clin Chem 1986;32;b64-70.

2. D.B.Sacks. *Diabetes mellitus*. In: Burtis CA, Ashwood ER, Bruns DE, eds. Tietz textbook of clinical chemistry and molecular diagnostics. 5th ed. St. Louis: Elsevier Saunders, 2012.

3. E.S. Kilpatrick, Z. Bloomgarden, P. Zimmet, *Is hemoglobin A1c a step forward for diagnosing of diabetes*. BMJ 2009;339:1288-90.

4. D.B. Sack, M. Arnold, G.L. Bakris, D.E. Bruns, A.R. Horvath, M.S. Kirkman, at al. *Guidelines and Recommendations for Laboratory Analysis in the Diagnosis and Management of Diabetes Mellitus.* Diabetes Care 2011;34:61-99.

5. T.Higgin *HbA1c- An analyte of increasing importance*. Clin Biochem 2012;45:1038-45.

6. D.M. Nathan, J. Kuenen, R. Borg, H. Zcheng, D Schenfeld, R.J. Heine, *Translating the A1c assay into estimated average glucose values, Diab.* Care 2008;31:1473-8.

7. American Diabetes Association,. *Standards of medical care in diabetes*. Diabetes Care 2011;34:S11-S61.

8. R. Bucala, A. Cerami, H. Vlassara, Advanced glycosylation end products in diabetic complications. Diabetes Rev 1995; 3: 258-68.

9. International Expert Committee Report on the role of the HbA1c assay in the diagnosis of diabetes, Diabetes Care 2009;32:1327-34.

Development of a New Amperometric Sensor for Adrenaline Based on the Carbon Electrode Modified with Ru(III) Complex

S. Redžić[1], E. Kahrović[2] and E. Turkušić[2*]

[1]University of Bihać, Biotechnical faculty, Luke Marjanovica bb 77 000 Bihać, Bosnia and Herzegovina
[2]University of Sarajevo, Faculty of Science, Department of Chemistry, Zmaja od Bosne 33-35, Sarajevo, Bosnia and Herzegovina

Abstract— **A new low-potential amperometric sensor for adrenaline based on glassy-carbon electrode modified by a water-insoluble redox mediator Sodium bis[N-2-oxyphenyl-5-bromosalicylideneiminato-*ONO*]ruthenate(III) complex using carbon ink was presented. FIA (Flow-Injection Analysis) amperometric measurements were performed at the operating potential of 100 mV (*versus* Ag/AgCl electrode) in 0.1 M phosphate buffer, pH 7.5 with flow rate 0.4 mL/min. The modified electrode shows a fast electric current response for adrenaline oxidation showing good reproducibility and stability. The sensor was tested in the range of 3-9 pH.**
It has a detection limit for adrenaline of $6.6 \cdot 10^{-2}$ mg/L (or $3.6 \cdot 10^{-4}$ mmol/L) (3δ) and a dynamic range of 0.5-25 mg/L adrenaline (i[μA] = 0,0506 *c* [mg/L] + 0,0573, r^2 = 0,99058).

Keywords— **Ru(III) complexes, Schiff Bases, Adrenaline, Modified electrode, Carbon ink, Amperometry, Flow-injection analyses.**

*Corresponding author: E. Turkušić is from the Faculty of Science, Department of Chemistry, Zmaja od Bosne 33-35, Sarajevo, Bosnia and Herzegovina (phone: 387-33-279-912; email: turkusic@gmail.com)

I. Introduction

Adrenaline is known as epinephrine, structure given in Fig. 1.

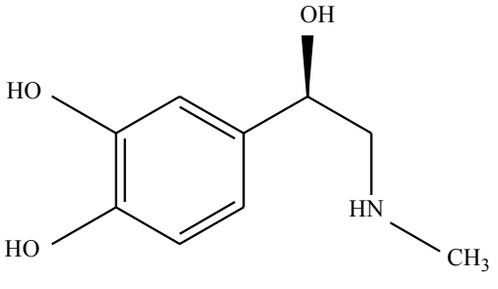

Fig.1. The structure of adrenaline [1]

Adrenaline is the hormone and one of the most important neurotransmitters that plays an important role in the mental stress and promotes a number of actions of the sympathetic nervous system [2]. It plays an important role as a mediator of stress caused by the development of anxiety disorders and depression. The concentration of adrenaline in the blood affects the regulation of a blood pressure, a heart rate, an immune system and a metabolism of glycogen. Adrenaline determination in the biological fluids is of great importance in medical diagnostics, mainly for patients suffering from Parkinson's disease. For this reason, there is a need for its quantitative determination in biological fluids and pharmaceutical preparations [3].

Different methods have been developed for adrenaline determination, for example: spectrophotometry [4], fluorimetry [5], colorimetry [6], liquid chromatography [7], capillary electrophoresis [8], chemiluminescence [9], electrochemiluminescence [10], amperometry [11], biamperometry [12], piezoelectric determination [13] and electrochemical determination with different modified electrodes [14]. The electrochemical methods are especially suitable for determination of adrenaline due to the speed determination, low cost and low limit of detection [15].

Many electrochemical sensors are developed for adrenaline determination in the presence of interferences [16, 17, 18]. Modification of electrodes based on carbon materials with suitable electron transfer mediator reduces the working potential, increases the sensitivity of the method and reduces the impact of interferences which is important for the adrenaline determination in the real samples [19]. Carbon electrodes with different polymer modifications: poly(caffeic acid), poly(L-aspartic acid), poly(indoleacetic acid), poly(L-methionine), 2-(4-Oxo-3-phenyl-3,4- dihydroquinazolinyl)-*N'*-phenyl-hydrazinecarbothioamid, valine, MnO_2 /Nafion, osmium complex and ruthenium complex (ruthenium oxide/ferrocyanide) for determination of adrenaline are reported [1, 11, 16, 20-25].

Ruthenium compounds have been the subject of increasing interest last decades for many reasons, especially due to their catalytic and anticancer activities. Ru(III) compounds with Schiff bases derived from salicylaldehyde and amines have been widely investigated due to the ability of these polydentate ligands to tune redox potential of complex species acting as catalysts and electron transfer mediators [28, 29, 30].

The aim of the paper was developing of a new sensor, prepared by surface modification of glassy-carbon electrode with water insoluble mediator Sodium bis[N-2-oxyphenyl-5-bromosalicylideneiminato-*ONO*]ruthenate(III) complex hereinafter referred as Na[Ru(N-Ph-O-5-Br-salim)$_2$].

II. Material and Methods

A. Reagents

The synthesis of Na[Ru(N-Ph-O-5-Br-salim)$_2$] was performed according to published procedure [26]. Adrenaline was purchased from Sigma-Aldrich, sodium dihydrogenphosphate and disodium hydrogenphosphate were purchased from Merck analytical grade (p.a). All other used reagents were of analytical grade purity (p.a. Merck). Phosphate buffer solution (0.1 M, pH 7.5) was prepared by mixing appropriate amounts of $NaH_2PO_4 \cdot 2H_2O$ and $Na_2HPO_4 \cdot 2H_2O$ in double distilled water and de-aerated by helium (99.995%, Messer Griesheim, Gumpoldskirchen, Austria).

Adrenaline solutions were prepared in the phosphate buffer (0.1 M, pH 7.5) just before use. All measurements were performed at ambient temperature.

B. Apparatus

The flow-injection system consisted of a high performance liquid chromatographic (HPLC) pump (Model 510, Waters, Milford, MA, USA), a sample injection valve (U6K, Waters), and a thin-layer electrochemical cell (CC5, BAS Bioanalytical Systems Inc., West Lafayette IN, USA). Teflon spacers (MF-1047, MF-1048, BAS) were used to adjust the thickness of the flow-through cell. A conventional three-electrode flow cell BAS 100 (BASi Dual 3mm Glassy carbon electrode MF-1000 for Thin -Layer Flowcells, BAS CC-5) was used for the experiments.

Glassy-carbon electrode was modified with Na[Ru(N-Ph-O-5-Br-salim)$_2$] complex and used as a working electrode (WE). The electrodes Ag/AgCl (3M KCl, model RE-1, BAS) and the back plate of flow cell were used as reference and counter electrode, respectively. The measurements were performed on the electrochemical workstation Autolab, potentiostat/galvanostat instrument (PGSTAT 12) using the corresponding software (Autolab Software version 4.9).

The pH values were measured using a pH meter (Thermo Orion, model 210+; Orion, Model SA 720) with the appropriate pH electrodes (SenTix 22 plus (A043019007).

C. Preparation of electrode

The mixture of Na[Ru(N-Ph-O-5-Br-salim)$_2$] as mediator and carbon ink (Electrodag 421SS PTFink, UN1210 PSN Printing ink, Acheson), mass ratio 1:1, was dissolved in acetone and applied on a glassy-carbon. The electrode was dried for 10 minutes at 60°C.

D. Measurement procedure

Flow-injection analyses (FIA) with the surface modified Na[Ru(N-Ph-O-5-Br-salim)$_2$] glassy-carbon electrode were performed at the applied potential of 100 mV (*vs* reference Ag/AgCl electrode) in 0.1 M phosphate buffer pH 7.5. The flow rate of the carrier buffer solution was 0.4 mL/min. 100 µL-portions of adrenaline solutions were injected. Peak heights were used to evaluate the results.

III. Results and Discussion

A. Amperometric determination of adrenaline

Current peak heights corresponding to the different adrenaline concentrations clearly demonstrate fast response and reproducibility of new sensor for adrenaline (Fig. 2).

Amperometric determination of adrenaline is based on the electrocatalytic oxidation on the glassy carbon electrode, surface modified with Sodium bis[N-2-oxyphenyl-5-bromosalicylideneiminato-*ONO*]ruthenate(III) complex**.** Adrenaline is oxidized to adrenaline-quinone (Scheme 1.) according to the proposed mechanism [1, 24, 27].

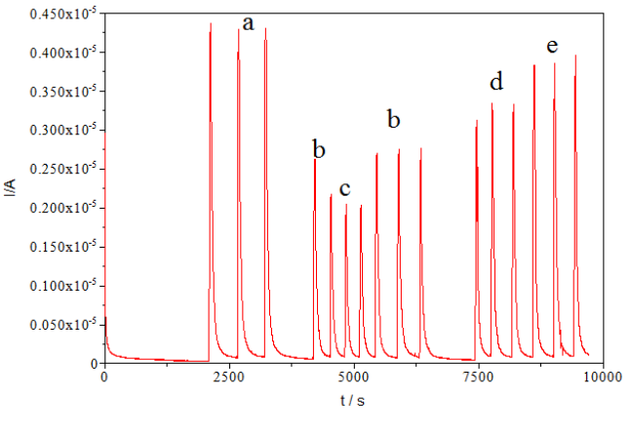

Fig. 2. Amperometric FI response of adrenaline with an Na[Ru(N-Ph-O-5-Br-salim)$_2$] carbon modified electrode. Concentration of adrenaline a) 1000, b) 200, c) 100, d) 300 and e) 500 mg/L, operating potential 100 mV vs. Ag/AgCl, flow rate 0.4 mL/min, injection volume 100 µL, 0.1 M phosphate buffer pH 7.5.

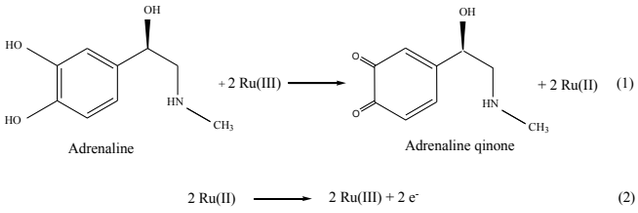

Schema 1: Mechanism of the catalytic adrenaline oxidation on the surface modified Na[Ru(N-Ph-O-5-Br-salim)$_2$] glassy-carbon electrode, according to reference [1]

B. Operating potential

The important parameter for the amperometric response of the sensor is the operating potential. Fig. 3. shows the dependence of the FI amperometric response and the background current of the potential in the range of -300 to 400 mV.

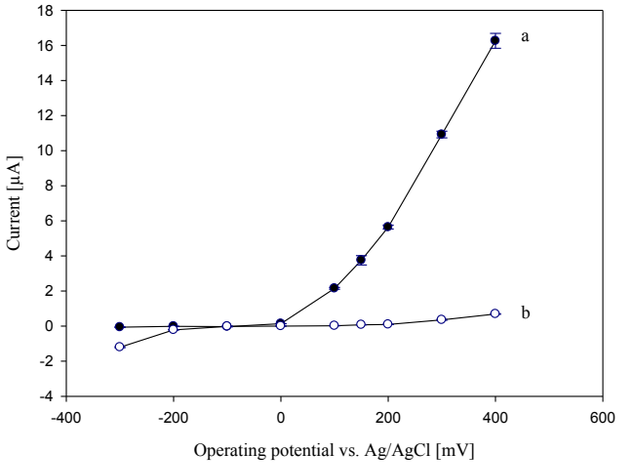

Fig. 3. Amperometric FI response on the applied operating potential. (a) current response of adrenaline concentration 200 mg/L and (b) background current. Electrode: Na[Ru(N-Ph-O-5-Br-salim)$_2$] modified carbon electrode, 0.1 M phosphate buffer pH 7.5, flow rate 0.4 mL/min, injection volume 100 µL.

The modified electrode demonstrates low background current in the broad potential range (-300 to +400 mV). Due to requirement to operate at low potential, which reduce interferences, 100 mV was used as optimal working potential.

C. Effect of pH

Fig. 4. shows the pH dependence of the amperometric response of adrenaline sensors in the range of 3-9. The comparison of background current with adrenaline current response shows that the background current is very unstable in the range of 3-6.6 pH. At higher pH values (7-9) background current is stabilized around zero and current response of adrenaline solutions increased. Although, the current response is higher at pH 9, the measurements were performed at pH 7.5 since there is a need for imitation of physiological ambient in biological fluids and pharmacological products.

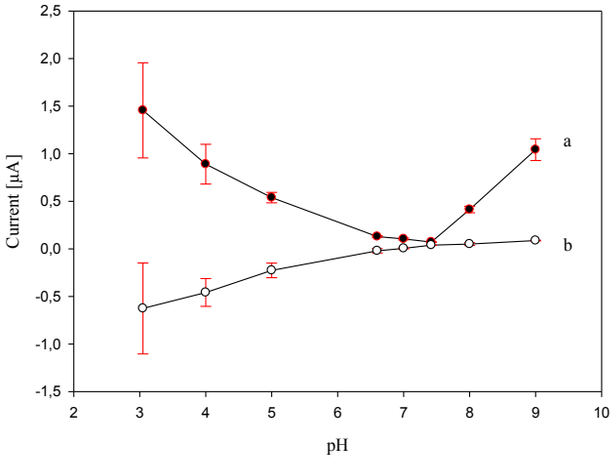

Fig. 4. Dependence of the amperometric response of the adrenaline sensor of the pH (0.1 M phosphate buffer pH 7.5). (a) current response of adrenaline concentration 200 mg/L and (b) background current. Electrode: Na[Ru(N-Ph-O-5-Br-salim)$_2$] modified carbon electrode, operating potential 0 mV, flow rate 0.4 mL/min, injection volume 100 µL.

D. Linearity, limit of detection and reproducibility

Linear relation between the amperometric peak current and the concentration was found in 0.5-25 mg/L adrenaline (Fig. 5) in 0.1 M phosphate buffer (pH 7.5): i[µA] = 0,0506 c [mg/L] + 0,0573, r^2 = 0,99058. For the concentrations above 25 mg/L, a slight deviation from linearity was observed.

The detection limit (given as 3δ) values calculated from 3 injection of 100 µL adrenaline at a concentration of 0.5 mg/L was determined to be $6.6 \cdot 10^{-2}$ mg/L (or $3.6 \cdot 10^{-4}$ mmol/L). Linearity and limit detection of sensor is shown in Fig. 6.

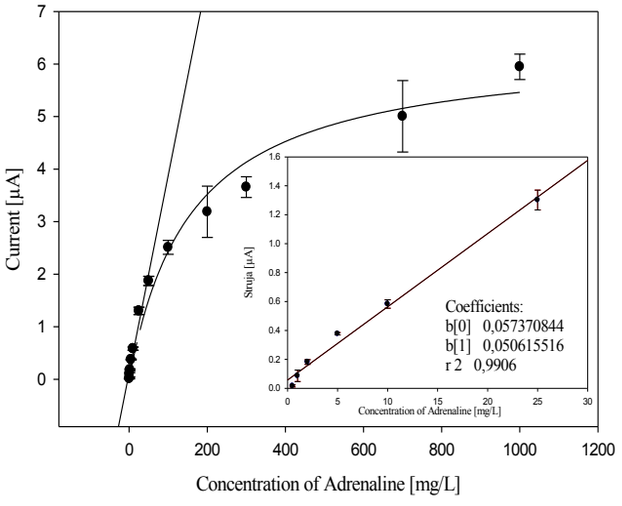

Fig. 5. Calibration curve for different concentrations of adrenaline (n=3). Electrode: Na[Ru(N-Ph-O-5-Br-salim)$_2$] modified carbon electrode, operating potential 100 mV vs. Ag/AgCl, flow rate, 0.4 mL/min, injection volume 100 µL, 0.1 M phosphate buffer pH 7.5.

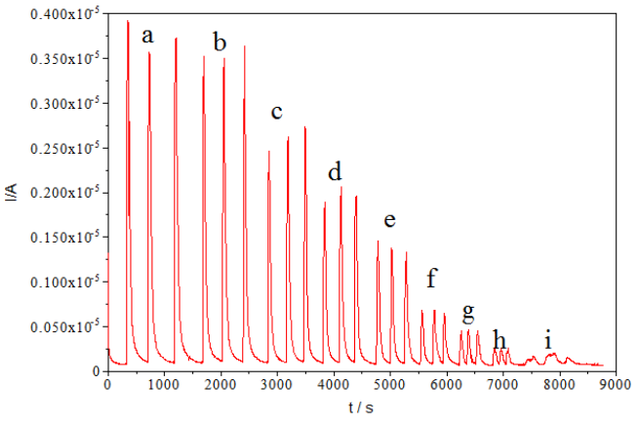

Fig. 6. Amperometric FI response of adrenaline with an Na[Ru(N-Ph-O-5-Br-salim)$_2$] carbon modified electrode. Concentration of adrenaline a) 300, b) 200, c) 100, d) 50, e) 25, f) 10, g) 5 and i) 1 mg/L adrenaline, operating potential 100 mV vs. Ag/AgCl, flow rate 0.4 mL/min, injection volume 100 µL, 0.1 M phosphate buffer pH 7.5.

IV. Conclusions

In the paper, a new amperometric sensor for adrenaline determination at physiological pH is reported. The surface modified glassy carbon electrode by stable ruthenium(III) complex, Sodium bis[N-2-oxyphenyl-5-bromosalicylideneiminato-*ONO*]ruthenate(III), showing fast current response, sensitivity and long-term stability is suitable for adrenaline determination in the range 0.5-25 mg/L. Further study will be focused on adrenaline determination in real samples, especially pharmaceutical products at higher pH values.

References

[1] J. B. Raoof, R.O, M. Baghayeri, A selective sensor based on a glassy carbon electrode modified with carbon nanotubes and ruthenium oxide/hexacyanoferrate film for simultaneous determination of ascorbic acid, epinephrine and uric acid, *Anal. Methods*, Volume: 3, 2011, pp 2367–2373.

[2] T. P. Huynh, K. C. C. Bikram, W. Lisowski, F. D'Souza, W.Kutner, Molecularly imprinted polymer of bis(2,2'-bithienyl)methanes for selective determination of adrenaline, *Bioelectrochemistry*, 2012, doi:10.1016/j.bioelechem.2012.07.003.

[3] I. M. Apetrei, D. Tutunaru, A. Nechita, C. Georgescu: Disposable amperometric biosensor for adrenaline detection, *Analele Universitati "Dunarea De Jos" Galati Medicina Fascicula XVII 2013*, No 1, 2013, pp 11-15.

[4] P. Solich, Ch. H. Polydorou, M. A. Koupparis, C. E. Efstathiou, Automated flow-injection spectrophotometric determination of catecholamines (epinephrine and isoproterenol) in pharmaceutical formulations based on ferrous complex formation, *Journal of Pharmaceutical and Biomedical Analysis*, Volume: 22, 2000, pp 781-789.

[5] J. Yang, G. Zhang, X. Wu, F. Huang, C. Lin, X. Cao, L. Sun, Y. Dinga, Fluorimetric determination of epinephrine with *o*-phenylenediamine, *Analytica Chimica Acta*, Volume: 363, 1998, pp 105-110.

[6] R. Baron, M. Zayatas, I. Willner, Dopamine-, L-DOPA-, adrenaline-, and noradrenaline-induced growth of Au nanoparticles: assays for the detection of neurotransmitters and of tyrosinase activity, *Anal. Chem.*, Volume: 77, Issue: 6, 2005, pp 1566-1571.

[7] C. Sabbioni, M. A. Saracino, R. Mandrioli, S. Pinzauti, S. Furlanetto, G. Gerra, M. A. Raggi, Simultaneous liquid chromatographic analysis of catecholamines and 4-hydroxy-3-methoxyphenylethylene glycol in human plasma. Comparison of amperometric and coulometric detection, *Journal of Chromatography A*, Volume: 1032, 2004, pp 65–71.

[8] P. Britz-Mckibbin, J. Wong, D. D. Y. Chen, Analysis of epinephrine from fifteen different dental anesthetic formulations by capillary electrophoresis, *J. Chromatogr. A*, Volume: 853, 1999, pp 535-540.

[9] J. Michalowski, P. Halaburda, Flow-injection chemiluminescence determination of epinephrine in pharmaceutical preparations using raw apple juice as enzyme source, *Talanta*, Volume: 55, 2001, pp 1165-1171.

[10] F. Li, H. Cui, X. Q. Lin, Determination of adrenaline by using inhibited $Ru(bpy)_3^{2+}$ electrochemiluminescence, *Anal. Chim. Acta*, Volume: 471,2002, pp 187-194.

[11] J. A. A. Ni, H. X. Ju, H. Y. Chen, D. Leech, Amperometric determination of epinephrine with an osmium complex and nafion double-layer membrane modified electrode, *Anal. Chim. Acta*, Volume: 378, 1999, pp 151-157.

[12] J. V. G. Mateo, A. Kojlo, Flow-injection biamperometric determination of epinephrine, *Journal of Pharmaceutical and Biomedical Analysis*, Volume: 15, 1997, pp 1821-1828.

[13] Z. Mo, X. Long, M. Zhang, Piezoelectric detection of ion pairs between sulphonate and catecholamines for flow injection analysis of pharmaceutical preparations, *Talanta*, Volume: 48, 1999, pp 643-648.

[14] E. Ozel, A. Hayat, S. Andreescu, Recent Developments in Electrochemical Sensors for the Detection of Neurotransmitters for Applications in Biomedicine, *Analytical Letters*, 2014, DOI: 10.1080/00032719.2014.976867.

[15] M. E. Ghica, C. M. A. Brett, Simple and efficient epinephrine sensor based on carbon nanotube modified carbon electrodes, *Analytical Letters*, Volume: 46, 2013, pp 1379-1393.

[16] H. Beitollahi, H. Karimi-Maleh, H. Khabazzadeh, Nanomolar and Selective Determination of Epinephrine in the Presence of Norepinephrine Using Carbon Paste Electrode Modified with Carbon Nanotubes and Novel 2-(4-Oxo-3-phenyl-3,4-dihydroquinazolinyl)-N '-phenyl-hydrazinecarbothioamide. *Anal. Chem.,* Volume: 80, Issue: 24, 2008, pp 9848-9851.

[17] X. Q. Lu, Y. Y. Li, J. Du, X. B. Zhou, Z. H. Xue, X. H. Liu, Z. H. Wang, A novel nanocomposites sensor for epinephrine detection in the presence of uric acids and ascorbic acids, *Electrochimica Acta,* Volume: 56, Issue: 21, 2011, pp 7261-7266.

[18] S. Kharian, N. Teymoori, M. A. Khalilzadeh, Multi-wall carbon nanotubes and TiO_2 as a sensor for electrocatalytic determination of epinephrine in the presence of p-chloranil as a mediator. *J. Solid State Electrochemistry,* Volume: 16, Issue: 2, 2012, pp 563-568.

[19] Emir Turkušić, *Uvod u hemijske senzore i biosenzore, Prirodno-matematički fakultet Univerziteta u Sarajevu*, 2012.

[20] W. Ren, H. Q. Luo, N. B. Li, Electrochemical behavior of epinephrine at a glassy carbon electrode modified by electrodeposited films of caffeic acid, *Sensors*, Volume: 6, 2006a, pp 80-89.

[21] Z. Y. Yu, X. C. Li, X. L. Wang, J. J. Li, K. W. Cao, Studies on the electrochemical behaviors of epinephrine at a poly(l-aspartic acid) modified glassy carbon electrode and its analytical application, *Int. J. Electrochem. Sci*., Volume: 6, 2011, pp 3890-3901.

[22] Y. Zhou, M. He, C. Huang, S. Dong, J. Zheng, A novel and simple biosensor based on poly(indoleacetic acid) film and its application for simultaneous electrochemical determination of dopamine and epinephrine in the presence of ascorbic acid, *J. Solid State Electrochem*., Volume: 16, 2012, pp 2203-2210.

[23] W. Ma, D. M. Sun, The electrochemical properties of dopamine, epinephrine and their simultaneous determination at a poly(L-methionine) modified electrode, *Russ. J. Electrochem*., Volume: 43, 2007, pp 1382-1389.

[24] M. Chen, X. Ma, X. Lin, Selective Determination of Epinephrine in the Presence of Ascorbic Acid and Dopamine Using a Glassy Carbon Electrode Modified with Valine, *International Journal of Chemistry,* Volume: 2, No 1, 2010, pp 206-211.

[25] X. Liu, D. Ye, L. Luo, Y. Ding, Y. Wang, Y. Chu, Highly sensitive determination of epinephrine by a MnO_2/Nafion modified glassy carbon electrode, *J. Electroanal. Chem*., Voume: 665, 2012, pp 1–5.

[26] E. Kahrović, A. Zahirović, E. Turkušić, Calf Thymus DNA Intercalation by Anionic Ru(III) Complexes Containing Tridentate Schiff Bases Derived from 5-X-Substituted Salicyladehyde and 2-Aminophenol, *J. Chem. Chem. Eng*., Volume: 8, 2014, pp 335-343.

[27] M. Aslanoglu, A. Kutluay, S. Karabulut, S. Abbasoglu, Voltammetric Determination of Adrenaline Using a Poly(1-Methylpyrrole) Modified Glassy Carbon Electrode, *Journal of the Chinese Chemical Society*, Volume: 55, 2008, pp 794-800.

[28] E. Turkušić, E. Kahrović, Development of new low potential amperometric sensor for L-cysteine based on carbon ink modification by Tetraethylamonium dichloro-bis[N-phenyl-5-bromosalicylideniminato-N,O]ruthenat(III), *Technics Technologies Education Management-TTEM*, Volume: 7/3, 2012, pp 1300-1303.

[29] E. Kahrović, E. Turkušić, New Ruthenium Complexes with Schiff Bases as Mediators for the Low Potential Amperometric Determination of Ascorbic Acid, Part II: Voltametric and Amperometric evidence of mediation with Bromo-derivative of Tetraethylamonium dichloro-bis[N-phenyl-5-halogeno-salicylideniminato-N,O]ruthenat(III), *HealthMED*, Volume: 6/3, 2012, pp 1046-1049.

[30] E. Kahrović, E. Turkušić, N. Ljubijankić S. Dehari, D. Dehari, and A. Bajsman, New Ruthenium Complexes with Schiff Bases as Mediators for the Low Potential Amperometric Determination of Ascorbic Acid, Part I: Voltametric and Amperometric evidence of mediation with Tetraethylamonium dichloro-bis[N-phenyl-5-chlorosalicylideniminato-N,O]ruthenat(III), *HealthMED*, Volume: 6/2, 2012, pp 699-702.

Bioelastična ekstramedularna koštana premosnica u lokomotornoj hirurgiji
Bioelastic extramedullary bone osteosynthesis in locomotor surgery

Zoran Hadžiahmetović [1], Narcisa Vavra Hadžiahmetović [2]

Klinički centar Univerziteta u Sarajevu, Sarajevo, Bosna i Hercegovina
[1] Institut za edukaciju, nauku i razvoj
[2] Klinika za fizikalnu medicinu i rehabilitaciju

Abstract— **The authors of this study will show experimental development, and then the clinical application of bioelastic extramedullary bone osteosynthesis (BEO). The main problem that has caused the work to develop BEO is the inability proper fixation of bones in small diaphysis in situations lack proclaimed osteosynthesis. In this respect, after the PC estimate material used basic task of experimental research, and it is determined that the reliability of the effect as BEO ekstramedulary binder in simple and complex fractures of small animals (13 dogs and 19 cats).**

By default the parameters of the research showed that a wide segment bioelastic BEO which is reflected in the prevention: shear, rotation, contraction and distraction.

The method is a new original surgical technique was introduced into clinical practice in 2006, dialed indication field. Final results compared with other alternative methods in favor of the application of BEO. Bypass has shown its strong foothold in strong comminuted fractures, interphalangeal and metacarpophalangeal necessary and arthrodesis with the installation of intercalary bone grafts bones of the hand with 12 applications (10 patients) at the Clinical Center University of Sarajevo in period 2007./2012.

Keywords— **bioelastic osteosynthesis, fractures, bone defects, arthrodesis**

I. UVOD

Osnovni problem u fiksaciji prijeloma malih kostiju u lokomotornoj hirurgiji jeste izbor adekvatne fiksacije. Ovo je posebno naglašeno kada se radi o defektima kostiju malih dijafiza.

Postavlja se pitanje koji koštani implantat, odnosno osteosintezu upotrijebiti ?.

Ukoliko se radi o maloj pločici sa vijcima često postoje problemi u smislu: neadekvatne (nedostatne) veličine, voluminoznosti, rigidnosti, korištenja specijalnog instrumentarija kao i visoke cjene implantata. Kada su u pitanju Kirschner igle (KI) i njihova intramedularna i/ili transkortikalna upotreba česte su infekcije oko igala, a i frekventan je gubitak fiksacije, lom, savijanje, migracija ili ispadanje. Vanjski fiksatori su ekstremno voluminozni, a njihova upotreba je vezana sa usko indikaciono područje. Oni također zahtjevaju specijalni instrumentarij i imaju visoku upotrebnu cijenu.

U cilju postizanja što boljeg elasticiteta kosti i širokog premoštavanja koštanog prijeloma prišlo se računarskom proračunu, odnosno pojedinačnom ispitivanju mehaničkog opterećenja jedne a zatim dvije Kirschner igle težine 12,0/24,0 g. dimenzija Ø 2,0 mm, L= 150 mm. Simulacijom se djelovalo silom Kg/N = 3/29,41, 5/49,03, 7/68.64. Ispitivala se deformacija na uvrtanje: statički momenat (M) Ncm i ostvareni ugao (α^0), kao i deformacija na savijanje bez uzdužne sile (KI/mm). Aksijalno opterećenje (kompresija-distrakcija) KI, kao i rigidnost odnosno elasticitet strukturne interkonekcije modela nisu mjereni jer su bili u koliziji sa specifičnostima eksperimentalnog ispitivanja. Utvrđeno je da je deformacija najmanja na uvrtanje kao i savijanje prilikom formiranja strukturnog bindera koji se sastoji od dvije KI uzdužno raspoređene pod uglom od 54^0 sa četiri serklažne žice na dva nivoa u svakom glavnom fragmentu kosti (1).

Ova simulacija je bila osnov za eksperimentalno istraživanje elastičnog koštano žičanog kompleksa na kostima malih životinja (psi i mačke). U tu svrhu inicijalno u tri slučaja prišlo se primjeni istovremenog intramedularnog i ekstramedularnog premoštavanja prijeloma sa KI i serklažom. Dalji cilj istraživanja je bio sa se utvrdi čvrstoća spoja dvije međusobno povezane KI i serklaže kroz rutinske procedure samo u ekstramedularnoj varijanti bez dodatne intramedularne potpore kod jednostavnih i kompleksnih prijeloma.

Nakon krajnje povoljnih početnih rezultata dalja aplikacija je bila isključivo ekstramedularna i nazvana je *Ekstramedularna Fiksacija Kiršner iglama i Serklažom (EFIKS).* Animalno istraživanje je provedeno u periodu 2001./2005. godina. U Kantonalnoj veterinarskoj stanici u Sarajevu u tom periodu operirano je 13 pasa i 19 mačaka sa prijelomima kostiju ekstremiteta nastalih u traumi. Praćeni su: cijeljenje prijeloma (radiografski), fiksacija implantata

(odnos alenteza – kost – meka tkiva), razvoj infekcije, nastanak deformiteta, zglobne kretnje i svakodnevne aktivnosti životinje (Slika 1.). Utvrđeno je da je EFIKS: čvrsta frakturna premosnica i kod nestabilnih prijeloma, ima širok segmentni bioelasticitet, dobro prevenira rotaciju, strig, angulaciju i distrakciju, dobro adaptira prijelomne okrajake i izuzetno je jeftina. Također evidentiran je i visoki stepen *bioelastičnosti osteosinteze (BEO),* odnosno direktna korelativnost bioelasticiteta sa uspostavljenim balansom između: koštanog kontakta, veličine kosti i dimenzije - pozicije implantata (1).

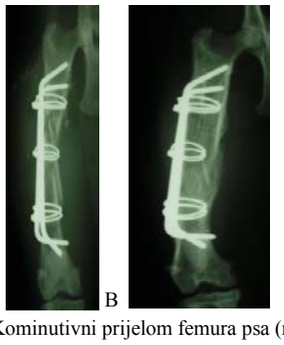

A B

Slika 1. Kominutivni prijelom femura psa (rtg.)

A. BEO nakon operativnog zahvata
B. BEO sanirani prijelom (2 mjeseca poslije operacije)

Metoda je kao originalna *(sec.Hadžiahmetović)* uvedena u rutinsku kliničku primjenu za operativnu fiksaciju prijeloma metakarpalnih kostiju i falangi na Klinikama za plastičnu i rekonstruktivnu hirurgiju i Urgentnu medicinu Kliničkog centra Univerziteta u Sarajevu 2006. godine (2,3,4,5).

Slijedeći navedene rezultate u tretmanu prijeloma u daljem razvoju premosnice postavljen je novi cilj istraživanja, a to je utvrditi:

- Kakva je primjenjivost BEO u stabilizaciji interkalarnog (uni/bi/trikortikalnog i cilindričnog) koštanog presadaka kod koštanih defekata falangi i metakarpalnih kostiju šake,
- U kom smislu je BEO na širokoj osnovi ravnomjernija i daje bolje biomehaničko uporište unutar koštane fuzije (artrodeze) te koliko je pouzdanija u odnosu na intramedularnu fiksaciju sa KI
- Da li je stabilizacija i konačna fuzija interkalarnog presatka u direktnoj korelaciji sa izborom implantata (6,7).

II. MATERIJAL I METODE

U periodu 2007.-2012. godina na Klinikama za plastičnu i rekonstruktivnu hirurgiju i Urgentnu medicinu KCUS operisano je 10 pacijenata sa koštanim defektima falangi i metakarpalnih kostiju. U svim slučajevima se radilo o traumatskom substratu, osim kod dva defekta koji su nastali nakon ekstripacije tumora, odnosno koštane ciste (Tabela 1.)

Tabela 1.

Br/Ost	Trauma/Tumor/ Cista	Artrodeza	Koštani presadak
1/1.	Phal.prox.pollicis (osteid osteoma)	MTCP + IP	Ilijačni (3 kortikalni)
2/2.*	Phal.prox.dig.IV, V (trauma)	MTCP + PIP	½+½ II metakarpala (cilindrični)
3/1.	Phal.med.dig.III (cista)	PIP	Slobodna fibula (cilindrični)
4/1.*	Phal.dist.indicis (trauma)	DIP	Ilijačni (kortikospongiozni)
5/1.*	Phal.prox.indicis (trauma)	MTCP + PIP	Ilijačni (2 kortikalni)
2/1.	Metacarpal.V (trauma)		Slobodna fibula (cilindrični)
6,7/2.	Phal.med.dig.IV (trauma)	PIP + DIP	Ilijačni (kortikospongiozni)
8/1.*	Metacarpal. III (trauma)		Radijalni (kortikospongiozni)
9,10/2.	Phal.med. dig. III (trauma)	PIP + DIP	Ilijačni (kortikospongiozni)

*1 dvostruki defekt falange, 4 otvoreni defekt **

Defekti su bili prosječne veličine 2,8 cm /1,5-3,2 cm/. Svi operativni zahvati su učinjeni naknadno, prosječno nakon 5 dana kod traumatskih defekata. Odnos muškaraca i žena je bio 7:3. Prosječna životna dob ispitanika iznosila je 29 godina.

Vrijeme praćenja je bilo od 3 do 6 mjeseci od operativnog zahvata.

Zadani parametri istraživanja su bili: radiografski (koštana konsolidacija, pozicija interkalarnog presatka, kolaps, resorpcija, skraćenje, rotacija prsta, infekcija kosti), funkcionalno (hvat šake-GMS, kretnje u susjednim zglobovima, ASŽ), strukturna stabilnost (pozicija svih sastavnica BEO i njen odnos sa koštanim presatkom).

III REZULTATI

Radiografski kod svih pacijenata je utvrđena potpuna fuzija od 6 do 16 sedmice bez skraćenja, resorpcije, rotacije presadka ili prsta.

Niti kod jednog pacijenta nije zabilježen postoperativni koštani infekt /kod 5 pacijenata je učinjena primarna hirurška obrada defekta i mekih tkiva. Ordinirana su antibiotika pre i postoperativno prema antibiogramu/.

Funkcionalnost šake u smislu grube motorne snage (GMS) uspostavljena je do 20 sedmice kod svih pacijenata a aktivnosti svakodnevnog života (ASŽ) kod 7 pacijenata nakon 16 sedmice.

Strukturna stabilnost svih BEO bila je uredna u posmatranom periodu.

Slika 2.

Aneurizmatska koštana cista srednje falange III prsta šake (rtg.)
Substitucija falange fibula graftom. BEO, ukočenje PIP i DIP zgloba tranzitorno - operacija 2007. godina

Slika 2 a.

Isti pacijent. Potpuna fuzija grafta na III prstu šake (rtg.)
Funkcionalna šaka - 2015. godina

IV DISKUSIJA

Rezultati istraživanja upoređeni su sa rezultatima koji su ostvarili Sabapathy i saradnici koji su fiksaciju interkalarnog presadka pokušali postići samo sa KI kod 15 pacijenata i 20 koštanih isključivo traumatskih defekata falangi. Imali su 6 dvostrukih defekata falangi i 7 otvorenih defekata veličine prosječno 3,3 cm /2,5 - 5,0 cm/ (8). Parametri istraživanja bili su identični. Operativni zahvati su provedeni također naknadno.

Radiografski je evidentirano da su imali: 16 fuzija presadaka u 6 sedmici, dva gubitka dužine za 15 i 20 % presadka kao rezultat resorpcije kosti, jednu pseudoartrozu /pokret 0 – 40 ° sa prihvatljivom stabilnosti/, jednu infekciju sa razvojem osteomijelitisa gdje se morala učiniti ekstrakcija presadka nakon 3 mjeseca.

Funkcionalnost šake je uspostavljena u smislu GMS i ASŽ nakon 16 sedmice.

Strukturna stabilnost nije uspostavljena kod 3 pacijenta kod kojih je evidentirana nedostatna stabilizacija presadka.

Definitivno kod 15% pacijenata ispitivane grupe evidentiran je loš izbor osteosintetskog materijala (implantata) što je doveo do poremećene koštane fuzije (8).

V ZAKLJUČAK

Kreirana BEO pokazala je svoje uporište kao metod izbora u stabilizaciji koštanih presadaka falangi i metakarpalnih kostiju šake kao i jednostavnih i kompleksnih dijafizarnih prijeloma kratkih, srednjih kostiju posebno nenosećih ekstremiteta.

Jednostavna je za provođenje. Dovoljno je elastična da ne stvara velike rigidne dijafizarne koštane segmente.

Jeftino zadovoljava sve savremene principe „biološke fiksacije“ prijeloma i osim serklažnog operativnog seta ne zahtijeva nabavku specijalnog instrumentarija.

U pojedinim situacijama potrebno je prevenirati fenomen poluge kosti, posebno kada je koštani defekt ili prijelomna linija izvan srednjeg dijafizarnog segmenta ili u situaciji loše kontaktne potpore. Ovo može inicirati i potrebu dodatnog korištenja serklažnih žica.Također redukcija mikrokretnji može se ostvariti povećanjem broja i debljine

KI, pogotovo ukoliko se očekuju snažnije mišićne aktivnosti.

REFERENCE

1. Hadžiahmetović Z. Krasni J. Osteosinteza tehnikom ekstramedularne fiksacije prijeloma Kirschner iglama i serklažom (EFIKS), Tr.Glas, 2006 ; 4 (3) : 27 – 30

2. Hadžiahmetovi Z. Uvođenje novih dijagnostičkih i/ili terapeutskih procedura, Info bilten , KCUS, 2006: (9 -10) : 19

3. Hadžiahmetović Z. Početna klinička iskustva u liječenju dijafizarnih prijeloma malih kostiju tehnikom originalne ekstramedularne osteosinteze, Med.Arh.; 2006, 60 (6) Supl.1: 9 – 12

4. Hadžiahmetović Z., Vavra – Hadžiahmetović N. Effects of Specific Forms of Extramedullary Fixation in Treatment of Diaphyseal Small Bone Fractures, HealthMED, 2008 ; 2 (4) ; 219 – 24

5. Hadžiahmetović Z. Operativno liječenje prijeloma koštanih defekata originalnom ekstramedularnom osteosintetskom premosnicom, Club M informator, 2012 : 4 (16) : 64-66

6. Hadžiahmetović Z. Biological extramedullary elastic osteosynthesis as a method of choice in the replacement of the hand bone defect with intercalated bone grafts, Folia Medica, 2012 ; 47 ; (2 suppl) : 18

7. Hadžiahmetović Z. Izbor osteosinteze pri nadomještanju koštanih defekata falangi šake autolognim interkalarnim presadcima, RADOVI Hrvatskog društva za znanost i umjetnost, XII-XIII, 2010./2011. : 80 – 187

8. Sabapathy SR, Venkatramani H, Giesen T, Ullah AS Primary bone grafting with pedicled flap cover for dorsal combined injuries of the digits,The Journal of Hand Surgery (European Volume, 2008) 33E: 1: 65–70

Adresa za korespondenciju:

Prof. dr .sc. Zoran Hadžiahmetović, Institut za naučnoistraživački rad i razvoj, Klinički centar Univerziteta u Sarajevu, 71000 Sarajevo, Bolnička 25, BiH (tel. 387-61-209-341; e-mail: h.vemi@bih.net.ba).

Patient Controlled Privacy and Encryption as a mean for more secure Electronic Health Records (EHR's)

Nihad Omerbegović[1]

[1] Faculty of Engineering and Information Technologies, International Burch University Sarajevo, Francuske Revolucije bb, 71000 Sarajevo, Bosnia and Herzegovina
{nihad.omerbegovic}@gmail.com

Abstract— **In this paper, some challenges of securing patient privacy in electronic health records will be discussed. We also argue that security in such systems should be enabled by encryption as well as access control. Furthermore, we argue for approaches that enable patients to generate and store encryption keys, so that the patient privacy is protected should the host data center be compromised. The main argument against such an approach is that encryption would interfere with the functionality of the system.**

Keywords— **Patient privacy, Security, Access Control, Electronic health record**

I. Introduction

The medical record, either paper-based or electronic, is a communication tool that supports clinical decision making and coordination of services, increases efficiency of care and improves scientific research. The documentation must be authenticated and, if it is handwritten, the entries must be legible.

Justices Warren and Brandeis define privacy as the right "to be let alone" [1]. According to Richard Rognehaugh, it is "the right of individuals to keep information about themselves from being disclosed to others; the claim of individuals to be let alone, from surveillance or interference from other individuals, organizations or the government" [2]. The information that is shared as a result of a clinical treatment is considered *confidential* and therefore must be protected [3]. The information can take various forms (including identification data, diagnoses, treatment, and laboratory results) and can be stored in multiple media (e.g., paper, video format, electronic files). Information from which the identity of the patient cannot be ascertained – for example, the number of patients with lung cancer in a given hospital – is not in this category.

The primary method of guaranteeing privacy in today's electronic systems is access control. In a system which relies only on access control, the servers that store data run an access control program, which verifies that any party accessing a patient's healthcare record has appropriate permissions. These access control systems keep a log of all accesses, providing communications that are securely encrypted. Although this has been a fairly effective approach, patients must trust the third party who is storing their data in their private health record.

Electronic medical records are open to potential abuses and threats. Some have pointed out that large amounts of sensitive healthcare information held in data centers is vulnerable to loss, leakage, or theft [4]. "In the last few years, personal health information on hundreds of thousands of people has been compromised because of security lapses at hospitals, insurance companies and government agencies" [5]. Privacy of information collected during health care processes is necessary because of significant economic, psychological, and social harm that can come to individuals when personal health information is disclosed [6]. Medical data is also misused by those who want to profit from it. For example, some companies make a business of buying and selling doctors' prescribing habits to pharmaceutical companies.

Businesses such as hospitals and law firms, which are required by law to respect users' privacy, "may be at risk of a lawsuit simply for using a cloud computing service, even if information is not leaked" [7].

Related Work

While reviewing related work, I noticed that hierarchical access control via encryption is not a new idea. Akl and Taylor [8] and later Sadhu [9] proposed constructions based on one-way functions which are very similar to what is described in Section 4.2. More recently, Hengartner and Steenkiste proposed a scheme for encryption-based access control based on hierarchical IBE [10]. Atallah et al presented a symmetric key scheme which allows not only for tree-based hierarchies, but also for arbitrary acyclic graphs [11]. Finally, recent work on attribute- based encryption [12, 13] enables encryption-based access control with more expressive policies; however it is not known how

to incorporate searchability in these schemes, so we will not discuss them here.

II. Patient Controlled Encription (PCE)

2.1 Goals of PCE

In an electronic health record, patients and healthcare providers can upload health data via medical devices and web applications. This data can be viewed or used later on. Also, patients may delegate access rights and allow family, friends, and specific healthcare providers to view or to edit parts of their record. Patients and their delegates may also want to efficiently perform searches over part or all of the record.

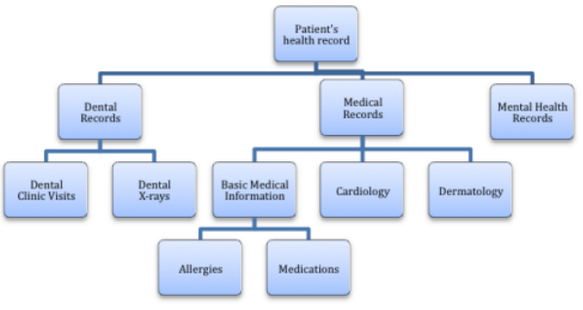

Fig. 1. A hierarchical health record

Let us consider the challenges that occur in a typical attempt to add security to such a system. How can patient allow others to access his record? Clearly he does not want to give out his entire decryption key, as that would allow the third party to read and modify his record or some parts of it. Let me now describe the PCE proposal. At a high level, a system using PCE allows the patient to use his decryption key to generate subkeys which will allow his delegates to search and access only certain parts of his record.
The goals of PCE are to:

Guarantee Strong Security In particular, PCE will:

1. Guarantee the patient's privacy: the patient should be confident that the administrators of the health data server will not learn anything about the patient's record, except the trivial information like the existence and size of the record.
2. Guarantee security in the case of server compromise: even if the server is compromised or stolen, the patient should be certain that his data has not been leaked, and
3. Guarantee correctness of the health record.

Maintain Functionality We want to maintain the above security without compromising the functionality of the server. This means the system should guarantee the following:

1. Efficient access to patient health records,
2. Easy sharing of parts of the record, and
3. Efficient searching over records.

2.2 Patient Health Structures

We assume that a patient's record is organized into a hierarchical data structure. There are multiple ways to decompose medical data into a hierarchical representation based on the use of different ontologies [14].
For example, a record may be decomposed at the top level into a set of mutually exclusive categories such as dental records, medical records, mental health data, and a category representing the set of all lab results obtained by the patient. The medical records category might be further broken down into subcategories for basic medical information (containing such subcategories as prescribed medications and known allergies), cardiologic data, dermatologic data, etc.

The key design criterion for PCE is that patients should be able to delegate access to any subset of these categories to their doctor, dentist, pharmacist, spouse, etc. We can notice that while a patient might wish to share his entire record with his doctor, he might not want to allow pharmacists, billing staff, or lab technicians to see any more information than is necessary. Thus, we propose a system in which a patient can grant access to specific potions of the data. As described above, the patient will generate and store his own secret key, which we will call the root key. Then he can use this root key to generate sub keys for various categories or subcategories. Data in each subcategory will be encrypted under the corresponding sub key. To delegate rights to read a particular category, he will generate the corresponding sub key, and send it to her doctor, dentist, etc.

Let us now consider the sample hierarchy displayed in Figure 1. Here, the patient might decide to grant his dentist access to both the "Dental Records" category and the "Basic Medical Info" category. This would allow the dentist to read all data concerning dental clinic visits, dental x-rays, allergies, and medications. However, the dentist would have no way of decrypting any of the information in the patient's mental health records, or his cardiologic data. Note that the server that stores the health information will not have access to the secret key, or any of the sub keys given to the doctor, and thus will be unable to decrypt any of the data. One advantage of a hierarchical structure is that it is easily extendable, where the patient (and potentially other parties to whom the patient grants the appropriate permissions) can add additional subcategories within any existing category.

Advantages The patient can easily give access to a category, without knowing all the types of files that might be included in it. Similarly, doctors can add subcategories with arbitrary names, without patient assistance. This will be particularly useful if we can't predict the names of all possible subcategories, i.e., if a doctor needs to add a category for a new type of test, or if categories are labeled by visiting dates.

Disadvantages The hierarchy is fixed so that there is only one way in which we can partition the record. If we want to give out access rights based on something else (e.g. based on document type or sensitivity of data) we will have to look at all the low-level categories involved, and give a separate decryption key for each. (in our example, giving a lab access to all X-rays would require giving separate keys for "Dental X-rays", "Cardiologic X-rays", and "Mental Health X-rays"). This problem might be partially avoided if we have several fixed hierarchies, and we encrypt each file under each hierarchy.

2.3 Preliminaries

Before we describe our proposal in more detail, we will make the following assumptions about the format of the patient's record. We assume that the patient's record is stored as a collection of entries, where each entry contains the name of a file, the name of the smallest category containing that file, a "locator tag" which the patient can use to refer to the file, and an encrypted version of the file itself. Some terminology that we will use later: For a hierarchical representation of data, we say that a given category cat_1 is an ancestor of another category cat_2 if cat_2 is contained within cat_1. For example, in Figure 1, "Medical Records" is an ancestor of "Allergies". We call a category a leaf category if it does not contain any other category. In Figure 1, "Dental Clinic Visits", "Dental X-Rays", "Allergies" etc. are all leaf categories. We sometimes refer to the name of a category as its label. We also give some notation: We will use $cat\ (i_1,..,i_n)$ to specify a category in our hierarchy, where (i_1) specifies that top level ancestor of the category, (i_1, i_2) specifies the next ancestor down the chain, and so on. For example, for the hierarchy in Figure 1, the "Allergies" category would be specified by $cat_{(MedicalRecords,BasicMedicalInformation,Allergies)}$ In a similar way, we will use $sk\ (i_1,..,i_n)$ to represent the decryption key for category $cat\ (i_1,..,i_n)$.

2.3 Basic PCE

We described the high level functionality of our PCE system. Let us now give a more formal description of the required properties. PCE system consists of four algorithms:

• A key generation algorithm **`PCEKeyGen`** which generates a root secret key and (in a public key system) public key for the patient.

• A key derivation algorithm **`PCEKeyDer`** which takes a secret key for a category, and the name of one of its subcategories, and generates the secret key for that subcategory.

• An encryption algorithm **`Enc`** which takes a public key and/or a secret key for a category, the name of that category, and a file, and encrypts that file for that category.

• A decryption algorithm **`Dec`** which takes the name of a category and the secret key for that category, and a cipher text encrypted for that category, and produces the decrypted file.

Two important properties that are required are *Correctness*, which means that any successfully encrypted document will be correctly decrypted given the appropriate decryption key, and *Security*, which says that an encryption of a document in a given category will not reveal information about that document as long as an adversary has not been given the decryption key for an ancestor category, even if he obtains many other decryption keys for other categories, and has access to encryption and decryption for all categories.

Thus, the health data server will store only encrypted files. When a patient wishes to grant access to a category to his doctor, he will run **`PCEKeyDer`** to generate the appropriate subkey and send it to the doctor. Then the doctor can retrieve all the encrypted files of that category from the server and decrypt them using this subkey.

III. WORK FLOW IN PRACTISE

Let us describe an instantiation of PCE. We will consider interactions between a patient Bill, his doctor Nadine, and the server which stores Bill's health records.

Creating User Accounts When patient Bill wants to sign up for an account, he needs to register as he would in any traditional EMR system. He connects to the server (via an SSL secure connection) and generates an account username and password that will be used in the future to identify his account and to authenticate to the server. Then, an application will be downloaded to his machine. This application will run locally and will perform the following tasks: first it will generate a public key pair *(pk B, sk B)*, which will be used to secure communications with other parties in the system. Then it will generate a root secret key *sk R* under which all Bill's health records will be encrypted. Finally, it will upload (via SSL) the public key *pk B*, which will be stored as part of Bill's health record. The *sk B* and *sk R* will be stored locally on Bill's machine.

At this point Bill can be offered the opportunity to upload some basic information such as birthdate, gender, height, etc. Bill will enter this information into the application. The application, which runs locally, derives the appropriate subkeys and from `sk R`, and choose random locator tags for each file. It uses the subkeys to encrypt Bill's information, and generate an encrypted index. It also uses the subkeys to generate the encrypted dictionary entry for each (file name, category name, locator tag). Finally, it will send the tags and the encrypted information and encrypted index to the server (via SSL). The server will store each encrypted file and encrypted index labeled by the corresponding tag.

Creating Provider Accounts When a provider organization wants to sign up for an account, it will register as in a traditional EMR system: customer will connect to the server via an SSL connection and establish an account username and credentials, which will be used in the future to identify the account and to authenticate to the server. A large organization can also have the opportunity to dynamically upload public keys corresponding to different parties within its staff.

Before an Appointment When Bill makes an appointment to see his provider, they exchange user names. If the provider is a large organization, Bill may also learn the identifier for the specific doctor he will be seeing.

Next, the doctor requests access to any necessary information as follows: The doctor logs in to the health server and enters Bill's user name, and her application downloads Bill's public key. Then the doctor encrypts the request for information under Bill's public key and upload the result to the server. Bill logs in to the server and his application downloads and decrypts this request and then presents it to him along with the doctor's username (and identifier). It also downloads the doctor's public key. If Bill agrees to allow access to the requested information, the application uses his root key `sk R` to locally generate subkeys for the appropriate categories. It encrypts these under the doctor's public key, and uploads them to the server. The doctor logs in to the server, and her application downloads the encrypted subkeys and then decrypts them. It also downloads the patient encrypted directory, and using the subkeys it decrypts the (file name, category name, locator tag) tuples for all the files that the doctor has access to. It presents these file names to the doctor (organized using the category names), who then selects the categories or individual files she wants to download. The application sends the corresponding locator tags to the server, and obtains the associated encrypted files. Finally, it decrypts the received files using the previously decrypted subkeys, and displays them to the doctor. When the doctor is done accessing this record, the application deletes all subkeys. (They can be retrieved again from the server when they are needed). The key idea of this approach is to avoid the use of e.g. smartcards as a direct input for encrypting and decrypting EHRs. In this example, before medical data is to be stored on an EHR server, the patient provides his smartcard only to generate a transaction code (TAC) which will be used as authorization secret. The encryption key is only based on the TAC and the patient's identity. When the EHR is to be read again, the patient gives the TAC to the health professional who needs to access the EHR. The novelty in this approach is that patients do not need to be present with their smartcards for decryption, but can provide the TAC via, e.g., phone.
This idea is illustrated in Figure 2 [15].

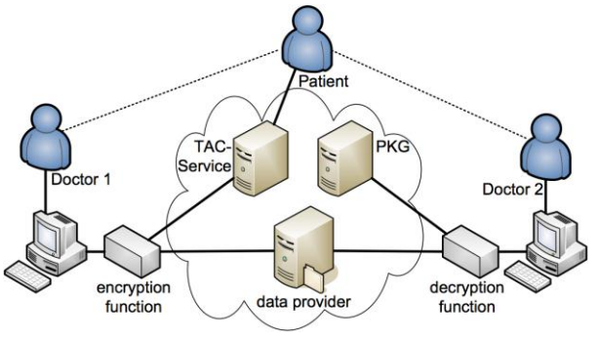

Fig. 2. Flexible security infrastructure for EHRs

After an appointment The doctor can request permissions to read and write additional categories. When the doctor wants to upload data to Bill's health record, she logs in to the health server. Her application downloads the necessary encrypted subkeys from the server. If no such keys have been uploaded, she requests them from patient Bill. The application decrypts the necessary subkeys, encrypts the data under those subkeys, and generates a corresponding encrypted index. For each file it also chooses a random locator tag and generates an encrypted directory entry. Finally, the application uploads the encrypted data, the encrypted index, the locator tag, and the directory entry for each file. When the doctor is done accessing this record, the application deletes all subkeys (they can be retrieved again from the server when they are needed).

IV. BUILDING PCE

4.1 Solution 1: Public Key PCE

So, how do we build a PCE? Here we show a construction that satisfies the properties in section 2, and that allows for public key encryption. In our basic scheme we need the following four algorithms:

• A key generation algorithm **PCEKeyGen**(1^k) → (PK_{root}, SK_{root}) which takes as input the security parameter k and generates a root decryption key SK_{root} and a public key PK_{root} for the patient's record.

• The key derivation algorithm **PCEKeyDer**($sk_{(i1,...,in-1)}$, (i_1,.., i_n)) → $sk_{(i1,...,in)}$ takes as input the name of a category (specified as a hierarchical list (i_1,..., i_n)), and the decryption key $sk_{(i1,...,in-1)}$ for the parent category $cat_{(i1,...,in-1)}$ (or SK_{root} for $n = 1$). It outputs a decryption key $sk_{(i1,..,in)}$ for category cat (i_1,...,i_n).

• The encryption algorithm **Enc** (PK_{root},(i_1, ...,i_n), m) → c takes as input a public key and a category specified as a list (i_1...,i_n) and a message m. It outputs an encryption of m for category $cat_{(i1,..,in)}$.

• The decryption algorithm **Dec** ($sk_{(i1,..,in)}$, c) → m takes as input a category name (i_1,...,i_n), a corresponding decryption key $sk_{(i1,...,in)}$ and a ciphertext c. It outputs decrypted message m if if the ciphertext was formed correctly for category $cat_{(i1,..,in)}$.

4.1.1 Basic Approach

A basic solution in this case is to use a CCA-secure Hierarchical Identity Based Encryption (HIBE) scheme. Shamir [16] proposed the concept of IBE as an encryption scheme in which any string (e.g. a name or email address) could be used as a public key. In the traditional IBE setting, there would also be a trusted authority who would issue the corresponding decryption key to the appropriate parties. HIBE, introduced by Gentry and Silverberg [17], allows for hierarchical identities: an encryptor encrypts a message using a list of strings id_1,...,id_L, and a party who had obtained the decryption key for id_1 could then delegate a key for id_1, id_2 for any string id_2, and so on.

The key innovation with the hierarchical structuring in PCE is that the patient plays the role of the trusted party. We replace the "identities" with the categories in hierarchical health record. Thus, in order to delegate access rights for a given category, the patient will generate the appropriate HIBE decryption key using that category as the identity and give the resulting key to the doctor, or friend, or family member.

Thus, we assume we are given a CCA secure HIBE scheme consisting of algorithms **HIBESetup**(1^k), which generates parameters **params** and a master secret key **mk** for the authority, **HIBEKeyGen**($sk_{(id1...,idn-1)}$, (id_1..., id_n)), which uses decryption key $sk_{(id1..., idn-1)}$ to generate decryption key $sk(id_{1...,}id_n)$, **HIBEEnc**(m, params, (id_1,...,id_n)), which encrypts a message m to identity (id_1,...,id_n), and **HIBEDec**(c, $sk_{(id1,...,idn)}$, (id_1,..,id_n)), which uses decryption key $sk(id_1,...,id_n)$ to decrypt a ciphertext intended for identity (id_1,...,id_n).

We build a PCE scheme as follows:

PCEKeyGen(1^k): Run **HIBESetup**(1^k) to obtain *params*, *mk*.

Output: PK_{root} = *params*, SK_{root} = *mk*.

PCEKeyDer($sk_{(i,...,in-1)}$, (i_1,..i_n)): Run **HIBEKeyGen**($sk_{(i1,...,in-1)}$, (i_1,...,i_n)) and output the resulting $sk_{(i1,...,in)}$.

Enc(PK_{root} , (i_1,.. i_n), m): Run **HIBEEnc**(m, PK_{root} , (i_1,...,i_n)), and output the resulting ciphertext c.

Dec($sk_{(i1,...,in)}$, (i_1,...,i_n); c): Run **HIBEDec**(c, $sk_{(i1,...,in)}$, (i_1,... i_n)), and output the resulting message m.

Security The security properties of PCE follow directly from the security properties of the underlying HIBE.

4.2 Solution 2: Symmetric key PCE

Here we show a construction for a similar, hierarchical set of categories, but which only allows for secret key encryption. The result is a construction built primarily from simple symmetric key primitives, which is much more efficient than the previous solution, but it does not allow public key encryption.

In our basic scheme we need the following four algorithms:

- The key generation algorithm **PCEKeyGen**(1^k) → SK_{root} which takes as input the security parameter k and generates a root decryption key for the patient SK_{root} .
- The key derivation algorithm **PCEKeyDer**($sk_{(i1,...,in-1)}$, (i_1,.., i_n)) → $sk(i_1,...,i_{n-1})$ takes as input the name of a category (specified as a hierarchical list (i_1,..., i_n)), and the decryption key $sk_{(i1,...in-1)}$ for the parent category $cat_{(i1,...,in-1)}$ (or SK_{root} for $n = 1$). It outputs a decryption key $sk_{(i1,...,in)}$ for category $cat_{(i1,...,in)}$.
- The encryption algorithm **Enc**($sk_{(i1,...,in)}$, (i_1,...,i_n), m) → c takes as input a public key, a message m, a category name specified as (i_1,...,i_n) and the corresponding decryption key $sk_{(i1,...,in)}$. It outputs an encryption of m for category $cat_{(i1,...,in)}$.
- A decryption algorithm **Dec**($sk_{(i1,...,in)}$, (i_1,...,i_n), c) → m takes as input the name of a category (i_1,..., i_n), a corresponding decryption key $sk_{(i1,...,in)}$ and a ciphertext c. It outputs decrypted message m if the ciphertext was formed correctly for category $cat_{(i1,...,in)}$.

4.2.1 Basic Approach

We will construct our PCE system from a pseudorandom function (or a keyed block cipher) $F : \{0,1\}^{s(k)} \times \{0,1\}^{p(k)} \rightarrow$

$\{0,1\}^{p(k)}$ for some polynomials s, p, and a CCA-secure encryption scheme, (**CCAEnc**, **CCADec**), with a keyspace $\{0,1\}^{p(k)}$.

PCEKeyGen(1^k): Choose $SK_{root} \rightarrow \{0,1\}^{p(k)}$.

PCEKeyDer($sk_{(i,...,in-1)}$, $(i_1,...,i_n)$): Compute and output $sk_{(i1,...,in)} = F\ sk_{(i1,...,in-1)}\ (i_n)$.

Enc($sk_{(i1,...,in)}$, $(i_1,..., i_n)$, m): Compute and output $c =$ **CCAEnc**($sk_{(i1,...,in)}$, m).

Dec($sk_{(i1,...,in)}$, $(i_1,...,i_n)$, c): Compute and output $m =$ **CCADec**($sk_{(i1,...,in)}$, c).

Security The security of the scheme can be trivially derived from the pseudorandom properties of the PRF and the CCA security of the encryption. Note also that we only encrypt files in leaf categories, so each key is used either for delegation or for encryption, but not for both.

Table 1. Properties of the schemes presented in Section 4.

Properties	Public Key PCE Sec 4.1	Symmetric Key PCE Sec 4.2
Upload without Key Distribution	Yes	No
Flexible Hierarchies	No	No
High Efficiency	No	Yes
Easy to Add Categories	Yes	Yes

V. CONCLUSIONS

Existing approaches to protect the privacy of EHRs are either insufficient with respect to strict privacy laws or they are too restrictive in their usage. For example, smartcard-based encryption systems require the patient to be always present to authorize access to medical records. In our approach, we propose a security architecture for EHR infrastructures that provides more flexibility but retains the security of patient-controlled encryption.

We have presented basic schemes for Patient Controlled Encryption, each appropriate for a different setting. Some of the more complex schemes can be part of the future work. Table 1 summarizes the advantages and disadvantages of these basic schemes. For a concrete design, we suggest to follow the set-up described in Section 3. We also concluded that it is possible and practical to achieve secure and protected EMR's while maintaining efficiency and functionality at the same time.

REFERENCES

1. Warren SD, Brandeis LD. The right to privacy. *Harvard Law Rev*. 1890;4:193.
2. Rognehaugh R. *The Health Information Technology Dictionary*. Gaithersburg, MD: Aspen; 1999:125.
3. Rinehart-Thompson LA, Harman LB. Privacy and confidentiality. In: Harman LB, ed. *Ethical Challenges in the Management of Health Information*. 2nd ed. Sudbury, MA: Jones and Bartlett; 2006:53.
4. M. Eric Johnson, Data Hemorrhages in the Health-Care Sector. Forthcoming in Financial Cryptography and Data Security, February 22-25, 2009.
5. Robert Pear. "Privacy Issue", New York Times, January 17, 2009.
6. Gostin LO, Turek-Brezina J, Powers M, Kozloff R, Faden R, Steinauer DD. Privacy and security of personal information in a new health care system. JAMA. 1993;270:2487-93.
7. Saul Hansell. "Does Cloud Computing Mean More Risks to Privacy?", New York Times, February 23, 2009.
8. Selim G. Akl and Peter D. Taylor. Cryptographic solution to a problem of access control in a hierarchy. ACM Trans. Comput. Syst., 1(3):239-248, 1983.
9. Ravi S. Sandhu. Cryptographic implementation of a tree hierarchy for access control. Inf. Process. Lett., 27(2):95-98, 1988.
10. Urs Hengartner and Peter Steenkiste. Exploiting hierarchical identity-based encryption for access control to pervasive computing information. In *SECURECOMM '05: Proceedings of the First International Conference on Security and Privacy for Emerging Areas in Communications Networks*, pages 384-396, Washington, DC, USA, 2005. IEEE Computer Society.
11. Mikhail J. Atallah, Marina Blanton, Nelly Fazio, and Keith B. Frikken. Dynamic and efficient key management for access hierarchies. ACM Trans. Inf. Syst. Secur., 12(3):1-43, 2009.
12. Amit Sahai and Brent Waters. Fuzzy identity-based encryption. In EUROCRYPT, pages 457-473, 2005.
13. Vipul Goyal, Omkant Pandey, Amit Sahai, and Brent Waters. Attribute-based encryption for fine-grained access control of encrypted data. In *ACM Conference on Computer and Communications Security*, pages 89-98, 2006.
14. Josh Benolah, Melisa Chase, Erik Horvitz. Patient controlled encryption: ensuring privacy of electronic medical records, *CCSW '09 Proceedings of the 2009 ACM workshop on Cloud computing security*, pages 103-114.
15. Thomas Hupperich, Hans Lohr, Ahmad Reza-Sadeghi and Marcel Winandy. Flexible Patient-Controlled Security for Electronic Health Records. *IHI '12 Proceedings of the 2nd ACM SIGHIT International Health Informatics Symposium* Pages 727-732
16. Adi Shamir. Identity-based cryptosystems and signature schemes. In George Robert Blakley and David Chaum, editors, Advances in Cryptology | CRYPTO '84, volume 196 of Lecture Notes in Computer Science, pages 47-53. Springer Verlag, 1985.
17. Craig Gentry and Alice Silverberg. Hierarchical ID-based cryptography. In Yuliang Zheng, editor, Advances in Cryptology | ASIACRYPT 2002, volume 2501 of Lecture Notes in Computer Science, pages 548-566. Springer Verlag, 2002.

DILEME PEDIJATARA U SUSRETU SA SUVREMENIM BIOTEHNOLOGIJAMA

Zubčević Smail

Pedijatrijska klinika Kliničkog centra Univeziteta u Sarajevu
Bosna i Hercegovina

Abstrakt – **Biotehnološka revolucija, čiji smo svjedoci, permanentno modificira način našeg života i razmišljanja. Sve moderne tehnologije primjenjene u medicini su tu da donesu neku korist, ali ograničenja koja dolaze sa njima i etičke dileme povezane sa istima se moraju stalno razmatrati. Debate u ovom području u Bosni i Hercegovini su uglavnom nedovoljne, a liječnici vrlo često ostavljeni u nekoj vrsti etičke neizvjesnosti i kontroverze.**

U ovom članku pokušavamo da se bavimo vrlo osjetljivim dijelom ovog problema koji se odnosi na djecu. Bosna i Hercegovina nema jedinstvenog tijela koje bi upravljalo ovim problemima, a takozvani etički komiteti u ustanovama zdravstvene zaštite izbjegavaju da postave jasne smjernice koje bi regulirale ovu problematiku.

Općenito, pedijatri, kao i drugi liječnici, imaju prilično uzak profesionalni fokus koji bi mogao biti nedovoljan za formuliranje javne politike u reguliranju biotehnologija. Moraju proširiti svoje znanje u smislu mogućnosti modernih biotehnologija, prije nego što postanu dovoljno kompetentni da uzmu udio u stvaranju politike u ovom segmentu. Ovaj članak bi trebao da pomogne u rasvjetljavanju nekoliko važnih segmenata, kao poticaj za dalju edukaciju u ovom smislu.

Jedno od rješenja koje predlažemo je formiranje neovisnih, interdisciplinarnih savjetodavnih tijela koja će se baviti etičkim pitanjima koje moderne biotehnologije donose u pedijatriju. Ta tijela bi trebala biti u stanju dati ekspertna mišljenja vladi u pogledu etičkih problema koje srećemo u zdravstvenoj zaštiti djece, moderirati javne i debate u okviru zakonodavnih i upravljačkih tijela, uzeti ulogu u pravljenju etičkih okvira u svakodnevnoj praksi i pomoći definirati prihvatljivu socijalnu politiku. Kao takva ona bi bila glavni faktor u odgovoru na etičke probleme i anticipiranju istih. Trebala bi djelovati na principu ubjeđivanja i konsensusa, kao stalno tijelo, ali i sa mogučnošću formiranja ad hoc komiteta kada se radi o određenim specifičnim pitanjima. Bila bi sačinjena od eksperata iz različitih oblasti: biotehnologije, koji po profesionalnom usmjerenju dolaze i iz medicinskog i iz inžinjerskog miljea, eksperata u oblasti zdravstvene njege pacijenata, sociologa, pravnih stručnjaka, teologa, filozofa, poduzetnika itd. Na ovaj način bi bile predstavljene različite vrijednosti i razmišljanja, što bi proces odluka učinilo kompletnijim.

Ključne riječi: **Etika, biotehnologije, pedijatrija**

I. UVOD

Razvoj biotehnologije posljednjih godina izaziva brojne etičke i društvene reakcije pojedinaca, javnog mnijenje, medija, nevladinih organizacija pa čak i političkih struktura. Pedijatri su prirodom svog posla usmjereni na zaštitu zdravlja najvulnerabilnijeg dijela populacije, te vrlo često imaju velike etičke i moralne probleme u donošenju adekvatnih odluka koje bi trebale pružiti što bolje mogućnosti liječenja i zdravlja djece. Cilj ovog prikaza je dati neke uvide u etička pitanja, dileme i kompromisa koji su vezani za razvoj biotehnologije u posljednjih nekoliko decenija.

Većina javnosti je jako optimistična kada se govori o sposobnosti biotehnologije da poboljša naš kvalitet života, stvara se pogrešan dojam da medicina je svemoćna i da za sve zdravstvene probleme postoji rješenje.

Istina je, živimo u doba u kojem se medicinska tehnologija razvija i poboljšava velikom brzinom, a dostupnost novih tretmana u razvijenim državama se povećava svakim danom. Situacija je mnogo kompleksnija u slabije razvijenim državama sa ograničenim resursima. Historija nas uči da sa svakim napretkom u medicinskoj nauci dolaze i dileme - naučne, socijalne, financijski, a pogotovo etičke i moralne.

Ove nedoumice se progresivno umnožavaju kada skupine ljudi koji dolaze iz različitih segmenta društva, sa izuzetno različitim stajalištima, odlučuju o platformama zdravstvene politike. U prvim desetljećima 21. stoljeća neke od ovih dilema postaju središnje tačke u planiranju daljeg razvoja biotehnologija i njihovog utjecaja na zdravstveni sistem

Kako jasnih odgovora obično nema, smatramo da će ova pitanja i dalje stvarati nedoumice u doglednoj budućnosti, naglašavajući potrebu za uključivanje što više ljudi različitih stručnih profila u ove diskusije, ali i držanja nekih osnovnih standarda etike u medicini [1].

Svu kompleksnost etičkih pitanja u pedijatriji vezanih za suvremeni razvoj biotehnologija bi bilo nemoguće obuhvatiti u jednom članku. Stoga ćemo ovdje predstaviti samo neke od bitnih aspekata vezanih za ova pitanja. Tu u prvom redu treba navesti etičke dileme u istraživanju novih biotehnoloških metoda u dječijoj populaciji, dostupnosti

rezultata novih tehnologija za dječiju populaciju zbog visokih finansijskih troškova, održavanju privatnosti, implikacijama daljeg razvoja istraživanja matičnih ćelija, mogućnostima kloniranja organa, te održavanju života pacijenata u dječijoj dobi gdje nema jasnog načina za poboljšanje stanja svijesti i kvalitete života.

II. Istraživanja novih biotehnoloških mogućnosti

Pitanje istraživanja novih biotehnoloških metoda u dijagnostici i pogotovo liječenju djece se samo nadovezuje na stara pitanja o etičnosti medicinskih istraživanja na djeci. Sadašnji rigorozni kriteriji na ovom planu kao posljedicu imaju da se ovakva ispitivanja rijetko provode u praksi, te na taj način djeca ostaju uskraćena za značajan broj modernih metoda liječenja jer nisu provedena potrebna ispitivanja u dječijoj populaciji. Situacija po ovom pitanju je u USA naročito došla u fokus od 1999. godine, kada je osamnaestogodišnji pacijent umro tokom sudjelovanja u ispitivanju genske terapije na Univerzitetu u Pennsylvaniji. Stručna javnost je oštro kritizirala instituciju jer nije uspjela adekvatno predstaviti ključne informacije u dokumentima o informiranom pristanku.

Ova epizoda je potaknula veliko preispitivanje među istraživačima i regulatorima, a mnogi univerziteti su uveli nove standarde u ispitivanja kao rezultat povećane pozornosti javnosti na obavljanje kliničkih ispitivanja u svijetu. U članku u Epidemiology Review iz 2002. godine Jeremy Sugarman, profesor bioetike i medicine na Johns Hopkins School of Medicine je napisao: «To je izuzetno važno kako bi se osiguralo da se istraživanje provodi odgovorno tokom cijelog ciklusa studije, od načina izbora sudionika do načina kako se podaci upisuju, analiziraju i objavljuju. Obraćanje pažnje na svaki aspekt provođenja istraživanja je potrebno za uspjeh u znanstvenom pothvatu i zaštitu sudionika studije i drugih učesnika od nepotrebnih ozljeda» [2].

Ovakva pitanja su dovoljno komplicirana kod adultnih pacijenata, da i ne spominjemo pedijatrijsku populaciju. Pacijenti, naročito oni teško oboljeli, su vrlo često spremni probati nešto novo; metodu, terapiju, čak i kada su liječnici svjesni i spremni prezentirati stav da nuspojave nisu u dovoljno istražene. Ta nekada velika navala volontera za istraživanje se mora kontrolirati od strane posebnih odbora za reviziju slučajeva, po mogućnosti i prije nego što pacijenti vide obrazac informiranog pristanka. Za ovakvo ponašanje postoje podaci i u kliničkoj praksi u našoj državi, čak i u mjeri da su volonteri nudili mito da budu uključeni u ispitivanje novih terapijskih mogućnosti. Stroga pravila selekcije u dječijoj populaciji su *conditio sine qua non* u istraživanju, jer informirani pristanak u principu daje druga osoba, roditelj.

III. Dostupnost novih tehnobioloških mogućnosti

Cijene zdravstvene zaštite rastu u cijelom svijetu, te tako i u Bosni i Hercegovini. Nova biotehnološka dostignuća su rezultat istraživanja koja su veoma skupa, te su i nove metode dugo vremena jako skupe. Uvođenje suvremenih dijagnostičkih i terapeutskih metoda predstavlja veliko finansijsko opterećenje za zdravstvene fondove. Odnos cijene modernih tretmana i izdavanja za zdravstvo ne ide u prilog pacijentima. Dostupnost suvremene dijagnostike i tretmana je veliki problem. Pacijenti i liječnici smatraju da je potrebno omogućiti najbolje dijagnostičke i terapijske metode, ali zdravstveni fondovi nisu uvijek dovoljno veliki za tako nešto i njihova hronično neracionalna upotreba ostavlja malo nade da u budućnosti možemo očekivati poboljšanje. Na taj način smatramo da će pristup novim dostignućima biotehnologije u našoj zamlji i dalje biti vrlo ograničen. Ovo predstavlja stalnu etičku dilemu za liječnike. Pedijatri moraju odlučiti kojem trenutku je potrebno reći «dosta» ograničenjima nove dijagnostike i tretmana koja nameću zdravstveni fondovi, imajući u glavi isključivo interese djeteta. Zdravstveni fondovi i poslodavci žongliraju sa aktulnim finansijskim problemima i rizicima neadekvatne dijagnostike i tretmana pacijenata, a da pri tome nemaju kontakt sa pacijentom. Pedijatar je osoba preko koje se prelama frustracija roditelja.

Etička pitanja ove vrste se ne mogu rješavati unutar ovakve formulacije i potrebno ju je na neki način nadići. Što se događa kada neki pacijenti ne mogu priuštiti vlastiti udjel u finansiranju određenog tretmana? Što ako zdravstveni fond odbije finansirati moderne dijagnostičke i terapijske pristupe? Takvi slučajevi nisu svakodnevni, ali se ipak pedijatri jako često sreću sa njima. Kako se postaviti u sukobu između bolesnika i zdravstvenog sistema? Ovaj sukob je dijelom ekonomski problem, ali dijelom i problem loše organizacije zdravstvene zaštite. Smatramo da pedijatar uvijek sa roditeljima treba razgovarati o suvremenim dijagnostičkim metadoma i tretmanima pacijenta bez obzira na njihovu dostupnost u datom momentu. Propust u informiranju roditelja ili staratelja djeteta o objektivnim mogućnostima medicine u liječenju njihovog djeteta se ne može opravdavati ekonomskim razlozima i slabom organizacijom zdravstvene zaštite. Ako ništa drugo, ne može se uskratiti mogućnost roditeljima ili starateljima pedijatrijskog pacijenta da spase život ili zdravlje svoga djeteta vlastitim finansiranjem liječenja. Liječnik u tom procesu mora biti izuzetno dobro informiran dosezima takvih metoda, stupnjem mogućeg poboljšanja kvalitete

života, da ne bi svojim nedovoljnim poznavanjem problematike doveo u zabludu roditelje ili staratelje djeteta.

IV. Zaštita privatnosti pedijatrijskih pacijenata

Zaštita privatnosti pacijenta je tema koja izaziva rastuću zabrinutost u javnosti. Zaštita ličnih podataka u vrijeme sve potpunije informatizacije društva spada u vrlo važne teme razvijenih zajednica, premda joj se u Bosni i Hercegovini ne pridaje veliki značaj, a i do sada nedovoljno formulirani zakoni o zaštiti privatnosti podataka se u praksi ne provode. Međutim, na pragu smo mnogo većeg problema u zaštiti podataka, a on se odnosi na zaštitu podataka o pacijentovom genomu, koji zahvaljujući modernoj biotehnologiji je danas moguće lako dešifrirati. U situaciji smo u kojoj naučnici posjeduju vještinu dešifriranja genetskog sistema osobe, te je sve vjerojatnija i mogućnost da dođe do ugrožavanja informacije o budućem zdravlju osobe koja postaje dostupna. Na primjer, sada je moguće znati da li će neko trogodišnje dijete razviti ozbiljne bolesti srca kasnije u životu. Smije li to znati budući poslodavac? Kako će to znanje utjecati na sposobnost pojedinca za dobivanje posla, osiguranje, ili hipoteke i kredita? [3]. Ovo predstavlja veliki problem kojim se društvo tek treba početi baviti. Ako postoji mogućnost liječenja tog djeteta za 500.000 ili milion konvertibilnih maraka, na koji način će zdravstveni fondovi reagirati na problem.

Biotehnologija nam donosi sve lakše mogućnosti dešifriranja ljudskog genoma, oprema koja je koštala stotine miliona danas košta nekoliko hiljada, i već su na vidiku jednostavni uređaji koji će iz kapi krvi, opremu od par hiljada konvertibilnih maraka i personalni računar omogućiti pojedincu potpun uvid u ljudski genom. Ovakav nastavak nekontrolirane primjene modernih biotehnoloških metoda otvara ogromne mogućnosti zloupotrebe, analiza DNK ima potencijal da uzdrma same korijene civilizacije [4]. Da li će se buduća djeca kreirati po unaprijed određenom planu, da li će evolucija kakvu danas poznajemo i priznajemo pretvoriti u dirigiranu evoluciji kojom upravlja par ljudi ili «komiteta»? Sa ovim mogućnostima još najbenignije izgleda situacija u kojoj budući mladoženja nakon što je došao do podataka o djevojčinom genomu pobjegne sa svadbe (ili obrnuto).

V. Mogućnosti genetskog savjetovanja i upravljanja

Kada se govori o napretcima u genetici neophodno je dalje razumijevanje veze DNK mutacija koje uzrokuju određene genetske bolesti i konkretnih posljedica na fenotipu. Testiranje embrija u traženju genetskih mutacija je trenutno moguće, međutim, svaka osoba u tome ne vidi ispravan etički čin. Koliko god je za neke ljude nepojmljivo da se trudnoća ne okonča abortusom ukoliko se tokom testiranja embrija nađu promjene koje upućuju na to da će dijete biti teško malformirano, za druge je činjenje prijevremenog prekida trudnoće i u ovoj situaciji ubistvo sa predumišljajem. Pedijatar koji liječi jedno dijete sa nekom kongenitalnom anomalijom ili bolešću uzrokovanoj genetskim faktorima treba biti u stanju dati savjet o prenatalnom genetskom testiranju za eventualne buduće trudnoće. Ovakav savjet lako dovodi do prije navedene situacije, te neki pedijatri ozbiljno razmišljaju o tome da li je sve ovo opravdano, ili je na neki način uvođenje eugenike «na mala vrata».

U slučaju ovakvog scenarija nema puno prostora za etička promišljanja općeg pedijatra, osim pružanja informacije koja je tražena od njih prilikom genetskog savjetovanja. Međutim, oni pedijatri koji pretežno rade sa djecom sa genetskim poremećajima su postavljeni pred prave etičke dileme. Strah od uvođenja eugenike kroz prenatalna testiranja se ne može smatrati neopravdanim. Mogućnost da prije rođenja odstranimo one za koje smatramo da nisu biološki potpuno vrijedni je zastrašujuća. Pored toga, vrlo često imamo situacije kada majke (roditelji) navode da prije prenatalnog testiranja nisu bili upoznati sa svim mogućim konsekvencama rezultata koje to ispitivanje donosi. Neka ispitivanja pokazuju da preko 92% onih koji su upozoreni da nose dijete sa sindromom Down su prijevremeno prekinuli svoju trudnoću. Često puta ove majke tvrde da su na neki način požurene s odlukom, te da im nije dana nikakva pozitivna povratna informaciju o tome kako dijete još uvijek može imati kvalitetan život. Navode da su u fokusu dobivanja informacija uglavnom bili negativni aspekti djeteta sa onesposobljenjem [5].

Kada se ovakva vrsta konsultacije radi idealno bi bilo da se podaci predstave na najobjektivniji mogući način, a zatim roditelji u potpunosti ostave da sami donesu odluku. Informacija bi morala biti potpuno oslobođena biasa na jednu ili drugu stranu. Neophodno je da pedijatri koji daju ovu informaciju ni na kakav način ne naglase da dijete sa onesposobljenjem ne može biti sretno dijete. Moderna biotehnologija se definitivno ne bi trebala upotrebljavati u situacijama gdje se ne može upotrijebiti na moralno i etički ispravan način.

Postoji i pritisak društva da se prave ovakvi testovi. Jednostavan test iz kapi krvi može dovesti osobu do najtežih mogućih odluka u životu. Pedijatri koji se bave genetskim savjetovanjem moraju biti od pomoći u donošenju te odluke, ali je za njih situacija moralno i etički vrlo složena [6] i značajno ovisna o njihovom svetonazoru.

Najteža je ona situacija gdje pedijatri misle da stvari idu

u pogrešnom pravcu, ali ne mogu ništa promijeniti. I u slučajevima kada neki oficijelni etički kodeksi dozvoljavaju neke postupke, pojedinac, pedijatar, često nije bez unutarnjih moralnih i etičkih dilemma [7]. Ukoliko budemo dozvolili prijevremeno prekidanje trudnoća djece koja nisu 100% genetski zdrava dovešćemo se u apsurdnu kreacionističku situaciju. Biotehnologija kojom danas raspolažemo nam to omogućava, mogućnosti komercijalizacije gore navedenog postoje i na nama je da postavimo regulatorna tijela koje će onemogućiti zloupotrebu i čuvati raznolikost ljudske vrste.

Ističe vrijeme da se u korijenu preduprijede neke stvari, a moguće je i da je već isteklo. Ne vidi se dovoljno napora i svijesti da se ovo pitanje u svijetu riješi na način koji bi osigurao prava pojedinca. Radne grupa američkog College of Physicians je objavila jedan takav napor u časopisu Annals of Internal Medicine, pod naslovom «Ethics in Practice: Managed Care and the Changing Health Care Environment" gdje su se pokušala precizirati etička načela za planove zdravstvenog sistema, korisnike i liječnike [8]. Iznijeto je mišljenje da sve stranke imaju etičku obavezu zaštite tajnosti podataka pacijenta u sistemu zdravstvene zaštite. Zauzet je stav da općenito identificirane informacije o pacijentu ne treba dijeliti bez pristanka pacijenta - osim u slučaju kada može biti ugroženo zdravlje i sigurnost drugih osoba ili javnosti, odnosno kako je propisano zakonom. Ipak, i ova izjava, međutim, ostavlja otvorenim pitanje o mjeri u kojoj prava pojedinca mogu biti potisnuta od strane «društvenih potreba». U Bosni i Hercegovini i dalje nema jasne javne debate o ovim problemima i rizikujemo da se donesu akti koji neće biti odraz potrebe zaštite pacijenta i čovjeka.

VI. Istraživanje matičnih ćelija

Istraživanja mogućnosti matičnih ćelija u liječenju različiti bolesti su danas vrlo važna tema za široki krug roditelja. Pedijatri su sve češće suočeni sa pitanjima mladih roditelja da li da se pohrane matične ćelije njihovih novorođenih beba i to ne predstavlja etički problem. Ali iza ovog, izgledom jednostavnog odgovora, krije se dosta nerazjašnjenih tema.

Istraživanje matičnih stanica je vruće pitanje za većinu svjetskih religija. Već pomalo pada u zaborav veliki zaostatak u ovim istraživanjima koji je nastupio u USA i EU sa početkom ovog stoljeća, nakon serije ograničenja istraživanja matičnih ćelija. To je dovelo do situacije u kojoj neke druge države, poput Kine, su nastavile istraživanja, ali kako nisu raspolagali dovoljnim istraživačkim resursima situacija danas nije u skladu sa onom koju smo predviđali koncem proteklog stoljeća. I danas ironično zvuči da se jedno znanstveno područje istraživanja, temeljeno na podacima i brojevima, može preformulirati u emocionalni problem. Ova rasprava dovodi do konflikta ljudi koji vjeruju da ovakva istraživanje jednog dana mogu donijeti lijekove za danas neizlječive bolesti i onih koji tvrde da se krši pravo na ljudski život.

Još 1999. godine American Society of Clinical Oncology je formulirao svoju politiku na način da «bilo da se radi o privatnom ili javnom finansiraranju, istraživači bi trebali biti svjesni etičkih pitanja koje se pojavljuju kada istraživanje uključuje embrije i fetalna tkiva, kloniranje ili druge kontroverzne pitanja». Sa druge strane, kroz historiju medicinska istraživanja često zahtijevaju balansiranje uočenih rizika i mogućih koristi. Ogroman potencijal istraživanja matičnih stanica za liječenje bolesti u kalkulaciji koristi i rizika sada jasno ide u prilog nastavka istraživanja, pa čak i ako to podrazumijeva etički osjetljiva područja. Osnovna doktrina medicine «ne štetiti» nas navodi da bi zaključak po ovom pitanju trebao biti da istraživanja matičnih stanica obećavaju veliki benefit i predstavljaju prioritet ako su etički temeljena na ovoj doktrini. Dobivanje matične stanice iz pacijenata, a da se pri tome ne nanosi ozbiljna šteta, može biti etički ispravno. Za razliku od ovoga, dobivanje matičnih stanica iz ljudskih embrija etički je vrlo problematično, jer predstavlja uništavanje tih embrija.

VII. Održavanje života

Mogućnosti održavanja života u modernim pedijatrijskim i neonatalnim jedinicama intenzivne njege i terapije, sa naprednim dostignućima u biotehnologiji postaju sve veće. Pedijatri koji rade na ovim odjelim su svakodnevno pod pritiskom donošenja odluka koje imaju dalekosežne posljedice, te mnoge etičke i moralne dileme.

Da li je moralno prihvatljivo dopustiti djetetu da umre? Intenzivne njege su stvorene sa ciljem liječenja potencijalno reverzibilnih životno ugrožavajućih patofizioloških stanja, i danas su opremeljene različitim «čudima» moderne biotehnologije. U prethodnoj rečenici je ključni izraz «potencijalno reverzibilna stanja». Ukoliko ne postoji razumna mogućnost da pacijent oporavi životno ugrožavajuće disfunkcije onda je nastavljanje metoda intenzivne njege beskorisno, rastrošno i neodgovorno. Većina stručnjaka smatra da ovakva djeca nemaju benefita od jedinice intenzivne njege i da im treba omogućiti dostajanstvenu smrt. Ali, ko je taj koji će prosuditi da li se radi o «potencijalno reverzibilnom stanju». Praksa nam govori da će većina pedijatara u jedinicama intenzivne njege postupati sa pacijentom kao da ima «potencijalno reverzibilno stanje» i kada je potpuno jasno da to nije

slučaj. Pedijatri će odbiti da na sebe preuzmu odgovornost uskraćivanja intenzivne njege i terapije, što dovodi do blokiranja jedinica intenzivne njege i nemogućnosti adekvatnog tretmana djece sa zbiljski «potencijalno reverzibilnim stanjima». Neophodno je jasnije razlikovanje djece koja zahtijevaju intenzivnu njegu i djece koja zahtijevaju palijativnu njegu [9].

Šta je važnije, život sam po sebi ili kvalitet života? Susrećemo se sa pacijentima koji se mogu u jedinicama intenzivne njege privremeno oporaviti, ali sa velikim posljedicama na fizičko i mentalno zdravlje, kao na primjer kod slučajeva teških hipoksično-ishemičnih encefalopatija ili neurodegenerativnih metaboličkih bolesti. Sa čisto etičke tačke gledišta pravo na život je fundamentalno pravo koje se ne može uslovljavati stvarima kao što je mentalno zdravlje ili sl. Sa druge strane, dijete u permanentno vegetativnom stanju nema nikakvog benefita od intenzivne njege, već mu ista može samo škoditi. Dijete u terminalnom stadiju teške mišićne spinalne atrofije može u nastavku svog života očekivati samo bol, što dovodi do toga da terapije koju mu produžuju život u stvari produžuju patnju do momenta neizbježne smrti. Možda je pravi način gledanja na problem taj da pravo na život kao takav i pravo na kvalitet života nisu suprostavljene već komplementarne kategorije [10]. Na taj način naši napori u održavanju života kao takvog su vođeni mogućnošću održanja prihvatljive kvalitete života kod ove djece.

Kada dijete na prijemu na intenzivnu njegu ne pokazuje jasne mogućnosti reverzibilnosti procesa koji ga je doveo u životno ugrožavajuće stanje pred pedijatre se postavlja dilema da li da se otpočne tretman za održavanje djeteta u životu, te se na taj način potencijalno dovedu u situaciju da kasnije to što su učinili trebaju povlačiti. Većina liječnika se slaže da etički gledano nema razlike između neuvođenja tretmana i isključivanja tretmana. I jedno i drugo treba biti rezultat odluke da ne postoji razumna mogućnost reverzije životno ugrožavajućeg stanja, bilo odmah na početku liječenja, ili tokom liječenja i nakon prikupljenih dodatnih informacija o pacijentovom stanju.

Ko je taj ko bi trebao donijeti konačnu odluku, liječnik, roditelji/staratelji, neko neovisno tijelo? Kroz dugi niz stoljeća ta odluka je praktično uvijek bila na liječnicima. Oni su tradicionalno uživali takvo povjerenje da roditelji nisu imali nikakvih dilema da oni trebaju odlučiti. «Doktor će znati najbolje» je bila rečenica koja je na neki način pokazivala poštovanje, ali i mogućnost da se ne zauzima jasan stav po ovom pitanju. Ovo (vjerovatno na sreću liječnika) nije više slučaj, kada se govori o medicinskoj struci postoji općenito nepovjerenje u ovu profesiju. Idealni scenario bi podrazumijevao zajedničku odluku roditelja/staratelja i liječnika, za što je potrebno da liječnik predoči detaljne informacije o stanju pacijenta, perspektivama, bez jasnog biasa, te omogući roditeljima/starateljima djeteta dovoljno vremena za razmišljanje, bez vršenja pritiska, te uz savjet da roditelji uključe u konsultaciju i druge profesionalce, kao što su npr. vjerski službenici, pravnici, socijalni radnici, psiholozi itd. Sve ovo treba da se odvija u uslovima uzajamnog poštovanja, uvažavajući tešku dilemu pred koju su roditelji/staratelji postavljeni.

VII. Kakva bi mogla biti rješenja

Svakodnevna praksa nas uči da većina pitanja koja su ovdje postavljena traže sistemski odgovor. Na žalost ni praksa u svijetu po ovom pitanju nam ne daje potpune vodiče kojim bi smo se mogli služiti. Dodatno opterećenje za našu zemlju predstavlja status slabo razvijene države sa vrlo ograničenim finansijskim i ljudskim resursima. U takvim uslovima postoji uvijek potreba za balansiranjem između onoga što je potrebno i onoga što je moguće. Ali, to nas ne sprječava da etičke principe u svom radu postavimo na visok nivo koristeći opće prihvaćene etičke standarde u zdravstvenim sistemima. Neophodno je jasno uspostavljanje principa koji mogu pokriti široki spektar situacija u kojim se pedijatri mogu naći. I u slučaju jasnog definiranja takvih principa nije neopravdano misliti da će liječnici i dalje tražiti širi panel ljudi u delikatnim odlukama koje mogu promijeniti život pojedinog pacijenta.

Kao jedno od rješenja predlažemo i formiranje neovisnih, interdisciplinarnih savjetodavnih tijela koja će se baviti etičkim pitanjima koje moderne biotehnologije donose u medicinu i pedijatriju. Ta tijela bi trebala biti u stanju dati ekspertna mišljenja vladi u pogledu etičkih problema koje srećemo u zdravstvenoj zaštiti djece, na osnovu čega bi se mogla početi stvarati jasnija zakonska regulativa, moderirati javne i debate u okviru zakonodavnih i upravljačkih tijela, uzeti ulogu u pravljenju etičkih okvira u svakodnevnoj praksi i pomoći definirati prihvatljivu zdravstvenu socijalnu politiku. Kao takva ta tijela bi bila glavni faktor u davanju odgovora na etičke probleme i anticipiranju istih. Trebala bi djelovati na principu razgovora, ubjeđivanja i konsensusa, bez preglasavanja. Organizirana bi bila kao stalno tijelo, ali sa mogučnošću formiranja *ad hoc* komiteta kada se radi o određenim specifičnim pitanjima. Trebala bi ih sačinjavati eksperti iz različitih oblasti: biotehnologije, koji po profesionalnom usmjerenju dolaze i iz medicinskog i iz inžinjerskog miljea, njege bolesnika, sociologije, pravnih nauka, teologije, filozofije, poduzetništva itd. Na ovaj način bi bili predstavljeni različiti segmenti društva, došle bi do izražaja različite vrijednosti i razmišljanja, a proces donošenja odluka bi se učinio kompletnijim.

I pored stvaranja ovakvih tijela na kraju bi pedijatri ipak

ostali sami u konačnom donešenju odluka kada se radi o pojedinačnom pacijentu. Dosadašnja edukacija pedijatara im ne daje dovoljno uvida u ovu problematiku. U razvijenim zemljama već dugo vremena postoji kontinuirana etička edukacija liječnika, pa i pedijatara, sa svim specifičnostima koje ona nosi. Samo dobro educirani pedijatri u smislu etičkih problema sa kojim se moderna medicina susreće, sa stalno obnovljenim uvidom u nova biotehnološka dostignuća i etička pitanja koja se sa njima postavljaju, mogu dati odgovore na ove probleme sa visokim moralnim i etičkim integritetom.

VIII. Reference

1. Beauchamp TL, Childress JF. eds. Principles of Biomedical Ethics. New York. Oxford University Press, 2001.
2. Sugarman J. Ethics in the Design and Conduct of Clinical Trials. Epidemiol Rev (2002) 24 (1): 54-58
3. Silverman E. The 5 Most Pressing Ethical Issues In Biotech Medicine. Biotechnology Healthcare 2004; 1(6): 41-6
4. Committee on Bioethics. Ethical issues with genetic testing in pediatrics. Pediatrics. 2001 Jun;107(6):1451-5.
5. Gonzales J. Ethics for the Pediatrician: Genetic Testing and Newborn Screening. Pediatrics in Review, 2011. (Online article).
6. Deans, et al. Non-invasive Prenatal testing for Single Gene Disorders: exploring the ethics. European Journal of Ethics 2011. (Online Article). DOI:10.1038/ejhg.2012.250http://pedsinreview.aappublications.org/content/32/11/490.short
7. Hester DM. Ethical Issues in Pediatrics. In: Guidance for Healthcare Ethics Committees, Hester DM and Schonfeld T eds. Cambridge University Press. Cambridge 2012
8. Povar GJ et al. Ethics in Practice: Managed Care and the Changing Health Care Environment: Medicine as a Profession Managed. Ann Intern Med. 2004;141(2):131-136
9. Feudtner Cl, Nathanson PG. Pediatric palliative care and pediatric medical ethics: opportunities and challenges. Pediatrics. 2014 Feb; 133 Suppl 1:S1-7
10. Sarnaik AP, Daphtary K, Sarnaik AA. Ethical Issues in Pediatric Intensive Care in Developing Countries: Combining Western Tecnology and Eastern Wisdom. Indian J Pediatr 2005; 72(4): 339-342.

Smail Zubčević, Pedijatrijska klinika, Klinički centar Univerziteta u Sarajevu, Patriotske lige 81, 71000 Sarajevo, Bosna i Hercegovina, tel 033566402, e-mail smail.zubcevic@gmail.com

The computer modelling and biomechanical analysis of musculoskeletal systems in The AnyBody Modeling System

Denis Spahić, Aleksandar Karač

University of Zenica/Faculty of Mechanical Engineering, Zenica, Bosnia and Herzegovina

Abstract— **This paper reviews The AnyBody Modeling System, designed for simulating the mechanics of the human body during different activities of daily living. Several features of the AnyBody System are presented, demonstrating the software capabilities and visualising the musculoskeletal model of the human body in action.**

Examples of a full-body model standing on a floor and doing a squat motion, with and without additional weight, and a free posture model in interaction with a piece of sport equipment are analysed, where the individual muscle forces, and the reaction forces in the human body joints are obtained.

In addition, the boundary conditions and the loads acting on the clavicle bone during the squat motion are exported for a subsequent numerical analysis. The output data and the mesh of the clavicle bone are imported into finite-element-based software. Obtained analysis demonstrates how the clavicle bone reacts with the muscle attachments and surrounding bones during performance of the analysed activities.

Keywords—**The Anybody Modeling System, inverse dynamics, biomechanics, the clavicle bone , Finite Element Analysis**

I. Introduction

The AnyBody Modeling System (AMS) is a software solution designed for simulating the mechanics of rigid multi-body systems – especially musculoskeletal ones. It was originally developed by a group of researchers from the Aalborg University [1], that has grown up in a spin-off company - AnyBody Technology [2]. The AMS is based on the application of general multi-body dynamics formalism [3], principles of the inverse dynamics [4] and the muscle recruitment optimization [5].

To develop multi-body dynamics models, the AMS provides a declarative, object-oriented modelling language - the AnyScript [6], which has a number of predefined classes that the user can create objects from. The predefined classes comprise basic data types, such as numbers and strings, mechanical object types, such as bones (called segments), joints of various types, drivers (functions of time determining values of different kinematics measures, which can also be used as the virtual motors when there are not defined muscles), forces, muscles, and operational and model management classes. One of the ideas behind the AnyScript is that its text-based format and object-oriented structure makes it easy to transfer elements between models. That means that a library of body segments could be built for the use in different analysis projects, and the models could be easily exchanged between users in collaboration on complex modelling tasks. Using the AnyScript modelling language, the user also controls the graphical appearance of the model by means of special objects with visualization capabilities (Fig. 1).

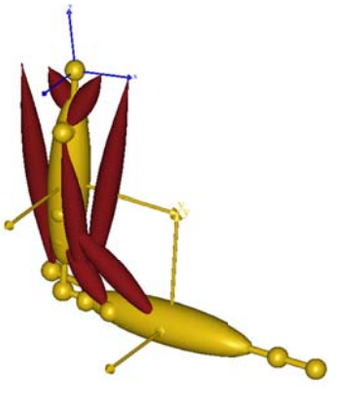

Fig. 1 Simplified model of an arm

As the input data the system requires motion and optionally external forces (measured or defined as objects in the AnyScript), from which the internal mechanical properties of a multi-body system are calculated (individual muscle forces, joint forces and moments, elastic energy in tendons, antagonistic muscle actions and much more). The motion could be applied in a different ways: (a) measured motion using a motion capture system (e.g. Vicon, Xsens, Kinetic, Animazoo, etc.) in a form of C3D or BVH data, (b) through the interface between a model and environment – where the model is driven by the motion from its environment (e.g. connection of the feet and hands with some parts of a machine), (c) manual input in the form of parameters which involve anatomical joint angles, or defining time-dependent drivers which control a kinematic measure (e.g. position and movements of hand, or centre of mass).

The AMS allows users to model just about any musculoskeletal system, be it a human or other creatures, and analyse reactions with them and an environment - which can be

something within the model (implant, e.g. knee or hip device), attached to it (exoskeleton, e.g. knee brace) or something interacting with the model (e.g. wheelchair, automotive seat, assistive device, piece of equipment).

Since musculoskeletal models of humans and animals are very complex and their accurate modelling from scratch would be an enormous task for most of users, the AMS comes with a full body model (Fig. 2), which is broadly and deeply validated [7], containing most bones, joints and muscles in the human physiognomy (roughly 1200 individual muscle fascicles). By default the body model represents the size and weight of an average European male (1.76m, 75kg), but the model can easily be scaled according to several scaling laws.

Fig. 2 The full human body model

In addition, users of the AMS are also provided with the AnyBody Managed Model Repository (AMMR) [8], which is the repository of musculoskeletal models that has been implemented for the AMS. Typically the models are originally developed by research projects at academic institutions or by AnyBody Technology in collaboration with academic institutions. The repository contains body and application models. The body models are generic models which can be applied in investigation/analysis and placed in the right context-application. The application models typically include a body model, specify optional parameters for it, and insert it into the environment/activity that is wished to be analysed.

According to the users' level, the AMS could be used in a several work flows. Standard work flow involves analyses of daily living activities (e.g. walking, lifting, exercising, pushing/pulling, etc.) in order to provide information about muscle activities and forces, joint reactions, kinematics of segments, mechanical cost, etc. In advance work flow users may use subject specific information (models of bones from CT or MRI scans, anthropometry data, strength of muscles, numbers of muscles or the position of their attachments, motion and external force data) and modify the mechanical and physical characteristics of the body model.

In addition to obtaining different sorts of output data, the AMS is also capable to export them to other software solutions for the subsequent analysis or post processing (Python, Matlab, Office applications). There are interfaces for exporting data to finite element modelling software (Abaqus and Ansys). In this way a very detailed and complex load scenarios on the bones could be applied and analysed. It is also possible to import various CAD models designed in 3D CAD design software SolidWorks (for example different pieces of furniture, sports equipment or machines) [9], put them in connection with the body model and make numerous analyses in order to optimise products for comfort or efficiency.

The main objective of this paper, besides the general introduction of the AMS, is to make several analyses in order to estimate loads in the selected human body joints and muscles, which are developed during the following activities: the squat of the body with/without dumbbells and the bench press.

II. Materials and Methods

A. Modelling the squat by utilising the standing model

For the purpose of the squat simulation of the body model, the standing model from the template library was used. This model has a few predefined features and some that can be modified:

- The model is supported by having both feet connected to the ground. The feet can move with the posture, but they are always supported by the connection with the floor.
- The posture of the model is controlled via anatomical angles for all major joints except the ankles.
- The model automatically balances its posture by means of the ankle angles such that its collective centre of mass remains vertically above the ankle joints.

By modifying the anatomical angles of the glenohumeral joint (flexion = 100 degrees, abduction = 90 degrees, external rotation = -20 degrees), the body model was set in the starting position.

The simulation time was chosen to be 2 sec with the resolution of 30 steps per second. During this time, the model changed its position by simultaneously varying the values of the knee flexion (from 0 to 90 degrees) and the hip flexion (from 0 to 45 degrees) of the both legs. It was done by following the sine functions defined by the drivers. Two positions of the model, for the time step 0 and 1sec, are presented in Figure 3.

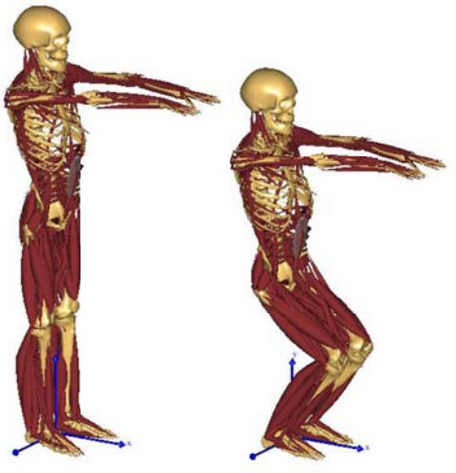

Fig. 3 Two positions of the model during the squat

An additional case was also investigated, with one change in the set-up. This time the model had two external forces (F=25N) acting on the position of the palms in the downwards direction. The scenario described the squat with the additional dumbbells.

As the last step, kinematics and inverse dynamics analyses were conducted. In addition, the loads that acted on the right clavicle bone were exported in the form of an xml file. Using available converter, as well as the tetrahedral mesh of the clavicle geometry, both provided by the AMS, this complex load scenario (applied loads and fixation conditions) was modelled and analysed using Abaqus [10]. The muscle attachments nodes and coupling constraints that were applied to the finite element model are presented in Figure 4.

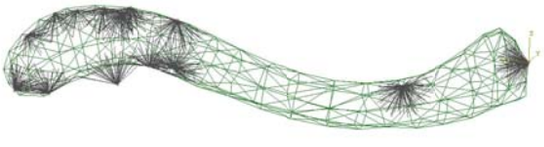

Fig. 4 The FE model of the clavicle bone

B. Modelling the bench press by utilising the free posture model

The bench press model is one of the examples available in the AMMR. It is based on the free posture model which is a good starting point for new applications involving the entire body. The initial posture of the model is set by changing the predefined anatomical angles in defined joints. The bench is simulated by reaction forces (forces that are unknown and must be determined by solving the equilibrium equations) between the head, thorax, pelvis, feet and the ground.

The barbell weight is defined as a segment of certain mass properties (m=30 kg), which is connected with hands by the spherical joints. The movement of the weight is defined by several drivers so that it simulates lowering and rising of the weight during the time period of 10 sec. The starting position of the model is shown in Figure 5.

Several analyses were carried out in order to investigate the reaction forces in the glenohumeral joint and the forces generated by the pectoralis muscle, taking into account various spacing between the hands on the barbell.

Fig. 5 The bench press model in the starting position

III. RESULTS

A. The squat model

Every object defined in the AMS model generates some form of the output data, either kinematic or dynamic. After having done the inverse dynamics analysis, using a standard graphing tool, the user can investigate huge amount of data presenting them in the form of 2D/3D charts.

As the prerequisite for the operation of the inverse dynamics, the kinematics analysis of the model is done first. The data obtained from this type of analysis could be used for various ergonomic studies. Taking into account the observed activity, the position, measured from the ground level, and velocity of the right hand are shown in Figures 6 and 7.

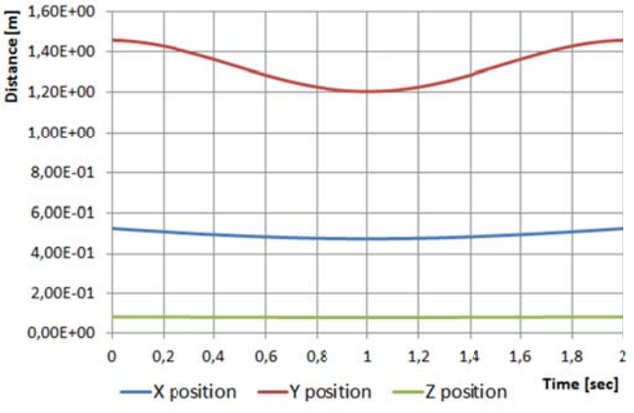

Fig. 6 X,Y and Z coordinates of the right hand

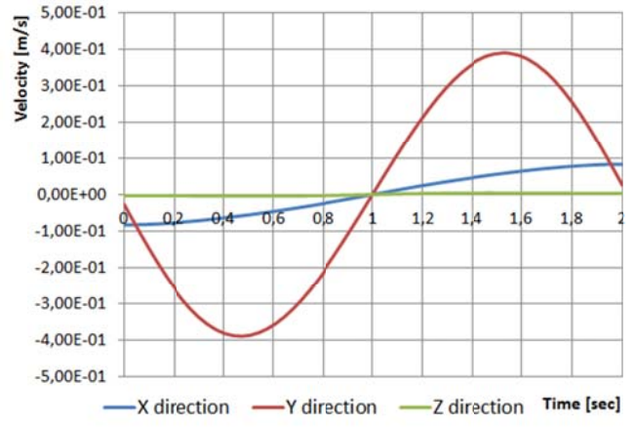

Fig. 7 Velocity of the right hand

The squat is compound, full body exercise that trains primarily the muscles of the tights, hips and buttocks, quadriceps (vastuslateralis, vastusmedialis, vastusintermedius and rectus femoris). The forces generated by this muscle group are shown in Figure 8.

Taking into account the position of the arms, the forces generated by the muscles from the upper body were also interesting information to investigate. Two different cases were analysed, with and without the additional dumbbells in the hands. In order to keep arms in the chosen position, the upper body muscles, especially the deltoid muscle, were activated as shown in Figures 9 and 10.

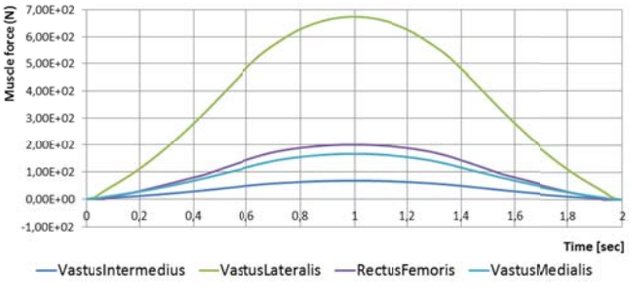

Fig. 8 Forces produced by the quadriceps muscle

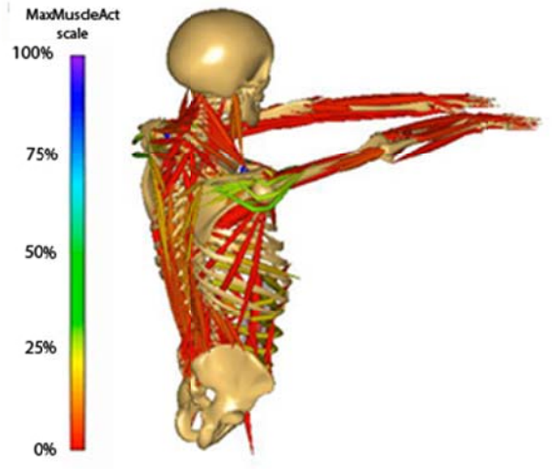

Fig. 9 The upper body muscle activity

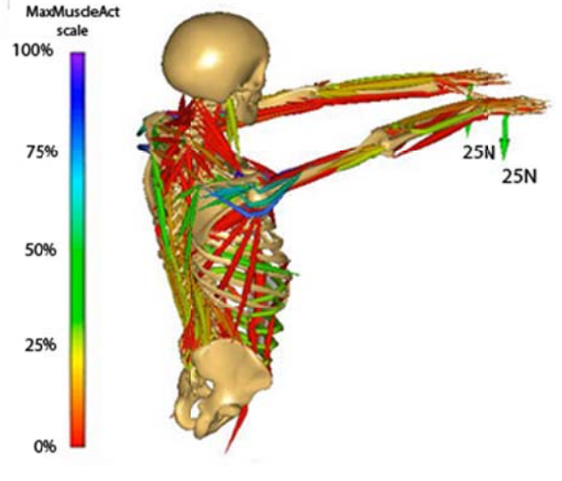

Fig. 10 The upper body muscle activity – the case with additional loads

Besides the muscle activity, many biomechanical researchers are also interested in joint reaction forces. Their values for the hip joint, generated during the observed activity, are presented in Figure 11.

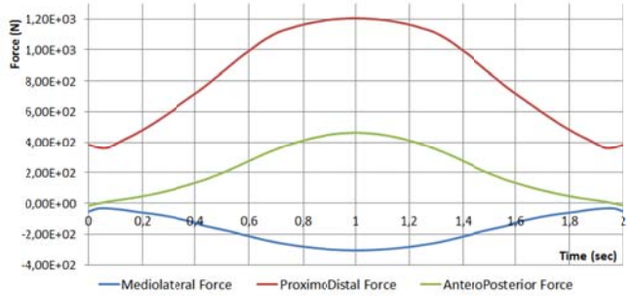

Fig. 11 Reaction forces in the hip joint

Figures 12 and 13 depict the von Mises stress distribution in the clavicle bone obtained from the FEM analyses. Although the mesh provided by the AMS is rather coarse, the results show noticeable quantitative distinction between two observed cases.

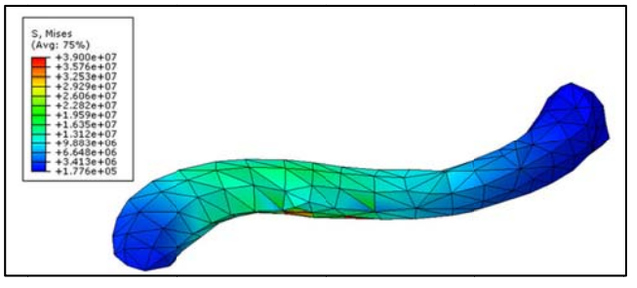

Fig. 12 Stress distribution in the clavicle bone – no additional loads

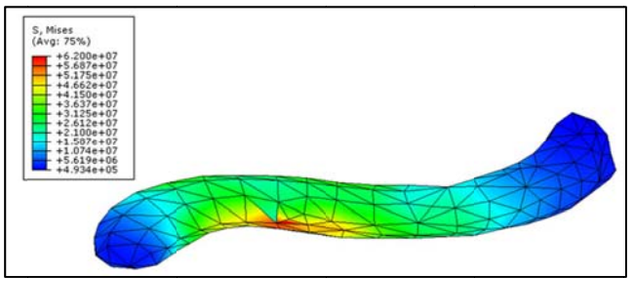

Fig. 13 Stress distribution in the clavicle bone – with additional loads

B. The bench press model

The bench press is an upper body strength training exercise that consists of pressing a weight upwards from a supine position. The exercise works the pectoralis muscles as well as supporting chest, arm, and shoulder muscles.

The position of the barbell, measured from the bench level, and the velocity in the Y direction are shown in Figures 14 and 15.

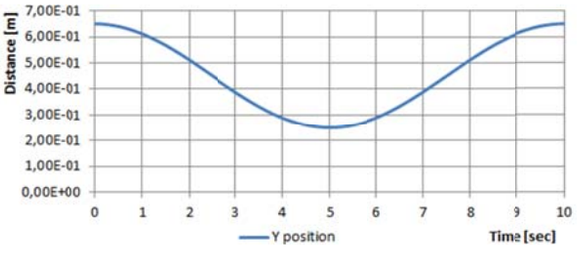

Fig. 14 Position of the barbell

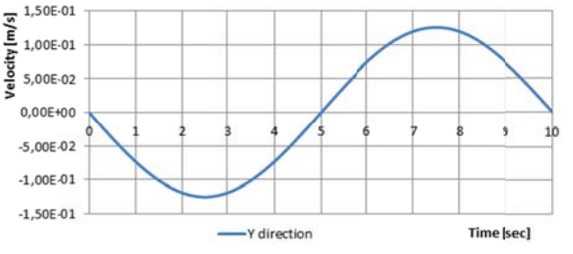

Fig. 15 Velocity of the barbell

The hands were symmetrically positioned in relation to the barbell middle plane. In order to investigate how the spacing of the hands affects the activity of the pectoralis muscle fascicles attached to the thorax and the reaction forces in the glenohumeral joint, two different cases were investigated: Case 1 – spacing between hands of 0,6 m (Fig. 16,18); Case 2 – spacing between hands 0,8 m (Fig. 17,19).

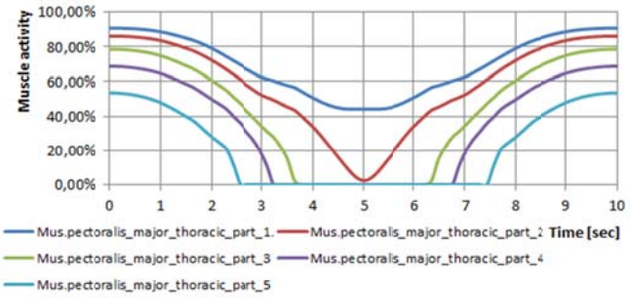

Fig. 16 Activity of the pectoralis muscle fascicles attached to the thorax – case 1

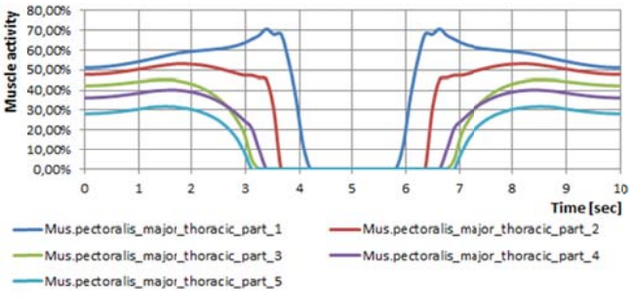

Fig. 17 Activity of the pectoralis muscle fascicles attached to the thorax – case 2

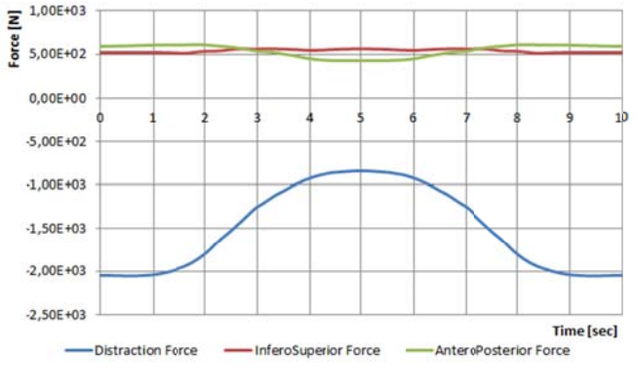

Fig. 18 Reaction forces in the GlenoHumeral joint – case 1

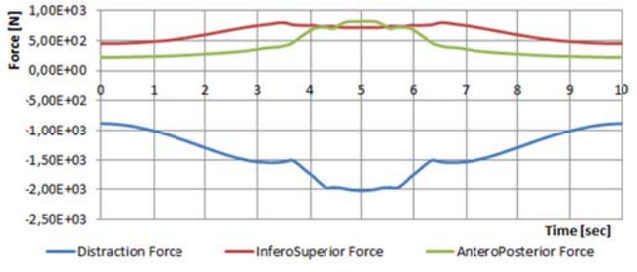

Fig. 19 Reaction forces in the GlenoHumeral joint – case 2

According to the obtained results, it is obvious that the bench press with the smaller distance between hands (case 1) would produce more activity in the pectoralis muscle and consequently better training results.

IV. Summary and Conclusions

Modelling humans and other creatures in the forms of musculoskeletal systems is very demanding task. It is virtually impossible to simulate realistic musculoskeletal systems by hand or even develop them bottom-up by general mathematical software. The only viable solution is to use a computer system designed for this particular purpose.

This paper gives a general overview of the AMS, the state-of-the-art software solution for modelling and simulating mechanics of musculosceletal systems. To this end, examples of two weight training exercises are presented using the full human body model from the AMMR (standing and free posture models).

Using the AnyScript modelling language certain details were programmed in order to simulate the movement of the analysed activities, which are always necessary input data for the subsequent inverse dynamics analysis.

Through the charts, various output results from the conducted kinematics and inverse dynamics analyses were presented, thus demonstrating great potentials of the AMS. Indeed, The AMS seems to be a powerful tool intended to the biomechanics researchers, designer engineers and physicians, interested in investigation of the musculoskeletal system of the human body and making optimised products to be in contact with humans.

ACNOWLEDGMENTS

Authors would like to thank Federal Ministry of Education and Science, Bosnia and Herzegovina, for their financial support intended for the purchase of the AMS.

REFERENCES

1. Aalborg University at http://www.enaau.dk
2. AnyBody Technology at http://www.anybodytech.com
3. P.E. Nikravesh, *Computer-Aided Analysis of Mechanical Systems*, Prantice Hall Inc.,Englewood Cliff,NJ,1988.
4. Gordon Robertson, Graham Caldwell, Joseph Hamill, Gary Kamen, Saunders Whittlesey, *Research Methods in Biomechanics,* Human Kinetics; 2nd edition, 2014.
5. Michael Damsgaard, John Rasmussen, SørenTørholm Christensen, EgidijusSurma, Mark dee Zee, Analysis of musculoskeletal systems in the AnyBody Modeling System, *Simulation Modelling Practice and Theory, Volume 14,* Issue 8, 2006, pp 1100 – 1111.
6. AnyScript community at http://www.anyscript.org
7. AnyBody Technology publication list at http://www.anybodytech.com/index.php?id=publications
8. AnyBody Model Repository at http://forge.anyscript.org/gf/
9. SolidWorks at http://www.solidworks.com
10. Abaqus at http://www.3ds.com

Mr.sc. Denis Spahić,Faculty of Mechanical Engineering, University of Zenica, Fakultetska1, 72 000Zenica, BiH (phone: 387-32-449-120; e-mail: dspahic@mf.unze.ba).

Three Dimensional Airway Tree Segmentation from Computed Tomography Lung Images

Nihad Mešanović[1], Haris Huseinagić[2] and Elnur Smajić[3]

[1] University Clinical Center Tuzla, IT Department, Tuzla, B&H
[2]University Clinical Center Tuzla, Radiology Department, Tuzla, B&H
[3]University Clinical Center Tuzla, Cardiology Department, Tuzla, B&H

Abstract— **One of the most important operations in analysis of medical images is segmentation. Computer aided detection (CAD) systems for analysis of medical images always involve segmentation of the image, as well as extraction of region of interest (ROI) and correct classification of area of interest. In this work, we are proposing a region growing algorithm for segmentation of lung structures, that is, airway segmentation. Due to the natural complex anatomical structure of the airways, with different branching levels, as well as originated noise and other artefacts in the CT image, the segmentation is more complex that other lung structures. A common method to segment the airway structure is region growing and semi-automated as well as fully automatic algorithms have been used for segmentation.**

This algorithm works in three dimensional space and the results are compared with the raw gray-scale volume image. The algorithm is using also morphological operators for accuracy. For evaluation of the results, three newly invented descriptors are used for efficient airway segmentation. The algorithm is tested on images from patients with lung CT scans. For verification of the results, we used Student t-test and Pearson correlation test that showed high correlation with the manual segmentation.

Keywords - **Airway Segmentation, CAD System, CT.**

I. Introduction

Computer aided diagnosis of lung CT image has been a remarkable step in medical image analysis, mainly in the early detection and diagnosis of lung abnormalities. Advanced image processing algorithms are applied on the images to clarify and enhance the image and then to separate the region of interest from the whole image. Computer-aided diagnosis (CAD) may be used as a second reader by analyzing nodules, tumors or lesions and as well as providing a malignancy estimate using computer vision and machine learning techniques. CAD may be used to solve the issues in diagnosis characterization, for example as the increased demand on radiologist's time caused by the large data volume, radiologist distraction in daily duties, and differences in radiologists' experience. Our main goal is to develop an effective CAD system that can assist radiologists in setting the right lung diagnosis. CAD systems for medical images usually involve the steps of segmentation the image, extraction of various region of interests (ROI) and classification of that regions. Different algorithms from different authors can be found for medical image segmentation such as thresholding [1], region growing [2, 3]. Different window width and level settings can also effect the image reconstruction [4]. These factors contribute to inaccuracies in the measured volume [5], resulting in inconsistency and uncertainty in detecting volume change in serial CT scans. Even for the identical imaging conditions, CT images will contain difference in image data, sometimes from the detector itself, noise received from the CT modality or the detectors, noise from the patient itself, or from the different procedures of the technician that is performing the scan.

Airway tree segmentation is the process of finding and extracting the anatomical structures that lead the air into the right and left lung. With the result of the segmentation, radiologists and medical practitioners can make measurements, check for abnormalities or lesions and generally be assisted in diagnosing diseases in the lung overalls. In this work, focus is set on the segmentation of the airway tree, the trachea and bronchi. Due to the natural complexity of the airway tree, with several branching levels, any noise or other artifacts present in the CT image, the segmentation can be affected in many ways. A common method to solve the problem of segmentation is region growing [6], and semi and fully automated region growing algorithms have been used to segment the airways [7-9]. In this process, the user provides one or more seed points inside the airway structure. From these points, a region is grown by recursively aggregating voxels that have a certain similarity test. Common similarity tests check differences in intensity between neighboring voxels. One common problem of region growing algorithms is leakage (Figure 1). In the case of the airway tree segmentation, a thin wall separates the structure from neighboring organs and air inside the lungs, so the noise or other artifacts can create holes in this wall and, since the airway and the interior surface of the lungs have similar voxel intensities due to partial volume effect, the entire lung area can be added to the segmented region. Another problem specific to airway tree segmentation is the

early collapse of branches, and in this case, the growing process stops too early and it only add partially segmented branches, so it can lead to bad segmentation.

Fig. 1 Characteristic leakage into lungs. Leakage usually occurs because the contrast of the bronchi wall is lowered by blurring caused by the partial volume effect

There is no universal segmentation algorithm that can be used in CAD (computer aided detection) applications for segmentation of human organs, or even, the same algorithm cannot be used for images from different diagnostic modalities. This paper propose an approach based on a region growing algorithm technique in order to segment the airway area from CT images and compare the results with the manual segmentation that is used as a ground truth, however, manual segmentation methods are labor intensive and subject of inter-observer errors and also subjective approach can lead to different results from different radiologists.

A. Overview of lung anatomy and previous work on airway segmentation

Human lungs consist of two major parts, the left lung and the right lung, and each lung is separated into lobes (Figure 2). Each lung is separated by lines, called fissures, and the right lungs have two fissures - major fissure and minor fissure. The left lung shows a slightly different structure, there is no defined minor fissure; it consists of only two lobes. Furthermore, each lobe is divided into more lung segments of which ten exist in each part of the lung. These segments contain branching trees (bronchi and bronchioles) that conduct blood and air into the distal regions where the gas exchange takes place (Figure 3). The bronchial tree has a pipe structure that is filled with air, and it starts at the trachea at the top and extends into the regions that are split into smaller and smaller branches. The splitting occurs usually in bifurcations, the parent branch splits up into two child branches, but trifurcations also exist.

The bronchi are further segmented into lobar bronchi that supply 5 lung lobes, segmental bronchi that supplies 20 segments, and sub-segmental bronchi. High-resolution multislice MSCT can show up bronchi segments of the 7th branching generation which can have diameters in the mm range, and the diameters of fourth generation airway in a typical CT image are about two or three voxels wide. The limitation of imaging resolution can add the blurring effects around airway wall and noise can lead to the different homogeneity of image intensities inside airway walls.

Segmentation of airway trees from CT images is critical for various clinical applications involving pulmonary diseases. Various algorithms have been proposed in the literature. Many of these algorithms have shown successful segmentation of the bronchi and trachea. However, for the higher generations of branches in the airway tree, current segmentation results still have room for improvement, indicated by a evaluation on 15 airway segmentation algorithms [10]. Schlathölter et al. [11] use a front-propagation algorithm for airway tree segmentation. Branchpoints are detected when the front splits up, while Tschirren et al proposed to keep an active region of spherical shape and to extended the region to i+1 possible branch [12]. A multi-threshold approach was adopted in [13] to increase robustness in growing airways trees. Pu et al. [14] used principal curvatures and directions in differentiating airways from other lung tissues in geometric space. The work of [15] focused on extending thin airways in the initial segmentation by computing the shortest paths inside a search sphere from end points. Previous work on airway segmentation mainly includes region growing methods [16-18], [9], morphology operators [19-21], and combinations of the region growing and morphological operators [22-24]. Other methods proposed in the past include rule based methods [25-26], energy function minimization [21], ROI modification-based techniques [27], as well as empirical methods [28-31].

II. MATERIALS AND METHODS

The main source of image data for implementation of this algorithm is images from the Picture Archiving and Communication System (PACS), a radiological system that is used for transferring the radiological images from the modalities to servers, and is available immediately to users, regardless to their location. PACS database in University Clinical Center Tuzla contains over 25.000.000 CT images, so for the testing and evaluation purposes images are used from PACS database. A total number of 15 patients were taken into consideration with total number of 6645 (average 443) slices. Low dose CT scans were done in full inspiration phase, without contrast, with the following parameters: 120 KVp, 100mAs with a single pitch of 1.25, 0.5 second rotation time and 0.6875 pixel spacing.

The algorithm consists of five steps (Figure 4):

1. First step is analyzing the image histogram for an optimal gray-value threshold Th_i is found for the segmentation of the airway tree, and the initial threshold is set to -1000 HU. Histogram thresholding is used for determination of the actual binary masks for the airway area. Binary masks are generated from input gray level CT data using an iterative thresholding algorithm, a better method than the conventional thresholding algorithm, in which the threshold is simply chosen as the minimum between the two maxima of the gray level histogram [32]. Afterwards, the sample mean of the gray values associated with the foreground pixels and the sample mean of the gray values associated with the background pixels are computed, and a new threshold value is determined as the average of these two sample means. The process is repeated until the threshold value does not change anymore, that means until the threshold in step i meets the following $Th_i=Th_{i+1}$.
2. Second step is analyzing the first slice of the CT series, the algorithm is finding the image center of gravity, and for the 5cmx5cm window region is looking for the oval or round shape that conforms the statement empirically found by consulting medical literature [28-31]: $100mm^2$ < Possible Trachea Area < $625\ mm^2$. If not found on the first slice, the algorithm is looking in consecutive ones until the tracheal area is found.
3. After the second step, the seed pixel for the region growing algorithm is selected in the trachea, and a 3D Region Growing (RG) with 4-connected neighbors is applied to the stack of CT images. Voxels are included in the grown region if their Hounsfield number is smaller than Th_i. The result is a binary mask (BM) of the airways tree, containing the trachea, the external airways, and the bronchi. To prevent the leakage into parenchyma, every time the new radius of segmented area in step i+1 is compared to the 150% radius of the previous area in step i. The leak is excluded by iteratively changing the threshold value (Figure 5). While region growing propagate, the skeleton and the current radius are calculated, and this information is used to prevent leakage in lung parenchyma. The algorithm terminates once the previous statement is fullled.
4. Morphological 3D closing is separately applied to BM for the inclusion the missing voxels corresponding to voxels that are excluded due to their high attenuation and partial volume effect, and the overall binary mask (OBM) is created, that contains airway tree and bronchial details.
5. Region growing may, due to partial volume effect, sometimes give unsatisfactory results, so we applied 1 voxel dilation (1 on x, 1 on y and 1 on z direction) to fill these gaps and to compensate for the lumen wall thickness.

The algorithm was tested by using Mevislab version 2.2 software and for evaluating the results, radiologists used Voxar workstation, on a standard diagnostic workstation.

B. Establishment of ground truth

In order to compare the result of our method, the perfect way is to compare it with the ground truth, however, manual tracing of the extracted region would be very time consuming. In the modern literature [16-18, 22, 24, 33, 34], there is no evidence of manual segmentation of the lung airways, and in the case of a high-resolution CT image that can include over 500 slices, it is very time consuming to draw the tracings slice-by-slice and difficult to maintain high accuracy of the human tracings in 3-D.

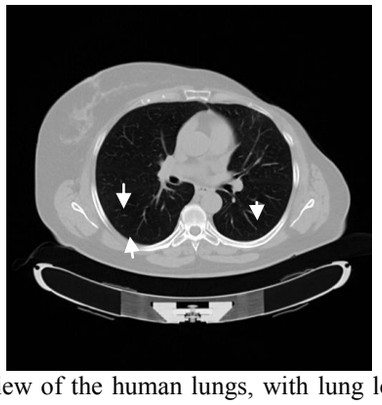

Fig. 2 Overview of the human lungs, with lung lobes, with fissures (lines shown with white arrows) between them. Image taken from PACS system, for better understanding of the human anatomy.

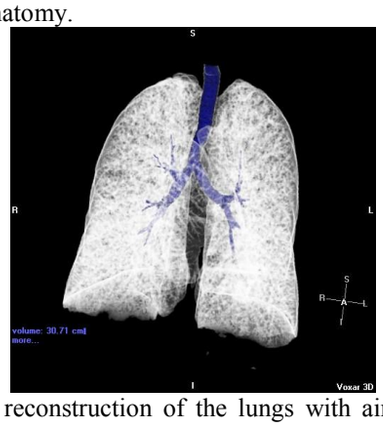

Fig 3 3D reconstruction of the lungs with airway trees superimposed on the lungs parenchyma. The volume shown on the image represents only the volume for the segmented area (blue). Image taken from PACS system, with segmented airway back projected on the human lungs.

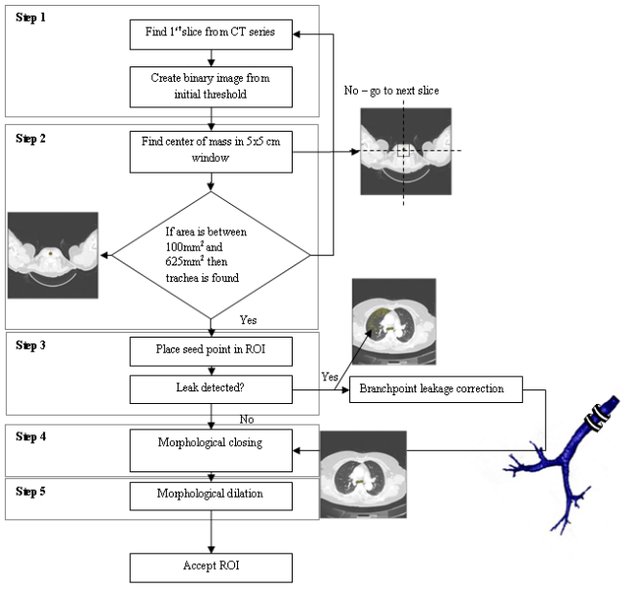

Fig 4 Detailed steps of automated airway tree detection method.

To test the results, we started with two radiologists with over 20 years of experience that helped to establish the airway segmentations ground truth. Radiologists first applied segmentation technique on the CT console, with the software that they are using for lung segmentation, in this case Voxar 3D workstation. All thin-section CT images obtained with volumetric acquisition were imported into the workstation in DICOM format by using a local area network. The first step in this procedure was to perform automatic segmentation of the bronchial lumen on the basis of noise filtering; this was followed by thresholding between two specified values; in this case, −1023 HU and −920 HU, however, radiologists did change these values in order to get satisfactory results. An observer placed a seed point within the lumen of the trachea on the first CT section of the volume. The software automatically reconstructed the bronchial binary volume from the voxels previously bithresholded. The binary volume was considered complete when all the connected voxels were involved. After the automatic processing, the radiologists edited the results to in order to delete false detections and add missing airway details. When the radiologists were satisfied with the edited results, the 3-D connected tree rooted at the trachea was extracted and saved for use as the ground truth. This procedure was repeated for each of the images in the validation data set. With this method the resulted area include the volume of the segmented airway area.

After establishing this area as the ground truth, we apply our segmentation method with region growing method on

the same set of patient data. Segmentation algorithm was performed by selecting the upper and lower threshold and keeping the intermediary results. We noticed that due to different anatomical and physiological state of each patient with different lung density, there is no fixed threshold that we can use, so the threshold for segmentation was adapted for each patient data. We made a quantitative evaluation by comparing the segmentation result with this algorithm of the segmented volume with the ground truth.

For evaluating segmentation methods, we considered the following factors for recognition: accuracy (agreement with ground truth) and efficiency (time taken for segmentation). In practice, it is almost impossible to establish true segmentation. In determining accuracy, it may be important to consider different landmark areas of the structure to be segmented depending on the application. To assess efficiency, computational and the user time is required for algorithm and operator training and for algorithm execution should be measured and analyzed. Accuracy, and efficiency are interdependent and segmentation methods are compared based on these factors.

Let I1 be the segmented area from image I. For any set of segmented voxels SA $\in$ I, let be the area representing the object defined by an object o in I obtained by using method RG, and let SA_1 be the corresponding segmented voxels with ground truth method. We use following measures for characterization of the accuracy:

False Negative Volume Area:

_____

False Positive Volume Area:

_____

True Positive Volume Area:

_____

The meaning of these measures is all expressed as a fraction of the volume of true overlaps. FNVA indicates the area fraction of tissue defined in SA_1 that was missed by method RG in area overlap. FPVA denotes the amount of tissue falsely identified by method RG as a area of the total amount of tissue in SA_1 TPVA describes the area of the total amount of tissue in SA_1 with which the object SARG overlaps.

The main purpose of the airway segmentation was developed for qualitative and quantitative purposes, and with this in mind, we created evaluation criteria for the evaluation of our method.

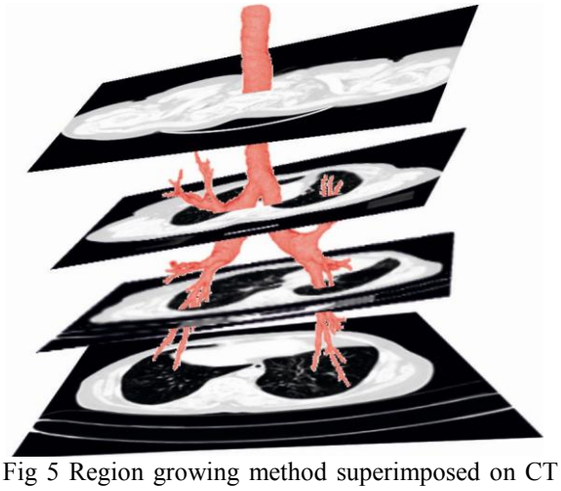

Fig 5 Region growing method superimposed on CT images.

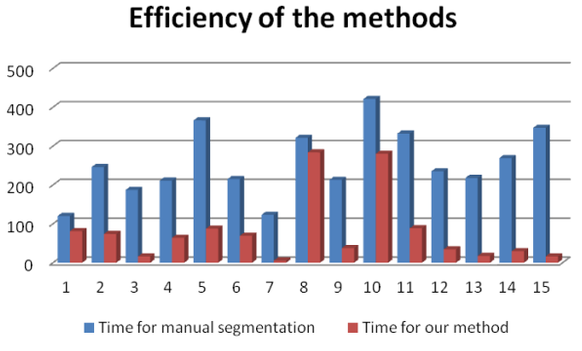

Fig. 6 Comparison of time needed for efficiency of the processes. We can conclude that the proposed method is faster than the manual segmentation. Average time for manual segmentation with commercial software is 245 seconds per patient; our method took 74 seconds per patient.

III. Results

With manual segmentation results, radiologists separately inspected images, and visually verified the correctness of the segmentations. The test outcome was satisfactory since accurate segmentation was achieved on about 95% of the test sample compared to the manual segmentation. To inspect the quality of the overall process, a Pearson and student T-test were used, to show how our method correlates with the proposed ground truth. The mean volume change (M=0.618, SD =3.1933, N= 15) was significantly greater than zero, t(15)=-0.75, providing evidence that our method is effective in airway segmentation in comparison with the ground truth. Pearson correlation coefficient is used as a

measure of similarity, and with the P=0.981, we can conclude that there is a significant correlation between our method and the ground truth. A 95 % C.I. about mean volume difference is (-1.1504, 2.386). Our method did outperformed the ground truth in 60% of thepatient test data, and the results can be seen in Figure 6.

IV. DISCUSSION

The main goal of this algorithm is to propose a method for airway segmentation to allow radiologists to move away from the working console as well as to avoid the need of expensive software applications provided by the different vendors. The algorithm main features are the use of adaptive thresholding, region growing and morphological operators. The algorithm, tested on 15 patients high-resolution CT scans, provides high performance, and segmentation quality, showing good accuracy in the airway segmentation, as stated by comparison against ground truth and by visual inspection by our radiologists. RG operations take approx 3 seconds per patient, and the algorithm execution time is about 74 seconds for a 500-slice CT scan, on a two quad-core Intel Xeon CPU workstation.

V. CONCLUSIONS

In this paper, we proposed a completely three-dimensional algorithm for automated lung segmentation in chest CT scans. It provides a good basis for a CAD system for airway segmentation and detection and is being integrated with the region growing based lung segmentation algorithm.

REFERENCES

1. Brown MS, McNitt-Gray MF, Goldin JG, Suh RD, Sayre JW, Aberle DR, Patient-specific models for lung nodule detection and surveillance in CT images, IEEE Transactions on Medical Imaging, 20:12, 2001.
2. Croisille P, Souto M, Cova M, Wood S, Afework Y, Kuhlman JE, Zerhouni EA, Pulmonary nodules: improved detection with vascular segmentation and extraction with spiral CT, Radiology, 197:2, 1995.
3. Harris K, Adams H, Lloyd D, Harvey D, The effect on apparent size of simulated pulmonary nodules of using three standard CT window settings, Clin Radiol, 47:2, 1993.
4. Winer-Muram HT, Jennings SG, Meyer CA, Liang Y, Aisen AM., Tarver RD, McGarry RC, Effect of varying CT section width on volumetric measurement of lung tumors and application of compensatory equations, Radiology, 229:1, 2003.
5. Gonzalez RC,Woods RE, Digital Image Processing, Addison-Wesley Longman Publishing, 2001.
6. Chiplunkar R, Reinhardt JM, Hoffman EA, Segmentation and quantification of the primary human airway tree, Proc. SPIE Medical Imaging. 3033, pp. 403-414, 1997.
7. Kiraly AP, Higgins WE, McLennan G, Hoffman EA, Reinhardt JM, Three-dimensional human airway segmentation methods for clinical virtual bronchoscopy, Academic Radiology 9:10, 2002.
8. Law TY, Heng PA, Automated extraction of bronchus from 3D CT images of lung based on genetic algorithm and 3D region growing, SPIE Proceedings on Medical Imaging, San Diego, CA, 3978, pp. 906-916, 2000.
9. Lo P, van Ginneken B, Reinhardt J, de Bruijne M, Extraction of airways from ct (exact'09), In Proceedings of the Second International Workshop on Pulmonary Image Analysis, pp. 175-189, 2009.
10. Schlathölter T, Lorenz C, Carlsen IC, Renisch S, Deschamps T, Simultaneous Segmentation and Tree Reconstruction of the Airways for Virtual Bronchoscopy, SPIE Medical Imaging 2002, Image Processing. San Diego, CA, pp. 103-113, 2002.
11. Tschirren, J., Hoffman, E., McLennan, G., Sonka, M.: „Intrathoracic airway trees: segmentation and airway morphology analysis from low-dose ct scans",IEEE Transactions Medical Imaging, 24:12, 2005.
12. Ginneken B, Baggerman W, van Rikxoort E, Robust segmentation and anatomical labeling of the airway tree from thoracic ct scans, Medical Image Computing and Computer-Assisted Intervention, 11:1, 2008.
13. Pu et al, A Differential Geometric Approach to Automated Segmentation of Human Airway Tree, IEEE Transactions on Medical Imaging, 30:2, 2011.
14. Lo P, Sporring J, Pedersen JJ, Bruijne M, Airway tree extraction with locally optimal paths, Medical Image Computing and Computer-Assisted Intervention, 12:2, 2009.
15. Chiplunkar R, Reinhardt JM, Hoffman EA, Segmentation and quantitation of the primary human airway tree, SPIE Medical Imaging, San Diego, CA: 1997.
16. Tozaki T, Kawata Y, Niki N, Ohmatsu H, Kakinuma R, Eguchi K, Kaneko M, Moriyama N, Pulmonary Organs Analysis for Differential Diagnosis Based on Thoracic Thin-section CT Images, IEEE Transactions on Nuclear Science, 45:6, 1998.
17. Mori K, Suenaga Y, Toriwaki J, Automated anatomical labeling of the bronchial branch and its application to the virtual bronchoscopy, IEEE Transactions on Medical Imaging, 19:2, 2000.
18. Pisupati C, Wolf L, Mitzner W, Zerhouni E, Mathematical morphology and its applications to image and signal processing, Kluwer Academic Publishers, 1996.
19. Prêteux F, Fetita CI, Grenier P, Capderou A, Modeling, segmentation, and caliber estimation of bronchi in high-resolution computerized tomography, Journal of Electronic Imaging, 18:1, 1999.
20. Fetita CI, Prêteux F, Quantitative 3D CT bronchography, Proceedings IEEE International Symposium on Biomedical Imaging (ISBI'02), Washington DC, 2002.
21. Bilgen D, Segmentation and analysis of the human airway tree from 3D X-ray CT images, The University of Iowa, IA, USA, Master's thesis, 2000.
22. Kiraly AP, 3D Image Analysis and Visualization of Tubular Structures, The Pennsylvania State University, Dept. of Computer Science and Engineering, Ph.D. dissertation, 2003.
23. Aykac D, Hoffman EA, McLennan G, Reinhardt JM, Segmentation and analysis of the human airway tree from 3D X-Ray CT images, IEEE Trans. Medical Imaging, 22:8, 2003.

24. Sonka M, Sundaramoorthy G, Hoffman EA, Knowledge-Based Segmentation of Intrathoracic Airways from Multidimensional High Resolution CT Images, Proceedings SPIE, 2168, 1994.
25. Park W, Hoffman EA, Sonka M, Segmentation of intrathoracic airway trees: a fuzzy logic approach, IEEE Transactions Medical Imaging, 17:8, 1998.
26. Kitasaka T, Mori K, Hasegawa H, Suenaga Y, Toriwaki J, Extraction of bronchus regions from 3D chest X-ray CT images by using structural features of bronchus, Computer Assisted Radiology and Surgery (CARS) 2003, International Congress Series 1256, pp. 240-245, 2003.
27. Holbert JM, Strollo DC, Imaging of the normal trachea. J Thorac Imaging 10:3, 1995.
28. Gamsu G, Webb WR, Computed tomography of the trachea: normal and abnormal. AJR Am J Roentgenol, 139: 2, 1982.
29. Vock P, Spiegel T, Fram EK, Effmann EL, CT assessment of the adult intrathoracic cross section of the trachea. J Comput Assist Tomogr; 8:6, 1984.
30. Breatnach E, Abbott GC, Fraser RG, Dimensions of the normal human trachea. AJR Am J Roentgenol, 142:5, 1983.
31. Hu S, Hofman EA, Reinhardt JM, Automatic Lung Segmentation for Accurate Quantitation of Volumetric X-Ray CT Images, IEEE Transactions on Medical Imaging, 20:6, 2001.
32. Palágyi K, Tschirren J, Hoffman EA, Sonka M, Quantitative analysis of pulmonary airway tree structures, Computers in Biology and Medicine, 36:9, 2006.
33. Tschirren J, McLennan G, Palágyi K, Hoffman EA, Sonka M, Matching and anatomical labeling of human airway tree, IEEE Transactions on Medical Imaging, 24:12, 2005.
34. Mesanovic N., Huseinagic, H., Mujagic, S., "3D Tracheobronchial Airway Tree Segmentation from Thorax CT Images", Biomedical Engineering: Applications, Basis and Communications Journal, Vol. 25:2, pp. 1-11, 2013.

Nihad Mešanović,University Clinical Center Tuzla,Trnovac bb, 75 000 Tuzla, BiH (phone: 387-35-303-445;
e-mail: nihad.mesanovic@ukctuzla.ba

SOFTVERSKO RJEŠENJE U DIFERENCIJACIJI I TRETMANU POREMEĆAJA ACIDO-BAZNOG STATUSA

Edin Begić[1], Mensur Mandžuka[2], Zijo Begić[3], Dušanka Bošković[2], Izet Mašić[1]

[1] Medicinski fakultet, Univerzitet u Sarajevu, BiH
[2] Elektrotehnički fakultet, Univerzitet u Sarajevu, BiH
[3] Pedijatrijska klinika, Klinički Centar Univerziteta u Sarajevu, Sarajevo, BiH

Sažetak— **Normalan acidobazni status (izohidrija) predstavlja vrijednost jona vodika u ekstracelularnoj tekućini unutar granica vrijednosti pH od 7,36 (44 nmol/L) do 7,44 (36nmol/L). Poremećaji acidobaznog statusa idu u dva smjera, u acidozu i alkalozu. Iz gasne analize arterijske krvi, može se utvrditi poremećaj, uvidjeti da li je nekompenzovan ili kompenzovan djelovanjem samih mehanizama organizma (puferski sistemi). Procesi koji dovode do narušavanja acidobaznog statusa su respiratorne i metaboličke prirode, i na osnovu njih je izvršena i sama klasifikacija poremećaja. Na osnovu analize krvi, dobivene informacije, uz podatak o tjelesnoj težini, se unose u softversko rješenje, i u prvom koraku se dobivaju informacije o kojoj se vrsti poremećaja acidobaznog statusa radi. U drugom koraku se određuje signifikantnost poremećaja, a treći korak bi predstavljao terapijski tretman. Softver nudi mogućnosti opcionalnog unošenja vrijednosti nivoa minerala, te na osnovu toga i upotpunjenje tretmana. Visok radni takt procesora u komercijalnim mobilnim uređajima nudi značajan računarski potencijal na dohvat ruke. S ciljem eliminacije potrebe za nabavkom specijaliziranog hardvera, te povećavanjem dostupnosti i mobilnosti sistema, rješenje je razvijano za Android platformu, koristeći programski jezik Java.**

Ključne riječi - **acidobazni status, poremećaj, tretman, Android.**

I. UVOD

Normalni acidobazni status organizma uključuje promjenu koncentracije vodikovih jona u ekstracelularnoj tekućini unutar uskih granica vrijednosti pH, od 7,36 (44nmol/L) do 7,44 (36nmol/L) [1]. Acidobazni status transcelularnog prostora se regulira aktivnim prijenosom kiselina, odnosno baza izvan ćelijskog prostora. Patološka stanja s povećanom koncentracijom vodikovih jona jesu acidoze, a alkaloze su stanja sa smanjenom koncentracijom vodikovih jona. Acidoza i alkaloza predstavljaju pojmove koji su vezani sa sistemske poremećaje koncentracije vodikovih jona. Poremećaji u koncentraciji, nastali u krvi, nazivaju se acidemija, odnosno alkalemija. Da bi se acidobazni status održao u fiziološkim granicama, organizam angažuje moćne regulatorne mehanizme: puferske sisteme, pluća, bubrege i koštani sistem. Puferski sistemi djeluju gotovo trenutno, ali imaju relativno mali kapacitet. Respiratorni sistem se aktiviše poslije nekoliko sati, a najmoćniji puferski kapacitet imaju bubrezi i koštani sistem, ali njima treba i najviše vremena. Puferski sistemi djeluju i u ekstracularnoj i intracelularnoj tekućini. Najvažniji ekstracelularni sistem je bikarbonantni puferski sistem, a intracelularni, proteinski i fosfatni puferski sistem [2]. S obzirom da imaju mogućnost da odstrane ugljen-dioksid izvan organizma, pluća mogu u velikoj mjeri da utiču na acidobazni status. Ako se ventilacija pluća duplira, pH vrijednost krvi će se povećati (alkaloza), a ako se ventilacija pluća smanji, i pH krvi će se smanjiti (acidoza). Ukupna moć puferisanja respiratornog sistema skoro je dvostruko veća od moći svih hemijskih puferskih sistema zajedno. Bubrežni sistem, djeluje puferski, tako što konzerviraju filtrirane bikarbonate, reguliraju titrabilni aciditet, te formiraju amonijačni jon. Uloga koštanog sistema je u korekciji hroničnih poremećaja acidobaznog statusa. U stanjima hronične acidoze, nastaje demineralizacija koštanog tkiva (oslobađanje kalcija i bikarbonata), čime se može kompenzirati poremećaj acidobaznog statusa.

II. POREMEĆAJI ACIDO-BAZNOG STATUSA

Uzroci acidobaznih poremećaja mogu biti metabolički ili disfunkcije respiratornog sistema. Prema tome poremećaji acidobaznog statusa obuhvataju četiri osnovna poremećaja: metaboličku i respiratornu acidozu, te metaboličku i respiratornu alkalozu. Prema promjeni pH vrijednosti krvi (ukoliko je uopće prisutan kompenzatorni mehanizam), sama kompenzacija može biti: potpuna – potpuna normalizacija pH vrijednosti uz očuvanost kompenzatornih mehanizama, subkompenzacija – nepotpuno korigovana pH vrijednost uz očuvanost kompenzatornih mehanizama i dekompenzacija-promijenjena pH vrijednost i odsustvo kompenzatornih mehanizama.

Metabolička acidoza (pH <7,35, smanjen nivo bikarbonata <24 mmol/L, kompenzatorna hiperventilacija-smanjen pCO_2) nastaje usljed povećanja količine vodikovih jona i usljed gubitka bikarbonatnih jona (povećani unos kiselina, povećana sinteza neisparljivih kiselina,

nagomilavanje metaboličkih kiselina, hronična bubrežna insuficijencija, distalna renalna tubularna acidoza, dijareja, maligni procesi, proksimalna renalna tubularna acidoza, Fanconijev sindrom, Wilsonova bolest). Bazni deficit je osnova metaboličke acidoze, te nastaje zbog nabrojanih etioloških faktora. Na račun smanjenja plazmatske koncentracije bikarbonata (služe za puferiranje vodikovih jona), povećava se koncentracija drugih aniona (radi postizanja i održavanja elektroneutralnosti). Anion može biti hlorid (Cl^-) ili anion neke druge metabolički proizvedene kiseline. Na osnovu toga razlikujemo: hiperhloremijske metaboličke acidoze (bubrežni poremćaji - intersticijski nefritis s azotemijom, hidronefroza, proksimalna i distalna renalna tubularna acidoza, gastrointestinalni uzroci - prolivi, uretero-enterostomija), metaboličke acidoze s anionskim manjkom (zatajivanje bubrega, dijabetička ketoacidoza, L-laktacidemija, unos salicilata) i njihove kombinacije (D-laktacidemija) [3]. Gap aniona (Na^+ (mmol/L) – (Cl^- (mmol/L) + HCO_3^- (mmol/L)) veći od 15 mmol/L upućuje, a veći od 25 mmol/L potvrđuje metaboličku acidozu, te na osnovu njegove vrijednosti može se odrediti da li se radi o acidozi s povećanim ili normalnim gapom aniona.

Osnovni uzrok respiratorne acidoze (pH <7,35, povišen pCO_2, kompenzatorno pad nivoa bikarbonata <24 mmol/L) je akutna ili hronična insuficijencija respiratornog sistema (akutna opstrukcija disajnih puteva, akutne restrikcijske bolesti pluća, akutna insuficijencija cirkulatornog sistema, depresija respiratornog centra, neurološke bolesti-poliomijelitis, polineuropatije, miastenija gravis, hronične opstrukcijske bolesti pluća, hronična inhibicija centra za disanje, bolesti zida grudnog koša, bolesti plućnog parenhima).

Metabolička alkaloza (pH >7,45, nivo bikarbonata>24 mmol/L, kompenzatorna hipoventilacija - povećan pCO_2) nastaje zbog gubitka kiselina ekstracelularne tekućine (gubitak HCl povraćanjem, hipokaliemija, hiperkalciemija, primjena diuretika koji ne štede kalij-furosemid, etakrinska kiselina) te usljed djelovanja faktora koji povećavaju koncentraciju bikarbonata u ekstraćelijskoj tečnosti (mliječno-alkalni sindrom, Connova bolest, Liddle-ov sindrom, terapijska primjena mineralokortikoida, primjena soli organskih kiselina, post hiperkapnijska stanja). Metaboličke alkaloze možemo podijeliti na one koje su ovisne o soli - Cl^- odgovorne (konstrikcijaska alkaloza, povraćanje, upotreba diuretika, unos antacida – hloridi ih ispravljaju) i na one koje o soli ne ovise- Cl^- rezistentne (ne koristi se natrijev hlorid u tretmanu, koristi se kalijev hlorid-prisutnost hlorida u mokraći).

Respiratorna alkaloza (pH >7,45, hiperventilacija – smanjen pCO_2, kompenzatorno smanjenje nivoa bikarbonata <24 mmol/L) je takav poremećaj acidobaznog statusa kod kojeg povećana alveolarna ventilacija uzrokuje smanjenje pCO_2, sljedstveno tome i smanjenje nivoa bikarbonata, te povećanje pH vrijednosti krvi. Dijeli se na akutnu (hiperventilacija zbog anksioznosti, visoka temperature, trovanje salicilatima, sepsa) i hroničnu (tumori mozga, encefalitis, ciroza jetre, koma, trudnoća).

Tabela 1. Poremećaji u koncentraciji jona i parcijalnog pritiska CO_2 nastali usljed poremećaja acido-baznog statusa (S-smanjeno, P – povećano, + - oznaka za primarni poremećaj)

	pH	**H^+**	**pCO_2**	**HCO_3^-**
Normalno	7,4	40 nmol/L	5,3 kPa	24 nmol/L
Respiratorna acidoza	S	P	P+	P
Respiratorna alkaloza	P	S	S+	S
Metabolička acidoza	S	P	S	S+
Metabolička alkaloza	P	S	P	P+

U svakodnevnoj praksi sreću se i složeni oblici poremećaja acido-baznog statusa (kombinacije pomenutih stanja). Mješoviti oblici mogu biti aditivni, kao kombinacija respiratorne i metaboličke acidoze (u dugotrajnoj šećernoj bolesti - kombinacija dijabetičke ketoacidoze i uremijske acidoze zbog dijabetičke nefropatije - teška acidemija). Kombinacija respiratorne i metaboličke alkaloze se najčešće viđa kod pacijenata koji su na respiratoru i nazogastričnoj sukciji – teška alkalemija. Kombinacije respiratorne alkaloze i metaboličke acidoze se javljaju u septičkom šoku i odlikuje se sniženom koncentracijom bikarbonata u plazmi i sniženim pCO_2. Respiratorna acidoza i metabolička alkaloza se javljaju kod hronične plućne opstruktivne bolesti, te prilikom upotrebe diuretika-povišena koncentracija bikarbonata u plazmi i povišen pCO_2.

Tačna dijagnoza je preduvjet pravilnog liječenja acido-baznih poremećaja. Na temelju anamneze, kliničke slike i laboratorijskih pretraga, možemo utvrditi postoji li poremećaj tjelesnih tekućina i acidobaznog statusa. Za laboratorijske pretrage uzima se arterijska krv, te je neophodna analiza pH, koncentracije bikarbonata i pCO_2 [4]. Terapija svih poremećaja se ogleda u etiološkom liječenju, kao i liječenju pratećih poremećaja koji mogu dovesti do pogoršanja samog poremećaja, sa posebnim osvrtom na koncentracije elektrolita u organizmu (poremećaji acidobaznog statusa, kao pratioca imaju i neki od poremećaja koncentracije elektrolita).

III. SOFTVERSKA DIJAGNOSTIKA POREMEĆAJA ACIDO-BAZNOG STATUSA

S ciljem maksimalne dostupnosti aplikacije razvijena je aplikacija za Android platformu u programskom jeziku Java. U 2012. godini tržišni udio Android uređaja iznosio je 75% na svjetskom tržištu, sa isporučenih 136 miliona uređaja [5]. Aplikacija zahtijeva unos ključnih parametara potrebnih za dijagnozu poremećaja acido-bazne ravnoteže:

- pH vrijednost krvi (normalna vrijednost 7.35-7.45),
- parcijalni pritisak ugljen-dioksida u krvi (izražen u kilopaskalima) (normalno 4.3-6.4 kPa),
- parcijalni pritisak kisika u krvi (izražen u kilopaskalima) (normalno 7.3-10.6 kPa),
- vrijednost bikarbonata izražena u mmol/L (normalno 24 mmol/L),
- bazni ekces i
- tjelesnu težinu pacijenta.

Dijagnoza acidobaznog poremećaja se postavlja na osnovu parametara dobivenih iz laboratorijskih nalaza arterijske krvi. Dijagnostička diferencija poremećaja acidobaznog statusa je vrlo specifična, te je jasno određena različitim parametrima (Slika 1.).

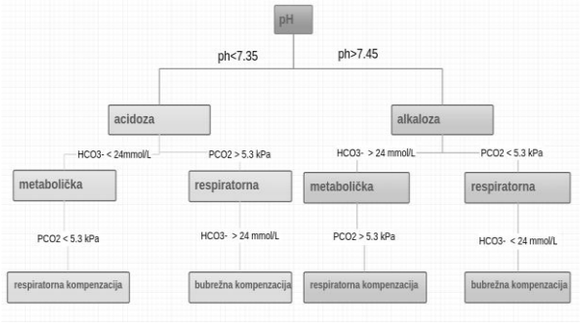

Slika 1. Dijagnoza acidobaznih poremećaja

Početni ekran aplikacije (Slika 2.) sadrži polja za unos već pomenutih podataka.

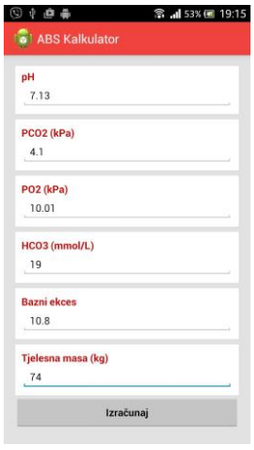

Slika 2. Početni ekran aplikacije

Podaci su karakteristični za određeni poremećaj ili kombinaciju poremećaja, te se na osnovu njih se može odrediti vrsta poremećaja, te kompenziranost poremećaja, odbrambenim mehanizmima organizma. Sljedeći korak predstavlja unos patoloških vrijednosti određenih elektrolita u organizmu (Slika 3. povišena vrijednost kalija – referentna vrijednost 3,5-5,2 mmol/L). Korisnik može odabrati i unijeti vrijednosti poremećaja jednog elemenata ili kombinaciju poremećenih vrijednosti više elemenata. Referetne vrijednosti natrija su 137 - 146 mmol/L , hlorida 101 - 111 mmol/L, kalcija 2,14 – 2,53 mmol/L, te magnezija 0,65 – 1,05 mmol/L.

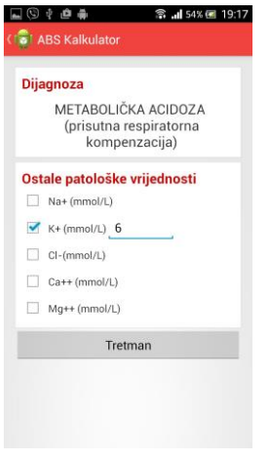

Slika 3. Dijagnoza poremećaja i prikaz opcionalnog unošenja dodatnih podataka

Na osnovu podataka unesenih sa Slike 2. i Slike 3. aplikacija preporučuje tretman pacijenta, sa tačno određenim vrijednostima neophodne terapije, na osnovu već zadatih

matematičkih formula i najnovijih smjernica za tretman određenog poremećaja (Slika 4.).

Slika 4. Tretman poremećaja

Osim što prikazuje terapiju samog poremećaja, navodi smjernice za rješavanje ostale problematike koja je striktno vezana za već postojeću dijagnozu koju pacijent ima. Na osnovu unesenih vrijednosti, aplikacija prepoznaje i uzima u obzir i kombinacije poremećaja acidobaznog statusa.

Pretrazivajući online rješenja, te literaturu iz oblasti telemedicine, došlo se do spoznaje da postoje mnoge Android i web aplikacije, koje u vidu kalkulatora daju opciju diferencijacije poremećaja, te neke od njih, određivanje njegove kompenziranosti. Ova aplikacija bi trebala biti pionir u savjetovanju terapije, uzimajući u obzir trenutno stanje pacijenta, njegove anamnesticke podatke, te već prisutne komorbiditete. S ciljem automatizacije procesa, buduća verzija aplikacije imat će funkcionalnost slikanja nalaza arterijske krvi. Unutar aplikacije vršila bi se analiza slike s ciljem izdvajanja neophodnih parametara. Biblioteka za optičko prepoznavanje karaktera omogućila bi automatsko popunjavanje polja neophodnih za dijagnozu poremećaja. Funkcionalnost bi bila omogućena kroz *open-source* Tessaract biblioteku, originalno razvijenu od strane Hewlett-Packard, a čiji dalji razvoj se od 2006. godine uključio i Google.

IV. Zaključak

Aplikacija predstavlja pomoć ljekaru u svakodnevnoj kliničkoj praksi te je orijentisana na tretman u jedinicima intenzivne njege. Lako je dostupna, praktična, te je izuzetno korisna u tretmanu metaboličke acidoze (smanjuje vrijeme potrebno za izračunavanje neophodne terapije-prilikom samog računanje potrebne vrijednosti natrijevog bikarbonata) i u terapiji metaboličke alkaloze (računanje viška bikarbonata). Rješenje sadrži smjernice za terapeutsko djelovanje svakog poremećaja, sa osvrtom na kolebanja oligoelemenata, te terapijskog djelovanja u slučaju njihovih poremećaja, što i u modernoj medicini predstavlja izazov u terapiji. Uključuje u terapiji i već postojeće komorbiditete pacijenta. Kombinacije poremećaja acido-baznog statusa mogu uveliko zakomplikovati rad ljekaru, te takve kombinacije predstavljaju i izazov prilikom pravljenja softverskog rješenja ovog tipa.

Literatura

1. Gamulin S., Marušić M., Kovač Z. i sur. *Patofiziologija*, knjiga prva, sedmo obnovljeno izdanje, Medicinska naklada, Zagreb, 2011.
2. Simonović-Živančević S., *Opšta patološka fiziologija*. Univerzitet u Kragujevcu, Kragujevac, 2006.
3. Jukić M i sur., *Intenzivna medicina*, Medicinska naklada, Zagreb, 2008.
4. Guyton C.A., Hall E.J., *Medicinska fiziologija*, Medicinska naklada, Zagreb, 2012.
5. Drake J., Lanier Z., Mulliner C., Fora P., Ridley S., Wicherski G., *Android Hacker's Handbook*, Wiley, SAD, 2014.

Edin Begić , Medicinski fakultet Sarajevo, BiH (phone: 387-61-303-375; e-mail: edinbegic90@gmail.com).

Farmaceutski inženjering

Mehović Semir[1], Dedić Mirza[2], Jordamović Nadir[3]

[1]JU Apoteke Sarajevo, Saliha Hadžihuseinovića Muveklita 11, 71000 Sarajevo,
[2]Farmaceutski fakultet, Univerzitet u Sarajevu, Zmaja od Bosne 8, 71000 Sarajevo
[3]Eli Lilly B-H doo, Koševo 9/2, 71000 Sarajevo

Sažetak: Farmaceutski inženjering je grana farmaceutske nauke i tehnologije, koji uključuje razvoj i proizvodnju farmaceutskih oblika. Sa ozbiljnim razvojem započeo je tek nedavno, a nastao je iz hemijskog i biomedicinskog inženjeringa. Danas obrazovanje iz oblasti farmaceutskog inženjeringa pokriva oko 210 fakulteta širom svijeta. Internacionalno društvo za farmaceutski inženjering (ISPE) okuplja preko 22.000 stručnjaka iz oblasti farmaceutskog inženjeringa. Farmaceutski inženjering uključuje mnoga naučna znanja iz biologije, hemije, medicine, farmacije, a za cilj ima unaprjeđenje razvojnih procesa i proizvodnje lijekova. Samim time, farmaceutski inženjeri su uključeni u procese koncepcije, dizajna, razvoja, proizvodnje, markiranja i pakovanja lijekova. Farmaceutski inženjering pokriva nekoliko specijalnosti: farmaceutska nauka i razvoj; biofarmaceutska proizvodnja; razvoj alternativnih modela za ispitivanje lijekova; razvoj farmaceutskih preparata koji su karakterisanih ciljanim i kontrolisanim otpuštanjem lijekova, ali i novim ljekovitim oblicima (transgeni, proteini, peptidi); klinička nauka; regulativna oblast; farmaceutski uređaji tj. projektiranje instrumenata, alata, ili implantata koji olakšavaju izradu, rukovanje ili upotrebu lijekova, kao i razvoj novih analitičkih metoda, te razvoj novih sistema dostave lijekova. Oblasti u farmaceutskom inženjeringu preklapaju se i sa drugim inženjerskim područjima, kao i neinženjerskim naučnim i medicinskim poljima.

Ključne riječi: farmacija, inženjering, nanotehnologija, dizajniranje lijekova.

I. Uvod

Napredak tehničkih i prirodnih nauka je posljednjih decenija više nego evidentan što je dovelo do toga da su one djelomično postale međusobno zavisne. Zaista, medicina, farmacija, hemija, biologija se ne bi mogle zamisliti bez naprednih tehnoloških otkrića, kao što su napredne dijagnostičke metode, laboratorijski aparati za kvantitativno i kvalitativno ispitivanje supstanci, te raznovrsni aparati koji se koriste u mnogobrojnim vrstama ispitivanja. Bilo je pitanje vremena kada će se tehničke i prirodne nauke spojiti i izgraditi jedan novi pravac razvoja nauke. Prvi sinergizam ove dvije, nekada zasebne, cjeline desio se početkom druge polovine XX vijeka kada je grupa elektroinženjera, članova Instituta radio inženjera (IRE), odlučila da se uključi u razmatranje postojećih problema u biologiji i medicini, a koje bi eventualno mogli riješiti oni [1]. Brojna istraživanja i otkrića su pogodovala tome da se veliki broj naučnika zainteresuje za ovu oblast, te je 1959. godine održana i Internacionalna konferencija za medicinski i biološki inženjering (Pariz, Francuska). Osnovna svrha konferencije je bila osnivanje Internacionalne federacije za medicinsku elektroniku i biološki inženjering (IFMEBE), odnosno danas poznatu kao Internacionalnu federaciju za medicinski i biološki inženjering (IFMBE). Ona danas broji preko 120.000 članova iz različitih naučnih oblasti, a u koju je učlanjeno oko 58 internacionalnih organizacija [2,3].

II. Farmaceutski inženjering

Kako nas je tome historija već naučila, farmacija je primijenjena nauka koja je proizašla isključivo iz prirodnih nauka kao što su biologija, hemija, botanika i dr. Tako je u ovom slučaju iz biomedicinskog i hemijskog inženjeringa proizašao i farmaceutski inženjering. Danas on predstavlja granu farmaceutske nauke i tehnologije, koji uključuje razvoj i proizvodnju farmaceutskih oblika.

Napredak na području farmaceutskog inženjeringa doprinio je i tome da se osnuje Društvo na internacionalnom nivou, a koje će okupljati farmaceutske inženjere i organizacije koje se bave farmaceutskom industrijom. Internacionalno društvo za farmaceutski inženjering (ISPE) predstavlja najveću svjetsku neprofitabilnu asocijaciju, koja unapređuje naučna, tehnička i regulativna područja farmaceutskog inženjeringa. Društvo je osnovano 1980. godine od strane nekoliko naučnika koji su vjerovali da je farmaceutskoj industriji neophodna dodatna organizacija po pitanju praktične aplikacije nauke i tehnologije. Zadnjih desetak godina ISPE objavljuje i časopis (*Pharmaceutical Engineering Magazine*), koji izlazi svaka dva mjeseca, donoseći najnovija saznanja o proizvodnim procesima i unapređenju kvalitete lijekova. ISPE danas okuplja preko 22.000 članova iz 90 zemalja širom svijeta [4].

A. Obrazovanje i vještine farmaceutskih inženjera

S obzirom da je potreba farmaceutske industrije za inženjerima naglo porasla proteklih decenija, te da su hemijski inženjeri morali prolaziti kroz dodatne kurseve obuke o farmaceutskim procesima i propisima, smatralo se neophodnim da se na fakultetima osnuje novi edukacijski smjer. Kroz zadnje dvije godine edukacije na fakultetu, studenti bi trebali imati dovoljno znanja o primjeni inženjerskih koncepata, naučnih zakona i principa u razvoju procesa za proizvodnju lijekova i farmaceutskih operacija. Prvi takav smjer osnovan je na *New* Jersey *Institute of Technology*, u Sjedinjenim Američkim Državama 2001. godine. Po završetku obrazovanja na ovom smjeru dobiva se zvanje mastera farmaceutskog inženjeringa [5]. Edukacija od dvije godine bi trebala obuhvatiti različite oblasti, gdje se na obje godine obrađuju teme iz tehnoloških i metodoloških područja farmacije (kristalizacija, miješanje prašaka, granulacija, kompresija, regulativa, organizacija proizvodnje itd.) [6]. Usmjereno obrazovanje od dvije godine bi im trebalo omogućiti vještine o primjenjivanju znanja iz matematike, fizike i inženjeringa na farmaceutske proizvodne procese; vještine dizajniranja sistema, komponente ili procesa; kompetentnost u multidisciplinovanim timovima; mogućnost identifikacije, formulacije i rješavanja problema farmaceutskog inženjeringa; razumijevanje profesionalne i etičke odgovornosti [7].

B. Područja rada farmaceutskih inženjera

Opšte specijalnosti koje pokriva farmaceutski inženjering su: farmaceutska nauka i razvoj - u širem smislu podrazumijeva testove i tehnike za otkrivanje, modificiranje ili projektovanje ljekovitih i pomoćnih supstanci; bio -/ farmaceutska proizvodnja - podrazumijeva optimalne procese za proizvodnju ljekovite supstance i proizvoda sa visokim kvalitetom i najboljom učinkovitosću; potom razvoj alternativnih modela (*ex vivo* i *in vitro*) za ispitivanje lijekova; razvoj farmaceutskih preparata koji su okarakterisani ciljanim i kontrolisanim otpuštanjem lijekova (nanomaterijali, biopolimeri), ali i novim ljekovitim oblicima (transgeni, proteini, peptidi); klinička nauka - podrazumijeva primjenu inženjerskih principa u vođenju studija za procjenu sigurnosti i učinkovitosti; regulativna oblast - koja koristi naučnu osnovu kroz regulaciju u donošenju odluka, sa naglaskom na analizu rizika i koristi; farmaceutski uređaji - projektiranje instrumenata, alata, ili implantata koji olakšavaju izradu, rukovanje ili upotrebu lijekova, kao i razvoj novih analitičkih metoda, te razvoj novih sistema dostave lijekova [8].

1. Dizajniranje alternativnih modela za ispitivanje lijekova

Svoja saznanja farmaceutski inežnjeri, zajedno sa ostalim naučnicima, mogu iskoristiti u razvijanju novih ćelijskih i tkivnih testova, kompjuterskih modela i drugih sofisticiranih metoda, a sve u cilju zamjene životinjskih modela na kojim se ispituju lijekovi. S obzirom da svaki originalni lijek mora proći pretklinička ispitivanja, zamjena životinja u ispitivanjima će doprinijeti u etičkom i materijalnom smislu, kao i bržem obavljanju ispitivanja i donošenju zaključaka o sigurnosti i efikasnosti lijeka [9]. Danas postoji čitav niz *in vitro* i *in silico* projekata koji su odobreni od strane glavnih zakonodavnih EU tijela, a koji su još u fazi razvoja. Neki od primjera su: *vitrocellomics* – *in vitro* model koji koristi humane embrione matične ćelije za testiranje lijekova u pretkliničkoj fazi; *exera* – trodimenzionalni *in vitro* model tkiva miša sa estrogenim receptorima, a koji služi za farmakološko - toksikološku analizu spojeva koji stupaju u interakciju sa nuklearnim receptorima; *esnats* – najnovija alternativna metoda testiranja koja koristi embrione matične ćelije za ispitivanje lijekova itd [10]. Inovativnost farmaceutskih inženjera se može ogledati i u tome da se nastoje uvesti 3D alternativni modeli za ispitivanje lijekova. Naime, do sada su se koristili samo 2D *in vitro* testovi koji i nisu sasvim adekvatni za predviđanje farmakodinamike i farmakokinetike lijeka u ljudskom organizmu. 3D alternativni modeli bi bili kombinacija *in vitro* i *in vivo* ćelijskih kultura u kojoj bi bila dodana i tzv. mikrookolina, koja bi oponašala prava tkiva i omogućila fiziološku ćelija-ćelija i ćelija-supstrat interakciju [11]. Dakle, neminovno je da će uskoro doći do razvoja alternativnih modela koji će moći skoro u potpunosti zamijeniti ispitivanja na životinjama. Međutim, ovi modeli moraju proći i rigorozne validacijske procese i uskladiti se sa zakonskim propisima, pa od momenta njihovog otkrića do primjenjivanja u praksi, može potrajati i do 10 godina [9].

2. Nanotehnologija i sinteza lijekova sa kontrolisanim i ciljanim otpuštanjem aktivne supstance

Razvoj lijekova sa kontrolisanim i ciljanim otpuštanjem aktivne supstance podrazumijjeva upotrebu nanotehnologije i biopolimera. Sama nanotehnologija predstavlja revoluciju u industriji, baziranu na integraciji više disciplina, a koja bi mogla uticati na skoro svaki dio čovjekovog života. U procesima nanotehnologije najviše se koriste principi iz nanoelektronike, nanomaterijala i nanobiotehnologije, gdje se farmaceutski inženjering svakako može uklopiti u područje nanobiotehnologije [12]. Nanotehnologija se, može se reći već tradicionalno, u farmaciji povezuje sa kontrolisanim i ciljanim otpuštanjem aktivne supstance iz

lijekova. Saradnjom farmaceutskih inženjera sa naučnicima iz drugih oblasti mogu se dizajnirati lijekovi za do sada neizlječive bolesti (karcinomi, Alchajmerova bolest, Parkinsova bolest itd.) [13]. Dosadašnjim saznanjima, farmaceutski inženjeri su uspjeli da dizajniraju nekoliko nanolijekova u različitim oblicima: polimerne nanopartikule – upotrebljene još prije 35 godina kao nosači za vakcine i hemoterapeutike; liposomi – koriste se kao nosači lijekova (uslijed njihove sposobnosti da preveniraju degradaciju lijekova, smanje incidencu neželjenih efekata i ciljano dostave aktivnu supstancu), te kao transdermalni ljekoviti oblici za visokomolekularne i hidrofobne lijekove i za okularnu primjenu lijekova; dendrimeri – koriste se za kontrolisano otpuštanje aktivne supstance; čvrsti lipidni nanonosači – mogu se primjenjivati na skoro sve načine, a osnovne karakteristike su dobra podnošljivost, visoka stabilnost, ciljana i kontrolisana dostava aktivne supstance; polimerne micele – mogu dospjeti do najnepristupačnijih dijelova ljudskog organizma i akumulirati veće količine aktivne supstance (korisno u liječenju karcinoma); nanokapsule – karakteriše ih niska gustoća i visok skladišni kapacitet, preuzimaju se uglavnom od strane mononuklearnih fagocita što omogućava njihovu akumulaciju u jetri i slezeni; keramičke i metalne nanopartikule – omogućavaju kontrolisano i ciljano otpuštanje aktivnih supstanci iz lijekova, služe za dostavljanje proteina i gena [14]. Neki od konkretnih primjera nanolijekova su: superparamagnetičke nanočestice željezo oksida koje se koriste za magnetsko - rezonantno skeniranje; nanoprašci za povećanje bioraspoloživosti slabo rastvorljivih lijekova; magnetski i optički aktivni materijali za liječenje karcinoma; nanohidroksiapatit koji se koristi kao implantat i za zamjenu kostiju; nanosenzori za precizniju (*point of care*) dijagnostiku [13]. Dakle, nanotehnologija predstavlja obećavajući trend proizvodnje novijih lijekova, gdje se lijekovi dizajniraju uz upotrebu savremene tehnologije koju farmaceutski inženjeri sasvim dobro razumiju. Međutim, treba reći da iako postoje brojni patenti nanolijekova, istih nema na tržištu uslijed nedostatka striktnih regulativnih i legislativnih smjernica, te nezainteresovanosti farmaceutske industrije [14].

3. Razvoj novih ljekovitih oblika i pristupa liječenju

Farmaceutski inženjeri svakako imaju mogućnost učestvovanja u razvoju novih ljekovitih oblika i novijim pristupima liječenju, kao što su genska terapija, inovativnija proizvodnja vakcina, dizajniranje lijekova proteinske strukture i inženjering biljaka [15].

Što se tiče dizajniranja lijekova proteinske strukture, ono je skoro pa nerazdvojivo od nanotehnologije, tako da se često ovi lijekovi inkorporiraju u liposome ili druge nanopartikule. Takođe, jedno od područja na kojim mogu raditi farmaceutski inženjeri je genska terapija. Ovo područje je veoma komplikovano i opširno, tako da zahtjeva angažman naučnika sa različitih područja, kao što su eksperti iz biotehnologije, medicine, biologije i genetičkog inženjeringa [16]. Danas je poznato preko 4000 genetski nasljednih bolesti, a broj gena koji ih kodiraju je još veći, što ukazuje na opširnost ovog područja. Upotreba transgenog materijala je veoma aktuelna tema danas i predstavlja budućnost liječenja mnogobrojnih oboljenja. Do sada je dizajnirano nekoliko metoda transdukcije gena: metoda rekombinantnog retrovirusa; rekombinantnog adenovirusa; adeno vezanog virusa; direktno iniciranje DNK (dezoksiribonukleinska kiselina); transfer gena pomoću partikula; dostavljanje gena pomoću liposoma. Genska terapija je definitivno obećavajuća metoda liječenja mnogih bolesti, sa dosta diskutabilnih situacija, kao što je potreba za permanentnom ili privremenom modifikacijom gena, da li se transfer gena treba obavljati *ex vivo* ili *in vivo*, koja ekspresija gena treba da se postigne itd.

Postoje indicije da se uskoro počnu proizvoditi i savremenije vakcine, koje će biti imati bolju podnošljivošć, a i neželjeni efekti će se svesti na minimum. Osim toga, novije vakcine će sadržati novije vrste produkata: jednomolekularne podjedinice antigena, virus slične čestice, monoklonalna antitijela i postojaće tzv. vakcine za gensku terapiju [15].

4. Pozicija farmaceutskih inženjera u kliničkoj praksi

Klinička nauka se u mnogome razvila, s obzirom da se njen početak bilježi početkom šesdesetih godina prošlog vijeka tj. nakon talidomidske krize. Razvojem farmaceutskog inženjeringa i sve većom upotrebom tehnologije u svim segmentima farmacije došlo je i do razvoja tzv. kliničkog inženjeringa. Prema smjernicama Američke asocijacije za srce, Američke asocijacije za medicinske instrumente i Američkog fakulteta za kliničke inženjere, klinički inženjeri su inženjeri koji su završili edukacijski program inženjerstva na akreditovanoj akademskoj ustanovi, a koji svoja naučna i tehnološka saznanja upotrebljavaju u cilju razvoja zdravstva i njihovih kliničkih aktivnosti. Kliničke aktivnosti u ovom slučaju podrazumijevaju direktnu brigu o pacijentu, klinička istraživanja i aktivnosti od javnog značaja sa ciljem poboljšanja zdravstvene brige. Osim navedenog, klinički inženjeri su neophodni u zdravstvenim ustanovama i zbog toga što doktori i farmaceuti ne razumiju u potpunosti funkcionisanje medicinskih aparata. Zapravo, u većini slučajeva medicinski aparati se ne razumiju u potpunosti niti se održavaju u skladu sa smjernicama koje daju proizvođači. Prisustvom kliničkih inženjera može se pružati

logistička podrška za svu medicinsku tehnologiju u bolnicama, može se pružiti adekvatan trening medicinskom osoblju po pitanju optimalnog rukovanja sa aparatima. Dakle, uloge kliničkog inženjera u sistemu zdravstva su višestruke: evaluacija nove medicinske tehnologije; dizajn, modifikacija i popravljanje sofisticirane medicinske opreme i sistema; procijenjivanje sigurnosti i testiranje performansi medicinske opreme; treniranje medicinskog osoblja kako bi rukovali sa medicinskim aparatima sigurno i efikasno; dizajn medicinskih aparata za klinička istraživanja; evaluacija novih neinvazivnih sistema praćenja liječenja itd.[15].

5. Regulativna oblast farmaceutskog inženjeringa

Regulativna oblast farmaceutskih inženjera se bavi kako zakonskim, tak i moralnim normama. Ove dvije norme predstavljaju dva različita pojma, ali su veoma često u interakciji. Regulativna oblast, u kojoj učestvuju farmaceutski inženjeri, koristi naučnu osnovu za donošenje konačnih odluka, a predmet koji se najčešće obrađuje je procjena i upravljanje rizikom [15]. Iako svjetska regulativna tijela, kao što su FDA (Organizacija za hranu i lijekove) i ICH (Internacionalna konferencija za harmonizaciju) svode rizik na minimum svojim smjernicama i regulativama (FDA Smjernice za validaciju procesa, ICH Q8 smjernice za razvoj lijekova), uvijek može doći do izuzetaka i potrebe za određenim timom koji će vršiti procjenu i upravljanje rizikom na nivou jedne farmaceutske kuće [17]. Procjena i upravljanje rizikom podrazumijeva da se provedu slijedeće aktivnosti: grupa farmaceutskih inženjera identifikuju rizik povezan sa upotrebom novije i nedovoljne poznate tehnologije/sistema; identifikovani rizik se analizira i evaluira, te se određuje da li je rizik prihvatljiv; redovno praćenje rizika nakon što se sistem implementuje. Za procjenu i upravljanje rizikom najvažnije je odabrati adekvatne stručnjake za to, koji u potpunosti razumiju dati problem i koji će samim tim postavljati prava pitanja i tražiti odgovore na njih [18].

III. ZAKLJUČAK

Sve veća potreba za najsavremenijom tehnologijom i inženjerskim principima u farmaceutskim procesima, rezultirala je nastankom farmaceutskog inženjeringa. Edukaciju iz ovog područja danas pokriva veliki broj fakulteta u SAD i u zemljama Zapadne Evrope, a nakon završenog fakulteta farmaceutski inženjer može učestvovati u velikom broju aktivnosti, koje zahtjevaju primjenu najsavremenijih saznanja iz tehnologije i inženjerstva. Ovo područje je još uvijek u fazi razvoja i teško je obuhvatiti sve oblasti kojim bi se mogli baviti inženjeri. Jednostavno rečeno, farmaceutski inženjeri primjenom elektrotehničkih i biomehaničkih principa mogu unaprijediti značajno ispitivanje, razvoj, testiranje i dizajniranje lijekova, te omogućiti liječenje do sad neizlječivih bolesti.

Za područje Bosne i Hercegovine, ali i cijelog Balkana, farmaceutski inženjering, kao i njegova primjena, je nedostižan pojam. Ne postoje ne uslovi niti na jednoj obrazovnoj ustanovi da se pruži edukacija za isti, niti postoje radni uslovi u kojim bi mogli ovi inženjeri raditi.

LITERATURA

1. Frederik Nebeker. Golden Accomplishments in Biomedical Engineering. IEEE History Center. New Jersey. 2002.
2. International Federation of Medical and Biological Engineering. History of IFMBE. Dostupno na: http://ifmbe.org/about-ifmbe/history-of-ifmbe/
3. Fagette Jr. P.H. The Biomedical Engineering Society: An Historical Perspective. Biomedical Engineering Society. 2004. USA, Landover, pp. 3-5.
4. International Society of Pharmaceutical Engineering. Dostupno na: http://www.ispe.org/about-ispe
5. Armenante P.M., Manfredi J.J., Howley M.A., Ostrove S.A. Core Courses and Core Activities in the Pharmaceutical Engineering Program at NJIT: A Re-evaluation of What Constitutes the Core Knowledge of an Emerging Engineering Field. International Conference on Engineering Education and Research. Ostrava, 2004. pp. 21-31.
6. Baron M., Lecoq O. Major in Pharmaceutical Engineering. Dostupno na: http://perso.mines-albi.fr/~schwartz/grad-school/Albi-Pharmaceutical-engineering.pdf
7. Rutgers School of Engineering. Master of Engineering in Pharmaceutical Engineering and Science. Piscataway, New Jersey. 2011.
8. Pharmaceutical engineering. Dostupno na: http://www.lsu.edu/studentorgs/ispe/Welcome_files/PHARMACEUTICAL%20ENGINEERING.pdf
9. Ranganatha N., Kuppast J. A review on alternatives to animal testing methods in drug development. Int J Pharmcy & Pharmac Sci. 2012; 4(5): 28-33.
10. Noqueiro E.M.. Alternative testing strategies: Progress report 2009. European Commission: Direcrtorate-General for Research. Brussels. 2009.

11. 3D Cell Culture: An Early-Stage Oncology Drug Discovery Tool. 3D Biomatrix, USA. 2012. Dostupno na: https://3dbiomatrix.com/wp-content/uploads/downloads/2012/04/3D-Biomatrix-White-Paper-Oncology-Drug-Discovery-Tool-.pdf
12. Ochekpe N.A., Olorunfemi P.O., Ngwuluka N.C. Nanotechnology and Drug Delivery Part 1: Background and Applications. Trop J Pharm Res. 2009; 8(3): 265-74.
13. Debjit B., Chiranjib R.M., Jayakar B.C. Role of nanotehcnology in novel drug delivery system. J Pharm Sci & Tech. 2009; 1(1): 20-35.
14. Ochekpe N.A., Olorunfemi P.O., Ngwuluka N.C. Nanotechnology and Drug Delivery Part 2: Nanostructures for Drug Delivery. Trop J Pharcm Res. 2009; 8(3): 275-87.
15. Bronzino J.D. The Biomedical Engineering Habbook. 2nd edition. Boca Raton: CRC Press LLC. 2000: pp. 1822-38; 1839-57; 2864-72.
16. Sooflyanl S.R., Baradaran B., Lotflpour F., Kazeml T., Mohammadnejad L. Gene Therapy, Early Promises, Subsequent Problems, and Recent Breakthroughs. Adv Pharm Bull. 2013; 3(2): 249-55.
17. Withcer M., Carbonell R., Odum J., Bigelow P., Lewis P., Zivitz M. Facility of the Future: Next Generation Biomanufacturing Forum. Pharm Eng. 2013; 33(2): 1-8.
18. Brady J. Risk Assessment: Issues and Challenges. Pharm Eng. 2015; 35(1): 1-8.

Investigation of Heart Rate Variability using Wavelet Packet Transform in Major Depressive Disorder

S.A. Akar[1], S. Kara[1] and V. Bilgiç[2]

[1] Institute of Biomedical Engineering, Fatih University, İstanbul, Turkey
[2]Psychiatry Department, Faculty of Medicine, Fatih University, İstanbul, Turkey

Abstract— **Depression is a common mood disorder that is characterized by impairment of mood regulation, and loss of interest in enjoyable activities. According to the previous studies, it has been reported that this disorder is related with elevated rates of cardiovascular morbidity and mortality. Therefore, as an important indicator for diagnosis and classification of cardiac dysfunctions, heart rate variability (HRV) has been widely used in depression. Differ from the previous studies in this field, wavelet packet transform (WPT) is used for determination of effective very low frequency (VLF), low frequency (LF), and high frequency (HF) bands in HRV signals of depressed patients in this study. Twenty patients who met the DSM-IV criteria for major depressive disorder and age, gender-matched twenty healthy controls were participated for this study. HRV data of these participants were first were recorded using the Brainamp ExG data acquisition system and then decomposed into sub-bands including VLF, LF, HF using WPT with 9 level Daubechies (db4) family and variations of energy in these bands were analyzed in MATLAB. The HRV measures as each sub-band average energy and sympathovagal balance (LF/HF ratio) were compared statistically between patients and controls. The results of this study indicates that especially the mean energy values of sub-frequency ranges in VLF band for each participant are higher than that the values of other bands as LF and HF. In addition, the mean energy values of the regions in LF band of control subjects are significantly lower than the same measure of patients. In contrast, in comparison with control subjects, patients with major depression exhibited low HF band energy. Finally, results indicate that sympathovagal balance that reflects the equilibrium between sympathetic and parasympathetic activity of the autonomic nervous system in patients was higher than that of control subjects indicating autonomic dysfunction throughout the entire experiment. It can be conclude that low cardiovagal activity in patients with major depression may contribute to the higher cardiac dysregulations of these patients.**

Keywords— **Major depressive disorder, heart rate variability, wavelet packet transform, sympathovagal balance.**

I. Introduction

Major depressive disorder is a common psychiatric condition comprising depression, loss of interest, pleasure and other symptoms [1]. Related to autonomic nervous system (ANS) dysfunction in patients, individuals suffering from depression often have decreased vagal tone, increased heart rate, fatigue, sleep disturbance, and sympathetic arousal [2]. Moreover, it has been reported that the existence of depressive disorder is associated with cardiovascular morbidity and mortality [3, 4]. Therefore, as a cost-effective and non-invasive procedure, heart rate variability (HRV) analysis has been widely used for assessing the cardiac autonomic modulation.

However, inconsistent results have been reported in these studies investigating HRV in depressive patients. In some of these studies, depressive patients show a reduction of HRV [5, 6] or no HRV difference compared to controls [7]. On the other hand, consistent with altered cardiac ANS function, increased heart rates have been reported in patients with depression and this situation has been suggested as an important risk factor for sudden cardiac death [4]. In most of these studies, ECG has been used for HRV analysis. Besides, as an easy, noninvasive and optical method, photoplethysmography (PPG) have also been proposed for HRV analysis in numerous studies [8, 9]. It has been reported that instead of the RR intervals of ECG signals, the peak-to-peak (PP) intervals in the PPG can be used for HRV analysis. In the frequency domain HRV analysis, the PPG data can be divided into very low frequency (VLF), low frequency (LF), and high frequency (HF) bands. Among them, the LF band (0.04-0.15 Hz) reflects both sympathetic and parasympathetic activities and the HF band (0.15-0.40 Hz) is only associated to parasympathetic activity [10]. Moreover, the ratio of the LF to HF power (LF/HF) that is an important characteristic for evaluating sympathovagal balance widely used another frequency domain HRV measures. The purpose of this study was to analyze frequency domain HRV features of depressive patients and healthy control subjects using PPG data. Unlike the previous researches in this field, wavelet packet transform (WPT) is used for determination VLF, LF, and HF bands and LF/HF ratio in PPG based HRV analysis of patients.

II. MATERIAL AND METHODS

A. Subjects and Experimental Procedure

20 depressed patients and 20 age and gender-matched healthy controls were studied in this research (Table 1). The patients with major depressive disorder, diagnosed by the Structured Clinical Interview for DSM-IV Axis-I Disorders, were recruited from Psychiatry Department of Fatih University, Sema Hospital. Fatih University ethics committee approved the study and an informed consent was obtained from all participants before the study. Patients with prior history of cardiovascular, pulmonary or other psychiatric diseases were excluded from the study.

Table 1 Demographical Data of the Participants

	Patients	Controls
Participants	20	20
Male / Female	12 / 8	11 / 9
Age	30.02 ± 4.14	28.45 ± 5.72

Data acquisition was started after a resting, adaptation period of approximately 3 min. PPG data were acquired for all subjects while they were instructed to sit on a chair without moving. For data collection, Brainamp ExG data acquisition system (Brain Products GmbH, Munich, Germany) and the associated software were used. The blood pulse sensor was strapped on to the index finger of subject's non-dominant hand and data were recorded for 5 minutes and sampled with 250 Hz.

B. Data Analysis

The data analysis was performed in MATLAB 7.6® software package. The obtained PPG signals were first preprocessed using the Butterworth filters as 8th order low-pass with 8 Hz cutoff frequency and 4th order high-pass with 10 Hz cutoff frequency in order to eliminate any motion artifact or noise. Then, an algorithm was implemented to find the peak-to-peak (PP) intervals of the data. The PP interval data were interpolated with a cubic spline interpolation and resampled with 4 Hz sampling frequency. In the last step of preprocessing, a sliding window average filter was used to select only the normal-to-normal beats of the data for HRV analysis without any occasional ectopies and/or arrhythmic beats. Finally, the data were decomposed into sub-bands with a 9 level db4 (daubechies) WPT. As a generalization of discrete wavelet transform, in WPT, both the approximation and detail coefficients are further decomposed at each level (Figure 1).

Therefore, using these decomposition 512 wavelet packets was obtained and between 1-9th nodes were defined as very low frequency, between 10-38th nodes were defined as low frequency (LF) and between 39-102th nodes were defined as high frequency (HF) bands.

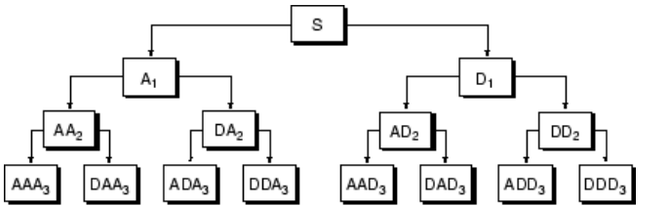

Fig.1 Illustration of WPT decomposition tree [11]

In these frequency bands, the mean RMS energy values of nodes were calculated using the following formula [12]

$$w_{rms,m,j} = \sqrt{\frac{1}{N}\sum\left|w_{m,j}(r)\right|^2} \quad (1)$$

where m denotes the decomposition level, N shows total number of elements in the packet, j is the index of node in each level, and r is an index for elements of the packet. The total energy was calculated as

$$E_{w_{rms,m,j}} = \sum_{j=0}^{2^M-1}\left|w_{rms,m,j}\right|^2 \quad (2)$$

where M is the last decomposition level. Then, the average energy values in each node were calculated for both patients and controls. The HRV measures as each sub-band average energy and sympathovagal balance (LF/HF ratio) were calculated in patients and controls.

C. Statistical Analysis

The results were evaluated statistically using the SPSS® (version 20.0) statistical software package. Levene's test was used to test the homogeneity of groups' variances. According to this test results, comparisons of HRV features between the patients and controls were compared using an independent sample Student's t-test.

III. RESULTS

In this study, PPG data were recorded from patients with depression and healthy controls to investigate frequency domain HRV features. A sample PPG data obtained from a patient in shown in Figure 2. In this figure, while horizontal axis shows time, the vertical axis illustrates PP intervals (PPint). Table 2 lists the calculated frequency domain HRV measures between depressive patients and control subjects.

We found statistically significant differences in extracted frequency domain measures of HRV between patients and control subjects.

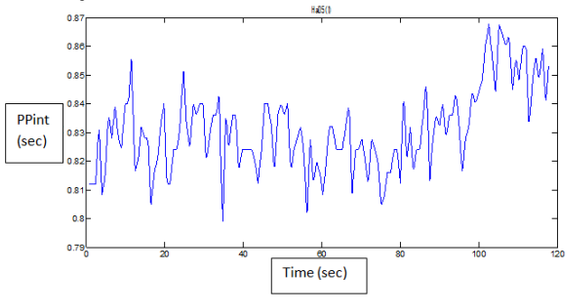

Fig.2 A sample PPG data of a patient subject

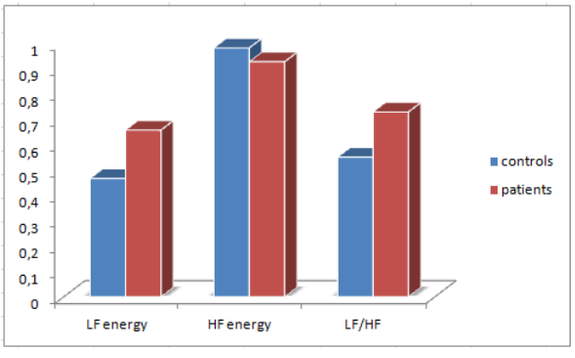

Fig.3 Comparison of HRV measures between patients and controls

Depressive patients had higher LF band energies and lower HF energy as compared to the control subjects' values as shown in Figure 3. Frequency domain analyses reveal that the patient group also exhibited significantly increased LF/HF ratio when compared to healthy subjects.

Table 2 Obtained HRV measures in patients and controls

	Patients	Controls
LF energy	0.6576 ± 0.34	0.4668 ± 0.19
HF energy	0.9273 ± 0.41	0.9819 ± 0.48
LF/HF ratio	0.729 ± 4.14	0.551 ± 5.72

IV. DISCUSSION AND CONCLUSION

It has been reported that altered autonomic function is related to higher rates of cardiac disease and morbidity in patients with depression. Therefore, HRV analysis has become a powerful and useful tool in clinical research to assess ANS dysfunction in these patients. We aimed to investigate the PPG based HRV frequency parameters using WPT. It was found that depressive patients had higher LF band energies and lower HF band energies. The decrease in HF power and related increase in LF/HF ratio in patients with depression are suggested as a result of reduced parasympathetic nerve activities and the imbalance of sympathetic and parasympathetic innervation, which may reflect dysregulation of sympathetic and parasympathetic coordination in depression [13]. Therefore, our findings suggest that depression is accompanied by dysfunction of the cardiac ANS. To understand the correlation between symptom severity of depression and dysregulations in cardiac autonomic activity, further studies in large number of participants will be required.

ACKNOWLEDGMENT

This study was funded by TÜBİTAK (The Scientific and Technical Research Council of Turkey) under project number 112E317.

REFERENCES

1. M. Ahmadlou, H. Adeli and A. Adeli, Fractality analysis of frontal brain in major depressive disorder, *International Journal of Psychophysiology* Volume: 85, 2012, pp 206–211.
2. I. S. Khawaja, J. J. Westermeyer, P. Gajwani, R. E. Feinstein, Depression and coronary artery disease: the association, mechanisms, and therapeutic implications, *Psychiatry (Edgemont)* Volume: 6, 2009, pp 38–51.
3. K. Sayar, H. Güleç, M. Gökçe, İ. Ak, Heart rate variability in depressed patients, *Bull Clin Psychopharmacol* Volume: 12, 2002, pp 130-133.
4. W. E. Severus, A. B. Littman, A. L. Stoll AL, Omega-3 fatty acids, homocysteine, and the increased risk of cardiovascular mortality in major depressive disorder. *Harv Rev Psychiatry* Volume: 9, 2001, pp 280-293.
5. J. H. M. Tulen, J. A. Bruijn, K. J. de Man, L. Pepplinkhuizen, A. H. van den Meiracker, A. J. Man in't Veld, Cardiovascular variability in major depressive disorder and effects of imipramine and mirtazapine. *Journal of Clinical Psychopharmacology* Volume: 16, 1996, pp 135–145.
6. P. K. Stein, R. M. Carney, K. E. Freedland, J. A. Skala, A. S. Jaffe, R. E. Kleiger, J. N. Rottman, Severe depression is associated with markedly reduced heart rate variability in patients with stable coronary heart disease. *Journal of Psychosomatic Research* Volume: 48, 2000, pp 493–500.
7. M. Moser, M. Lehofer, R. Hoehn-Saric, D. R. McLeod, G. Hildebrandt, B. Steinbrenner, M. Voica, P. Liebmann, G. Zapotoczky, Increased heart rate in depressed subjects in spite of unchanged autonomic balance. *Journal of Affective Disorders* Volume: 48, 1998, pp 115–124.
8. Y. Yoon, J. H. Cho, G. Yoon, Non-constrained Blood Pressure Monitoring Using ECG and PPG for Personal Healthcare. *J Med Syst* Volume: 33, 2009, pp 261-266.
9. N. Selvaraj, A. Jaryal et al. Assessment of heart rate variability derived from finger-tip photoplethysmography as compared to electrocardiography. *J Med Eng Technol* Volume: 32(6), 2008, pp 479-84.

10. Anonymous, Heart rate variability. Standards of measurement, physiological interpretation, and clinical use. Task Force of the European Society of Cardiology and the North American Society of Pacing and Electrophysiology. *Eur Heart J* Volume: 17(3), 1996, pp 354-81.
11. Matlab Wavelet packets, access time: February 2015, http://www.mathworks.com/help/wavelet/ug/waveletpackets.html
12. J C Goswami, A K. Chan, *Fundamentals of Wavelets Theory, Algorithms, and Applications*. A Wiley Interscience Pub. 1999.
13. Y. Wang, X. Zhao, A. O'Neil, et al., Altered cardiac autonomic nervous function in depression, *BMC Psychiatry*, Volume: 13, 2013, pp 187-193.

Corresponding Author:
S.A. Akar is with the Institute of Biomedical Engineering, University of Fatih, İstanbul, 34500 Büyükçekmece, Turkey (phone: +90 (212) 8663300-2643; e-mail: saimeakar@fatih.edu.tr).

In vitro models to determine the pharmacokinetic parameters

Pehlivanović Belma[1]

[1] PhD student at Faculty of Pharmacy, University of Sarajevo, Sarajevo, Bosnia and Hercegovina

Abstract— **The pharmaceutical industry seeks to more efficient and precise determination of the main pharmacokinetic parameters of existing and new drugs, and therefor uses new in vitro models that show a high degree of correlation with in vivo response.**

Determination of intestinal absorption, metabolic transformations and metabolic profile of drugs is carried out using the laboratory in vitro models, which represent innovative basis for determination of absorption, distribution, metabolism and elimination (ADME) of drugs .

The aim of this paper is to present three most important in vitro models, their properties and applications in the pharmaceutical industry when determining the pharmacokinetic parameters.

The rapid development of the pharmaceutical industry expressed the need for in vitro models for the determination of pharmacokinetic parameters in the laboratories that want to increase their operational efficiency and effectiveness.

Keywords— **Pharmacokinetics, drugs, parameters, in vitro models**

I. Introduction

The prediction of human pharmacokinetic and disposition attributes of new drugs from preclinical data has become a mainstay of drug metabolism and pharmacokinetics organizations within pharmaceutical research and development operations. In the vast majority of large research and development groups, the nomination of new compounds into the development phase requires a prediction of what the human pharmacokinetics will be.

Models have been developed to assess important human disposition attributes during the drug design phase so that scientist can simultaneously optimize absorption, distribution, metabolism, and excretion properties and pharmacological potency. These models and methods are standard in modern drug discovery, and are a critical element to successful drug discovery[1]

The majority of drugs available on the market are in oral dosage forms. For the assessment of permeability and oral drug absorption and metabolism, in vitro and high throughput systems, such as the parallel artificial membrane permeability assay (PAMPA) and cell-based systems exist to relate drug permeability to absorption, especially for compounds that do not undergo intestinal metabolism.

The most popular high-throughput screening tool for drug permeability is human colon carcinoma (Caco-2) or transfected Madin-Darby canine kidney (MDCK) cells [2].

II. In vitro models to determine the pharmacokinetic parameters

A. Caco-2 cell lines

A popular in vitro model is the Caco-2 cell line, derived from human colon carcinoma cells that contains the P-glycoprotein (Pgp). Studying the permeability of compounds across a Caco-2 cell monolayer is an established in vitro model to screen for oral absorption and to evaluate the mechanism of transport.

In culture, they differentiate spontaneously into polarised intestinal cells possessing an apical brush border and tight junctions between adjacent cells, and they express hydrolases and typical microvillar transporters. This cell line was first used as a model for studying differentiation in the intestinal epithelium, and later for estimating the relative contributions of paracellular and transcellular passage in drug absorption. Caco-2 cells, despite their colonic origin, express in culture the majority of the morphological and functional characteristics of small intestinal absorptive cells, including phase I and phase II enzymes, detected either by measurement of their activities toward specific substrates, or by immunological techniques [1].

The Caco-2 permeability model is also considered to be the industry reference standard for in vitro prediction of in vivo human intestinal permeability, bioavailability and drug-drug interactions (DDIs) of orally administered drugs.

The development of the Caco-2 cell has greatly facilitated progress and led to the testing of diverse drug classes as Pgp. More recent development involved transfection with the cytochrome P450 gene and stimulation by butyrate to provide the added P450 activity. The incubation system, the donor and receiving compartments separated by the cell monolayer, is an efficient, high-throughput system for examination of whether newly developed pharmaceuticals are substrates of cytochrome P450 3A4 and/or P-glycoprotein such that interactions with other drugs may be predicted [2].

Most studies with Caco-2 monolayers were performed to determine whether a drug is actively or passively transported across the intestinal epithelium, and to provide new insights into the regulation of drug transport. So Caco-2 model has become the gold standard to relate drug permeability to oral drug absorption [3].

B. Parallel artificial membrane permeability assay

Parallel artificial membrane permeability assay is a model which determines the permeability of substances from a donor compartment, through a lipid-infused artificial membrane into an acceptor compartment.

A multi-well microtitre plate is used for the donor and a membrane/acceptor compartment is placed on top; the whole assembly is commonly referred to as a "sandwich". At the beginning of the test, the drug is added to the donor compartment, and the acceptor compartment is drug-free. After an incubation period which may include stirring, the sandwich is separated and the amount of drug is measured in each compartment. Mass balance allows calculation of drug that remains in the membrane.

To date, PAMPA models have been developed that ehibit a high degree of correlation with permeation across a variety of barriers, including Caco-2 cultures, the gastrointestinal tract, blood–brain barrier and skin. The donor and/or acceptor compartments may contain solubilizing agents, or additives that bind the drugs as they permeate.

To improve the in vitro - in vivo correlation and performance of the PAMPA method, the lipid, pH and chemical composition of the system is often designed with biomimetic considerations in mind.

Furtherrmore, PAMPA only measures permeability by passive diffusion whereas the Caco-2 permeability assay also assesses active uptake/efflux and paracellular transport. Therefore, a good correlation is observed between the Caco-2 permeability assay and PAMPA if the compound crosses the membrane by passive diffusion alone.

If the compound is a substrate for active efflux then the PAMPA overestimates the permeability and if the compound undergoes active uptake or paracellular then the PAMPA underestimates the permeability [4,5].

C. Madin-Darby Canine Kidney cells

Apart from Caco-2 cells other models that are most frequently used for ADME studies are MDCK cells. When the MDCK cells are cultured under standard conditions, they differentiate into polarized columnar epithelial cells and form tight cellular junction. The main advantage of MDCK cells is shorter culture time, which can be equal to 24 hours.

A good correlation was reported between permeation of passively absorbed drugs in Caco-2 and MDCK cells. The permeability coefficients of hydrophilic compounds are usually lower in Cacco-2 cells than in MDCK cells.

Whereas Caco-2 cells originate from human colon adenocarcinoma cells, MDCK cells are from dog kidney cells, and thus the expression levels of intestinal transporters would be different in these two cell lines [6].

III. CONCLUSION

In vitro models can be used to study the ADME properties of drugs or general chemicals. Caco-2 cell lines can be performed to estimate the absorption of compounds through the lining of the gastro-intestinal tract. The versatility of Caco-2 cells is demonstrated by the fact that, even to this day, they are serving as the basis for the creation of innovative new models that are contributing to our understanding of drug efflux transporters such as P-glycoprotein.

As financial and other factors in pharmaceutical development continue to strain timelines and resources, PAMPA will most likely continue to play an ever-increasing role in laboratories wishing to increase their operating efficiencies and success rate.

REFERENCES

1. Hunter J, Jepson MA, Tsuruo T, Simmons NL, and Hirst BH Functional expression of P-glycoprotein in apical membranes of human intestinal caco-2 cells. kinetics of vinblastine secretion and interaction with modulators. J Biol Chem 268: 199, 14991-14997.
2. Cummins CL, Mangravite LM, and Benet LZ, Characterizing the expression of CYP3A4 and efflux transporters (P-gp, MRP1, and MRP2) in CYP3A4-transfected Caco-2 cells after induction with sodium butyrate and the phorbol ester 12-O-tetradecanoylphorbol-13-acetate. Pharm Res18:2001,1102-1109
3. Hidalgo IJ, Raub TJ, and Borchardt RT. Characterization of the human colon carcinoma cell line (Caco-2) as a model system for intestinal epithelial permeability. Gastroenterology 96: 1989; 736-749.
4. Bermejo, M. et al. PAMPA – a drug absorption in vitro model 7. Comparing rat in situ, Caco-2, and PAMPA permeability of fluoroquinolones. Pharm. Sci., 21:2004; 429-432
5. Avdeef, A. et al. Caco-2 permeability of weakly basic drugs predicted with the Double-Sink PAMPA pKaflux method. Pharm. Sci., 24:2005; 333-349
6. Shane C. Gad, *Preclinical Development Handbook: ADME and Biopharmaceutical properties,* John Whiley and Sons Inc, 2008.

Analysis of sub-cerebellar regions in patients with Chiari Malformations

Engin Akar[1], Sadık Kara[1], Hidayet Akdemir[2] and Adem Kırış[3]

[1] Institute of Biomedical Engineering, Fatih University, Istanbul, Turkey
[2]Department of Neurosurgery, Medicana International Hospital, Istanbul, Turkey
[3]Department of Radiology, Mehmet Akif Ersoy Cardio-Thoracic Surgery Training and Research Hospital, Istanbul, Turkey

Abstract— **Chiari Malformations are serious neurological defects involving herniation of hindbrain tissues such as cerebellar tonsils, brainstem and IV. ventricle into the spinal canal through the foramen magnum. By the severity of cerebellar descent, these malformations are classified into four different types. Clinically the least obvious and the mildest one is named as type I and defined as the descent of cerebellar tonsils into the cervical canal more than 5 mm. Magnetic Resonance Images (MRI) of brain in the sagittal plane provides the best clues in the diagnosis of the Chiari Malformation type I (CM-I). Previous studies investigated the morphological characteristics of cerebellum and nearby regions such as brain stem and fourth ventricle. Aim of this study is to analyze the cerebellar regions in chiari patients and healthy controls to search for the discriminative properties between the two groups. Sagittal brain MRI of eleven chiari patients and gender matched controls were used in order to examine the area of sub-cerebellar tissues such as gray matter (GM) and white matter (WM) and the area ratio between GM and WM. A graphical user interface (GUI) for implementing image processing techniques was developed using MATLAB environment. By means of GUI, the region embracing the whole cerebellum tissue on the mid-sagittal MR images were manually extracted. In addition, using Statistical Parametric Mapping (SPM) package the MRI slices were segmented into GM and WM tissues. Using the extracted cerebellum region as a mask, the cerebellar GM and WM tissues were achieved and the corresponding areas were computed by counting the number of pixels on each GM and WM slice. According to the statistical results, it has been found that cerebellar GM areas of the patients are significantly higher than the values of controls. As a consequence, this approach may provide a discriminative feature between patients with CM-I and health control subjects.**

Keywords— **Chiari malformation, magnetic resonance imaging, segmentation, gray matter, white matter**

I. Introduction

Chiari Malformations are a group of developmental anomalies that involve the herniation of cerebellar tonsils, brainstem and IV. ventricle into the spinal canal through the foramen magnum [1]. The mildest of these anomalies is designated as Chiari Malformation type I (CM-I) and radiologically defined as the downward displacement of the cerebellar tonsils below the foramen magnum more than 5 mm [2]. Chiari Patients may show several symptoms of different severity ranges. The most frequent one is the headache in the back of the head. Another common condition is the pain in neck and shoulders [3]. Additionally, a number of secondary symptoms have been reported such as ataxia which is the presence of abnormal, uncoordinated movements, dysarthria which is a motor speech system problem, balance problems, dizziness and muscle weakness [4]. Midline sagittal MR images provide a proper view for the diagnosis of the anomaly. In addition, A cine phase-contrast MRI may also be used for the cerebrospinal fluid (CSF) flow assessment for diagnostic purposes [5]. Surgical procedure used for the treatment of Chiari is posterior fossa decompression. The aim of this operation is to create more space around the herniation and bring back natural circulation of CSF [6].

Several studies have been made to investigate the neurological conditions of CM-I. In these studies, linear and volumetric measurements were carried out using the MRI slices and computer tomography (CT) scans of brain for the evaluation of morphological characteristics of posterior cranial fossa (PCF) [5, 7-9]. As a linear criterion, the length of the tonsillar descent was measured as an indicator of the Chiari severity. Moreover, the volume of PCF, CSF and the whole brain were calculated for the volumetric evaluation of CM-I [5, 8]. Additional studies were also carried out for the assessment of the CSF flow and velocity in order to understand the effects of CSF flow dynamics on the symptoms intensity of the Chiari anomaly [10, 11].

Previous studies investigating the PCF features [5, 7-9] and CSF flow dynamics [10, 11] have provided valuable information related to CM-I; nevertheless, there are still unclear points regarding the pathophysiology and symptomatology of this anomaly. Therefore, the aim of this study is to search for some elucidatory and discriminative features in order to contribute the ongoing redefinition of Chiari anomaly. In the present study, the areas of cerebellar substructures such as white matter (WM) and gray matter (GM) were calculated and the ratio between these area values were found in order to investigate the morphological variations between the Chiari patients and healthy controls.

II. Material and Methods

A. Subjects and MRI Acquisition

Brain images of 11 healthy subjects (5 males and 6 females, 16 - 50 years age range) and 11 Chiari I patients (4 males and 7 females, 16 - 55 years age range) were used in this study (Table 1). The experimental procedures of the present study were approved by the Ethical Committee of Fatih University. The image data were obtained from the MRI records of Department of Radiology, Mehmet Akif Ersoy Cardio-Thoracic Surgery Training and Research Hospital and Medicana International Hospital, İstanbul. T1-weighted human brain MRI were acquired from a Siemens Symphony Magnetom Aera 1.5 T MR scanner (Erlangen, Germany). Image parameters: sagittal slices of 5mm, echo time 9.8 ms, repetition time 511 ms, flip angle 90º, FOV 23 cm, and matrix size 512x512.

B. Image Processing

The image processing procedures which consists of four steps were carried out using the midline sagittal MRI slices. For the facilitation of these procedures, a graphical user interface (GUI) was built using the MATLAB 8.2® user interface development environment. The initial step of image processing is filtering of MRI images based on 2D median filtering using a 3×3 kernel in order to improve the signal to noise ratio. Secondly, the region that contained the entire cerebellum was manually extracted from the midline sagittal brain images in order to use as a mask for obtaining cerebellar GM and WM (Figure 1a and 1b). In the third place, the sagittal MRI slices were registered to SPM8 utility and the WM and GM images were produced as a result of this application. After that, using the MATLAB based GUI, the masking operations were performed to get the images that contained solely the cerebellar GM and WM tissues (Figure 1c and 1d). In the final step, the areas of GM and WM regions were calculated by counting the nonzero pixels in these regions and by multiplying the result with the distance of each pixel in mm in both vertical and horizontal dimensions.

C. Statistical Analysis

SPSS® (version 20.0) statistical software package were used the evaluate the results statistically. The independent sample Student's t-test was used to compare the results of area analysis between the patients and controls. Levene's test was used to test the homogeneity of groups' variances.

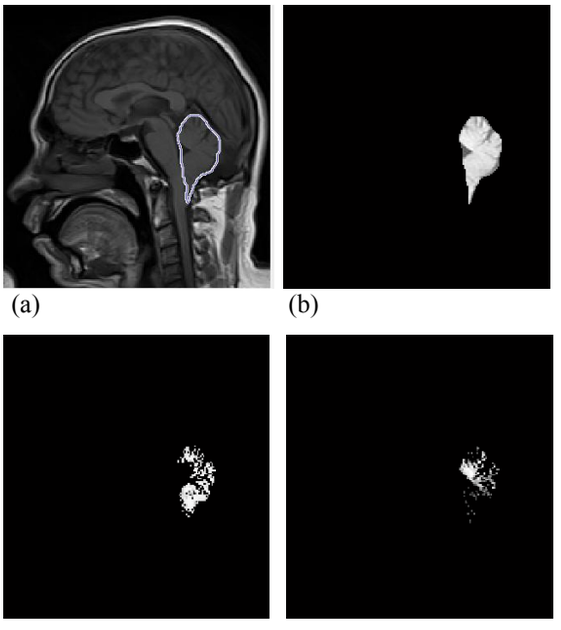

Fig 1. Manual Extraction and GM and WM segmentation processes. (a) Determination of cerebellum borders, (b) extracted cerebellar region, (c) segmented gray matter tissue, (d) segmented white matter tissue.

III. Results

In this study, MRI records of patients with Chiari and healthy controls were recorded and image segmentation procedures were performed on the acquired images in order to investigate the variations in cerebellar tissues. The areas calculated for cerebellar GM and WM and the ratios between them are listed in Table 1.

Table 1 Demographical data of subjects and the results of area analysis

	Patients	Controls
Participants	11	1
Male / Female	4 / 7	5 / 6
Age	38,64 ± 8,39	37,64 ± 8,88
Cerebellar GM area	856,03 ± 131,88	644,31 ± 75,82
Cerebellar WM area	424,79 ± 138,04	481,41 ± 83,58
GM / WM area ratio	2,41 ± 1,46	1,37 ± 0,24

The results of this study showed that the GM area of cerebellum in patients with Chiari was significantly higher ($p < 0.001$) than the corresponding area values of healthy controls as shown in Figure 2.

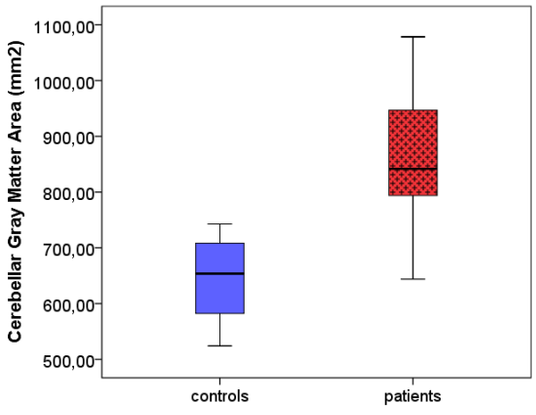

Fig. 2 Comparison of GM area between patients and controls

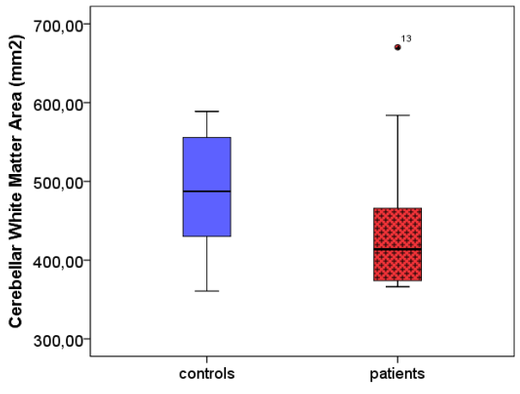

Fig. 3 Comparison of WM area between patients and controls

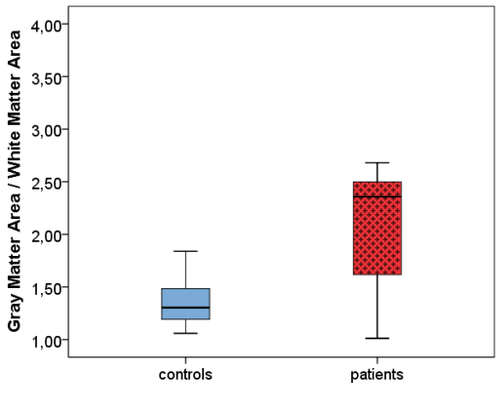

Fig. 4 Comparison of WM area between patients and controls

We could not find a significant difference in cerebellar white matter area between Chiari patients and healthy controls ($p = 0{,}261$) which is shown in Figure 3. Finally, our results demonstrated that the ratios between the cerebellar GM and WM were significantly higher ($p = 0{,}041$) in patients than the ones in controls. The box-plot diagram in Figure 4 displays this condition.

IV. Conclusions

CM-I is a neurological disorder of hindbrain tissues which is characterized by the descent of cerebellar tonsils more than 5 mm into the cervical canal through the foramen magnum. It has been reported that patients with chiari have smaller volumes of PCF and CSF compared to the healthy controls [5]. Additionally, some studies indicated that patients with chiari have altered dynamics of CSF flow and velocity [10, 11].

According to the results of some previous studies, the exact mechanism of the pathophysiology of Chiari is not well understood which leads to the difficulties in treatment and management of patients [10, 12]. Therefore, the purpose of the present study is to find new informative characteristics by performing an area analysis on cerebellar structures including GM and WM. The results indicated that Chiari patients have larger GM area values compared to controls. Similarly the ratio between the GM and WM area values are lower in controls. Thus, our findings suggest that altered physical conditions in CM-I may result in changes in cerebellar GM and WM. To confirm our results, further studies should be performed with a larger number of participants and based on new analysis techniques.

References

1. P. R. Choudhury, P. Sarda, P. Baruah, S. Singh, A magnetic resonance imaging study of congenital Chiari malformations. OA Case Reports 2013 Aug 08;2(8):73.
2. A. D. Elster, M. Y. M. Chen, Chiari I malformations: clinical and radiologic reappraisal. Radiology 1992;183:347–53.
3. A. Talal, O. M. Amer and el-Shmam, Chiari Malformation Type I: A New MRI Classification Magn Reson Imaging. 1997;15(4):397-403.
4. R. Yassari, D. Frim, Evaluation and management of the Chiari malformation type 1 for the primary care pediatrician. Pediatr Clin North Am. 2004 Apr; 51(2): 477-90.
5. T. H. Milhorat, M. W. Chou, E. M. Trinidad, R. W. Kula, M. Mandell, C. Wolpert, M. C. Speer, 1999. Chiari I Malformation Redefined: Clinical and Radiographic Findings for 364 Symptomatic Patients. Congress of Neurological Surgeons Volume 44(5) pp 1005-1017.
6. P. Kunert, M. Janowski, A. Zakrzewska, et al. Comparison of results between two different techniques of cranio-cervical decompression in patients with Chiari malformation. Neurol Neurochir Pol 2009;43:337–45.

7. H. Nylan, K. G. Krogness, 1978. Size of posterior fossa in Chiari type I malformation in adults. Acta Neurochir (Wien). 40, 233-242.
8. R. E. Clatterbuck, E. P. Sipos, 1997. The efficient calculation of neurosurgically relevant volumes from computed tomographic scans using Cavalieri's direct estimator. Neurosurgery 40, 339-343.
9. S. Aydin, H. Hanimoglu, T. Tanriverdi, E. Yentur, M. Y. Kaynar, 2005. Chiari type I malformations in adults: a morphometric analysis of the posterior cranial fossa. Surg Neurol. 64(3), 237-41
10. S. Linge, V. Haughton, A. E. Løvgren, K. A. Mardal, A. Helgeland, H. P. Langtangen, 2011.Effect of tonsillar herniation on cyclic CSF flow studied with computational flow analysis. Am. J. Neuroradiol. 32(8), 1474–1481.
11. E. C. Clarke, D. F. Fletcher, M. A. Stoodley, L. E. Bilston, 2011. Computational fluid dynamics modeling of cerebrospinal fluid pressure in Chiari malformation and syringomyelia. Journal of Biomechanics 46, 1801 - 1809.
12. M. Nishikawa, H. Sakamoto, A. Hakuba, N. Nakanishi, Y. Inoue, 1997. Pathogenesis of Chiari malformation: A morphometric study of the posterior cranial fossa. J Neurosurg 86, 40-47

Corresponding Author:
E. Akar is with the Institute of Biomedical Engineering, University of Fatih, İstanbul, 34500 Büyükçekmece, Turkey (phone: +90 (212) 8663300-2643; e-mail: enginakar@st.fatih.edu.tr).

KONTINUIRANI ELEKTROKARDIOGRAFSKI HOLTER MONITORING DJEČIJE DOBI

Zijo Begić, Senka Mesihović Dinarević, Almira Kadić, Mirza Halimić
Pedijatrijska klinika, KCU Sarajevo, Bosna i Hercegovina

Sažetak - **Kontinuirani dinamički dvadeset četveročasovni elektrokardiografski (Holter) monitoring je vrlo važna metoda u dijagnostici i tretmanu aritmija dječije dobi. Aritmije su poremećaji frekvencije i regularnosti ritma srca, koje nastaju kao posljedica poremećaja u stvaranju i/ili provođenju podražaja u specifičnoj ili radnoj muskulaturi srca. Za razliku od odraslih, mehanizam nastanka aritmija u djece je raznovrsniji (kruženje, naknadni potencijal, automatizmi).**

Cilj rada: Prikaz mjesta i uloga metode u svakodnevnom kliničkom radu pedijatrijskog kardiologa.

Materijal i metode: Istraživanje je imalo retrospektivni i analitički karakter, te je obuhvatilo period april 2003.- januar 2015. (podaci prikupljani iz „Registra EKG Holter monitoringa").

Rezultati:U nepunih 12 godina, kod 2616 pacijenta je urađen kontinuirani EKG Holter monitoring, dječaka 1329(50,8%), a pacijenti su bili starosne dobi od rođenja do 19.godine života. Registracija neonatusa i dojenčadi je bilo 45 (1,7%), male djece 69 (2,6%), predškolske 262 (10%), školske 893 (34,1%), djeca u pubertetu i adolescenciji 1350 (51,6%). Kod 1775 pacijenta (67,8%) Holter je rađen prvi put, a kontrolnih 841(32,2%). Indikacije za provođenje Holtera su bile: aritmije 1075 (41,1%), prekordijalna bol 626 (23,9%), sumnja na preeksiktacije i/ili preekscitacije 276 (10,5%), krize svijesti 213 (8,1%), nekorigirane urođene/stečene mane srca 116 (4,4%), operisane mane srca 99 (3,7%), hipertenzija 81 (3,1%), kontrola rada pejsmejkera 43 (1,6%), ostali uzroci 87 (3,3 %). Otpusne dijagnoze nakon urađenog EKG Holter monitoringa su nesignifikantne aritmije 1189 (45,4%), lutajući centar vodič 579 (22,1 %), preekscitacije 444 (17 %), benigne ventrikularne ekstrasistole 165 (6,3%), atrioventrikularni blokovi 84 (3,2 %), sinusna pauza 63 (2,4%), ostali poremećaji ritma 92 (3,5 %). U pomenutom periodu su registrovana 54 slučaja WPW (Wolf Parkinson White) sindroma, koji su u najvećem broju slučajeva bili udruženi sa paroksizmalnom supraventrikularnom tahikardijom i čine većinu otpusnih dijagnoza preekscitacija. Kod 124 (4,7%) pacijenta se primjenjuje antiaritmijska terapija. Implanitrano je 27 pacemakera, u radiofrekventna ablacija je rađena u 23 slučaja.

Zaključak: Razvoj pedijatrijske kardiohirurgije je inicirao i razvoj pedijatrijske aritmologije kao imperativni segment pedijatrijske kardiologije. Kontinuirani EKG Holter monitoring je postao nazamjenljiva metoda u svakodnevnoj dijagnostici i terapiji aritmija dječije dobi.

Ključne riječi - **pedijatrijske aritmije, dvadest četveročasovni EKG Holter monitoring, razvoj.**

I. UVOD

Pedijatrijska aritmologija koja se bavi aritmijama (disaritmijama) dječije dobi, je još uvijek nedovoljno istraženo područje pedijatrijske kardiologije/kardiohirurgije čija razvijenost predstavlja glavni parametar ocjene razvijenosti medicine, prvenstveno radi smanjenja perinatalnog mortaliteta. Incidenca signifikantnih aritmija djece je 2%, a ako govorimo o svim nesignifikantnim poremećajima ritma do 25%. Osnovni mehanizam za stvaranje aritmija je uzrokovan nestabilnošću membranskog potencijala u ćelijama srca, koji povećava automatizam i one postaju ektopični centri koji mijenjaju normalan redoslijed stvaranja i provoĎenja nadražaja u drugim dijelovima srca. Patofiziološki klasično se navode tri mehanizma nastanka disritmija: pojava kruženja u nekom dijelu srca, pojava naknadnih potencijala ili neuobičajenih pojava automatizma. Kod djece najčešće je vezan za pojavu kružnih mehanizama, a uzroci mogu biti različiti: intrakardijalni i ekstrakardijalni. Vjerovatno je pomjeranje istraživanja na nivo ćelijskih poremećaja pravi put za razumijevanje geneze aritmija. Postoje brojne mogućnosti klasifikacije srčanih aritmija koje se osnivaju na kliničkim i elektrokardiografskim kriterijima. Dijele se na poremećaje ritma za sinusni čvor (nenormalno stvaranje ili odavanje impulsa), poremećaji ritma uslijed stvaranja ektopičnih impulsa i poremećaje ritma zbog oštećenja provoĎenja impulsa U odnosu ma mjesto nastanka dijele se na atrijalne i ventrikuarne, a klinički na poremećaje brzine rada srca (bradiaritmije i tahiaritmije), poremećaje ritma (ekstrasistole) i poremećaje sprovoĎenja (blokove). Mogu se prezentovati akutno ili hronično i nastati u svim životnim dobima djeteta. Najčešća aritmija dječije dobi je sinusna tahikardija, a najznačajnija paroksizmalna supraventrikularna tahikardija Osnovni simptomi disritmija su: osjećaj opće slabosti, zamaranje, palpitacije, hipotenzija, vrtoglavica, mučnina, bljedoća, marmorizacija, preznojavanje hladnim znojem, crvenilo lica (zajapurenost), iako i najteže disritmije mogu godinama ostati asimptomatske. Na disritmiju možemo posumnjati prema spomenutim anamnestičkim podacima, pozitivnim fizikalnim kliničkim nalazom (venske pulzacuje vrata, promjene pulsa, disritmičnost akcije), a dijagnoza se postavlja na osnovi niza dijagnostičkih pretraga: elektrokardiografije (EKG), kontinuiranog elektrokardiografskog

dvadeset-četverosatnog holter monitoringa, metoda trajnog praćenja srčanog ritma (transtelefonski EKG i loop-rekorder), ehokardiografski (pa čak i fetalnom ehokardiografijom), scintigrafijom, tilt-table testom, ergometrijom, ezofagealnom elektrofiziologijom, elektrofiziološkim ispitivanjem uz programiranu elektrostimulaciju (PES) srca, intrakardijalnom elektrofiziologijom.

Senzitivnost pojedinih metoda je za različite aritmije različita. Terapijski najznačajniji vid liječenja je baziran na primjeni antiaritmijskih lijekova i primjeni elektroterapije (elektrostimulacija, elektrokardioverzija, defibrilacija, implantacija, radiofrekventna ablacija). Terapijski pristup je često nažalost individualan. Kontinuirani dinamički dvadeset-četveročasovni elektrokardiografski monitoring je suverena dijagnostička metoda (zlatni standard) aritmija dječje dobi.

II. Cilj rada

Cilj rada je prikaz mjesta i uloga metode dinamičkog 24h EKG holter monitoringa u svakodnevnom kliničkom radu pedijatrijskog kardiologa. Naime početkom razvoja pedijatrijske kardiohirurgije u BiH, koje je započeo aprila 1997. godine, razvoj aritmologije se pokazao neophodnim i bez barem kontinuiranog holter monitoringa bilo je nezamislivo ozbiljno pristupiti ovom problemu.

III. Materijal i metode

Istraživanje je imalo retrospektivni i analitički karakter, te je obuhvatilo period april 2003.- januar 2015. (podaci prikupljani iz „Registra EKG Holter monitoringa“ Pedijatrijske klinike, KCU Sarajevo). Po protokolu je kod 2616 pacijenta djece urađen je dinamički kontinuirani EKG Holter monitoring. Sve registracije su učinjene tokom hospitalizacije uz vođenje dnevnika aktivnosti i evidencijom subjektivnih tegoba, u trajanju od prosječno 24h sa registracijom najčeće između sto i dvjesto hiljada otkucaja, odnosno QRS kompleksa. Pokušaji provođenja metode u kućnim uslovima se nisu pokazali primjenjivim u našim uslovima. Sam aparat je baterijski kasetni rekorder sa ugrađenim satom, te elektodama za snimanje prekordijalnih odvoda na grudnom košu pacijenta. U principu u svakom momentu se registruju tri odvoda. Dnevnik aktivnosti tokom registracije bilje ži pacijent, dijete ili roditelj kako bi omogućili utvrđivanje korelacije pacijentovih satsimptoma i aktivnosti pacijenta sa pojavom eventualnih aritmija. Vođenje dnevnika, doziranje aktivnosti (trčanje uz stepenište, primjena test trake, i slično), kontrolu subjektivnih tegoba i provjeru elektroda nadzire pedijatrijska nadležna medicinska sestra,. koja prebacuje kasetu na softverski sistem, gdje pedijatrijski kardiolog vrši očitavanje. Elektroničkoj obradi otkucaja, registraciji i predočenim rezultatima mogu smetati neispravnost aparata, nepravilno postavljenje elektrode, kvašenje aparata, blizina magnetnog polja, aparati sa visokim naponima, metali i slično. Na snimku tada imamo veči broj artefakata, bizarnih slika , koje se ne bi snemjeli pogrešno interpretirati.

IV. Rezultati

Dječaka je bilo 1329 (50,8%), a pacijenti su bili starosne dobi od rođenja do 19. godine života. Registracija neonatusa i dojenčadi je bilo 45 (1,7%), male djece 69 (2,6%), predškolske 262 (10%), školske 893 (34,1%), djeca u pubertetu i adolescenciji 1350 (51,6%) (grafikon 1.).

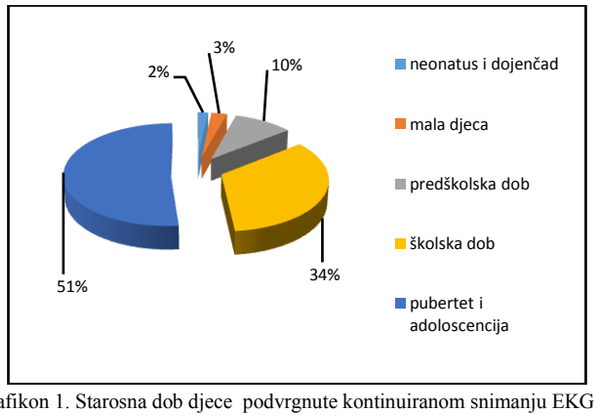

Grafikon 1. Starosna dob djece podvrgnute kontinuiranom snimanju EKG Holter monitoringu

Kod 1775 pacijenta (67,8%) Holter je rađen prvi put, a kontrolnih EKG Holter monitoringa je bilo 41 (32,2%).

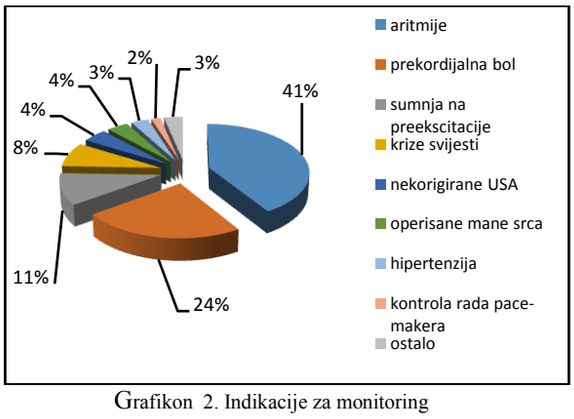

Grafikon 2. Indikacije za monitoring

Indikacije za provođenje Holtera su bile: aritmije 1075 (41,1%), prekordijalna bol 626 (23,9%), sumnja na preeksiktacije i/ili preekscitacije 276 (10,5%), krize svijesti

213 (8,1%), nekorigirane urođene/stečene mane srca 116 (4,4%), operisane mane srca 99 (3,7%), hipertenzije 81 (3,1%), kontrola rada pejsmejkera 43 (1,6%), ostali uzroci 87 (3,3 %) (grafikon 2.).

Otpusne dijagnoze nakon urađenog EKG Holter monitoringa su nesignifikantne aritmije 1189 (45,4%), lutajući centar vodič 579 (22,1 %), preekscitacije 444 (17 %), benigne ventrikularne ekstrasistole 165 (6,3%), atrioventrikularni blokovi 84 (3,2 %), sinusna pauza 63 (2,4%), te ostali poremećaji ritma 92 (3,5 %) (grafikon 3.).

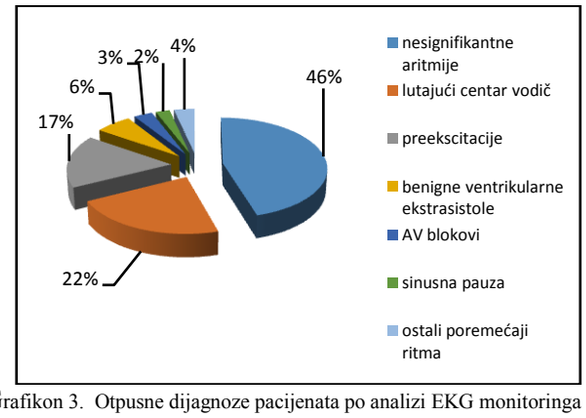

Grafikon 3. Otpusne dijagnoze pacijenata po analizi EKG monitoringa

U pomenutom periodu su registrovana 54 slučaja WPW (Wolf Parkinson White) sindroma, koji su u najvećem broju slučajeva bili udruženi sa paroksizmalnom supraventrikularnom tahikardijom i čine većinu otpusnih dijagnoza preekscitacija.

Kod 124 (4,7%) pacijenta se primjenjuje antiaritmijska terapija. Implanitrano je 27 pacemakera, a radiofrekventna ablacija je rađena u 23 slučaja.

V. Diskusija

Broj registracija dinamičkog dvadestčetveročasovnog EKG Holter monitoringa, prosječno oko 220 pedijatrijskih pacijenata godišnje je reprezentativan i dobar za sticanje iskustva i znanja, ali se postavlja pitanje racionalnosti, bolje saradnje sa pedijatrijskim kardiolozima u Federaciji BiH, preciziranjem indikacija registracija, vremena kontrola i slično. Ne postoji signifikantna razlika u polnoj strukturi, a prevaga djece u pogledu uzrasne dobi preko 50% u pubertetu i adolescencije je posljedica neurohormonskih zbivanja i poznata i saglasna rezultatima drugih autora. Prisutno pomeranje registracije poremećaja ritma u rano neonatalno i dojenačko razdoblje (1,7%), koje će razvojem fetalne ehokardiografije rezultirati i detekcijom fetalnih aritmija intrauterinome dijagnostikom i liječenjem (fetalna ehokardiografija, izravna intrauterina primjena lijeka u fetalnu cirkulaciju ili primjena lijeka preko majke), će biti još prisutnije [1,2,].

Postoji nekoliko otvorenih pitanja koja izbijaju u prvi plan. Najintrigantnije je pitanje incizijskih aritmija, koje nastaju nakon operativne korekcije urođenih srčanih mana (USM) i na ćemu se bazirana današnja i buduća istraživanja ove oblasti.

Moderna pedijatrijska kardiologija se danas uglavnom bavi urođenim srčanim manama. Incidenca urođenih mana srca je 0,8-1% i predstavljaju 23% svih urođenih anomalija, te su najčešće urođene anomalije [3,4]. Posljednjih godina smo svjedoci intenzivnog razvoja pedijatrijske kardiohirurgije (napredak u dijagnostici, interventnoj dijagnostici, neonatalnom zbrinjavanju, perfuziji, anesteziji, kardiohirurškim tehnikama,...) i sve većih mogućnosti hirurškog liječenja većine urođenih anomalija srca, pa i najkompleksnijih [5]. U najvećem broju slučajeva urođene anomalije srca zahtjevaju operativno liječenje (oko 60%), katkada i u više navrata. Danak razvoja i uspjeha pedijatrijske kardiohirurgije je pojava brojnih incizijskih (postoperacijskih) aritmija [6]. Hemodinamski USM se dijele na urođene anomalija srca bez šanta (opstruktivne), urođene anomalije srca sa šantom i kompleksne urođene anomalije srca. Anomalije sa šantom dijelimo na acijanogene sa lijevo-desnim i cijanogene sa desno-lijevim šantom..

Proces nastajanja incizijskih aritmija, u vidu puteva kruženja električnih impulsa, se javlja oko ožiljaka na mjestima hirurških incizija atrija ili ventrikula, oko provodnika (conduit), zakrpa (patch) i sličnih artefekata. Incizijske aritmije su najčešće trajne mada mogu biti i prolazne, ali i progresivno evolutivne [7]. Neke kongenitalne anomalije srca imaju disritmiju koja je često udružena uz njih ili čak sastavni dio same anomalije poput Morbus Ebsteina, transpozicije velikih krvnih sudova, trikuspidne atrezije, totalnog anomalnog venskog utoka, atrijalnog septalnog defekta, atrioventrikularnog septalnog defekta. Nakon operativne korekcije kongenitalne anomalije srca najčešći poremećaji ritma su postoperativni blok desne grane, atrioventrikularni blok II stepena tipa Mobitz 2, atrioventrikularni blok III stepena, blok lijeve grane, paroksizmalna supraventrikularna tahikardija, kod veće djece i atrijalna fibrilacija [8]. Najteže disritmije se javljaju nakon zamjene valvule i u ovim postoperativnim valvularnim anomalijama incidenca postoperativnog kompletnog bloka se javlja u incidenci 60-80% uz trombozu, hipovolemiju i dehidraciju naročito kod mlađe djece [9]. Obzirom da su urođene anomalije srca evolutivnog karaktera njihova rana dijagnostika je imperativna, a potpuna objektivizacija zbog složene hemodinamike

i anatomije, udruženosti sa drugim anomalijama od krucijalnog značaja za pedijatrijskog kardiohirurga. Kod djece kod kojih odgađamo operativni tretman kongenitalne anomalije srca postoji veći rizik pojave incizijskih aritmija [10]. Empirijski je utvrđena veća učestalost poremećaja ritma nakon operacije kongenitalnih anomalija srca prvenstveno kompleksnog tipa, kod transpozicije velikih krvnih sudova, ventrikularnog septalnog defekta, koarktacije aorte, aortne stenoze, atrioventrikularnog septalnog defekta, pa i atrijalnog septalnog defekta kao i svih kongenitalnih anomalija srca gdje se hirurški vrši intervencija u okolini aortalne valvule ili na nivou interventrikularnog septuma [11]. Operativna tehnika urođene anomalije srca utiče na vrstu incizijskih aritmija [12]. Incizijske aritmije su naročito čest uzrok iznenadne srčane smrti u djece, pa i odraslih, naročito nakon operisane kongenitalne aortalne stenoze, Tetralogije Fallot, transpozicije velikih krvnih sudova i kod ovih operisanih kongenitalnih anomalija potrebna je posebna pažnja [11,12].

Često odluku o tretmanu pojedine urođene anomalije srca (transkateterizaciono, hibrid operacija, palijativna korekcija, radikalna korekcija) donosimo na osnovu nastanka vitalno ugrožavajućih aritmija [13]. U ovom momentu je upravo pojava incizijskih aritmija jedan od odlučujućih parametara za preferenciju određene operativne tehnike. Neprepoznate i neadekvatno liječene incizijske disritmije mogu biti neposredni i još češće, kasniji uzrok smrti [1,14]. Uvijek se moraju posmatrati kroz prizmu rasta i razvoja djeteta kao specificuma samog za sebe, a čije se interakcije sa urođenim anomalijama srca i incizijskim aritmijama mnogoznačne [15]. Ovo je jedan od razloga dinamičnog razvoja pedijatrijske ritmologije. Sa druge strane dijagnostika i tretman incizijskih aritmija prate ovaj trend uglavnom putem invazivnih procedura i novih lijekova [16]. Naših 116 zapisa EKG Holter monitoringa kod neoperisanih USA i 99 zapisa operisanih srčanih mana, te implantiranih 27 pejsmejkera često i nakon pojave totalnog AV bloka nakon operacije USM, što ukupno čini 8,3% svih registracija sugeriše veličinu problema.

Sa druge strane terapija, ne samo incizijskih aritmija, je kompleksna. Novija tehnička dostignuća elektroterapije uz otkrivanje novih lijekova nije uspjela razriješiti mnogobrojne dileme.

U ovom momentu je implantirano 27 pejsmejkera , kod nas u preko 50% slučajeva, radi totalnog AV bloka nakon operativne korekcije USM ili nakon kongenitalnog bloka, pa i abolesti SA čvora. Radiofrekventnu ablaciju smo imali kod 23 pacijenta, sa zadovoljavajućim rezultatom kod 75% pacijenata. Naših 4,7 % zapisa je bilo u cilju ordiniranja terapije ili kontrole terapije od ukupnog broja od 22,6% registriranih signifikantnih poremećaja ritma (preekscitacije, sinusne pauze, AV blokovi).

Farmakoterapijski tretman je uglavnom baziran na primjeni pet grupa lijekova; grupa I blokatori brzog ulaska natrija u ćeliju sa svoje tri podgrupe: kinidin, prokainamid, dizopiramid odnosno lidokain, meksiliten, tokainmid, fenition flekanaidpropafenon, enkainid, cibenzolin i lorkainid, grupa II - antagonisti β1 adrenergičkih receptora - propranolol, ormidol, atenolol, metoprolol i nadalol), grupa III - blokatori kalijumskih kanala – amjodaron, sotalol, bretilium, grupa IV – blokatori kalcijevih kanala-digoksin, verapamil, adenozin, diltiazem i neklasifirani antiaritmici – atropin, adrenalin, izoprenalin, kalcijum hlorid, magnezijum hlorid [17]. U našoj svakodnevnoj praksi najčešće koristimo blokatore kalijumskih kanala i beta blokatore, dok u jedinicama intenzivne njega, češće koristimo blokatore kalijumskih kanala i neklasificirane antiarimtike. Sotalol hidhlorid najviše koristimo sa zadovoljavajućim uspjehom.

Terapiju najčešće dajemo u vidu monoterapije ali i kombinovane antiaritmijske terapije i druge terapije. Posebno bi trebalo apostrofirati primjenu kombinovanog liječenja gojaznih sa metforminom i sotalolom, pa i antihipertenzivima tipa ACE inhibitora. Nedostaci medikamentozne terapije aritmija su opterećenost redovitim uzimanjem lijeka, recidivom aritmija, psihološkim posljedicama svijesti o bolesti, nuspojava lijekova, rizikom interakcija, potrebom za trajnim nadzorom bolesnika, čestih specijalističkih pregleda, kao i upotrebe dijagnostičkih metoda, te povremenih hospitalizacija zbog recidiva aritmija i/ili evaulacija. Kritičnost, samokritičnost u vidu obrade terapije prognoze bi morali biti naš imperativ, ne zaboravljajući naše socijalne i društvene okvire.

VI. ZAKLJUČAK

Razvoj pedijatrijske kardiohirurgije je inicirao i razvoj pedijatrijske aritmologije kao imperativni segment pedijatrijske kardiologije. Kontinuirani EKG Holter monitoring je postao nazamjenljiva metoda u svakodnevnoj dijagnostici i terapiji aritmija dječije dobi. Obzirom da kontinuirani EKG holter monitoring nije dostatan potrebama bilo bi važno ovladati dječijom elektrofiziologijom, kao i metodama radiofrekventne kateterske ablacije (krio i termo terapije), uz tehničko praćenje implantacije suvremenijih i zahtjevnijih pejsmejkera, imajući u vidu posebnosti elektrostimulacije srca u djece, sve češća endovensku ugradnju, intraoperaciona testiranja, sigurnu kontrolu i samokontrolu sve složenijh aparata. Incizijske aritmije će biti i dalje

otvoreno pitanje i predmet budućih istraživanja. Dječija aritmologija nije ekstenzija adultne aritmologije i puno više postavlja pitanja, nego što daje apsolutne odgovore u ovom momentu.

LITERATURA

1. Rubart M., Zipes D. P. Arrhythmias, Sudden Death and Syncope. U: Bonow R.O., Mann D.L., Zipes D.P., Libby P. Braunwald's Heart Disease: A Textbook of Cardiovascular Medicine. 9th ed. Philadelphia: Saunders Elsevier. 2011. 660-669.
2. Hanash C.R., Crosson J.E. Emergency diagnosis and management of pediatric arrhythmias. *J Emerg Trauma Shock.* [Online]. 2010. 251-260.
3. Jovanović I., Đukić M., Parezanović V., Ilić S. UroĐene srčane mane. U: Ostojić M., Kanjuh V., Beleslin B. Kardiologija. Beograd: Zavod za udžbenike. 2011. 588.
4. Massin M., Malekzadeh-Milani S.G., Demanetz H., Wauthy P., Deuvaert F.E., Dessy H., Verbeet T. Prevalence of early postoperative arrhythmias in children with delayed open-heart surgery for severe congenital heart disease. *Acta Clin Belg*. 2010. 386-391.
5. Pflaumer A. Perspectives in ablation of arrhythmias in children and patients with congenital heart disease. *Intern Med J.* 2012. 70-76.
6. Malčić I. Osobitosti aritmija u dječjoj dobi. U: Begovac M., i sur. Aritmije u liječničkoj praksi. Zagreb: Školska knjiga. 2010. 94.
7. Prijić S., AĐić O., Košutić J., Stajević M., Ninić S., Kuburović V., i sur. Značaj magnetne rezonancije u praćenju bolesnika sa Tetralogijom Fallot. U: Zdravković D., ĐorĐević M. Problemi u pedijatriji 2012. Beograd: Zavod za udžbenike. 2013. 132-147.
8. Grujić M., MrĐa S., Mujović N., Kocijančić A. Tahikardije. U: Grujić M. Srčane aritmije. Beograd: Kosmos; 2010. 166.
9. Prijić S., Košutić J., Vukomanović V., Stajević M., Ninić S. Savremeni pristup dijagnostici i liječenju aortne stenoze kod djece. U: Zdravković D. Problemi u pedijatriji 2010. Beograd: Zavod za udžbenike. 2011. 419-432.
10. Alp H., Narin C., Baysal T., Sarıgül A. The prevalence of and risk factors for early postoperative arrhythmias in children after cardiac surgery. [Online]. 2013. 85
11. Gist K. M., Erickson B. A., Schuchardt E. L., Morose M., Kaufman J., Da Cruz E., Mitchell M. B., et al. Tachyarrhythmia following Norwood Operation: A Single Center Experience. *Cardiology in the Young* - 46th Annual Meeting of the Association for European Paediatric and Congenital Cardiology, AEPC with joint sessions with the Japanese Society of Pediatric Cardiology and Cardiac Surgery, Istanbul, May 23-26, 2012, Cambridge University Press, May 2012. 22 (1).4.
12. Buljević B. Uzroci i intrauterino liječenje fetalnih aritmija. U: Malčić I., Škrablin-Kučić S. i sur. Fetalna i neonatalna kardiologija. Zagreb: Medicinska naklada. 2011. 182-200.
13. Baumgartner H., i sur. ESC Guidelines for the management of grown-up congenital heart disease (new version 2010): The Task Force on the Management of Grown-up Congenital Heart Disease of the European Society of Cardiology (ESC). *Eur Heart J.* 2010. 31 (23), 2915-2957.
14. Košutić J., Stajević M., Šehić I., Ugrinović B., Vukomanović V., Rakić S., i sur. Indikacije i optimalan uzrast za hiruršku korekciju izolovanog otvora meĐukomorske pregrade. U: Zdravković D. Problemi u pedijatriji 2010. Beograd: Zavod za udžbenike. 2011. 321-328.
15. Ofori-Amanfo G., Cheifetz I.M. Pediatric postoperative cardiac care. *Crit Care Clin.* 2013. 29(2), 185-202.
16. Bagatin J., Carević V. Novi lijekovi u kardiologiji. *Medicus.* 2010. 19(2), 225-229.
17. Begić Z. Poremećaji srčanog ritma dječije dobi (preporuke-algoritmi dijagnostike i tretmana). PECS, VIII Ljetna pedijatrijska škola, Sarajevo, 2010. 75-99.

Zijo Begić, Pedijatrijska klinika, Klinički centar Univerziteta u Sarajevu, Patriotske lige 81, 71000 Sarajevo, Bosna i Hercegovina, tel 033566405, e-mail: begiczijo@gmail.com

Concept and Implementation of Fuzzy Set Theory Technique for Image Enhancement Purposes

Emrah Irmak[1], Kadir Ileri[2] and Ali Ozkahraman[2]

1 Karabuk University / Biomedical Engineering Department, Karabuk, Turkey
2 Karabuk University / Electrical and Electronics Engineering Department, Karabuk, Turkey

Abstract— **Fuzzy set theory has become a crucial tool in image processing including image enhancement, edge detection, noise detection, noise removal, image segmentation, geometric measurement, scene analysis etc. Among these image enhancement is widely used for some important specific areas such as medical, photography and selenography. The main goal of image enhancement is to process a given image so that the result is more suitable than the original image for a particular profession. In this paper very short basics of image enhancement using fuzzy logic are introduced and application of image enhancement concept is presented using fuzzy set theory with s-shaped membership function for medical, color and gray scale images. The proposed technique is able to improve the contrast of medical images, color images and gray scale images by means of software techniques. In this paper, an algorithm is explained and implemented to enhance images using fuzzy technique with s-shape membership function.**

Keywords— **fuzzy logic, image enhancement, membership function, contrast stretching.**

I. INTRODUCTION

Image enhancement is widely used in computer graphics. It is a popular sub-area of image processing. Image enhancement is the improvement of image quality to a better and more understandable level for visual appearance [1]. The main goal of image enhancement is to process a given image so that the result is more suitable than the original image for a particular profession [2]. One important point is that the enhancement doesn't increase the intrinsic information content of the data, but it increases the dynamic range of the intensity values of pixels so that intrinsic information can be detected easily.

Image enhancement techniques can be divided into two main groups;

- *Spatial Domain Methods* operate directly on pixels. Fuzzy logic image enhancement method can be included into this group. The operation can be formulated as;

$$g(x, y) = T[f(x, y)] \quad (1)$$

where g is output image, f is the input image and T is an operation on f defined over some neighborhood of (x, y).

- *Frequency Domain Methods* operate on Fourier transform of an image [3]. These methods enhance an image $f(x, y)$ by convoluting the image with a linear, position invariant operator. The operation can be formulated as;

$$g(x, y) = f(x, y)*h(x, y) \quad (2)$$

where g is output, f is input image and h is transfer function [4].

Figure 1 shows the common algorithm of image enhancement process. The image to be enhanced is taken into computer environment, decision about selecting appropriate image enhancement technique is made, image is gone under enhancement process and enhanced image is displayed.

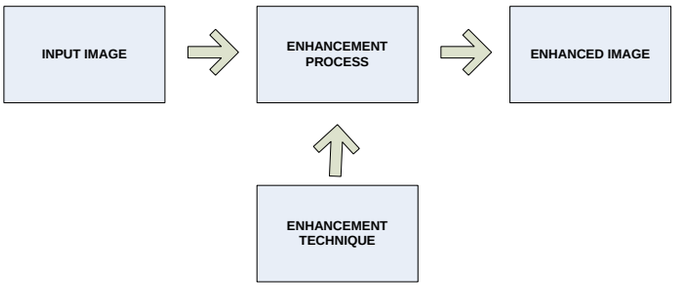

Figure 1: Image Enhancement Algorithm

A. Fuzzy Set Definition

Being natural is an important property of fuzzy sets. To make idea more clear let us think that we would like to define a set of levels of difficulty that share the property difficulty. In conventional set theory, we are assumed to determine critical edge, say difficulty level 50. All difficulty levels between 0 and 50 are elements of this set; the others do not belong to the set. However difficulty is a matter of degree. Therefore, a fuzzy set can specify this model much better. To define this set, we also need two different critical edges, say difficulty levels 50 and 100. All of the difficulty levels that are less than 50 are elements of the set whereas difficulty levels greater than 100 are not elements of the set

and difficulty levels between 50 and 100 are the elements of the set to some degree. Some degree statement is the key point of the fuzzy set theory.

The basic property of fuzzy logic is that it is a decision-making algorithm. Making a decision is one of the most important procedures in the real life. The objective of making a decision is to get an optimal or a nearly optimal solution from input information using a membership function [5].

Fuzzy set theory was first proposed by Zadeh in 1965, and was first used in control by Mamdani.

Fuzzy set is a set that allows elements to belong to it to a particular extent. A fuzzy set is defined by a membership function that maps elements of a given domain into values in [0, 1].

II. Methodology and Implementation

The problem whether a pixel should become darker or brighter than it already is, can be thought as the main field of interest of the fuzzy logic image enhancement. Figure 2 is the key point algorithm of the proposed method. The first step is to take image into computer environment, the next step is to compute the histogram of the image in question and accordingly to decide whether image histogram is appropriate for s-shape membership function or not. If histogram range lies down in a narrow band this means that fuzzy logic s-shape image enhancement method is suitable for this specific aim. The following step is to convert image to fuzzy plane. Next is to modify membership function using proper modification formula. Stretching contrast is the next step of the proposed method. The last step is to convert image to original plane and to display the enhanced image.

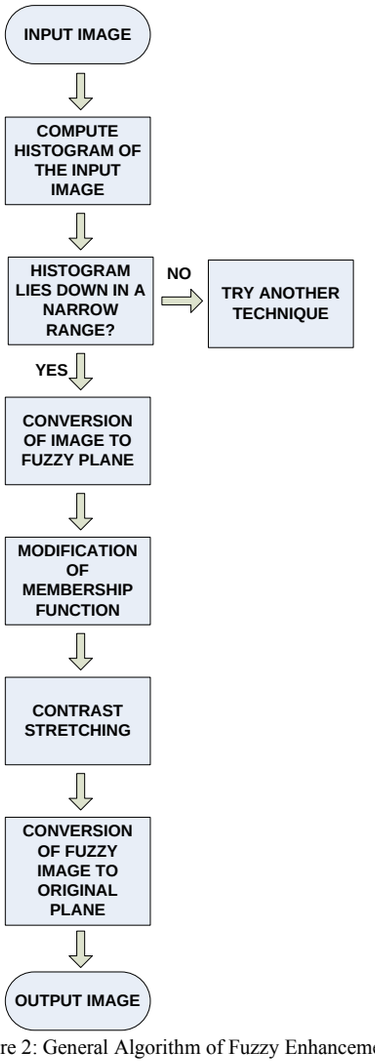

Figure 2: General Algorithm of Fuzzy Enhancement

Algorithm:

Step-1: Compute histogram of the image. If the range of intensity values in the histogram of the image is small (in other words, if the range of the intensity value lies down in a narrow band) then fuzzy logic enhancement technique with s-shape membership function is appropriate for image enhancement process.

Step-2: After choosing the fuzzy logic enhancement with s-shape membership function, specify minimum intensity value (g_{min}) and maximum intensity value (g_{max}) of the image.

Step-3: Once the minimum and maximum intensity values found, convert image to fuzzy plane by shifting minimum intensity value to 0, maximum intensity value to 1,

and other intensity values between 0 and 1 using fuzzy formula below. This process is called *fuzzification* [6].

Conversion to Fuzzy Plane:

$$\mu_{(g)} = \frac{g - g_{min}}{g_{max} - g_{min}} \quad (3)$$

Step-4: Now all the image data is on the fuzzy plane. At this point modification of membership function and contrast stretching are the next steps. As stated before it is determined that s-shape membership function modification is appropriate for images whose range of intensity values range in a narrow band.

S-Shape Membership Function:

$$S(z; a, b, c) = \begin{cases} 0 & z < a \\ 2\left(\frac{z-a}{c-a}\right)^2 & a \le z \le b \\ 1 - 2\left(\frac{z-c}{c-a}\right)^2 & b < z \le c \\ 1 & z > c \end{cases} \quad (4)$$

This spline-based curve is a mapping on the vector z, and is named because of its S-shape. The parameters a and c locate the extremes of the sloped portion of the curve where b is arithmetic mean of a and c.

Step-5: Stretch the image contrast by multiplying each pixel intensity value in the image by a constant value.

Step-6: The last step is the defuzzification the image and test of the enhanced image [7].

III. IMPLEMENTATION AND EXPERIMENTAL RESULTS

Figure 3 is the original color image to be enhanced whereas Figure 4 shows the enhanced color image after fuzzy logic with s-shape membership function enhancement process. Equation 4 is applied to the each color layers which are red, green and blue of color image.

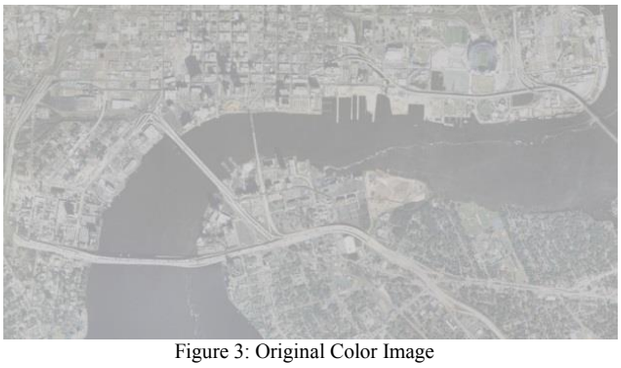

Figure 3: Original Color Image

Figure 4: Enhanced Color Image

Figure 5 is the original grayscale image of moon to be enhanced and Figure 6 shows the enhanced moon image. For a lunarian or a space scientist enhanced image, Figure 6, is more illustrative in an astrionics perspective.

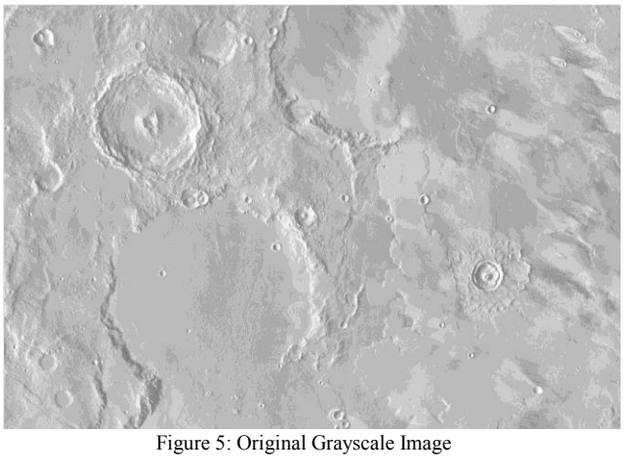

Figure 5: Original Grayscale Image

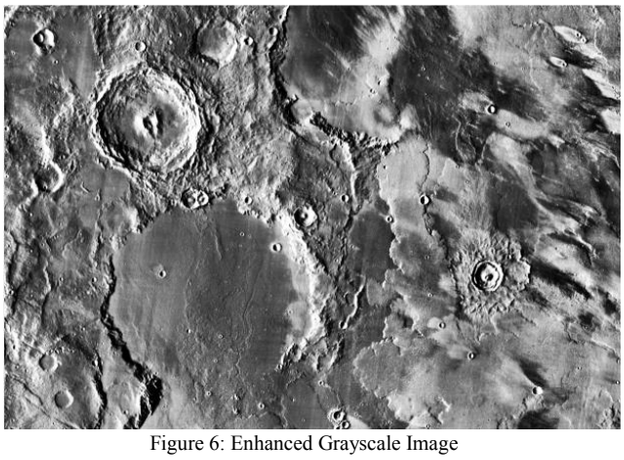

Figure 6: Enhanced Grayscale Image

Figure 7 is the mr image to be enhanced of a patient and Figure 8 shows the enhanced mr image. Since information

gained from medical images acquired in the clinical track of events is usually of a complementary nature, proper visual appearance of useful data obtained from the images is often desired [8]. For a doctor, radiologist or a physician image in Figure 8 which is the enhanced image is more informative in a medical point of view.

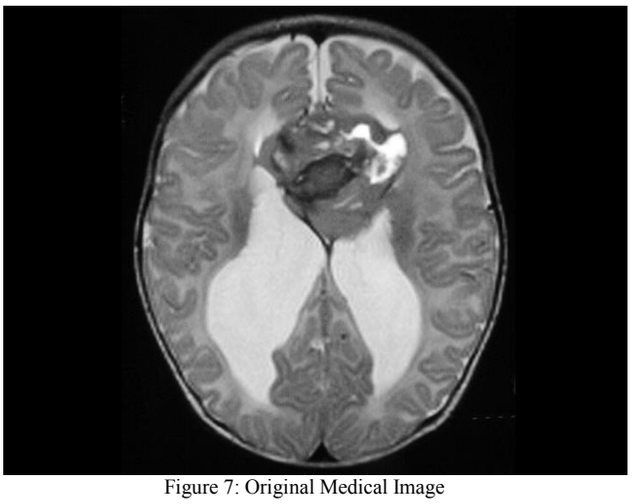

Figure 7: Original Medical Image

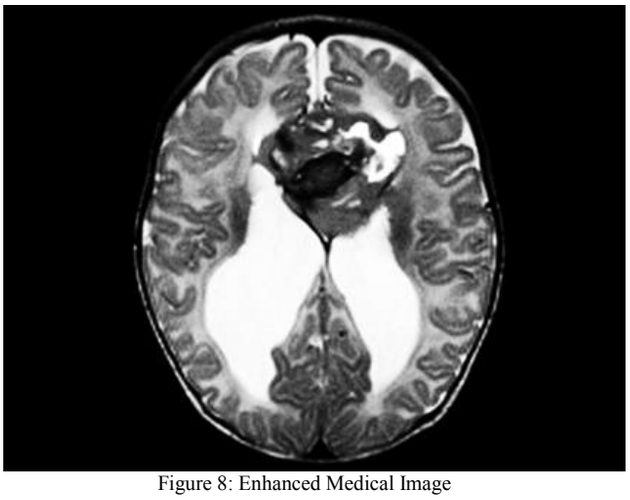

Figure 8: Enhanced Medical Image

IV. Conclusion and Future Work

The scope of image enhancement algorithms includes a wide spectrum of subjects including medical image enhancement, color image enhancement and grayscale image enhancement [9]. In this paper the requirements and conditions of using proposed technique have been determined and correspondingly usage of image enhancement has been presented for a daily color image, an astronomy image (an image of the moon) and a medical image (Mr Image of a patient's brain) using fuzzy logic with s-shape membership function image enhancement technique. The algorithm has been successfully applied and desired enhanced images have been showed. In the future work, it is planned to integrate this MATLAB and C# software to the Digital Signal Processors (FPGA's).

References

1. Chowdhury, M.M.H. Islam, M.E. Begum, N. Bhuiyan, M.A. "Digital image enhancement with fuzzy rule-based filtering", 10th international conference on Computer and Information Technology (ICCIT). 27-29 Dec. 2007.
2. M. R. Ramesh Kumar, R. K. Gupta, V. Dayal. Theme oriented enhancement of sea surface temperature in thermal infrared avhrr images. Journal of the Indian Society of Remote Sensing December 1987, Volume 15, Issue 2, pp 43-51.
3. K. Venkateshwarlu, Assist. Prof. Anju Bala. Image enhancement using fuzzy inference system. Master of engineering in Computer Sciences and Engineering. Thapar University, Patiala, June 2010.
4. Guo Xian Jiu; Jiang Feng Jiao; Li Xiang, "Image enhancement method based on fuzzy set and subdivision," Awareness Science and Technology (iCAST), 2011 3rd International Conference on , vol., no., pp.174,176, 27-30 Sept. 2011.
5. Hong TP, Lee CY (1996) Induction of fuzzy rules and membership functions from training examples. Fuzzy Sets Syst 84:33–47.
6. Prof. Mrs. Preethi S.J, Prof. Mrs. K. Rajeswari. Membership Function modification for Image Enhancement using fuzzy logic. International Journal of Emerging Trends & Technology in Computer Science (IJETTCS). Volume 2, Issue 2, March – April 2013.
7. Tarun Mahashwari, Amit Asthana. Image Enhancement Using Fuzzy Technique. IJRREST International Journal Of Research Review In Engineering Science & Technology (ISSN 2278–6643) Volume-2, Issue-2, June-2013.
8. Irmak Emrah, Ercelebi Ergun. Ertas Ahmet H. Brain tumor detection using monomodal intensity based medical image registration and MATLAB. Turkish Journal of Electrical Engineering & Computer Sciences (Turk J Elec Eng & Comp Sci). DOI: 10.3906/elk-1403-75. (IN PRESS).
9. Rafael C. Gonzalez, Digital image Processing, Prentice Hall, 2008.

Development of domain specific language and IDE for Internet of Things applications in remote patient monitoring

A.Salihbegovic [1], E. Kaljic[1], T. Eterovic[1] and S.Ribic [1]

[1] Faculty of Electrical engineering, University of Sarajevo, Bosnia Herzegovina

Abstract— **Paper is devoted to presentation of the results achieved so far in the area of research and development of software design tools helping designers to design and develop applications in the domain of internet of things (IoT). Three main areas of applications of internet of things paradigm are targeted: smart home, telemedicine e.g. remote patient monitoring and intelligent transportation.**

The development of visual domain specific language code named DSL-4-IOT, is defined as graphical high level language that is abstracting in its building blocks many specifics, peculiarities and heterogeneity of sensors, actuators, communication media and protocols, physically organized within wired or wireless sensor nodes, that are specific for internet of thing devices.

Selection of sensors, actuators and devices is done by IoT application designer, only on the functional level demanded by specific application. The devices are selected from the rich application library of DSL-4-IOT designer, or if not existing within library modules, the designer can easily add new device, entering its technical data like device manufacturer and type, sensors and/or actuators integrated or hooked to device, communication media and underlying protocol.

After configuring IoT application using DSL-4-IOT designer, the software suite shall output clear system architecture with bill of material and specifications of all hardware devices and components needed for build-up of the system, as well as configuration files, that are downloaded to open source runtime software application.

While entering the configuration data into DSL-4-IOT designer, user is also specifying the way how ambient monitoring and control and patient monitoring interface shall look like. User interface is web application that can be presented on any PC device, mobile phone or tablet with Internet connection and standard web browser. User can view and interact with the IoT application from anywhere where Internet is available.

Keywords— **Internet of things, telemedicine, remote patient monitoring, smart home, wearable biomedical sensors,**

I. INTRODUCTION

Application development challenges, heterogeneity of devices (physical variables sensors, biometric sensors) , different software implementation (Android, iOS, Linux), different interaction modes (pub/sub, request/response, command) and different engineering units (deg C, deg F, bar, etc.) are the ecosystem in which the designers of the Internet of Things (IoT) applications are creating their projects[1], [2].

Designers of IoT applications should be relieved of most of these diversities and specifics (wide range of hardware and software entities running on specific platforms, middleware specific features), and be able to use integrated development environment (IDE) based on domain specific high level language which in its entities would abstract most of these intricacies and specifics in hardware, software, communication media and protocols. Furthermore, the language should be capable to support large scale design of these systems by combining several design blocks and saving them in application libraries, importing them, reconfiguring and parameterizing with ease for new tags and locations, enabling reusability and scalability [3].

Furthermore, the scope of the language and design tools based on that language should span several application area of IoT, including environmental monitoring and control where patient(s) is/are living, with remote monitoring of its biomedical parameters and health condition.

II. STRUCTURE AND FUNCTIONALITY OF DSL-4-IOT LANGUAGE

The vast versatility of the types of sensors and actuators as well as heterogeneity of communication medias and protocols that are immanent, are facing design engineer within the domains of Internet of things applications. Understandably, all this is posing burden on designer to acquire knowledge and learn many specifics that are far beyond the functionalities and application requirements that he/she wants to build into the system.

Therefore, there are many efforts going on among researchers and developers to develop higher level domain specific language that will abstract many of these specifics and peculiarities into building blocks and library modules from which he/she is designing its application, specifying the devices and hardware needed for designed system acquisition and deployment on the application site [4].

We in our research project, have opted for the development of one visual domain specific language that shall empower IoT application designer with a visual high level

language and based on it, a design Editor named DSL-4-IoT. The Editor enables designer to configure the system structure, select devices, sensors and actuators either from built-in library devices available in Designer itself, or enter the ones that he/she selects, parametrizing the metadata available from manufacturer's design literature. These device modules can then be saved and included in built-in library modules for future use.

The development of the DSL-4-IoT language is based on the class of visual domain specific modelling languages (VDSMLs) that are using UML formal presentations and abstract syntax in a metamodel. The front end of the Editor has been developed in JavaScript.

The layout of DSL-4-IoT Editor-designer is shown on Fig. 1.

In the command bar, the Editor is providing the necessary tools for opening and saving the applications configuration, together with additional commands for manipulation of individual or groups of block structures (group, copy, paste, delete, undo, redo, resize, etc.).

Labelling of the block structures on the hierarchical level of generic blocks (system, subsystem, devices, device channels, etc.) is enabled using the "Text" button.

The remaining two buttons are intended for generation of textual configuration files with extension "items", and "sitemap" that are used directly in the runtime execution.

The last button further right is used to call external program named "Rule editor" , that enables the designer to configure any logical, sequential or temporal relationships between "items" created in previous step of entering configuration program, where „items" are the logical representation of physical channels of the configured devices (sensor inputs or actuator or command outputs), or variables associated with messages obtained via web services, SMS messages or emails. In broader terms, items are objects that can be read or written to in order to interact with them. Items can be bound to bindings, i.e. for reading the value or status from device channel input or for updating output channel on the device output going to some actuator. More on this can be found in documentation on OpenHAB project [5].

Bellow the higher abstract layer of DSL-4-IoT domain specific language, there is a lot of additional glue code that is running in OpenHAB runtime to:

- Interface disparate hardware and software Components
- Interface software components and middleware
- Map code for device and software components

This glue code which is running in runtime executing DSL-4-IoT tools developed configuration files has been selected as Java based OpenHAB 1.x open source project, widely popular in the IoT community.

In order to abstract mentioned heterogeneity of various IoT devices, sensing and actuating physical devices are described as entities in high level manner and then these

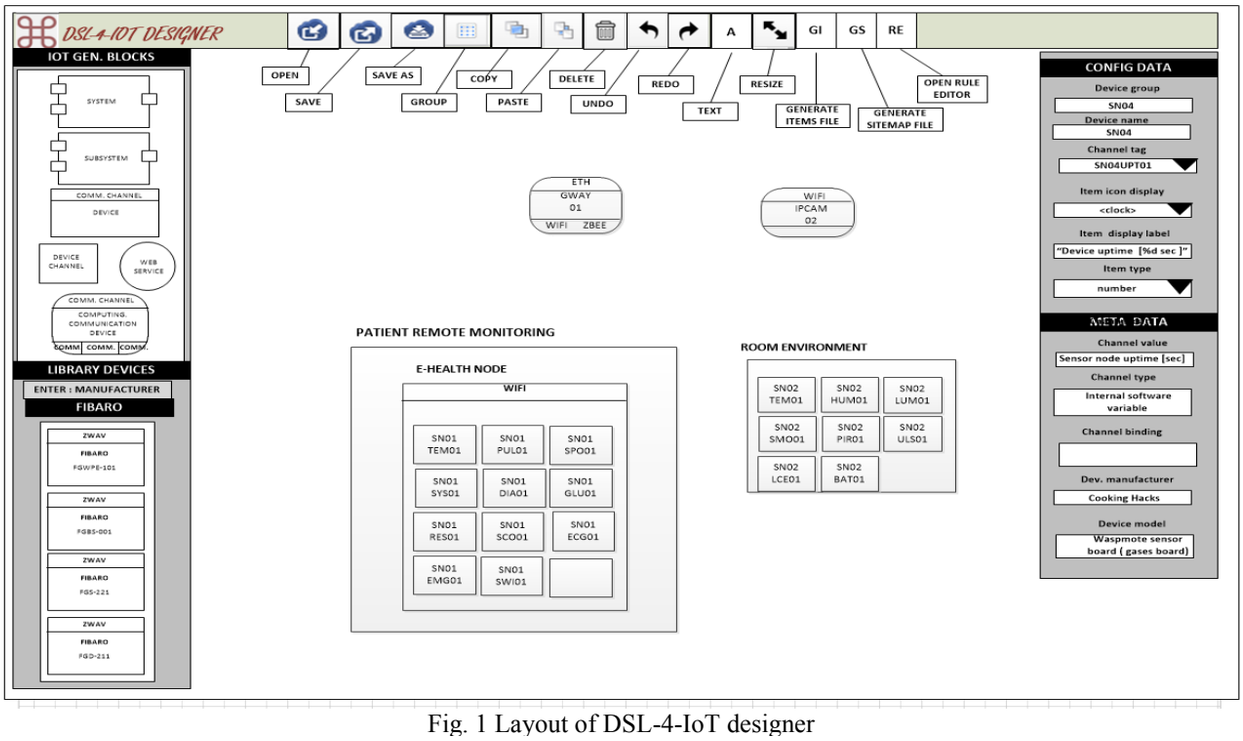

Fig. 1 Layout of DSL-4-IoT designer

resources are instantiated as many times as necessary with the distinct tag names, to represent all physical and virtual devices included in the particular project application.

Scalability of operations within the IoT system application logic that connects "items" in interconnected wireless sensory networks of devices and users is solved with hierarchical clustering consisting of:

- system
- subsystem
- device (autonomous and powered)
-physical or virtual channel

Use of this hierarchical structure enables: project partitioning at physical level, project partitioning at functional level, and to define scope from which software components shall produce or consume data.

DSL-4-IOT compiler within Designer is mainly composed of a parser and configuration files generator. Configuration files generator (items, rules, sitemap) generates formatted text outputs that can be directly downloaded and executed within OpenHAB runtime engine.

Both tools rely on declarative domain-specific language used to graphically represent IoT system topology and "items" embedded in this topology.

Runtime libraries are JavaScript coded based on OpenHAB runtime engine used, as mentioned earlier, to execute application described with generated configuration files.

DSL-4-IOT for configured IOT system structure, exports the data into one JSON array. This array keeps information about position of all the items within configuration, relationships between items and groups, value of all configured fields associated with items and of datatypes. JSON configuration array includes OpenHAB specific fields and associated rules. This array is typically huge in size, and is useful as container from which it is possible to restore the state for further editing and setting up of sensory network configuration.

From the configuration stored in JSON array format, it is possible to export data to wider scope of integration platforms for home automation including remote patient monitoring for new health centers, one of them being OpenHAB. OpenHAB runtime engine requires five kinds of configuration files: Items, Rules, Persistence, Scripts and Sitemaps. These text files differ by file extension and internal structure.

Items in OpenHAB 1.x runtime can be defined using configuration files located in subfolder configurations/items, relative to OpenHAB installation directory. Item definition files have the file extension *.items. Groups are also defined in the *.items file.

A special conversion program scans the JSON document received from the visual DSL-4-IOT configuration Editor. Each cell in this document which is of type iot.device becomes item, and cells which are recognized as embedding cells became groups. The items are stored inside groups.

Sitemaps are used to create elements of a user interface. They are stored in OpenHAB runtime directory configurations/sitemaps. Each file has *.sitemap extension. The structure is similar to above described items configuration file. The very first line has an element called Sitemap, and it is followed in next lines by some of elements: Color picker, Chart, Frame, Group, Image, List, Selection, Set point, Slider, Switch, Text, Video, Webview. [5]. All of them, except Frame, describe user interface elements in single line.

The file which defines rules for IOT application configuration has extension *.rules. A rule file can contain multiple rules, and consists of three sections:

Imports, Variable Declarations and Rules.

Next chapter describing experimental testbed shall demonstrate how these rules are used to establish relationships and functionalities between both environmental and biophysical variables measured on patient and in the room environment where he lives.

III. EXPERIMENTAL TESTBED FOR PROOF OF DEVELOPED DESIGN TOOLS

For proof of concept and versatility of developed visual domain specific language and development environment based on DSL-4-IoT Designer, the experimental testbed has been built and implemented composed of the variety of wireless static and mobile sensory nodes with multiplicity of sensors, actuators, communication channels and protocols from various manufacturers. From the point of view of IoT application domains, two most frequent domains were chosen to be presented, by selection of the types of sensors and their functionality: smart home and remote patient monitoring.

Sensors and actuators used in build-up of experimental testbed have been either autonomous with integral communication transceiver channel, or hooked up to large number of wireless devices (nodes), based on different communication technologies (Wi-Fi, ZigBee, Z-wave, Bluetooth, NFC,) and protocols (HTTP, TCP/IP, UDP, MQTT, Modbus, SimpliciTI, serial protocols etc.). This topology is depicted on the following Fig. 2.

Experimental testbed is physically divided in several domains:

-Central domain which is located in room 2-29 (acting as central nurse monitoring ward),

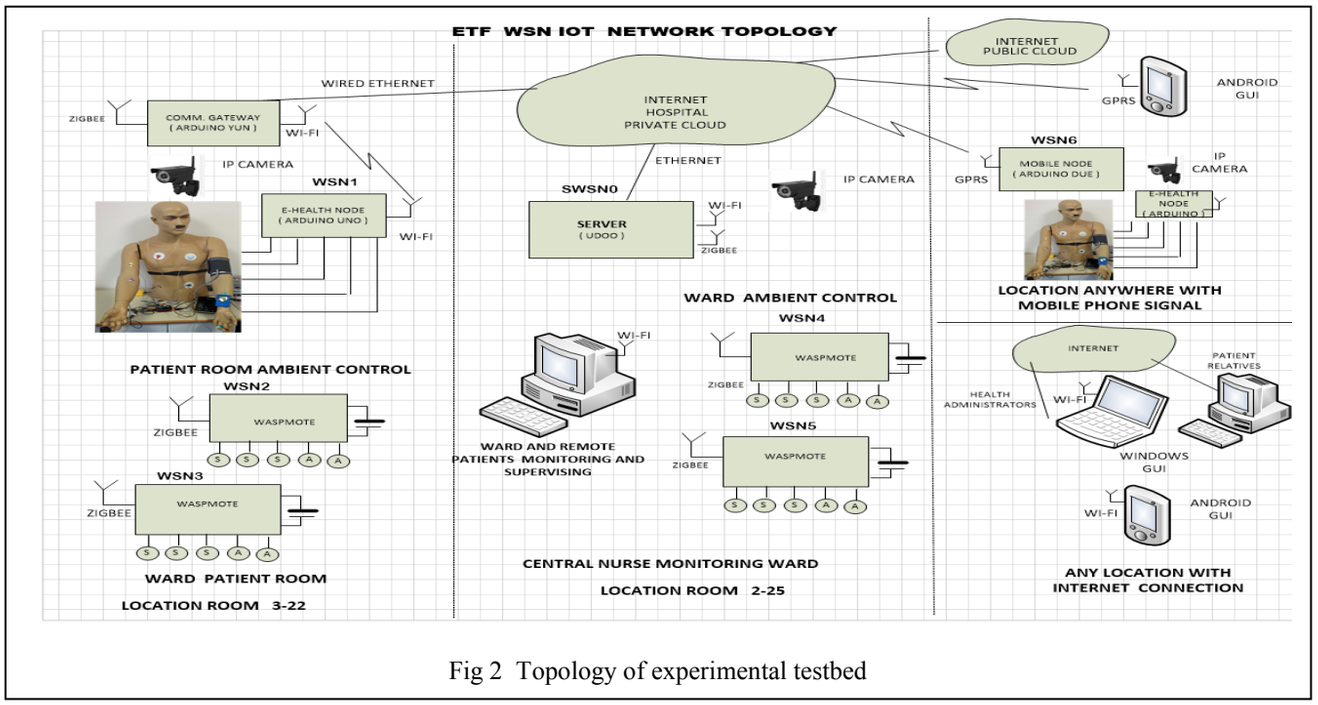

Fig 2 Topology of experimental testbed

- Remote domain which is located in room 3-22 (ward patient monitoring room)

-Mobile domain (like central lab within the hospital, or outpatients staying at their homes), which can be located anywhere within the reach of telecom mobile network signal.

Central domain is housing core server (SWSN0) built on Arduino compatible UDOO computer based on embedded computer with Freescale i.MX 6 ARM Cortex-A9 1 GHz quad-core processor and 1 GB of RAM. UDOO based server executes open source OpenHAB runtime software which is based on the OSGi container, and is powered from 5V DC power source (USB port).

Remote patient monitoring , located in room 3-22, consists of ZigBee wireless sensor nodes (WSN2 & WSN3) for monitoring and control of environmental parameters (temperature, humidity, luminosity, presence, position, proximity, air pollution with various pollutants, patient movement, weight, opened and closed room and bathroom doors and window, flooding on the bathroom floor, wet bed sheets bellow the patient, etc.) as well as actuating and controlling functions (switching On and OFF room and bathroom lights, changing room set point on thermostat, opening and closing or positioning in any intermittent position blinds on windows, opening or closing of the windows, etc.). These wireless sensory nodes are based on Libelium Waspmote hardware built on ATmega1281 microcontroller with powered with onboard battery of 6600 mAh providing 2-3 years autonomy.

E-Health wireless node (WSN1) is based on the Arduino Uno board, e-Health sensor shield and Wi-Fi module [6]. e-Health sensor shield acquires biometric data and enable applications where human patient local and/or remote monitoring is needed, using 10 different biomedical sensors:

- pulse (heartbeat rate), oxygen in blood (SPO2), airflow (breathing), body temperature, electrocardiogram (ECG), glucometer, galvanic skin response (GSR - sweating), blood pressure (sphygmomanometer), patient position (accelerometer) and muscle/electromyography sensor (EMG).

Fig. 3 is illustrating how these biometric sensors are connected to patient being simulated with the doll, all connected individually to e-Health node from Libelium.

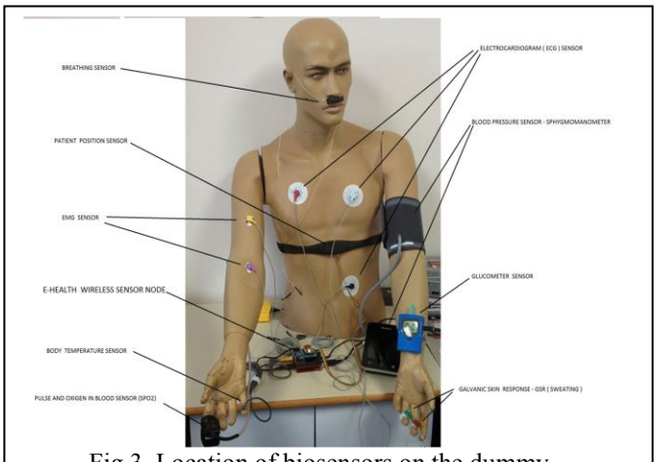

Fig 3. Location of biosensors on the dummy

These sensors are not certified for applications with human beings and are only demonstrating the concept, but provide real life platform for adequate testing of developed software design tools.

Arduino Uno board is built on ATmega 328 microcontroller an

d is powered via USB connector from 5 V DC supply, hence does not have autonomy because of the higher power requirements. This is not important since the node is stationary and is located in patient room where power supply is available.

In order to enable connection of wireless nodes from a patient room 3-22 to the server in the central nurse monitoring ward (room 2-29), the communication gateway is used. Communication gateway is implemented using Arduino Yún with Wi-Fi and ZigBee/802.15.4 communication modules [7]. This gateway mode also requires USB connected 5 V DC power supply. All Arduino boards used in this experimental testbed come with tiny built-in kernel and boot loader for application development and downloading in provided Arduino development environment[8].

Mobile domain that can be installed at any remote patient location, is based on the GPRS mobile node, and Android based mobile phones and tablets. GPRS mobile node is implemented using Arduino Due board and GPRS shield. For communication between GRPS mobile node and server, OpenHAB REST API was used, utilizing my.openHAB cloud service[9].

Central monitoring ward and patient room (rooms 2-29 and 3-22), are covered by video surveillance enabling visual supervision and feedback of the activities performed at these two locations, implemented with IP cameras. Video streams from IP cameras are taken in MJPEG format and presented to the user within OpenHAB web interface on desktop and laptop computers, or HABDroid application on Android based mobile phones [10].

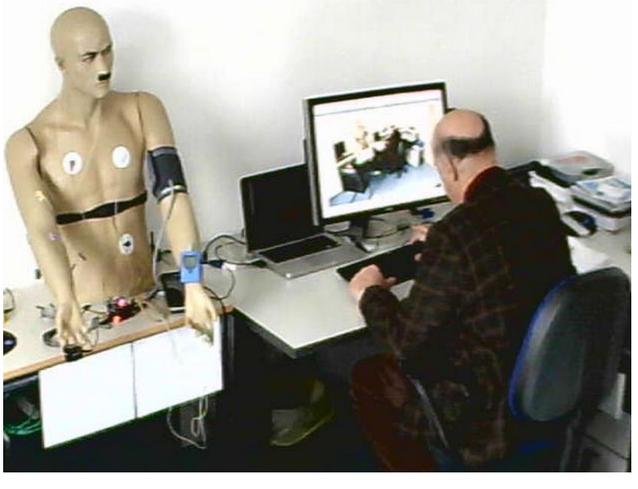

Fig. 4 IP camera monitoring of patient room

IP cameras are equipped with IR (infrared) light that enable full night vision of the patient room even in total darkness. The view of the camera in patient room with dummy doll for patient is shown on the Fig. 4.

User interface that provides monitoring as well as full control of all devices that have been implemented within described IoT experimental testbed, is provided as web application in any web browser that has JavaScript runtime engine included, connecting to IP address of the server (SWSNO). The interface can be accessed either on desktop or laptop computer or any smartphone or tablet with Android or Apple iOS Operating system.

Fig. 5 is showing how this display looks like for the biometric data acquired from patient and presented in window which is open from main screen selecting WSN1 node (e-Health node).

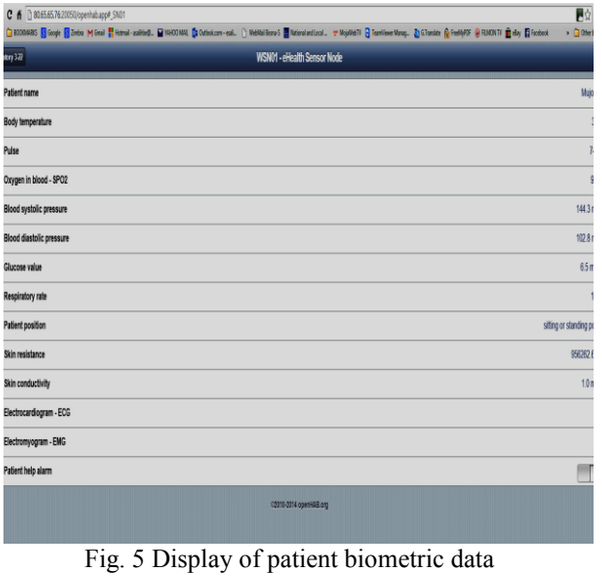

Fig. 5 Display of patient biometric data

IV. DESIGNING FUNCTIONALITIES IN THE SYSTEM

Functionality of the remote patient monitoring as well as monitoring and control of the environmental conditions, is implemented using rules Editor which is generating one more configuration file necessary for runtime execution of the designed IoT application on server (SWSN0).

The examples of these functionalities created with Rule Editors are:

When (any measured biometric parameter or combination of is outside of the permissible limits)

Then

- Send visual and audible alarm to nurse in central monitoring ward to appear on her screen
- Send SMS message to mobile phone or smart watch of

doctor on duty, or any other relevant phone number

- Send email message to any email address defined Log the data for any post mortem analysis that might be required.
- Send email message to any email address defined Log the data for any post mortem analysis that might be required.

The message contains all data identifying the patient name and location with the time of medical event.

Rule editor enables the IoT designer to create any kind of conditions based on combination of continuously measured biometric and environmental variables, time of the day, day in the week etc. to generate warning or alarm message send to addresses previously mentioned recipients.

Example for this is detection of event when patient is out of bed for longer of 10 min. (detected by smart bed weight sensor) in period of 10 in the evening till 7 in the morning, and he/she is not in standing or sitting position (detected by patient position accelerometer), and has entered in room toilet (detected by door sensor). Coincidence of these events might indicate that the patient has collapsed while in toilet and need urgent attention, that can be also checked on video camera monitoring patient location.

Even the condition that the patient lying in smart bed has suddenly become wet and need nurse attention to change bed sheets, can be detected by humidity sensor.

The patient from his side, has full control of the environmental conditions in the room where he is staying, controlling lights, room temperature, windows openings, blinds on the windows, calling for nurse attention etc. using standard smart phone or tablet, while some actions, like switching the lights on when he stand-up from the bed, while room luminosity is bellow certain percentage (or depending of the time of the day), are done by the IoT system automatically.

All the measured parameters, medical events and video recordings are continuously logged in the hospital database for medical records, and can be also send to public clouds with protected access requiring full authentication and authorisation.

V. CONCLUSIONS

The development of IoT application design environment based on the high level visual programming language in form of Editor within the class of visual domain specific modelling languages (VSDL) using formal presentations and abstract syntax has been presented in this paper. The front end of the Editor is based on JavaScript language.

The runtime execution of IoT application configuration files, generated with this Editor is carried out by OpenHAB runtime engine developed within the framework of "OpenHAB" open source project.

Further extension in the development of the software design tools is planned to add new IoT devices into DSL-4-IoT library, which shall remove the burden from application designers to add new devices not available in the library.

The usability of developed software tools for application software design of IoT application has been demonstrated on the experimental testbed that has included remote patient monitoring and smart home examples. Remote patient monitoring has been demonstrated on the set of 10 noncertified biosensors, which are connected to wireless node and require connection with stationary patient.

Extensive research and fast developing biosensors which are wearable and wirelessly connected to hub sensory node, allowing the patients full freedom of movement while wearing them, shall enable that, the IoT applications like the one demonstrated in this paper, become affordable and widespread[11], [12], [13].

ACKNOWLEDGMENT

The paper has been prepared and written on the results achieved within the project that was financially supported by the Federal ministry for education and science, Federation of Bosnia Herzegovina.

REFERENCES

[1] J. Gubbi, R. Buyya, S. Marusic, and M. Palaniswami, "Internet of Things (IoT): A vision, architectural elements, and future directions," Future Generation Computer Systems, vol. 29, pp. 1645-1660, 2013

[2] J. Clerk S. Zhang, The Application of Internet of Things in the Intelligent Medical Management, journal of Shandong polytechnic university, 2012, vol. 26, no. 3, pp. 87-89.

[3] J. Kiljander, J. Takalo-Mattila, M. Etelapera, J.-P. Soininen, and K. Keinanen. Enabling end-users to configure smart environ-ments. In Applications and the Internet SAINT), 2011 IEEE/IPSJ 11th International Symposium on, pages 303–308, 2011.

[4] T. S. Lopez, D. C. Ranasinghe, M. Harrison, D. McFarlane, "Adding sense to the Internet of Things An architecture framework for smart object systems," Personal and Ubiquitous Computing, vol. 16, no. 3, pp. 291-308, 2012

[5] OpenHAB : open source project web site, http://www.openhab.org/ / [Accessed on: 10.1.2015]

[6] e-Health Sensor Platform for Biometric and Medical applications http://www.libelium.com/130220224710/ , [Accessed on: 10.1.2015]

[7] Waspmote: Libelium wireless sensory network ,http://www.libelium .com/products/waspmote/ [Accessed on: 10.1.2015]

[8] Arduino products, http://arduino.cc/en/Main/Products [Accessed on: 28.2.2015]

[9] My.openHAB , https://my.openhab.org/ , [Accessed on: 10.1.2015]

[10] HABDroid – Android application for openHAB, https://github.com/openhab/openhab/wiki/HABDroid, [Accessed on: 10.1.2015]

[11] M. Nadeski,"Efficient portable medical device design straategy", Embedded Computing design, June 10, 2014

[12] K.Hung, Y.T. Zhang and B. Tai. "Wearable Medical Devices for Tele-Home Healthcare, Engineering in Medicine and Biology Society, 2004.

[13] Z.Feng,M. Smith," Measuring heart rate and blood oxygen levels for portable medical and wearable devices", Embedded Computing design, June 5, 2014

Turning the Challenge into Opportunity – A Strategic Framework for the Biomedical Engineering Development in Bosnia and Herzegovina

S. Mustoo[1] and L. Gurbeta[2]

[1] Verlab Ltd Sarajevo, Medical Device Verification Laboratory, Sarajevo, Bosnia and Herzegovina
[2] Faculty of Electrical Engineering, University of Sarajevo, Bosnia and Herzegovina

Abstract — **In respect with growing population, health care systems are becoming main priority in social-economy policies. Within the modern health care system, overcoming challenges in human health protection, disease prevention, treatment and rehabilitation of patients require engineering involvement. Investment in biomedical engineering (BME) creates a base for progress in many fields, from cutting health care expenses, better quality and accuracy in diagnosis and patient treatment, increase of medical therapies reliability and, finally, improved populations' life quality. Economic growth, improvement and competitiveness of the country through BME require highly educated engineers, appropriate legislative in accordance with World Health Organization (WHO) and government support. Main goal of this article is to present the basic strategic framework necessary for BME development in Bosnia and Herzegovina, with potential to influence economic growth. This cause-a-consequent connection between economic growth and BME is still unexplored in Bosnia and Herzegovina. Discussing the BME phenomena in Bosnia and Herzegovina has a great significance since it can determine the possible reason for increase in its internal and external funding. The future holds so far unexplored possibilities in the field of BME in Bosnia and Herzegovina, which can lead to social and economic progress, and the first step toward it is to create a strategic framework as a foundation.**

Keywords— **biomedical engineering, strategic framework, education, knowledge society, economic growth & development**

I. Introduction – The Mystery Around Biomedical Engineering Significance

In industrial society, work force and capital were considered to be key factors of manufacturing. In modern society (late 1970s), information and communication technologies played key role in manufacturing. Since the late years of 20th century human knowledge became driving force of society change and improvement. That is the way that informational society became knowledge society [1]. Since 1950s technological innovations became central growth driving force of economy leaders due to expansion of research focused institutions, where researchers and engineers played essential role in human wellbeing improvement. Importance of BME research can be overlooked from three main aspects.

First, scientific research aspect, is valued by number of publications and research output. About half of Europe scientific publication tackled the BME issue [2]. Second, economic aspect, consider return of investment in BME research activities. This segment is best described in *Health Economics Research Group* and *Office of Health Economics* (2008) report: *What's it worth?* - where is highlighted that every pound invested in BME brings 39 pennies each year, in long term [3] with no tendency to interrupt the process of creating investment benefits. Connection between research investment and economic growth is best shown on United Kingdom (UK) example. Through long term investments in BME, UK succeeded to make most important and most efficient sector in economy after financial. They made it possible through commercial use of research results. Similar study was conducted in United States of America (USA) that showed that every US$1 spent by *National Institutes of Health* (NIH) usually generates US$2.21 in 12 months [4]. On the other side, *US National Academies of Science*, states their opinion on BME in article "*Rising above the gathering storm"*, pointed out the fact that without competitive and highly educated engineers and entrepreneurship development, American economy would lose position of world leader due to growing competition [5]. Third aspect refers to health and social benefits of the population. In that manner population benefits from BME researches mostly through new discoveries which improve health (healthy working population), extend populations' life expectance and increased populations' life standard. At the same time, this aspect is connected to economic expenses/ cuts of health care system. BME innovations can unburden health care systems which are mostly under debts especially in transition countries. It is these reasons why current state, possibilities, challenges and future development of BME in Bosnia and Herzegovina should be discussed while awareness of this question should be spread through politicians, government and population.

II. WEALTH OF NATIONS & BIOMEDICAL ENGINEERING COMMITEMENT

National point of view

Many countries have benefited from BME commitment. Singapore, for example, a few decades ago, was emerging biotech cluster with the main aim to position itself as a world-class research and development center due to government financial support. As key advantages, Singapore has used an educated and skilled work force, government funding, favorable business and legal environment, and government supported research institutes. Ten years ago, Singapore has decided to put a national focus on BME, taking into account changes in the world economy, striving for the rapid economic development, especially after gaining statehood in 1965. It should be noted that until 1960s, Singapore's economy had an attribute as a labor-intensive economy due to the low level of educated work force, strikes, high unemployment rate, and a rapidly growing population. By 1970, Singapore was focused to industrial and technical education of the work force.

This strategy of economic growth was successful until the mid-1970s, when developed countries have exceeded the development of high-tech production. Therefore, the Singaporean government decided to focus on production based on skills, added value, technology, as well as the production of electronics. After the first major recession in 1985, Singapore was looking for new areas for economic growth. Bearing in mind the population of less than 4 million (same as Bosnia and Herzegovina), and few natural resources, the government of Singapore has decided to focus on human capital as the most important resource. In other words, Singaporean economy was built on knowledge, skills and innovation.

It was late 90s of 20th century, when Singapore recognized biomedicine as an area with huge growth potential. The growth was conducted through two phases. First, from 2000 to 2005 foundations were set by pointing out the importance of human and intellectual capital. Once the foundation were set, in the second phase (2006 to 2010) Singapore has focused on strengthening capabilities in clinical research to improve populations' health care, which contributed to the economy and society in general.

Government investment in BME, in Singapore, by the end of 2014 was about 3.5% of gross domestic product (GDP) [4a].

During the recessions governments tend to cut expenses in research and education. On the other hand, the Swedish Ministry of Finance held the view that investment in research infrastructure is what creates future economic growth and should not be subject to financial cuts [6], which was recipe for economy recovery. In the same period Canadian government actually decided to, among other things, halve investment in BME research. However, the economic revival was not caused by these cuts, but only thanks to the fact that during this period the US increased imports of Canadian products.

In addition to the United States and European Union countries, the possibilities of BME research has been recognized by India and Brazil, which are slowly becoming important players in the field of science. Asian countries have also speeded up its research activities by combining education, investment and involvement of local governments. The reason for this are precisely the benefits mentioned above.

Individual point of view

One of the formal definitions of BME engineer is an expert who "builds on scientific understandings of disease and to design new healthcare technologies" [7]. Therefore, BME engineers can design and develop devices, instruments and/or programs to solve specific clinical problem, thanks to broad knowledge in the field of technology and medicine.

Becoming a BME engineer usually requires a minimum four years of university education. However, attending the second and third cycle of university programs offer much greater opportunities for promotion into the top BME researcher and expert.

According to CNN research from 2013, BME engineer took the title of the best job in the United States, as this work brings high job satisfaction, low stress, high income and earnings, high contribution to society and flexible work. Also in 2014, Forbes has rated BME engineer to be the most desirable job within health care sector.

Also, there is a need for BME engineers in Europe, since BME sector is leading competitive European sector with the market size of 95 billion EUR, which operates in favorable European legislation framework since the European Union tends to build the European Research Area by 2020.

While in most countries, universities compete to bring world top students on their universities, in Bosnia and Herzegovina we are witnessing a lack of BME study programs which are the main precondition of any possibility for job systematization in this field. Absence of BME study programs is the main obstacle to "produce" skilled BME engineers, and in the end to create and develop BME sector in Bosnia and Herzegovina.

III. STRATEGIC FRAMEWORK BIOMEDICAL ENGINEERING IN BOSNIA AND HERZEGOVINA

As already mentioned, BME has the potential for rapid development of countries with low GDP through the integration

of social sciences insights and technological innovation, from concept to production. This article presents entirely new idea, a development accelerator of Bosnia and Herzegovina through the BME commitment supported by medicine, electrical engineering, mechanical engineering and economics postulates. Acceptance and implementation of this idea demands governmental, academic and industrial support. The following text provides strategic framework for BME development in Bosnia and Herzegovina through four key factors that must be developed and balanced in the coming years in order to provide economic recovery based on knowledge and innovation, instead of low-cost work force.

Creating a strategic framework for the BME development in Bosnia and Herzegovina is indicated by the fact that in comparison with neighboring countries, the countries of EU28 and EU4 and five countries which are our largest export partners, Bosnia and Herzegovina has the lowest GDP per capita for 2013 and 2012 [7]. Given that industrial production remains burdened by debt, tangled in the post-war privatization process, with the necessity of huge investments in equipment that Bosnia and Herzegovina isn't currently financially capable to deliver. Recovery and development should be based, according to the views of the authors of this article, on investment in knowledge and competence of human resources. Favorable geopolitical area, with highly educated, capable and competent professionals, as well as a favorable business environment can very quickly distinguish Bosna and Herzegovina as desirable destination for foreign investment. Therefore, BME can be a trigger for the economic growth of the country through the implementation of the strategic framework presented in this paper. Four key factors are following:

Support body. As a starting point in the strategic framework implementation body responsible for development of BME in Bosnia and Herzegovina should be established. That support body can be an existing body, Society for Medical and Biological Engineering (DMBIUBIH), which brings together a large number of university professors, doctors, engineers and technicians in the field of medical, biological, electrical, mechanical engineering, pharmacy and other related science fields and can help the government in determining the strategic direction related to BME. The society should be invited to make proposals for the creation of pioneering model for productive international cooperation of biomedical engineers, application of university programs, cross-cultural learning, foundation of BME research, etc. Effective functioning DMBUBIH would solve the problem of inferiority of BME in Bosnia and Herzegovina. Also, the society could be responsible for linking education and research with industry.

One of the currently most noticeable indicators of the inferiority of the scientific research sector in relation to the environment is little presence of our researches in international scientific meetings, their minor appearance in scientific literature (indexed journals), inability to organize the scientific events such as conferences, little or almost no publishing activities, lack of journals and periodicals in libraries and above all very little interest of young people for post-graduate studies and doctoral research (PhD in future studies) and work in the scientific research field.

State / Government. Next step in implementing this framework is the government's strategic orientation, i.e. commitment and innovation, research and science funding. Investing is just one side of the medal of BME development strategy. Well-coordinated, national approach is essential. This segment will be the most difficult to change since the statistics do not show determination and commitment of previous policy options towards science. According to the Federal Ministry of Science and Education, the share of allocations for science as a % of GDP at the level of Federation of Bosnia and Herzegovina has grown significantly over the period 2008-2013 year. Investments in this area in 1990 of 1.5% have never reached above this level. The largest part of public and higher education institutions funding were in amount of 1,912,718 KM [7a] which is a clear expression of the lack of focus of political structures in knowledge and science. Taking into account that the scientific research funding lies on the Entities jurisdiction, it is clear that changes and restructures are required but are the most difficult.

Environment. Involvement of government can result in supportive business and regulatory environment. Members of society DMBIUBIH are also working on writing proposals for changes legislative regarding scientific research in our country. Bosnia and Herzegovina will have to work hard to create a favorable business environment for investors and the first step is to gather scientific elite under support body so application for European grants can be made. According to the Federal Institute for Development Programming (2013) on the ease of doing business, Bosnia and Herzegovina has dropped one place compared to 2013, and is located at 131 position (out of 189 countries). [8] In this year's Index of Economic Freedom our country is ranked among 185 country on 103 place with the score 57.3 points [8a] which is the same number of points as last year.

University. Final, long term, step in strategic framework implementation refers to the study BME study program creating, with the aim to produce and train competent experts. In cooperation with the Society for Medical and Biological Engineering in Bosnia and Herzegovina an important role is reflected in talent attracting. Taking into account the small Bosnian population, it is necessary to consider the holistic strategy of talent attracting, locally and internationally. International BME experts can provide mentoring to young Bosnian scientists. If our University provide a high quality study

program, this will result in increased number of foreign students, who may also affect BME improvement in Bosnia and Herzegovina during their study period. BME is a discipline that cannot be sustained within the traditional professional organizational structure. University of Sarajevo, as the largest and oldest educational institution in Bosnia and Herzegovina, has a leading role in the intellectual and educational capital creation. However, the University of Sarajevo has still no faculty / department / stream in BME filed. By creating BME study programs University of Sarajevo would be the only public educational institution that can enable multidisciplinary training of students linking knowledge, experience and techniques in the wider field of electrical engineering with biomedical practices.

The funds should be directed towards organizing an interdisciplinary program at the University of Sarajevo, which would allow:

- Intellectual integration of medicine, electrical engineering, mechanical engineering, IT, natural sciences at the undergraduate and graduate level.
- Integration and Cooperation with the market (health institutions, industry, etc....).
- The conditions in which the program staff and students can work as part of teams for large BME projects (regional and / or international level)
- The conditions for staff and students mobility at the prestigious world BME universities and institutes, in order to transfer knowledge in Bosnia and Herzegovina.

BME study program should also provide students mobility in other countries, which could result in domestic BME engineers with wider knowledge and cultural horizons and can ensure long term modernization of healthcare system.

IV. Conclusion

Technology has had a dramatic impact on every sphere of life, including the medical care. As the BME has evolved, in particular over the last fifty years, ethical issues have become important regarding processing of biomedical signals, biotechnology, biomechanics, biosensors, medicine, economics and biology.

Since the BME is still at its infancy in Bosnia and Herzegovina, initially it is necessary to thoughtfully and strategically access creating a favorable environment that will later provide sustainable BME development.

Business climate, government, university and support body are key players in this process, and their balanced, efficient and professional approach may be essential.

This article may be common start point for BME engineers, business entities and politicians in order to present Bosnia and Herzegovina as a country that base its development on knowledge, innovation and high qualified engineers. Creating high-quality BME study programs and, further, ensuring employment of BME engineers Bosnia and Herzegovina will prevent drain brain of its top students and outstanding experts.

In Bosnia and Herzegovina it is necessary to create a favorable business environment for BME investments. Flexibility and openness to BME innovations can become a trigger for the transformation of Bosnia and Herzegovina in a competitive and prosperous economy. On the other hand, an appropriate legislative framework is a must for intellectual property protection.

Investing in BME in Bosnia and Herzegovina should attract foreign investments and develop new capacities such as production of new drugs, new laboratories and other medical and engineering facilities as well as modernize existing facilities. Thus, through an integrated system of government support, regulatory framework, research and development, and educated and qualified engineers, Bosnia and Herzegovina could become initially regional and then European BME center.

References

1. European Medical Research Councils (EMRC). *A Stronger Biomedical Research for a Better European Future.* European Science Foundation, 2011.
2. Health Economics Research Group (HERG), Brunel University i Office of Health Economics (OHE), RAND Europe. Medical Research: *What's it worth? Estimating the economic benefits from medical research in the UK.* For the Medical Research Council, the Welcome Trust and the Academy of Medical Sciences, 2008.
3. M. Colin. *Science economics: What science is really worth*? Nature: 2010.
4. P.L. Chuan Singapore Betting on Biomedical Science." Issues in Science & Technology (Innovation Policy around the World): 2007. November 27, 2014. http://issues.org/26-3/poh/
5. US National Academies of Science. *Rising above the gathering storm*. Energizing and Employing America for a Brighter Economic Future, 2007.
6. The Academy of Medical Science. *Biomedical research – a platform for increasing health and wealth in UK*. 2011.
7. Ministarstvo obrazovanja i nauke FBiH. *Izvještaj o razvoju Federacije Bosne i Hercegovine.* FMON: 2013.
8. Federalni zavod za programiranje razvoja. *Lakoća poslovanja 2014:* Bosna i Hercegovina. FZPZ: 2013.

S. Mustoo is with the Verification Laboratory "Verlab" Ismeta Mujezinovića 30, Sarajevo, B&H (phone: 387-33-569-540; e-mail: sabrina@verlab.ba).

IoT Wireless Sensor Networks for Healthcare Applications

Dejana Ugrenovic[1], Gordana Gardasevic[1], Darko Golic[2], Vera Gazdic[2]
[1]Faculty of Electrical Engineering, University of Banja Luka, Banja Luka, BiH
[2]Clinic for Anesthesiology and Intensive Care, University Hospital Clinical Centre Banja Luka, BiH

Abstract—**Internet of Things (IoT) is a paradigm that marks the convergence of the existing Internet to the new platform by allowing unambiguous IP addressing and access to physical objects. Currently, the emerging IoT field are the healthcare and biomedical applications. The aim of this paper is to report the preliminary research results for the IoT healthcare scenario based on 6LoWPAN (IPv6 over Low power Wireless Personal Area Networks) protocol stack within the Contiki operating system. In order to evaluate the performances, we measured the throughput and packet loss rate.**

Keywords—**Internet of Things, Wireless Sensor Networks, 6LoWPAN, Healthcare, Contiki.**

I. Introduction

The IoT (Internet of Things) healthcare applications represent an emerging research field in the past few years [1,2]. Ubiquitous IoT healthcare system aims to provide remote monitoring of patient health status in real time, prevention of critical patient conditions, life quality improvement of the elderly through the smart environment, medical and drugs database administration, etc.

Wireless Sensor Networks (WSNs) have had the increased deployment in the recent years and have earned the significant importance in different areas [3]. Such networks are composed of distributed nodes that can sense the environment, collect relevant information and communicate with other nodes. It has been recognized that IoT WSN deployments for smart health services will play a key role in supporting broad goals of medical applications.

6LoWPAN **(**IPv6 over Low power Wireless Personal Area Networks) is a protocol stack, based on IPv6 protocol, that is used and designed primarily for WSNs [4]. Contiki is an open source operating system for sensor netwoks, implemented in C programming language [5]. It has the event-driven kernel and supports preemptive multithreading that can be applied on a per-process basis. Contiki also contains Cooja.

Our long-term research plan is directed towards the creation of distributed and scalable IoT healthcare monitoring system. The specific sensor parameters (ECG, heart rate, blood oxygen saturation, temperature, blood pressure, etc.) that follow the patient's condition will be transferred by platform to the appropriate IP end-devices (Web servers, mobile devices) to enable their analysis and remote data access. In this paper we report preliminary results obtained by implementing the IoT healthcare testbed based on Contiki's 6LoWPAN protocol stack and Cooja network simulator.

The paper is outlined as follows: Section II describes the platform, simulation setup and selected topologies. Section III presents simulation results in terms of throughput and packet loss rate. The conclusions are drawn in Section IV.

II. Simulation Setup

The platform chosen for the simulation is Tmote Sky. This platform consists of 8 MHz, 16-bit RISC processor with TI MSP430F1611 10kB RAM, 1MB Flash memory and Chipcon CC2420 transceiver at 2.4GHz, with a transmission range of about 100 meters. The physical and MAC (Medium Access Control) layer is specified by standard IEEE 802.15.4. Radio duty cycling (RDC) model that enables low power consumption is Contiki MAC.

The Fig.1 illustrates the simple network topology used for simulation purposes. The topology contains one node that receives data (server node), marked with number 1, and other six sensor nodes (client nodes) that send different sensor data, marked with numbers 2, 3, 4, 5, 6 and 7. Client nodes send different types of data in specific packet form, thus representing the traffic properties of electrocardiogram signal (ECG), body temperature, blood oxygen saturation, respiration rate, glucose level and blood pressure. In this paper, we investigated two different scenarios. In the first scenario, each node sends data to the server with the same Packet Send Interval (PSI) and with the same payload value, while in second scenario each node sends data to server with different PSI and with different payload value. Packets representing the ECG signal are sent with the highest value of packet sending frequency and payload size, while other nodes have lower values of packet sending frequency and payload size, based on [6]. In each scenario, the total number of packets generated is 3000. Two different evaluation metrics were selected for both scenarios: the throughput and Packet Loss Rate (PLR). Table 1 shows values of simulation parameters (payload and PSI) for different types of transmitted biomedical data.

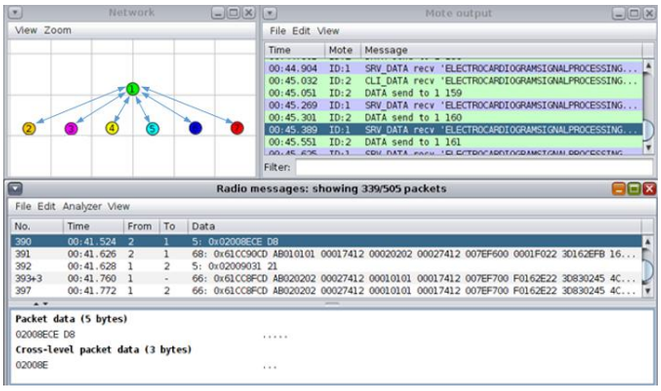

Fig. 1 Simulation scenario for testing IoT healthcare performances

Table 1 Sensor data parameters

Type of data	Payload	Packet Send Interval
ECG	40 bytes	250ms
Body temperature	1 byte	100s
Blood oxygen saturation	5 bytes	100s
Respiration rate	1 byte	40s
Glucose level	3 bytes	2s
Blood pressure	2 bytes	40s

III. Simulation Results

Fig. 2 shows the throughput results as a function of PSI, for the first scenario. The throughput is higher in the first scenario due to offered traffic, but PLR is increased too as the number of nodes increases. Table 2 summarizes results for different scenarios and traffic parameters. The better performances, in terms of PLR, are obtained by second scenario, where each node sends data to server with different PSI and different payload size.

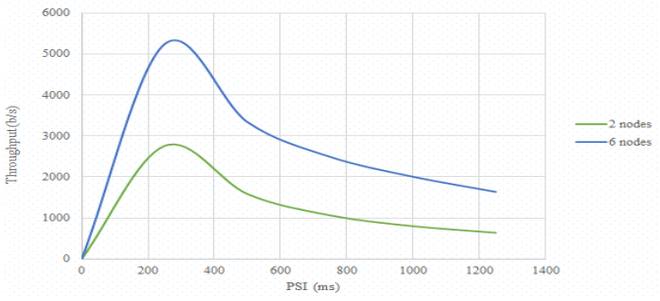

Fig. 2 Throughput for the first scenario as a function of PSI

Table 2 Simulation results

Topology	Parameters	Throughput [b/s]	Packet Loss Rate [%]
First scenario: two nodes	PSI = 250ms Payload =50 bytes	2756.72	0.86
Second scenario: two nodes (aggregate traffic)	PSI_1=250ms, PSI_2=40s $Payload_1$=40bytes, $Payload_2$=14bytes	1182.37	0.32
Second scenario: six nodes	PSI_1=250ms, PSI_2=100s, PSI_3=100s, PSI_4=40s, PSI_5=2s, PSI_6=40s	1162.82	0.33

IV. Conclusions

IoT-driven healthcare monitoring system employs sensors to collect relevant biomedical information. Data are transferred wirelessly by platform to appropriate IP end-devices to enable real-time visibility of the patient's condition. The preliminary simulation results are encouraging, especially due to low PLR, and are providing the insight into the possibilities of implementing such a distributed and scalable model in real medical environments. As the next steps, we will test more complex multihop topologies for different sensor and data transmission parameters.

ACKNOWLEDGMENT

The research was supported by NORBOTECH (NORway-BOsnia TECHnology Transfer) project, within the Programme in Higher Education, Research and Development; financed by Norwegian Ministry of Foreign Affairs.

REFERENCES

1. Yuan Zhang, Limin Sun, Houbing Song, and Xiaojun Cao, "Ubiquitous WSN for Healthcare: Recent Advances and Future Prospects", *IEEE Internet of Things Journal*, vol. 1, no. 4, pp. 311-318. August 2014.
2. Gia, T.N.; Thanigaivelan, N.K.; Rahmani, A.-M.; Westerlund, T.; Liljeberg, P.; Tenhunen, H., "Customizing 6LoWPAN networks towards Internet-of-Things based ubiquitous healthcare systems," NORCHIP, 2014 , vol., no., pp.1,6, 27-28 Oct. 2014.
3. I.F. Akyildiz, W. Su, Y. Sankarasubramaniam, E. Cayirci, Wireless sensor networks: a survey, *Computer Networks*, Volume 38, Issue 4, 15 March 2002, pp. 393-422, ISSN 1389-1286.
4. N. Kushalnagar, G. Montenegro and C. Schumacher. IPv6 over Low power wireless personal area networks (6LoWPAN): overview, assumptions, problem statement, and goals. RFC 4919.
5. Contiki Operating System, http://www.contiki-os.org/
6. W. Mehmood, A.B. Mnaouer, A. Hassan, R. Tabish, B. Gaabab, F. Touati, "Performance Evaluation of 6LoWPAN Based Networks for Ubiquitous Health Monitoring System", in ICWN paper, Las Vegas Nevada, USA, 2014.

Dejana Ugrenovic is with the Faculty of Electrical Engineering, University of Banja Luka, Patre 5, 78 000 Banja Luka, BiH (phone: 387-66-686-770;e-mail:ugrenovic.dejana@gmail.com)

Theoretical and Experimental UV-Vis Spectroscopic Analysis Of Chamazulene

M. Salihovic and A Sapcanin

Faculty of Pharmacy, University of Sarajevo, Zmaja od Bosne 8, 71000 Sarajevo, Bosnia and Herzegovina

Abstract— **In the present research, UV/Vis spectra of chamazulene was recorded. Density Functional Theory (DFT) B3LYP level using 6-31G(d) basis set have been carried out to investigate the structure of chamazulen, and to investigate the UV/Vis spectra and some additional properties. Correlation coefficients were used to compare the experimentally observed and theoretically computed vibrational frequencies for compound. Calculations were done using software Spartan 10. The theoretical characterization matched the experimental measurements, showing a good correlation. Experimental data showed that chamazulene have absorption maximum at 340 nm to 530 nm. The position of λmax did not much different with theoretical calculation. The calculated density of states showed excellent agreement with UV/Vis diffuse reflectance spectra predicting the absorption maximum at 310 nm (calculated 332 nm) to 530 nm (calculated 516 nm). The calculated values are lower than the experimental absorption maximum. The reason for the discrepancies between the theory and experiment can be the vibrational effects, which are not taken into account and hydrogen bonding with the solvent molecules. DFT calculations have been used extensively for calculating a wide variety of molecular properties such as equilibrium structure, charge distribution UV/Vis, FTIR and NMR spectra, and provide reliable results which are in agreement with experimental data.**

Keywords— **UV/Vis spectra, density functional theory (DFT), chamazulene.**

I. INTRODUCTION

Chamazulene (1,4-dimethyl-7-ethylazulene) is an aromatic chemical compound obtained by steam distilation in of a variety of plants including chamomile (*Matricaria chamomilla*), wormwood (*Artemisia absinthium*), and yarrow (*Achillea millefolium*). It is a blue-violet derivative of azulene which is synthesized from the sesquiterpene matricin [1, 11]. For the quantitative determination of essential oil, total azulenes and chamazulene in chamomile, are used to various methods such as gravimetry, spectrophotometry in the visible region and gas chromatography [7].

Density Functional Theory (DFT) has been accepted by the quantum chemistry community as reliable and effective approach for the computation of molecular structure, vibration frequencies and energies of chemical reactions [2, 3]. DFT calculations provide excellent agreement with experimental vibrational frequencies of investigated compounds [12]. In this study, UV/Vis spectra of chamazulene was recorded. The purpose of this work is to determine the chamazulene of essential oil from Bosnia and Herzegovina chamomile samples by UV/Vis method, to compare DFT study with Spectral Behavior of isolated chamazulene. The Beck´s three-parameter exchange functional with the Lee, Yang and Parr correlation functional (B3LYP),developed by Truhlar et al. were used to perform theoretical calculations on the structure, the UV/Vis spectra and some additional properties of the investigated compound [13, 14, 15].

II. MATERIALS AND METHODS

A. Materials

Chamomile tea commercially available from Bosnian markets was used in this study. All the reagents and chemicals were purchased from Sigma-Aldrich Co. LLC.

B. Investigated compounds

The compound chamazulene was studied for their experimental and theoretical properties. Structure of investigated compound is presented in Fig. 1.

Fig. 1 Structure of chamazulene

C. UV-Vis spectrometry and Thin Layer Chromatography (TLC) analysis

The methods for chamazulene determination in chamomile essential oil was developed based on silica gel G thin layer chromatography (TLC) and UV-spectrophotometry.

The sample was dissolved in ethanol and applied to precoated TLC. The chromatographic separations were done on the silica gel F254. TLC plates developed with dichlorme-

than: etylacetat (9:2 v/v). Detection was performed under UV lamp at 254 nm and the evaluation of the chromatographic plate was based on processing of chromatographic images. Then Rf value was calculated and compared with literature data [9].

Ultraviolet Spectra were recorded using LAMBDA 25, PerkinElmer UV-Vis Spectrometer, and ethanol was used as solvent for the dilution of sample as well as blank.

D. Theoretical calculations

All the calculations were carried out with the Spartan 10 software. The geometries were optimized using the method: B3LYP basis set: 6-31G(d) as shown in Fig.2.

The harmonic vibration frequencies were calculated by this method and the results were compared with experimental spectra. This method was used for calculating UV/Vis spectra of dyes at the B3LYP/6-31G (d) level for chamazulene.

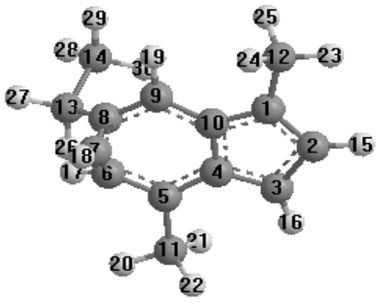

Fig. 2 Structure of chamazulene

III. RESULTS AND DISCUSSION

TLC and UV/Vis dats of the prepared chamazulene

TLC study of the isolated compound was found (Rf=0.80) almost similar to that of the literature (Rf=0.78) data so this study concludes that the isolated compound may be chamazulene. After that chamazulene was determined directly by measuring absorbance at 310 nm to 530 nm.

Experimental and theoretical UV/Vis spectral data

The electronic spectra of the chamazulene exhibit two characteristic broad bands at 340 nm and 530 nm (Table 1).

Table 1. Experimental and theoretical UV/Vis spectral data.

Compound	λmax [nm] (experimental)	λmax [nm] (computation)	Intensity
Chamazulene	225	228	1.1687
	266	264	0.0529
	340	332	0.0184
	530	516	0.0183

The chamazulene exhibits the absorption maximum at 340 nm to 530 nm (Figure 3a). The position of λmax did not much different with theoretical calculation (Figure 3b). The calculated density of states showed excellent agreement with UV–Vis diffuse reflectance spectra predicting the absorption maximum at 310 nm (calculated 332 nm) to 530 nm (calculated 516 nm). The calculated values are lower than the experimental absorption maximun (Table 1). The reason for the discrepancies between the theory and experiment can be the vibrational effects, which are not taken into account and hydrogen bonding with the solvent molecules.

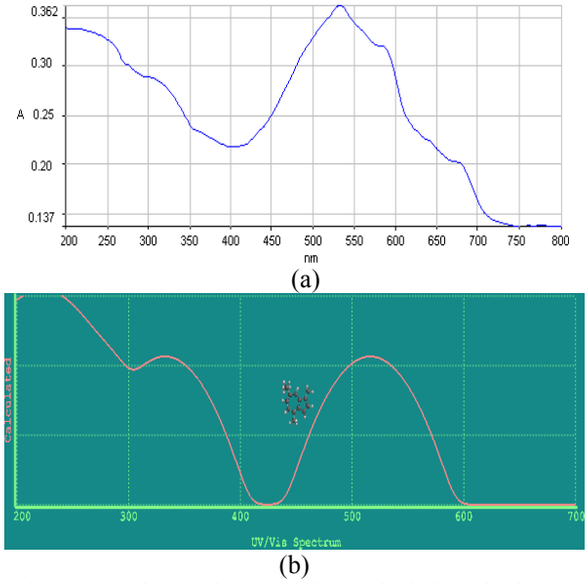

(a)

(b)

Fig. 3 Experimental (a) and theoretical (b) calculation of UV/Vis absorption spectra of Chamazulene

DFT calculations for structural and electronic properties

Optimized molecular structures of chamazulene of the most stable form are shown in Figure 2. Molekular orbital calculations provide a detailed description of orbitals inclu-

ding spatial characteristics, nodal patterns and individual atom contributions. The contour plots of the frontier orbitals for the ground state are shown in Figure 4, including the Highest Occupied Molecular Orbital (HOMO) and Lowest Unoccupied Molecular Orbital (LUMO). It interesting to see that both orbitals are substantially distributed over the conjugation plane. It can be seen from the Figure 4 that the HOMO orbitals are located on the substituted molecule while LUMO orbitals resemble those obtained for the un-substituted molecule and therefore the substitution has an influence on the electron donation ability, but only a small impact on electron acceptance ability. It can be seen that the energy gaps between HOMO and LUMO of chamazulene is 3.19 Hartree. The values of the HOMO and LUMO energy gap explained the eventual charge transfer interaction taking place within the molecules. The lower the HOMO–LUMO energy gap, the lighter and less stable/more reactive the molecule. [4]. The energy gaps between HOMO and LUMO of guaiazulene is 3.20 Hartree [10]. Chamazulene is more reactive than guaiazulene because it has lower value of the HOMO and LUMO energy gap.

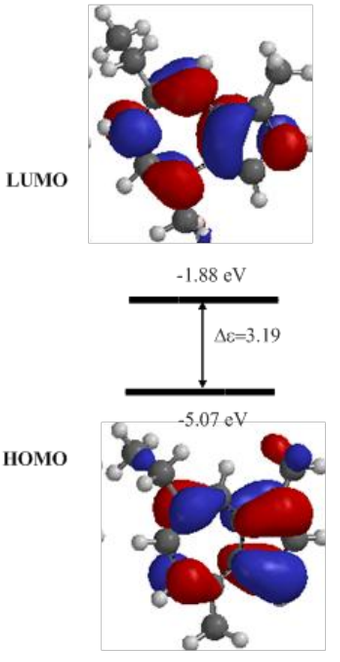

Fig. 4 Frontier molecular orbitals of chamazulene

Atomic charges for chamazulene

Atomic charges of chamazulene showed in Table 2. These data show that the atomic charge has been affected by the presence of substituent of rings [5, 6, 8] as shown in the Table 2.

Table 2. Atomic charges of chamazulene

Atom	Atom type (MM2)	Charge Huckel	Atom	Atom type (MM2)	Charge Huckel	Atom	Atom type (MM2)	Charge Huckel
C(1)	C Alkene	-0.095	C(13)	C Alkane	0.184	H(25)	H	0.047
C(2)	C Alkene	-0.0434	C(14)	C Alkane	-0.109	H(26)	H	0.248
C(3)	C Alkene	-0.418	H(15)	H	0.028	H(27)	H	0.035
C(4)	C Alkene	-0.074	H(16)	H	0.028	H(28)	H	0.036
C(5)	C Alkene	-0.249	H(17)	H	0.286	H(29)	H	0.042
C(6)	C Alkene	0.249	H(18)	H	0.029	H(30)	H	0.043
C(7)	C Alkene	0.142	H(19)	H	0.021	H(31)		
C(8)	C Alkene	0.417	H(20)	H	0.037			
C(9)	C Alkene	-0.177	H(21)	H	0.040			
C(10)	C Alkene	-0.182	H(22)	H	0.041			
C(11)	C Alkane	-0.146	H(23)	H	0.039			
C(12)	C Alkane	-0.15	H(24)	H	0.046			

The data (Table 2.) show that the high estatomic charge in molecule is at [C(3) -0.418)] and the next charge value is at [C(5) -0.249]. These data show clearly that these three atoms are the most reactive toward the substitution reactions.

IV. CONCLUSIONS

Selected structural parameters of the optimized geometries of the chamazulene have been obtained by DFT calculations. The electronic spectra of the chamazulene fundamental modes have been precisely assigned and analyzed and the theoretical results were compared with the experimental values. Conducted research provides data about electronic spectra and structural information of chamazulene. The theoretical characterization matched the experimental measurements and showing a good correlation

REFERENCES

1. A. Meisels, A. Weizmann. The structure of chamazulene. J.Am.Chem.Soc. (1953) 75(15), 3865-3866.
2. A. Beyramabadi, A. Morsali, Intramolecular proton transfer of 2-[(2,4dimethylphenyl) iminomethyl]-3,5-dimethoxyphenol Schiff-base ligand: A density functional theory (DFT) study. *Int J. Phys. Sci*., *Volume: 6*, Issue: 7, 2011, pp 1780-1788
3. A. H Kadhum, A. A. Al-Amiery, M. Shikara, A. Mohamad, Synthesis, structureelucidation and DFT studies of new thiadiazoles.*Int. J. Phys. Sci*., *Volume: 6*, Issue: 29, 2011, pp 6692-6697
4. A. H Kadhum, A. A. Al-Amiery, A. Y. Musa, A. Mohamad, The antioxidant activity of new coumarin derivatives. *Int. J. Mol. Sci*., 12 , 2011, pp 5747-5761.A. H Kadhum, A. Mohamad, A. A Al-Amiery, M.S Takriff, Antimicrobial and antioxidant activities of new metal complexes derived from 3-aminocoumarin. *Molecules*, 16, 2011, pp 6969-6984.
5. A. H Kadhum, B.A Wasmi, A Mohamad, A. A Al-Amiery, M.S Takriff, Preparation, characterization, and theoretical studies of azelaic acid derived from oleic acid by use of novel ozonolysis method. *Res. Chem. Inter. Med*., *Volume: 38*, Issue: 2, 2012, pp 659-668.
6. L. Z Padula, R. V. D Rondina, J. D Coussio, Quantitative determination of essential oil total azulenes and chamazulene in german chamomile matricaria chamomilla cultivated in argentina. *Planta Medica Volume: 30*, Issue: 3, 1976, pp 273-280
7. J. W Peters, W. N. B Lanzilotta, J Lemon, L.C Seefeldt, X-ray crystal structure of the Fe-only hydrogenase (CpI) from *Clostridium pasteurianum* to 1.8 Angstrom resolution. *Science*, 282, 1998, pp 1853-1858
8. L. Roth and G. Rupp, Roth Collection of Natural Products Data, *VCH Verlagsgesellschaft, Weinheim*. 1995, pp 100-228.
9. S. Špirtović-Halilović, M. Salihović**,** A. Osmanović, E. Veljović, S. Trifunović, S. Roca, Z. Ašimović, D. Završnik, DFT study of guaiazulene. *Congress of the Chemists and Chemical Engineers of Bosnia and Herzegovina*, 2014, Sarajevo. PP-PTC-02.
10. H Safayhi, J Sabieraj, E. R Sailer, H.P Ammon, "Chamazulene: An antioxidant-type inhibitor of leukotriene B4 formation". *Planta medica Volume: 60*, Issue: 5, 1994, pp 410–413.
11. A. Özgür P. Cemal, S Mustafa, NMR spectroscopic study and DFT calculations of vibrational Analyses, GIAO NMR shieldings and $^{1}J_{CH}$, $^{1}J_{CC}$ spin-spin coupling Constants of 1,7-diaminoheptane. *Bull. Chem. Soc. Ethiop. Volume: 23*, Issue: 1, 2009, pp 85-96.
12. Axel D.Becke, Densityfunctional thermochemistry. III. The role of exact exchange, *J. Chem. Phys*. 98, 1993, pp 5648-5652
13. Lee, Chengteh and Yang, Weitao and Parr, Robert G, Development of the Colle-Salvetti correlation-energy formula into a functional of the electron density, *Phys. Rev. B* 37, *Volume: 37*, Issue: 2, 1988, pp 785-789.
14. Y. Zhao, D. G Truhlar, Benchmark databases for nonbonded interactions and their use to test density functional theory, *Journal of Chemical Theory and Computation, Volume: 1*, Issue: 3, 2005, pp 415-432.

Corresponding author: Aida Šapčanin,
Faculty of Pharmacy, University of Sarajevo, Zmaja od Bosne 8, 71000 Sarajevo, Bosnia and Herzegovina,
phone number: +387 33 586 187
e.mail: ida@bih.net.ba

Treatment of iatrogenic dissection of the left subclavian artery

Haris Huseinagić[1], Suad Jaganjac[2], Mirza Moranjkić[1], Nihad Mešanović[1]
[1] Department of Radiology and nuclear medicine, University Clinical Centre, Tuzla, Bosnia and Herzegovina
[2]Schön Klinik Hamburg Eilbek, Abteilung für Radiologie, Hamburg, Germany
[1] Department of Neurosurgery, University Clinical Centre, Tuzla, Bosnia and Herzegovina
[1] Department of IT, University Clinical Centre, Tuzla, Bosnia and Herzegovina

Abstract— **Dissection and treatment of subclavian artery are rarely in the medical literature. Dissection is usually the result of catheterization, anomalies port aortae or occurs after trauma. We present the case of women aged 60 years whose main symptom is painful and cold left hand. Stenosis of left subclavian artery immediately distal to the origin of the left vertebral artery was found and angioplasty was performed. The second intervention was followed after 8 months with the aim of stent.**

Keywords— **subclavian artery dissection. balloon expandable stent.**

I. Introduction

Treatment of subclavian artery stenosis with percutaneous transluminal angioplasty (PTA) has been the treatment of choice for symptomatic lesions [1]. Percutaneous transluminal angioplasty (PTA) is less invasive than surgery [2-4]. Complications of PTA are dissection, distal embolization, and hematoma [5].

Arteriosclerosis is the main cause of subclavian artery stenosis and less frequently are: thrombaangitis obliterans, Takayasu arteritis, giant cell arteritis, fibromuscular dysplasia and granulomatous arteritis [6]. Indications for endovascular treatment of subclavian artery stenosis are injuries of subclavian artery with shunts or aneurysm. Regardless of etiology, the left subclavian artery is more often affected than the right subclavian artery. Arteriosclerotic lesions occur predominantly proximal to the origin of vertebral arteries while lesions in giant cell arteritis affecting the distal subclavian artery and axillary artery [7]. Based on the systemic nature of atherosclerosis we found in 80% of patients accompanying lesions of supra aortic arterial branches. Clinically, subclavian artery stenosis are usually asymptomatic as the reduced flow through the ipsilateral vertebral artery is compensated through the contralateral vertebral artery over circulus arteriosus.

We present a case of endovascular stent treatment of a spontaneous dissection of the left subclavian artery. Stent placement was complicated by the shape and extent of dissection leaf, closing the orifice of left subclavian artery.

Fig. 1 Transfemoral aortic arch angiography with selective subclavian angiography and selective transcubital intraarterial digital subtraction angiography

A 60-year-old woman with a history of generalized arteriosclerosis and stenotic changes in both iliac arteries and hemodynamically relevant stenosis of the left subclavian artery proximal to the exit of vertebral artery clinically manifested by dizziness, blurred vision without ataxia, symptoms of brachial ischemia during exercise with cold left arm and pain during stress.

Fig. 2 The lesion was crossed with a 0.035-inch angled guidewire

The initial clinical examinations included blood pressure measurements in both arms, Doppler sonography and Computerized tomography arteriography of the cervicobrachial arteries during exercise and at rest. Systolic blood pressure was lower on the affected, left side (50 mm Hg).

Transfemoral aortic arch angiography with selective subclavian angiography and selective transcubital intraarterial digital subtraction angiography (Fig. 1) were performed in March 2013.

The patient received 100 mg of aspirin three days before the interventional treatment. The procedure was performed under local anesthesia. Intravenous heparin was administered during the procedure to maintain an adequate activated clotting time between 250 and 350. Into the left brachial artery we introduced a 6-French sheath. Under road-mapping, the lesion was crossed with a 0.035-inch angled guidewire (Fig. 2). The lesion was predilated with an angioplasty balloon.

Control DSA after PTA indicated a sufficient blood flow in blood vessel with dissection of the wall that did not seem hemodynamically relevant. An absence of stenosis or residual stenosis less than 30% of the arterial diameter was considered a technical success. The clinical condition of the patient is partially improved as a reduction in the difference in blood pressure between the treated and the untreated arms was less than 20 mm Hg.

Fig. 4 In the ostium of subclavian artery we found two lumens, the first, false lumen, which is bigger and has direct communication with the vertebral artery, and the second, considerably smaller, true lumen having contact with distal subclavian artery

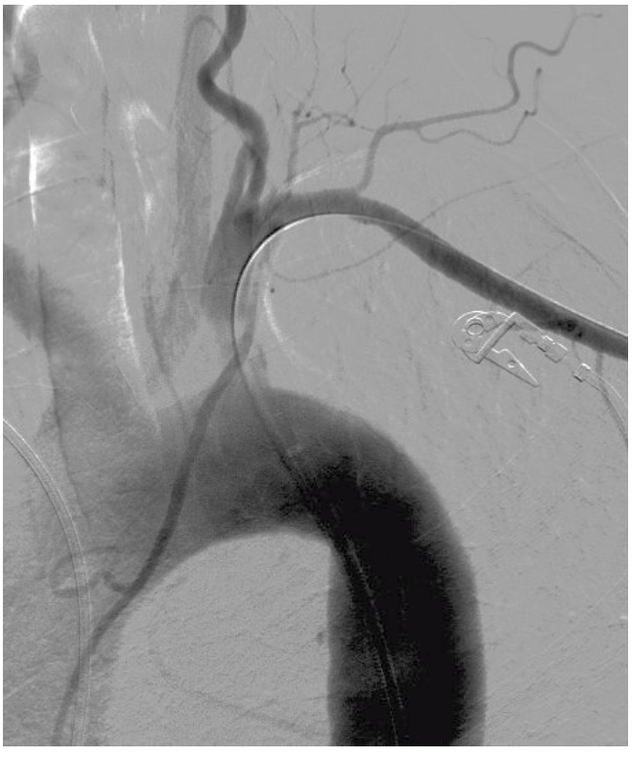

Fig. 3 Terumo-wire was successfully placed through the true lumen in the distal position of the left subclavian artery in RAO position

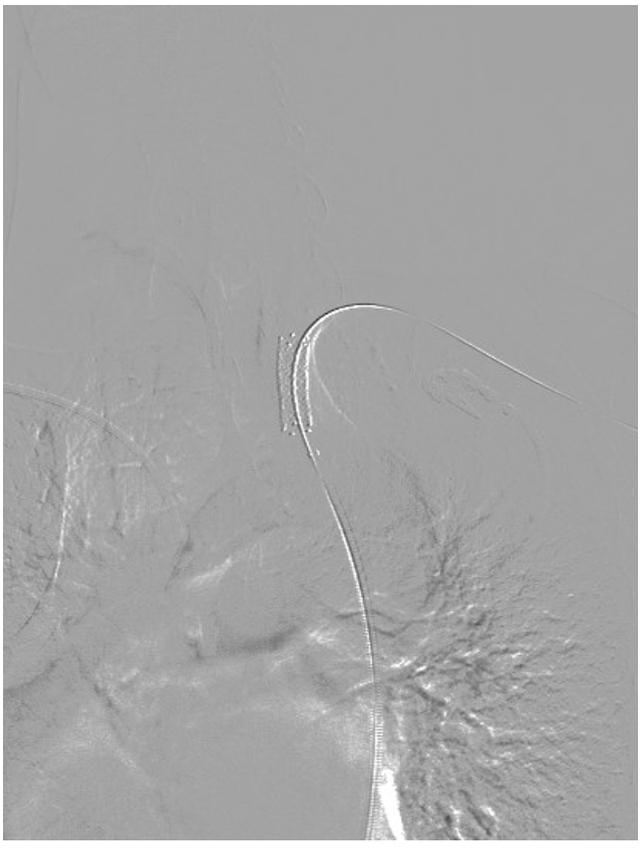

Fig. 6 The lesion was predilated with an angioplasty balloon followed by deployment of a balloon expandable stent.

Fig. 5 Angiographic control showed closing of the false lumen, an open vertebral artery and fast filling of distal subclavian artery with contrast medium

Reintervention was performed using left femoral access in October 2014. Discrete restenosis of the left subclavian artery with insufficient filling of contrast agent in the distal part of subclavian artery and the longitudinal dissection until the vertebral artery was registered on DSA in the LAO position.

Terumo wire is trying to reach the distal subclavian artery. This maneuver remains unsuccessful after multiple attempts. By changing the position from LAO to RAO, becomes clear why it is not possible to place Terumo wire in the distal part of the subclavian artery. In the ostium of subclavian artery we found two lumens, the first, false lumen, which is bigger and has direct communication with the vertebral artery, and the second, considerably smaller, true lumen having contact with distal subclavian artery (Fig. 3).

Terumo-wire was successfully placed through the true lumen in the distal position of the left subclavian artery in RAO position (Fig. 4). After placement of Terumo wire follows protective percutaneous transluminal angioplasty using a balloon expandable stent measuring 8 mm x 3 cm. The lesion was predilated with an angioplasty balloon followed by deployment of a balloon expandable stent. Stent size was selected according to the diameter of the adjacent normal subclavian artery (Fig. 5).

PTA was performed via the left transfemoral approach with an H1 head-hunter catheter (William Cook Europe, Bjaeverskov, Denmark). The catheter was placed proximal to the true lumen of dissection and a 160-cm-long J guidewire with a 3-mm radius (William Cook Europe) was carefully advanced through the true lumen of left subclavia artery. The tip of the guidewire remained deep in the left axillary artery during the placement of catheter.

The angiographic catheter was then exchanged for a balloon catheter with stent. Polyethylene balloon catheters (William Cook Europe) with maximal pressures up to 12 atm (1.2 x 106 Pa) was used. The balloon length was 4 cm, and its diameter was 8 mm.

Angiographic control showed closing of the false lumen, an open vertebral artery and fast filling of distal subclavian artery with contrast medium (Fig. 6). Upon completion of the intervention ipsilateral brachial and radial arteries pulse was palpable. Before the intervention, the pulse was not palpable. After the intervention is applied therapeutic dose

of low molecular heparin for 48 hours, followed by aspirin 100 mg and clopidogrel 75 mg/day for 6 weeks.

The literature states that the intervention is technically successful in 88% to 100% in stenoses and 46% to 100% in patients with occlusion. Complications are listed as embolic occlusion in 3% and apoplexy in 2% of patients. Mortality is stated in 0.6% of cases. Short-term results of endovascular intervention and extrathoracic operations are very good. However long-term results are significantly better in the group of operated patients.

II. Discussion

Subclavian artery dissection has been described as occurring primarily during catheterization, with coexisting anomalies of the aortic arch, or with traumatic injury [8]. A spontaneous or minimally traumatic subclavian artery dissection is a rare event and has only recently been described [5, 9-11]. The precise pathogenesis of any arterial dissection remain unclear [12]. It has been associated with hypertension, vasculopathy, trauma, drug abuse, migraine, or minimal trauma associated with sport activities [13].

Spontaneous or minimally traumatic subclavian artery dissection revealed a total of 3 cases in our literature review.

The clinical presentation of subclavian artery dissection has included vertigo, dizziness, thoracic pain, back pain, and left--arm paresthesias, followed by any neurological symptoms [1]. In any case of suspected vertebral artery dissection without a clear cause, it has been proposed that it may be worthwhile to obtain imaging of the subclavian artery [2, 14-16]. All patients should undergo conventional angiography with any suspected dissection, to confirm the diagnosis, elucidate abnormal flow patterns, and perform possible endovascular treatment if indicated [4].

Possible complications of subclavian artery dissection include false aneurysm, intramural hemorrhage, thrombosis, or emboli to the head and neck or left upper extremity. If ischemia results from subclavian artery dissection, endovascular treatment is treatment of [17, 18].

III. Conclusions

Endovascular stenting for subclavian artery dissection should be to avoid complications such as left arm ischemia, stroke, and endoleak, and where feasible, an appropriate preoperative assessment should be carried out.

References

1. Acikel S, Dilli A, Sari M, Keyik B, Kilic H, Dogan M, et al. Achilles tendon of descending aorta: intimal tear distal to the left subclavian artery and anterograde dissection of descending aorta. International journal of cardiology. 2013;162(2):e43-6.
2. Chen Q, Hou K, Zhang ZX, Zhu YQ, Song TY. Acute occlusion of the left subclavian artery with artery dissection. Chinese medical journal. 2006;119(3):255-8.
3. Schmitter SP, Marx M, Bernstein R, Wack J, Semba CP, Dake MD. Angioplasty-induced subclavian artery dissection in a patient with internal mammary artery graft: treatment with endovascular stent and stent-graft. AJR American journal of roentgenology. 1995;165(2):449-51.
4. Guhathakurta S, Agarwal R, Borker S, Sharma AK. Chronic dissection of the left subclavian artery with pseudocoarctation. Texas Heart Institute journal / from the Texas Heart Institute of St Luke's Episcopal Hospital, Texas Children's Hospital. 2003;30(3):221-4.
5. Marik PE, McLaughlin MT. Spontaneous subclavian artery dissection: a pain in the neck diagnosis. BMJ case reports. 2013;2013.
6. Tochii M, Ando M, Takagi Y, Kaneko K, Ishida M, Akita K, et al. Iatrogenic type A aortic dissection after catheter intervention for the left subclavian artery. Annals of thoracic and cardiovascular surgery : official journal of the Association of Thoracic and Cardiovascular Surgeons of Asia. 2010;16(6):451-3.
7. Myers SI, Harward TR, Cagle L. Isolated subclavian artery dissection after blunt trauma. Surgery. 1991;109(3 Pt 1):336-8.
8. Nakamura K, Nakamura E, Matsuyama M, Niina K, Ishii H. Spontaneous left subclavian artery dissection with concurrent thrombosis and embolic occlusion of the lower limbs: report of a case. Surgery today. 2010;40(7):658-61.
9. Ananthakrishnan G, Bhat R, Zealley I. Spontaneous subclavian artery dissection causing ischemia of the arm: diagnosis and endovascular management. Cardiovascular and interventional radiology. 2009;32(2):326-8.
10. Fernandes AF, Lange MC, Piovesan EJ, Zamproni LN, Germiniani FM, Zetola VF. Spontaneous subclavian artery dissection in a young woman with migraine: an unusual etiology of stroke. Arquivos de neuro-psiquiatria. 2010;68(3):475-6.
11. Garewal M, Selhorst JB. Subclavian artery dissection and triple infarction of the nervous system. Archives of neurology. 2005;62(12):1917-9.
12. Iwamuro Y, Nakahara I, Tanaka M, Higashi T, Watanabe Y, Harada K, et al. Occlusion of the vertebral artery secondary to dissection of the subclavian artery--case report. Neurologia medico-chirurgica. 2005;45(2):97-9.
13. Barbesier M, Duncanson ER, Mackey-Bojack SM, Roe SJ, Thomas LC. Sudden death due to spontaneous acute dissection of the left subclavian artery with rupture during postpartum period: a case report. International journal of legal medicine. 2013;127(2):453-7.
14. Kitamura H, Kimura A, Fukaya S, Okawa Y, Komeda M. Emergent total arch replacement for acute type A aortic dissection with aberrant right subclavian artery in a systemic lupus erythematosus patient. General thoracic and cardiovascular surgery. 2013.

15. Stanley GA, Arko FR, 3rd, Foteh MI, Jessen ME, DiMaio JM. Hybrid endovascular treatment of an anomalous right subclavian artery dissection in a patient with Marfan syndrome. The Annals of thoracic surgery. 2012;94(2):639-41.
16. Knobloch K, von Falck C, Teebken O, Krettek C. Scapulothoracic dissociation with subclavian artery dissection following a severe motorbike accident. European journal of cardio-thoracic surgery : official journal of the European Association for Cardio-thoracic Surgery. 2006;30(4):671.
17. Yoshida K, Tobe S. Dissection and rupture of the left subclavian artery presenting as hemothorax in a patient with von Recklinghausen's disease. The Japanese journal of thoracic and cardiovascular surgery : official publication of the Japanese Association for Thoracic Surgery = Nihon Kyobu Geka Gakkai zasshi. 2005;53(2):117-9.
18. Scheffler P, Uder M, Gross J, Pindur G. Dissection of the proximal subclavian artery with consecutive thrombosis and embolic occlusion of the hand arteries after playing golf. The American journal of sports medicine. 2003;31(1):137-40.

H. Huseinagić is with the Faculty of Medicine, University of Tuzla, Univerzitetska 1, 75 000 Tuzla, BiH (phone: 387-35-303-504; e-mail: haris.huseinagic@ukctuzla.ba).

Evaluation of the amount of used OnyX

Haris Huseinagić[1], Mirza Moranjkić[2], Nihad Mešanović[3], Zahida Ademović[4], Amela Begić[4]
[1] Department of Radiology and nuclear medicine, University Clinical Centre, Tuzla, Bosnia and Herzegovina
[2] Department of Neurosurgery, University Clinical Centre, Tuzla, Bosnia and Herzegovina
[3] Department of IT, University Clinical Centre, Tuzla, Bosnia and Herzegovina
[4]University of Tuzla, Tuzla, Bosnia and Herzegovina

Abstract — **A report on initial experiences in working with liquid embolic agent (Onyx) in the embolisation of arteriovenous brain malformations.**

METHOD Embolization of the brain AVM was performed in 7 patients (5 women and 2 men, mean age 30.6 years (median 33, range of 16-41 years) in the period from December 2013 to December 2014. Clinically, 7 patients were presented with seizures, hemorrhage from the AVM in 2 patients, subarachnoid hemorrhage from concomitant aneurysm in one patient, disorders of vision in one patient and one patient was diagnosed with AVM accidentally. The average size of the AVM was 3.7 cm (median 4, the range from 2- 7 cm).

RESULTS In all seven patients carried a total of 8 embolization procedures with a total of 22 embolisation of artery feeders. Mean reduction in size of the AVM was 75% (median 80%, the range of 40% - 100%). We did not achieved total obliteration, no embolization was preceded to a surgical procedure or radiosurgery. In our relatively small sample, there was not one death or permanent complications.

CONCLUSION Onyx is a safe means of embolisation of cerebral AVM. Complete obliteration of the AVM of the brain is only possible with small malformations. Great AVM of the brain can be treated by repeated embolisation, surgicaly or radiosurgicaly after the original embolisation. Modern approach to the treatment of brain AVM embolisation may be embolisation alone, or a combination of embolisation with surgery or stereotaxic radiosurgery. Embolisation is used to reduce the size of the AVM or to prepare the patient for the surgical procedure.

All procedures were performed using embolization Onyx EVOH (ethylene vinyl alcohol) copolymer dissolved in DMSO (dimethyl sulfoxide), with a suspension of micronized tantalum powder.

Keywords— **arteriovenous brain malformations. AVM, embolisation, Onyx.**

I. Introduction

The ethylene vinyl alcohol copolymer, Onyx(R) (ev3, Inc., MN, USA), is an embolic agent used in the management of arteriovenous malformations (AVMs) and was approved by the US FDA in 2005. Use of Onyx has resulted in higher curative rates compared with previous embolic agents such as N-butyl-2-cyanoacrylate. Onyx has several advantages over previous embolic agents. For instance, Onyx is a copolymer and does not adhere to catheters but solidifies slowly owing to the diffusion of its solvent dimethyl sulfoxide. [1]. Intracranial arteriovenous malformations (AVMs) have a cumulative risk of hemorrhage and refractory seizures. Pre-surgical Onyx embolization of cerebral AVMs improves clinical outcome [2]. Cerebral arteriovenous malformations (AVMs) have an estimated 2-4% annual risk of hemorrhage [3]. Endovascular approaches to arteriovenous malformations (AVMs) are often necessary to define and help treat these often complex lesions. Angiography provides important information to help plan surgically or radio surgical approaches. Modern embolization techniques allow AVMs to be treated with the goals of making surgery safer and easier, eliminating high-risk features in patients with AVMs who are otherwise not candidates for treatment, and even potentially curing the patient of the lesion. Liquid embolic agents have significantly advanced what is possible with endovascular treatment of AVMs [4]. Onyx was first described in the 1990s. It is a non-adhesive and radiolucent compound. Onyx-based closure of the lumen of the targeted vessel is obtained by means of precipitation. The process is enhanced peripherally to the main flux of the injected mixture. This facilitates angiographic monitoring of embolization at any stage. The degree of lumen closure is associated with the location of the vessel. Supratentorial and cortical locations are most advantageous. Dense and plexiform

structure of AVM nidus as well as a low number of supplying vessels and a single superficial drainage vein are usually advantageous for Onyx administration.

Unfavorable factors include nidus drainage into multiple compartments as well as multiarterial supply of the AVM, particularly from meningeal arteries, en-passant arteries or perforating feeders. Onyx appears to be a safe and efficient material for embolization of cerebral AVMs, also in cases of intracranial bleeding associated with AVM.

Curative embolization of small cerebral AVMs is an efficient and safe alternative to neurosurgical and radiosurgical methods. Careful angiographic assessment of individual arteriovenous malformations should be performed before each Onyx administration [5].

Ruptured brain arteriovenous malformations (bAVMs) are at increased risk of re-hemorrhage, but management has historically been conservative [6]. Onyx was first introduced on December 2013. Here we present our local experience in the UCC Tuzla over a 12-month period.

II. Materials and methods

A. Patients

Between December 2013 and December 2014, 7 patients (5 women, 2 men) with AVMs were treated by embolization with Onyx. The 7 patients with embolization were a mean of 30,6 years old (median, 33; range, 16 – 41 years).

Clinically, 7 patients were present with seizures, bleeding from the AVM in 2 patients, subarachnoid hemorrhage from concomitant aneurysm in one patient, disorders of vision in one patient and one patient was diagnosed with AVM accidentally.

The average size of the AVM was 3.7 cm (median 4, the range of 2-7 cm). Grading according to Spetzler and Martin [7] was grade I in 2, grade II in 4, and grade III in 1.

B. Morphology of Cerebral arteriovenous malformations

There was one large right frontoparietal AVM. One patient had a left posterior temporal AVM, and another had a left temporo-parieto-occipital AVM. Two patients had left occipital AVMs, and two had right frontal AVMs. The size of these AVMs ranged from 2 to 7 cm (mean, 3.7 cm). Based on the Spetzler-Martin classification of AVMs [8] two (25%) were grade I, four (58%) were grade II, and one was with grade III.

The grade-I and grade-II AVMs (6/7, 83%) were embolized with the clear intent to completely occlude the malformation if feasible. The grade-III AVM (1/7, 17%) had embolisation with the intent to reduce the volume of malformation and in a future to repeat embolisation and completely occlude the malformation.

C. Embolisation techniques

Onyx is a non-adhesive liquid embolic agent [9, 10] supplied in vials. Each vial contains tantalum and ethylene-vinyl alcohol copolymer, dimethyl sulfoxide (DMSO). The copolymer dissolved in DMSO is prepared in three different concentrations: 6.0%, 6.5%, and 8.0%. To ensure proper mixing of the tantalum powder, the vials are kept on a shaker (Vortex II) for at least 20 minutes. Onyx viscosities of 18, 20, and 34 cP have respective concentrations of 6.0%, 6.5%, and 8.0%, and accordingly it is formulated as Onyx 18, Onyx 20, and Onyx 34.

Diffusion of DMSO is initiated by precipitation of the copolymer if the mixture comes into contact with an aqueous solution. The process of precipitation of the copolymer begins on the surface while the core is still liquid. The result is a soft, non-adherent mass, with a lava-like consistency of flow within blood vessels.

During an injection of Onyx, the mixture does not fragment. In our study we used Onyx 18 as the embolization agent in all patients. All Onyx embolizations were carried out under general anaesthesia. A 6-French (6F) arterial sheath was

placed in the right femoral artery. Diagnostic cerebral angiography was performed.

A guiding catheter was inserted in either an internal carotid artery or a dominant vertebral artery. With an aid of a 0.008-inch guidewire (Mirage, ev3 Neurovascular), a flow-directed microcatheter (Marathon, ev3 Neurovascular) was navigated to the nidus of AVM.

The feeding pedicle of the AVM should be occluded by the reflux of Onyx along the microcatheter up to 2 cm retrogradely.

The microcatheter was flushed with DMSO, and the microcatheter was slowly filled with Onyx for no less than 40 seconds under continuous visual control using subtracted fluoroscopy, Onyx was slowly and progressively injected into the nidus.

As soon as early embolisation of the draining vein was evident or reflux was noted along the microcatheter, the injection was stopped. After 1 to 2 minutes injection could be resumed.

III. Results

In all seven patients, we carried a total of 8 embolization procedures with a total of 22 feeder artery embolization. Mean reduction in size of the AVM is 75% (median 80%, the range of 40% - 100%). We did not achieve total obliteration in any of cases.

There was no procedural morbidity or mortality, procedural intracranial haemorrhage or instance of a stuck or retained microcatheter.

In the six patients with AVMs in whom maximal volume reduction was attempted, four (4/6, 70%) achieved a more-than-80% volume reduction.

There was no major permanent neurological deficit or mortality in this group of patients. The other two patients were planned for repeated embolization.

A. Case illustrations

Case 1

A 27-year-old man presented with headache, nausea and occasionally double vision. Computed tomography showed intraventricular haemorrhage, CT angiography delineated size and extent of a frontal AVM. We completely occluded the AVM using single 1.4 ml Onyx embolization The patient was discharged from hospital 3 days after the procedure.

Case 2

A 32-year-old woman presented with headache only. CT and CTA imaging showed a 6-cm left temporo-parietal AVM with superficial cortical and deep, straight sinus venous drainage. The patient was prepared for embolisation. (Fig. 1) The first session of embolisation partially occluded the superficial cortical part of the AVM. A second session of embolisation 3 months later through the left middle cerebral artery achieved a subtotal occlusion (Fig. 2).

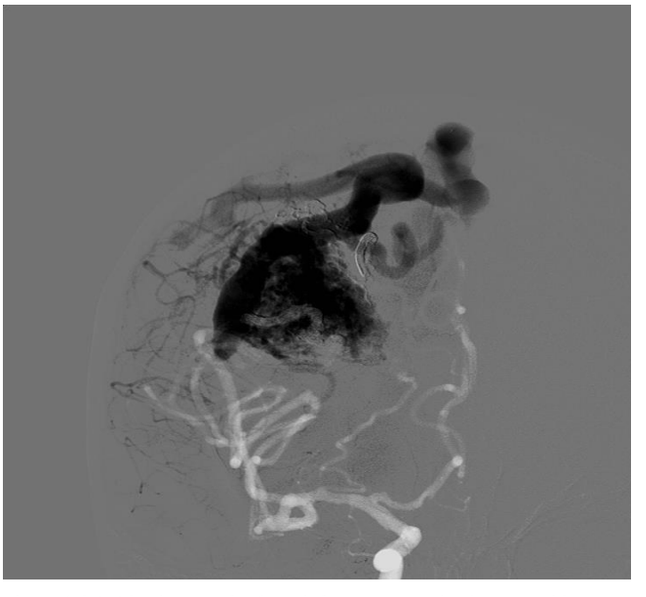

Figure 1 2D DSA image of a 6-cm left temporo-parietal AVM with superficial cortical and deep, straight sinus venous drainage.

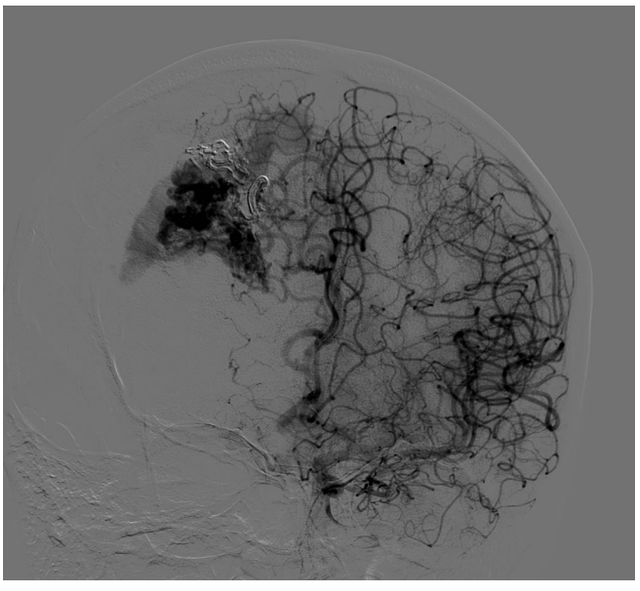

Figure 2 A second session of embolisation 3 months later through the left middle cerebral artery achieved a subtotal occlusion.

IV. Discussion

The annual hemorrhage rate of intracranial arteriovenous malformations (AVMs) varies from 2 to 4% [11]. The aim of AVM treatment is total occlusion to prevent future haemorrhage. Successful AVM treatment could be achieved only with the availability of different treatment modalities.

The radiosurgery is the treatment for small AVMs located in eloquent areas. The standard treatment for ruptured AVMs located in non-eloquent areas is microsurgery. A review of the literature showed data to support Onyx treatment efficacy in AVM cure and AVM size reduction (Table 1). In centres using Onyx embolization alone as their primary treatment for cerebral AVM, neurological morbidity of 8 to 8.5% and mortality of 3% have been reported, with a complete occlusion rates as high as 49 to 54%.

Stuck, broken and retained microcatheters were described in earlier reported series. The key to avoiding stuck, broken and retained microcatheters is strict adhesion to reflux length, as well as injection time. A DMSO-compatible detachable catheter may be considered to be an alternative solution. Before embolisation, the degree of achieved AVM occlusion cannot be absolutely

Table 1. Literature review of Onyx embolisation with the intent of endovascular cure and/or primary aim of volume reduction for subsequent microsurgery or radiosurgery

Case series	No. of patients	Angiographic cure	Permanent neurological deficit	Procedure-related death	Other technical complications (No. of patients)
Mounlayer et al. 2007	94	49% (26/53)	8.5% (8/94)	3.2% (3/94)	Retained microcatheter (4), distal rupture of arterial feeder (5)
Weber et al. 2007	94	20% (19/94)	9.6% (9/94)	0%	Stuck microcatheter (9). distal perforation (4)
van Rooij et al. 2007	44	16%. (7/44)	4.6% (2/44)	2.3% (1)	Glued microcatheter (2)
Katsardis et al. 2008	101	54% (28/52)	8% (8/101)	3% (3/101)	Stuck microcatheter (1)
Panagiotopouios et al. 2009	82	24.4% (20/82)	3.8% (3/82)	2.4% (2/82)	-
Song et al. 2007	70	18.6% (13/70)	7.1% (5/70)	1.4% (1/70)	-
Jahan et al. 2001	23	Average: 63%*	4% (1/23)	0%-	-
Weber et al 2007	47	Mean: 85±18% *	Disabling: 9%: nondisab: 21%	0%'	Stuck microcatheter (4), vessel perforation (5)
Natarajan et al. 2008	28	Average: 74±18%‘	1/28 (3.6%)	0%'	Stuck microcatheter (2). vessel perforation (1)
Velat et al. 2003	20	Median: 50±25%"	10% (2/20)	5% (1/20)'	-

predicted. The Onyx cast has high radio-opacity and can hide the rest of the nidus making it difficult to visualise the course. This situation can result in unwanted placement of Onyx into the venous part of the malformation. The aim of embolization of large AVMs is volume reduction. The nidus should be without fragments. Any residual nidus should be at the periphery of the Onyx cast.

The reasons for recurrence after glue embolisation are pedicle embolisation and recanalisation of the thrombosed portion of nidus. Onyx nidal embolisation theoretically eliminates possibility for recurrence after glue embolisation. In the literature, the recurrence rate of Onyx AVM embolisation has been reported to be between 0% and 4.8%, main-ly during the initial 3 to 4 months [5]. Based on a magnetic resonance angiography after 3 months, and a digital subtraction angiography after 6-month in our patients, there was no evidence of recurrence. We believe that Onyx will prove to be a promising agent for cerebral AVM embolisation.

V. Conclusions

Onyx is a safe, promising agent for cerebral AVM embolisation. Complete obliteration of the AVM of the brain is only possible with small malformations. Great AVM of the brain can be treated by repeated embolization, surgicaly or radiosurgicaly, after the initial embolization.

Modern approach to the treatment of brain AVM embolisation may be alone, or a combination of embolization with surgery or stereotaxic radiosurgery. Embolisation is used to reduce the size of the AVM or to prepare the patient for the surgical procedure.

References

1. Lanzino G, Burrows AM, Cloft HJ. Onyx embolization. Journal of neurosurgery. 2014;120(2):375-6.
2. Kim ST, Jeong HW, Seo J. Onyx Embolization of Dural Arteriovenous Fistula, using Scepter C Balloon Catheter: a Case Report. Neurointervention. 2013;8(2):110-4.
3. Spiotta AM, Miranpuri AS, Vargas J, Magarick J, Turner RD, Turk AS, et al. Balloon augmented Onyx embolization utilizing a dual lumen balloon catheter: utility in the treatment of a variety of head and neck lesions. Journal of neurointerventional surgery. 2014;6(7):547-55.
4. Khaja MS, Park AW, Swee W, Evans AJ, Fritz Angle J, Turba UC, et al. Treatment of type II endoleak using Onyx with long-term imaging follow-up. Cardiovascular and interventional radiology. 2014;37(3):613-22.
5. Jia JB, Green CS, Cohen AJ, Helmy M. CT and radiographic appearance of extracranial Onyx embolization. Clinical radiology. 2014.
6. Gao X, Liang G, Li Z, Wang X, Yu C, Cao P, et al. Transarterial coil-augmented Onyx embolization for brain arteriovenous malformation. Technique and experience in 22 consecutive patients. Interventional neuroradiology : journal of peritherapeutic neuroradiology, surgical procedures and related neurosciences. 2014;20(1):83-90.
7. Yen CP, Schlesinger D, Sheehan JP. Natural history of cerebral arteriovenous malformations and the risk of hemorrhage after radiosurgery. Progress in neurological surgery. 2013;27:5-21.
8. Jeon HJ, Park KY, Kim SY, Lee JW, Huh SK, Lee KC. Surgical outcomes after classifying Grade III arteriovenous malformations according to Lawton's modified Spetzler-Martin grading system. Clinical neurology and neurosurgery. 2014;124:72-80.
9. Szajner M, Roman T, Markowicz J, Szczerbo-Trojanowska M. Onyx((R)) in endovascular treatment of cerebral arteriovenous malformations - a review. Polish journal of radiology / Polish Medical Society of Radiology. 2013;78(3):35-41.
10. Wu Q, Wang HD, Zhang QR, Zhang X. Parent artery occlusion with Onyx for distal aneurysms of posterior inferior cerebellar artery: a single-centre experience in a series of 15 patients. Neurology India. 2013;61(3):265-9.
11. Ramalingaiah AH, Prasad C, Sabharwal PS, Saini J, Pandey P. Transarterial treatment of direct carotico-cavernous fistulas with coils and Onyx. Neuroradiology. 2013;55(10):1213-20.

H. Huseinagić is with the Faculty of Medicine, University of Tuzla, Univerzitetska 1, 75 000 Tuzla, BiH (phone: 387-35-303-504; e-mail: haris.huseinagic@ukctuzla.ba).

Three-dimensional rotational angiography in the control of the results of endovascular coiling of intracranial aneurysms

Haris Huseinagić[1], Mirza Moranjkić[1], Nihad Mešanović[1]

[1] Department of Radiology and nuclear medicine, University Clinical Centre, Tuzla, Bosnia and Herzegovina
[1] Department of Neurosurgery, University Clinical Centre, Tuzla, Bosnia and Herzegovina
[1] Department of IT, University Clinical Centre, Tuzla, Bosnia and Herzegovina

Abstract— **The process of endovascular treatment of cerebral aneurysms requires intensive use of 3D rotational angiography in planning and monitoring the entire process. 3D RA allows unlimited manipulation of model blood vessels and defining the morphology of the aneurysm without using radiation.**

The purpose of the study was to compare the results of the analysis of residue or recurrence of the aneurysm after endovascular treatment using 3D RA and 2D digital subtraction. Method. In 68 patients with 76 cerebral aneurysms, we made regular controls using both techniques, 2D DSA and 3D RA. Residual and recurrent aneurysms are classified into five stages, and the pictures taken by both modalities are compared. Results. 2D DSA detected the residual and recurrent aneurysm in 53.70% of cases (29/54 aneurysms), and 3D RA in 66.67% (36/54 aneurysms). In nine cases in 2D DSA did not detected residues of which was discovered in 3D RA, and 3 cases of 2D DSA reveals little short neck aneurysm, which is on the 3D RA, in fact, a small aneurysm. In five cases from the use of 3D RA reduced the level of classification aneurysm.

Conclusion: 3D RA reveals more residues aneurysms.

Keywords— **3D RA, 2D DSA, endovascular treatment of cerebral aneurysms.**

I. Introduction

Recent neurointerventional and neurosurgical technologies require an understanding of lesions and adjacent structures in three dimensions [1]. 3D angiography is a true technical revolution that allows improvement in the quality and safety of diagnostic and endovascular treatment procedures [2]. Geometric characteristics and arrangement of the cerebral vessels are assumed to be related to the development of vascular diseases [3]. The use of image-guided interventional radiological techniques is increasing in prevalence and complexity. Imaging system developments have helped improve the information available to interventionalists to plan and guide procedures. Information on doses to patients resulting from alternative imaging techniques or protocols is useful for both the process of justifying particular procedures and in optimizing the resultant exposures. Such information is not always available, especially for new or developing imaging techniques [4]. 3D imaging is a valuable adjunct in neuroangiography for visualization and measurement of cerebral aneurysms and for determination of the optimum projection for intervention. To enable spatially accurate 3D reconstruction the system must correct for geometrical distortion in the image intensifier television system as well as for deviations in gantry motion [5]. Dome-to-neck ratio of intracranial aneurysms is an important predictor of outcomes of endovascular coiling. 3D imaging techniques are increasingly used in evaluating the dome-to-neck ratio of aneurysms for intervention [6]. Cerebral aneurysms must be monitored for varying periods after surgical and/or endovascular treatment and the duration of follow-up will depend on the type of therapy and the immediate post-operative outcome. Surgical clipping for intracranial aneurysms is a valid treatment but the metal clips generate artefacts so that follow-up monitoring still relies on catheter angiography [7]. A gold standard of cerebral vessel imaging remains the digital subtraction angiography (DSA) performed in three projections. However, in specific clinical cases, many additional projections are required, or a complete visualization of a lesion may even be impossible with 2D angiography. Three-dimensional (3D) reconstructions of rotational angiography were reported to improve the performance of DSA significantly [8].

II. Materials and methods

Patients

Between February 2014 and December 2014, 68 consecutive patients [35 female (26–77 years, mean 53) and 33 male (24–67 years, mean 49); age range, 24–77 years; mean age, 51 years] were prospectively enrolled in this study and were examined with cerebral 3DRA. All patients had a known intracranial aneurysm, for which it was decided they should undergo 3DRA to plan endovascular or neurosurgical treatment. Clinically, 33 patients had Hunt and Hess score of 0; 8 had score I; 8 had score II; 5 had score III; 3

had score IV; and 11 had score V. 16 of 33 patients with Hunt and Hess score 0 had a symptomatic cerebral aneurysm. Written informed consent was obtained from patients or their relatives after full explanation of the nature of the diagnostic and interventional procedures.

We included 68 3D datasets of 1 vascular tree of 68 patients with at least 1 intracranial aneurysm on the 3D dataset and a complete cerebral DSA performed between February 2014 and December 2014. A complete DSA consisted of 3-vessel angiography in 53 patients and 4-vessel angiography in 15 patients, for a total of 219 vessels. 68 3D datasets were reevaluated on the workstation. The presence, location, and size of additional aneurysms were also assessed. The size of aneurysm was defined as the maximal diameter as measured on 3DRA. Data base that served as a reference consisted of results of re-evaluation of 3DRA data. The location of aneurysm were classified into carotid artery, middle cerebral artery, anterior cerebral artery, and posterior circulation. We reviewed and the DSA images of the corresponding 68 vascular trees in 2 or 4 projections on a PACS workstation for the presence and location of additional aneurysms. Results were compared with the findings in the reference data base. Number, location, and size of false-negative and false-positive additional aneurysms were recorded. The location of neurysm was classified as carotid artery, middle cerebral artery, anterior cerebral artery, and posterior circulation.

3DRA

3D rotational angiograms were performed under general anesthesia by using an angiographic system (Integris BV 5000, Philips Medical Systems, Best, The Netherlands) running the software Integris 3DRA, release 4.2. By means of a transfemoral approach with the Seldinger technique, DSA was performed by using a standard diagnostic 5-F catheter (GEN selective, IMAGER II, Boston Scientific, Natick, Mass.).

The tip of the diagnostic catheter was placed in the cervical portion of the internal carotid artery or vertebral artery proximal to the skull base. Selective four-vessel injections were performed in the anteroposterior, lateral, and oblique projections.

3DRA of the corresponding vessels was then performed. Contrast material was injected with a total amount of 18 ml and a flow-rate of 3 ml/s using power injector (Angiomat Illumena, Liebel-Flarsheim, Cincinatti, Ohio). The image acquisition was performed during the 3DRA using a range of 180 degrees with a rotational speed of up to 30 degrees/s. Systemic blood pressure was monitored during the entire examination.

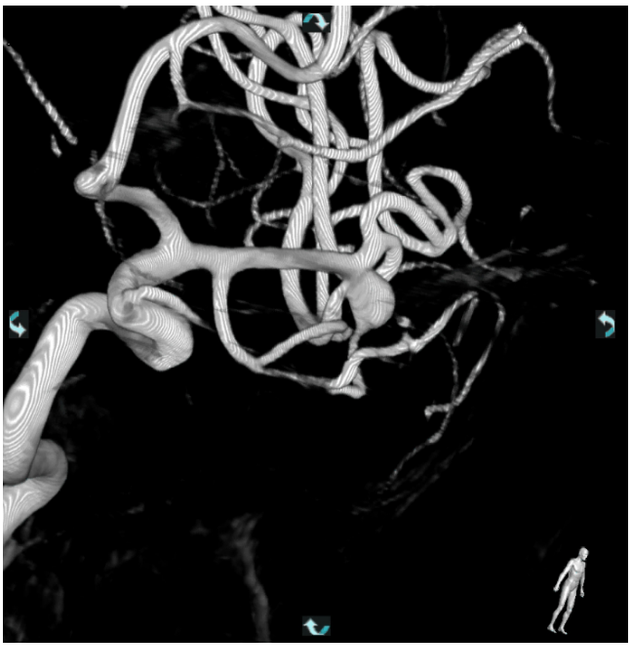

Figure 1. 3DRA of the vessels with aneurysm on arteria cerebri media. Contrast material was injected with a total amount of 18 ml and a flow-rate of 3 ml/s using power injector.

Statistical Analysis

A χ^2 test (2-tailed) was used for comparison of the proportion of aneurysms $\leq$ 3 mm in additional aneurysms, the proportion of aneurysms $\leq$ 3 mm missed on DSA and in all additional aneurysms as detected on 3DRA, and the location (classified as carotid artery, middle cerebral artery, anterior cerebral artery, and posterior circulation) of additional aneurysms missed on DSA versus the location of all additional aneurysms.

III. Results

In 68 3D datasets, 68 target aneurysms and 8 additional aneurysms were detected for a total of 76 aneurysms. The mean size of 68 target aneurysms was 7.4 mm (median, 6; range, 1–32 mm). The mean size of 8 additional aneurysms was 3.54 mm (median, 3; range, 0.5–17 mm). Of 8 additional aneurysms, 5 (65%) were $\leq$ 3 mm; and of 68 target aneurysms, 1 (17%) were $\leq$ 3 mm. The proportion of aneurysms $\leq$ 3 mm was significantly higher in additional aneurysms (5 of 8, 65%) than in target aneurysms (1 of 68, 17%) χ^2,P <.0001).

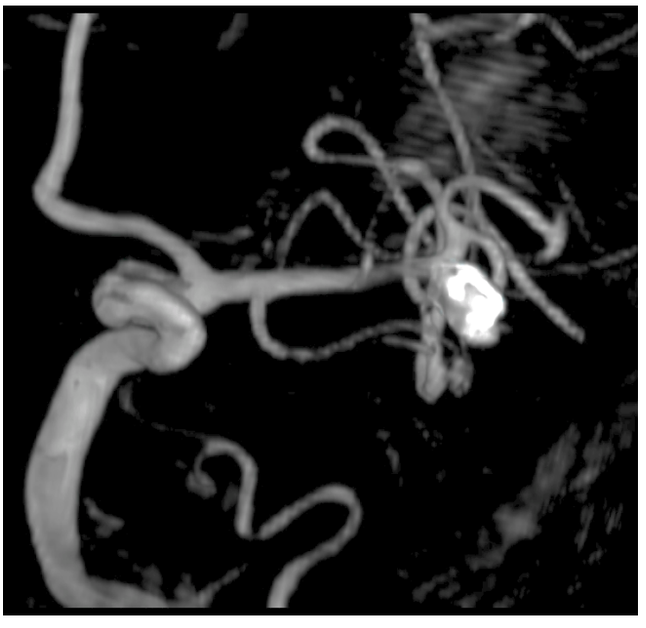

Figure 2 The image acquisition was performed during the 3DRA after procedure of embolisation.

Results of Observers

Of 8 additional aneurysms, 2 (29%) were missed on DSA (Figs 1–5). The mean size of the missed aneurysms was 1.94 mm (median, 2; range, 0.5– 4 mm). Of 2 missed aneurysms, 7 (96%) were ≤ 3 mm. The proportion of aneurysms ≤ 3 mm in missed additional aneurysms (7 of 8, 96%) was significantly higher than that in all additional aneurysms (5 of 8, 65%) χ^2,P < .0035.

The location of 8 missed additional aneurysms was the anterior cerebral artery in 2 (22%), the carotid artery in 3 (37%), the middle cerebral artery in 2 (26%), and the posterior circulation in 1 (7%). With the χ^2 test, the location of missed additional aneurysms was not different from the location of all additional aneurysms. Two false-positive aneurysms were observed on DSA, 1 on the ophthalmic artery and 1 in the middle cerebral artery.

Data entry procedures and statistical analysis were performed with a statistical software system (SPSS for windows, version 16.0.1 EV, Chicago, Ill.).

IV. Discussion

In this study, we found that 2 of 8 small additional aneurysms that were apparent on 3DRA of 68 vascular trees in 68 patients with a target aneurysm were missed on DSA. All except 1 of the missed aneurysms were 3 mm or smaller, and the smallest aneurysm was 0.5 mm. In addition, we found no significant difference in distribution of missed aneurysms compared with all additional aneurysms.

The phenomenon of angiographically occult additional aneurysms found during surgery of symptomatic aneurysms is well known in the surgical literature. An incidence of 3.7% and 4.9% of angiographically occult microaneurysms of 2 mm or smaller was reported [9, 10]. In a series of 1012 symptomatic aneurysms, 377 additional aneurysms, of which 169 (12.2% of all aneurysms) were 2 mm or smaller [11]. If technically possible, these microaneurysms were clipped or wrapped to prevent their growth and rupture. Although the clinical significance of the presence of additional small aneurysms may be subject to debate [12, 13], in our opinion, accurate detection of these small aneurysms may have consequences in the selection of patients for choice of therapy (coiling or clipping) and in the frequency and duration of follow-up. For example, in patients with target aneurysms suitable for both coiling and clipping, the presence of additional aneurysms that cannot be coiled may direct the therapy of choice to clipping if these additional aneurysms can be clipped in the same surgical procedure (Figs 2– 4A–C,5A–D). In patients who are treated for the target aneurysm but are left with untreated small additional aneurysms, imaging follow-up strategy may be more frequent and more prolonged to detect growth of these small aneurysms in a timely manner. If small additional aneurysms remain undetected, patients may be wrongly considered to have a single instead of multiple aneurysms. In epidemiologic studies concerning multiplicity of aneurysms, this may have consequences for determination of risk factors and outcome [13, 14].

In our experience, 3DRA is a major step forward in the detection and evaluation of intracranial aneurysms. The postprocessing capabilities of a 3D dataset allow viewing in any desired projection in high resolution without hindering overprojecting bony structures. This makes small aneurysms more obvious than those on the limited number of projections of DSA [15-19]. In addition, complex vascular areas such as the anterior communicating artery complex can easily be unraveled and evaluated for the presence of aneurysms or vascular variations such as fenestrations [20]. Measurement of aneurysm diameter and aneurysm volume can be performed accurately without the need for correction for magnification [16]. Another advantage of 3DRA over DSA is its relative operator independency: After catheterization of the desired vessel, acquisition of the rotational run is standard procedure. Extensive postprocessing can be performed easily for scientific purposes, even many years after acquisition if the dataset is exported from the work-

station to an external data-storage medium. On the other hand, DSA of intracranial vessels requires more experience and skill of the operator with respect to the decision of whether and which additional projections should be made. Image postprocessing is limited to window and width adjustment and pixel shifting, and storage of raw data is usually limited in time. A disadvantage of 3DRA with respect to DSA is the higher contrast load per acquisitioned run (18 – 24 versus 6 – 8 mL), longer acquisition time (6 – 8 seconds), and in- creased patient radiation dose. In uncooperative patients, such as some patients with acute subarachnoid hemorrhage, patient movement may degrade image quality. In our study, most 3DRA datasets were acquired in patients under general anesthesia before coiling of the target aneurysm. Total patient contrast load and radiation dose can be decreased when only 3DRA acquisitions are obtained of all vessels, without preceding DSA runs. In this way, not only are the total contrast load and radiation dose roughly the same as those for DSA, but aneurysm imaging is also optimized. Currently, this is our protocol in cooperative patients with suspected intracranial aneurysms. Our findings indicate that DSA may no longer be considered the gold standard for detection of intracranial aneurysms in studies that evaluate aneurysm-detection rates of noninvasive image techniques such as CTA and MRA. Both of these imaging techniques are inaccurate and unreliable in the detection of aneurysms of 3 mm and smaller [21, 22]. In our sixty eight 3D datasets of single vascular trees, 68 aneurysms were detected and 1 of these (17%) were 3 mm or smaller. Thus, a considerable proportion of intracranial aneurysms can potentially be missed with CTA and MRA. Future studies concerning CTA and MRA in intracranial aneurysms should be compared with 3DRA instead of DSA.

V. CONCLUSIONS

3DRA depicts considerably more small additional aneurysms than DSA. In selected patients, accurate detection of these aneurysms may have consequences for choice of treatment technique and for the frequency and duration of imaging follow-up. In cooperative patients with suggestion of intracranial aneurysms, 3- to 4-vessel 3DRA only (without preceding DSA runs) should be recommended as the optimal image strategy.

REFERENCES

1. Abe T, Hirohata M, Tanaka N, Uchiyama Y, Kojima K, Fujimoto K, et al. Clinical benefits of rotational 3D angiography in endovascular treatment of ruptured cerebral aneurysm. AJNR Am J Neuroradiol. 2002;23(4):686-8.
2. Anxionnat R, Bracard S, Macho J, Da Costa E, Vaillant R, Launay L, et al. 3D angiography. Clinical interest. First applications in interventional neuroradiology. J Neuroradiol. 1998;25(4):251-62.
3. Bogunovic H, Pozo JM, Cardenes R, Frangi AF. Automatic identification of internal carotid artery from 3DRA images. Conf Proc IEEE Eng Med Biol Soc. 2010;2010:5343-6.
4. Bridcut RR, Murphy E, Workman A, Flynn P, Winder RJ. Patient dose from 3D rotational neurovascular studies. Br J Radiol. 2007;80(953):362-6.
5. Bridcut RR, Winder RJ, Workman A, Flynn P. Assessment of distortion in a three-dimensional rotational angiography system. Br J Radiol. 2002;75(891):266-70.
6. Brinjikji W, Cloft H, Lanzino G, Kallmes DF. Comparison of 2D digital subtraction angiography and 3D rotational angiography in the evaluation of dome-to-neck ratio. AJNR Am J Neuroradiol. 2009;30(4):831-4.
7. Budai C, Cirillo L, Patruno F, Dall'olio M, Princiotta C, Leonardi M. Flat panel angiography images in the post-operative follow-up of surgically clipped intracranial aneurysms. Neuroradiol J. 2014;27(2):203-6.
8. Ciescinski J, Serafin Z, Strzesniewski P, Lasek W, Beuth W. DSA volumetric 3D reconstructions of intracranial aneurysms: A pictorial essay. Pol J Radiol. 2012;77(2):47-53.
9. Karasawa H, Matsumoto H, Naito H, Sugiyama K, Ueno J, Kin H. Angiographically unrecognized microaneurysms: intraoperative observation and operative technique. Acta neurochirurgica. 1997;139(5):416-9; discussion 9-20.
10. Inamasu J, Suga S, Horiguchi T, Akaji K, Mayanagi K, Kawase T. Cerebral microaneurysms found incidentally during aneurysm surgery. Neurological research. 2001;23(4):304-8.
11. Yasargil MG. The advent of microsurgery. The Mount Sinai journal of medicine, New York. 1997;64(3):164-5.
12. Wermer MJ, van der Schaaf IC, Algra A, Rinkel GJ. Risk of rupture of unruptured intracranial aneurysms in relation to patient and aneurysm characteristics: an updated meta-analysis. Stroke; a journal of cerebral circulation. 2007;38(4):1404-10.
13. Kaminogo M, Yonekura M, Shibata S. Incidence and outcome of multiple intracranial aneurysms in a defined population. Stroke; a journal of cerebral circulation. 2003;34(1):16-21.
14. Juvela S. Risk factors for multiple intracranial aneurysms. Stroke; a journal of cerebral circulation. 2000;31(2):392-7.
15. Anxionnat R, Bracard S, Ducrocq X, Trousset Y, Launay L, Kerrien E, et al. Intracranial aneurysms: clinical value of 3D digital subtraction angiography in the therapeutic decision and endovascular treatment. Radiology. 2001;218(3):799-808.
16. Tanoue S, Kiyosue H, Kenai H, Nakamura T, Yamashita M, Mori H. Three-dimensional reconstructed images after rotational angiography in the evaluation of intracranial aneurysms: surgical correlation. Neurosurgery. 2000;47(4):866-71.
17. Sugahara T, Korogi Y, Nakashima K, Hamatake S, Honda S, Takahashi M. Comparison of 2D and 3D digital subtraction angiography in evaluation of intracranial aneurysms. AJNR American journal of neuroradiology. 2002;23(9):1545-52.
18. Hochmuth A, Spetzger U, Schumacher M. Comparison of three-dimensional rotational angiography with digital subtraction angiography in the assessment of ruptured cerebral aneurysms. AJNR American journal of neuroradiology. 2002;23(7):1199-205.
19. Beck J, Rohde S, Berkefeld J, Seifert V, Raabe A. Size and location of ruptured and unruptured intracranial aneurysms measured by 3-dimensional rotational angiography. Surgical neurology. 2006;65(1):18-25; discussion -7.
20. de Gast AN, van Rooij WJ, Sluzewski M. Fenestrations of the anterior communicating artery: incidence on 3D angiography and relationship to aneurysms. AJNR American journal of neuroradiology. 2008;29(2):296-8.

21. Kouskouras C, Charitanti A, Giavroglou C, Foroglou N, Selviaridis P, Kontopoulos V, et al. Intracranial aneurysms: evaluation using CTA and MRA. Correlation with DSA and intraoperative findings. Neuroradiology. 2004;46(10):842-50.
22. Jayaraman MV, Mayo-Smith WW, Tung GA, Haas RA, Rogg JM, Mehta NR, et al. Detection of intracranial aneurysms: multi-detector row CT angiography compared with DSA. Radiology. 2004;230(2):510-8..

H. Huseinagić is with the Faculty of Medicine, University of Tuzla, Univerzitetska 1, 75 000 Tuzla, BiH (phone: 387-35-303-504; e-mail: haris.huseinagic@ukctuzla.ba).

BioEcomat (BEC) - Machine for recycling biotech drugs

A.B. Adna Sijerčić
Iternational Burch University/Genetics and Bioengineering, IBU student, Sarajevo, Bosnia and Herzegovina

Abstract - **Biotechnological drugs are drugs that are produced using living organisms. Modern biotechnological drugs are the result of the latest scientific achievements and production of researchers of different profiles. These drugs are a new challenge for industry, and the number of applications for obtaining traffic is continuously growing.**
These drugs are manufactured and usually genetically modified, and there is possibility that they "escape" in outside world (by wrong recycling) and they could cause genetic pollution and poisoning of the environment, maybe new "modern" disease. BioEcomat (BEC) is a machine that automatically recycles old, unusable biotehnological drugs, and ejects the confirmation of a transaction that can be desired in designated places exchanged for money or other medicines. The machine has a database of over 4000 medications, and code reader to recognize what you want to recycle.

Keywords – **Biotechnology, biotech drugs, pharmacy, genetical mutations, environment.**

INTRODUCTION

Hazard of genetic engineering (environmental risks) is genetic pollution - once GMO (bacteria, fungus or virus) escapes into the environment, it will be impossible to stop it or destroy it. Unlike nuclear waste, which diminishes over time (half-life), genetical waste is multiplied and strengthened. (Thieman, 2008.)

BIOTECHNOLOGY OF DRUGS
Biotechnological drugs are those drugs that are produced using living organisms such as, for example, yeast, bacteria or mammalian cells. *Real bioreactor is a living cell !!*
These are large molecules of complex structure.
Although some biotech drugs were used many centuries ago, modern biotechnological drugs are the result of the latest scientific achievements and sophisticated production technology with the participation of researchers of different profiles such as pharmacologists, pharmacists, doctors, immunologists, biologists. These drugs are a new challenge for researchers and industry, and the number of applications for obtaining traffic is continuously growing.
Biologically similar drugs are special part, which are similar to natural active molecules after the those do not exist in nature.Biologically similar drugs are resulting in biotechnological development and production. This is subject to special procedures for testing the efficacy and safety. (Squassina, 2010)

A growing number of biotechnology products which are candidates for drugs, increases the need for staff trained in all phases of production and control of these products. (Squassina, 2010)

LITERATURE REVIEW

FEATURES OF CLASSIC AND BIOLOGICAL DRUGS
One of the features of synthetic and semisynthetic classic drugs is small molecule relatively simple chemical synthesis. Other one is extraction of the biologically active molecule of human or animal origin (insulin, heparin, HGH, coagulation factors, albumin)
Biotechnological drugs need better yield, purity and safety of drugs that exist in the mammalian organism (Insulin, HGH). Modificated molecule or a molecule which can not be extracted from biological material (erythropoietin, interferon, interleukin, growth faktri)
There are significant differences between the production of classicmdrugs and biologics (biological drugs). *Classical drugs* are products with formulation, their starting material is defined, there are few controls during the manufacturing process, it's easy control of the end product and large series are produced. *Biotechnology drugs* are produced by purification, their starting material could be different, there are numerous of controls and checks during the production of drug, complex tests are arranged at the end product which is more complicated because manufacturing process is a product-specific, and at the end the amount of production is small (grams or kilograms). (Guidance for Industry pharmacogenomic, 2005)

For the production of biotech drugs you need suitable microorganisms or cells genetically modified (inserted naturally occurring or synthetic nucleotides) and then after purification, the product is used in human or veterinary medicine (Fig.1. – Biotech drug)

Fig.1. – Epogen, Epoetin Biotech drug – medicine for End Stage Renal Disease (ESRD)

System with expression of the corresponding genes is necessary. Another necessary is a system for producing compatible with microorganism and cells, and purifying system is necessary too.
Fourth necessary thing is preserving the characteristics of the active substance.
The pharmaceutical formulation is needed eg. PEGylation (modification of polyethylene glycol) protein stabilization, protection from proteolysis, elimination half-life extension of time, attenuation of immune response, increasing the solubility, lower aggregation.

The flow of production of biotechnological drugs:
You first need to modify products in order to use it for drugs (GMP). Then you need the Bank of cells - cells work - starting material - Celiac cultivation harvest - treatment - pharmaceutical formulation.
The critical phase is purification which means eliminating the risk of contaminants, and of course the process must be validated.
Risks are toxicity, unsuitable biological activity, immunogenicity, oncogenicity and infection.

These things are covered by GMP control in biopharmaceutical:
• The Bank of cells,
• The process of fermentation and culturing,
• The process of purification,
• The active principle,
• The pharmaceutical formulation and the method of packaging,
• The product itself

Types of expression systems for biotech drugs are
• Bacteria - insulin- no glycosylation, short cycle
•Yeast- factors growth-modified glycosylation
• Mammalian cells- antibodies - glycosylation, long cycle
• Skin-AT III - a long cycle

The new generation of biotech drugs in the future is as follows:
• nucleic acids: antisense RNA, DNA itself, RNAi
• gene therapy
• therapies cells
-autolog - (cells of the patient, immune acceptable)
-allogene - (human donor cells)
-stem cell - (Stem cell or germ is an undifferentiated cell that has unlimited capacity division),
-xenotransplants - (transplant whose donor and recipient belong to different species (eg. transfer from animal to human)).
(Guidance for Industry pharmacogenomic, 2005)

BIOLOGICS
The products of living organisms are large and complex molecules which are sensitive to environmental influences during the production of active molecules, storage and formulations. (Thieman, 2008.)
Production of a specific biologics was unknown until 20 years ago and is constantly changing. There must be talented and skillful researchers for searching bilogics. Still, this group of drugs is extensively studied (the top of modern science). The specific production facilities are required. (Thieman, 2008.)

BIOTECH WEAPONS
Biotech weapon is being developed through a union of natural and engineering sciences. (Squassina, 2010)

Ultra-damage:
When choosing a mode of attack with biotechnological weapons, there are two choices: nucleotide sequences (DNA) or protein structure. This means that it may cause physiological disorder in the body by causing damage to the ultra-gene or protein structure. Precise ultra-damage to targets such as genes and proteins is one of the peculiarities of biotechnological weapons and all other weapons directly damage the muscles and organs.

Secrecy (occultation):
Detection and prediction of concrete effects of the weapons of the enemy is almost impossible. Only after the obvious incapacity of its forces, the enemy will realize that it is attacked. In this sense, biotech weapon is the weapon which is deffined with extremely tactical nature.

The ability to control it and capacity for regeneration:
The degree of damage that biotech weapons produce at a given time can be examined in a laboratory to determine accurately. It can even provide an antidote or treatment. The provision of such bioinformation to the enemy would be a "grace" to him.

Difficulties in taking measures to protect the enemy:
Due to the number of living (micro-) organisms which can be used in the construction of military, Biotechnology armies are dangerous and nonethical because so much of the human genome and proteome may be attacked and damaged in so many ways, the final diagnosis and prompt treatment is difficult. Types of gene or protein structure such as the specific key. Only the designer of such weapons has the key, and the enemy is not really able to find a "profile" for that key. (Squassina, 2010)

CONCLUSION

I believe that biotechnology of drugs opens entirely new scientific way for us and provides many features necessary for a better future and progress in the future.
It is interesting because of its broad and truly significant range of applications and because is solves unsolved mysteries and medical problems, issues and diseases.
It provides new hope for curing some serious diseases, which so far has not been curable with ordinary pharmaceutical and medical devices and methods.

Fig.2.- Superior and imagined look of BEC

THE AIM OF THE PROJECT

The aim of this study is to inform people about the differences, advantages, disadvantages and opportunities that are offered with biotech drugs.
The aim is also to, in some way, encourage or at least slowly introduce the possibility of the development of biotechnology drugs within BiH.

MY VISION

My vision is solution to the problem of recycling biotehnological drugs and genetically modified drugs to prevent genetic pollution and poisoning of the environment and its inhabitants (maximum effectiveness)
The machine (slot machine) that swallows the old unusable biologicals, and ejects the appropriate confirmation of the transaction would be called ***BioEcomat (BEC).*** It is a machine that automatically recycles old, unusable bitehnological drugs, and ejects the confirmation of a transaction that can be, as you desire, exchanged for money or other medicines, in designated places. (Fig.2.-superior look of BEC)
The machine has a database of over 4000 medications to recognize what you want to recycle (and what kind of content should certify that you throw). First you have to bring your code to code reader. Code is located on the package of each drug, in order to determine type of the drug, the validity of the drug; and also you need to bring code located on your health card to code reader in order to establish a person's identity, to prevent illegal exploitation services of BEC, and if all goes well – you'll get an offer (proffer) for printing confirmation that you can accept or reject.
But except that, code reader has much more important function. Not all biotech drugs are recycled in same way. Some of them must be destroyed instantly as recycled, and others must be stored properly in order for further procedure, testing and usage in laboratory. So as I already said, the most important function of code reader is to recognise by code, which drug must be destroyed and which one stored. Code reader decides that by help of huge biotech drugs code data base entered previously in system, which is promptly and properly serviced and updated. So how BEC machine works? Firstly let me tell you something about destruction and proper storage of DNA. Because most of biotech drugs have purified DNA or RNA mixed with some other chemicals, best option to make those bottles or ampoules DNA free is to use Bleach which is the most frequently used, cheap and works really well (we clean all lab benches daily with bleach) (Tomaž Skrbinšek, 2013) that is best and cheapest method for DNA destruction. This solution needs to be diluted containing different correctly measured amounts of: distilled water, Sodium Hypochlorite and some other disinfectant. Or for example: you mix 10mL of household bleach with 90mL of water to create a 10% solution of bleach (Debbie, 2012) , like we do in a "recipe" for lab disinfection, and you always need to make a new solution when disinfecting. Other method for destruction is autoclaving, but autoclaving under the standard conditions of 121°C for 20 min won't sufficiently remove amplifiability from the model DNA and it was found to be a possible source of laboratory contamination. However, the amplifiable template is possible to be surelly removed after autoclaving at 121°C for 80 min (Tetsushi, 2013). Now methods for DNA storage, birds on branch knows that freezing temperatures stops or slows down metabolic processes of almost all living beings, so same thing happens with DNA and RNA, and they become "alive" again with rise of a temperatures. Ultra low temperature LAB freezers generally operate between user-set ranges from -40°C to -86°C whereas models described as low temperature laboratory freezers can be set from -10°C to -40°C, depending on make and model. DNA: Plasmids at -20C, Genomic at 4C. DNA can fall out of solution if stored at -20C. With plasmids that is no problem because you can vortex them and get them back into solution. Genomic DNA is dangerous to vortex because you might break the DNA. RNA: Is less stable than DNA so we store it at -80.(Fig.3, Fig.4 – lab freezer) But you should be able to store it at 20C too. (Protocol Online, 1999-2013)

Fig 3. A 52 cubic foot Norlake Laboratory Freezer

Fig 4. Nor-Lake Ultra-Low Freezer

So now when you know everything I will tell you how should BEC machine work. Code reader recognise by code, should BEC destroy or store that given biotech drug. When you put your medicine trough opening on machine, it will automatically, previously decided by code, move it into appropriate case. If it moves it into case for destruction, special Bleach pump (automatically mixing all needed contents) will spray the inserted medicine, and store it in another box contained in back part of BEC machine. If BEC moves medicine into storage case part, it will store biotech drugs on -20°C, which is good temperature for DNA and RNA storage. And if BEC recognise by code that medicine date is expired it will automatically move it into case for destruction. BioEcomat will contain chip inside, so when it gets full, red bulb will switch on, and thanks to that chip it will alarm company to empty containers. But even without that alarm BEC lab workers will empty BEC machine every ten days because some DNA and RNA need even lower temperatures after ten days of storage on -20°C. Transport trucks for BIOECOMAT recycled material will, of course, have proper containers for destructed material and storage freezers. Material from destruction case will be taken to BEC labs for safety autoclaving to predict contamination for every case. Autoclaving will be done at 121°C for 80 min, because this is the safety guaranteed method. Material from storage part will be taken directly to huge drive in BAC lab freezers to store on -86°C. BEC trucks would drive into room with this freezers and unload cases with material directly from transport freezers into BEC lab freezers for further procedure and testing. This is my idea for great improvement for stopping biotech contamination.

As I imagine BioEcomat, would be placed in several locations in Bosnia and Herzegovina, and abroad. Primarily in Sarajevo, we would set first-BioEcomat along with all hour pharmacies (state pharmacies), firstly experimentally. Later BEC would be introduced to private pharmacies too, but with time the company behind the machines would aim to put it at the malls which have any medical content (pharmacies, drugstores,cosmetic markets...). Also, later with the slot for biotech drugs, machines for the recycling of ordinary remedies, would be set too.

REFERENCES

1. Debbie Kolozsvari, January 2012 - Reviewed by: Institutional Biosafety Committee - Biosafety info sheet: Disinfection using bleach
2. Directorate-General for Research and Innovation. Biotechnologies, Agriculture, Food. European Union. 2010
3. Guidance for Industry pharmacogenomic Data Submissions, US Food and Drug Administration. March 2005
4. Protocol Online (1999-2013)
5. Squassina A, Manchia M, Manolopoulos VG, Artac M, Lappa-Manakou C, Karkabouna S, Mitropoulos K, Del Zompo M, Patrinos GP (August 2010). "Realities and expectations of pharmacogenomics and personalized medicine: impact of translating genetic knowledge into clinical practice". *Pharmacogenomic*
6. Tetsushi Suyama and Mamoru Kawaharasaki National Institute of Advanced Industrial Science and Technology (AIST), Tsukuba, Ibaraki, Japan BioTechniques, Vol. 55, No. 6, December 2013 - Decomposition of waste DNA with extended autoclaving under unsaturated steam
7. Thieman, W.J.; Palladino, M.A. (2008). *Introduction to Biotechnology*. Pearson/Benjamin Cummings
8. Tomaž Skrbinšek, University of Ljubljana, 2013
9. Tovatech LLC, 11 Harrison Court, South Orange, NJ 07079, USA

Uporedba postproceduralnih ishoda kod pacijenata tretiranih različitim vrstama stentova

L. Divović Mustafić[1], M. A. Kulić[2]

[1]UKCS/Institut za bolest srca- Klinika za kardiohirurgiju, mr.sci.med., Sarajevo, Bosna i Hercegovina
[2]UKCS/ Institut za bolesti srca- Klinika za kardiologiju, doc. dr., Sarajevo, Bosna i Hercegovina

Abstrakt: PROBLEM: Perkutana koronarna intervencija (PCI- Percutaneus coronary intervention) je interventna kardiološka procedura kojom se uz pomoć stentova (Drug eluting stent-ova i Bare metal stent-ova) tretiraju aterosklerotske promjene unutar koronarnih krvnih sudova. „Drug eluting" stentovi (DES) reduciraju mogućnost nastanka postproceduralnih komplikacija lokaliziranim otpuštanjem visokih koncentracija bioaktivne supstance postproceduralno. Stabilna angina pektoris jeste klinička manifestacija ishemijske bolesti srca, a koja svoje osobine nije mijenjala tokom perioda od 60 dana.

CILJEVI ISTRAŽIVANJA: Utvrditi demografske karakteristike i riziko faktore u odnosu na posmatrane grupe. Ehokardiografski utvrditi vrijednost Ejekcione frakcije (%) i gibljivost zidova miokarda kod ispitanika u periodu od uključenja u studiju do postproceduralnih 6 mjeseci. Utvrditi zahvaćenost koronarki u odnosu na posmatrane grupe, MACE postproceduralno te potrebu za rekateterizacijom na osnovu ponovne pojave anginoznih tegoba i pozitivnog ergometrijskog testa. Utvrditi cost effectiveness procedure u zavisnosti od vrste stenta.

METODOLOGIJA ISTRAŽIVANJA: Istraživanje je bilo retrospektivno-prospektivno, komparativno u periodu 2010- 2013 godine. Uzorak istraživanja je 100 pacijenata u Klinici za kardiohirurgiju UKCS kojima je PCI-om tretiran lijevi koronarni sistem. Pacijenti su podijeljeni u: radnu skupinu (50 pacijenata sa implantiranim DES-om), te kontrolnu skupinu (50 pacijenata sa implantiranim BMS-om). Pacijenti su kontrolisani u prvih 6 mjeseci postproceduralno.

REZULTATI ISTRAŽIVANJA: Razlika među demografskim karakteristikama nije značajna. Zastupljenost riziko faktora kod pacijenata tretiranih DES-om, nije veća, izuzev kod pacijenata sa diabetes melitusom tip 2. 6 mjeseci postproceduralno, vrijednost EF je porasla kod obje grupe ispitanika, statistički signifikantno kod pacijenata tretiranih DES-om. Preproceduralno su kod pacijenata tretiranih DES-om, prisutne veće i rasprostranjenije promjene gibljivosti zida lijevog ventrikla. Te promjene nakon 6 mjeseci pokazuju početne znake poboljšanja statistički signifikantno. DES su postavljeni u prosjeku više unutar proksimalnog segmenta, kao i unutar širih i dužih segmenata koronarke. Neke od MACE parametara nisu pokazale statistički signifikantnu razliku u zastupljenosti u odnosu na posmatrane grupe. Potreba za rekateterizacijom, na osnovu ponovne pojave anginoznih tegoba, kao i ergometrijskog nalaza postproceduralno, je značajnija u grupi pacijenata tretiranih BMS-om. Dužina hospitalizacije, kod obje grupe pacijenata je u prosjeku ista. Cost effectiveness je veća kod pacijenata tretiranih DES-om.

ZAKLJUČAK: Pacijenti sa DES-om imaju bolji klinički, ehokardiografski i angiografski ishod, u odnosu na pacijente sa BMS-om.

Ključne riječi: PCI (Perkutana koronarna intervencija), Kateterizacija srca, Stabilna angina pektoris, DES (Drug eluting stent), BMS (Bare metal stent)

I. Uvod

A. Definicija Angine pektoris

Angina pektoris (AP) predstavlja kliničku manifestaciju ishemijske bolesti srca. Javlja se najčešće kod muške populacije starije od 50 godina životne dobi, te kod žena preko 60 godina životne dobi. O stabilnoj angini pektoris se može govoriti kada se njene karakteristike ne mijenjaju tokom perioda od 60 dana. Stabilna angina pektoris se može manifestirati u vidu stezanja, pritiska, bola u području iza grudne kosti, najčešće provocirana fizičkim naporom, emocionalnim stresom, hladnoćom, sa tipičnom propagacijom prema vratu, ramenima, području između plećki, lijevoj podlaktici, korijenu vrata, vilici, epigastriju. Traje vremenski period od 2-5 min. Tipa je „cresendo-decresendo.

Simptomi koji mogu pratiti anginozni napad su slabost, mučnina, nagon na povraćanje, preznojavanje, gušenje. Sam naziv „Angina pectoris" potiče od latinskih riječi „angere" što znači gušiti te „pectus", gudni koš. AP nastaje kao posljedica formiranja aterosklerotskog plaka, a koji nastaje nakon aktivacije endotela na bifurkacionim mjestima, te na mjestima turbulentnog toka krvi.

B. Postavljanje dijagnoze stabilne angine pektoris

Dijagnostičke procedure se mogu podijeliti na neinvazivne, pod kojima se podrazumijeva: elektrokardiogram (EKG), 24-satni Holter monitoring, ergometrijski test, perfuziona scintigrafija miokarda, ultrazvuk srca, MSCT. Koronarna angiografija jeste invazivna kardiološka procedura, kojom se vizualizacija koronarnih krvnih sudova postiže pomoću ručno ubrizganog jodnog kontrastnog sredstva, vidljivog X zrakama. Kontrast se uvodi u krv pomoću katetera, metodom po Sel-

dingeru, a pristupno mjesto jeste najčešće art. femoralis dextra ili art. radialis dextra. Procedura se obavlja u tzv. Cath. – labu.

C. T*erapija pacijenata sa stabilnom anginom pektoris*

Terapija pacijenata sa stabilnom anginom pektoris se može podijeliti na medikamentoznu, koja podrazumijeva primjenu: beta blokatora, ACE inhibitora, nitro preparata, blokatora kalcijevih kanala, statina, acetilsalicilne kiseline, heparina (nefrakcionisani i niskomolekularni), tienopiridina, ivabradin, te metaboličkih agensa. U terapijske procedure se ubraja perkutana transluminalna koronarna angioplastika (PTCA), koju je 1977. godine, prvi put izveo doktor Andreas Gruentzig u Cirihu. PTCA kao interventna terapijska metoda, podrazumijeva koronarnu angiografiju sa balon dilatacijom. Dalji napredak medicine dovodi do primjene stentova u terapijske svrhe. Stentovi predstavljaju metalne, mrežolike potpornice, cilindričnog oblika, sa funkcijom da plasirani unutar krvnog sudu isti drže prohodnim, na mjestu postojeće stenoze ili okluzije, uzrokovane aterosklerotskim plakom.

Karakteristike idealnog stenta bi bile netrombogenost, fleksibilnost u neekspandibilnoj formi, a u ekspandibilnoj stabilna potpora unutar lumena koronarnog krvnog suda, te sposobnost radioopacifikacije. DES ima sposobnost otpuštanja visoke koncentracije biološki aktivne supstace u prvih 30 dana postproseduralno, a koja reducira mogućnost nastanka postproceduralnih komplikacija. Lijekovi koji se otpuštaju imaju antiinflamatorni i/ili imunomodulatorni, te antiproliferativni efekat.

II. Materijal i metode

Istraživanje je bilo retrospektivno-prospektivna, komparativno u periodu 2010- 2013 godine. Uzorak istraživanja je 100 pacijenata u Klinici za kardiohirurgiju UKCS kojima je PCI-om tretiran lijevi koronarni sistem. Pacijenti su podijeljeni u: radnu skupinu (50 pacijenata sa implantiranim DES-om), te kontrolnu skupinu (50 pacijenata sa implantiranim BMS-om). Pacijenti su kontrolisani u prvih 6 mjeseci postproceduralno.

Kriteriji za uključenje u studiju su bili: pacijenti sa tegobama po tipu angine pektoris, pacijenti sa pozitivnim ergometrijskim testom, urađenim ergometrijskim testom, MSCT-om, scintigrafijom miokarda.

Kriteriji za isključivanje iz studije su bili: pacijenti sa akutnim koronarnim sindromom (ACS), LM stenozom, stenozom RCA, kombiniranom CAD(Coronary Artery Disease) i valvularnom patologijom, dokazanom alergijom na kontrastno sredstvo, acetilsalicilnu kiselinu, klopidogrel, prethodno dijagnosticiranim hroničnim sistemskim bolestima, prethodno dijagnosticiranim malignim bolestima, hroničnom bubrežnom insuficijencijom, smrtni ishod u periodu trajanja studije.

Iz istorije bolesti hospitaliziranih pacijenata su uzeti: demografski podaci, podaci o prisustvu riziko faktora, prethodno urađene ehokardiografske pretrage, te koronarografski nalaz.

Tokom perioda praćenja posmatrani su slijedeći parametri: prisutnost ponovnih anginoznih tegoba, te njihova klinička manifestacija: EKG, krvni pritisak, frekvenca rada srca, te ehokardiografski nalaz 6 mjeseci postproceduralno kod svih ispitanika, te učestalost potrebe za ponovnu rekateterizaciju.

III. Rezultati

Ne postoji statistički značajna razlika u učestalosti pacijenata muškog i ženskog spola između posmatranih grupa [$\chi^2(1)=0.000$, P>0.05]. U prosjeku, pacijenti muškog spola koji su tretirani sa DES stentom su bili mlađe životne dobi (=58.66, SD=9.42) u odnosu na pacijente muškog spola koji su tretirani sa BMS stentom (=61.16, SD=9.79). Ova razlika, također, nije statistički signifikantna [$t(74)=1.135$, P>0.05].

Ne postoji statistički značajna razlika u učestalosti hipertenzije između posmatranih grupa [$\chi^2(1)=1.478$, P>0.05], dislipidemije [$\chi^2(1)=0.000$, P>0.05], pušačkog statusa [$\chi^2(2)=1.742$, P>0.05], pozitivne porodične anamneze [$\chi^2(1)=0.000$, P>0.05], dok je visoko statistički značajna razlika u učestalosti diabetes melitusa kod pacijenata između posmatranih grupa [$\chi^2(1)=16.877$, P<0.001].

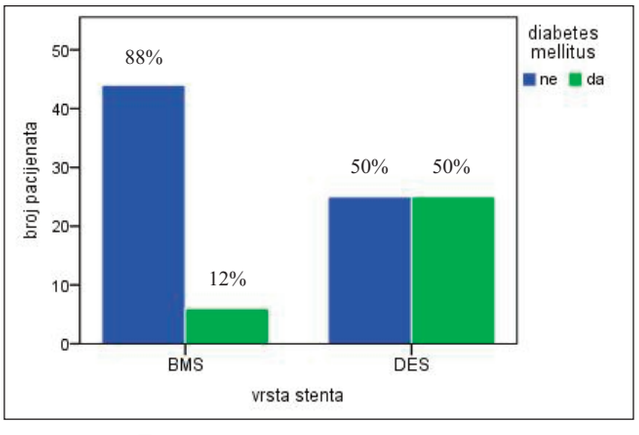

Fig. 1 Učestalost D. M tip 2 kod pacijenata u zavisnosti od vrste implantiranog stenta

Pacijenti tretirani sa DES-om, imali su veću ejekcionu frakciju nakon 6 mjeseci (=47.10, SD=10.91) u odnosu na vrijednost ejekcione frakcije na početku (=45.68, SD=10.23). Ova razlika [-1.42%; 95%CI (-2.63; -0.21)] je statistički signifikantna $t(49)=-2.350$, P=0.023, odnosno P<0.05.

Tabela 1 E. F. na početku i nakon postproceduralnih 6 mjeseci

vrsta stenta		ejekciona frakcija	Mean	N	Std. Deviation	Std. Error Mean
BMS	Pair 1	na početku	48,51	50	8,559	1,223
		nakon 6 mjeseci	48,90	50	9,136	1,305
DES	Pair 1	na početku	45,68	50	10,297	1,456
		nakon 6 mjeseci	47,10	50	10,905	1,542

Na početku istraživanja, postoji signifikantnost u učestalosti: akineza anteriorno [$\chi^2(1)=6.832$; P=0.016] i akineza septalno [$\chi^2(1)=5.482$; P=0.034] između posmatranih grupa. Nakon 6 mjeseci, postoji signifikantnost u učestalosti: akineza anteriorno [$\chi^2(1)=6.775$; P=0.017], akineza septalno [$\chi^2(1)=5.741$; P=0.031] između posmatranih grupa. Unutar grupe pacijenata tretiranih DES-om, na početku ispitivanja bilo je 34% pacijenata sa akinezom anteriorno, naspram 28% poslije 6 mjeseci.

Što se tiče akineze septalno taj odnos je u grupi pacijenata tretiranih DES-om, 34%: 26%.

Analiza reziduala ukazuje da su BMS, više od očekivanog, postavljani na srednji i distalni segment, dok su DES, više od očekivanog, postavljani na proksimalni segment zahvaćen promjenama. Vrijednost [$\chi^2(2)=18.297$, P<0.001] je visoko statistički značajna.

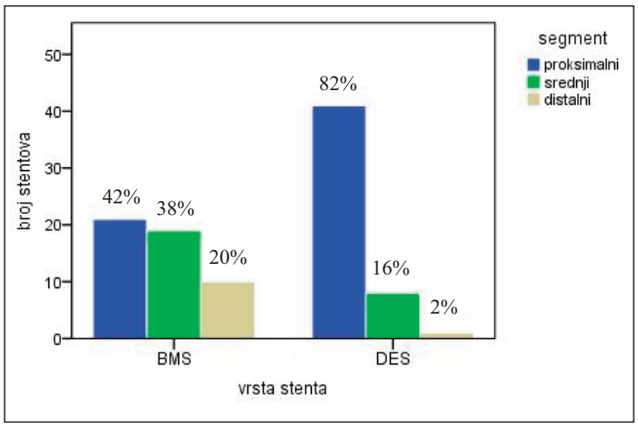

Fig. 2 Učestalost segmenta zahvaćenog promjenom prema posmatranim grupama

U prosjeku, DES stentovi su plasirani na šire segmente (mm) zahvaćene promjenom [=3.41, SD=0.42; 95%CI (3.29; 3.52)] u odnosu na BMS stentove [=3.05, SD=0.33; 95%CI (2.95; 3.14)].

Ova razlika [0.36 mm; 95%CI (0.21; 0.51)] je visoko statistički signifikantna [$t(98)=4.793$, P<0.001].

Tabela 2. Širina segmenta (mm) zahvaćenog promjenom

Vrsta stenta		N	Minimum	Maximum	Mean		SD
		Statistic	Statistic	Statistic	Statistic	Std. Error	Statistic
BMS	Širina stenta (mm)	50	2.50	4.00	3.046	0.046	0.326
	Valid N	50					
DES	Širina stenta (mm)	50	2.75	4.00	3.410	0.059	0.419
	Valid N	50					

U prosjeku, DES stentovi su plasirani na duže segmente (mm) zahvaćene promjenom [=19.28, SD=6.15; 95% CI (17.53; 21.03)] u odnosu na BMS stentove [=16.20, SD= 3.23; 95% CI (15.28; 17.12)]. Ova razlika [3.08 mm; 95% CI (1.13; 5.03)] je statistički signifikantna [$t(98)=3.134$; P<0.01]

Tabela 3. Dužina segmenta (mm) zahvaćenog promjenom

vrsta stenta		N	Minimum	Maximum	Mean		SD
		Statistic	Statistic	Statistic	Statistic	Std. Error	Statistic
BMS	Dužina stenta (mm)	50	8.0	26.0	16.200	0.4562	3.2262
	Valid N	50					
DES	Dužina stenta (mm)	50	12.0	33.0	19.280	0.8704	6.1546
	Valid N	50					

U prosjeku, DES stentovi su plasirani na krvne sudove sa većim procentualnim suženjem [=90.30, SD=6.79; 95%CI (88.37; 92.23)] u odnosu na BMS stentove [=84.50, SD=9.49; 95% CI (81.80; 87.20)]. Ova razlika [5.80%; 95%CI (1.65; 9.08)] je statistički signifikantna [$t(98)=3.515$; P<0.05]

Tabela 4. Procentualno suženje (stenoza) zahvaćenog krvnog suda

Vrsta stenta		N	Minimum	Maximum	Mean		SD
		Statistic	Statistic	Statistic	Statistic	Std. Error	Statistic
BMS	Procenat stenoze	50	60.0	95.0	84.500	1.342	9.489
	Valid N	50					
DES	Procenat stenoze	50	70.0	98.0	90.300	0.960	6.789
	Valid N	50					

Major Adverse Cardiac Events (MACE) postproceduralno podrazumijevao je pojavu akutnog infarkta miokarda postproceduralno, ICV, kao i pojava restenoze. Ne postoji statistički značajna razlika u učestalosti infarkta miokarda postproceduralno [$\chi^2(1)=1.010$, P>0.05], učestalosti moždanog udara [$\chi^2(1)=3.093$, P>0.05], te učestalosti rekateterizacije između posmatranih grupa [$\chi^2(1)=0.000$, P>0.05]. Kod jedne

pacijentice, koja je tretirana sa BMS stentom, urađena je rekateterizacija, te se kod iste pacijenticee javila restenoza. Kod jednog pacijenta koji je tretiran DES-om, urađena je rekateterizacija, dok restenoza nije evidentirana.

Postoji statistički značajna razlika u postproceduralnoj pojavi anginoznih tegoba između posmatranih grupa [$\chi^2(1)$= 10.526, P=0.003, odnosno P<0.01].

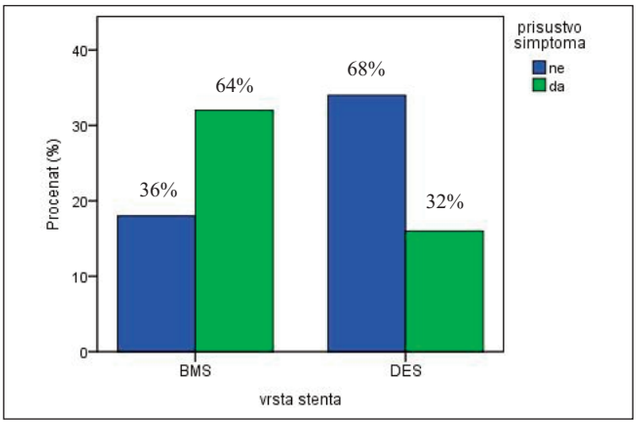

Fig. 3 Postproceduralna pojava simptoma

Postoji statistički značajna razlika u ergometrijskom nalazu između posmatranih grupa [$\chi^2(2)$=8.400, P=0.011, odnosno P<0.05].

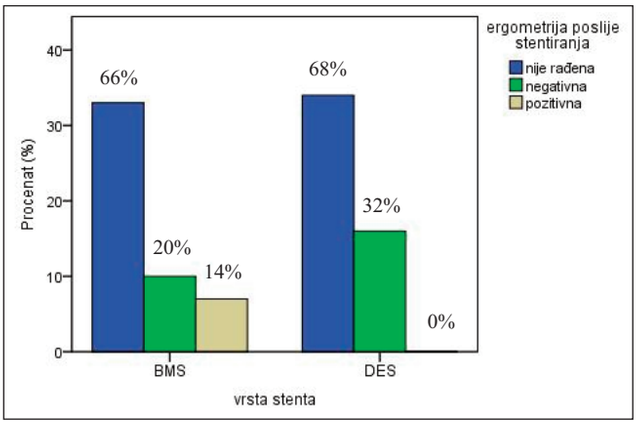

Fig 4. Ergometrijski test postproceduralno

Ne postoji statistički signifikantnost u dužini trajanja hospitalizacije u odnosu na spol, prema posmatranim grupama (ženski spol [t(22) = -0.496, P>0.05]) (muški spol[t(74) = -0.200, P>0.05]).

Cijena koštanja 3 dana hospitalizacije sa kateterizacijom i plasiranjem BMS-a iznosi ukupno 4 274,0 KM, dok uzimajući u obzir isto za DES cijena iznosi 5 944,0 KM. Cijena koštanja jednog dana hospitalizacije iznosi 158,0 KM. Dužina hospitalizacije za pacijente tretirane BMS-om u prosjeku je iznosila 3, odnosno 4 dana. Kumulativno je potrošeno 119 672,0 KM za 28 pacijenata koji su hospitalizirani 3 dana, odnosno 57 616,0 KM za 13 pacijenata hospitaliziranih 4 dana. Dužina hospitalizacije za pacijente tretirane DES-om u prosjeku je takođe iznosila 3 odnosno 4 dana. Kumulativno je potrošeno 154 544,0 KM za 26 pacijenata koji su bili hospitalizirani 3 dana, odnosno 67 122, 0 KM za 11 pacijenata koji su hospitalizirani 4 dana.

IV. Diskusija

Yoshinobu O., Neville K. i sar. su u svom istraživanju provedenom 2009. godine utvrdili da spol ne utiče na to da li pacijenta treba tretirani BMS-om ili DES-om. Oni su sproveli retrospektivnu kohortnu studiju na 4 936 pacijenata od kojih je 28.2% bilo ženskog spola. Praćena je pojava MACE u periodu od naredne 3 godine i nađeno je da spol ne igra ulogu u pojavi MACE u zavisnosti od vrste plasiranog stenta. Iz ovoga se da zaključiti da spol ne bi trebao imati uticaja na to da li se pacijentu treba implantirati BMS ili DES (1).

N. Shammas, G. Shammas i sar. su vršili istraživanje efekta implantacije DES-a na pacijente u zavisnosti od njihove starosne dobi. Pacijenti su podijeljeni u dvije grupe: mlađe životne dobi (< 65 godina) i starije životne dobi (> 65 godina). Istraživanje je trajalo 2 godine. Došlo se do zaključka da ne postoji statistički značajna razlika između dvije grupe pacijenata u potrebi za rekateterizacijom, trombozom stenta, te pojavom nefatalnog infarkta miokarda (p=0.71). Iz ovoga proizilazi da je u ovom slučaju bilo potpuno irelevantno da li će se DES implantirati mlađim ili starijim pacijentima (2).

Garg, Normand i sar. su ispitivali pojavu restenoze, akutnog infarkta miokarda, u zavisnosti od vrste implantiranog stenta kod pacijenata sa diabetes meiltusom tip 2. Ispitivanje je trajalo od 2003.-2004. godine, a pacijenti su praćeni tokom tri naredne godine. Ishod ispitivanja je utvrdio da je grupa pacijenata tretiranih DES-om u korelaciji sa nižom stopom pojave akutnog infarkta miokarda (p=0.02), te manjom potrebom za revaskularizacijom, u odnosu na grupu pacijenata tretiranih BMS-om (p<0.001) (3).

Mehrpooya, Ghasemi i sar. autori su rada koji pokazuje efekat implantacije DES na koronarne krvne sudove sa 70% stenozom. U studiju je bilo uključeno 40 pacijenata, kod kojih je angiografski dokazano prisustvo 70% stenoze na koronarnom krvnom sudu (nije precizirano kome). Svim pacijentima je implantiran DES, a ehokardiografska procjena je vršena nakon procedure te jedan mjesec poslije procedure. Srednja vrijednost EF prije procedure bila je 33.33%, da bi poslije PCI bila 44.87% (p<0.000). U istom radu je vršena procjena poboljšanja pokretljivosti zida miokarda nakon implantacije DES, a kod pacijenata sa 70% stenozom na LAD. Procjena je

vršena preproceduralno, te postproceduralno nakon jednog mjeseca od strane istog kardiologa- ultrasoničara, a kontrolisano je od strane druga dva. Svi pacijenti (100%), imali su abnormalnosti u pokretljivosti zidova miokarda, koja je nakon mjeseca dana procentualno pala na 65% (4).

Hesham, Abdel- Moniem i sar. su vršili istraživanje kojim su željeli pokazati uticaj plasiranja stenta (nije definisana vrsta stenta), na segmentalnu pokretljivost zidova miokarda. Uzeto je u obzir 25 pacijenata sa hroničnom stabilnom anginom pektoris koji su preproceduralno imali procijenjenu EF višu od 50%. Ispitivanje je trajalo od januara do septembra 2010. godine, a pacijenti su praćeni dan, te 6 mjeseci postproceduralno. Procjena je vršena preko pulsnog tkivnog doplera. Ispitivanja su pokazala da postoji signifikantno poboljšanje u snazi srčanog mišića, na račun septalnog, anteriornog, lateralnog i inferiornog zida ($p<0.01$) (5).

Jin Oh Na, Jin Won Kim i ostali su ispitivali efekat različite vrste stenova u slučaju njihove implantacije unutar koronarnih krvnih sudova sa lezijom širom od 3.5mm. Ispitivanje je trajalo od 2002.-2007. godine, a uzeto je u obzir 240 pacijenata. Klinički i angiografski ishodi su evaluirani nakon 6 mjeseci. Ispitivanje je pokazalo da je pojava in- stent restenoze bila značajnija u grupi pacijenata tretiranih BMS-om ($p=0.007$), a sa druge strane potreba za revaskularizacijom ($p=0.62$) kao i MACE ($p=0.86$)nisu pokazali statistički signifikantnu razliku između ove dvije grupe (6).

Calais, Lagerqvist i sar. su ispitivali efekat različite vrste stentova u zavisnosti od mjesta implantacije. U obzir su uzeli LAD, LCX. Podaci su uzeti iz SCAAR (Swedish angiography and angioplasty registry). Od 2005- 2011. godine su uzeti u obzir svi pacijenti koji su imali proksimalne lezije stentirane DES-om ili BMS-om. Rezultati su ukazali da su proksimalne lezije LAD tretirane DES-om imale manju incidencu restenoze u odnosu na pacijente tretirane sa BMS-om. Kod pacijenata sa proksimalnom lezijom LCX ne postoji statistički značajna razlika u pojavi restenoze u zavisnosti od vrste implantiranog stenta ($p<0.001$) (7).

Hansen, Kaiser i sar. su ispitivali efekat implantacije dvije vrste stenta u zavisnosti od veličine (dijametra) koronarnog krvnog suda. MACE je praćen dvije godine postproceduralno. Rezultati su pokazali da DES reducira MACE u periodu od dvije godine kod ženskog ($p<0.0001$) i muškog ($p=0.003$) pola kod velikih koronarnih krvnih sudova (8).

Maarten, Laarman i sar. su vršili ispitivanje u kome je sudjelovalo 200 pacijenata, kod kojih je registrovana okluzija koronarnog krvnog suda. Polovini pacijenata je implantiran DES-om, a drugoj polovini BMS. Posmatrala se između ostalog i pojava in- stent restenoze u vremenskom periodu od 6 mjeseci postproceduralno. Ispitivanja su pokazala da je in- stent restenoza u pacijenata tretiranih DES-om bila prisutna sa 7%, a 36% u drugoj grupi pacijenata tretiranih BMS-om ($p<0.001$) (9).

Marroquin, Faith Selzer i sar. su ispitivali efekat implantacije DES-a u odnosu na BMS kod pacijenata kod kojih je dijametar ciljanog krvnog suda bio manji od 2.5mm ili veći od 3.75 mm, a ciljana lezija duža od 30mm. U obzir je uzeto 6551 pacijenta. Kontrola je vršena tokom godine dana, a praćena pojava infarkta miokarda. Tokom godine nije bilo statistički signifikantne razlike između ove dvije grupe pacijenata kada se radi o infarktu miokardu, dok je potreba za revaskularizacijom bila značajno niža kod pacijenata tretiranih DES-om (10).

Nienaber, Akin i sar. su od 2005- 2006. godine bili nosioci studije čija je osnova bila komparacija DES- ova i BMS- ova. U studiju je bilo uključeno 6384 pacijenta, a ishodi PCI su praćeni 3, 6, 9 i 12 mjeseci postproceduralno. Rezultati su pokazali da je pojava akutnog infarkta miokarda postproceduralno bila 3.2% za pacijente tretirane DES-om, a u grupi pacijenata sa BMS-om 6.0% ($p<0.01$). Moždani udar je u grupi pacijenata tretiranih DES-om bio prisutan sa 1.2%, nasuprot grupi pacijenata sa BMS-om gdje se javio sa 2.7% ($p<0.05$). Potreba za revaskularizacijom je u grupi pacijenata tretiranih DES-om bila prisutna sa 10.4% nasuprot 14.9% koliko je bila zastupljena u grupi pacijenata sa BMS-om ($p<0.01$). Što se tiče postproceduralne tromboze stenta nije bilo statistički signifikantne razlike. U grupi pacijenata sa DES-om tromboza se javila 3.7%, nasuprot 4.3% koliko je bila prisutna u grupi pacijenata sa BMS-om ($p=0.57$) (11).

Prednost DES nad BMS u redukciji postproceduralne pojave MACE, detaljno je iznijet u velikim studijama *Basket* (12).

S obzirom da mnoga istraživanja negiraju ergometrijski test kao dijagnostički prediktor u procjeni prohodnosti stentova postproceduralno, bit će navedeno istraživanje, koje govori u prilog korištenja ergometrijskog testa kao validne dijagnostičke procedure. *Mohan i Dhall i sar.* su vršili ispitivanje postproceduralno prateći 80 pacijenata i to 41 sa BMS-om i 39 sa DES-om. Pacijenti su praćeni u vremenskom periodu od 6-9 mjeseci postproceduralno. Restenoza se javila kod 29 pacijenata, i to 20 pacijenata sa BMS-om, te 9 pacijenata sa DES-om. U tom vremenskom periodu je 79 pacijenata radilo ergometrijski test, koji se pokazao pozitivan kod 25 pacijenata, a kod ostatka je bio negativan. Nezavisno od toga rađena je rekateterizacija, nakon koje je pokazano da od 29 pacijenata sa restenozom, njih 22 su imali istovremeno i pozitivan ergometrijski test ($p=0.000$) (13).

Veliki broj studija ukazuje na veću potrebu za revaskularizacijom nakon implantacije BMS, signifikantno više nego nakon implantacije DES-a (14) (15).

Da bi se vršila procjena cost effectiveness potrebno je prvo definisati pojam QALY. QALY (Quality Adjusted Life Yearmjera) jeste mjera "opterećenja bolešću", t.j. efekat zdravstvenog problema na život pacijenta, evaluirano kroz finansijski aspekt medicinske intervencije, morbiditeta, mortaliteta.

Uzimajući u obzir veliki broj studija, dolazi se do zaključka da u procjeni ova dva aspekta, veliku ulogu ima finansijsko stanje zemlje. Tako razvijene zemlje sjeverne Evrope i SAD-a, dugoročnije gledaju na to koliko jedan pacijent finansijski košta državu. Politika tih zemalja je takva, da implantacijom DES-a, smanjuju finansijski teret u budućnosti, jer reducirajući pojavu postproceduralnih komplikacija, smanjuju novčani iznos koji država mora izdvojiti da bi pacijenta ponovno dijagnostički i terapeutski zbrinula. U slabije razvijenim zemljama, kao i u zemljama u razvoju, implantacija DES-a je kontrolisana, i u strogim indikativnim okvirima (16) (17) (18).

V. Zaključak

Bez obzira na cijenu koštanja stenta, cost effectiveness je veća kod pacijenata tretiranih DES-om. Potreba za rekaterizacijom je veća u grupi pacijenata tretiranih BMS-om postproceduralno. Pacijenti tretirani DES-om imaju bolji klinički, kao i ehokardiografski ishod postproceduralno.

REFERENCE

1. Yoshinobu O., M.D., Neville K., MA, Joost D., M.D., Garcia- Garcia H. M., M.D., M.Sc., Gonzalo N., M.D., Cheng J. M., M.Sc. et al, Impact of Sex on 3-Year Outcome After Percutaneous Coronary Intervention Using Bare- Metal and Drug- Eluting Stents in Previously Untreated Coronary Artery Disease Insights From the Research (Rapamycin- Eluting Stent Evaluated at Rotterdam Cardiology Hospital) and T- Search (Taxus-Stent Evaluated at Rotterdam Cardiology Hospital), J Am Coll Cardiol Intv. 2009; 2 (7):603- 610. doi:10.1016 /j.jcin.2009.03.016.
2. Shammas N. W., Shammas G. A., Sharis P., Jerin M.,Age Differences in Long Term Outcomes of Coronary Patients Treated with Drug Eluting Stents at a Tertiary Medical Center Midwest, Cardiovascular Research Foundation, 1236 E Rusholme, Suite 300, Davenport, IA 52803, USA Received 15 April 2013; Revised 21 May 2013; Accepted 21 May 2013., Journal of Aging Research Volume 2013 (2013), Article ID 471026, 4 pages http://dx.doi.org/10.1155/2013/471026.
3. Garg P., MBBS, M.Sc., Normand S. T., Ph.D., Silbaugh T. S., B.Sc., Wolf R. E., M.Sc., Zelevinsky K., BA, Lovett A., et al. Drug-Eluting or Bare-Metal Stenting in Patients With Diabetes Mellitus, results From the Massachusetts Data Analysis Center Registry, PubMed, Circulation. 2008 Nov 25;118(22):2277-85, 7p following 2285. doi: 10.1161/CIRCULATIONAHA.108.820159. Epub 2008 Nov 10.
4. Mehrpooya M., Ghasemi M., Ramin E., Shahrzad I., Vatan K. K., Improvement in Left Ventricular Ejection Fraction and Wall Motion Abnormality after Successful Angioplasty and Stenting of Chronic Coronary Obstruction, Medical Sciences - Seyed Al Shohada Heart Hospital - Urmia – Iran, Nationalpark- Forschung in der Schweiz (Switzerland research Park Journal), Vol. 102, No. 10 (2013).
5. Hesham R., Abdel-Moniem A., Email S., and El- Batran M. M.B.B., Evaluation of Myocardial Function in Patients with Chronic Stable Angina and Apparent Normal Ventricular Function (Tissue Doppler Study Before and After PCI), Eur Heart J Supplements, Volume 14, Issue suppl A, Pp. A14-A19.
6. Oh Na J. M. D., Won Kim J. M. D., Ph. D. Ung Choi C. M. D., Choi Un J. M. D., Yong Shin S. M. D., Euy Lim H. M. D., Ph. D. et al. Bare-metal stents versus drug-eluting stents in large (≥3.5 mm) single coronary artery: Angiographic and clinical outcomes at 6 months, J of Cardiol, Volume 54, Issue 1, Pages 108-114, August 2009.
7. Calais F.; Lagerqvist B.; James S.; Leppert J.; Fröbert O. TCT-603, Proximal Coronary Artery Stenting: DES Versus BMS and LAD Versus the Rest, J Am Coll CArdiol. 2012;60(17_S):.doi:10.1016/j.jacc.2012.08.640.
8. Hansen K. W., Kaiser C., Hvelplund A., Soerensen R., Madsen J. K., Jensen J. S. et al., Improved two-year outcomes after drug-eluting versus bare-metal stent implantation in women and men with large coronary arteries: importance of vessel size, International Journal of Cardiology, Volume 169, Issue 1, Pages 29–34, October 25, 2013.
9. Maarten J. S., M. D., Ph. D., Laarman G. J, M. D., Ph. D., Rahel B. M., M. D., Ph. D., Kelder J. C., M. D., A.R. Bosschaert M., M. D., Kiemeneij F., M. D., Ph. D. et al. Primary Stenting of Totally Occluded Native Coronary Arteries II (PRISON II) A Randomized Comparison of Bare Metal Stent Implantation With Sirolimus-Eluting Stent Implantation for the Treatment of Total Coronary Occlusions, http://circ.ahajournals.org/content/114/9/921.short.
10. Marroquin O. C., M.D., Selzer F., Ph.D., Mulukutla S. R., M.D., Williams D. O., M.D., Vlachos H. A., M.Sc., Wilensky R. L., M.D., et al., A Comparison of Bare-Metal and Drug-Eluting Stents for Off-Label Indications, N Engl J Med 2008; 358:342-352January 24, 2008DOI: 10.1056/NEJMoa0706258.
11. Nienaber C. A., Akin I., Schneider S., Senges J., Fetsch T., Tebbe U. et all. , Clinical outcomes after sirolimus-eluting, paclitaxel-eluting, and bare metal stents (from the first phase of the prospective multicenter German DES.DE Registry), Am J Cardiol. 2009 Nov 15;104 (10):1362-9. doi: 10.1016/j.amjcard.2009.06.058. Epub 2009 Sep 26.
12. Pfisterer M., Brunner-La Rocca H. P., Rickenbache P., Hunziker P., Mueller C., Nietlispach F. et all., Long-term benefit–risk balance of drug-eluting vs. bare-metal stents in daily practice: doesstent diameter matter? Three-year follow-up of BASKET, Eur Heart J. 2009 Jan;30(1):16-24. doi: 10.1093/eurheartj/ehn516. Epub 2008 Nov 25.
13. Mohan S., MBBS M.D. DNB FICA FCCP and Dhall A., SM MBBS M.D. D.M., A comparative study of restenosis rates in bare metal and drug-eluting stents, http://www.ncbi.nlm.nih.gov/pmc/articles/PMC3005409/.
14. Jack V. Tu, M. D., Ph.D., Bowen J., B.Sc.Phm., M.Sc., Chiu M., M.Sc., T. Ko D., M.D., M.Sc., C. Austin P., Ph.D., He Y., M.D., Ph.D. et all.,Effectiveness and Safety of Drug Eluting Stents in Ontario, N Engl J Med 2007; 357:1393-1402October 4, 2007DOI: 10.1056/NEJMoa071076.
15. Marzocchi A. M. D., Saia F. MD Ph. D., Piovaccari G. M. D., Manari A.M.D., Aurier E., M. D., Benassi A. M. D. et all., Long-Term Safety and Efficacy of Drug-Eluting Stents: Two-Year Results of the REAL (REgistro AngiopLastiche dell'Emilia Romagna) Multicenter Registry, Circulation. 2007 Jun 26;115(25):3181-8. Epub 2007 Jun 11.
16. Oliva G., Cost-Effectiveness of Drug-Eluting Stents: Implications for Clinical Practice and Healthcare Costs, Rev Esp Cardiol. 2006;59:865-8. - Vol. 59 Num.09.
17. Stefanini G. G, M. D., Holmes D. R., Jr., M.D., Drug-Eluting Coronary-Artery Stents, N Engl J Med 2013; 368:254-265 January 17, 2013DOI: 10.1056/NEJMra1210816.
18. Schafer P. E., Sacrinty M. T., Cohen D. J., Kutcher M. A., Gandhi S. K., Santos R. M. et all., Cost-effectiveness of drug-eluting stents versus bare metal stents in clinical practice. Circ Cardiovasc Qual Outcomes. 2011 Jul;4(4):408-15. doi: 10.1161/CIRCOUTCOMES.110.960187. Epub 2011 Jun.

Lejla Divović Mustafić, mr. sci. med., Univerzitetski Klinički centar Sarajevo, Institut za bolesti srca, Klinika za kardiohirurgiju, Sarajevo, BiH (mob. 0038761 171 990; e-mail: lejla.divovic@gmail.com)

Radioiodine therapy of differentiated thyroid cancer

Sumeja Kaimović[1], Arnela Hairlahović[1]

[1]Medicinski fakultet, Sarajevo, BiH

Abstract- **As one example of the success of biomedicine and bioengineering in the area of the endocrine system can be considered the use of positron emission tomography and radiopharmaceuticals in the diagnosis and treatment of different diseases of the thyroid gland.**
Radioactive iodine is used in the treatment of differentiated thyroid carcinoma (glandule thyroidea) and therapeutic treatment of indolent hyperthyroidism caused by the thyroid gland adenomas.
RAI is defined as the systemic administration of 131-sodium or potassium iodide (131) for the selective irradiation of the thyroid gland remains, non- resectionable or incompletely resectionable .
Based on these two primary objectives, there are two main treatment options:
1- Radioactive ablation- postoperative additional option that is used to remove the remains of glandular tissue.
2- The treatment of non- resectionable or incompletely resectionable lesion, as curative or palliative treatment or as an addition to primary treatment of cancer.
The decision about whether to radioactive iodine was used with the intention of treating or with the intention of palliative treatment, should be individual for each patient and should take into consideration factors such as: operability, iodine preference, location of the lesion, tumor characteristics, age and health status patient, and the potential risks that the process brings with it.
General risk from the use of radioactive iodine is the decimation low while the benefits are many.
It is important to note that biomedical engineering in the field of endocrinology and counting contributes to cure patients with differentiated carcinoma crutch glands, and so that is presently in clinical trials latest molecular targeted therapy.

Keywords- **differentiated thyroid cancer, radioiodine therapy, radioactiv ablation**

I. INTRODUCTION

As one of examples of the success in biomedicine and bioengineering in the field of endocrine system can be considered the use of positron emission tomography and radiopharmaceuticals in the diagnosis and treatment of various diseases thyroid gland. Thanks to PET -functional imaging technique that produces a three-dimensional image of functional processes in the body and thanks to the different radiopharmaceuticals which in its composition contain iodine, provides not only a visual representation of the thyroid gland, but also its metabolic activity.

Radiotraser that is used for diagnostic purposes on patients with thyroid disease is I-123, and radioteraser that is used for therapeutic purposes I-131.

Radioactive iodine (RAI) is used in two cases:
- the treatmant of differentiated thyroid cancer,
- the treatment hyperthyroidism caused by therapeutic indolent thyroid adenomas

II. DIFFERENTIATED THYROID CANCER (DTC)

Differentiated thyroid cancer (DTC) is defined as a carcinoma deriving from the follicular epithelium and retaining basic biological characteristics of healthy thyroid tissue, including expression of the sodium iodide symporter (NIS), the key cellular feature for iodine uptake. DTC is an uncommon disease clinically, but worldwide, its incidence shows a noticeable increase.
DTC most often refers to the follicular and papillary carcinoma of the thyroid gland.
Although the 10-year survival rate in cases of distant metastasis is approximately 25–40%, the 10-year overall cause-specific survival for DTC patients as a whole is estimated at approximately 85%. [1]

Since no other cells in the body can't absorb iodine, radioactive iodine can be used to destroy any thyroid cells while all other cells in the body are not affected. The majority of radioactive iodine, therefore, will be absorbed by remaining thyroid cells, regardless of if they have cancer.

III. RADIOIODINE THERAPY - RAIT

RAIT is defined as the systemic administration of 131-sodium or potassium iodide (131I) for selective irradiation of thyroid remnants, microscopic DTC or other nonresectable or incompletely resectable DTC, or both purposes. Based on the primary goal of the RAIT, there are two main forms of the procedure

The first form, radioiodine ablation, is an post-surgical adjuvant option that is used to remove the remnants of thyroid tissue. Ablation also may detect previously occult metastases and serves to treat any microscopic tumour deposits. Therefore, radioiodine ablation may reduce long-term morbidity and possibly, mortality.

The second form of RAIT, radioiodine treatment of nonresectable or incompletely resectable lesions, e.g. microscopic disease, macroscopic local tumor or lymph node or distant metastases, is performed as curative or palliative therapy either as a component of primary treatment of DTC or to address persistent or recurrent disease. [1]

Radioiodine ablation after total or near-total thyroidectomy is a standard procedure in patients with DTC.

Radioiodine treatment of nonresectable or incompletely resectable tumour, has shown in various investigations to be effective in eradicating disease, slowing disease progression or providing symptomatic relief. [1]

The results of RAIT are superior for microscopic or small macroscopic tumors than for larger lesions. Therefore, the feasibility of partial or complete resection of macroscopic lesions should always be checked as a first treatment option. [1]

The decision on whether or not to give RAIT with the intention of cure or palliation should be individualised to the patient and should consider the fallowing factors:

1. *Operability* – except in cases of high risk of surgical complications, excision is most preferred first-line treatment for persistent or recurrent DTC, and especially in cases of lesions limited to the thyrod bed or neck lymph nodes.
2. *Iodine avidity* - before starting a RAIT, it is necessary to check are cances cells iodine-avid, due RAIT exerts no benefit in the absence of iodine-avid tissue
3. *Disease site* –whilst limph, lung and most soft tissue metastases have high rates of cure by RAIT with or without surgery, cure of bone and brain metastses are relatively rare.
4. *Tumour characteristics* – patients with less differentiated tumor have a greater risk of relaps and a reduced survival,
5. *Patient age* - patients who are older, e.g. >45 years of age, at thyroid cancer diagnosis often present with more aggressive tumor and have a reduced age adjusted disease-free and overall survival [7]; therefore, older age at diagnosis could be a factor favouring RAIT when the indication for this intervention is not definite.
6. *Patient health status* - inability to tolerate surgery or other potential therapeuthic interventions, e.g. chemotherapy, could make RAIT the prefered or the only therapeutic option;
7. *Potential risks of the precedure* – whilst RAIT is generally well-tolerated, it is not without short- and long-term toxicity, which includes second primary malignancy. These potentional risks sholud be weighted against expected benefits od the intervention. [1]

Before treatment we need to prepare the patient. First thing we need to do is pass trought pathology of the tumor, the TNM classification, than get acquainted with the entire history of a disease, do laboratory and other relevant tests. A special aspect of patient preparation is an increasing of thyroid-stimulating hormon so the uptake of radioactive iodine could be as high as possible. We achive this by using a recombinant human TSH (rhTSH) or pausing of substitional therapy if the patient use it (2 weeks before the procedure for T3, and 4 weeks before the procedure for T4), also it necessary to reduce the iodine in food. [3]
The dose to use is individual for each patient and depends on tumor size and age of the patient.

A. Contraindiations

Absolute:

1. Pregnancy
2. Breastfeeding

Relative:

1. Bone narrow depression if administration of high 131I activities is intended.
2. Pulmonary function restriction if a significant pulmonary 131I accumulation is expected in lung metastases
3. Salivary gland function restriction especially if 131I accumulation in known lesions is questionable
4. Presents of neurological symptoms or damage when inflammation and local edema caused by the RAIT of the metastases could generate severe compression effects. [1]

B. Side effects of treatment with radioactive iodine

Side effects of treatment with radioactive iodine are different depending on age, comorbidity, and a dose of radioactive iodine that is applied.

Possible short-term side effects include:
- Inflammation of the salivary glands
- Dry mouth
- Short-term changes in taste and smell senses - it usually spontaneously resolved within 4-8 weeks
- Nausea, which usually takes a few days
- Pain and swelling in the neck

Possible long-term side effects include:

- Blockage of the tear duct
- A temporary testosterone reduction in men
- temporary amenorrhea or dysmenorrhea in women
- temporarily bone marrow disorder
- Disorders of pulmonary function
- The occurrence of other tumors - it is a rare complication. [2]

IV. Conclusion

Radioactive iodine therapy (radioiodine tretmnant ablation) has been used since the 1950s. The risk is extremely low, and the potential benefits are quite high.

It is important to mention that biomedical engineering in the domain of endocrinology increases in quantity daily contributes to cure patients with differentiated thyroid carcinoma. Currently, there is a clinical trial of the latest molecular target therapy.

Top researched therapies are analogues of vitamin A, retinoids, which by binding to its receptors, increase expression of NIS and radioiodine uptake in tumor cells. However, cancer cells except the deficient expression of NIS have many metabolic defects, and these defects can be, for example, reducing the accumulation or retaining of radioactive iodine and consequently effectiveness of RAIT.

Screening expression of retinoid receptors in patients can increase the rate of therapeutic response and narrow the treated population. Of interest, a recent case report suggests that retinoids may exert therapeutic biological effects independent of enhancing RAIT. [1]

REFERENCES

1. Guidelines for radioiodine therapy of differentiatedthyroid cancer, M. Luster & S. E. Clarke & M. Dietlein & M. Lassmann &P. Lind & W. J. G. Oyen & J. Tennvall & E. Bombardieri, EANM 2008
2. Thyroid gland cancer at http://www.cybermed.hr/centri_a_z/rak_stitne_zlijezde/rak_stitne_zlijezde_faq
3. Thyroid cancer treatment at http://www.cancerresearchuk.org/about-cancer/type/thyroid-cancer/treatment/radiotherapy/radioactive-iodine-treatment-for-thyroid-cancer

Numerical and experimental stress analysis of an external fixation system

E. Mešić, V. Avdić and N. Pervan

Mechanical Engineering Faculty/Department of Mechanical Design, University of Sarajevo, Bosnia and Herzegovina

Abstract— **This paper presents research results of a stress analysis of a Sarafix external fixation system, applied to an unstable tibia fracture. A stress analysis was performed using FEA and experimental stress measurements using strain gauges. Research was performed on the Sarafix external fixation system controlling values and directions of principal stresses at the measuring points in the case of axial compression. Sarafix proved to be mechanically stable, confirming good clinical results in the treatment of bone fractures.**

Keywords— **Computer Aided Design (CAD), Finite Element Analysis (FEA), experimental stress analysis, CATIA, principal stresses.**

I. Introduction

After J.F. Malgaigne invented the external fixator in 1840, their selection and application was generally carried out on empirical grounds and accumulated experience in clinical orthopedics and traumatology [1]. In order to promote and carry out necessary research to improve fixation, a development of a theoretical analysis of problems fixation based on the principles of structural mechanics is pursued.

The external fixator is a medical device for the immobilization of fractures or serious damage to the structure of extremities. External fixation is a method of fracture immobilization achieved by the application of pins or wires into or through a bone and their binding to the outer frame. The above basic concept of the method has not changed since its origin, but progress is reflected through the development of new design solutions and materials used. In the last two decades, a closer link between medical science and other disciplines of science (Technics, Medical Engineering, Biomechanics etc.) has been created, with the aim of multidisciplinary solving contemporary medical problems. One example of association of scientists of different profiles for the purpose of designing and improving medical equipment is the application of methods of external fixation and the development of systems for external fixation.

The idea for the development of the external fixator Sarafix was developed by a group of orthopaedists of "prim.dr. Abdulah Nakas" General Hospital in Sarajevo under siege, in May 1992 [2]. The idea was triggered by the insufficient number of existing fixators, as the result of the expansion of the war activities in Bosnia and Herzegovina. Shortly after, the first fixator called Sarajevo war fixator - Sarafix (Fig. 1) was produced.

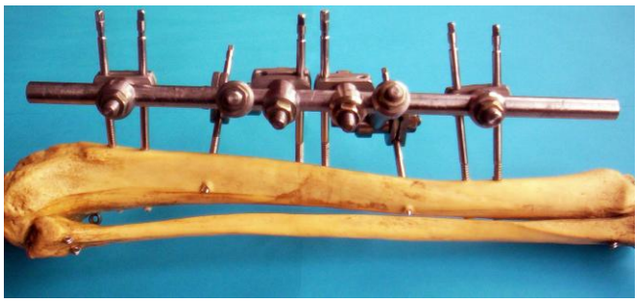

Fig. 1 Analyzed configuration of the Sarafix external fixation system

During the war, the Sarafix found its highest application in the treatment of extensive gunshot-explosive fractures of long bones of the extremities. Today, in peacetime traumatology, it is used in accidental injury in traffic accidents and industrial trauma.

Sarafix external fixation system represents a unilateral, biplanar external fixator which belongs to a group of modular fixators with one-half pins. Owing to the high flexibility and mobility, its application is possible to the complete human skeleton. Sarafix is the holder of numerous awards and prizes at international exhibitions of innovations, and gold medals at the exhibitions of innovations Brussels Eureka 95 and Geneva 1996, and Sarajevo's Sixth of April Award for 2001 should be emphasized.

II. Objective and Methods

All commercial fixators, now in use, passed a biomechanical study before their first application. Mechanical testing of Sarafix fixator was not performed before its clinical application, because of the war-time circumstances in which it originated. Complete mechanical research of the fixator, besides the examination of its stiffness to the loads to which it was exposed after the application, includes the analysis of stresses (von Mises and principal stresses) on the characteristic location of fixator design. Extensive studies of the mechanical research of the Sarafix fixator were carried out within the thesis [3]. Due to the limited scope of this paper, only the results of the axial compression tests will be presented.

With the aim of determining stability of external fixators, various sensors and transducers are set up on their designs [4]. During the past few years, except of performing the

experimental testing, there has been an increased use of geometrical modeling and finite element analysis (FEA), in order to more fully describe the behaviour of the fixator and its components during the loading [5].

This paper presents results of stress analysis of the most used configuration of the Sarafix external fixator in the case of an unstable tibial fracture. An open fracture at the middle of tibia with fracture gap of 50 mm (severe extensive injury with a considerable defect of bone structure) was examined. The most complicated aspect of bone fractures, both in terms of complexity of treatment and structural stresses of external fixator, is an open fracture. In the case of open fractures, in the initial phase of treatment, the full load is transferred through the fixator. The analyzed configuration of the Sarafix fixator contains four one-half pins in proximal and distal bone segment (Fig. 1 and 2).

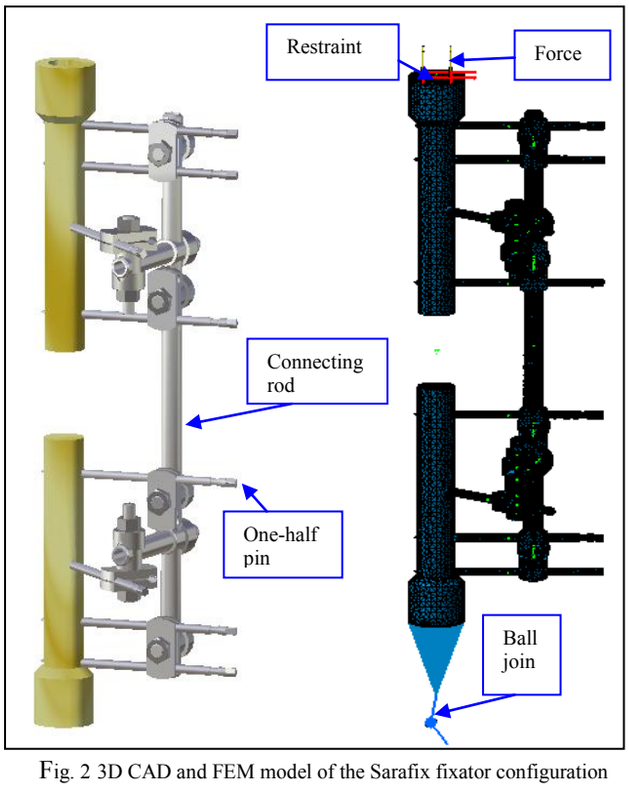

Fig. 2 3D CAD and FEM model of the Sarafix fixator configuration

The mechanical stability analysis of the Sarafix fixator was carried out using FEA and experimental analysis under axial compression.

CAD modeling of the Sarafix fixator and FEA were carried out at the *Laboratory for Computer Aided Design - CADlab* of the *Mechanical Engineering Faculty Sarajevo*. The first step consisted of forming a 3D geometrical model of the analyzed Sarafix fixator configuration, whereupon the FEA was performed on the model using CAD/CAM/CAE (Computer Aided Design/Computer Aided Manufacturing/Computer Aided Engineering) system CATIA [6, 7]. During the structural FEA, values of von Mises stresses were observed at two control points in the middle of the fixator connecting rod. The intensity and direction of principal stresses were monitored and analyzed at the same points.

Understanding the physical behaviour of the model is a basic prerequisite for successful process of modeling real systems. Before that, it is necessary to make numerous assumptions related to modeling: structure, joints between the components, boundary conditions, loads, materials, etc. Fig. 2 shows the CAD and finite element method (FEM) model of the analyzed Sarafix fixator configuration after pre-processing. During the processes of the linear FEA, the material of wooden bone models was defined as orthotropic, while materials of the fixator design were modeled as isotropic. The FEM model consisted of solid finite elements of a linear (TE4) and parabolic tetrahedron (TE10) type. Join elements of the spider type were used for modeling the joints between the components of the Sarafix fixator. The following joints were used: Fastened connection, Contact connection and Bolt tightening connection. The modeling of the influence of supports was performed using a Smooth virtual part. At the end of the proximal bone segment, the axial load in the form of surface force (Force density) was applied in the direction of the z axis of the Cartesian coordinate system. A displacement constraint of the Sarafix FEM model was derived by using the Ball join restraint on the model of distal bone segment. Likewise, a displacement constraint at the model of proximal bone segment was performed by using the User-defined restraint, which prevented the two translations in direction of x and y axis of the Cartesian coordinate system [8].

Experimental stress analysis was conducted at the *Laboratory for materials testing* and *Laboratory for mechanical design testing* of the *Mechanical Engineering Faculty Sarajevo* (Fig. 3). At the Laboratory for materials testing, the examination of the analyzed configuration of the Sarafix fixator on the axial compression was performed, using a universal material testing machine (Zwick GmbH & Co., Ulm, Germany, model 143501). The analyzed configuration of the Sarafix fixator was attached to proximal and distal tibia bone segments modeled with cylindrical wooden bars with known physical properties. During the testing, the intensity of the load (0 to 600 N at the rate of 5 N/s) on the model of proximal segment of the tibia was controlled, using the force transducer (U2A, HBM-Hottinger Baldwin Messtechnik GmbH, Darmstadt, Germany). A wooden model of the proximal and distal bone segments are supported on the ball joint supports [9].

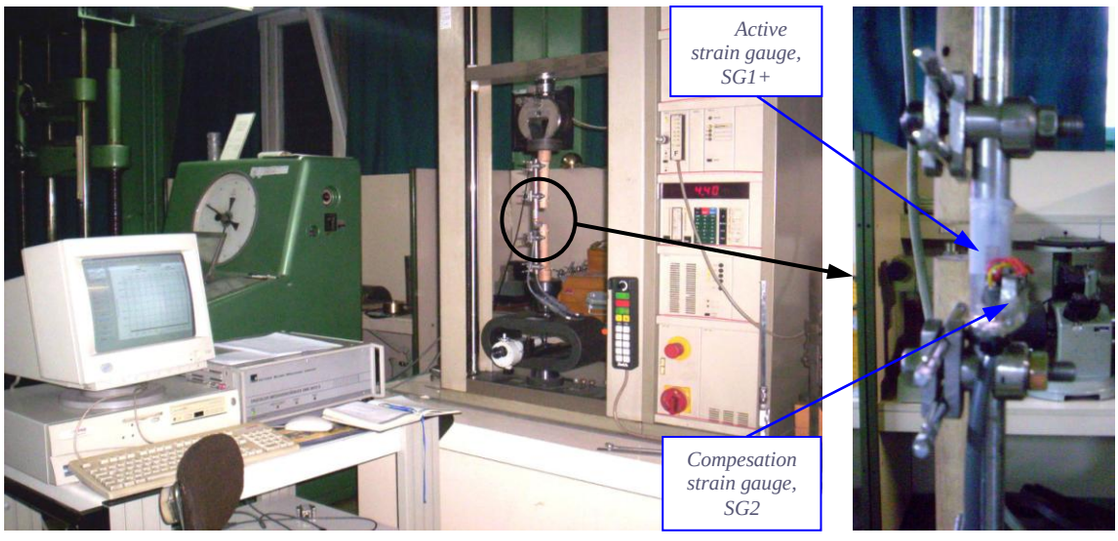

Fig. 3 Set-up for experimental testing on axial compression

Tensometric measurement equipment (Laboratory for mechanical design testing) was used to control and monitor the value of the dominant principal stress on the two measurement points at the middle of the fixator connecting rod. The following equipment from the HBM manufacturer was used:

- digital measuring amplifier system (DMC) 9012A,
- computer with software for acquisition, monitoring and processing of measurement results – Catman, and
- four strain gauges (type 3/120LY11) connected in two Wheatstone half-bridges.

The strain gauges were placed on the opposite sides of the Sarafix fixator connecting rod at the same locations where intensities of maximum and minimum principal stresses were monitored during the FEA. Thereafter, the strain gauges were connected with the DMC system and computer through two separate channels. In this way, the maximum and minimum principal strains on the measuring points were measured independently [10].

This measurement method was applied because the connecting rod was subjected to a compound strain, which consisted of bending strain and axial compressive strain. The connecting rod, due to the axial compression at the proximal segment of the bone model, is exposed to the combined loading (eccentric pressure), which consists of a combination of bending and axial compression. This form of the strain is manifested by the unequal distribution of tensile and compression stresses along the longitudinal section of a connecting rod, i.e. neutral line does not coincide with the axis of symmetry of the fixator connecting rod. Therefore, the two separate Wheatstone half-bridges were formed and connected with the DMC system via two measurement channels. Wheatstone half-bridges consist of active strain gauge SG1 and compensation (inactive) strain gauge SG2 (Fig. 3). The compensating strain gauges were placed near the active strain gauges on a plate tied to a connecting rod. Compensating strain gauges are used to compensate the effect of temperature on the measurement and they are of the same type as the active ones. The plate and connecting rod are made of the same material.

III. Stress Analysis

The principal stresses of the stress tensor are the distinctive values of the stress tensor, while their direction vectors are the principal directions or eigenvectors [11]. When the coordinate system is chosen to coincide with the eigenvectors of the stress tensor, the stress tensor is represented by a diagonal matrix:

$$\boldsymbol{\sigma} = \begin{bmatrix} \sigma_1 & 0 & 0 \\ 0 & \sigma_2 & 0 \\ 0 & 0 & \sigma_3 \end{bmatrix} \quad (1)$$

where: σ_1, σ_2 and σ_3 are the principal stresses.

The values of the principal and von Mises stress were controlled on two locations at the middle of the fixator connecting rod during the FEA. The measuring point closer to the model of the bone segment was marked with MP- and

the point on the opposite side of the connecting rod was marked with MP+ (Fig. 4).

Compressive stresses, which were recorded at the measuring point MP- have a higher intensity compared to the tensile stress at the MP+. This is a direct consequence of the appearance of an eccentric compression that exposed fixator connecting rod. The direction of the maximum principal stress (σ_1) on the measuring point MP+ coincides with the direction of z axis, i.e. the axis of symmetry of the connecting rod. Likewise, the direction of the minimum principal stress (σ_3) on the MP- coincides with the axis of symmetry of the connecting rod. The minimum principal stress compared to the other two principal stresses at the MP- is dominant. Within the Fig. 4 a view B is given where directions and intensities of the principal stresses on the measuring points are presented. Note that at the MP+ the maximum principal stress is in fact the tensile stress, while at the MP- the minimum principal stress is actually the compressive stress. Also, it can be seen that the dominant principal stresses (σ_1 and σ_3) are in the bending plane of the fixator which is not parallel with AP (anterior-posterior) plane. For this reason, the vectors of the dominant principal stresses do not match either (Fig. 4, View B). Previously performed FEA determined the direction and intensity of the principal stresses. Also, it was noted that the intensities of the other two principal stresses at the measuring points were negligible compared to the maximum (σ_1 on MP+) and minimum (σ_3 on MP-) principal stress (Table 1). Active strain gauges are placed on the opposite sides of the connecting rod at the nearest and farthest point from the model of the bone, so that their longitudinal axis coincides with the directions of dominant principal strains (ε_1 and ε_3) at the measuring points [12]. The strain, registered by Wheatstone half-bridge with one active and one compensation strain gauge, is given by the relation:

$$\varepsilon = \frac{4}{k} \cdot \frac{U_A}{U_E} \tag{2}$$

where:

k - is gauge factor, U_A – is bridge output voltage and U_E – is excitation voltage (bridge input), [13].

The dominant principal stresses at the measuring points (MP+ and MP-) are determined through the relations:

$$\begin{aligned} \sigma_1 &= \varepsilon_1 E \\ \sigma_3 &= \varepsilon_3 E \end{aligned} \tag{3}$$

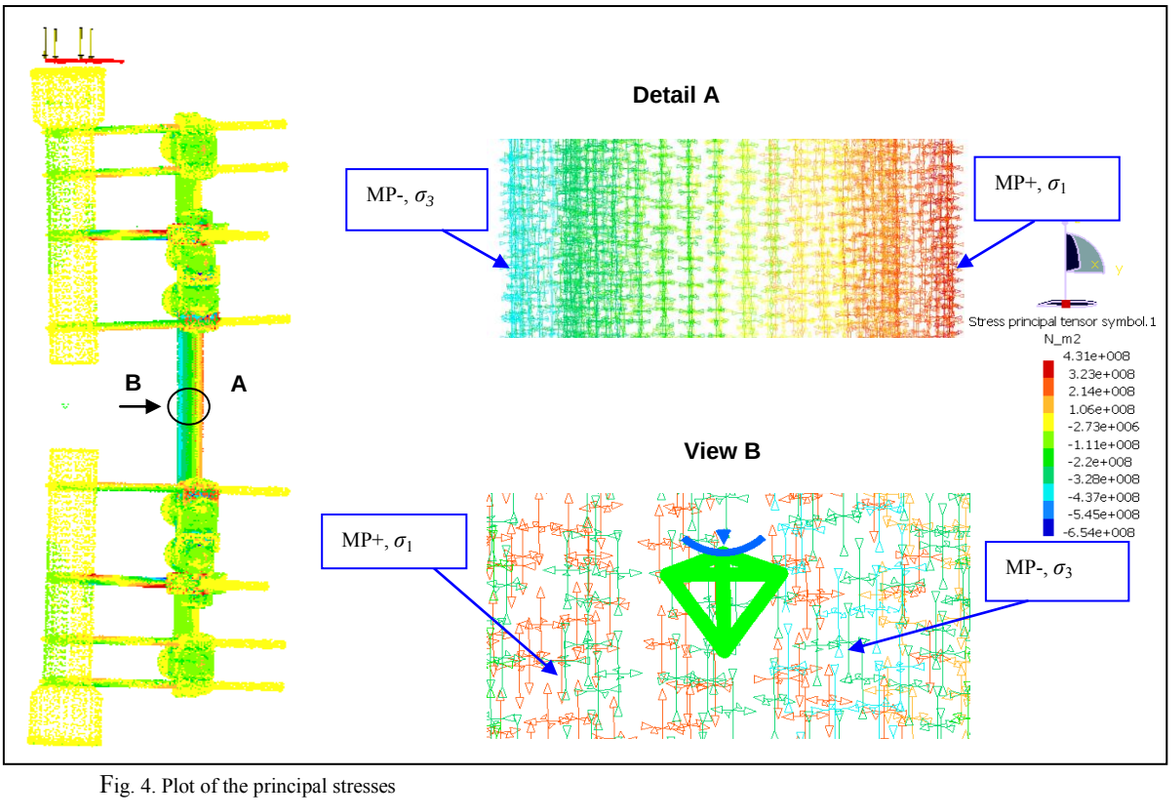

Fig. 4. Plot of the principal stresses

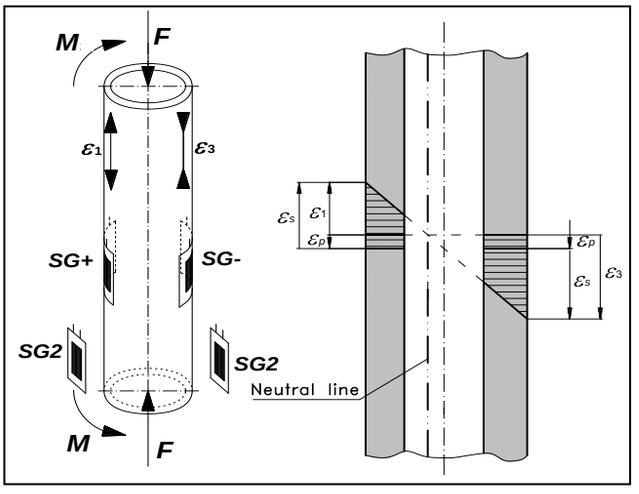

Fig 5. Arrangement of strain gauges and distribution of loads and strains in the longitudinal section of the connecting rod

Simultaneous measuring of the largest positive and negative principal strains on the opposite sides of the fixator connecting rod was carried out independently at two measurement points (Fig. 5).

In the following analysis, the strain gauge placed on the side of the connecting rod closer to the bone model will be referred to as SG-, while a strain gauge placed on the opposite side will have a label SG+. This way of setting up strain gauges enables the measurement of the greatest positive principal strain (ε_1) at the measuring point MP+, on the basis of which the intensity of the maximum principal stress (σ_1) is determined. Analogously, on the measuring point MP-, the greatest negative principal strain (ε_3) was measured, on the basis of which the intensity of the minimum principal stress (σ_3) is determined. The minimum principal stress compared to the other two principal stresses at the point MP- is dominant.

Independently measured total strains at the measuring point consisted of the compressive and bending strain. The total (principal) strains are defined by the principle of superposition, as follows:

$$\varepsilon_1 = -\varepsilon_p + \varepsilon_s = -\frac{F}{AE} + \frac{M}{EZ}$$
$$\varepsilon_3 = -\varepsilon_p - \varepsilon_s = -\frac{F}{AE} - \frac{M}{EZ} \qquad (4)$$

where:
ε_p – is the strain component caused by the axial compressive force,
ε_s – the strain component caused by the bending moment,
A – the area cross-section of the fixator connecting rod,
E – modulus of elasticity,
M – bending moment,
Z – section modulus of the fixator connecting rod.

In this case of load, the bending strain was significantly higher than the compression strain ($|\varepsilon_s| \gg \varepsilon_p$). Distribution of the strains in the longitudinal section of the fixator connecting rod is shown schematically in the Fig. 5. Acquisition, display and processing of measurement results are performed using the HBM Catman software.

IV. Results

In order to achieve a direct comparison of results of the FEA and experimental analysis, all parameters of geometry, materials, loads, restrains on the FEM model are set according to experimental settings.

Table 1 shows the intensities of principal and von Mises stresses generated at the measuring points in the case of maximum axial compression force. The value of the maximum principal stress (σ_1) at the MP+ was significantly higher than the other two principal stresses (σ_2 and σ_3). Likewise, the value of the minimum principal stress (σ_3) at the MP- was significantly higher than the other two principal stresses (σ_1 and σ_2).

Table 1. Maximum values of principal stresses at the measuring points

Location	***Principal stresses***	***Methods***	
		FEA, MPa	***Exper.*** , MPa
MP+, SG+	$\boldsymbol{\sigma_1}$	330	334
	$\boldsymbol{\sigma_2}$	0,2	-
	$\boldsymbol{\sigma_3}$	0,001	-
MP-, SG-	$\boldsymbol{\sigma_1}$	-0,003	-
	$\boldsymbol{\sigma_2}$	-0,4	-
	$\boldsymbol{\sigma_3}$	-355	-368

The maximum deviations of the results obtained by FEA in relation to the results obtained by experimental testing are range: the principal stress σ_1 to 1,2%, and the principal stress σ_3 to 3,6% (Fig. 6).

Principal stresses with the negative sign represent compressive stress. It is noted that at the MP+ all principal stresses are positive, while at the MP- all principal stresses are negative (Table 1). The maximum values of maximum principal stress at the control points is σ_3 = 368 MPa and they are lower than the yield strength of the material of the fixator connecting rod (σ_v = 650 MPa).

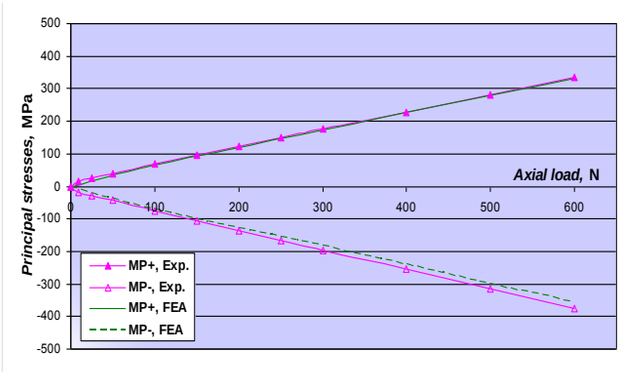

Fig 8. Comparative diagram of the principal stresses (σ_1 on MP+) and (σ_3 on MP-)

V. Conclusion

The conducted research has shown that there is a linear dependence between the loads and stresses generated on the connecting rod, as a result of the absence of large displacement and plastic deformation of the fixator components. The above fact is also a basic requirement for the fixator's stability in terms of preserving anatomical reduction of bone fragments in the postoperative load conditions. Detailed data of the stability of external fixation systems are needed by the orthopedic surgeon to predict successful healing of a fracture. The stability provided by the Sarafix fixator has been proven by mechanical research, confirming good clinical results in the treatment of bone fractures.

Comparing the results of FEA and experimental analysis of principal stresses at the measuring points reveals their good agreement. We can conclude that the developed FEM model of the Sarafix fixator was verified.

The CAD/CAM/CAE system CATIA can be successfully used in the development of CAD models, FEA and computer simulations of the process from different areas of technics and medical engineering. Using the developed CAD/FEM model of the Sarafix fixator, it is possible to control displacements and stresses generated at any point of the bone-fixator system. It is anticipated that this model will provide useful information to surgeons who use Sarafix external fixator for fracture fixation.

Due to extreme flexibility of the formed 3D geometrical model, rapid changes were enabled not only to the geometry and position of components and fixator, but also to the materials applied in the external fixation (from stainless steels to radio-transparent composite materials). In this way, conditions for design optimization of the external fixator are created, which would significantly shorten time and reduce development costs of medical devices for external fixation of bones. In addition, the application of such models greatly reduces the volume of conventional preclinical experimental testing of fixators.

REFERENCES

1. M.A. Karunakar, M.J. Bosse: Principles of External Fixation, Chapter 7, *Rockwood & Green's: Fractures*, 5th edition, 2001.
2. Š. Đozić, *Biomehaničke karakteristike unilateralnog, biplanarnog Sarajevskog ratnog fiksatora "Sarafix" u liječenju strijelno-eksplozivnih akcidentalnih prijeloma dugih kostiju ekstremiteta*, Ph.D. Dissertation, Faculty of Medicine, University of Sarajevo, Sarajevo, BiH, 2011.
3. E. Mešić, *Doprinos razvoju integrisanog CAD/KBE sistema za konstruisanje i redizajniranje medicinskih aparata za spoljašnju fiksaciju kosti*, Ph.D. Dissertation, Mechanical Engineering Faculty, University of Sarajevo, Sarajevo, BiH, 2013.
4. D. Jasinska-Choromanska, I. Sadzynski: "Monitoring Technique of Bone Fracture Healing Using External Fixators", *39th International Conference, Experimental Stress Analysis*, 2001, pp. 35-40.
5. H. Radke, D.N. Aron, A. Applewhite, G. Zhang: Biomechanical Analysis of Unilateral External Skeletal Fixators Combined with IM-Pin and without IM-Pin Using Finite-Element Method, *Veterinary Surgery*, *35*, 2006, pp. 15-23.
6. R. Cozzens, *Advanced CATIA V5 Workbook: Knowledgeware and Workbenches Release 16*, Southern Utah University, Schroff Development Corporation, 2006.
7. N.G. Zamani, *CATIA V5 FEA Tutorials Release 19*, University of Windsor, Schroff Development Corporation, 2010.
8. E. Mesic, A. Muminovic & N. Repcic: "Geometrical Modelling and Structural Analysis of the Sarafix Fixator Configurations", *Annals of DAAAM for 2012 & Proceedings of the 23rd International DAAAM Symposium*, ISBN 978-3-901509-91-9, ISSN 2304-1382, pp 0069 - 0074, Editor: B. Katalinic, Published by DAAAM International, Vienna, Austria 2012.
9. E. Mešic, A. Muminovic and N. Repcic, "Mechanical Stability Analysis of the External Fixation System Sarafix". *Proceedings of the 12th International Design Conference – DESIGN 2012*, *Section: Design methods, Session D435: Life science and design for healthcare*, Editors: Marjanovic D., Storga M., Pavkovic N., Bojcetic N., May 21-24, Cavtat-Dubrovnik, Croatia, 2012,pp.1029-1038,ISSN1848-4700.
10. Hoffmann K., "Applying the Wheatstone Bridge Circuit", *Hottinger Baldwin Messetechnik GmbH*, 1987.
11. O.C. Zienkiewicz, R.L Taylor, J.Z. Zhu, *The Finite Element Method: Its Basis and Fundamentals*, 6th edition, Butterworth-Heinemann, Oxford, 2005.
12. E. Mešić, A. Muminović, N. Repčić, "Structural Analysis and Experimental Testing of External Fixator System Under Axial Compression", *13th International Research/Expert Conference, Trends in the Development of Machinery and Associated Technology-TMT 2009*, Hammamet, Tunisia, 2009, pp. 497-500.
13. A.S. Khan, X. Wang, *Strain Measurements and Stress Analysis*, Prentice-Hall, New Jersey, USA, 2001.

Doc.D.Sc. Elmedin Mešić is with the Mechanical Engineering Faculty/ Department of Mechanical Design, University of Sarajevo, Vilsonovo setaliste 9, 71000 Sarajevo, Bosnia and Herzegovina (phone: 387-33-729-834; e-mail: mesic@mef.unsa.ba).

Internet of Things za zdravstvenu zaštitu - Novi nivo ''smart'' usluga u zdravstvu

Daliborka Mačinković

Fond zdravstvenog osiguranja Republike Srpske/Informacione tehnologije, Banja Luka, BiH, RS

Abstract — **Ovaj rad razmatra mogućnosti koje pruža *Internet of Things (IoT)* u oblasti zdravstvene zaštite - kao novi nivo pametnih usluga u zdravstvu. Budućnost zdravstvene zaštite se opisuje mnogim konceptima kao što *su pervasive healthcare (pHelath), ubiquitous healthcare (uHealth), mobile healthcare (mHealth), electronic healthcare (eHealth), telehealth, telemedicine*. Tradicionalne zdravstvene usluge su vezane za pružanje zdravstvenih usluga isključivo u zdravstvenim ustanovama, IoT za zdravstvenu zaštitu ukazuje na mogućnost pružanja zdravstvenih usluga u određenim okolnostima kod kuće ili bilo gdje, bilo kad (*Anytime, Anywhere, In-home Smart Healthcare Services)*. IoT uključuje postojanje senzora koji prikupljaju podatke o pacijentu, mikrokontrolera koji procesiraju, analiziraju podatke i bežično komuniciraju, mikroprocesora koji omogućuju bogate grafičke korisničke interfejse, zdravstvenih-specifičnih gejtveja koji podatke sa senzora dalje analiziraju i transportuju do korisnika. IoT treba da prati procese prikupljanja podataka sa senzora, obradu korisnih informacija, vizuelizaciju znanja o objektu, reaktivnost kao novi nivo usluga u zdravstvu. Primjeri senzora koji se mogu implementirati za praćenje vitalnih parametara pacijenta su *Blood Pressure Sensor (sphygmomanometer), Body Temperature Sensor, Glucometer Sensor, Sensor Electrocardiogram (ECG), Pulse and Oxygen in Blood Sensor (SPO2), Patient Position Sensor (Accelerometer), Airflow Sensor (Breathing), Galvanic Skin Response(GSR)* i drugi. Najznačajnije funkcionalnosti koje uključuje IoT za zdravstvenu zaštitu su: praćenje i monitoring objekata (ljudi, opreme, medikamenata), udaljeni servisi za dijagnostiku, prvu pomoć, upravljanje tretmanima, upravljanje novim informacijama o zdravstvenoj zaštiti, međusaradnja sa drugim zdravstvenim ustanovama. Tehnologije koje obećavaju rješavanje trenutnih izazova obrade podataka u realnom vremenu su inteligentno procesiranje *in-memory analytics, contex-aware computing, predictive analytics, streaming analytics*. Sa tehnološkog stanovišta potrebno je razmotriti mogućnosti senzorskih uređaja za prikupljanje podataka, komunikacione mogućnosti, servise za upravljanje, aplikacije. Sa poslovnog stanovišta potrebno je razmotriti kako dobijene informacije koristiti u postojećim sistemima zdravstvene zaštite kao novi nivo pametnih usluga.**

Keywords—**Internet of Things za zdravstvo, senzori, real-time obrada podataka, monitoring objekata, udaljeni servisi za dijagnostiku.**

I. Uvod

Internet of Things je nova paradigma koja umrežavanjem objekata iz svakodnevnog života i senzora gradi platforme koje trebaju pružiti nove usluge za razne oblasti poput transporta i logistike, pametnog okruženja, korisničkog socijalnog domena, domena zdravstvene zaštite. Cilj rada jeste da ukaže na trenutne mogućnosti upotrebe senzorskih uređaja za zdravstvo i mogućnosti njihove integracije u kompleksan sistem zdravstvene zaštite. Posebno su izdvojeni procesi koji se odvijaju u IoT ekosistemu praćeni određenim tehnologijama.

Postoje brojne definicije *Internet of Things* i može se reći da je to ideja o inteligentnim stvarima ili objektima, koji mogu biti locirani, adresirani i kontrolisani preko Interneta, generišu velike količine podataka koje je potrebno obraditi u realnom vremenu i koji trebaju proizvesti određene događaje kao kontrole i komande [1].

Internet of Things je tehnološka revolucija koja predstavlja budućnost računarstva i komunikacija i njegov razvoj počiva na dinamičkim tehničkim inovacijama u brojnim važnim poljima od bežičnih senzora do nanotehnologija [2].

Potvrda o eksploziji razvoja IoT objekata je dokaz o rapidnom povećanju povezanih objekata u IP mrežu i predviđanjima o umrežavanju 50 milijardi uređaja do 2020. godine.

IoT za zdravstvenu zaštitu uključuje postojanje senzora koji prikupljaju podatke o pacijentu, mikrokontrolera koji procesiraju, analiziraju podatke i bežično komuniciraju, mikroprocesora koji omogućavju bogate grafičke korisničke interfejse, zdravstvenih-specifičnih gejtveja koji podatke sa senzora dalje analiziraju i transportuju.

IoT za zdravstvenu zaštitu treba da prati proces povezivanja fizičkog i virtuelnog svijeta - objekata kao što su ljudski organi, zgrade, oprema, osoblja pomoću senzora i mikroprocesorskih čipova, u internet i omogući stvaranje podataka, generisanje znanja o objektima i reaktivnost u zdravstvenom sistemu. Prikupljanje podataka sa senzora, obrada u realnom vremenu, napredna analitika trebaju omogućiti bogatstvo inteligencije za planiranje, upravljanje i donošenje odluka u zdravstvenom sistemu.

Sa tehnološkog stanovišta potrebno je razmotriti mogućnosti senzorskih uređaja, prikupljanje podataka, mrežne mogućnosti, servise, aplikacije.

Sa poslovnog stanovišta potrebno je razmotriti kako dobijene informacije koristiti u postojećim sistemima zdravstvene zaštite kao novi nivo usluga u zdravstvu.

Rad je organizovan u pet poglavlja. Nakon uvoda u drugom poglavlju predstavlja se IoT putem toka procesa sa odgovarajućim tehnologijama. *Internet of Things* treba da prati procese prikupljanja podataka sa senzora, obradu korisnih informacija, vizuelizaciju znanja o objektu, reaktivnost kao novi nivo zdravstvenih usluga. U trećem poglavlju predstavljaju se grupisane funkcionalnosti koje se mogu dobiti korišćenjem IoT rješenja. U četvrtom poglavlju predstavljaju se primjeri personalizovanih samo-pratećih proizvoda koji trebaju otvoriti nove mogućnosti zdravstvene zaštite. U petom poglavlju daje se zaključak rada o značaju i mogućnostima IoT za zdravstvenu zaštitu i potrebi kreiranja novog nivoa zdravstvenih usluga koji su ovim radom ukazani.

II. PROCESI I TEHNOLOGIJE IOT-A ZA NOVI NIVO USLUGA U ZDRAVSTVU

Istraživanje i razvoj u oblasti "pametnih" usluga u zdravstvenom sistemu obuhvata tehnologije prikupljanja podataka sa senzorskih uređaja, obradu podataka u realnom vremenu, transfer informacija bežičnim tehnologijama, čovjek-mašina interfejs, upravljive uređaje, interoperabilnost i integraciju sa naslijeđenim bolničkim sistemima i elektronskim zdravstvenim kartonom.

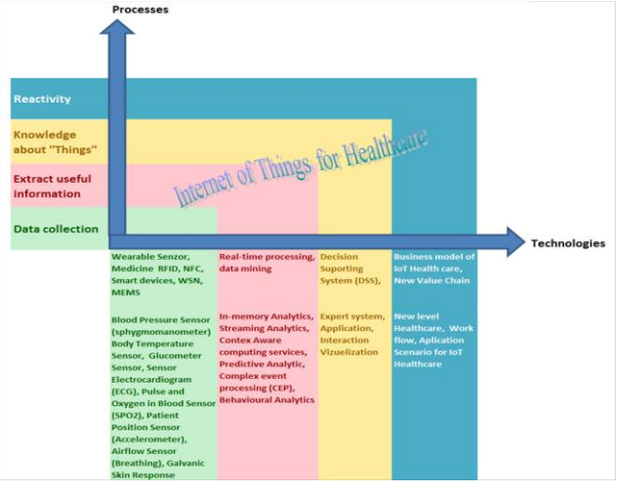

Sl. 1 Procesi i tehnologije IoT-a za zdravstvenu zaštitu

Tradicionalne zdravstvene usluge su vezane za pružanje zdravstvenih usluga isključivo u zdravstvenim ustanovama. Budućnost zdravstvene zaštite se opisuje mnogim konceptima kao što su *pervasive healthcare (pHealth), ubiquitous healthcare (uHealth), mobile healthcare (mHealth), electronic healthcare (eHealth), telehealth, telemedicina.* Razvijanje *Internet of Things* za zdravstvenu zaštitu ukazuje na mogućnost pružanja zdravstvenih usluga u određenim okolnostima kod kuće ili bilo gdje, bilo kad - *Anytime, Anywhere, In-home Smart Healthcare Services*, kao novi nivo usluga u zdravstvu.

Internet of Things prati procese prikupljanja podataka sa senzorskih uređaja, obradu i izdvajanje korisnih informacija prema korisniku u različitim fazama, vizuelizaciju znanja o objektu putem mobilnih, web aplikacija, određenu reaktivnost kao novi nivo usluga uključene u postojeći zdravstveni sistem koji treba predstaviti preciznim scenarijom i poslovnim modelom. Navedeni procesi su podržani odgovarajućim tehnologijama prikazanim na sl. 1, koje trebaju omogućiti uspješan tok svakog pojedinačnog procesa.

Vrste senzora koji se mogu implementirati za praćenje vitalnih parametara pacijenta su *Blood Pressure Sensor (sphygmomanometer), Body Temperature Sensor, Glucometer Sensor, Sensor Electrocardiogram (ECG), Pulse and Oxygen in Blood Sensor (SPO2), Patient Position Sensor (Accelerometer), Airflow Sensor (Breathing), Galvanic Skin Response(GSR)* i dr.

Biomedicinski signali dobijaju se putem specijalnih uređaja sa pacijentovog tijela kao što su bežični senzori na tijelu ili van tijela sa odgovarajućim mrežnim tehnologijama. Razne multimedijalne informacije koncentrisane oko pacijenta mogu se prikupljati sa video kamere, mikrofona, ili senzora pokreta i vibracija. Ostale vrste senzora uspješno prate resurse zdravstvenog sistema medikamente, opremu, prostorije i mogu značajno doprijenijeti uspješnijem funkcionisanju zdravstvenog sistema.

Obrada podataka prikupljenih sa različitih vrsta senzorskih uređaja zahtijeva različita stanja obrade i može teći u različitim fazama lokalno, na internetu, u računarskom oblaku (*cloud computing*). Putem standarda i komunikacionih protokola Wi-Fi, BLE, ANT, ZigBee, USB, i 2G, 3G i 4G moguć je prenos relevantnih podataka do korisnika. Kako većina podataka može biti smještena u računarskom oblaku, važno je uzeti u obzir privatnost podataka, sigurnost, vlasništvo i pristup. Proizvođači servisa za računarski oblak, razvijaju usluge posebno za biosenzore i zdravstvenu oblast, prikupljanje podataka i skladištenje.

Tenologije koje obećavaju rješavanje trenutnih izazova, izdvajanja korisnih informacija iz ogromne količine prikupljenih podataka sa senzora, jesu u obliku inteligentnog procesiranja *in-memory analytics, contex-aware computing*, *predictive analytics*, zatim obrada podataka koji dolaze u neograničenom toku *streaming analytics*. Posebnim algoritmima potrebno je izdvojiti informacije od važnosti i učiniti dostupnim korisniku.

U sledećem procesu informacije trebaju biti čitljive od strane ljudi i upotrebljive (human-readable, human-usable). Tele-medicinske aplikacije pokrivaju područje hitne zdravstvene zaštite, kućne njege, nadgledanje pacijenata kao tele-kardiologija, tele-radiologija, tele-patologija, tele-dermatologija, tele-oftamologija, tele-psihijatrija i tele-hirurgija, aplikacije za praćenje starijih ljudi i pravilne upotrebe lijekova. Ove aplikacije omogućavaju pravovremenu i i ekspertsku medicinsku uslugu u nepristupačnim lokacijama, kao što su ruralna područja, ambulante, brodovi, vozovi, avioni kao i u kućnom okruženju.

Premiještanje telemedicine sa deskotop platfomi na bežične i mobilne konfiguracije ima značajan uticaj na budućnost zdravstvene zaštite. Mobilni i bežični koncepti u zdravstvenoj zaštiti su usko povezani sa bio-monitoringom i kućnim monitoringom. Bio-monitoring koristi mobilne mreže uključujući fiziološki monitoring parametara kao što su srčani ritam, *electrocardiogram (ECG), electroencephalogram (EEG) monitoring, blood pressure, blood oximetry*, i druge fiziološke signale. Alternativa korišćenja uključuje monitoring fizičkih aktivnosti kao što su kretanje (*movement*), gastro mjerenja (*gastrointestinal telemetry)* i praćenje lokacije. Korišćenjem mobilne tehnologije, zapis o pacijentu može biti dostupan profesionalcima za zdravstvenu zaštitu sa bilo koje lokacije koji se konektuju sa interne mreže zdravstvene ustanove. Ljekari mogu imati "sveprisutni" pristup pacijentovoj istoriji, laboratorijskim rezultatima, farmaceutskim podacima, podacima o osiguranju i medicinskim resursima [3].

U radu [4] identifikovani su makro trendovi razvoja tehnologija koji trebaju doprinijeti rješavanju trenutnih izazova IoT-a: minijaturizacija uređaja, napredak u RFID tehnologiji, Internet Protocol version Six (IPv6), poboljšanja u komunikacijama protok i kašnjenja, real-time analitika, adaptiranje cloud tehnologija i sigurnosti.

Dio ključenih tehnologija IoT-a prema [5] su senzori i aktuatori, Wireless Sensor Network (WSN), Intelligent and Interactive Packaging (I2Pack), real-time embedded system, MicroElectroMechanical Systems (MEMS), mobile internet access, cloud computing, Radio Frequency IDentification (RFID), Machine-to-Machine (M2M) communication, human machine interaction (HMI), middleware, Service Oriented Architecture (SOA), Enterprise Information System (EIS), data mining.

Većina poslovnih modela je fokusirana na dijelove sistema odnosno arhitekturu IoT sistema.

Prema [6] sistem se ne može shvatiti proučavanjem njegovih dijelova odvojenih od entiteta, temelj za poslovni model treba da posmatra prirodu ekosistema IoT-a i fokusira se na aktivnosti umjesto na dijelove. Prethodna istraživanja predlažu integraciju aktera, različitih tokova resursa, i razmjenu vrijednosti između njih za mapirnje u ekosistemske operacije.

U radu [7] predstavljen je sistem sistemskog pogleda (tj. "arhitektura"), prema kojoj je platforma organizacija stvari (npr. tehnologije i komplementarne imovine), a zajednica je organizacija ljudi, a poslovni ekosistem je organizacija ekonomskih aktera.

Srž IoT ekosistema se odnosi na međusobne veze fizičkog svijeta stvari sa virtuelnim svijetom interneta, softvera i hardverske platforme, standarda i najčešće se koristi za omogućavanje interkonekcije [8].

Neophodno je pojedinačna rješenja integrisati u postojeće zdravstvene sisteme kao kompleksno rješenje i kreirati nove pametne usluge kao reaktivnost zdravstvenog sistema.

III. FUNKCIONALNOSTI IOT ZA ZDRAVSTVENU ZAŠTITU

Najznačajnije funkcionalnosti IoT za zdravstvenu zaštitu grupisane su kao: praćenje i monitoring objekata (ljudi-pacijenata, osoblja, opreme, medikamenata), udaljeni servisi za dijagnostiku, prvu pomoć, upravljanje tretmanima, upravljanje informacijama o zdravstvenoj zaštiti, međusaradnja sa zdravstvenim ustanovama [5].

A. Praćenje i nadgledanje

Svi obekti u zdravstvenom sistemu (pacijenti, osoblje, lijekovi, oprema) mogu biti praćeni i nadgledani korišćenjem senzorskih uređaja. Praćenje i lociranje inventara, opreme, materijala i imovine. Praćenje radnih tokova u bolnicama za poboljšanje rada i uklanjanje uskih grla. Praćenjem i identifikaciom mogu se izbjeći greške terapija, uzimanje lijekova (doza, vrijeme). WHO (*World Health Organization*) je objavila da 50% populacije ne uzima pravilno lijekove, što ukazuje na doprinos IoT tehnologija [9].

B. Udaljeni servisi

Zdravstveni servisi kao što su pružanje prve pomoći, moždani udar, dijeta i upravljanje lijekovima, telemedicina i udaljena dijagnoza, zdravstvene socijalne mreže, mogu biti isporučene udaljeno putem interneta i uređaja. Različiti bežični pristupi pacijentu bilo gdje i bilo kada mogu omogućiti pružanje udaljenih zdravstvenih usluga. Senzorski uređaji omogućavaju dijagnostiku real-time putem zdravsvenih indikatora koje prikupljaju i prenose bežično.

C. Upravljanje informacijama

Sve zdravstvene informacije (logistika, dijagnose, terapije, lijekovi, upravljanje, finansije i dnevne aktivnosti) mogu biti prikupljenje, upravljive i korišćene putem lanca vrijednosti u integrisanom zdravstvenom sistemu.

D. Organizaciona saradnja

Zdravstveni informacioni sistemi se mogu proširiti pružanjem usluga kod kuće, bilo gdje, bilo kad, pomoću IoT rješenja i integrisati ove usluge u zdravstveni sistem. Moguća je međusaradnja i razmjena dobijenih novih podataka između zdravstvenih ustanova.

IV. PERSONALIZOVANI SAMO-PRATEĆI PROIZVODI

Jedno od područja velikog rasta IoT jeste mjerenje individualnih zdravstvenih metrika putem samo-pratećih gadžeta, smart-telefona sa senzorskim proširenjima, kliničkog udaljenog praćenja, nosivih senzora flastera, bezbroj biorelevantnih aplikacija. Novi trend jeste multi-senzor platforma koja u sebi sadrži nekoliko senzora u obliku pametnog sata, narukvicu senzora, nosivih senzora, flaster za nadgledanje, nadgledanje i napredno testiranje krvi, mozak-računar interfejs, neuro-senzing, mapiranje emocija [10].

A. Pametni satovi i narukvice senzori

Narukvica (*Wristband*) senzori su prethodnik pametnih-satova (*Smartwatches*). Jedana od prvih primjera narukvice senzora jeste korišćenje akcelerometra za mjerenje koraka, udaljenosti, zatim su uslijedila proširenja mjerenjem kalorija, tempa, nivoa intenziteta, u odnosu na aktivno-neaktivno vrijeme, GPS-a, praćenje otkucaja srca, interaktivnog treninga. Tri nove generacije proizvoda dodaju nove funkcionalnosti na standardnu metriku ukupnih koraka, udaljenost i kalorije. *Mio Active* dodaje otkucaje srca, *LarkLife* identifikuje vrstu aktivnosti, omogućuje praćenje press dijeta, mjerenje sna, i koristi se u kombinaciji metrike za personalizovane preporuke o promjenama koje korisnik može napraviti da bude bolje [11]. *Amiigo* narukvice i obuća mjere tip vježbanja, temperaturu tijela i nivo kiseonika u krvi putem infracrvenog senzora [12]. Multi-senzor narukvica su uređaji takođe u razvoju za kliničku upotrebu, kao primjer, epilepsiju. Jedan tim stvorio je narukvicu za otkrivanje konvulsivnih napada kroz elektrodermalne aktivnosti i akcelerometar, kao koristan napredak u odnosu na lab-based metode EEG kao uređaj se može nositi kontinuirano [13].

B. Nosivi senzori i flasteri za nadgledanje

Procjenjuje se da će 80 miliona nosivih senzora biti u upotrebi za zdravstvene aplikacije do 2017. godine [14]. Sljedeća generacija flastera koristi bogatu tehnologiju senzora kako bi se omogućilo da flasteri bežično prenose informacije i uključe se u dvosmjernu komunikaciju u realnom vremenu. *Sano Intelligence*-a jednokratni flaster za kontinuirano praćenje krvi, namijenjen je za mjerenje glukoze u krvi i nivoa kalija, mjerenje bubrežne funkcije i ravnoteže elektrolita. Obećavajući koncept su rastezljive elektronske tetovaže za kontinuirano praćenje vitalnih znakova kao što su otkucaji srca, moždanih aktivnosti, temperature tijela i nivoa hidratacije [15]. Nosivi senzor flasteri su takođe korisni za praćenje srca (*Zio Patch iRhythm*) mogu se nositi za praćenje srčanog ritma i upozoravaju aritmiju [16]. Još jedan zanimljiv primjer novih tehnologija je kontinuirano praćenje krvnog pritiska, gdje umjesto glomaznih traka za ruku, tu je mala ruka-flaster sa elektrodama koja mijenja impedanciju tkiva i pretvara ga u čitanje krvnog pritiska preko senzora [17]. Također obećavajuća je ideja koristeći glucometer kao platformu. Hemičari su razvili metodu kako vezati kratkim segmentima DNK na veliki broj potencijalnih molekula koji bi mogli biti prisutni u krvi, vodi ili hrani. Do sada, ovaj *glucometer-as-a-platforma* metoda se koristi za otkrivanje kokaina, interferon, adenozin, i uranijuma [18],[19].

C. Neprekidni IoT monitoring i napredak u testiranju krvi

Ključno očekivanje za IoT uređaje je da oni omogućuju neprekidno praćenje i real-time prenos podataka, idealno u realnom vremenu povratne informacije i personalizovane preporuke [20]. Testiranje krvi je još jedna oblast u kojoj tehnologije senzora i druge inovacije ubrzano napreduju. Umjesto odlaska u laboratoriju, korisnici mogu ubosti svoje prste kod kuće sa lancetom, staviti krv na laboratorijsku karticu, poslati mail na kartici za analizu, i vidjeti rezultate na webu. *ZRT Laboratory* nudi test krvi na licu mjesta, *Talking20* pozivajući se na 20 aminokiselina koje čine proteini u organizmu, nudi suvo testiranje krvi na licu mjesta, pet markera, vitamina B1 i B9, i hormona: testosteron, estradiol, progesteron. Za kliničke dijagnostičare, postoje nova rješenja *i-STAT System* iz *Abbott Labs* testiranja krvi na mjestu njege. Ovo je ručni krvni analizator koji u realnom vremenu daje rezultate laboratorijskih-kvalitata, za 25 različitih krvnih markera uključujući hemoglobin, hematokrit, glukoze, kalij, kalcij, pH, urea nitrogen (BUN), kreatinin i laktata. Rezultati se mogu koristiti odmah na licu mjesta, a prenose liječnicima u realnom vremenu za konsultacije. Još jedan inovativni pravac u testiranju krvi fokusira se na razvoj testova za patologije koje nisu bile prethodno mjerljive. Jedan od primjera je i novo dostupna *Ridge* dijag-

nostika, krvni test za depresiju, mjerenje nivoa u serumu od devet biomarkera (alfa1 antitripsina, apolipoproteina CIII, mozak-izvedeni neurotropski faktor, kortizola, epidermalni faktor rasta, mijeloperoksidaza, prolaktin, resistin i rastvorljivi faktor nekroze tumora alfa tip II receptor) [21]. Isti krvni markeri se mogu koristiti za otkrivanje drugih prediktivnih stanja. Na primjer, kod dijabetičara, nivoi 1AC hemoglobina su prediktivna početna stanja, od deset godina, i mogao bi biti meta za rano preventivnu intervenciju [22].

D. Brain-Computer interfejs (BCIs), neuro-senzorstvo, emocionalno-mapiranje

U narednom periodu, očekivanja su da će biti omogućeno mnogo veće razumijevanje mozga. Naredna generacija korisnika EEG-a može iskoristiti poboljšanja raznih senzorskih tehnologija posebno u prenosu podatka niskoenergetskim Bluetooth-om i tehnologijama baterija. To bi moglo značiti mnogo udobniji, nenametljivi i vizualno atraktivan-nosivi elektronski-mozak monitor koji bi mogao biti na raspolaganju da se nosi 24/7, neprestano prikuplja podatke i pakuje ih u korisne aplikacije u realnom vremenu. EEG proizvodi druge generacije *InteraXon* i *Axio, Veritas Scientific* uređaj za otkrivanje laži, na *TruthWave* razvijene su na osnovu dostupnih korisnik-EEG tehnologija. Standardna neuronaučna tehnika se koristi za otkrivanje moždane aktivnosti, kada se prepoza lice osobe registruje se odgovor P300 iz vrste aktivnosti mozga poznat kao dagađajem vezan potencijal (*event related potentials -ERPs*). Veliki broj firmi i akademskih laboratorija rade na mjerenju emocija, poznatim kao efekti. Ovo je na neki način digitalna implementacija i produženje rada istraživanja emocija pionira Paul Ekman, koji je razvio FACS (Facial Action Coding System), sada poznat kao FACE (izraz lica, podizanje, blagost, emocije), da taksonomizira svaki ljudski izraz lica. Dvije kompanije, *Affectiva i Affectiva Interfaces*, koristite računarske web kamere i eye-tracking tehnologije za čitanje mikroekspresija lica, uglavnom u svrhu neuromarketinga (npr; određivanje biofizičkog odziva učesnika za potrošačku marku ili zabavni proizvod kao što su TV emisije ili film). *Affectiva* koristi multi-senzor narukvicu koja snima GSR, temperaturu i akcelerometar pored tehnologije webcam eye-tracking. Čak i bez EEG ili Eye-tracking, neki stepeni emocija, kao što su nivo stresa mogu biti otkriveni s drugim mjerenjima dobijenim od senzora kao što je GSR [23].

E. Pametni telefon i periferije

Mobilni telefon je platforma za mnoge aktivnosti, inicijalno za komunikaciju, zatim i za računarstvo, a sada za kvantifikovano praćenje, čemu je doprinio stalni pristup internetu. Tako je osnovna funkcionalnost telefona, glas u kombinaciji s automatizovanim algoritmima, rezultovala novom generaciom IoT prediktivne aplikacije, za detekciju npr. Parkinsonove bolesti. Program mašinskog učenja analizira različite glasovne kvalitete u uzorku kao što su vokalni tremor, snaga izdaha i fluktuacije vilice, jezika i usne za procjenu prisutnosti i ozbiljnosti Parkinsonove bolesti [24].

Pametni telefoni kao dio IoT aplikacije, sa proširenjima kao što su *AliveCor* elektrodiagramom (EKG) za monitoring srca, pametni telefon sa sistemom za ultrazvuk imaging *MobiSante-a*, *CellScope* otoskop (pregled srednjeg uha), dermascope (za snimanje slike na koži). Prateći trendove u razvoju senzora, minijaturizacija i poboljšanje funkcionalnosti, lako je zamisliti da je za neke aplikacije očekivati, da naredne generacije *sensortech* bi mogle uključivati direktnu integraciju senzora u smartphone platformu umjesto da budu periferije uz hardver. Jedan primjer za to je *LifeWatch V*, smartphone sa uobičajenim paketom senzora za mjerenje EKG, tjelesne masti, broja otkucaja srca, stresa, temperature, zasićenosti krvi i nivoa glukoze u krvi [25].

Android-baziran na ideji [10], senzora ugrađen direktno u hardver, je takođe vidljiv u Google Project Glass. Project Glass definiše novu kategoriju nosivog računarstva, gdje mala kamera i računarski čvor montiran na uglu naočala mogu pretraživati internet i prikazati rezultate u realnom vremenu ispred očiju. U budućnosti, moglo bi biti posebnih izdanja projekta Glass ili druge slične multi-senzor platforme sa ugrađenim mikroprocesorom za spajanje niza funkcionalnosti kao što su EEG, praćenje oka, broj otkucaja srca, GSR, akcelerometar, temperatura, GPS, i internet pretragu i rezultate prikazati u definisanoj kategoriji ljudski uvećane platforme za informacije u realnom vremenu, komunikaciju, povratne informacije i optimizaciju performansi.

V. ZAKLJUČAK

Rad je ukazao na mogućnosti i značaj razvoja *Internet of Things* za zdravstvenu zaštitu. IoT je posmatran kao proces povezivanja fizičkog i virtuelnog svijeta, objekata kao što su ljudski organi i zdravstveni resursi, pri čemu nastaju novi izvori zdravstvenih podataka prikupjeni sa senzora iz kojih je moguće generisati znanje o objektima i postići reaktivnosti u zdravstvenom sistemu. Predstavljeni su senzori koji mogu prikupiti podatke o vitalnim parametrima pacijenata. Putem novih komunikacionih protokola moguć je prenos relevantnih podataka do korisnika u realnom vremenu. Obrada podatka zahtijeva napredne analitičke tehnologije za izdvajanje relevantnih informacija iz ogromne količine podataka koji neprestano pristižu sa senzora. Korisnik treba imati pristup podacima putem savremenih aplikacija. Posebano je naglašena potreba intergracije novih

podataka u zdravstveni sistem, za dobijanje vrijednih usluga kao novog nivoa pametnih usluga u zdravstvu. Predstavljeni su personalizovani samo-prateći proizvodi kao gadžeti, nosivi senzori, flaster senzori, pametni satovi senzori, narukvica senzor, novih metoda udaljenog testiranja krvi, tendencije integracije mobilnih telefona i senzora. *Internet of Things* je oblast koja se tek razvija, ali ogroman značaj za zdravstvenu primjenu se može uočiti već u prvim rješenjima.

REFERENCE

1. National Intelligence Council. Disruptive Technologies Globa-Trends 2025. Six Technologies with Potential Impacts on US Interests Out to 2025. 2008., [online] http://www.fas.org/irp/nic/ disruptive.pdf [accessed dec. 2014.]
2. ITU Internet Reports 2005: (2005). The Internet of Things-Executive Summary, [online] www.itu.int/osg/spu/ publications/internetofthings [Accessed jan.2015.]
3. D. Vouyioukas, I. Maglogiannis, "Communication Issues in Pervasive Healthcare Systems and Applications Pervasive and Smart Technologies for Healthcare: Ubiquitous Methodologies and Tools", IGI Press Pages 197-227 2010
4. InternetOfThings[Online]. htps://www.ida.gov.sg/~/media/Files /Infocomm%20Landscape/Technology/TechnologyRoadmap/InternetOfThings.pdf [Accessed nov. 2014.]
5. Z. PANG, Technologies and Architectures of the Internet-of-Things (IoT) for Health and Well-being, Doctoral Thesis in Electronic and Computer Systems KTH – Royal Institute of Technology Stockholm,Sweden, January 2013
6. Battistella, C., Colucci, K., De Toni, A.F., & Nonino, F. 2013. Methodology of Business Ecosystems Network Analysis: A Case Study in Telecom Italia Future Centre. Technological Forecasting & Social Change,80: 1194–1210.
7. Muegge, S. 2013. Platforms, Communities, and Business Ecosystems:Lessons Learned About Technology Entrepreneurship in an Interconnected World. Technology Innovation Management Review, 3(2): 5-15. http://timreview.ca/article/655
8. Mazhelis, O., Luoma, E., & Warma, H. 2012. Defining an Internet-of-Things Ecosystem. In S. Andreev, S. Balandin, & Y. Koucheryavy (Eds.). Internet of Things, Smart Spaces, and Next Generation Networking – Lecture Notes in Computer Science, Volume 7469: 1-14. Berlin:Springer
9. Dolan, B. Lloyds Pharmacies to sell Proteus smart pills, sensors. Mobihealthnews. 2012. Available online: http://mobihealthnews.com/15820/lloyds-pharmacies-to-sell-proteus-smartpills-sensors/ (accessed on 31 October 2012).
10. M.Swan, "Sensor Mania! The Internet of Things, Wearable Computing, Objectiv Metrics, and the Quantified Self 2.0", J. Sens. Actuator Netw. 2012, 1, 217-253; doi:10.3390/ jsan1030217
11. Jung, S. Larklife Looks to Help You Improve Your Health and Your Sleep. 2012. medGadget. Available online: http://techcrunch.com/2012/10/17/amiigo-is-a-fitness-bracelet-plus-app-thatknows-what-type-of-exercise-youre-doing-and-what-its-doing-to-you/ [accessed dec.2014.]
12. Lomas, N. Amiigo Is A Fitness Bracelet (Plus App) That Knows What Type Of Exercise You're Doing—And What It's Doing To You. TechCrunch. 2012, online:http://techcrunch.com/2012/10/17/amiigo-is-a-fitness-bracelet-plus-app-that-knows-what-type-ofexercise-youre-doing-and-what-its-doing-to-you/ [accessed dec. 2014.]
13. Poh, M.Z.; Swenson, N.C.; Picard, R.W. A wearable sensor for unobtrusive, long-term assessment of electrodermal activity. IEEE Trans. Biomed. Eng. 2010, 57, 1243–1252.
14. Prakash, D.; Berlin, E. Adhesive-Based Technologies Stick to Home Healthcare. 2012. Medical Device and Diagnostic Industry, online: http://www.mddionline.com/article/ adhesivetechnologies-home-healthcare [accessed dec. 2014].
15. Talbot, D.; Sutton, K. Making Stretchable Electronics. 2012. MIT Technology Review, online: http://www.technologyreview.com/ demo/428944/making-stretchableelectronics/[accessed dec.2014.]
16. Wearable Sensor Patches iRhythm: A Zio Patch for Cardiac Arrhythmias online: http://internetmedicine.com/irhythm/ [accessed dec. 2014]
17. Ostrovsky, G. New Startup Develops Continuous Blood Pressure Measurement without a Counter-Pressure Cuff. 2012. medGadget, online: http://medgadget.com/2012/02/newstartup-develops-ontinuous-blood-pressure-measurement-without-a-counter-pressure-cuff.html [accessed 12.2014.]
18. Ahlberg, L. Pocket chemistry: DNA Helps Glucose Meters Measure More Than Sugar, 2012. Available online: http://news.illinois.edu/news/11/0725glucose_meter_YiLu.html [accessed dec.2014.]
19. Xiang, Y.; Lu, Y. Using personal glucose meters and functional DNA sensors to quantify a variety of analytical targets. Nat. Chem. 2011, 3, 697–703.
20. Lewis, N. Remote Patient Monitoring Market to Double By 2016. 2012. InformationWeek Healthcare. Available Online: http://www.informationweek.com/healthcare/mobile-wireless/remote-patient-monitoring-market-to-doub/240004291 [accessed dec. 2014.]
21. Papakostas, G.I.; Shelton, R.C.; Kinrys, G.; Henry, M.E.; Bakow, B.R.; Lipkin, S.H.; Pi, B.; Thurmond, L.; Bilello, J.A. Assessment of a multi-assay, serum-based biological diagnostic test for major depressive disorder: A Pilot and Replication Study. Mol. Psychiatry 2011, doi:10.1038/mp.2011.166.
22. Heianza, Y.; Arase, Y.; Fujihara, K.; Tsuji, H.; Saito, K.; Hsieh, S.; Kodama, S.; Shimano, H.;Yamada, N.; Hara, S.; Sone, H. High normal HbA(1c) levels were associated with impaired insulin secretion without escalating insulin resistance in Japanese individuals: The Toranomon Hospital Health Management Center Study 8 (TOPICS 8). Diabet. Med. 2012, 29, 1285–1290.
23. Villarejo, M.V.; Zapirain, B.G.; Zorrilla, A.M. A stress sensor based on Galvanic Skin Response(GSR) controlled by ZigBee. Sensors 2012, 12, 6075–6101.
24. Parikh, R. Interview with Max Little, Ph.D., Director of the Parkinson's Voice Initiative.medGadget. 2012. Available online: http://medgadget.com/2012/08/interview-with-max-little-phd-director-of-the-parkinsons-voice-initiative.html[acc. dec.2014.]
25. Stomp, W. LifeWatch V: Android-based Healthcare Smartphone Packed with Medical Sensors.medGaget. 2012. Available online: http://medgadget.com/2012/07/lifewatch-v-android-basedhealthcare-smartphone-packed-with-medical-sensors.html (accessed dec. 2014).

Sleep stage classification using AR Burg and C4.5 classifier

Nejra Arnaut, Abdulhamit Subasi

International Burch University, Faculty of Engineering and IT, Electrical and Electronics Department,
Sarajevo, Bosnia and Herzegovina

Abstract-**In this study, an effective automatic novel system for sleep staging that is based on AR Burg and C4.5 decision tree method is constructed in order to enhance pertinence of automatized sleep staging classification. It is of huge significance to analyze human sleep during various life cycles. Sleep stage classification process is long-term and demanding job performed by sleep professionals. Traditional sleep staging technique is the study of polysomnograms (PSGs) records from a sleep laboratory. One of the most significant signals in PSGs are electroencephalogram (EEG) signals. However, it is challenging and complex job to accurately record and analyze these EEG signals. The main aim of this study is to solve this problem. For processing of EEG signal is used AR Burg signal processing technique. The AR Burg features were extracted from characteristic waves of EEG signals were used to classify various sleep stages. C. 4.5 decision tree classification methods is used for automatic classification of various sleep stages based on AR Burg features that are extracted from the a single Electroencephalogram (EEG) Fpz-Cz channel. Features extracted from EEG signals using AR Burg method were fed into C4.5 decision tree classifier to distinguish between various sleep stages, such as wakefulness (W), rapid eye movement (REM), non-rapid eye movement sleep stages (NREM-1, NREM-2, NREM-3 and NREM-4) and Movement time (M). EEG sleep recording used to prove the efficiency of the system, proposed in this study, are taken from the publically available Sleep-EDF database (expanded). Obtained overall classification accuracy is 91.01 %. The efficiency of the proposed automatic system for sleep stage classification is proved with obtained experimental results.**

Keywords- **Classification, Sleep stages, AR Burg, Decision Trees, C 4.5.**

I. INTRODUCTION

Sleep analysis is an issue which received great attention in recent time in medicine, but also in theoretical area. In this study, an automatic intelligent system for sleep stage analysis and classification is proposed. It is of great importance to have automatic intelligent sleep stage analysis and classification system since sleep analysis can be employed to detect different neurological diseases such as insomnia, narcolepsy and many others diseases [1]. According to Rechtschaffen and Kales (R&K) sleep scoring standard [2], there are two main sleep stages, namely, rapid eye movement (REM) and non-rapid eye movement (NREM). NREM stage is divided into four sub-stages: NREM1, NREM2, NREM3 and NREM4. Each of these sub-stages characterizes specific part of sleep duration with unique time and frequency [2]. Through whole night of human sleep, these five stages will occur begin with awake to stage NREM4.

NREM1 sleep stage is represented as transition time between sleep and wakefulness time, characterized with high amplitude of theta waves. At NREM 2 sleep stage, brain starts to create blasts of rapid, rhythmic brain wave movement that we called sleep spindles. NREM3 is characterized as transition between NREM2 and NREM3, where delta waves starts to occur and that are dominant in NREM4 sleep stage. During this stage, brain movement is transformed from NREM4 s to NREM1 sleep stages [3, 4].

Sleep specialist use some regular methods for sleep stage classification based on visual examination strategy. In this type of methods, large data information is required for analysis, from eight EEG channels, EMG and EOG. Results with EOG and EMG are not so precious, because they are able to change states for diverse sleep stages. For sleep stage classification most significant role has EEG signals, but other signals such as EMG, EOG and ECG are also significant. Importance of EMG signals is to separate REM and NREM1 stage, while EOG is used to detect eye movement in NREM1 and REM sleep stages [5].

This paper is organized as follows. In Sections 2, materials and methods used in this study are discussed. In this section, dataset used in this study is explained. Also, AR Burg feature extraction method and decision tree classifier used in this study is presented. In section 3, experimental results obtained in this study are presented. Conclusion and possible future improvements are given in Section 4.

II. MATERIALS AND METHODS

A. Experimental Dataset

Dataset extracted from publicly available SC Sleep-EDF Database [Expanded][1] is used to evaluate the performances of the system proposed in this study. This database contains 61 polysomnograms (PSGs) with related experts' sleeps stage annotation files called hypnograms. This database is the results of two different studies. The first study was conducted between 1987 and 1991 and included 79 healthy Caucasians with age between 25 and 101. PSG record

[1] http://www.physionet.org/physiobank/database/sleep-edfx/

duration lasted for about 20 hours. EEG sampling frequency was 100 Hz. The second study was conducted in 1994 and included 22 Caucasian males and females being having with minor problems in falling asleep. EEG signals in study also had sampling frequency of 100 Hz. Every polysomnogramic record consists of EEG (Fpz-Cz and Pz-Oz electrode placements), Electrooculogram (EOG), sub mental chim electromyogram (EMG) and an event marker [6, 7, 8]. Sleep stages in this database are W, R, 1, 2, 3, 4, M (movement time) and ? (not scored). These sleep stages were decided based to Rechtschaffen & Kales criteria [2] .

B. Burg method

Using Burg's method for AR spectral estimation with respect of Levinson Durbin recursion, minimization the forward and backward prediction errors is established. The primary advantages of the Burg method is capability to resolve closely spaced sinusoids in low level signal and estimation of short data records which will ensure their AR power spectral density to be closed the true values. The main difference between all other AR estimation methods and Burg is property of method to calculate the reflection coefficients, without estimation of autocorrelation function.

The performance of stable AR model should include some factors such as: appropriate algorithm for the data, providing data length, selection of data orders value and stationary level. Data order value is dependent of number of data coefficient and evaluated using different criteria. According to data order value, it is possible to identify frequency details of data and corresponding peaks. In the case of low value, it not possible to record peaks in frequency spectrum; while high value cause spurious peaks that are not part of original data. Reason for low accuracy of the system are high-order models, long data records and high signal to- noise ratios.

The reflection coefficient is established by [9, 10, 11, 12]:

$$Kp = -2\sum_{n-p+1}^{N} {}^{e}f,_{p-1}(n)e_{b,p-1}(n-1) \Big/ \sum_{n-p+1}^{N} [|e_{f,p-1}(n)|^2 + |e_{b,p-1}(n-1)|^2]$$

PSD estimation of Burg system is formed by:

$P_{burg}(f) = e_p/|1 + \sum_{k=1}^{p} e_p\, a_p(k) e^{-2j\pi fk}|^2$, where $e_p = e_{f,p} + e_{b,p}$ is the total least-squared error [9, 10].

C. Decision Tree Algorithms

One of main fundamental machine learning methods are decision trees (DTs). They are useful for high dimensional data. It is tree data structure easily understand, because of their form and contain of nodes and leaves. According to value of attributes of case, DTs will assign class value to case. DT is known as universal approximations which map linear and nonlinear relationships and don't need a lot of training data for learning. DT has two types of nodes [13, 14]:

- root node
- internal nodes

The root node is associated with all training samples which are usually divided in two or more classes, which will cause investigation of samples and divide root node to internal nodes. When leaf nodes are reached in internal node, it is possible to read class label. In the case of binary DT, every node divide itself into two new nodes, while nonbinary DT divide itself in three new or more nodes [13, 14].

C 4.5 is one of DT implementation algorithms. The basic purpose of C4.5 algorithm is capability to predict missed values of features using knowledge of related domains. Also, it is possible to reduce the three size without attending accuracy by: replacement and subtree raising. It is done by replacing subtree with a leaf node, and later with most frequently used tree.

When reduction of tree is not effective, C4.5 will create decision rules. The procedure of creating decision rule procedure is given below [13, 14]:

- Rule 1: If (A = x_1 and B = y_1), Classification = Class 1;
- Rule 2: If (A = x_2 and C = z_1), Classification = Class 2;
- Rule 3: If (A = x_2 and C = z_2), Classification = Class 1.

Those rules can be placed together in order to provide smaller set of decision rules for tree. C. 4.5 methods is used for automatic classification of various sleep stages based on AR Burg features that are extracted from one single Electroencephalogram (EEG) Fpz-Cz channel.

III. RESULTS AND DISCUSION

Classification of EEG signals consists of data acquisition, biomedical signal processing and feature extraction, and classification. MATLAB R2013 was used for biomedical signal processing, while performance of machine learning tools was tested in Weka, due to their good implementation and simplicity of use.

In this study, only one record (SC400E100) was employed to test performances of our proposed system. In this study, Fpz-Cz channel was analyzed. This record was divided into

smaller segments with duration of 30s each in the first step. In the second step, features were extracted by means of AR Burg signal processing technique. Extracted features are used for automatic classification of various sleep stages by using C 4.5 method. The performance of C4.5 machine learning algorithm determines how well system proposed in this study performs.

When C 4.5 machine learning tools is used, it has to be decided on how to create training and testing dataset. In order to create training and testing dataset, 10-fold cross-validation (CV) was used in this study. With 10-fold CV, entire dataset (after AR feature extraction) is divided into 10 folds of approximately same sizes. In 10-fold CV, 9 folds are used for training and remaining one fold is used for testing. Such procedure is repeated 10 times. Overall 10-fold CV accuracy is the average of achieved 10 individual accuracies. Performances of the system proposed in this study were evaluated by means of CV overall accuracy rate.

In this study, by means of AR Burg feature extraction methods, 6 sleep stages, namely, Wakefulness, NREM1, NREM2, NREM3, NREM4 and REM, were considered as 6 different classes in order to perform classification task. In total for all six classes, 1736 instances were extracted. System prosed in this study, ARBURG + C 4.5, was able to correctly classify 1580 instances or 91.0138 % of all instances, what is very high classification rate.

Table 1 Obtained performance results for C4.5 classifier

Correctly Classified Instances	1580	91.0138 %
Incorrectly Classified Instances	156	8.9862 %

CONCLUSION AND FUTURE WORK

In this study, novel automatic system for sleep stage classification is proposed. This system is the highly-performing mix of feature extractor and classifier. Six different sleep stages, namely Wakefulness, NREM1, NREM2, NREM3, NREM4 and REM, were analyzed and classified. AR Burg algorithm was employed as feature extractor and C 4.5 decision tree method was used as classifier. System proposed in this study achieves high overall accuracy of 91.01 %. Obtained results shows that C 4.5 decision tree classifier has noteworthy function for capturing and interpreting of sleep stage data and can help medical workers with deciding on correct diagnosis and treatments. In future work, more records will be used to prove high performances of system proposed I this study. Also, different feature extraction and classification techniques will be employed in order to find the most accurate sleep stage classification system.

REFERENCES

[1] K. Šušmáková, "Human Sleep and Sleep EEG," *Measurement Science Review,* vol. 4, no. 2, pp. 59-74, 2004.

[2] A. Rechtschaffen and A. Kales, A Manual of Standardized Terminology, Techniques and Scoring System for Sleep Stages of Human Subjects, MD, USA: US Department of Health, Education, and Welfare:, 1968.

[3] K. Lovell and C. Liszewski, "Summary: Normal Sleep Patterns and Sleep Disorders," 2015. [Online]. Available: http://learn.chm.msu.edu/neuroed/neurobiology_disease/content/otheresources/sleepdisorders.pdf. [Accessed 8 February 2015].

[4] K. Venkatesh, S. Poonguzhali, K. Mohanavelu and K. Adalarasu, "Sleep Stages Classification Using Neural Network with Single Channel EEG," *International Journal of Recent Advances in Engineering & Technology (IJRAET),* vol. 2, no. 8, pp. 5-8, 2014.

[5] F. Ebrahimi, M. Mikaeili, E. Estrada and H. Nazeran, "Automatic Sleep Stage Classification Based on EEG Signals by Using Neural Networks and Wavelet Packet Coefficients," in *30th Annual International IEEE EMBS Conference*, Vancouver, British Columbia, Canada, 2008.

[6] B. Kemp, A. H. Zwinderman, B. Tuk, H. A. Kamphuisen and J. J. Oberye, "Analysis of a Sleep-Dependent Neuronal Feedback Loop: The Slow-Wave Microcontinuity of the EEG," *IEEE Transactions on Biomedical Engineering,* vol. 47, no. 9, pp. 1185-1194 , September 2000.

[7] A. L. Goldberger, L. A. N. Amaral, L. Glass, J. M. Hausdorff, P. C. Ivanov, R. G. Mark, J. E. Mietus, G. B. Moody, C.-K. Peng and H. E. Stanley, "PhysioBank, PhysioToolkit, and PhysioNet: Components of a New Research Resource for Complex Physiologic Signals," *Circulation,* vol. 101, no. 23, pp. 215-220, 13 June 2000.

[8] M. Mourtazaev, B. Kemp, A. Zwinderman and H. Kamphuisen, "Age and gender affect different characteristics of slow waves in the sleep EEG," *Sleep,* vol. 7, p. 557–564, 1995.

[9] E. Alickovic and A. Subasi, "Classification of ECG signals for cardiovascular diseases detection using different signal processing techniques and machine learning method," Sarajevo, 2012.

[10] A. Subasi, E. Erçelebi, A. Alkan and E. Koklukaya, "Comparison of subspace-based methods with AR parametric," *Computers in Biology and Medicine,* pp. pp 196,199, 2004.

[11] İ. Güler, M. K. Kiymik, M. Akin and A. Alkan, "AR spectral analysis of EEG signals by using maximum likelihood estimation," *Computers in Biology and Medicine,* vol. 31, no. 6, pp. 443-444, 2001.

[12] O. Faust, R. U. Acharya, A. R. Allen and C. M. Lin, "Analysis of EEG signals during epileptic and alcoholic states using AR," *IRBM,* vol. 29, no. 1, pp. 44-52, 2008.

[13] S. Ruggier, "Efficient C4.5 [classification algorithm]," *IEEE Transactions on Knowledge and Data Engineering,* vol. 41, no. 2, pp. 438 - 444, 2002.

[14] O. A. Omitaomu, Lecture Notes in Data Mining, M. W. Berry and M. Browne , Eds., World Scientific Pub Co Inc, 2006.

Tissue Welding with 980nm and 1064nm lasers: Effect of Pulse Modulation

Dž. Katana[1], H.Ö. Tabakoğlu[2]

[1] The Institute of Biomedical Engineering/Department of Biomedical Engineering, Fatih University, Istanbul, Turkey
[2] The Institute of Biomedical Engineering/Department of Biomedical Engineering, Fatih University, Istanbul, Turkey

Abstract— **Lasers have alreday become irreplacable tools in biological applications and in modern medicine as it has the power to cauterize as it cuts, vaporize the tissue and reduce the surgical trauma. Laser tissue welding is a process that utilizes use of laser energy to join or bond tissues and has proven to be effective in clinical applications, such as tissue incision closure. Study was performed on 18 Wister rats (randomly selected) weighing 200-220g in order to study side effects of 980nm and 1064nm laser pulse modulation for which is known to cause milder thermal damages when compared to CW mode. Incisions were made on dorsal region and closed by laser irradiation at 1W for 10 seconds (exposure time) and 5J per spot. Post surgically animals were divided into two groups and sacrificed at 4th and 7th day. Once samples were taken and tissue processed, histological analyses were performed by quantifying thermal changes on tissues by determining and analyzing hypothermal area, granulation and coagulation area as well as the length of the incision line. It was found that closure of incision line was better and thighter at 7th day post-irradiation than at 4th. The incision line length and hypothermal area were less in samples irradiated with 980nm laser than those irradiated with 1064nm laser yet the difference was not significant. Granulation area differed significantly at 4th day where the same pattern was not observed at 7th day. Coagulation area was present in samples of both groups with no statistical difference.**

Keywords— **Pulse modulation, 980nm & 1064nm lasers, photothermal side effects.**

I. Introduction

Based on their power output, lasers can be classified into two groups, continuous mode lasers (CW) and pulse mode lasers [1]. CW operation mode of a laser is a mode which is constantly being pumped and which continually emits light [2]. Optical power of pulse mode lasers is in a pulse form measured on specific time scale at certain repetition rate [1]. The outcome is a laser beam which is 'on' half of the time and 'off' half of the time. One of the main advantages of pulsed operated lasers is their capacity of producing very short pulses with a very high intensity whose duration can range from couple of milliseconds to several femtoseconds and this way can minimize collateral thermal damage [3].

Lasers have adapted well and found use in different areas including tissue welding because of their unique ability of bringing thermal apposition of tissue [5]. Laser tissue welding (LTW) is a process which utilizes use of laser energy in order to bond or join tissue. The major advantages of the laser tissue welding are: direct water tight incision closure, less scar formation, and none of foreign-body reactions against the suture materials. It does not require the insertion of foreign material in the tissue, problems related to undesirable reactions are avoided or eliminated and thus enabling faster wound healing and reduced operative time [4]. Successful LTW primarily relies on factors, such as: the wavelength of laser, optical and thermal properties of tissues, spot size, laser power, exposure time, pulse duration and repetition rate [6,10]. The main disadvantages of the laser procedure are the possible thermal damage (hyperthermia, coagulation, carbonization, vaporization), determining the end-point of the procedure and lack of reproducibility [4].

Lasers as CO2, Er:YAG and Ho:YAG were in use for many years beacuse of their good absorption rate but new studies have showed that longer exposure and high power can cause some side effects such as thermal damage which is the reason why diode lasers were introduced into LTW (800-1064nm). 980nm laser has good absorption in water and hemoglobin [16], allowing controlled tissue ablation and providing a bloodless field for most surgical procedures compared to 1064nm laser light which readily penetrates through the epidermis and reaches the dermis but often damages and chars surrounding tissue causing excessive bleeding with bigger hypothermal area [7,11]. Researches indicate that 980nm laser is lalso effective in wound healing [15] and that it can increase the rate of cell growth within hours of light exposure [13,14]. On the other hand, 980nm wavelength does not reach deeper layers and can result in excessive damage to the epidermis and other healthy skin structures where 1064nm wavelength leads to delayed healing period due to incomplete wound brindging and causes severe thermal side effects [9].

The aim of this study was to examine side effects of 980nm and 1064nm wavelength pulsed modulation for which is know that causes milder thermal damages when compared to CW mode.

II. Materials and Methods

A. AKT-Epidermis dual wavelength laser system

AKT Dual Wavelength Laser System for skin applications is an ultimate laser system with two wavelengths, 980nm and 1064nm, designed to produce radiation with maximum output power of 2 watts. These wavelengths can be used individually or in a combined beam form.

In this study wavelengths were used individually as we were interested in the effects of 980nm and 1064nm laser pulse modulation. Laser parameters (duration, on-off time and power) were chosen according to the previous studies in this area:

1W for 10 seconds and 5J per spot for pulsed mode

(980nm) On Time= 050 Off Time= 050 Duration= 010s Current= 75%

(1064nm) On Time= 050 Off Time= 050 Duration= 010s Current= 80%.

B. Animals and surgery

The research was carried out under a protocol approved by the Institutional Animal Research and Care Ethic Committee at Boğaziçi University, Istanbul. The study was conducted on eighteen (18) randomly selected, male and female Wistar rats, albino rat, one of the most popular rats used for laboratory research. Animals were weighing 200-220g. Rats were housed in plastic cages in vivarium with the controlled temperature (22°±2°C).

18 Wistar rats, male and female were anesthetized with anesthesia solution containing Ketamine (75-100mg/kg) and Xylazine (10mg/kg) by intraperitoneal injection. Hair at the spot of application was shaved, more precisely dorsal region where 0.5cm full incisions were made along parallel but vertical axis on each rat's skin (0.75mm thick). As making incisions resulted in appearance of bleeding, the blood had to be removed and the incision spots had to be cleaned which was accomplished by compressing the site of incisions. This way potential light absorption by blood was prevented. When the surgery was completed rats were divided into two groups (4^{th} day and 7^{th} day).

C. Post-surgery and closure method

Once the surgery was performed, the length and the thickness of the full incisions were checked by using digital caliper. Animals were not given any food or water for the next 24 hours. During 7 days, the healing progress of full incisions was observed where 4th and 7th day were chosen to be control days. Half of the animals were sacrificed at 4th and the other half at 7th day after the irradiation closure of the incisions. On these days, tissue samples closed by AKT-Epidermis Dual Wavelength Laser System were collected and fixed in Formaldehyde Solutions for further histology testing.

Following irradiation closure of the incision, half of the animals were sacrificed at 4th day, and the rest at 7th day. After, the wound sites excised with at least 5mm margin and fixed in Formaldehyde Solution (37% Ph. Eur. Bp Usp, Mercck KGaA 64271 Dermsdart Germany) and the tissue samples were stored in the solution at 4° C.

D. Tissue Processing

The samples contained in plastic cassettes placed in tissue processing machine for 18h where dehydration, clearance and filling with paraffin took place through a series of processing in graded alcohol, xylene and paraffin respectively. The tissues were embedded in paraffin using paraffin embedding machine, Hot (Leica EG 1150 H) and Cold Plate (Leica EG 1150 C). The paraffin blocks were than stored in refrigerator for 24 hours to get well-solidified. Once the excess water is removed and tissue samples placed and supported with a substance that will allow its cutting into thin sections, the process of sectioning was performed.

The paraffin blocked samples were cut into slices in 12 and 14 micron with Tissue Sectioning Machine RM 2255 and then collected on the slides and placed in the incubator for 24 hours to remove excess paraffin from the tissue.

Hematoxylin and Eosin (H&E) staining was used for histological examinations. This stain is one of the main stains and it gives idea about general tissue structure.

E. Microscopic Examination

Under light microscope (Nikon), 4x magnifications and high resolution images were captured with Nikon camera and Imaging software (NIS Elements D 2.30) was used to quantify parameters which gave idea on how successfully an incision closed was by analyzing thermal effects/hypothermal area, granulation and coagulation area and measuring the length of the incision line.

F. Statistical analysis

Histological comparison between two groups (hypothermal area, granulation and coagulation area and the length of the incision line) followed by the arithmetic mean, standard deviation and Student T-test were determined in order to test for statistical differences in the set of data at p= 0.05 level for 980nm and 1064nm wavelength pulsed mode groups.

III. Results

As the aim was studying the side effects of both, 980nm and 1064nm wavelength pulse modulation lasers, a histological comparative study was completed by quantifying thermal changes in tissues by determining and analyzing hypothermal area, granulation and coagulation area as well as the length of the incision line. The areas of interest were photographed and compared.

Histological analyses showed that wound closure for both lasers at 4th day post-irradiation was not fully completed, in other words, there were still some visible openings though the closure was tighter in samples treated with 980nm laser (Fig. 1). The wound closure for both lasers was better at 7th day post-irradiation (Fig. 2).

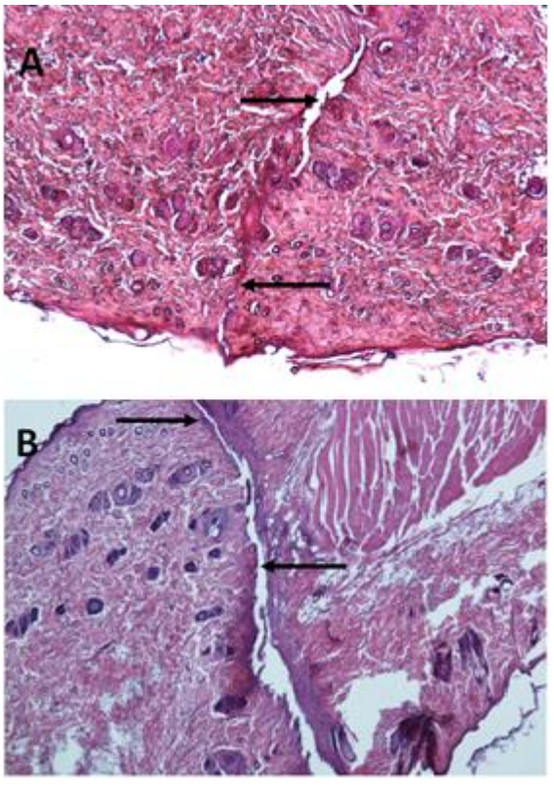

Fig. 1 The incision line appearance at 4th day post-irradiation
A-samples treated with 980nm; B-samples treated with 1064nm

Arithmetic mean of the incision line's length at 7th day post-irradiation in both groups (980nm irradiated and 1064nm irradiated samples) was less than the mean at 4th day post-irradiation which indicates that wound closure is stronger and thighter at 7th day post-irradiation. The incision line's lenght in samples irradiated with 1064nm laser was longer than in ones irradiated with 980nm laser but statistically there was no significant difference between arithmetic mean of the incision line's lengths at 4th and 7th day between these two lasers as $p>0.05$.

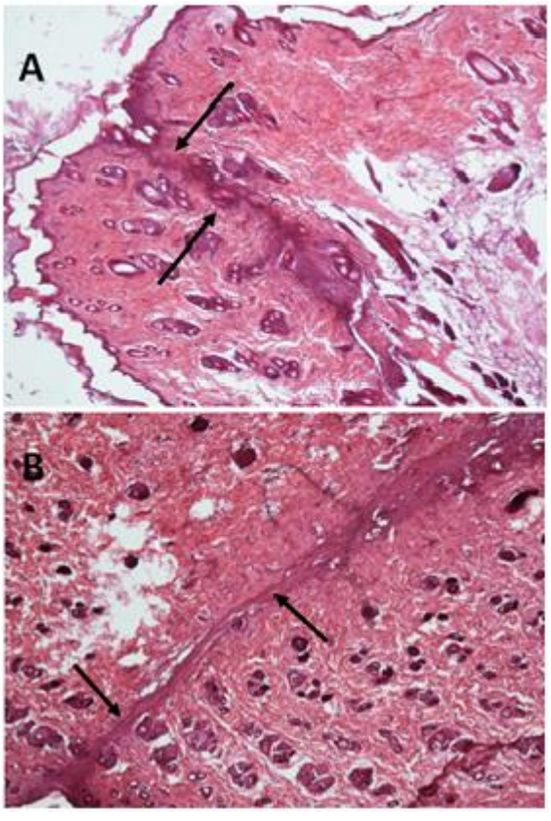

Fig. 2 The incision line appearance at 7th day post-irradiation
A-samples treated with 980nm; B-samples treated with 1064nm

Thermal alterations were observed in samples treated with both lasers. They were histologically assessed by measuring the thermal area, hypothermal area and granulation area. Histological examination showed a notable tissue alteration in irradiated regions in both 980nm and 1064nm laser. Side effects were more noticeable at 4th day post-irradition for both lasers thus more present in samples irradiated with 1064nm laser (Fig. 3).

All the thermal changes reduced at 7th day in both groups (Fig. 4). Again, there was no noticable significant statistical difference found in side effects mean at 4th and 7th day for both lasers except for the A-G (granulation area). A-G mean at 4th day in 980nm and 1064nm irradiated samples was found to differ significantly ($p<0.05$). The same patteren was not observed at 7th day (Fig. 5).

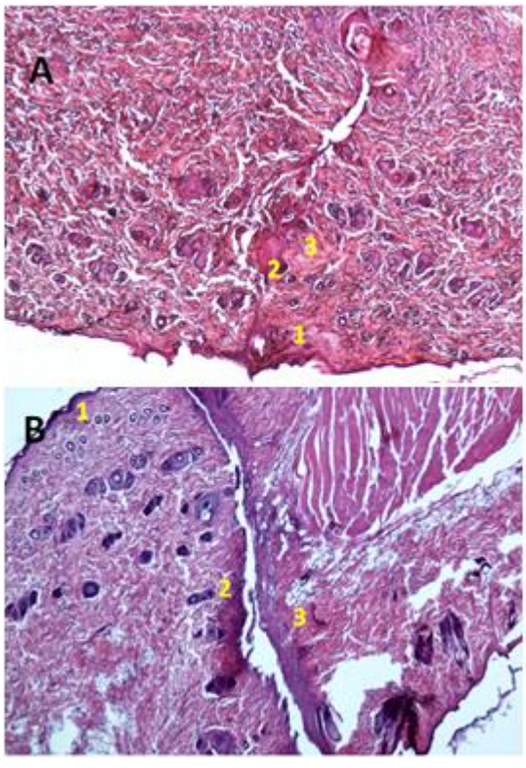

Fig. 3 The Coagulation Area (1), Granulation Area (2) and Hypothermal Area (3) appearance at 4th day post-irradiation; A-samples treated with 980nm; B-samples treated with 1064nm

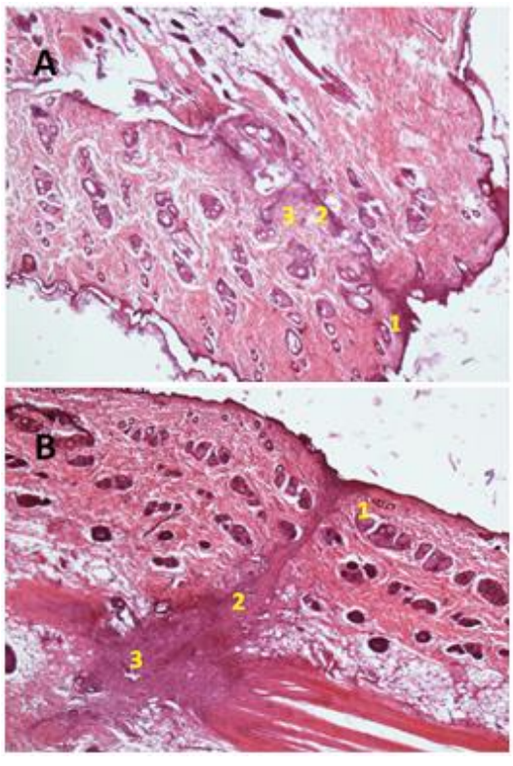

Fig. 4 The Coagulation Area (1), Granulation Area (2) and Hypothermal Area (3) appearance at 7th day post-irradiation; A-samples treated with 980nm; B-samples treated with 1064nm

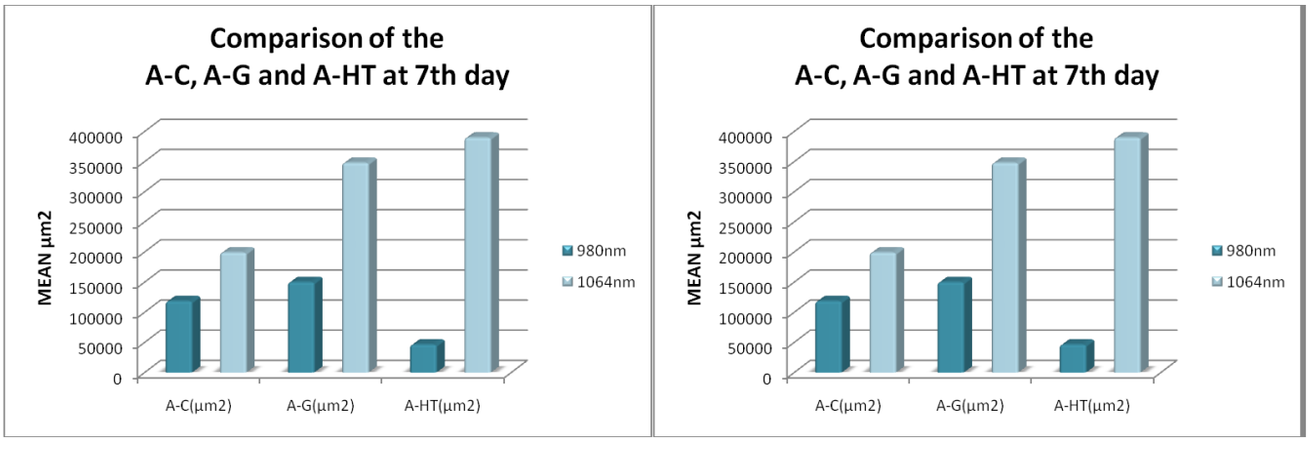

Fig. 5 Graphical representation of Arithmetic Mean for the Coagulation Area A-C, Granulation Area A-G and Hypothermal Area A-HT at 4th and 7th post-irradiation day for 980nm and 1064nm laser

IV. Discussion

Pulse mode coagulation gives milder thermal damage to the tissue when compared to CW mode coagulation. One of the main advantages of pulsed operated lasers is their capacity of producing very short pulses with a very high intensity.

980nm laser has good absorption in water and hemoglobin, allowing controlled tissue ablation and providing a bloodless field for most surgical procedures compared to 1064nm laser light which readily penetrates through the epidermis and reaches the dermis but often damages and chars surrounding tissue causing excessive bleeding with bigger hypothermal area. The absorption peak of 980nm laser by melanin is not as high as the absorption peak of 780nm and 815nm diode lasers, which gives this laser an advantage of better penetration into deeper tissue layers, approximately 3mm to 4mm [7].

The 1064nm laser among all non-ablative laser sources holds the most prominent position. This laser is also known to mainly produce photothermal effects on the irradiated skin due its penetrativity and it is easily absorbed by melanocytes [8,12].

As the objective of the research was to evaluate side effects of 980nm and 1064 nm wavelength pulse modulation, a histological comparative study was completed by quantifying thermal changes in tissues by determining and analyzing hypothermal area, granulation and coagulation area in the region adjacent to the irradiated site from either side of the incision line. Also, as the length of the incision line was measured.

The results have showed that arithmetic mean for coagulation area (A-C) and hypothermal area (A-HT) (μm2) does not differ significantly as $p>0.05$ for 4th and 7th days but with higher mean for 1064nm laser at 4th and 7th day. Reduction of previously mentioned areas was noticed at 7th day for both lasers but with higher arithmetic mean for 1064nm laser. Thus it can be concluded that side effects diminish by time for both lasers.

Granulation area (A-G) at 4th day in 980nm and 1064nm irradiated samples was found to differ significantly ($p<0.05$). The same patteren was not observed at 7th day where the reduction of granulation area was noticed in both groups.

Moreover, histological analyses have showed that wound closure for both lasers at 4th day post-irradiation was not fully completed, in other words, there were still some noticeable openings (Fig. 3). The complete wound bridging for both lasers was noted at 7th day post-irradiation though the closure was tighter in samples irradiated with 980nm laser (Fig. 4).

Arithmetic mean of the incision line's length at 7th day post-irradiation in both groups (980nm irradiated and 1064nm irradiated samples) was less than the mean at 4th day post-irradiation which indicates that wound closure is stronger and tighter at 7th day post-irradiation. The incision line's length in samples irradiated with 1064nm laser was longer than in ones irradiated with 980nm laser but still there was no significant statistical difference between arithmetic mean of the incision line's lengths at 4th and 7th day between two groups ($p>0.05$).

V. Conclusions

980nm and 1064nm lasers operated in pulse mode have shown to be good nominees for skin wound closure. Side effects in both groups caused by the laser irradiation were noticed at 4th and 7th days after wound closure but more present at 4th day in samples irradiated with 1064nm laser. Reduction of A-C, A-G and A-HT was noticeable at 7th day in both groups. The reduction in incision line's length has also been noticed at 7th day. Therefore, it can be concluded that the side effects, results of 980nm and 1064 nm irradiation, get smaller with time. Everything being taken in account, we may conclude that both lasers were effective in wound closure with both of them causing side effects with no significant statistical difference between them at 4th and 7th day post-irradiation except A-G at 4th day.

ACKNOWLEDGMENT

The authors thank Boğazici University, The Institute of Biomedical Engineering Biophotonic laborotory for allowing us to use their equipment, devices and materials and for making this research possible.

REFERENCES

1. http:// diowavelaser.com
2. Rudiger Paschotta, *Encyclopedia of laser physics and technology*, John Wiley and Sons; 1 edition, New Jersey, 2008.
3. Parasan N. Prasad, *Introduction to Biophotonics, Wiley-Interscience*; 1 edition, New Jersey, 2003.
4. K. Kyunghan, G. Zhixiong, Ultrafast Radiation Heat Transfer in Laser Tissue Welding and Soldering, *Taylor & Francis Volume: 46,* Issue: A, 2004, pp 23-40.
5. A. M. Gobin, D. P. O'Neal, D. M. Watkins, N. J. Halas, R. A. Drezek, J. L. West, Near infrared laser tissue welding using nanoshells as an exogenous absorber, *Lasers Surg. Med. Volume: 37*, Issue: 2, 2005, pp 123–129.
6. L. S. Bass, M. R. Treat, Laser tissue welding: A comprehensive review of current and future clinical applications, *Lasers Surg. Med. Volume: 17*, Issue: 4, 1995, pp 315–349.
7. I. Cilesiz, S. Thomsen, A. J. Welch, E. K. Chan, Controlled temperature tissue fusion: Ho:YAG laser welding of rat intestine *in vivo*, part two, *Lasers Surg. Med. Volume: 21*, Issue: 3, 1997, pp 278–286.

8. A. Rosenbach, C. M. Williams, T. S. Alster, Comparison of the Q-switched alexandrite (755 Nm) and Q-switched Nd:Yag (1064 Nm) lasers in the treatment of benign melanocytic nevi, *Dermatologic Surgery Volume: 23*, Issue: 4, 1997, pp 239–244.
9. M. H. Khan, R. R. Anderson, R. K. Sink, D. Manstein, D. Eimerl, Intradermally Focused Infrared Laser Pulses: Thermal Effects at Defined Tissue Depths, *Lasers in Surgery and Medicine Volume: 36*, Issue: 4, 2005, pp 1–11.
10. Markholf H. Niemz, *Laser-Tissue interactions*, Springer; 2 edition, New York, 2007.
11. G. Murat, D. Zeynep, H. O. Tabakoglu, B. Ozguncem, Closure of skin incisions by 980-nm diode laser welding, *Lab. Med. Sci. Volume: 21*, Issue: 1, 2006, pp 5-10.
12. J. Parker, I. Hamzavi, Q-switched Nd:YAG 1064-nm laser for the treatment of acne-Induced postinflammatory hyperpigmentation, *Journal of the American Academy of Dermatology Volume: 60*, Issue: 5, 2009, pp 198.
13. C. C. Dierickx, The role of deep heating for noninvasive skin rejuvenation, *Lasers Surg. Med. Volume: 38*, Issue: 9, 2006, pp 799-807.
14. D. S. Mark, C. Scott, Effects of Infrared laser exporsure in a cellular model of wound healing Lasers, *Lasers Surg. Med. Volume: 38*, Issue: 9, 2006, pp 699-703.
15. H. O. Tabakoglu, D. K. Zeynep, Tissue welding with 980-nm diode laser system: preliminary study for determination of optimal parameters, *Photonic Therapeutics and Diagnostics Volume: 6078*, Issue: 39, 2006, pp 177-183.
16. H. O. Tabakoglu, T. Nermin, G. Murat, The effect of irradiance level in 980-nm diode laser skin welding, *Photomedicine and Laser Surg. Volume: 28*, Issue:4, 2010, pp 453-458.

Dž. Katana, The Institute of Biomedical Engineering, Fatih University, 34500 Büyükçekmece, 34000 Istanbul, Turkey (phone: 905-35-078-39-78; e-mail: dzanakatana@hotmail.com)

Texture-based automatic polyp detection in colonoscopy videos

A. Avramović and I. Ševo

Faculty of Electrical Engineering, University of Banja Luka, Bosnia and Herzegovina

Abstract— **Analysis of colonoscopy, endoscopy and smart pill videos are often used during the diagnostic procedure, so automatic detection of colon polyps, tumors and internal bleeding can be helpful. Automatic video analysis can ease or improve diagnostic process in cases where physician needs to analyze long-duration videos in order to check if there are signs of early tumor stage or bleeding. Automatic detection of regions of interest and video annotation can be used to mark relevant frames and enable faster and more efficient diagnosis. In this paper, a method for texture analysis of colonoscopy video is presented. Different texture descriptors are extracted from regions containing polyps and compared with the texture descriptors taken from the regions of healthy tissue and other non-informative regions. The goal was to systematically assess the possibilities for automatic detection of colon polyps in colonoscopy videos based on their texture.**

Keywords— **Colonoscopy, polyp, texture.**

I. Introduction

Colon polyps are clumps of cells forming at the lining of the colon. Although most colon polyps are harmless, over time some of the untreated polyps can develop into colon cancer. Thus, it is important to have regular polyp screening, especially for the higher risk population (seniors, smokers or persons with history of colon cancer within the family). One of the most efficient screening methods is colonoscopy, which is an endoscopic bowel examination with camera on a flexible tube passed through the anus. Although colonoscopy is efficient method for finding and removal of the polyps, it is an uncomfortable procedure for the patient. As an alternative, non invasive virtual colonoscopy, based on CT and MR scans can be used, but still with limited possibilities for diagnosis [1], whereas other methods include customized blood tests [2]. Another screening approach involves Smart Pill technology [3] [4]. It is a minimally invasive approach that gives direct view to the inside of the colon. Patient swallows the pill, approximately 2 cm long, equipped with a camera, which provides video of the interior with 2–8 frames per second. This way, patient is treated with an easy to swallow and dispose capsule, without need for sedation, radiation or air-inflation. Since capsule may provide long duration videos, overview of the screening results can be time consuming. Therefore, automatic detection of polyps during the unattended video processing would be useful for faster and efficient diagnosing. Breakthrough of colonoscopy and smart pill technology increased attention to the problem of polyp detection.

A number of papers considers the classification of polyp images obtained from the various medical studies [3] [4] [5]. Common approach of these studies include partitioning of images, extracted from the videos, into the polyp class and non-polyp class, as well as offline classification. In this research we consider the possibilities to automatically detect polyps during the video processing, according to their texture. We also suggest the framework for simple survey of the video in frame by frame manner. The main idea was to introduce an algorithm able to process the video, as fast as possible. During the processing, the regions of interest would be adequately labeled, allowing physicians to easily find and overview the frames with the most interesting content.

This paper is further organized as follows. Section II briefly describes the proposed solution; Section III introduces descriptor used for texture analysis. Section IV describes used data and research methodology in details, while Section V describes classification approach, In Section VI the experiments are described and a detailed analysis of the results are given and Section VII gives concluding remarks.

II. Proposed framework

The goal of the analysis of colonoscopy and smart pill videos is the detection and labeling of regions showing interesting events, i.e. the polyps in this particular research. The proposed framework was designed to achieve two basic goals: (1) high detection efficiency and (2) fast execution. High efficiency means achieving high true positive rate (detection of the region showing polyps) and low false positive rate (not detecting the regions showing healthy tissue). Fast execution is important to enable multiple runs over the long duration videos, since unattended video analysis may require processing with different parameters. In order to achieve fast execution, proposed framework avoids the usage of the computationally expensive statistical learning techniques. It is based on the simple comparison of the processed region with ground truth dataset that provides the knowledge of what should be detected. The final result of the analysis should be annotation of the regions showing

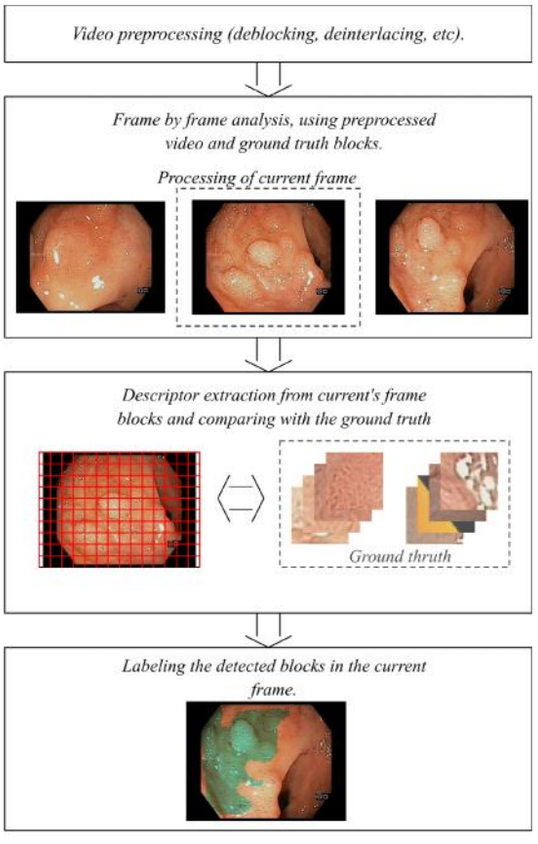

Fig. 1 Block scheme of the proposed framework (best view in color).

polyps if the specific frame if exists. If one region (group of pixels, blocks) is detected it is denoted as *Positive*, otherwise it is denoted as *Negative*.

Proposed solution contains several phases: (1) video preprocessing, (2) frame by frame analysis, (3) descriptor extraction from current block, (4) comparing with the ground truth dataset, and (5) labeling the current block as either *Positive* or *Negative*. The block scheme of the proposed method is given in Fig. 1.

III. Texture descriptors

A. Local Binary Pattern

The first version of Local Binary Pattern (LBP) exploits local texture features of *3x3* neighborhood in order to produce 256-bins occurrence histogram used for texture description. The central pixels is compared with interpolated values of the neighborhood pixels to produce *8*-bit binary number which is assigned one of the $2^8 = 256$ unique values. Later, Ojala *et. al.* [4] introduced rotation invariant and uniform version of the descriptor, using only uniform patterns. One specific patterns is declared as uniform if *8*-bit binary number has at most two 0/1 changes.

We used multi-resolution pattern analysis, as proposed in [4], to extract feature vectors from all three color bands separately, after which we concatenated them in one 162 dimensional texture descriptor (rgbLBP). Also, we implemented a multispectral version of LBP in which one pixel is processed in color, thus yielding a sparse descriptor with large dimensionality (concLBP) of 1000.

B. CENTRIST

CENTRIST is another efficient local texture descriptor which uses a similar pattern analysis as LBP. It is a histogram obtained from the image after Census Transform [5]. Census Transform uses *3x3* neighborhood to calculate binary pattern. CENTRIST also uses division of image space into 31 subblocks in two levels. Since we use CENTRIST to describe of *64x64* size blocks we avoid further block division to reduce descriptor dimensionality. Feature vector is extracted from each color band separately and later concatenated into one descriptor with total dimensionality of 762.

IV. Used data and methodology

The colonoscopy high resolution video of *576x768* pixels, showing the usual screening and intervention procedure, is used as input. In order to provide the knowledge for the ground truth dataset, frames containing polyps were extracted from the video and divided into blocks of size *64x64* pixels. Several blocks from the polyp region were manually extracted and labeled as *Positive*. On the other hand, several blocks showing healthy tissue were joined with non-informative blocks and labeled as *Negative*. Examples of the *Positive* and *Negative* blocks are given in Fig. 2 and Fig. 3, respectively. By visual comparison of block from these two classes, we can notice that *Positive* blocks have specific wrinkled pattern different from the Negative block texture. Therefore, we used texture descriptors, proven to have good classifying abilities, namely Local Binary Pattern [5] and CENTRIST [6].

From each block from *Positive* and *Negative* class texture descriptor was extracted in order to obtain the ground truth knowledge. Colonoscopy video was analyzed in frame by frame manner. Each frame is divided into overlapping blocks of size *64x64* so that the same texture descriptors can be extracted from these blocks. In order to detect the region containing polyp at the current frame, the descriptor from each block was compared with the ground truth descriptors, i.e. descriptors from the training set. Evaluation of the possibilities of automatic polyp detection in colonoscopy video is done with the simple framework described in Section II.

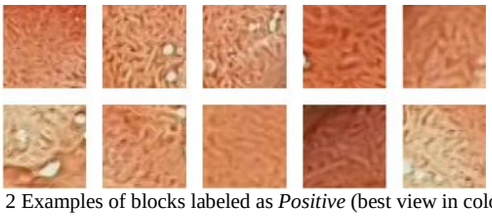

Fig. 2 Examples of blocks labeled as *Positive* (best view in color).

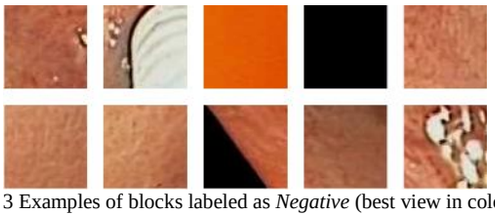

Fig. 3 Examples of blocks labeled as *Negative* (best view in color).

As it was earlier described, the ground truth is taken from manually labeled blocks. All texture descriptors described in previous Section are tested with nine frames extracted from video, given in Fig. 4. These frames are chosen to enable testing typical cases, thus we have: (1) frames with polyps, (2) frames with healthy tissue and (3) non informative frames. In all experiments, we used the same parameters. The block overlapping is used with the step 8 and sensitivity is set to 2 (highest possible).

In order to evaluate the true positive/false negative ratio, we manually labeled the polyp regions on three test frames (the first row on Fig. 4) to obtain ground truth mask. The ground truth mask is later compared with the output mask.

V. Classification approach

If texture descriptor of the current block is closer to *Positive* texture descriptor that to *Negative* texture descriptor, the current block is labeled as *Positive*. Otherwise, it is declared as *Negative*. In order to avoid coarse division the overlapping of the blocks is enabled as well. Therefore, one pixel can be examined during the processing of several blocks. Level of sensitivity could be controlled with the number of detection required to declare one pixel as *Positive*. Generally, if we denote the size of the block as B and the block step (number of pixels between centers of two overlapped blocks) as St, one pixel can be examined within N blocks, where N is:

$$N = (B/St)^2 \qquad (1)$$

If lower sensitivity is required, the higher number of *Positive* detections will be needed in order to declare one pixel *Positive*. Therefore, sensitivity S is inversely proportional to the number of *Positive* detections. If we denote the number of required detections with D, the highest sensitivity is in the case when $D = N/2$ and the lowest sensitivity is in the case when $D = N$. Generally, we can introduce:

$$S = N/D \qquad (2)$$

where S is in the range $[1,2]$.

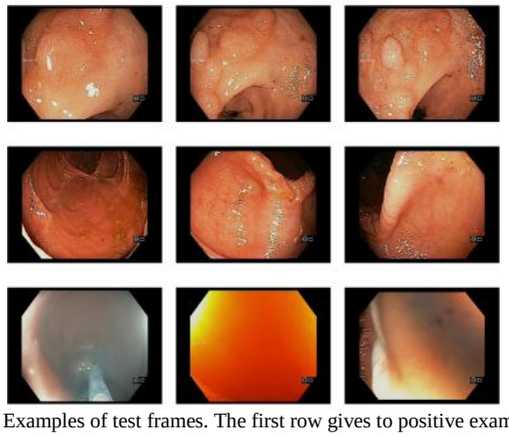

Fig. 4 Examples of test frames. The first row gives to positive examples, frames with polyp regions. The second row show frames with healthy tissue, and the third row gives examples of non-informative frames (best view in color).

We used two different approaches to determine if one block is closer to *Positive* or *Negative* class:

- **NearestMean**: This approach calculates the average texture descriptor for both *Positive* and *Negative* ground truth blocks. Current block is labeled as *Positive* if the Euclidean distance of block's descriptor is smaller from the *Mean Positive* than from the *Mean Negative* descriptor.
- **NearestNeighbor**: This approach includes the calculation of Euclidean distance of the block's descriptor from all descriptors extracted from *Positive* and *Negative* blocks. Than the smallest distance is used to decide how to label the current block.

We can notice that *NearestMean* and *NearestNeighbor* are two opposite approaches. *NearestMean* uses only one characteristic descriptors that should describe all blocks from the class which is less informative, but less time consuming. Contrary, *NearestNeighbor* approach uses a diversity of class descriptors but it is more time consuming.

VI. Experiments

A. Experimental setup

The proposed framework as well as texture descriptors were implemented in C#. Descriptors are tested with both *NearestMean* and *NearestNeighbor* approach. Euclidean

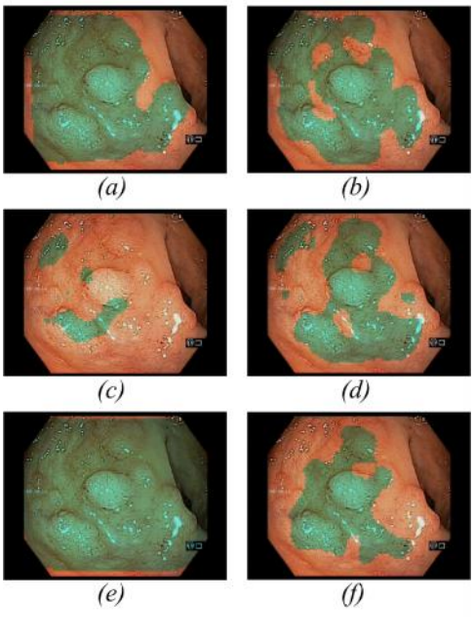

Fig. 5 Results of processing one positive frame with different descriptors and different approaches: (a) CENTRIST with *NearestMean*, (b) CENTRIST with *NearestNeighbor*, (c) rgbLBP with *NearestMean*, (d) LBPriu2 with *NearestNeighbor*, (e) concLBP with *NearestMean*, and (f) concLBP with *NearestNeighbor*. Green areas are detected regions of interest (best view in color).

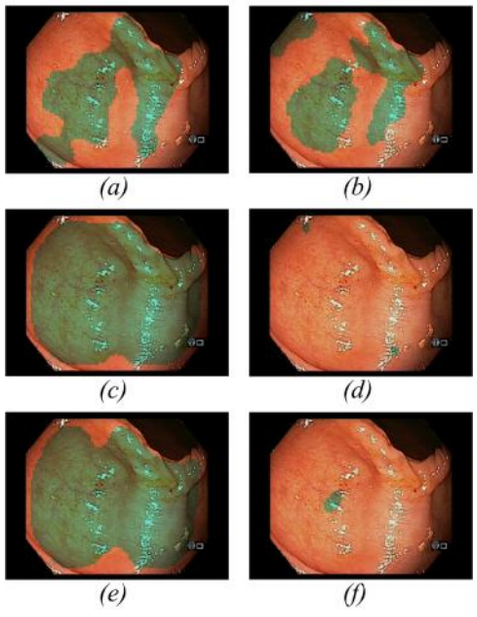

Fig. 6 Results of processing one negative frame with different descriptors and different approaches: (a) CENTRIST with *NearestMean*, (b) CENTRIST with *NearestNeighbor*, (c) rgbLBP with *NearestMean*, (d) LBPriu2 with *NearestNeighbor*, (e) concLBP with *NearestMean*, and (f) concLBP with *NearestNeighbor*. Green areas are detected regions of interest (best view in color).

distance was used as distance measure between descriptors in each case. The aim of these experiments was to examine if the proposed approach is able to satisfy two major goals mentioned in Section II. Since faster and more accurate processing is desirable, we also examined the time consumption of proposed approaches.

B. Results

Examples of the output frame processed with different descriptors and different detection approaches for one positive and one negative frame are given on Fig. 5 and Fig. 6, respectively. By examining the results in all these cases we can give several observations. CENTRIST-based approaches have good performance for detection of polyp regions for the positive frame, but large false positive rate for negative frame. The reason for this may be the very similar wrinkled texture of both polyp and certain regions of healthy tissue. Nevertheless, *Nearest-Neighbor* approach combined with LBP descriptor gives significantly smaller false positive rate comparing to CENTRIST descriptor. For both positive and negative frame, the *NearestNeighbor* approach gives better true positive/true negative detection comparing to *NearestMean* approach. In the case when non informative frame is processed, we can notice small true positive rate, due to wrinkled texture of regions with distinct reflection artifact. We can conclude that texture can be used for efficient automatic polyp detection, but the reduction of the false positive rate is required. The ways to achieve that include customized descriptor as well as inclusion of color and morphology description.

C. Time consumption

The fast execution of the proposed solution is of significant importance, thus the time consumption was analyzed as well. Since the proposed solution uses frame by frame video processing approach, in Table 1. we give the averaged processing time for one frame for the different descriptors and classification approaches. All experiments are executed on computer with Intel Core i3-3320 CPU on 3.3 GHz. We can notice that methods based on rgbLBP descriptor are significantly more time demanding. The reason for this can be found in computational expenses of interpolation needed for multi-resolution analysis in every spectral band. On the other hand, concLBP is less time demanding since it uses analysis on single resolution, jointly from all spectral bands. CENTRIST based methods are the fastest since it uses the simplest calculation for feature detection. Also, it is interesting to notice that *NearestNeighbor* approach does not consume additional time comparing to *NearestMean.* Reason for this is the small number of ground truth block used in

Table 1 Averaged frame processing time consumption for different descriptors and classification approaches, in the cases where 8 pixel and 16 pixel step is used.

Descriptor and classification approach	8 pixel step	16 pixel step
CENTRIST with *NearestMean*	2 seconds	1 second
CENTRIST with *NearestNeighbor*	2 seconds	1 second
rgbLBP with *NearestMean*	120 seconds	29 seconds
rgbLBP with *NearestNeighbor*	120 seconds	30 seconds
concLBP with *NearestMean*	23 seconds	5 seconds
concLBP with *NearestNeighbor*	23 seconds	5 seconds

Table 2 Averaged true positive/false negative for different descriptors and classification approaches.

Descriptor and classification approach	True positive	False negative
CENTRIST with *NearestMean*	95%	5%
CENTRIST with *NearestNeighbor*	90%	10%
rgbLBP with *NearestMean*	97%	3%
rgbLBP with *NearestNeighbor*	90%	10%
concLBP with *NearestMean*	97%	3%
concLBP with *NearestNeighbor*	85%	15%

this experiment. Nevertheless, time consumption is high manly because of the high resolution of processed images and the large number of examined blocks due to the small step. We can notice significantly smaller time consumption in the case when pixel offset is increased, but larger step produces more coarser region labeling.

D. Detection accuracy

As it was described before, detection accuracy is evaluated comparing of the output mask and the manually labeled mask. Averaged true positive and false negative values obtained in this comparison, for the different descriptors, are given in the Table 2. In all cases step 8 and sensitivity 2 is used. By analysis of the results we can notice high percentage of true positive detections. On the other side, there is a significant percentage of false positive detections, especially when the *NearestMean* classification approach is used, which can result in significant false detections on negative frames.

VII. CONCLUSIONS

In this paper we examined possibilities for automatic polyp detection in colonoscopy video of high resolution, based on texture analysis. We analyzed three different texture descriptors and two classification approaches. Overlapping of blocks is used to deal with coarse classification. We concluded that automatic detection is possible with the cost of high false positive rate, so future work will include color and morphology description.

The second interesting point is that classification based on *NearestNeighbor* approach reduces false positive rate without significant time consumption. Also, customization of texture description will be considered in future work.

ACKNOWLEDGMENT

The research was supported by NORBOTECH (NORwayBOsnia TECHnology Transfer) project for Programme in Higher Education, Research and Development by Norwegian Ministry of Foreign Affairs, and by the Ministry of Science and Technology of the Republic of Srpska under contract 19/6-020/961-187/14.

REFERENCES

1. Z. Wang, L. Li, J. Anderson, D. Harrington and Z. Liang, Computer Aided Detection and Diagnosis of Colon Polyps with Morphological and Texture Features, *Medical Imaging 2004: Image Processing, Proceedings of SPIE Vol. 5370,* 2004.
2. L.A. Alexandre, J. Casteleiro and N. Nobreinst, Polyp Detection in Endoscopic Video Using SVMs, *Lecture Notes in Computer Science Volume 4702, pp 358-365,* Springer 2007.
3. M. Franz, M. Scholz, I. Henze, S. Rockl and L. I. Gomez, Detection of colon polyps by a novel, polymer pattern-based full blood test, *Journal of Translational Medicine* 2013, *11:278 doi:10.1186/1479-5876-11-278*
4. B. Li, M. Q.-H. Meng and J. Y. W. Lau, Computer-aided small bowel tumor detection for capsule endoscopy, *Artificial Intelligence in Medicine, Elsvier Volume: 52,* 2011 , pp 11-16.
5. B. Li and M. Q.-H., Computer-based detection of bleeding and ulcer in wireless capsule endoscopy images by chromaticity moments, *Computers in Biology and Medicine, Elsvier Volume: 39,* 2009 , pp 141-147.
6. T. Ojala, M. Pietikainen and T. Maenppa, Multiresolution gray-scale and rotation invariant texture classification with local binary patterns, *IEEE Transaction on Pattern Analysis and Machine Intelligence, Volume: 24,* 2002 , pp 971-987.
7. J. Wu and J. Regh, CENTRIST: A visual descriptor for scene categorization, *IEEE Transaction on Pattern Analysis and Machine Intelligence, Volume: 33,* 2011 , pp 1489-1501.

A. Avramović is with the Faculty of Electrical Engineering, University of Banja Luka, Patre 5, 78000 Banja Luka, BiH (e-mail: aleksej@etfbl.net)

I. Ševo is with the Faculty of Electrical Engineering, University of Banja Luka, Patre 5, 78000 Banja Luka, BiH (e-mail: igor.sevo@etfbl.net)

The validation of smartphone's built-in cameras for heart rate extraction

J. Nišić[1], N. Beganović[1], E. Zaimović[1], L. Goletić[1], E. Hujdur[1] and A. Šećerbegović[1]
[1] Faculty of Electrical Engineering, University of Tuzla, Tuzla, Bosnia and Herzegovina

Abstract - **The revolution of mobile devices has lead to the development of different applications for monitoring individual's health and wellbeing. Various smartphone's features can be utilized for the acquisition of different signals such as electrocardiogram, heart rate, position, location etc. Measuring heart rate is of great importance for the prevention and treatment of cardiovascular diseases. Several applications have already been introduced for heart rate measurement by placing fingertip on the back of smartphone's camera. In this paper, we have tested smartphone's front-camera for the recording of individual's face and extraction of photoplethysmography signal. Mobile application records skin color changes from face in real time and extracts average intensity of RGB components for each frame. The obtained photoplethysmography signal is being processed in real time and different filtering operations are being applied in order to increase accuracy of extracted heart rate values. iPhone application was developed and tested on ten individuals in daylight with good light conditions. Texas Instruments Chronos EZ430 watch along with Blue Robin heart rate monitor were used for validation. Our results demonstrate that low-resolution front-facing camera has potential for contact-free heart rate estimation, compared to commonly used back camera.**

Keywords - **heart rate, photoplethysmography, smartphone, camera.**

I. INTRODUCTION

Smartphones have become an indispensable part of everyday life. Various integrated sensors allow mobile devices to communicate with its environment and collect data in order to measure different physical quantities. This allows smartphones to transform into powerful mobile measurement systems. Special attention has been give to the ability of smartphones to measure various health parameters like heart rate (HR)[1-3], blood pressure[4][5], posture[6][7] etc. Heart rate is one of the most important health indicators, which is measured as the number of times the heart beats per minute. When the body is in a good condition, the heart needs less effort and fewer beats per minute to pump blood through the blood vessels to the muscles. Heart rate is also changing depending on the human's emotional and mental state. It depends on the situation and enviroment in which measurment is being performed. Using smartphone for heart rate measurement allows for monitoring in a non-clinical enviroment, which leads to the reduction of the noise caused by fear of clinical surroundings. In the literature, as well as in the commercial application stores, there are several types of applications for HR measurement. These applications demand direct contact with the smartphone camera, usually fingertip, in order to detect small changes in the skin's color. By using various digital signal processing techniques, it is possible to estimate heart rate with small error rate[1-3]. Previous studies demonstrated that non-contact heart rate monitoring also provides reliable results [8][9]. In this paper, we have tested smartphone's built-in front camera for contact-free heart rate monitoring. Instead of the fingertip, individual's face is used for detecting different color changes and it generates a photoplethysmography (PPG) signal. Face detection is necessary in order to select particular face feature, usually the forehead, for better quality of the obtained PPG signal. iPhone application is developed and described that utilizes the front-facing camera and provides the user with reliable heart rate measurements. Our results demonstrate that front camera can reliably detect heart rate changes, compared to commerical heart rate monitor.

II. WORKING PRINCIPLE

Photoplethysmography (PPG) presents an optical method for the detection of blood volume changes [13]. In order to obtain PPG signal, it is necessary to have a light source and photosensitive detector. Measurement methods can be reflective or transmissive light, which depends on whether the light source and the detector are on the same side or the opposite. Today's fast digital cameras allow for the acquisition of reflective PPG signal, without any contact with the patient. In this paper, PPG is extracted from video sequence and it contains pulses that reflect changes in vascular blood volume of the visible skin within each cardiac beat. Photoplethysmography has been used for estimation of heart rate [9], heart rate variability [10], oxygen saturation [11], respiration rate [12] etc .

Since smartphones have already been involved into healthcare service delivery, their built-in cameras were also tested for the detection of PPG signal. Back camera of the smartphone is usually designed with superior performances, compared to the front camera. Since the front camera is designed for video calls, it compromises image quality and size in order to make it possible to transfer the video signal with as less as possible jerkiness and freezing percentages

as well as black frames ratio. Smartphone that has been used in this paper has 1.2-megapixel sensors in front camera, while its back camera contains 8-megapixel sensors, which allows for better recording quality in low-light conditions. Unlike the front-facing camera, rear camera supports optical image focus and stabilization, while this needs to be done manually when using the front one. These specifications clearly show that much better results can be achieved with much less effort using the rear camera, but in this paper we wanted to investigate the quality of PPG signal with front-facing camera in a well-lit environment. One of the biggest advantages of using the front camera for heart rate detection is easier handling because the user can exactly see what he is recording. This allows for proper positioning of the individual's face, which can minimize noise due to the movement.

Obtained video recording was executed with 25 frames per second. This frame rate can be used for heart rate estimation, due to the fact that heart rate frequency bandwidth is considered between 0.7 and 4 Hz, which corresponds to the heart rate range between 45 and 200 bpm. As each digital image is composed of red, green and blue (RGB) color components, it is necessary to use the component, which has the highest amplitude in heart rate frequency domain. Previous research demonstrated that green color component has the biggest hemoglobin absorption [8][9] and it was also used for our testing. After the initial recording with smartphone, all signal processing operations were executed offline, using MATLAB (The MathWorks, Inc.).

Figure 1 shows average color intensities for each channel during one measurement and confirms the fact that blood volume changes of the green component are prevailing compared to others in time domain.

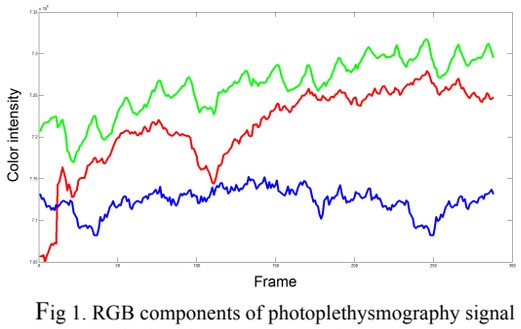

Fig 1. RGB components of photoplethysmography signal obtained by smartphone's front camera

In order to extract heart rate values, preprocessing operations are required in order to remove the noise due to the movement and light changes. Average intensity of the green component is being filtered using slightly modified moving average filter (since it is non-causal system in its original form [14]) (Eq. 1)

$$y[n] = \frac{1}{M}\sum_{k=0}^{M-1} x[n-k] \quad (1)$$

where *y[n]* is the output value (color intensity for current frame), *x[n – k]* is the input signal (color intensity for previous frames) and *M* is the window width. We have used M = 9 samples because it provided best results. Heart rate was estimated in frequency domain (Eq. 4),

$$HR = 60 * f_{max} \quad (2)$$

where f_{max} is the frequency of the highest peak in heart rate frequency range (0.7 – 4 Hz).

Validation of the results was performed using professional device with declared accuracy 99% - Texas Instruments Chronos EZ430 watch (Figure 2) along with BM Innovations BM - CS5 chest strap. EZ430 Chronos is a highly integrated mobile development tool of Texas Instruments in form of a sport watch. The watch was used as a heart rate monitor – it wirelessly collects data obtained from chest strap and shows heart rate results on the LCD display.

Fig. 2 Texas Instruments EZ430 Chronos watch and BlueRobin Heart rate monitor

III. Implementation

The application consists of two subsystems: iPhone application used for signal acquisition and MATLAB script for post-processing and final calculations (Fig. 3). The following subsections contain detailed explanation of the designed system.

A. Initial setup

Implemented application uses iPhone's front camera for continuous video recording. Video session used 25 fps

recording frame rate (although the device supports frame rates up to 240 fps) because it was enough for heart rate estimation and to keep CPU usage less intensive. This would enable to use the smartphone for signal processing in real time with minimal battery discharge. Apple iPhone 6, which was used in this paper, features Apple A8 chipset built on 64-bit architecture and M8 motion co-processor [16]. With this configuration, it was possible to execute complex calculations along with the acquisition of the signals from camera. The application is multithreaded and consists of the separated modules for ensuring effective user interaction and signal processing at the same time. Video session was recorded for 10 seconds after initial stabilization, which lasts several seconds.

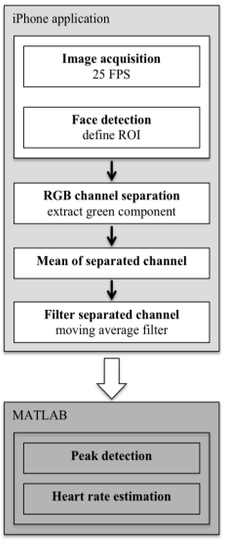

Fig. 3 Structure of the implemented system

The application uses non-compressed video data directly from the video memory and reads only values of green component intensity. These values are being averaged for each region of interest in real time immediately after they are written into the buffer. Region of interest has been defined by Apple's face detection API. These averaged values are input signal for MA filter and its output is being stored locally so it could be exported after finishing measurement. All processing operations, from face detection to filtering, have been done repeatedly for each acquired frame. During the measurement and performance, inspection and benchmarking have shown 27% CPU utilization percentage. These values are satisfying for the design of energy-efficient application, as well as to make it usable on older devices with less processing power. After basic processing, the signal is ready for extraction and further analysis in MATLAB. Screenshot of implemented application is shown in Figure 4.

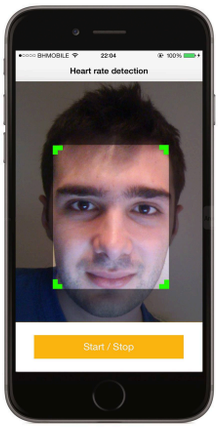

Fig. 4 Screenshot of the application during the measurement

IV. Results

10 subjects (3 females and 7 males) at the age of 24 ± 3 took a part in field-testing and experiments with the application. They were instructed to sit and hold smartphone in a hand at a distance of 20 cm from their face during the 15 seconds long measurement process. Tests were performed indoor in a well-lit environment and subjects were measuring their heart rate with the earlier described BlueRobin heart rate monitor along with the iPhone application.

Table 1 Estimated mean heart rates

Subject	Reference-watch (BPM)	Front-camera (BPM)	Back-camera (BPM)	Front-camera Mean error	Front-camera Mean error
1	61	60	61	1	0
2	66	63	64	3	2
3	93	94	94	1	1
4	110	110	112	0	2
5	77	78	77	1	0
6	82	82	82	0	0
7	71	72	72	1	1
8	64	64	64	0	0
9	110	110	109	0	1
10	61	58	62	3	1
		Mean error rates		**1**	**0.8**

After the first test, each individual was asked to repeat the measurement, by placing the fingertip on the rear camera,

which was done in our previous work [15]. Results of this experiment together with relative errors of estimation are shown in Table 1.

Our results demonstrate that mean and standard deviation error values when using front-facing camera has 1±1.48 beats per minute deviations compared to the reference Chronos watch. When compared to the back camera, results are slightly better with 0.8±1.09 beats per minute. Front-facing camera provided satisfactory results, compared to the back-camera. It must be taken into account that front-facing camera estimates heart rate values from video recording of the face, which is more susceptible to noise due to the motion artifact and light fluctuations. On the other hand, application using more powerful back camera requires direct contact with fingertip, where previously mentioned artifacts are lower. Figure 5 displays the results of performed measurements with different applications and reference watch.

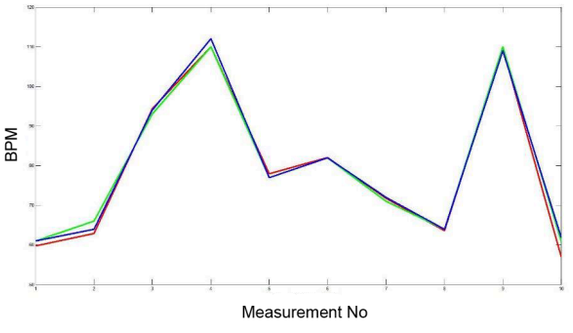

Fig 5. Results achieved using different measurement methods: reference (green); fingerprint (blue); face (red)

CONCLUSION

In this paper, we have successfully designed and implemented smartphone-based contactless heart rate measurement system. Our results demonstrate that smartphone's built-in cameras can estimate heart rate values, where front-face camera extracts PPG signals from individual's face and back-camera from fingertip. Although back camera application reported slightly better results, application based on front-facing camera demonstrated that it could provide respectable results in short term monitoring. The future studies will be focused on minimization of noise due to the sensitivity of light conditions, as well on the improvement of software image stabilization.

REFERENCES

1. D. Grimaldi, Y. Kurylyak, F. Lamonaca, and A. Nastro, "Photoplethysmography detection by smartphone's videocamera," 6th *IEEE Int Conf IDAACS*, vol. 1, 2011, pp. 488-491
2. C. G. Scully, J. Lee, J. Meyer, A. M. Gorbach, D. Granquist-Fraser, Y. Mendelson, and K. H. Chon, "Physiological parameter monitoring from optical recordings with a mobile phone," *IEEE Trans Biomed Eng*, vol. 59, no. 2, pp. 303-306, 2012
3. P. Pelegris, K. Banitsas, T. Orbach, and K. Marias, "A novel method to detect heart beat rate using a mobile phone," *IEEE Conf Proc EMBS*, pp. 5488-5491, 2010
4. V. Chandrasekaran, R. Dantu, S. Jonnada, S. Thiyagaraja, K.P. Subbu, "Cuffless Differential Blood Pressure Estimation Using Smart Phones," *IEEE Trans Biomed Eng*, vol.60, no.4, pp.1080-1089, 2013
5. H. Li, H. Zhao, "Systolic blood pressure estimation using Android smart phones," 6th *Int Conf BMEI*, pp. 260-264, 2013
6. S. Nishiguchi, M. Yamada, K. Nagai et al., "Reliability and validity of gait analysis by android-based smartphone," *Telemedicine and E-Health*, vol. 18, pp. 292–296, 2012
7. J. Dai, X. Bai, X, Z. Yang, Z. Shen, D. Xua, "Mobile phone-based pervasive fall detection", *Pervasive Ubiquitous Computing*, vol. *14*, pp. 633–643, 2010
8. W. Verkruysse, L. O. Svaasand, and J. S. Nelson, "Remote plethysmographic imaging using ambient light," *Optics Express* vol. 16, no. 26, pp. 21434–21445, 2008
9. M.Z. Poh, D.J. McDuff and R.W. Picard. "Non-contact, automated cardiac pulse measurements using video imaging and blind source separation." *Optics Express*, vol. 18, no. 10, pp. 10762-10774, 2010
10. K. Srinivas, Dr. L. Ram Gopal Reddy, R. Srinivas, "Estimation of heart rate variability from peripheral pulse wave using PPG sensor" *3rd Kuala Lumpur International Conference on Biomedical Engineering 2006 IFMBE Proceedings*, vol. 15, pp. 325-328, 2007
11. K. Shafqat, R.M. Langford, S.K. Pal, P.A. Kyriacou, "Estimation of Venous oxygenation saturation using the finger Photoplethysmograph (PPG) waveform," *Engineering in Medicine and Biology Society (EMBC), Annual International Conference of the IEEE*, pp. 2905-2908, Aug. 2012
12. Chon K.H., Dash S., Kihwan Ju, "Estimation of Respiratory Rate From Photoplethysmogram Data Using Time–Frequency Spectral Estimation," *Biomedical Engineering, IEEE Transactions on*, vol.56, no.8, pp. 2054-2063, Aug. 2009
13. J. Allen, "Photoplethysmography and its application in clinical physiological measurement", *Physiological Measurement*, vol. 28, no. 3, 2007
14. Steven W. Smith, "The Scientist and Engineer's Guide to Digital Signal Processing" *California Technical Publishing*, 1997.
15. J. Nišić: "Heart rate measurement using iOS application", *XIII International Scientific – Professional Symposium INFOTEH*, I. Sarajevo, Bosnia and Herzegovina, pp. 1151-1155, Mar. 2014
16. Apple iOS Developer Library, *Apple, Inc.* at http://developer.apple.com/library/ios

Smartphone-based remote health monitoring: opportunities and challenges

A. Šećerbegović[1], N. Suljanović[1] and A. Mujčić[1]

[1] Faculty of Electrical Engineering, University of Tuzla, Tuzla, Bosnia and Herzegovina

Abstract— **The transformation of healthcare service delivery from hospital-centric models toward patient-centric models is rapidly evolving. The emergence of wireless technologies and powerful mobile devices opened up opportunities for real-time remote health monitoring. Different mobile health (mHealth) applications are being deployed on smartphone devices, which allow patients to actively participate in their healthcare management and decision-making process. Smartphones, equipped with wireless connectivity features and powerful processing capabilities, are usually used as a data aggregation and communication nodes. In this paper, we have discussed opportunities and challenges in smartphone-based remote health monitoring systems, with special attention to cardiovascular disease monitoring and camera-based estimation of vital signs. Distribution of processing operations for different components of monitoring system, including sensor nodes, smartphone device and cloud/server component is introduced. This proves to be of high importance, in order to resolve issues such as reliability, power consumption, security, accuracy, user acceptance etc. The usage of personalized smartphone-based emergency detection model is proposed, which would allow for early detection of possible chronic disease deterioration and help in the reduction of false alarms. This paper highlights that up-to-date smartphones can meet requirements for efficient remote monitoring, although several challenges still need to be resolved.**

Keywords— **mHealth, smartphone, power consumption, signal processing**

I. Introduction

The revolution of today's mobile devices has lead the patients toward self-centered healthcare services, compared to the previously hospital-based devices and tests. Several factors contributed to the rapid integration of smartphone devices into healthcare systems. Small, non-invasive, unobtrusive and inexpensive wireless sensors have become widely available to the patients, from fitness-based accessories to vital signs acquisition devices. Wireless technologies such as Bluetooth, have enabled simple integration of smartphone devices with sensor nodes. Number of smartphone's users globally is on the rise constantly, with the prediction of more than 2 billion in 2016 [1]. Their availability and affordable prices contributed to their utilization in all sphere's of life, including healthcare. Another major advantage is the possibility of programming and designing personalized applications, which can provide patients with data collection and analysis, previously considered impossible.

In this paper, we have discussed the opportunities and challenges, surrounding smartphone's usage in remote health monitoring. Although above listed advantages are rapidly contributing to the integration of smartphone devices in healthcare service delivery, several aspects still need to be considered. We have elaborated the drawbacks and benefits of using smartphone itself in data acquisition process, with its built-in cameras and applications in cardiovascular diseases monitoring. Another big challenge for these systems is power consumption, due to the fact that data transmission from sensor via smartphone to the cloud contributes to rapid battery draining. Optimal distribution of processing operations that would increase reliability and user acceptance is explained, along with personalization of smartphone-based application for emergency situation detection. The personalized smartphone-based emergency model is introduced which can help in providing early detection of possible patient's deterioration and minimizing false alarms.

II. Smartphone in remote monitoring

Various numbers of diseases can have enormous benefit from continuous remote monitoring. For example, cardiovascular diseases require close monitoring of patient's electrocardiogram (ECG), which was previously only attainable in hospitalized environment with medical personnel on hand. With wireless sensor nodes now easily available, greater mobility of the patient and continuous acquisition of the signals is opening opportunities for real-time analysis, emergency detection and prevention of serious collapse, such as heart attack.

When integrating smartphone device in healthcare service delivery or vital signs estimation, two different aspects can be considered. First one can be applied with healthy population, in order to use the remote monitoring system for periodic vital signs estimation (Figure 1). Applications that can be used for this type of health assessment have already

been introduced [2-4]. A convenient way to acquire vital signs such as heart rate, heart rate variability and respiration rate, without additional accessory devices, is to obtain video recording with smartphone device. Another example is getting insight into patient's posture and possible fall detection, with simple smartphone's accelerometer sensor [4]. However, continuous monitoring would require specialized device – a sensor node, along with smartphone due to the fact that smartphone's main functions are not the monitoring on vital signs, whereas Internet access, phone calls are essential features. Therefore, smartphone in this scenario would only have connection with other healthcare-related devices, such as sensors or cloud. This is explained in second approach, which is basically standard framework for remote patient monitoring (Figure 2). In the following subsections, challenges and opportunities for both aspects are described in detail.

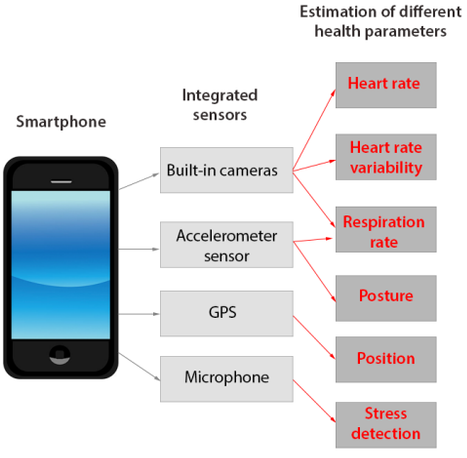

Fig. 1 Estimation of different health parameters using smartphone's built-in sensors for periodic measurement

A. Smartphone as an acquisition tool for periodic health assessment

Occasional insight into patient's health status can be useful when performing different exercises or feeling stressed. With recent developments in technology, this is available to anyone who owns a smartphone device. The working principle is as follows: photoplethysmographic (PPG) signal presents a puslatile signal that corresponds to blood volume changes due to heart beating. PPG signal can be measured non-invasively at the skin surface by detecting changes in light intensity[5]. Smartphone's built-in cameras can be used for the recording of patient's skin, on different body parts. Extraction of PPG signal from video recording is easily achieveable, by selecting specific region of interest (ROI) and averaging pixel values of each frame. Further processing of PPG signal provides heart rate (HR) and heart rate variability[6], which can be used for further analysis and possible detection of cardiac abnormalities. Additional built-in sensors and features are used for different purposes, such as stress detection[7] from smartphone's microphone, respiration rate estimation [8] etc. The main advantage of these systems is that they use smartphone for acquisition of biomedical signals without requiring additional equipment like sensors, cables, electrodes etc. The difficulties like battery charging, misplacement of electrodes, and noise due to the movement of sensor nodes are avoided, which proves to be comfortable and convenient for the patients.

Future developments in this area can be directed to the estimation of other important vital signs, such as blood pressure. For middle-aged and older individuals, it is necessary to frequently measure blood pressure values, as it is an important indicator of cardiovascular diseases. Although several researchers have addressed this problem [9][10], it is still not user acceptable in terms of measurement process or calibration procedures. Challenges of vitals signs estimation with smartphone's built-in cameras are mostly related to the acquisition and processing of PPG signal. In order to achieve high accuracy, minimal movement of the subject is required. Additional load is placed on the processing part of smartphone. Processor intensive operations for processing of video and high frame rate values are contributing to faster battery draining, which raises the cost of implementing these applications in real life monitoring.

B. Smartphone for continuous remote monitoring

The basic framework of patient remote health monitoring with smartphone devices includes three distinctive components, as seen in Figure 2.

Fig. 2 Framework for remote patient monitoring system, with smartphone as a processing tool

Wireless sensor nodes are connected to the gateway, usually smartphone device for further transmission or analysis of acquired signals. Patient monitoring systems based

on mobile devices have primarily relied on their communication services for analysis of biomedical data. A large number of systems have taken the advantage of standard communication features such as SMS and MMS messaging, as well as the wireless communication technologies like Wi-Fi or GPRS to transfer the collected data to a remote location, usually server. Higher computational power, increased performance memory and faster data communication are contributing to better user experience of different smartphone's functions [11-15]. Although this type of monitoring is more convenient for the patient, there are key issues that need to be addressed. Security is one of the main concerns when transferring patient's health data to remote location. Power consumption is the main drawback of today's smartphone operation. However, in the process of long term monitoring, they are also the main culprits for constant need for battery charging.

Possible solution to the power consumption problem is to define specific distribution of the operations to the components of mHealth framework. Wireless sensor nodes can be efficient in acquisition of biomedical signals, with possibility of performing signal processing operations [16]. It is also well known that transmission of the signals is requiring higher battery levels. This can be solved by initiating a periodic communication between smartphone and sensor, for the transmission of the signals. Recent wireless technology - Bluetooth low energy is the first candidate that can be employed in this scenario, due to the low energy consumption and broad implementation in new smartphone devices. Compared to the standard Bluetooth, it has low-duty-cycle transmissions allowing for the device to faster go to sleep mode and preserve battery levels. After wireless sensor node initiates connection with smartphones, specific processing can be performed and allow patient to have real-time analysis of his health status in his hand. This can all be done without the need for medical personnel or hospital equipment.

III. Personalized Smartphone-Based Emergency Model

In the previous section, it is highlighted that smartphone device, as well as the wireless sensors nodes, can perform certain signal processing operations, but not all. We have already stated that it is essential to define which processing for which signals is executed on a specific platform (sensor, smartphone, cloud) in order to allow patient for seamless, comfortable and reliable monitoring in real time. However, in terms of dealing with chronic diseases such as heart-related problems, hypertension, asthma etc., it is assumed that patient will be using the system for longer periods of time. In these situations, possible sudden deteriorations of patient's health require timely detection. Building a personalized model for specific patient could help in solving this problem.

Figure 3 displays the proposed personalized smartphone-based emergency detection model. Periodic signal processing can be executed on wireless sensor nodes or smartphone. This processing needs to be as minimized as possible, due to the previously mentioned power consumption challenges. By performing a comparison with previously collected data, a preliminary decision about the urgency of situation is to be made. Three different levels are presented, including low level – which would only require interaction with the patient, e.g. the electrode is not properly placed; middle level of emergency would establish a wireless connection to the medical facility or upload the data to the cloud, in order to perform complex analysis on a powerful resource. This analysis can result in raising an alarm to the medical professionals if needed. Finally, high level of emergency would suggest that system detected a serious deviation from previous data, and that the patient is not responding to the alerts. This means that immediate communication is established to the medical facility, for an emergency intervention. Minimum amount data that needs to be transmitted includes alarm message and last reading of acquired vital signs. Additional information about the patient, such as his location via GPS system, his posture via accelerometer sensors can also be transmitted or uploaded to the cloud.

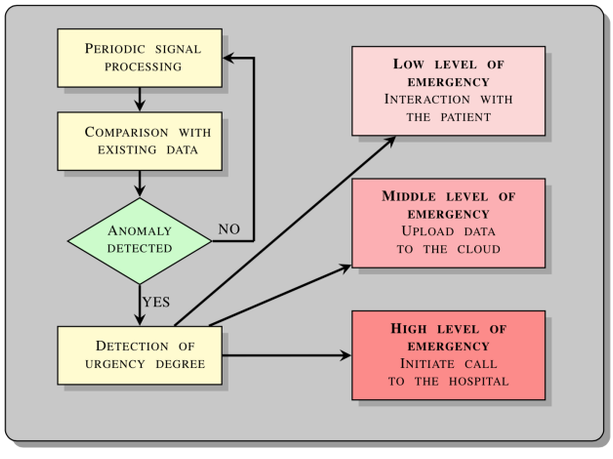

Fig. 3 Personalized smartphone-based emergency detection model

Although suggested emergency model would ideally be personalized for each patient and work only with the data obtained from him, it still needs to have some important issues resolved.

- The determination of vital parameters to be monitored is important, due to the fact that preference should be given to those parameters that will first indicate potential health deterioration. Most important vital signs include heart rate, blood pressure, respiration rate and temperature where heart rate and respiratory rate prove to be the most important predictors of patient's cardiovascular instabilities [17]. These parameters can easily be measured, with wireless sensor nodes or they can be derived from PPG signal. Smartphone's built-in cameras can be used for obtaining PPG signal, and provide patient with fast and reliable results. However, for specific monitoring it would be best if the selected vital signs or signals are proposed by medical professional.
- Reduction in power consumption can be achieved when limiting continuous streaming of signals from wireless sensor node to smartphone. Although periodic streaming can easily be achieved, optimum scenario would involve only streaming of the data when anomaly is detected. This means that constant processing of acquired data would be required. One of the possible solutions to this aspect would be to use data quickest change detection algorithm [18], which would be utilized for deployment of fast and energy-efficient algorithms for specific biomedical signal processing. These algorithms are designed in order to detect change in patient's health parameters quickly and efficiently. Initial calibration for particular patient needs to be executed, in order to gather sufficient amount of data for reliable prediction and raising the alarm, when the patient's health status parameters are outside previously specified limits.
- Streaming of obtained biomedical signals from sensor nodes to smartphone device or cloud are to be avoided, except in the emergency situations. In our previous work [14], we have tested smartphone for three different scenarios, where Android smartphone was used as for constant acquisition of ECG signals. As seen in Figure 4, power of battery draining is becoming higher with constant transmission of the data via Bluetooth and Wi-Fi wireless connections. Almost same amount of power is used for signal processing on the smartphone, although with advancements in smartphone's CPU and performance capabilities, this value can be minimized. This means that sending signals in a continuous form to the cloud would not be recommended, although cloud-based processing is based on resource-free platforms [19].

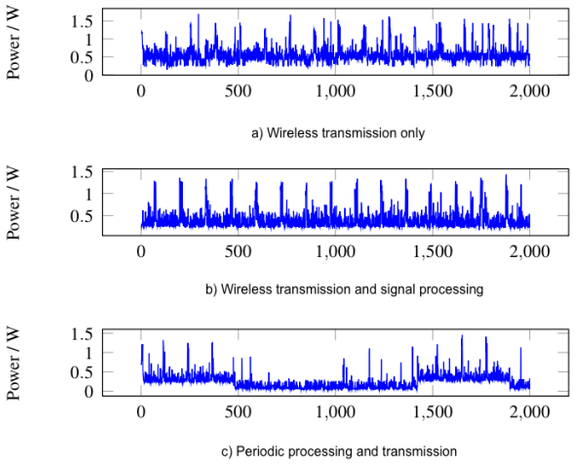

Fig. 4 Power-consumption of smartphone with different processing applications [14]

Above listed challenges and proposed solutions can be implemented in smartphone devices, in order to provide the patient with user-acceptable, reliable and accurate healthcare service, by using up-to-date smartphones.

IV. CONCLUSION

The penetration of smartphone devices is rapidly growing, as well as their technology improvement, lower prices and new features. Healthcare systems are influenced by smartphone's revolution as well, with their integration in patient's surveillance as well as the professional's work. In this paper, we have discussed in what way smartphone devices can be utilized to improve current remote health monitoring systems. A personalized smartphone-based emergency model for the detection of patient's health deterioration is presented, along with discussion of its key functionalities. With proper distribution of signal processing operations and specific data transmission, we believe that up-to-date smartphones can provide user with effective monitoring with additional improvements in the future.

ACKNOWLEDGMENT

This study is part of the "Norbotech project", supported by the Norwegian Ministry of Foreign Affairs Programme in Higher Education, Research and Development (HERD) in the Western Balkans 2010 – 2014 within the field of ICT.

REFERENCES

1. InMarketer Report, Smartphone Users and Penetration Worldwide 2013-2018, 2014.
2. S. Kwon, H. Kim, K. S. Park, Validation of heart rate extraction using video imaging on a built-in camera system of a smartphone, *IEEE EMBS*, pp.2174-2177, 2012.
3. M. J. Gregoski, M. Mueller, A. Vertegel, et al., Development and Validation of a Smartphone Heart Rate Acquisition Application for Health Promotion and Wellness Telehealth Applications, International Journal of Telemedicine and Applications, 2012.
4. Y. He, Y. Li, S.D. Bao, Fall detection by built-in tri-accelerometer of smartphone," *IEEE BHI,* pp.184-187, 2012.
5. J. Allen, Photoplethysmography and its application in clinical physiological measurement, *Physiological Measurement*, 2007.
6. R.C. Peng, X.L. Zhou, W.H. Lin, and Y.T. Zhang, Extraction of Heart Rate Variability from Smartphone Photoplethysmograms, Computational and Mathematical Methods in Medicine, 2015.
7. H. Lu et al, StressSense: detecting stress in unconstrained acoustic environments using smartphones, *Proc UbiComp*, 2012.
8. T. Pechprasarn, S. Pongnumkul, S, Estimation of respiratory rate from smartphone's acceleration data," *ECTI-CON*, 2013.
9. V. Chandrasekaran, R. Dantu, S. Jonnada, S. Thiyagaraja and K.P. Subbu, Cuffless Differential Blood Pressure Estimation Using Smart Phones, *IEEE Transactions on Biomedical Engineering,* , vol.60, no.4, pp.1080-1089, 2013.
10. H. Li, H. Zhao, Systolic blood pressure estimation using Android smart phones, Int Conf BMEI, pp.260-264, 2013.
11. R.G. Lee, K.C. Chen, C.C. Hsiao, C.L. Tseng, A mobile care system with alert mechanism, *IEEE Trans Inf Technology Biomed*, vol. 11, no. 5, pp. 507-517, 2007.
12. N. M. Grzywacz, Complex Biomedical Systems: From Basic Science to Translation, *Pulse, IEEE Volume: 3*, Issue: 4, 2012 , pp 22-26.
13. A. Šećerbegović, A. Mujčić, N. Suljanović, M. Nurkić, J. Tasič: "The research mHealth platform for ECG monitoring", *11th International Conference on Telecommunications CONTEL 2011*, June 15–17, 2011, Graz, Austria, pp. 103-108
14. Jae Min K, Yoo T, Hee Chan K, A wrist-worn integrated health monitoring instrument with a tele-reporting device for telemedicine and telecare. Instrum Meas IEEE Trans 55(5):1655–1661.
15. Oresko JJ, Jin Z, Cheng J, Huang S, Sun Y, Duschl H, Cheng AC (2010) A wearable smartphone-based platform for real-time cardiovascular disease detection via electrocardiogram processing. Inf Technol Biomed IEEE Trans 14(3):734–740
16. F. Rincon, F, P.R. Grassi, P.R, N. Khaled, D. Atienza, D. Sciuto, Automated real-time atrial fibrillation detection on a wearable wireless sensor platform,"*IEEE EMBC,* pp.2472-2475, 2012.
17. R. M. Schein, N. Hazday, M. Pena, B.H.Ruben. C.L. Sprung, Clinical antecedents to in-hospital cardiopulmonary arrest, *Chest*, 98(6), pp.1388-1392, 1990.
18. C. Alvarez, D. Smith-Norris, A. Agarwal, Biomedical diagnostic system for device coding. *Systems Conference (SysCon)*, 2013, DOI: 10.1109/SysCon.2013.6549872.
19. X. Wang, Q. Gui, B. Liu, Z. Jin, Y. Chen. Enabling Smart Personalized Healthcare: A Hybrid Mobile-Cloud Approach for ECG Telemonitoring, *IEEE Trans Bio Health* Informatics, 2014.

A. Šećerbegović is with the Faculty of Electrical Engineering, University of Tuzla, Franjevačka 2, 75 000 Tuzla, BiH (phone: 387-35-259-600; e-mail: alma.secerbegovic@untz.ba).

ULOGA RENTGEN DIJAGNOSTIKE U PEDIJATRIJSKOJ PRAKSI

Nedim Begić[1], Zijo Begić[2], Edin Begić[1], Amra Dobrača, Mensur Mandžuka[3]
[1] Medicinski fakultet, Univerzitet u Sarajevo, BiH
[2] Pedijatrijska klinika, KCU Sarajevo, BiH
[3] Elektrotehnički fakultet, Univerzitet u Sarajevu, BiH

Sažetak — **Uvod: Rentgen dijagnostika se u svakodnevnom radu kod pedijatrijske populacije koristi kao značajan dijagnostički i terapijski postupak. Najstarija je, ali još vrlo značajna metoda konvencionalne radiologije. Dobiva se djelovanjem rentgenskih zraka iz rentgenske cijevi na poseban film koji kao medij za prikaz različitih tkivnih gustoća nije dovoljno osjetljiv. Moguće je prikazati i razlikovati samo veće razlike u gustoći tkiva (patološke procese). Cilj rada: Prikaz, uloga i značaj, poduzetih rentgenoloških metoda u svakodnevnom radu sa djecom u okviru primarne i sekundarne zdravstvene zaštite. Materijal i metode: Istraživanje je obuhvatilo 2691 pacijenta (18,32 % od ukupnog broja stanovnika opštine, odnosno 23,43 % participanata korištenja zdravstvene zaštite) u dobi od rođenja pa do kraja 18-te godine života, tokom kalendarske 2014 godine, u „Domu zdravlja Breza“, Breza, Bosna i Hercegovina. Istraživanje je imalo retrospektivni i deskriptivni karakter. Rezultati: Protekle godine je urađeno ukupno 4719 rentgenoloških procedura od čega 530 kod djece (11,23%). Od toga je bilo 222 (41,89%) rentgenskih snimaka kostiju (sumnja i/ili povrede, razvojni poremećaji i bolesti kostiju i zglobova), 198 pluća i srca (37,36%), 48 zuba i vilice (9,06 %) , 48 paranazalnih sinusa, (9,06 %), 8 rtg nativnih snimaka abdomena/uro trakta (1,51%) i 6 snimaka stranog/ili sumnje na strana tijela u mekim tkivima ili digestivnom sistemu (1,13%). Rentgen snimanje su indicirali pedijatri u 301 slucaju,(56,79%), specijalisti urgentne medicine i ljekari opšte prakse u 181 slučaju (34,15%), te stomatolozi u 48 slučajeva (9,06 %). Zaključak: Rentgen dijagnostika je nezamjenljiv segment svakodnevnog rada primarne i sekundarne zdravstvene zaštite dječije populacije. Rentgenološke metode u svakodnevnom radu sa pedijatrijskom populacijom, zajedno sa drugim dijagnostičkim i terapeutskim metodama, uveliko pomažu u postavljanju pravovremene i ispravne dijagnoze, te u adekvatnoj terapiji. Istovremeno omogućavaju dobru trijažu, odnosno skrining, za eventualni tretman u tercijarnim ustanovama zdravstvene zaštite.**

Ključne riječi — **rtg dijagnostika, pedijatrijska populacija, značaj**

I. UVOD

Rentgen dijagnostika se u svakodnevnom radu kod pedijatrijske populacije koristi kao značajan dijagnostički i terapijski postupak.

Početak radiologije vezan je za Wilhelma Conrada Rontgena koji je 1895. godine (prije 120 godina) napravio prvi snimak ruke. Dotadašnje posmatranje bolesnika odnosno patoloških procesa u organizmu je bilo moguće na operacionom ili obdukcijskom stolu. Do 1967. godine radiologija se razvijala isključivo u okviru klasičnog dobivanja analogne slike. Analogna rentgenska slika nastaje posrednim ili neposrednim bilježenjem efekata rentgenskih zraka, koje iz fokusa rentgenske cijevi prolaze kroz objekt koji se snima i izazovu fotohemijski efekt na rentgenskom filmu.

Rentgenska era je trajala sve do 1967 godine kada uvođenjem računara u proces dobivanja digitalne radiolške slike po principu kompjuterizovane tomografije se dešavaju izuzetno brze tehničke inovacije koje dovode do razvoja kompjuterizovane tomografije, ultrazvuka, magnetne rezonance, angiografija, termovizije, pozitron emisione tomografije, te interventne radiologije, pa sve do današnjih in vivo mjerenja i praćenja bioloških procesa u ćelijama (jedro ćelije).

Rentgen dijagnostika je najstarija, ali još vrlo značajna metoda konvencionalne radiologije. Dobiva se djelovanjem rentgenskih zraka iz rentgenske cijevi na poseban film koji kao medij za prikaz različitih tkivnih gustoća nije dovoljno osjetljiv. Moguće je prikazati i razlikovati samo veće razlike u gustoći tkiva (patološke procese).

U svakodnevnoj primarnoj i sekundarnoj zdravstvenoj zaštiti, pogotovo dječije populacije ima nemjerljivu korist, radi dostupnosti, ekonomičnosti, lakog rukovanja i relativno kvalitetnog rezultata odnosno slike.

II. MATERIJAL I METODE

Istraživanje je obuhvatilo 2691 pacijenta (18,32 % od ukupnog broja stanovnika opštine, odnosno 23,43 % participanata korištenja zdravstvene zaštite) u dobi od rođenja pa do kraja 18-te godine života, tokom kalendarske 2014 godine, u „Domu zdravlja Breza“, Breza, Bosna i Hercegovina. Istraživanje je imalo retrospektivni i deskriptivni karakter.

.

III. REZULTATI

Protekle godine je urađeno ukupno 4719 rentgenoloških procedura od čega 530 kod djece (11,23%) – 61,2 % muške djece, sa prevagom djece školske dobi – 47%.

Od toga je bilo 222 (41,89%) rentgenskih snimaka kostiju (sumnja i/ili povrede, razvojni poremećaji i bolesti kostiju i zglobova), 198 pluća i srca (37,36%), 48 zuba i vilice (9,06 %) , 48 paranazalnih sinusa, (9,06 %), 8 rtg nativnih snimaka abdomena/uro trakta (1,51%) i 6 snimaka stranog/ili sumnje na strana

tijela u mekim tkivima ili digestivnom sistemu (1,13%) (grafikon 1.).

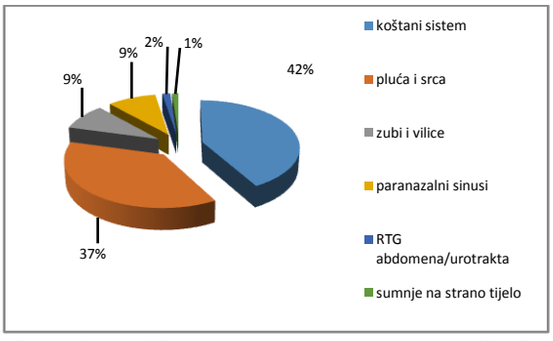

Grafikon 1. Vrste RTG snimaka u svakodnevnom radu s pedijatrijskom populacijom

Rentgen snimanje su indicirali pedijatri u 301 slucaju, (56,79%), specijalisti urgentne medicine i ljekari opšte prakse u 181 slučaju (34,15%), te stomatolozi u 48 slučajeva (9,06 %) (grafikon 2.).

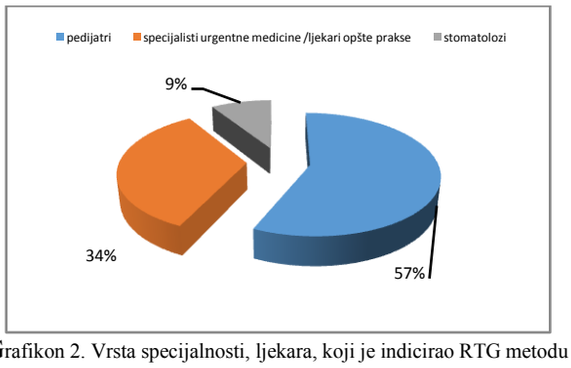

Grafikon 2. Vrsta specijalnosti, ljekara, koji je indicirao RTG metodu

IV. DISKUSIJA

Rentgenska era u radiologiji u vidu klasične radiologije od 1895 do 1967 godine je inicirala razvoj kompletne medicine, a i njenih pojedinih grana, prvenstveno radiologije, hirurških disciplina, internističkih disciplina i osebno pedijatrije. Pedijatrija koja se bavi djetetom od rođenja pa do kraja adolescencije, bolesnim i zdravim, predstavlja medicinu razvojne dobi. U tom periodu djeca su izložena normalnim procesima rasta i razvoja koji su specifični i karakteristični ali i mnogobrojnim patološkim procesima.

Dječija dob je vulnerabilna faza i u pogledu nesreća. Nesretni slučajevi dječije dobi su u razvijenim zemljama i zemljama u razvoju vodeći uzroci mortaliteta do 14-te godine života (saobraćaj, padovi, aspiracija ili gutanje stranog tijela, trovanja, gušenja, strangulacija, utapljanje, opekotine, mehaničke ozljede, eksplozivne naprave i oružja, sportske ozljede) [1].

Razlikujemo tipične nesreće u pojedinim razdobljima djetinjstva i zahvaljujući njima uzimajući u obzir dob djeteta, socijalno-ekonomsko stanje porodice smo u stanju preduzimati neke mjere za njihovo sprečavanje. Smatra se da na jednu smrtnu nesreću dolazi više od 200 nesreća koje zahtijevaju liječenje.

U svakodnevnoj pedijatrijskoj kliničkoj praksi pogotovo u jedinicama hitne pomoći unutar domova zdravlja gdje obično svu službu vrše specijalisti urgentne medicine i/ili ljekari opšte prakse u tretmanu a pogotovo dijagnostici rentgen dijagnostika je od ogromnog značaja. Zapravo ne postoji oštećenje muskularnog tkiva koje se ne bi moglo detektovati rentgen snimkom. Tokom našeg jednogodišnjeg praćenja u sklopu primjene svih rentgenoloških metoda evidentirali smo u preko 40% slučajeva primjenu metode u cilju snimanja osteomuskularnog sistema.

U ukupnom dječijem morbiditetu prvo mjesto zauzimaju upale respiratornog sistema zbog osobitosti dišnih organa djece. Smatra se da do kraja predškolskog perioda djeca u prosjeku imaju 6 do 9 akutnih infekcija dišnih organa. Rentgen snimak plućnog tkiva je od neprocjenjive koristi pogotovo za pedijatre radi utvrđivanja eventualne upale pluća (slika 1.).

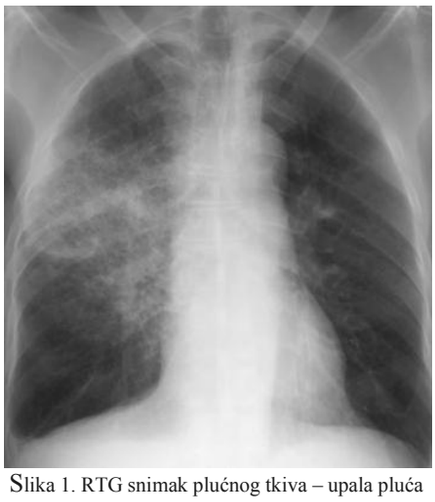

Slika 1. RTG snimak plućnog tkiva – upala pluća

Rentgenska slika pluća ne samo da govori za patološko-anatomski oblik pneumonije nego dopušta da diferenciramo i uzročnika na osnovu dobi, laboratorijske dijagnostike i na osnovu epidemioloških okolnosti i sezonskih varijacija.

Educiran pedijatar će biti u stanju i na osnovu izgleda plućnog vaskularnog crteža kao i procjene oblika i veličine srčane sjene (slika 2.) da zaključi da li eventualno uz fizikalni nalaz i elektrokardiografiju dijete ima bolest srca (urođenu ili stečenu srčanu manu). Rentgen slike pluća i srca smo radili kod naših 37 % pacijenata.

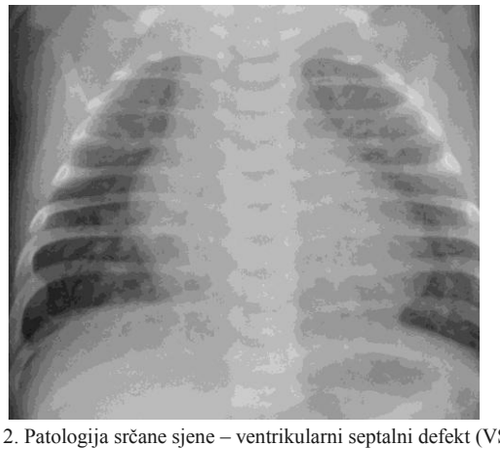

Slika 2. Patologija srčane sjene – ventrikularni septalni defekt (VSD)

Savremena zaštita zdravlja zuba, kao i eventualne traume lica, pa i sumnja na strano tijelo uz relativno česte upale sinusa uveliko koriste rentgen dijagnostiku. Stomatologija sa svim svojim disciplinama, maksilofacijalna hirurgija i otorinolaringologija i danas kao glavnu metodu detekcije koriste rentgen snimak zuba, vilice i paranzalnih sinusa. Skoro petina (18%) svih rentgenskih metoda smo koristili u tretmanu djece [2].

Specijalisti urgentne medicine kao i pedijatri bez obzira na laboratorijsku dijagnostiku su često u dilemi pri sumnji na postojanje akutnog abdomena u djece. Bol u trbuhu je diferencijalno-dijagnostički vrlo širok ali sa rentgen dijagnostikom akutni apendicitis, Meckelov divertikulitis, ileus, krvareći ulkus, se ne bi smjeli previdjeti (slika 3.) [3].

Slika 3. Opstrukcija u gastrointestinalnom sistemu [4]

U dječijoj dobi pogotovo kod manje djece se susrećemo i sa stranim tijelom bilo respiratornog ali i digestivnog sistema. Najčešće se radi o djeci predškolskog perioda sa karakterističnom kliničkom slikom a dopuna rentgen dijagnostikom nam uveliko pomaže u postupku i liječenju. Apostrofirajući primjenu rentgen dijagnostike u svakodnevnom radu ustanova primarne i sekundarne zdravsvene zaštite djece evidentno je da je rentgen dijagnostika nezamjenjiva [5]. Ima se utisak da najviše pomoći od rentgen dijagnostike u svakodnevnom radu imaju pedijatri kao i specijalisti urgentne medicine, odnosno dežurni ljekari u jedinicama hitne pomoći. Svakodnevna pedijatrijska praksa u domenu primarne i sekundarne zdravstvene zaštite uz dobru edukaciju i minimum tehničkih pomagala, kao i primjenu rentgenskih metoda može dobro odgovarati svojoj ulozi [6].

V. Zaključak

Rentgen dijagnostika je nezamjenljiv segment svakodnevnog rada primarne i sekundarne zdravstvene zaštite dječije populacije. Rentgenološke metode u svakodnevnom radu sa pedijatrijskom populacijom, zajedno sa drugim dijagnostičkim i terapeutskim metodama, uveliko pomažu u postavljanju pravovremene i ispravne dijagnoze, te u adekvatnoj terapiji. Dobri rezultati rentgen dijagnostike su evidentni u procjeni pogotovo preloma kostiju, akutnih infiltrativnih promjena pluća, kardiomegalije, bolesti zuba, upala sinusa, nivoa zraka pri akutnom abdomenu, verifikaciji i lokalizaciji stranog tijela, konkremenata urinarnog sistema i slično. Primjena rentgenoloških metoda omogućava dobru trijažu, odnosno skrining, za eventualni tretman u tercijarnim ustanovama zdravstvene zaštite.

Literatura

1. Mardešić D. i sur. Pedijatrija. Medicinska naklada, Zagreb, 2003.
2. Lovrinčević A., Lincender L., Vegar Zubović S., Klančević M. Opća i specijalna radiologija, Medicinski fakultet, Sarajevo, 2009.
3. Meštrović J i sur. Hitna stanja u pedijatriji. Medicinska naklada, Zagreb, 2012.
4. Turk, E. , Tan, A. , Karaca, F. , Edırne, Y. and Karaca, I. (2013) Postoperative intestinal obstruction caused by Meckel's diverticulitis after appendectomy. Open Journal of Pediatrics, **3**, 346-349.
5. Ristić D.I. Urgentna medicina kroz primjere iz prakse. Obeležja, Beograd, 2003.
6. Jukić M i sur. Intenzivna medicina, Medicinska naklada, Zagreb, 2008.

Nedim Begić, Medicinski fakultet Univerziteta u Sarajevu, Čekaluša 90, 71000 Sarajevo, Bosna i Hercegovina, tel +387 61 324-461, e-mail:nedim_begic91@hotmail.com

Non-contact video-based heart rate and heart rate variability extraction from different body regions

A. Alić[1], B. Bajrić[1], A. Hodžić[1], O. Kamerić[1], A. Bašić[1] and A. Šećerbegović[1]

[1]Faculty of Electrical Engineering, University of Tuzla, Bosnia and Herzegovina

***Abstract*— Cardiovascular diseases are among leading causes of mortality around the world. Long-term monitoring of different cardiac parameters could help in prevention of heart attack or detection of life-threatening arrhythmias. With modern technology development, cheap and accessible methods for different vital signs estimation have emerged. Video-based non-contact heart rate estimation has already been implemented in literature, usually based on individual's face. In this paper, different body parts were used for estimation including forehead and palm. Heart rate and heart rate variability values were calculated based on photoplethysmography (PPG) signal, which was extracted from video recording. Video recordings were obtained by using professional camera where five individuals were filmed before and after mild exercise. As interframe compression methods degrade the quality of PPG signal, uncompressed video format was used. Separation of the observed signals was executed using Independent Component Analysis (ICA) method for obtaining red, green and blue components from acquired PPG signal. The validation of heart rate and heart rate variability was performed by using 12-channel electrocardiogram recording device. Our results demonstrate that non-contact method for heart rate and heart rate variability estimation shows sufficiently good results, assuming normal light conditions and minimal movement of the subject.**

***Keywords*— Photoplethysmography (PPG), heart rate, heart rate variability (HRV), independent component analysis (ICA)**

I. Introduction

Frequent measurement of heart rate (HR), as one of the most important indicators of human's health, can help in heart attack prevention or early detection of various diseases. Traditional HR measurement methods require medical examination by equipment based on optical and electronic sensors and skin-contact. Electrocardiogram (ECG) based methods are using electrodes or chest straps that might cause skin irritation. Inexpensive commercial heart rate watches and sensors are available on the market as well. However, special attention has been given to the non-contact method by using video. Following the rapid technological advancements and emergence of fast digital cameras, several methods for non-contact heart rate and heart rate variability have been described [1-3]. With improvements of smartphone's built-in cameras, introduced methods are allowing for vital signs monitoring anywhere and anytime.

In this paper we have used uncompressed video recording for the acquisition of two important vital signs: heart rate and heart rate variability. Heart rate is one of the most important indicators of cardiovascular health, while heart rate variability (HRV) is often used for the detection of several diseases such as myocardial infarction and dysfunction, diabetic neuropathy etc.[4] Different signal processing methods were applied in order to extract reliable and noise-free photoplethysmography signal. In this paper, we have chosen to test independent component analysis (ICA)[5], as a reliable method for separating red, green and blue (RGB) components from video recording, as suggested in [1]. Five individuals participated in the recordings, during relax state and after mild exercise. Video recordings of subject's face and palm were used for the detection of blood volume changes. Heart rate values as well as the two time-domain parameters of HRV were validated with standard 12-channel ECG recording device.

II. Experimental method

Non-contact photoplethysmography, also known as imaging photoplethysmography has gained attention in recent years. Photoplethysmography presents an optical measurement method of blood volume changes based on light reflection of the individual's skin. Imaging photoplethysmography has been used for estimation of different vital signs, including heart rate [1], heart rate variability [2][3], respiration rate [6] etc.

A. Measurement process

For this study two experiments were performed, each one with the purpose of approving accuracy of non-contact video based method for heart rate extraction.

The recordings for first experiment were made with subject still with minimal motion, without any particular changes in behavior. After first video had been obtained, subjects were asked to perform mild exercise for several minutes. Second recording was performed immediately after exercise. Recordings were conducted indoors with only sunlight entering through windows as source of illumination. Signals were extracted from non-compressed video format.

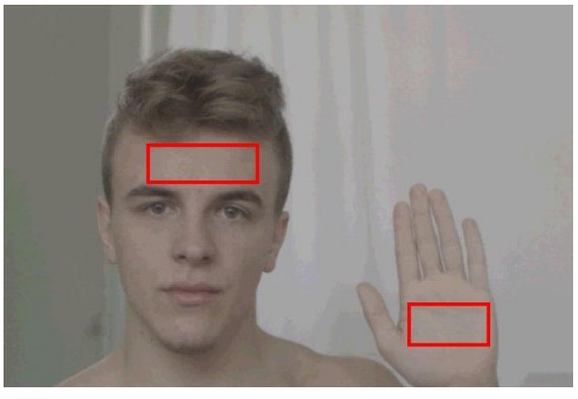

Fig 1. Two selected ROIs for HR estimation

All video recordings lasted for one minute. Professional RED camera with frame rate of 50 fps and 3072 x 1728 pixels resolution was used. Before the filming started, subjects have been connected to 12-channel ECG device in order to obtain "gold standard" heart rate values. Once a recording was successfully acquired, two regions of interest (ROI) were extracted: forehead, size 300x100 and palm 100x50 pixels as shown in Figure 1.

B. Data processing

All algorithms and calculations were analyzed in MATLAB. ROI is decomposed into red, green, and blue channels for each frame and spatially averaged to form the raw PPG signals. Green channel of the RGB signal contains the most information about the HR due to the fact that hemoglobin has maximum absorption for the green components [7]. It should be noted that red and blue channels also contain visible blood volume pulsations. After loading RGB matrix with channels values gathered from video frames, preprocessing operations as suggested in [1] were executed.

Detrending of the obtained PPG signal [8] is an implementation of time-varying high-pass FIR filter, which can successfully remove noise artifacts, introduced in raw PPG signals, due to the individual's movement and light changes. Normalization of filtered PPG signal is executed by using the following equation

$$PPG_i = \frac{\mathrm{PPG_i} - \overline{PPG}_\mathrm{i}}{\sigma_{PPG_i}} \quad (1)$$

Where PPG_i represents each data point of PPG i-th component, $\overline{PPG}_\mathrm{i}$ is average of all the sample data points and σ_{PPG_i} is standard deviation. Figure 2 demonstrates synchronized ECG and PPG signals from forehead. Both signals were resampled to the same frequency (256 Hz). It is evident to see how the ECG signal precedes PPG signal, which corresponds to the cardiac cycle. After the contraction of the heart, blood volume pulse travels through different blood vessels and can be evident on the peripheral parts of the body, such as forehead. R peaks in ECG signal are corresponding to the peaks in PPG signal. R peaks are detected by using Pan-Tompkins algorithm [10], while peaks in PPG signal are traced by customized first-derivative based algorithm. Photoplethysmography signal from palm is demonstrated in Figure 3, where is visible the noise of the signal due to the movement.

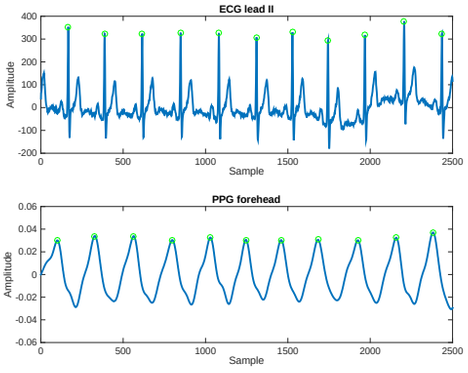

Fig 2. ECG signal from lead II and processed PPG signal from forehead

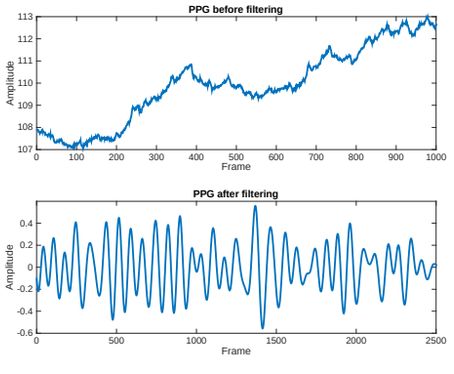

Fig 3. Raw and processed PPG signal from palm

The Independent Component Analysis (ICA) [5][9] is applied in order to separate three independent sources of extracted RGB signal. In order to determine spectral content of PPG and heart rate frequency, obtained PPG signal was analyzed in frequency domain. The component with the highest peak in heart rate frequency range was selected for further signal processing, as suggested in [2]. Two time-domain parameters of heart rate variability were calculated as well. Average interval value (AVNN) and standard deviation (STDNN) between normal heart beats are calculated based on reference ECG signal as well as the PPG signal from forehead. Considering the fact that peaks in PPG signals need to be annotated in order to calculate HRV parameters, band-pass filtering was performed. Operational range for band-pass filter in our experiment was between 0.7 and 4 Hz, which corresponds to heart rate values between 40 and 240 beats per minute.

III. RESULTS

Five male individuals aged between 20 and 25 years, male were participating in the experiment. None of the subjects involved in this study had any heart disease, cardiovascular nuisance and no history of diabetes. Obtained reference values of heart rate, as well as the estimated values, mean square errors and standard deviations for face and palm are shown in Tables 1 i 2.

Table 1. Results obtained by using PPG signal from forehead compared to the ECG signal

No.	State of the subject	Mean HR from ECG (reference)	Mean HR from forehead	Mean error (forehead)	Mean square error
1	Relax	63.8493	63.8264	0.0229	0.0005
2	Relax	96.6478	96.5556	0.0922	0.0085
3	Relax	50.5123	50.5019	0.0104	0.0001
4	Relax	80,2798	79.8083	0.4715	0.2223
5	Relax	90.5049	90.8884	0.3835	0.1471
6	Exercise	94.6102	94.9750	0.3648	0.1331
7	Exercise	123.7328	123.7962	0.0634	0.0040
8	Exercise	85.0225	84.8453	0.1772	0.0314
9	Exercise	103.2213	103.2436	0.0223	0.0005
10	Exercise	111.1264	111.1920	0.0656	0.0043

When comparing heart rate values obtained from forehead, our results report 0.19 ± 0.16 beats per minute, deviations from reference ECG signal. With palm PPG signal, results of estimation are slightly worse 0.34 ± 0.27 beats per minute. This can be explained by the fact that PPG signal from palm contained greater amount of noise due to the movement, during recording.

Heart rate variability time-domain parameters were calculated for each individual and are shown in Table 3. Total mean error rate and standard deviation for AVNN, when comparing reference ECG values and PPG signal from forehead, is 0.0477 ± 0.13699, while for STDNN is 0.01165 ± 0.01146. Our results demonstrate that HRV parameters can be successfully estimated by PPG signal as well.

Table 2. Results obtained by using PPG signal from palm compared to the ECG signal

No.	State of the subject	Mean HR from ECG (reference)	Mean HR from palm	Deviation (palm)	Mean square error
1	Relax	63.8493	63.9208	0.507	0.2570
2	Relax	96.6478	96.7250	0.2616	0.0684
3	Relax	50.5123	50.3283	0.8427	0.7101
4	Relax	80,2798	79.9167	1.0075	1.0151
5	Relax	90.5049	91.2093	1.6163	2.6124
6	Exercise	94.6102	95.0873	0.0395	0.0016
7	Exercise	123.7328	123.9170	0.2967	0.0880
8	Exercise	85.0225	84.7132	18.8134	1.8821
9	Exercise	103.2213	103.0691	0.0247	0.0006
10	Exercise	111.1264	110.2192	0.9492	0.9009

Table 3. HRV parameters obtained by using PPG signal from forehead compared to the ECG signal

No.	State of the subject	AVNN from ECG (reference)	AVNN from forehead	STDNN from ECG	STDNN from forehead
1	Relax	0.9421	0.0476	0.9465	0.0506
2	Relax	0.6225	0.0332	0.6262	0.0353
3	Relax	1.1944	0.0864	1.1901	0.1157
4	Relax	0.7503	0.0471	0.7489	0.0728
5	Relax	0.6829	0.0469	0.6655	0.0415
6	Exercise	0.6348	0.0193	0.6355	0.0229
7	Exercise	0.4851	0.009	0.4857	0.0376
8	Exercise	0.7067	0.0226	0.708	0.0331
9	Exercise	0.5816	0.0136	0.5828	0.0167
10	Exercise	0.5388	0.0272	0.5392	0.022

IV. CONCLUSION

In this paper we have used video recording to obtain photoplethysmography signal from different regions (forehead and palm). PPG signal obtained from forehead section that was used for estimation of heart rate values

shows higher accuracy compared to the palm. This can be explained by the fact that forehead is closer to the heart and is less susceptible to noise due to the motion artifact and light fluctuations. Two parameters of heart rate variability in ECG signal showed high correlation with pulse rate variability, obtained from PPG signal. In the future, various signal processing methods will be explored for better assessment of PPG signal along with other parameters of heart rate variability.

REFERENCES

[1] W. Verkruysse, L. O. Svaasand, and J. S. Nelson, "Remote plethysmographic imaging using ambient light," Opt. Expr., vol. 16, pp. 21434– 21445, Dec. 2008

[2]] M.-Z. Poh, D. J. McDuff, and R. W. Picard. Advancements in noncontact, multiparameter physiological measurements using a webcam. IEEE Trans. on Biomedical Engineering, 2011

[3] S. Kwon, H. Kim, and K. S. Park. Validation of heart rate extraction using video imaging on a built-in camera system of a smartphone. In EMBS, 2012.

[4] E. Gil, M. Orini, R. Bailón, J. M. Vergara, L. Mainardi, and P. Laguna, "Photoplethysmography pulse rate variability as a surrogate measurement of heart rate variability during non-stationary conditions," *Physiological Measurement*, vol. 31, no. 9, pp. 1271–1290, 2010.

[5] J.-F. Cardoso, "High-order contrasts for independent component analysis (ICA)", Neural Comput. 11(1), 157–192, 1999

[6] W. Karlen et al., "Respiratory rate assessment from imaging photoplethysmography", *IEEE Int Conf EMBS*, 2014.

[6] W. G. Zijlstra, A. Buursma, and W.P. Meeuwsen van der Roest. Absorption spectra of human fetal and adult oxyhemoglobin, deoxyhemoglobin, carboxyhemoglobin, and methemoglobin ,. Clinical Chemistry, 37(9):1633– 1638, September 1991

[7] M. P. Tarvainen, P. O. Ranta-Aho, and P. A. Karjalainen, "An advanced detrending method with application to HRV analysis," IEEE Trans. Biomed. Eng., vol. 49, no. 2, pp. 172–175, Feb. 2002.

[8] A. Hyvärinen, "Independent component analysis: algorithms and applications," Neural Networks, vol. 13, pp. 411-430, June 2000

[9] S. Kwon, H. Kim, and K. S. Park. Validation of heart rate extraction using video imaging on a built-in camera system of a smartphone, *IEEE* EMBS, 2012.

[10] J. Pan, W. J. Tompkins, "A Real-Time QRS Detection Algorithm," *IEEE Trans Biomed* Eng, vol. BME-32, no.3, pp.230-236, 1985.

A. Alic is a student at Faculty of Electrical Engineering, University of Tuzla, BiH (e-mail: alicamra@hotmail.com)

Which Particle Sizes and Nutrient Media Should be Used to Identify The Presence of Microorganisms in the Operating Rooms?

Y. Ülgen[1], S. Yalvarmış[1] and A. Ak[2]

[1] Bogazici University/Institute of Biomedical Engineering, Istanbul, Turkey
[2]Erzincan University/Dept. of Biomedical Engineering, Erzincan,Turkey

Abstract— **In the operating rooms and intensive care units, air quality plays a key role in preventing hospital acquired infections which occur due to airborne microbiological agents. The aim of this project is to observe which particle sizes and nutrient medias should be used in order to identify concentrations of airborne bacteria/fungi in the operating rooms by using three different methods which are passive sampling, active sampling and particle counting methods respectively and to evaluate the quality of air by comparing these three sampling techniques. Following the general cleaning of the operating rooms which is in accordance with ISO 144644-1:1999 (E) standard related to clean room and associated environments, measurements are performed at temperatures between 21 and 25^{0}C with 37-75% relative humidity. In consequence of indications, for microbiological evaluation of air quality in the operating room by using active sampling methods, the best results are acquired with using Tryptic Soy Agar (TSA) and 5% Sheep Blood Agar with particle sizes between 4,1 and 7,1 μm.**

Keywords— **Particle counting, air quality, airborne bacteria, microbiological sampling.**

I. Introduction

Despite modern operating room (OR) design techniques, sterilization efforts and regulations, mortality attributable to nosocomial infections is still a problem [1, 2, 3].

The level of sterilization in an OR is assessed by the measurement of bacteria and air borne particle concentrations [4, 5]. Bacteria do exist in the OR's under normal conditions; but should be limited to 30 CFU/m^2 at rest; and to 180 CFU/m^2 when operational [6,7]. Microbiological sampling is the commonly used in determining the risks of infection. Table 1 illustrates the microbiological classification of OR's by passive sampling [8].

II. Methodology

A. Particle Counting

For particle counting, FLUKE, model 983 particle counter is used (Fig. 1). This counter has a flow rate of 2,83 L / min. The particle counter has 6 channels which can classify the particles into 6 groups according to the size of particles: > 0.3μm, > 0.5 μm, > 1.0 μm, > 2.0 μm, > 5.0 μm and > 10.0 μm. Measurements are taken from the operating table top; repeated six times, with a sampling time of 1 minute, in 10 min. intervals.

Table 1 Microbiological Classification of OR's

	Bacteria (CFU/m^2)	Fungi (CFU/m^2)
Very Clean	0 to 10	0 to 2
Clean	11 to 20	3 to 4
Acceptable	21 to 50	5 to 10
Contaminated	51 to 150	11 to 30
Highly Contaminated	>150	>30

B. Microbiological Sampling

In passive and active samplings, six different nutrient media are used: Sheep Blood Agar 5%, Müller Hinton agar, Nutrient agar, Tryptic Soy agar and Eozin Methylene Blue agar for bacteria; Sabouraud's Dextrose Agar for fungi in petri dishes of 9 cm diameter and 1/155 m^2 surface area.

Petri dishes are placed at four corners (A,B,C and D) of the room and on the operating table (E) and exposed to air for 30, 60, 120 and 240 minutes, for collection. Viable particles collected on a variety of nutrient agar are then incubated for 72 hours at 37^{0}C, for counting and identification.

Colony forming units CFU/m^2 are calculated as,

$$x = 155.k/p.d \quad (1)$$

where,
x=number of bacteria/fungi per m^2 per minute,
k=counted number of colonies,
p=total number of petri dishes used for collection,
d=exposed time in minutes.

The New-Star Andersen Six-stage Viable active Particle Sampler is a multi-orifice cascade impactor which is normally used to measure the concentration and particle sizes (0.65, 1.1, 2.1, 3,3, 4.7 and 7.0 mm) of aerobic bacteria and fungi in the ambient air (Table 1).

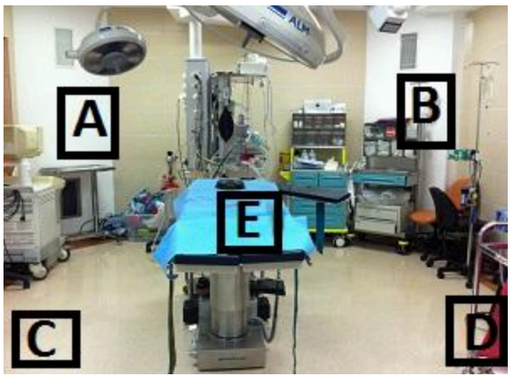

Fig. 1 Passive sampling locations

This instrument has been widely used as a standard for enumerating the viable particles in a microbial aerosol. The sampler is calibrated (at 28,3 l/min) so that all particles collected, regardless of physical size, shape, or density are sized aerodynamically and can be directly related to human lung deposition.

Colony forming units are calculated as, CFU/m^3 = number of bacteria/fungi colonies/total sampled air volume.

III. Results

Measurements with the particle counter are displayed in Table 2. Active sampling results are given in Table 3, expressed as colony forming units per unit volume. Results with passive sampling following incubation for bacteria and fungi colonies per unit area are shown in Table 4.

Table 2 Particle counting according to ISO 14644.

Particle Sizes (µm)	Number of Particles/m^3
0,3	4547687
0,5	352197
1	73078
2	27688
5	3640
10	1812

Table 3 Bacteria and Fungi (CFU/m^3)

Viable particle size	TSA	NA	EMBA	SDA	SBA	MHA
7.1 and above	3,53	4,16	4,90	5,77	6,80	8,01
4.7 and 7.1	4,71	5,55	6,54	7,70	9,07	10,68
3.3 and 4.7	0,00	0,00	0,00	0,00	0,00	0,00
2.1 and 3.3	1,18	1,39	1,63	1,92	2,27	2,67
1.1 and 2.1	2,36	2,77	3,27	3,85	4,53	5,34
0.65 and 1.1	1,18	1,39	1,63	1,92	2,27	2,67

Table 4 Bacteria and Fungi (CFU/m^2)

		30 min	60 min	120 min	240 min
TSA	A	10,3	7,8	10,3	4,5
	B	10,3	5,2	2,6	2,6
	C	5,2	12,9	5,2	4,5
	D	10,3	7,8	1,3	2,6
	E	87,8	10,3	5,2	7,1
NA	A	10,3	2,6	2,6	3,9
	B	5,2	10,3	2,6	0,0
	C	10,3	7,8	2,6	3,9
	D	0,0	2,6	0,0	0,6
	E	20,7	0,0	1,3	1,3
EMBA	A	237	85	60	27
	B	377	98	51	25
	C	180	134	42	28
	D	206	100	28	19
	E	175	74	41	33
SDA	A	5,2	2,6	2,6	1,3
	B	0,0	7,8	1,3	0,0
	C	0,0	0,0	>645,8	1,9
	D	5,2	0,0	2,6	0,6
	E	0,0	5,2	0,0	1,3
KKA	A	5,2	0,0	0,0	1,3
	B	0,0	7,8	2,6	2,6
	C	10,3	15,5	3,9	1,3
	D	0,0	0,0	0,0	1,3
	E	0,0	5,2	2,6	1,9
MH	A	5,2	2,6	2,6	1,3
	B	0,0	5,2	1,3	1,9
	C	0,0	0,0	2,6	1,9
	D	0,0	0,0	2,6	0,0
	E	0,0	5,2	5,2	0,0

Influence of airborne particles on viable microorganisms sampling is considered as the ratio of CFU to number of particles, as shown in Table 4.

Table 4 Ratios of viable microorganisms to particles: CFU/# of particles

Sizes	TSA	NA	EMBA	SDA	SBA	MHA
0,65-1,1	5,3	0.0	403,1	0.0	0.0	0.0
1,1-2,1	28,2	0.0	1187,5	0.0	98,5	70,8
2,1-3,3	68,4	0.0	4163	134,3	201,4	267,9
3,3-4,7	0.0	0.0	15290	0.0	415,6	415,6
4,7-7,1	1554,5	396,9	24144	0.0	396,9	396,9

IV. DISCUSSION

From this study, it is concluded that the type of nutrients that are suitable for microbiological evaluation of OR's are Tryptic Soy agar and 5% Ship Blood agar, with particle sizes between 4,1 and 7,1 μm.

Bacterial microorganisms are living organisms of diameter 0,3 μm or greater. Fungi have sizes of 2 to 10 μm.

The microorganisms that favorably multiply in the Tryptic Soy agar are Escherichia coli, Staphylococcus aureus, Streptococcus pyogens, candida alnbicans, Salmonella typhimurium and Pseudomonas aeruginosa.

Other microorganisms such as Staphylococcus aureus, Staphylococcus agalactiae, Listeria monocytogenes, Bacillus cereus and Clostridium perfringes will grow in the nutrient medium of Ship Blood agar.

REFERENCES

1. M. Altındiş, D. Karaaslan, "Ameliyathanelerde sterilizasyon ve havalandırma ilkeleri," Kocatepe Tıp Dergisi, vol. 2, s. 29-36, 2001.
2. S. Başkan, "Cerrahi alan infeksiyonlarının önlenmesi: Ameliyathane Koşulları Nasıl Olmalı?"Hastane Infeksiyonları Dergisi,vol. 7, s. 161-167, 2003.
3. A. E. Andersson, I.Bergh, J. Karlsson, B. I. Eriksson, K. Nilsson, "Traffic flow in the operating room: An explorative and descriptive study on air quality during orthopedic trauma implant surgery," American Journal of Infection Control, vol. 40, s. 750-5, 2012.
4. M.L. Cristina, A.M. Spagnolo, M. Sartini, D. Panatto, R. Gasparini, P. Orlando, G. Ottria, F. Perdelli, "Can Particulate Air Sampling Predict Microbial Load in Operating Theatres for Arthroplasty?" PLOS ONE, Vol. 7, s. 1-6, 2012.
5. A. Uzunköy, "Cerrahi alan enfeksiyonlarında ameliyathanenin rolü," Harran Üniversitesi Tıp Fakültesi Dergisi, vol. 1, s. 38-48, 2004.
6. M. Çakmakçı, "Ameliyathane ve Cerrahi İnfeksiyonlar," Hastane Infeksiyonları Dergisi, vol. 3, s. 140-146, 1999.
7. G.-H. Wan, F.-F. Chung, C.-S. Tang, "Long-term surveillance of air quality in medical center operating rooms," Am J Infect Control, vol. 39, s. 302- 308, 2011.
8. B. Kozazeybek, A. Ordu, A. Ayyıldız ve ark. "Cerrahi merkezilerinde ameliyathane hava temizliği ölçümlerinde farklı yöntemlerin irdelenmesi: 3 merkezli bir çalışma," Hastane infeskiyonları dergisi, Vol. 4, Sayı 3, s. 164-174, 2000.
9. Hawkey, P.H., Mccormick, A., A. Simpson, R.A.: Selective and differential medium for the primary isolation of members of the proteae. J. Clin. Microbiol. 23; 600-603, 1986.
10. United States Pharmacopeia XXVI, Chapter "Microbial Limit Tests", 1995.

Corresponding author:

Yekta Ülgen is the Director of the Institute of Biomedical Engineering, Bogazici University, Istanbul 34684 Turkey. (phone: 0905325065024; e-mail: ulgeny@boun.edu.tr)

Surface EMG pattern recognitionby using DWT feature extraction and SVMclassifier

Ermin Podrug, Abdulhamit Subasi

Faculty of Engineering and Information Technologies, International Burch University, Sarajevo, Bosnia and Herzegovina

Abstract—**In this study we proposed a surface electromyogram (EMG) pattern classification approach for the recognition of different myoelectric signals. EMG signals are used in human motion pattern recognition. In exoskeleton robot control, EMG signals are used in the detection of the electrical activity associated with muscle contraction and obtained by measurement of the electrical activity of a muscle during contraction. Since different categories of contraction can cause EMG signals to vary, the recognition performance also affected by this variation. In order to eliminate this variation in EMG signal during contraction, different time and frequency techniques are used for feature extraction from surface EMG signals. Then a set of feature selection method based on different statistical techniques is developed so that the high-dimensional features can be reduced by a supervised feature reduction algorithm. Then, support vector machine (SVM) is used to classify the EMG signals. The experimental results show the high accuracy of the proposed system and also revealed that it is betterfor EMG signals from the same type of muscle contraction, whether dynamic or isometric, are consistently used in both the training and validation phases. The methodology developed in this study has potential applications in exoskeleton robot control and rehabilitation.**

Keywords—**EMG, DWT feature extraction, SVM classifier, pattern recognition, myoelectric signals.**

I. Introduction

Electromyography (EMG) is an electrodiagnostic medicine technique for evaluating and recording the electrical activity produced by skeletal muscles [1]. The recognition of limb motions from the electromyogram (EMG) plays an important role in both health care and engineering. For example, there is evidence that intensive therapy has beneficial affection there habilitation progress of stroke patients, and such kind of therapies require detection of the intention of the patient's activity[2,3].EMG pattern recognition systems have been widely used in many man-machine interface applications such as multi- function prosthesis, electrical wheelchairs, virtual mouse, keyboard and virtual world etc.[4]

As the acquired surface EMG signals are often blended with signals that are coming from other muscles and therefore have much noise, the obtaining of pure EMG signals is difficult.[5] If we want identifiable EMG signals, we need to use some sort of feature. EMG signals are non-stationary, and because of that we can't use just time-domain or frequency features. Time-frequency analysis methods, as wavlet transform is, can ensure signal informations in time-domain and also frequency-domain.[6]

II. Materials & methods

A. EMG Data Acquisition

The data set of EMG signals that we used in this paper is obtained from Machine Learning Repository.[7]

Protocol: Three male and one female subjects (age 25 to 30), who have experienced aggression in scenariossuch as physical fighting, took part in the experiment. Throughout 20 individual experiments,each subject had to perform ten normal and ten aggressive activities. Regarding the rights of the subjects involved, ethical regulations and safety precaution have been followed based on the code of ethics of the British psychological society. The regulations explain the ethical legislations to be applied when experiments with human subjects are conducted. According to the experimental setup and the precautions taken, the ultimate risk of injuries was minimal. The subjects were aware that since their involvement in this series of experiments was voluntary, it was made clear that they could withdraw at any time from the study.

Instrumentation: The Essex robotic arena was the main experimental hall where the data collection took place. With area 4x5.5m, the subjects expressed aggressive physical activities at random locations. A professional kick-boxing standing bag has been used, 1.75m tall, with a human figure drawn on its body. The subjects' performance has been recorded by the Delsys EMG apparatus, interfacing human activity with myoelectrical contractions. Based on this context, the data acquisition process involved eight skin-surface electrodes placed on the upper arms (biceps and triceps), and upper legs(thighs and hamstrings).

Data setup: The overall number of electrodes is 8, which corresponds to 8 input time series one for a muscle channel (ch1-8). Each time series contains ~10000 samples (~15 actions per experimental session for each subject).

EMG signal obtained from data set is shown in figure 1.

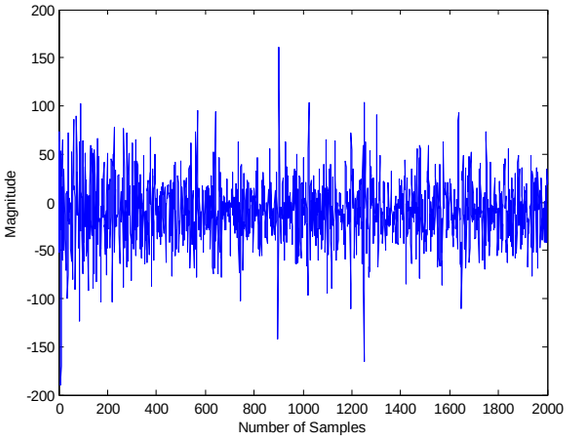

Fig. 1 Raw EMG signal

B. Methods

Multi-scale Principal Component Analysis for De-noising

Multi-scale PCA (MSPCA) combines the ability of PCA to take out the cross-correlation between the variables, to split deterministic characteristic from stochastic processes for de-noising EMG signals. To combine the abilities ofPCA and wavelets, the measurements for each variable are dividedinto its wavelet coefficients. The PCA of the covariance matrix of the coefficients at each scale is calculated one by one and their autocorrelation is approximately de-correlated because of the wavelet decomposition. The amount of principal components to be captivated at each scale is not transformed by the wavelet decomposition since it does not affect the core relationship between the variables at any scale. As a result, existing techniques like, cross validation, screen test, or parallel analysis may be used for the data matrix in the time domain or to every wavelet coefficient to choose the proper amount of components [8, 9,10]

Discrete Wavelet Transformation(DWT)

The discrete wavelet transformation (DWT) uses digital filtering techniques in order to obtain a time-scale representation of a digital signal. DWT employs two sets of functions, called scaling functions $\varphi(t)$ and wavelet functions $\psi(t)$, which are associated with low-pass filters h(n) and high-pass filters g(n) [9-12].

The brake down of the signal into different frequency bands is acquired by successive high-pass and low-pass filtering of time domain signals, followed by downsampling by two. As a result, the J-th level DWT performed on N samples of digital signals sampled with frequency Fs is a set of detail coefficients cDi, i = 1 to J and approximation coefficients cAJ, concatenated into a single matrix of length N[9-13]

Distribution of energy of the EMG signal in time and frequency is represented by the extracted discrete wavelet coefficients. Using statistics over the wavelet coefficient sets helped in decreasing the dimensionality of the extracted feature vectors [14]. The statistical features used in this paper are the following:

- Mean of the absolute of each sub-band coefficients values.
- Average power of the each sub-band of wavelet coefficients.
- Standard deviation each sub-band of the coefficients.
- Ratio of the absolute mean values of adjacent sub-bands.

Support vector machine (SVM)

Basically, the support vector machine is a binary learning machine with some highlyelegant properties.To explain how the machine works, it is perhaps easiest to start with the case of separable patterns that arise in the context of pattern classification. This basic idea is elongated in a principled way to deal with the more difficult case of nonlinearly segregative patterns. A notion that is central to the development of the support vector learning algorithm is the inner-product kernel between a ―support vector" x_i and a vector x drawn from the input data space. Most importantly, the support vectors consist of a small subset of data points extracted by the learning algorithm from the training sample itself. Indeed, it is because of this central property that the learning algorithm, involved in theconstruction of a support vector machine, is also referred to as a kernel method. However, unlike the suboptimal kernel method, the kernel method basic to the design of a support vector machine is optimal, with the optimality beingrooted in convex optimization. However, this highly desirable feature of the machine isachieved at the cost of increased computational complexity[15].

III. Results and Discussion

In this study, DWT feature extraction and support vector machine (SVM) algorithm has been applied for EMG signal classification. First MSPCA is applied for de-noising EMG

signals and then DWT feature extraction technique is applied for surface EMG classification.

K-fold cross-validation method is applied for predicting the error rate of SVM classifier.

The number of true negatives (TN), true positives (TP), false positives (FP) and false negatives (FN) are used as a measurement to evaluate the performance of classifier. Different definitions are used to explain the results on different domains. The specificity, sensitivity and accuracy are widely used in diagnostic and detection tests and defined as follows.

$$\text{Sensitivity} = TP/(TP+FN)\ x100\% \quad (1)$$

$$\text{Specificity} = TN/(TN+FP)\ x100\% \quad (2)$$

$$\text{Accuracy} = (TP+TN)/(TN+TP+FN+FP)\ x100\% \quad (3)$$

SVM classification algorithm is applied and the results are presented in Table 1.

Table 1 Results

Movement	Accuracy (%)
Bowing	95.8
Clapping	98.6
Handshaking	84.7
Hugging	86.1
Jumping	81.9
Running	93.1
Seating	97.2
Standing	95.9
Walking	100
Waving	88.9
TOTAL	92.2

As seen from the table the classification accuracy of SVM is 92.22%. Furthermore, advantage of using DWT and SVM method is to have capability of modelling high dimensional feature space. Hence, more accurate data are provided to the SVM classifier by using DWT decomposition and MSPCA de-noising.

Total classification accuracy of our approach is the best when compared to other studies which used the same EMG data set. Since, MSPCA de-noising method is not utilized in other studies. According to comparison results it can be seen easily that appropriate and coherent decomposition and de-noising methods perform better on surface EMG signal classification.

IV. Conclusion

In this study, we have found out DWT decomposition method with MSPCA de-noising and SVM classifier gives an acceptable accuracy for surface EMG signals. This study achieved significantly better performance by using MSPCA de-noising. SVM classifier with DWT feature extraction method accomplished good performance with MSPCA de-noising over the ten EMG signal patterns. While examining coherence between methods, we realized how higher accuracy can be achieved by rearranging the parameters of the SVM classifier. Generally it is not efficient to use default parameters of classifiers since they have been set for common purpose. The classification accuracy with MSPCA de-noising, DWT feature extraction and SVM with a nonlinear kernel (C=300, γ=0.001) combination.

References

1. Kamen, Gary. Electromyographic Kinesiology. In Robertson, DGE et al. Research Methods in Biomechanics. Champaign, IL: Human Kinetics Publ., 2004.
2. P. S. Lum, C. G. Burgar, P. C. Shor, etal., Robot-assisted movement training compared with conventional therapy techniques for the rehabilitation of upper limb motor function after stroke, Arch. Phys. Med. Rehabil .83(7) (2002)952–959.
3. R. Riener, T. Nef, G. Colombo, Robot-aided neuro rehabilitation of the upper extremities, Med. Biol. Eng. Comput. 43(1)(2005)2–10.
4. M. A. Oskoei, H. Hu, Myoelectric control systems—a survey, Biomed. Signal Process. Control 2(4)(2007)275–294.
5. D. Farina, M.F. Lucas, C. Doncarli, Optimized wavelets for blind separation of non-stationary surface myoelectric signals, IEEE Trans. Biomed. Eng. 55 (1) (2008).
6. M. Khezri, M. Jahed, A novel approach to recognize hand movements via sEMG patterns, in: Proceedings of the 29th Annual International Conference of the IEEE Engineering in Medicine and Biology Society, Lyon, France, 2007, pp. 4907–4910.
7. Lichman, M. (2013). UCI Machine Learning Repository [http://archive.ics.uci.edu/ml]. Irvine, CA: University of California, School of Information and Computer Science.
8. Strang, G.; Nguyen, T. Wavelets and Filter Banks; Wellesley Cambridge Press: Wellesley, MA, USA, 1996.
9. Bakshi, B. R. (1998). Multiscale PCA with Application to Multivariate Statistical Process Monitoring. AIChE Journal.
10. E. Gokgoz, A. Subasi, Comparison of decision tree algorithms for EMG signal classification Biomedical Signal Processing and Control, 18 (2015), 138–144.
11. E. Gokgoz, A. Subasi, "Effect of Multiscale PCA de-noising on EMG signal classification for Diagnosis of Neuromuscular Disorders ", Journal of Medical Systems, 38(4):31,1-10, April 2014.
12. Polikar, R. The Wavelet Tutorial, 1996.Available online:http://person.hst.aau.dk/enk/ST8/wavelet_tutotial.pdf (accessed on 10 February 2015).
13. Tamara GrujicSupuk, Ana KuzmanicSkelin and MajaCic, Design, Development and Testing of a Low-Cost sEMG System and Its Use in Recording Muscle Activity in Human Gait, *Sensors* **2014**, *14*(5), 8235-8258.

14. Kandaswamy, A., Kumar, C.S., Ramanathan, R.P., Jayaraman, S., Malmurugan, N. Neural classification of lung sounds using wavelet coefficients. Computers in Biology and Medicine 34 (2004), pp. 523-537.
15. Simon Haykin,Neural Networks andLearning Machines, Third Edition, Pearson Education, Inc.2009.

Measurement in medicine – Past, present, future

A.Badnjevic[1], L. Gurbeta[1], D.Boskovic[2] and Z.Dzemic[3]

[1]Verlab Ltd Sarajevo, Medical Device Verification Laboratory, Sarajevo, Bosnia and Herzegovina
[2]Faculty of Electrical Engineering, University of Sarajevo, Sarajevo, Bosnia and Herzegovina
[3] Institute of Metrology of Bosnia and Herzegovina, Sarajevo, Bosnia and Herzegovina

Abstract— **In addition to knowledge and experience of medical doctors, correct diagnosis and appropriate patient treatment largely depend on accuracy and functionality of medical devices. In a large number of serious medical situations proper functionality of medical devices is crucial for patients. Therefore it is necessary to carry out as strict and independent testing of functionalities of medical devices as possible and to obtain the most accurate and reliable diagnosis and patient treatment.**

This paper presents the results of study conducted by the Institute of Metrology of Bosnia and Herzegovina (IMBIH) that highlight the necessity of introducing metrology into medicine and defining standard regulations for inspections of medical devices. As it has been previously done for other kinds of devices that are under jurisdiction of the Institute of Metrology of BH, this research provides a foundation for the introduction of medical devices into the legal metrology system with precisely defined units of measurement, their ranges and errors.

The study was based upon data collected through three clinical centers, 25 hospitals, 63 health centers and 320 private health institutions in BH over the course of one year.

As a result of this study, the medical devices that have been introduced into the legal metrology system in BH include ECG devices, defibrillators, patient monitors, respirators, anesthesia machines, dialysis machines, pediatric and neonatal incubators, therapeutic ultrasounds, infusion pumps and perfusors. Furthermore, standard inspection regulations for the aforementioned medical devices are also defined. Additionally, a national laboratory for the inspection of medical devices was established and it currently operates under the ISO 17020 standard.

With the introduction of medical devices into the legal metrology system and with the establishment of a fully operational national laboratory for inspection of medical devices, we expect that the reliability of medical devices in diagnosis and patient care will increase and that the costs of the health care system in BH will be reduced.

Keywords— **medical device, healthcare system, legislative, standard, metrology**

I. MEDICAL DEVICES UNDER LEGAL METROLOGY – MOTIVATION

Around the world, there are variety of health care systems each with its own characteristics and organizational structure according to nation resources, requirements and needs. Bearing this in mind it is very difficult to give general definition of health care system. Basically, it can be defined as normatively accepted system of society and government in protecting and improving the health of population, with all system factors affecting organized and constantly evolving as part of general country social system [1]. Each health care system consists of medical institutions which in addition to personnel and infrastructure must possess the necessary equipment in order to perform the correct diagnosis and treatment of their patients. In addition to the knowledge and experience of medical doctors, in patient diagnosis and treatment, it is necessary to have the correct and tested medical apparatus.

Diversity and innovativeness of medical devices, as a result of evolving field of biomedical engineering, significantly contribute to improvement in quality and efficiency of healthcare services. European commission define medical device as any instrument, apparatus, appliance, software, material or other article, whether used alone or in combination, including the software intended by its manufacturer to be used specifically for diagnostic and/or therapeutic purposes. Covering a wide range of products, from bandages to the most sophisticated life-supporting products used in diagnosis, prevention, monitoring, and treatment of diseases proper functionality of medical devices is crucial. In particular, it is important in life critical situations, when doctors have no more than 10 minutes to make a decision according to diagnosis based on readings of medical devices [2]. Unfortunately, between 40,000 and 80,000 patients around the world, die due to the malfunctioning of medical apparatus [3] and over 10,000 patients get seriously injured [4]. Due to these facts, withdraw of series of medical devices from market by its manufacturers have been registered in the past [5].

The health care system of Bosnia and Herzegovina is very complicated and time consuming for its end users. It consists of three levels and over 20 sub-levels including different ministries, agencies and other institutions. Each of these levels and sub-levels suffer consequences of apparent fragmentation of the system on one, and the diversity of laws and regulations in some parts of the country, on the other hand. All

this significantly contributes to different treatment of patients, different possibilities of access to health services, as well differences in quality of provided services [6].

The aspect of safety of medical apparatus in health care system around the world is regulated by different agencies or by applying international managing standards for health care institutions which ensure that safety of medical devices is checked once a year. On the other hand, the aspect of safety of medical apparatus in health care system of BH is left to manufacturers or distributors of medical equipment, allowing them a certain kind of monopoly.

In order to comply with the recommendations of the World Health Organization (WHO), and international standards for medical devices that are applied in developed countries of Europe and the rest of the world, as mentioned, it is necessary to apply the law in the field of metrology for medical apparatus. In that way every medical device is considered as a legal metrology which is regularly checked for deviations of output values. These deviations must not exceed the defined limits in order for medical device to be safe for use on patients. International standards and norms concerning medical devices are Medical Device Directive 93/42 / EEC [8], Medical Electrical Equipment ISO 60601 [9] and Safety Testing of Medical Devices ISO 62353 [10]. In addition, the international standard ISO 17020 defines the system of competence management of laboratories that deals with the inspection [11].

At the state level, in Bosnia and Herzegovina, Institute of Metrology (IMBIH) which is an integral part of the European Association of National Metrology Institutes (EURAMET) has legal jurisdiction over measurement devices. Among other things, IMBIH has the task to realize a base of standards in Bosnia and Herzegovina, to provide traceability of national standards to international standards and to prescribe metrological standard requirements and reference materials [7]. Metrological legislation in the field of medicine, as well as for other existing measures and gauges, should be defined by IMBIH. Currently legal metrology covers regulations for flow meters, gas meters, electricity meters, heat meters, water meters, mass scales, pressure gauges, ionizing radiation and other. In order to introduce medical devices in legal metrology, due to previously discussed safety importance of medical devices, it is necessary to conduct a study through the entire health care system of Bosnia and Herzegovina in order to provide the necessary information to define the laws and regulations in the field of metrology in medicine.

II. MEASUREMENT IN MEDICINE IN BOSNIA AND HERZEGOVINA

A. Methods

The study entitled "Measurement in medicine" was carried through all public and private health facilities including three clinical centers, 26 hospitals, 63 health centers and 320 private institutions. The study was conducted by national team appointed by the IMBIH.

The research and writing of the study lasted six months. All health care institutions were asked to define electrical medical devices that they use by name of manufacturer and model.

Based on results of processing collected data, the team from the IMBIH suggested which medical devices should be defined as legal metrology and become subject to regular verifications in accordance with the ISO 17020 standard. For every proposed medical device it was necessary to precisely define which outputs must be annually verified and the minimum characteristics of etalons that will be used in verification (inspection).

B. Results

The results of research and study have shown that currently in Bosnia and Herzegovina there are a number of medical devices aged over 20 years. In most cases these medical devices are not subjects of any service, or any kind of inspection.

Medical devices of newer generation, as shown in the study, went under authorized preventive and corrective maintenance in different ways. In some health institutions preventive service is scheduled annually, while in some institutions four times per a year, with a great impact for the budget of the health care institution and for the overall health care system. This is another kind of previously mentioned monopoly.

As a part of preventive service, an authorized service center performs also certification of apparatuses. Certification process report is usually a work order document. This document only reports the result of the certification: whether the device passed or failed. The work order document contains neither any information about device output values measurement, nor the reference to the certification standard.

Based on all collected data, as well as on the basis of international standards for medical equipment and metrology, IMBIH team proposed 10 different medical devices to be introduced in legal metrology. The proposed medical devices are used in critical patients care and are an integral part of every intensive care unit, operating rooms, and emergency care. The proposed devices are: ECG, defibrillator, patient

monitor, infusion pums, perfusors, respirator, anesthesia machine, dialysis machine, neonatal and pediatric incubator and therapeutic ultrasound.

Table 1. Overview of the medical devices and their output values in legal metrology

No.	Medical device	Output value
1	ECG	Voltage amplitude output
		Heart rate measured during time interval of 1 minute
2	Defibrillator	Energy output
3	Patient monitor	ECG parameters
		Respiration
		NIBP
		IBP
		Body skin temperature
		Standard SpO2
		CO2
4	Infusomat	Flow
5	Perfusion	Flow
6	Respirator	Flow
		Flow
		Volume
7	Anesthesia machine	Flow
		Flow
		Volume
		Concentration of anesthesia gasses
8	Dialysis machine	Conductivity
		Temperature
		Pressure
9	Incubators	Air temperature
		Body skin temperature
		O_2concentracion
		Relative humidity
		Mass
10	Therapeutic ultrasound	Power output

For these medical devices output values that will be subject to regular inspections are defined. Table 1 presents medical devices introduced into legal metrology and their respective output values which are subject to regular inspections.

As a result of the study, legal regulations were published in the Official Journal of Bosnia and Herzegovina, listing the medical devices that have become legal metrology. Regulations also define inspection rules and allowed deviation limits for each of the measures listed in the Table 1.

Safety inspection of medical devices in health care system can be performed only by the unbiased, impartial and independent laboratory accredited according to the ISO 17020 standard and appointed by the state. The laboratory for inspection of medical devices must possess the equipment calibrated by a calibration laboratory accredited and operating in accordance with the ISO 17025 standard. Therefore, traceability can be traced back to the international standards for all devices that are subject of verification process.

Regulations also define that the inspection of medical devices in health care institution is done once in a year.

III. CONCLUSIONS

The primary role of any health care system is to provide effective, accurate, safe and equal service to all patients. Introduction of medical equipment in legal metrology is one of the steps for regulation and standardization of the health care system in Bosnia and Herzegovina.

In this way lobby of private companies in the distribution and maintenance of medical equipment can be reduced. Also, unbiased control of measuring instruments is performed, using etalons that have documented traceability to international standards.

The most important is that all the steps also increase safety and reliability in health care, resulting in better and more reliable patient diagnosis and treatment.

REFERENCES

1. Boris Hrabač, *Zdravstveni sistemi i podsistemi, Sveučilište u Mostaru. 2013/2014*
2. BMJ Quality & Safety at *http://qualitysafety.bmj.com/*
3. Journal of the American Medical Association at*http://jama.jamanetwork.com/journal.aspx*
4. Electrical safety of medical equipment at*http://www.ewh.ieee.org/r8/uae/Elect_Safety_Med_Equip.pdf*
5. Fierce Medical Devices at*http://www.fiercemedicaldevices.com/story/ge-recalls-scanners-after-patient-crushed-death/2013-07-29*
6. Ervin Mujkić, *Sistem zdravstva u Bosni i Hercegovini: stanje i pravci moguće reforme,*Fondacija Centar za javno pravo
7. IMBH at *http://www.met.gov.ba/*
8. Medical Device Directive 93/42 / EEC at http://eur-lex.europa.eu/LexUriServ/LexUriServ.do?uri=CONSLEG:1993L0042:20071011:en:PDF

9. Medical Electrical Equipment ISO 60601, General requirements for basic safety and essential performance, IEC 60601-1-11:2010
10. Safety Testing of Medical Devices ISO 62353/2014
11. Europena Comission, Medical Devices. Guidence document at*http://ec.europa.eu/health/medical-devices/files/meddev/2_1-1___04-1994_en.pdf*

A. Badnjević is with the Verification Laboratory "Verlab" Ismeta Mujezinovića 30, Sarajevo, B&H (phone: 387-61-213-599; e-mail: almir@verlab.ba).

Overview for computer aided detection of aortic diseases

Elnur Smajić[1], Nihad Mešanović[2]

[1]University Clinical Center Tuzla, Clinic for internal diseases, Cardiology department, Tuzla, Bosnia and Herzegovina
[2]University Clinical Center Tuzla, Sector for information technologies, Tuzla, Bosnia and Herzegovina

Abstract- **Aortic diseases are the greatest challenge of our time to diagnose as well as treat contribute to the wide spectrum of arterial diseases: aortic aneurysms, acute aortic syndromes (AAS) including aortic dissection (AD), penetrating atherosclerotic ulcer and atherosclerotic and inflammatory affections, as well as genetic diseases (e.g. Marfan syndrome) and congenital abnormalities including the coarctation of the aorta. AAS is often the first sign of the disease, which needs rapid diagnosis and decision-making to reduce the extremely poor prognosis. Recently, the published data demonstrated that the overall global death rate from aortic aneurysms and AD increased between 1990 and 2010 with higher rates for men. The burden increases with age, and men are more often affected than women. On the other hand the diagnostic methods for imaging the aorta have improved significantly, particularly by the development of multi-slice computed tomography (MSCT) and magnetic resonance imaging (MRI) technologies, due the ability to obtain a complete 3D dataset of the entire aorta. The new published data demonstrated that, the drop in mortality of aortic dissection was greatest among patients getting surgical repair. The reason for the improvement in mortality in operative patients might have been subtle improvements on various fronts. This may partly be because of advancements in noninvasive diagnostic technology, such as the development of multidetector CT resulting in rapid high definition CT angiography from neck to abdomen, leading to increased detection of dissection. Computer aided detection (CAD) has been a revolutionary step in the early diagnosing of aortic diseases. Since the cardiologist must be able to quickly propose diagnosis for the patient, a high degree of accuracy in CAD models is required within a minimum amount of time. In this paper we described the principles of CAD systems, development methods and implementation of proposed methods for aortic diseases. CAD analysis can be used in daily routines and may contribute to more efficient diagnosis and in treatment of aortic diseases.**

Key words- **Aortic diseases, Computer aided detection**.

I.INTRODUCTION

Today's, acute and chronic coronary artery disease and/or ischemic heart disease is under the control of myocardial revascularization (coronary artery bypass grafting- CABG and percutaneous coronary intervention- PCI), particularly percutaneous coronary intervention. In the meantime, PCI has become one of the most frequently performed therapeutic interventions in medicine, and progress has resulted in a steady decline of periprocedural adverse events, resulting in excellent outcomes with both revascularization techniques [1].

Although valvular heart disease (VHD) is less common in industrialized countries than coronary artery disease, heart failure (HF), or hypertension, there is a great interest in this field because VHD is frequent and often requires intervention. Decision-making for intervention is complex. New evidence was accumulated, particularly on risk stratification; in addition, diagnostic methods in particular echocardiography and therapeutic options have changed due to further development of surgical valve repair and the introduction of percutaneous interventional technique mainly transcatheter aortic valve implantation (TAVI) and percutaneous edge-to-edge valve repair. These changes re mainly related to patients with aortic stenosis (AS) and mitral regurgitation (MR). Thus, VHD is a problem that is almost solved [2].

In addition to coronary and peripheral artery diseases, aortic diseases contribute to the wide spectrum of arterial diseases: aortic aneurysms, acute aortic syndromes (AAS) including aortic dissection (AD), intramural haematoma (IMH), penetrating atherosclerotic ulcer (PAU) and traumatic aortic injury (TAI), pseudoaneurysm, aortic rupture, atherosclerotic and inflammatory affections, as well as genetic diseases (e.g. Marfan syndrome) and congenital abnormalities including the coarctation of the aorta (CoA). Similarly to other arterial diseases, aortic diseases may be diagnosed after a long period of subclinical development or they may have an acute presentation. Acute aortic syndrome is often the first sign of the disease, which needs rapid diagnosis and decision making to reduce the extremely poor prognosis. The Global Burden Disease 2010 project demonstrated that the overall global death rate from aortic aneurysms and AD increased from 2.49 per 100 000 to 2.78 per 100 000 inhabitants between 1990 and 2010, with higher rates for men. On the other hand the prevalence and

incidence of abdominal aortic aneurysms have declined over the last two decades. The burden increases with age, and men are more often affected than women. The ESC's Task Force on Aortic Dissection, published in 2001, was one of the first documents in the world relating to disease of the aorta and was endorsed by the American College of Cardiology (ACC). Since that time, the diagnostic methods for imaging the aorta have improved significantly, particularly by the development of multi-slice computed tomography (MSCT) and magnetic resonance imaging (MRI) technologies, due the ability to obtain a complete 3D dataset of the entire aorta. During the past decade, advances in multidetector CT (MDCT) and MRI have led to their current role as the techniques of choice for the evaluation of the entire spectrum od aortic diseases [3,4].

To the contrary of coronary artery disease and valvular heart disease, aortic diseases are still the greatest challenge of our time to diagnose as well as treat. Lack of adequate percutaneous intervention in aortic diseases, preferred surgical procedures, so that the management of aortic diseases is quite demanding. The new published data demonstrated that, the drop in mortality of aortic dissection was greatest among patients getting surgical repair. The reason for the improvement in mortality in operative patients might have been subtle improvements on various fronts. This may partly be because of advancements in noninvasive diagnostic technology, such as the development of multidetector CT resulting in rapid high definition CT angiography from neck to abdomen, leading to increased detection of dissection [5].

Computer Aided Detection (CAD) is a computer system that process and analyze an image (mammogram, US, CT-scan, MRI) combining elements of artificial intelligence (AI) and digital image processing (postprocessing). Image segmentation is the process of partitioning an image into regions by grouping together neighborhood pixels based on the some predefined similarity criterion. The similarity criterion can be determined using specific properties or features of pictures elements (pixels) representing objects in the image. In other words, segmentation is a pixel classification technique that allows the formation of regions of similarities in the image. In some applications segmentation may be useful to classify image pixels into anatomical regions, such as bones, muscles, and blood vessels, while in others into pathological regions, such as cancer, tumor, tissue deformities and multiple sclerosis lesions. Segmentation is an important tool in medical image processing and it has been useful in many applications. The applications include detection of the coronary border in angiograms, multiple sclerosis lesion quantification, surgery simulations, surgical planning, measuring tumor volume and its response to therapy, functional mapping, automated classification of blood cells, studying brain development, detection of microcalcification on mammograms, image registration, atlas matching, heart image extraction from cardiac cine angiograms, detection of tumors etc [6].

On the other hand, the goal of medical visualization is to produce clear and informative pieces of images of the important structures in a data set but simple approaches have limited performance on visualization of heart and other organs. Volume visualization can be used either directly with the whole volume data or after a segmentation algorithm. For both cases, volume rendering is an important technique since it displays 3D images directly from the original data set and provides automatic combinations of the selected image transformations such as opacity and color. Different approaches regarding cardiac segmentation for a variety of modalities have been widely described in the literature in the past years and range from 2D methods to more complex, model based, and approaches. In the past few years several software applications have been presented in the literature, which allows fast image processing pipelines by using a graphical user interface where different processing blocks can be interconnected [6].

II. COMPUTER AIDED DETECTION IN THE DIAGNOSIS OF AORTIC DISEASES

A. Healthy vs Diseased Aortae

Over the past few decades, research into diagnostic radiology has provided more tools for handling symptoms of cardiac disease. For diagnosing chest pain, several studies have demonstrated that a contrast-enhanced CT scan of thoracic cavity is an effective, accurate, and noninvasive method with a high negative predictive value for cardiac diseases. One particular method is Triple Rule-Out (TRO) protocol in which the coronary arteries, pulmonary arteries, thoracic aorta, and other intrathoracic structures are highlighted in the CT scan. By examining the scan for signs of serious heart conditions, for instance coronary stenosis, pulmonary embolism, and AD, TRO images can be used to determine if a patient should be released or admitted for further evaluation. This method results in the cutting of cost and time involved with diagnosing a patient [7].

With the purpose of designing a CAD system for aortic diseases to assist radiologists, it developed two automated diagnostic processes for determining whether an aortic object, in a contrast-enhanced CT image, is healthy or diseased. The diagnostic process currently detects two aortic diseases, AD and PAU. Two criteria for signs of these diseases were established for the system to be utilized in its decision making process: for AD, if it cross-section of the aorta in an image is not circle-like; for PAU, if it the aorta

contains objects with Hounsfield Units (HU) values higher than normal along its wall [7].

In the case of an AD, blood flows into the media layer of a deteriorated section of the aortic wall and creates a new lumen. From the perspective of a CT image, the lumen is separated into two pieces and the differences in blood pressure between the two lumens cause distortions in their shapes. The functions of the diagnostic process were designed based on edge oriented methods and should be capable of recognizing a circle-like object in an image. In the output, this process identifies aortic objects with a circle-like shape as healthy and any aortic object that does not meet that criterion as a possible candidate for aortic disease. The AD detection process had a sensitivity of 0.8218 and a specificity of 0.9907. This indicates that this process is capable of identifying a healthy aorta shape but not fully able to recognize all types created by an aorta dissection. The most common error occurred when the aorta dissection caused the aorta to shrink but still maintained a circle-like shape [7].

In the case of PAU, an ulceration of an atheromatous plaque erodes the intima causing a hematoma in the media of the aorta. In contrast-enhanced CT slices, a PAU appears as a contrast-filled, pouch-like protrusion of the aorta or as a thickened aortic wall in absence of an intimal flap or a false lumen. The HU around the PAU can be higher than the normal lumen for two reasons. First, contrast media become temporarily trapped in these pouches and increase its concentration in this area. Second, the calcified plaque that causes PAU has a high HU value and lines the intima around the PAU. The functions for the diagnostic process were created using interest point operators to locate these objects of higher than average intensity within an aortic object. In the output every aortic object that meets this criterion is labeled as a PAU object and sign of a PAU. Otherwise, the aortic object as a whole is labeled as healthy. The PAU detection process scored a sensitivity of 0.7587 and a specificity of 0.9700. This process mostly avoided incorrect identification of PAU. This is likely due to the success of this segmentation process with removing artifacts and noise. Regarding the sensitivity, this process was able to distinguish a majority of the PAU. When it overlooked a PAU, this was because the PAU had an intensity that was similar to the lumen. But, criteria still unaddressed for identifying aortic diseases include significant changes in the size (increasing or decreasing) of aorta, appearance of intimal flaps which are dark lines contained within the lumen, and detection of PAU on the boundary based on shape. Several studies have confirmed the feasibility of this approach, providing good coronary, pulmonary, and aortic image quality with negative predictive values in the range of 99.4% to 100%. Relative disadvantages of a TRO include increased scan length, additional radiation exposure, 20% to 50% more contrast volume (to maintain pulmonary artery opacification), and added protocol complexity [7,8].

It is known that connective tissue disorders, such as Marfan's syndrome and Familial Thoracic Aortic Aneurysm syndrome, are at increased risk of developing aortic aneurysm and dissection. Early detection of connective tissue disorders is potentially an important tool in prophylactic treatment of these severe diseases. Automated and accurate segmentation (unlike manually) of the aorta in 4D (3D + time) MR image data and a CAD method using independent component analysis (ICA) can help in this issue. 4D MR image data can show a set of validated quantitative indices of aortic morphology and motion. The aorta is visible as a candy cane or a bit like a question mark tilted left. The mean of the diseased is seen to be a bit dilated compared to the mean of the healthy subjects, which corresponds to clinical observations. The diseased are seen to have a dilation at the ascending aorta, and both, a dilation of the ascending and descending aorta, apparently including a dilation around the beginning of the descending aorta. It can be observed that the diseased subjects seem to have a thicker arch and in particular a thicker ascending aorta. The diseased subjects also appear to have a thicker ascending aorta and a flatter aortic arch. The mean shape is unfortunately not precise enough, as a descriptor, to separate the two classes using a simple distance measure or canonical discriminant analysis. The automated 4D segmentation result produced accurate aortic surfaces. The CAD method distinguished between normal and diseased subjects with a classification accuracy of 96.8 %, using features showing correspondence to clinical observations of connective tissue disorder [9].

Since its introduction in the late 1980s, 2-dimensional phase contrast MRI (2D PC-MRI) has become a routine part of standard-of-care cardiac MRI for the assessment of regional blood flow in the heart and great vessels. More recently, time-resolved PC-MRI with velocity encoding along all three flow directions and three-dimensional (3D) anatomic coverage (also termed '4D flow MRI') has been developed and applied for the evaluation of cardiovascular hemodynamics in multiple regions of the human body. A number of studies have demonstrated the potential of 4D flow MRI to provide an improved assessment of hemodynamics which might aid in the diagnosis and therapeutic management of cardiovascular diseases. Some of the earliest and best studied applications of 4D flow MRI are the macroscopic visualization and 3D quantification of thoracic aorta hemodynamics. One particular area of clinical interest is patients with bicuspid aortic valve (BAV) who have an ascending aortic aneurysm or are at risk of aneurysm formations and dissection. Recent data using 4D

flow MRI has shown high velocity flow jets impinging on the ascending aortic wall and resulting in increased WSS in these regions and additional results demonstrate increased helical flow in the ascending aorta of BAV patients. This type of assessment is unique to 4D flow MRI. A second application of 4D flow MRI in the thoracic aorta is aortic arch and descending aorta assessment in patients with aortic coarctation. Using 4D flow MRI to assess this cohort of patients has proven to provide useful characteristics about the impact of coarctation and coarctation repair on flow features throughout the aorta. Patients with aortic coarctation tend to have flow jet eccentricity following the coarctation resulting in jet impingement along the descending aorta [10].

B. Aortic dissection

There are many methods for detection of aortic dissection. We already described one of the particular method (TRO protocol) for detection of aortic dissection. Very interesting issue in this topic is pathogenesis of aortic dissection. Most aortic dissections occur with transverse tear along the greater curvature of the aorta a few centimeters above the aortic valve. Mechanical stress in the aortic wall is proportional to blood pressure and vessel diameter. Wall abnormalities may also promote dissections. Several studies have visualized aortic root motion where in the root is displaced downward during systole and returns to its previous position in diastole. Recent MRI studies in healthy subjects revealed an axial downward motion and a clockwise axial twist during systole. The force driving the aortic annulus motion is the ventricular traction accompanying every heartbeat. This force is transmitted to the aortic root, the ascending aorta, the transverse aortic arch, and supra-aortic vessels. Thus, aortic root motion has direct influence on the deformation of the aorta and on the mechanical stress exerted on the aortic wall [11].
Beller CJ et al. were investigated, in cardiac patients with a finite element model of the aortic root, arch, and branches of the arch using ANSYS 5,7 software, influence of aortic root displacement and pressure on the aortic wall stress. Aortic root motion is increased in patients with aortic insufficiency (they have increased stroke volume), but reduced in patients with hypokinesis of the left ventricle. They showed that the right lateral aspect of the ascending aorta a few centimeter above sinotubular junction experienced increased longitudinal stress with increased axial displacement, pressure, and aortic wall stiffness. This may explain why circumferential intimal tears and aortic dissections occur more often in this location. Functional downward displacement of the aortic root seemed to be as much of a risk factor for dissection as hypertension. Increased stiffness was also found to enhance the effects of root motion on aortic wall stress. For all the above reasons, in patients possibly at risk of dissection, aortic root movement should be considered an additional risk factor [11].

C. Aortic aneurysm

There are many methods for the detection of aortic aneurysms. One method is based on graph cut theory (modified Boykov and Jollys method) for segmenting the aneurismal sac of an abdominal aortic aneurysm (AAA) both from multi-slice MR and CT scan examinations. It is a semi-automatic method to segment the lumen and the aortic wall from a stack of axial images covering the abdominal aorta from the renal arteries down to the iliacs. A comparison with manual tracing demonstrates that this semi-automatic segmentation is as precise as an expert. It works independently on MRI and CT-scan volumes. This semi-automatic method provides reliable contours of the abdominal aorta from CT-scan or MRI, allowing rapid and reproducible evaluations of AAA. The overall procedure including initialization, segmentation and touch up takes roughly less than one minute. This is fairly small compared to manual segmentation. As a rule of thumb, our experts took between 4 and 8 minutes to segment a 20-slice MRI volume and between 7 and 12 minutes for a 40-slice CT scan volume. The deployment of this approach in clinical practice would provide cardiologists with key parameters allowing the follow up of patients with AAA [12].
Sakalihasan et al. by means of combined positron emission tomography and computes tomography (PET-CT) examination, observed positive correlation between clinically unstable AAA and positive uptake of 18F-fluoro-2-deoxy-glucose (FDG) in the aneurysm wall. Elevated FDG uptake was also related to the presence of a high density of inflammatory cells in the aneurismal aortic wall. Further studies have been confirmed these observations. In study of Xu et al. was performed comparison of wall stress analysis and PET-CT images of AAA. The lumen boundary was segmented semi-automatically by using the region growing method, wich traces the perimeter of the lumen by seeking pixels of a selected range of intensities. The segmented lumen contours were then assembled in 3D, and luminal surface was constructed by using cubic B splines. Similar procedures were followed for the segmentation and reconstruction of the outer wall surface. Stress analysis was performed for all the reconstructed aneurysm models by using a finite element method code ADINA 8,2 (Automatic Dynamic Incremental nonlinear Analysis). This finite element analysis of wall stress shows that the stress distribution is highly dependent on 3D geometric features of the aneurysms, and that areas of maximum stress do not

occur at the maximum diameter. The location of high wall stress correlates well with the site of high FDG uptake shown by the PET-CT fusion image. At the same sites, for different periods of time, further CT scan examinations revealed rupture of aortic aneurysm. So, there is a potential link between accelerated metabolism in aortic aneurysm wall and high mechanical stresses experienced by the wall. PET imaging combined with wall stress analysis could potentially give more reliable predictions of the risk of aneurysm rupture. PET-CT scan and finite element analysis are able to monitor the development and evolution of AAA [13].

III. Computer aided detection in the treatment of aortic diseases

In addition to the role of information technologies in the diagnosis of aortic diseases, it has a great relevance in the therapeutic methods of aortic diseases. Simulation of stent placement enables clinicians to determine which devices are appropriate for an individual patient [14].

Egger et al. presented automatic segmentation, both the lumen and outer wall of the aorta that allows clinicians to determine if intervention is warranted and if so, which stenting device is most appropriate, and where it should be positioned. It is possible to perform an analysis to determine if intervention is required and acquire measurements necessary to select the proper stenting device. But, the diaphragm has signal intensity characteristics very similar to that of thrombus, and in the presence of a dissection the segmentation of outer wall may incorrectly exlude one of the channels (false lumen). Automatic vs manual segmentation showed better results in simulation of stent placement [14].

In the paper of Zheng et al. were presented a fully automatic aorta segmentation and valve landmark detection in C-arm CT with applications to transcatheter aortic valve implantation (TAVI) [15]. The initial clinical trial demonstrated the usefulness of this sistem in the TAVI workflow, providing a proper angulation to avoid large tilting of prosthetic valve after deployment. However, automatic segmentation of the aorta in a C-arm CT volume is far more challenging. The aortic arch and descending aorta may be captured in some volumes, but missing in others. To adress this challenge, the whole aorta is split into four parts: aortic root, ascending aorta, aortic arch, and descending aorta using part based model. The aortic root is detected and segmented as the first step using marginal space learning [16]. Assembling all the aortic parts together, it get an initial surface mesh of the aorta. Besides segmenting the aorta, it also detect eight aortic valve landmarks: three aortic hinge points, three aortic commissure points, and left and right coronary ostia since they are important in both surgery planning and providing visual guidance during surgery. This approach is computationally efficient, taking about 1,4 seconds to process a volume on a computer [15].

Capelli et al. explore the feasibility of TAVI in patients which are currently borderline cases for a percutaneous approach. Three-dimensional models of the implantation sites were reconstructed from CT images. Within these realistic geometries, TAVI with an Edwards Sapien stent was simulated using finite element modelling. Finite element analysis proved that TAVI was morphologically feasible. After the implantation, stress distribution showed no risks of immediate device failure and geometric orifice areas increased with low risk of obstruction of the coronary arteries. Maximum principal stresses in the arterial walls were higher in the model with native outflow tract. Finite element analyses can both refine patient selection and characterise device mechanical performance in TAVI, overall impacting on procedural safety in the early introduction of percutaneous heart valve devices in new patient populations [17].

Treatment of patients with Marfan's syndrome is a particular challenge. Standard surgical management of aortic root aneurysm in Marfan patients is either total root replacement or valve-sparing root replacement. The placement of a personalised external aortic root support (PEARS), relatively new technique, was introduced in 2004 as a conservative approach for Marfan patients. PEARS technology employs spatial data from MRI or CT images to create a CAD model from which a replica of the individual aorta is made by rapid prototyping. On this former, a mesh support, customised for the individual patient, is manufactured from a macroporous textile knitted from a medical grade polymer yarn. The mesh is positioned around the aorta, closely applied from the aortoventricular junction to beyond the brachiocephalic artery. This way of operation were no deaths or cerebrovascular, aortic or valve-related events. These early outcomes are better than published results for the more radical extirpative root replacement operations. After proof of principle and prospective evaluation, the technique has undergone Health Technology Appraisal by the British National Institute for Health and Care Excellence (NICE) [18, 19].

IV. Conclusion

This article provides an overview of clinical applications of Computer Aided Detection (CAD) in aortic diseases. CAD established its role in medical imaging, and steps forward to fill new, more demanding positions in medical practice. On the one hand, aortic diseases represent a diagnostic and therapeutic challenge for cardiologists, but on the other hand

the progress of computer-aided detection is particularly in the diagnosis and treatment of aortic diseases. We can conclude that CAD is powerfooll tool in the diagnosis, monitoring, predicting of complications and therapeutic interventions of aortic diseases.

REFERENCES

1. S. Windecker, Ph. Kolh, F. Alfonso, J. Ph. Collet, J. Cremer, V. Falk, G. Filippatos, C. Hamm, S. J. Head, P. Ju¨ni, A. P. Kappetein, A. Kastrati, J. Knuuti, U. Landmesser, G. Laufer, F. J. Neumann, D. J. Richter, P. Schauerte,M. S. Uva, G. G. Stefanini, D. P. Taggart, L. Torracca, M. Valgimigli,W. Wijns, and A. Witkowski. 2014 ESC/EACTS Guidelines on myocardial revascularization The Task Force on Myocardial Revascularization of the European Society of Cardiology (ESC) and the European Association for Cardio-Thoracic Surgery (EACTS) Developed with the special contribution of the European Association of Percutaneous Cardiovascular Interventions (EAPCI). European Heart Journal (2014) 33, 2451-2496.

2. A. Vahanian, O. Alfieri, F. Andreotti, M. J. Antunes, G. Baro´n-Esquivias, H. Baumgartner, M. A. Borger, T. P. Carrel, M. DeBonis, A. Evangelista, V. Falk, B. Iung, P. Lancellotti, L. Pierard, S. Price, H. J. Scha¨fers, G. Schuler, J. Stepinska, K. Swedberg, J. Takkenberg, U. Otto Von Oppell, S. Windecker, J. L. Zamorano, M. Zembala. Guidelines on the management of valvular heart disease (version 2012) The Joint Task Force on the Management of Valvular Heart Disease of the European Society of Cardiology (ESC) and the European Association for Cardio-Thoracic Surgery (EACTS). European Heart Journal (2012) 33, 2451–2496.

3. R. Erbel, V. Aboyans, C. Boileau, E. Bossone, R. Di Bartolomeo, H. Eggebrecht, A. Evangelista, V. Falk, H. Frank, O. Gaemperli, M. Grabenwo¨ger, A. Haverich, B. Iung, A. J. Manolis, F. Meijboom, Ch. A. Nienaber, M. Roffi, H. Rousseau, U. Sechtem, P. A. Sirnes, R. S. von Allmen, Ch. J. M. Vrints. 2014 ESC Guidelines on the diagnosis and treatment of aortic diseases Document covering acute and chronic aortic diseases of the thoracic and abdominal aorta of the adult The Task Force for the Diagnosis and Treatment of Aortic Diseases of the European Society of Cardiology (ESC). European Heart Journal (2014) 35, 2873–2926.

4. D. Litmanovich, A. A. Bankier, L. Cantin, V. Raptopoulus, Ph. M. Boiselle. CT and MRI in diseases of the aorta. AJR 2009;193:928-940.

5. P. S. Mody et al. Trends in aortic dissection hospitalizations, interventions, and outcomes among Medicare beneficiaries in the United States, 2000-2011. Circ Cardiovasc Qual Outcomes 2014.

6. N. Mešanović, E. Smajić. Overview of open source software for computer aided detection in cardiology. Symposium Cro e-Cardiology 2012, March 15-17, 2012, Osijek, Croatia.

7. M. Gayhart, H. Arisawa. Automated detection of healthy and diseased aortae from images obtained by contrast-enhanced CT scan. Hindawi Publishing corporation, Computational and Mathematical Methods in Medicine, volume 2013, article ID 107871, 7 pages.

8. T. S. Cook, M. Galperin-Aizenberg, H. I. Litt. Coronary and Cardiac Computed Tomography in the Emergency Room: Current Status and Future Directions. J Thorac Imaging 2013;28:204–216.

9. M. S. Hansen, F. Zhao, H. Zhang, B. K. Ersbøll, A. Wahle, T. Scholz and M. Sonka. Detection of Connective Tissue Disorders from 4D Aortic MR Images using Independent Component Analysis, MICCAI- Medical Image Computing and Computer-Assisted Intervention, 2006.

10. Z. Stankovic, B. D. Allen, J. Garcia, K. B. Jarvis, M. Markl. 4D Flow imaging with MRI. Cardiovasc Diagn Ther 2014;4(2):173-192.

11. C. J. Beller, M. R. Labrosse, M. J. Thubrikar, F. Robicsek. Role of aortic root motion in the pathogenesis of aortic dissection. Circulation 2004;109:763-769.

12. A. A. Duquette, P. M. Jodoin, O. Bouchot, A. Lalande. 3D Segmentation of abdominal aorta from CT-scan and MR images. Computerized Medical Imaging and Graphics 2012;36:294-303.

13. X. Y. Xu, A. Borghi, A. Nchimi, J. Leung, P. Gomez, Z. Cheng, J. O. Defraigne, N. Sakalihasan. High levels of 18F-FDG uptake in aortic aneurysm wall are associated with high wall stress. Eur J Vasc Endovasc Surg 2010;39:295-301.

14. J. Egger, B. Freisleben, R. Setser, R. Renapuraar, C. Biermann, T. O'Donnell. Aorta Segmentation for Stent Simulation. Medical Image Computing and Computer-Assisted Intervention, Workshop on Cardiovascular Interventional Imaging and Biophysical Modelling 2009; 10 pages.

15. Y. Zheng, M. John, R. Liao, J. Boese, U. Kirschstein, B. Georgescu, S. K. Zhou, J. Kemfert, T. Walther, G. Brockmann, D. Comaniciu. Automatic aorta segmentation and valve landmark detection in C-arm: Application to aortic valve implantation. International Conference on Medical Image Computing and Computer-Assisted Intervention 01/2010; 13(Pt 1):476-83.

16. Y. Zheng, A. Barbu, B. Georgescu, M. Scheuering, D. Comaniciu. Four-chamber heart modeling and automatic segmentation for 3D cardiac CT volumes using marginal space learning and steerable features. IEEE Trans. Medical Imaging 27, 11, 2008, pp 1668-1681.

17. C. Capelli, G. M. Bosi, E. Cerri, J. Nordmeyer, T. Odenwald, P. Bonhoeffer, F. Migliavacca, A. M. Taylor, S. Schievano. Patient-specific simulations of transcatheter aortic valve stent implantation. Med Biol Eng Comput. 2012 Feb;50(2):183-92.

18. T. Treasure, J. J. Takkenberg, T. Golesworthy, F. Rega, M. Petrou, U. Rosendahl, R. Mohiaddin, M. Rubens, W. Thornton, B. Lees, J. Pepper. Personalised external aortic root support (PEARS) in Marfan syndrome: Analysis of 1-9 year outcomes by intention-to-treat in a cohort of the first 30 consecutive patients to receive a novel tissue and valve-conserving procedure, compared with the published results of aortic root replacement. Heart 2014; 100(12):969-75.

19. F. J. Criado. Aortic dissection: a 250-year perspective. 8th current Trends in Aortic and Cardiothoracic Surgery Conference; Houston, 29-30 april 2011.

Elnur Smajić, University Clinical Center Tuzla, Tuzla, Trnovac bb, 75000 Tuzla (phone:387-35-303-110;387-61-185-437,elnur.smajic@ukctuzla.ba)

AC and DC Coupling of Electrocardiograph in Mobile Monitoring Applications

D. Jurić[1] and A. Akšamović[1]

[1] University of Sarajevo, Faculty of Electrical Engineering, Sarajevo, Bosnia and Herzegovina

***Abstract*-- Recording of ECG signals is becoming more and more commonplace in the modern world today. An increasing number of smartphones, wearables and other devices have ECG signal detection, recording and analysis capability. These mobile devices have imposed upon them a different set of constraints when compared to the classic holter or ambulatory electrocardiographs such as to have low power consumption, to be lightweight and to be compact. DC coupling of ECG has become a solution to address these issues that come up before a biomedical equipment designer. Still DC coupling has its own design requirements and they are in this paper compared to design requirements of AC coupling. Analog front end requirements are discussed in terms of filtering, conversion, power consumption and compactness of size. Digital back end requirements are discussed in terms of processor number of bits required for each method and amount of digital filtering each method requires to obtain an acceptable ECG signal. Applicability of both methods to mobile electrocardiograph design is then discussed.**

Electrocardiograph as a device is mature and well developed technology. Still the advances in electronics and microcontrolers that enable evermore complex digital signal processing algorithms to be used in electrocardiography [1]. The goal of this research is to uncover whether or not the DC coupled, digital filtering intensive electrocardiography is more suitable to mobile monitoring aplications that the conventional AC coupled, analog filtering intensive electrocardiography.

Firstly to obtain a valid and usable signal in electrocardiography is a somewhat difficult chalendge due to the various sources of noise that saturate the and obsucure the valuable information that the ECG signal carries [2]. Sources of noise are various and are both high and low frequency artifacts. Example of a low frequency artifact would be the bias that the electrode-skin interface brings to the signal, while an example of a high frequency artifact would be the RF noise and noise coming from neon lights. Usually the biggest source of noise in Electrocardiography is the 50 Hz interference that comes from power lines [2].

In order to reduce the 50 Hz noise there are two courses of action. First one is filtering the signal using passive and active analog filters as well as with digital filters [3]. Second course of action is to maximize the Common-Mode-Rejection (CMR) of the circuit [4]. Usually the instrumentation amplifier that is most commonly used as a first stage amplifier for a single Electrocardiograph lead has a very high CMR, usually of about 100 or more decibels. This is an ideal situation value because the signal aquisition elements that preceed the instumentation amplifier in the signal path have a degree of mismatch in their resistance due to component tolerances and electrode positioning on the body [5].

For the initial design a single lead Electrocardiograph design with dry stainless steel electrodes was chosen. This was done because it is easy to scale to multiple lead designs and also to implement a different type of electrodes if neccessary. Also longterm monitoring aplication are usually done using various dry electrodes because of the subjects comfort and because the conventional wet Ag/AgCl electrodes dry out during time. For the design of a bioamplifier a AD621 instrumentation amplifier was used for the first stage amplification, while for the second stage a UA741 opreational amplifier was used. Before the first stage amplification signal was filtered using a passive first order RC low pass filter with a cut-off frequency of 286 Hz in order to remove RF interference from the signal. Between stage one and stage two amplifiers a passive first order RC high pass filter with a cut-off frequency of 1.5 Hz was used to remove the DC component form the signal.

Our first course of action was to directly connect the subject to the bioamplifier common. This proved inadequate for it failed to produce a readable ECG signal on an oscilloscope. Next course of action was to

implement a circuit called Right-Leg-Drive in order to reduce the level of common mode voltage [improving cmr using RLD TI]. Role of the Right-Leg-Drive is to invert and amplify the common mode voltage and then feed it back into the body of the patient thus reducing it's level.

In first attempt a simple amplification an inverting of the comon mode voltage taken from the gain seting resistor of the insturmentation amplifer using a ua741operational amplifier was implemented. This imediately produced a readable ECG signal on the oscilloscope screen as shown on Figure 1.

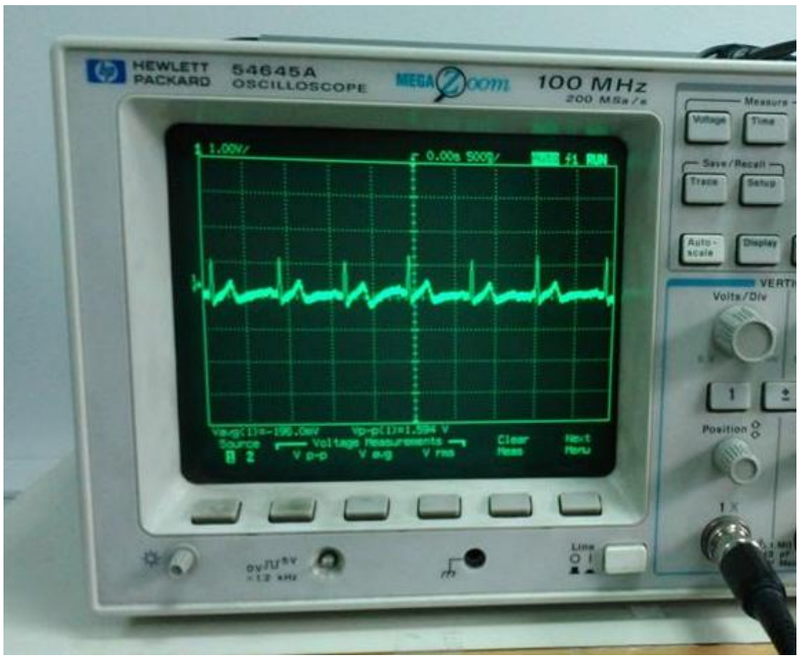

Figure 1.

Since the Right-Leg-Drive creates a closed loop system with the patient, leads, LPF filter and insturmentation amplifier it is neccesary to make sure that the circuit is stable in all conditions. The electrodes together with leads cables are especially problematic because their resistance and capacitance is not fixed but varies greately as a functon of their placement and position making the poles that they introduce into the sistem imposible to cancel out. Also the level of induced noise in the ECG cabels will depend on their position in respect of the power lines. Because of this it is important to carefully chose the amplification of RLD so that it leaves a sufficient level of stability margin. This can be done by introducing a capacitor in a RLD operational amplifer feedback loop [6].

After the signal has been adequately amplified modern ΔΣ AD converters with a high number of bits enable the ECG signal to be digitized without an intensive analog filtering [7]. After digitization by such a AD converter signal can be digitally filtered and manipulated using the standard techniques for digital signal processing. This approach reduces the size of the Analog-Front-End (AFE) portion of the Electrocardiograph which also assumed to leads to reduced power consumption making the system especially well suited for mobile long term monitoring applicatons [8] and wireless sensor networks [9]. Examining whether this approach is more power efficient than the conventional one that relies more on analog preparation of the signal will be the next stage of the research.

Keywords— **Electrocardiograph, Biopotentials amplifier, Right-Leg-Drive**

REFERENCES

1. Sonal K. Jagtap, M.D. Uplane, „*A Real Time Approach: ECG Noise Reduction in Chebyshev Type II Digital Filter*“, International Journal of Computer Applications (0975 – 8887) Volume 49– No.9, July 2012
2. Leif Sörnmo, Pablo Laguna, Electrocardiogram (ECG) Signal Processing, Wiley Encyclopedia of Biomedical Engineering; 2006
3. Seema Nayak, M.K. Soni, Dipali Bansal, Filtering Techniques for ECG Signal Processing, IJREAS Volume 2, Issue 2, 2012
4. Bill Crone, „*Common-Mode Rejection: How It Relates to ECG Subsystems and the Techniques Used to Provide Superior Performance*“, Analog Devices, Inc, 2011
5. Venkatesh Acharya, „*Improving Common-Mode Rejection Using the Right Leg Drive Amplifier*“, Texas Instruments, Inc, SBAA188–July 2011
6. Bruce B. Winter, John G. Webster, „*Driven-Right-Leg Circuit Design*“ IEEE Transactions on Biomedical Engineering, Vol. BME-30, No. 1, January 1983
7. Karthik Soundarapandian, Mark Berarducci, „*Analog Front-End Design for ECG Systems Using Delta-Sigma ADCs“*, Texas Instruments, Inc, SBAA160A–April 2010
8. Yu Mike Chi, Tzyy-Ping Jung, „*Dry-Contact and Noncontact Biopotential Electrodes: Methodological Review“*, IEEE Reviews in Biomedical Engineering, Vol. 3, 2010
9. Yu M. Chi, Gert Cauwenberghs, „*Wireless Non-contact EEG/ECG Electrodes for Body Sensor Networks“* International Conference on Body Sensor Networks, pg. 297 – 301, 2010

Primjena neuronskih mreža u razvoju lijekova

Haseljić Naida[1], Smajović Alisa[2]

[1]Farmaceutski fakultet Univerziteta u Sarajevu, PhD Student, Sarajevo, Bosna i Hercegovina
[2]Farmaceutski fakultet Univerziteta u Sarajevu, Katedra za farmaceutsku informatiku, Sarajevo, Bosna i Hercegovina

Abstract-**Najsavršeniji danas poznati stroj za obradu podataka je ljudski um. Računarski ekvivalent ljudskoj obradi podataka je umjetna neuronska mreža (engl. Artificial Neural Network, ANN). Neuronska mreža je skup međusobno povezanih jednostavnih procesnih elemenata, jedinica ili čvorova čija se funkcionalnost temelji na biološkom neuronu. Umjetna neuronska mreža predstavlja umjetnu repliku ljudskog mozga kojom se nastoji simulirati postupak učenja. Analogija s pravom biološkom mrežom nije u potpunosti adekvatna jer postoje mnogi fenomeni nervnog sistema koji nisu modelirani umjetnim neuronskim mrežama, kao što postoje i karakteristike umjetnih neuronskih mreža koje se ne slažu s onima bioloških sistema. Umjetna inteligencija i neuronske mreže razvijaju se s ciljem praktične primjene, to jeste, kvalitetnije obrade podataka, kako bi se unaprijedili i ubrzali procesi zaključivanja u nauci i tehnologiji. Umjetne neuronske mreže su moćan alat za simulaciju brojnih nelinearnih sistema i primijenjene su u rješavanju mnogih kompleksnih problema iz oblasti farmaceutskih istraživanja, inženjeringa, psihologije i medicinske hemije. U ovom radu su navedene mogućnosti primjene umjetnih neuronskih mreža u razvoju lijekova QSAR (Quantitative structure–activity relationship) metodama. QSAR povezuje fizičko-hemijske osobine spojeva sa njihovom hemijskom ili biološkom aktivnošću. QSAR modeli bazirani na umjetnim neuronskim mrežama su široko korišteni kao metoda predviđanja u virtualnom screening-u (VS). U kliničkim istraživanjima je vrlo važno utvrditi sigurnost i učinkovitost postojećih lijekova. Screening u laboratoriju i optimizacija spojeva su skupe i spore metode, ali bioinformatika može značajno pomoći u kliničkim istraživanjima za navedene svrhe pružajući mogućnost predviđanja toksičnosti lijekova i aktivnosti kod netestiranih, potencijalnih lijekova. Navedeno je moguće postići zbog dostupnosti bioinformatičkih alata i metoda VS-a koje omogućavaju testiranje svih potrebnih hipoteza prije kliničkih ispitivanja. Očekuje se da će upotreba neuronskih mreža dovesti do napretka u pretkliničkim ispitivanjima, ubrzanja u screeningu i identifikaciji novih, do sada nepoznatih molekula i formiranju eksperimentalnih modela koji do sada nisu bili izvodivi.**

Keywords-**neuronske mreže, QSAR,lijekovi**

I. UVOD

Naučnici su stalno u potrazi za sistemom koji bi oponašao ljudsku inteligenciju i sve mogućnosti obrade podataka ljudskog mozga [1]. Računarski ekvivalent ljudskoj obradi podataka je umjetna neuronska mreža (engl. *Artificial Neural Network, ANN*). Neuronska mreža je skup međusobno povezanih jednostavnih procesnih elemenata, jedinica ili čvorova čija se funkcionalnost temelji na biološkom neuronu. Umjetna neuronska mreža je umjetna replika ljudskog mozga kojom se nastoji simulirati postupak učenja. Njome su implementirani pojednostavljeni modeli biološke neuronske mreže. Analogija s pravom biološkom mrežom nije u potpunosti adekvatna jer postoje mnogi fenomeni nervnog sistema koji nisu modelirani umjetnim neuronskim mrežama, kao što postoje i karakteristike umjetnih neuronskih mreža koje se ne slažu s onima bioloških sistema [2]. Umjetna inteligencija i neuronske mreže razvijaju se s ciljem praktične primjene, tj. kvalitetnije obrade podataka, kako bi se unaprijedili i ubrzali procesi zaključivanja u nauci i tehnologiji.

U prošlosti je identifikacija ljekovitih supstanci vršena uglavnom kroz nasumično eksperimentiranje što nije bilo naročito učinkovito obzirom da je mehanizam djelovanja uspješnog lijeka uglavnom ostajao nedorečen. U 1960-im godinama se počeo razvijati alternativni pristup u razvoju lijekova sa fokusom na QSAR (*quantitative structure–activity relationship*) koji se zasniva na korištenju poznatih odgovora (aktivnosti) spojeva jednostavnih struktura kako bi se predvidio odgovor kompleksnih spojeva, nakon čega se spojevi sa željenim osobinama nastavljaju ispitivati [1, 3]. Koristeći metodu regresije, Hansch je uspostavio vezu između fizičkohemijskih osobina i biološke aktivnosti. Rezultat ovog pristupa bila je jednačina koja opisuje, kvantitativno, vezu između biološke aktivnosti supstance i njene hemijske strukture.

U QSAR biološka aktivnost, a u QSPR (*Quantitative structure–property relationship*) farmakokinetičke osobine, mogu biti povezane sa fizičkohemijskim osobinama. QSAR/QSPR modeliranje se koristi kako bi se postavio matematički izraz koji povezuje odabrane parametre sa fizičkohemijskim osobinama serija supstanci iste vrste. QSAR pristup se koristi kako bi se predvidjela korelacija i optimizirale molekularne strukture koje se koriste u studijama i kako bi se razumjeli mehanizmi djelovanja lijekova [4]. QSAR/QSPR model zasnovan je na regresijskoj analizi. Matematičke metode regresije su toliko bitne u QSAR/QSPR modeliranju da će izbor metode regresije u većini slučajeva odrediti da li će rezultujući model biti uspješan ili ne. Odabir ispravne metode i danas predstavlja izazov za istraživače [5].

Neuronske mreže su vrsta matematičkih modela koji su dizajnirani tako da procesiraju ulazne informacije i generiraju skrivene modele odnosa. Glavna prednost umjetnih neuronskih mreža u odnosu na statističke modele je ta da za njih nije neophodan rigidno strukturiran eksperimentalni dizajn. One dobro raspoznaju obrasce i dobro donose odluke na temelju nepreciznih ulaznih podataka [1, 2, 6]. Pored toga, umjetne neuronske mreže mogu naći povezanost ovisnih i varijabli bez specificirane matematičke funkcije. Zbog toga su veoma upotrebljive u

rješavanju nelinearnih problema [6]. Neuronske mreže odlično rješavaju probleme klasifikacije i predviđanja i općenito sve probleme kod kojih postoji odnos između prediktorskih (ulaznih) i zavisnih (izlaznih) varijabli, bez obzira na visoku složenost te veze (nelinearnost). Nedostatak je tendencija za prekomjernom specijalizacijom modela i poteškoća u utvrđivanju koji su deskriptori najznačajniji za dobiveni model. U QSAR/QSPR studijama najčešćese koriste neuronske mreže s radijalnim baznim funkcijama (engl. *radial basis neural networks* RBNN) i generalizirane regresijske neuronske mreže (GRNN) [5].

Cilj ovoga rada je bio dati kratak pregled mogućnosti primjene neuronskih mreža u potrazi za novim lijekovima, nadopunjujući i dajući korak i dalje od QSAR analize. Prema svojoj definiciji, neuronske mreže bi, manipulišući s većim obimom podataka, mogle brže i kvalitetnije predvidjeti molekule s potencijalnom primjenom u farmakoterapiji.

A. *Poređenje biološkog i umjetnog neurona*

Ljudski mozak sastoji se od velikog broja neurona, pri čemu postoji i više od 100 vrsta istih. Svaki od neurona ima svoju funkciju i svaki gradi veze sa 10^4 drugih neurona. Sastoji se od tijela, dendrita, aksona i završnih ploča, kao što je prikazano na Slici 1-A. Informacije se prenose kroz tijelo stanice u vidu akcijskog potencijala sa dvije strane ćelijskog zida neurona [6].

Umjetna neuronska mreža također se sastoji od umjetnih neurona, tj. procesnih elemenata koji prenose informacije u mreži i čija se funkcionalnost temelji na biološkom neuronu. Umjetni neuron je zamišljen kao jednostavna jedinica koja prima informacije, obrađuje ih i šalje dalje drugim neuronima u mreži. Konekcije među neuronima variraju u *težini*, koja je definirana *koeficijentom težine*. Model umjetnog neurona je prikazan na Slici 1-B i na Slici 2 [3, 6, 7].

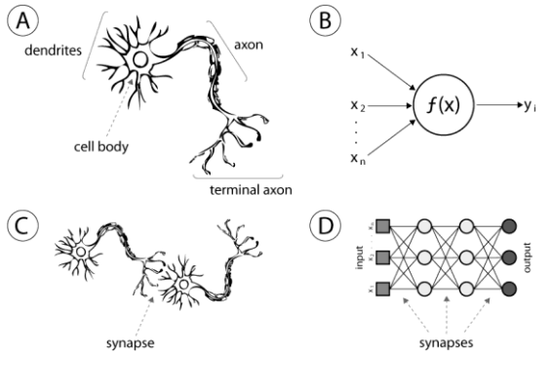

Slika 1. Model umjetnog neurona

Elementi modela umjetnog neurona su:

a) Skup sinapsi odnosno ulaza od kojih svaki ima svoju jačinu tj. težinu;
b) Sumator za sabiranje ulaza otežanih odgovarajućim sinapsama neurona. Ove operacije računaju linearnu kombinaciju ulaza;
c) Aktivacijska funkcija koja ograničava amplitudu izlaza neurona [8].

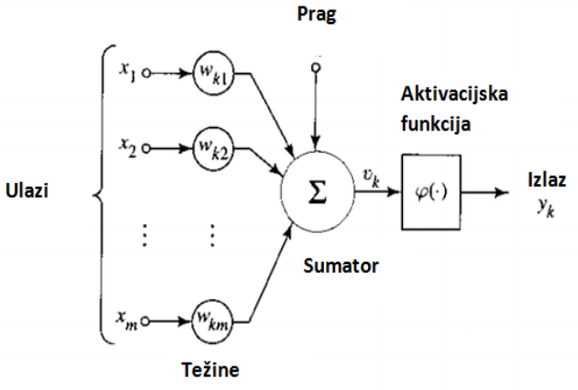

Slika 2. Model neurona

Neuroni u umjetnoj mreži su raspoređeni u slojeve. Umjetne mreže imaju tri sloja:

1. Ulazni sloj (prima ulaz iz okoline, tj. nezavisnu varijablu sistema);
2. Skriveni sloj (svi neuroni u slojevima koji nisu ni ulazni ni izlazni);
3. Izlazni sloj(generira zavisnu varijablu)

Kada potencijal dođe do aksona biološkog neurona otpuštaju se hemijski signali u sinaptički prostor. Hemijske supstance prelaze sinaptički prostor i na sljedećem neuronu otvaraju ili zatvaraju kanale kroz koje prolaze naelektrisane molekule, remete normalni potencijal stanice i stvaraju novi potencijal (signal). Signal još nije informacija jer se još ne prenosi dalje kroz tijelo. Stvaranje signala je po principu „sve ili ništa“. U tijelu stanice se sumiraju svi potencijali od 10^4 neurona s kojima jedan neuron komunicira i ako ukupni napon pređe aktivacijski prag, neuron generiše akcijski potencijal koji se ponovo dalje prenosi tijelom neurona [6]. Postoji analogija između neuronskih mreža i aktivnosti bioloških neurona koji sumiraju ulazne signale, procijenjene jačinom sinaptičkih veza i šalju izlazne signale koji su ograničeni nekim maksimalnim vrijednostima [1].

Funkcionalnost biološkog neurona najjednostavnije oponaša McCulloch-Pitts model umjetnog neurona, tzv. Threshold Logic Unit (TLU). Analogija u ovom modelu neurona je izložena u nastavku. Signali su opisani numeričkim izrazom i na ulazu u neuron se množe *težinskim faktorom* koji opisuje jakost sinapse i brojni je ekvivalent stvarnog podražaja jednog neurona prema drugom. Zatim se

svi signali sumiraju, kao što se sumiraju i potencijali u biološkom neuronu. Ako je dobiveni iznos sume iznad definiranog praga podražaja, neuron proizvodi izlazni signal.

Umjetne neuronske mreže su moćan alat za simulaciju brojnih nelinearnih sistema i primijenjene su u rješavanju mnogih kompleksnih problema iz oblasti farmaceutskih istraživanja. QSAR povezuje fizičko-hemijske osobine spojeva sa njihovom hemijskom ili biološkom aktivnošću. Pod ovim osobinama se podrazumijeva nekoliko važnih parametara, kao što su molekularna težina, volumen, elektronegativnost, logP, akceptori vodika, donori vodika i molarna refrakcija [1].

Struktura ciljnog proteina često nije poznata. U takvim slučajevima, potencijalni lijekovi se mogu analizirati eksperimentalnim tehnikama i preko zajedničkih strukturnih osobina. Takve metode bazirane na farmakoforu, ili ligandu, uključuju npr. 3D-QSAR tehnike. Primjeri popularnih metoda 3D-QSAR su komparativna analiza molekularnog polja (CoMFA), komparativna analiza molekularnih indeksa sličnosti (CoMSIA) i GRID. Osnovna ideja CoMFA je povezanost biološke aktivnosti molekule sa sa njenim elektrostatskim i prostornim interakcijama. Molekule (ligandi) koje se proučavaju su poredane strukturalno u 3D mreži. CoMSIA uzima u obzir hidrofobne parametre. Tako dobiveni deskriptori se zatim analiziraju statističkim metodama, kao na primjer tehnikama parcijalnih najmanjih kvadrata, u svrhu dobivanja korelacije između aktivnosti i polja, što dovodi do 3D-QSAR modela liganda. GRID je sličan CoMFA, i također se može koristiti kako bi se utvrdile energetske interakcije između sonde i liganda. Osim toga, GRID se može koristiti i za izračunavanje energije vodikovih veza. U 4D-QSAR četvrta dimenzija predstavlja konformacije, orijentacije ili protonirana stanja za svaku molekulu. 5-D QSAR ide korak dalje omogućavajući promjene u mjestu vezivanja za receptor i ligand topologiju. Dodavanje učinaka solvacije dovodi do 6D-QSAR koja je omogućila, u kombinaciji s fleksibilnim spajanjem, relativno tačnu identifikaciju endokrinih poremećaja sa potencijalnim lijekovima. Povećanje broja parametara je dovelo do zahtjeva da se pristupima umjetne inteligencije dobije korelacija između molekularnih i drugih osobina i promatrane aktivnosti. Statističke i kompjuterske tehnike učenja, kao što je multipla linearna regresija (MLR), analiza glavnih sastavnica ili parcijalnih najmanjih kvadrata bi se u tom slučaju mogle koristiti za rješavanje problema [3]. Ligandi mogu biti predstavljeni strukturnim i drugim deskriptorima. Izbor deskriptora je važan korak u bilo kojoj QSAR studiji. Drugi važan korak je identifikacija uzoraka koje koreliraju sa aktivnošću. Nadalje, spojevi koji pokazuju obećavajuća svojstva mogu biti upoređeni sa drugim spojevima kako bi se identificirali drugi potencijalni lijekovi koji dijele važne osobine. Prema tome, evidentno je da pristupi umjetne inteligencije za selekciju osobine, prepoznavanje uzorka, klasifikaciju i grupiranje mogu biti primijenjeni za rješavanje navedenih problema [1].

QSAR modeli bazirani na umjetnim neuronskim mrežama su široko korišteni kao metoda predviđanja u virtualnom screening-u (VS). U kliničkim istraživanjima je vrlo važno utvrditi sigurnost i učinkovitost postojećih lijekova. Screening u laboratoriju i optimizacija spojeva su skupe i spore metode, ali bioinformatika može značajno pomoći u kliničkim istraživanjima za navedene svrhe pružajući mogućnost predviđanja toksičnosti lijekova i aktivnosti kod netestiranih potencijalnih lijekova. Navedeno je moguće postići zbog dostupnosti bioinformatičkih alata i metoda VS-a koje omogućavaju testiranje svih potrebnih hipoteza prije kliničkih ispitivanja [1].

B. *Dosadašnja istraživanja na polju primjene neuronskih mreža u razvoju lijekova*

Imajući u vidu da je upotreba neuronskih mreža u polju farmacije sve veća, veliki je broj studija koji prikazuju njihovu primjenu. U nastavku će biti navedeno samo nekoliko.

Kolhicin je inibitor polimerizacije tubulina koji sprječava proliferaciju ćelija i time ima potencijal kao antineoplastik. Strukturne karakteristike koje određuju njegovu aktivnost nisu razjašnjene te je razvijena SOM (samoorganizirajuća) mreža kako bi se dobio kvantitativni 3D model koji opisuje seriju kolhicinoida. Na taj način su se dobile dvodimenzionalne mape izabranih površinskih svojstava molekule koje služe za vizuelizaciju interakcija pojedinih spojeva sa njihovim biološkim receptorima [9].

Trovanje organofosfornim jedinjenjima vodi do formiranja inhibirane acetilholinesteraze što rezultira akumulacijom acetilholina i holinergičke krize. U preporukama za tretman trovanja su antimuskarinski agens atropin i acetilholinesteraza reaktivator (oxim). Atropin blokira efekat nakupljenog acetilholina, dok oksim defosfolizira molekulu enzima i povraća njenu aktivnost. Umjetne neuronske mreže su korištene za predviđanje pravilne strukture novih acetilholinesteraza reaktivatora [10].

U okviru nastavka proučavanja derivata tetrahidrokinolona izučavana je citotoksičnost 38 supstanci, ali ne i korelacija specifičnosti za tumorske ćelije i hemijskih deskriptora. U tu svrhu korištena je linearna regresija sa umjetnim neuronskim mrežama [11].

Potencijalni antiHIV lijekovi su inhibitori nukleozidne reverzne transkiptaze. Spojevi 1-[2-Hidroksietoksi(metil)-6-(feniltio)-timina] (HEPT) inhibiraju alosterično mjesto enzima i manje su toksični i stabilniji nego nenukleozidni inhibitori (NNRTI). Modelirana je anti-HIV aktivnost HEPT derivata uz korištenje grafičkih teoretskih deskriptora kod kojih je razmatrana udaljenost i povezanost [12].

Također su proučavani spojevi koji ciljaju reverznu transkriptazu i to 4, 5, 6, 7-Tetrahidro-5-metilimidazo[4, 5, 1-jk][1, 4]benzodiazepin-2(1H)-on (TIBO) derivati kao

nenukleozidni inhibitori (NNRTI). Osamdeset i dva TIBO derivata su proučavana troslojnim neuronskim mrežama kako bi se dobili podaci o QSAR ovih spojeva. Identificirani su relevantni faktori koji kontrolišu aktivnost anti-HIV-1 TIBO derivata. Rezultati su u skladu sa rezultatima prethodnih studija na HEPT derivatima i pokazuju značaj parametra hidrofobnosti u QSAR modeliranju TIBO derivata [13].

Kanabinoidi (spojevi izolovani iz *Cannabis sativa*) se koriste u različite medicinske svrhe. Proučavan je uticaj nekoliko molekularnih deskriptora na psihoaktivnost 50 kanabinoida kako bi se dobio model za procjenu psihoaktivnosti novih kanabinoida. Prvo je izvršena selekcija molekularnih deskriptora, a zatim i kreirana dva modela neuronskih mreža kako bi se konstruirao adekvatan model za klasifikaciju novih kanabinoida. Prvi model je bio MLP sa back propagacijom, dok je drugi bio Kohonenova mreža. Rezultati su upoređeni i pokazano je da su obje tehnike omogućile veliki procenat tačnosti u razgraničavanju psihoaktivnih i psihoneaktivnih spojeva. Kohonenova mreža je bila superiornija u odnosu na MLP [14].

Struktura tiobenzamida i derivata kinolizidina i njihova aktivnost protiv virusa gripe proučavana je elektronskom topološkom metodom (ETM) i modelom umjetne neuronske mreže kako bi se dobio QSAR model sa skeletom koji najznačajnije opisuje aktivnost [15].

Proučavani su i antimikrobni peptidi kao potencijalni netoksični spojevi za liječenje bakterijskih infekcija. Bioinformatičke strategije mogu inspirisati dizajn novih peptida sa poboljšanom aktivnošću. Umjetne neuronske mreže koje uzimaju podatke o fizičkohemijskim svojstvima ovih peptida se mogu koristiti da se identificiraju aktivni peptidi i da se procijeni njihova antimikrobna aktivnost, a pokazale su veliku tačnost koja korelira sa eksperimentalnim podacima [16].

Korišten je QSAR sa multiplom linearnom regresijom u proučavanju HEPT derivata sa značajnom anti-HIV aktivnošću i određeno je 37 različitih deskriptora. Model se pokazao veoma tačnim u predviđanju [17]. Poređeni su SOM-QSAR, CoMSA i za seriju dihidrofolat reduktaza inhibitora [18].

Neuronske mreže korištene su i u QSAR studiji 66 mono i bis kvaternih amonijumovih soli koje djeluju kao antagonisti neuralnih nikotinskih receptora za acetilholingdje je ciljna vrijednost bila maksimalna vrijednost inhibicije [19].

434 pozitivna alosterična modulatora glutamat receptora subtip 4 čija se aktivacija pokazala efikasna u modelu Parkinsonove bolesti kod glodara su korištena za treniranje mreže. Model je korišten za skrining baze od 450 000 spojeva koji bi mogli imati djelovanje [20].

Neuronske mreže imaju posebne prednosti u klasifikaciji kompleksnih podataka. One prepoznaju tačna ciljana mjesta unutar podataka u sklopu različitih tipova obrazaca. U literaturi je prikazan eksperiment u kojem je korištena neuronska mreža sa devet ulaza uz jedan bias čvor i jedan izlaz koji odgovara predviđanju. U pitanju je bila u potpunosti povezana mreža, a algoritam učenja je bio tipa *backpropagation*. Svaki od 5 skrivenih čvorova je bio specijaliziran za jedan od tipova protein - ligand interakcije koje su bile sastavni dio trening seta podataka. Dobri ligandi pokazuju visok afinitet ka vezivnim mjestima, ali mehanizam vezivanja ima visoko variranje. Neuronske mreže i suglasne metode daju dva pristupa da dopuste mreži učenje da prezentuje višestruke obrasce za vezivanje liganda. Ovi obrasci mogu podrazumijevati da ligand ima najveći afinitet da se ostvari kroz vodikove veze ili kroz hidrofobne reakcije. Afinitet za vezivanje iz jedinstvenog izvora sa jednom metodom je sigurna metoda u određivanju afiniteta za vezivanje liganda za ciljani protein. Jedna od negativnih strana u upotrebi mreža u ovom slučaju je prespecijalizacija modela [21].

Particioni koeficijent predstavlja mjeru hidrofobnosti, odnosno hidrofilnosti supstance. ANN se uspješno može korisiti u razvoju QSPR modela kako bi predvidio n-oktanol/voda particioni koeficijent heterogenog seta organskih ljekovitih supstanci. Deskriptri koji se pojavljuju u QSPR modelu pružaju informacije o različitim osobinama molekula koje mogu učestvovati u intermolekularnim interakcijama koje utiču na particioni koeficijent. Dobar odnos između predviđenih i dobivenih rezultata pokazuju validnost modela. U ovu svrhu korištena je neuronska mreža sa *backpropagation* algoritmom učenja. Težine su podešene tako da smanje grešku između očekivanih i izračunatih vrijednosti. Kako su na početku eksperimenta date opisne varijable odabralo se nadgledano učenje. Nakon nekoliko pokušaja postavljena su 4 neurona unutar skrivenog sloja. Neuronska mreža je trenirana sa 110 lijekova.Izračunate statističke vrijednosti su pokazale da ovaj model pokazuje svu superiornost vještačkih neuronskih mreža. Rezultati su pokazali da vještačke neuronske mreže mogu tačno prikazati odnos između strukturnih parametara i particionog koeficijenta različitih ljekovitih supstanci i predvidjeti $\log P_{o/w}$ novih derivata [22].

II. ZAKLJUČAK

Računarske metode u razvoju i testiranju lijekova su sve više u upotrebi i postaju standardni model u potrazi za novom ljekovitom molekulom. Ograničenja računarskih modela se pokušavaju prevazići upotrebom umjetne inteligencije i neuronskih mreža.

Neuronske mreže su veoma pouzdane za raspoznavanje uzoraka koji nemaju linearnu povezanost i koji se ne mogu

povezati matematičkom niti statističkom funkcijom. Imaju i ogromnu, već primjenjivu, ulogu u pretraživanju i analizi baza podataka sa velikom tačnošću. Svrha neuronskih mreža je brzo dobivanje rezultata, a da se pri tome ne moraju izvoditi dugotrajni i skupocijeni eksperimenti.Njihova upotrebna vrijednost je već dokazana i u studijama o modelima kvantitativne povezanosti strukture i aktivnosti (QSAR). Očekuje se da će upotreba neuronskih mreža dovesti do napretka u pretkliničkim ispitivanjima, ubrzanja u screeningu i identifikaciji novih, dosad nepoznatih, molekula i formiranju eksperimentalnih modela koji dosada nisu bili izvodivi.

III. LITERATURA

1. W. Duch, K. Swaminathan, J. Meller,*Artificial Intelligence Approaches for Rational Drug Design and Discovery*,Current Pharmaceutical Design, 2007.
2. G.V.Maltarollo, K.M. Honório, A.B.Ferreira da Silva,*Applications of Artificial Neural Networks in Chemical Problems*. In: K. Suzuki, editor,*Artificial Neural Networks - Architectures and Applications*. InTech, 2013, pp 203-223.
3. K. Gashteovski, I. Trenchev, N. Borisova, I. Todorin, G. Iliev,*Neural networks – basic principles for construction, their application in drug design and genetic algorithms*, Faculty of Mathematics & Natural Science, 2011.
4. S. K. Singh, S. Saini et al., Quantitative Structure Pharmacokinetic Relationship Using Artificial Neural Network: A Review. *International Journal of Pharmaceutical Sciences and Drug Research*, *Volume: 1*, Issue: 3, 2009, pp. 144-153.
5. Liu Peixun, Wei Long, Current Mathematical Methods Used in QSAR/QSPR Studies,*Int. J. Mol. Sci., Volume: 10*, Issue: 5, 2009, pp. 1978-1998.
6. V. Sutariya, A. Groshev, P. Sadana, D. Bhatia, Y. Pathak, Artificial Neural Network in Drug Delivery and Pharmaceutical Research. *The Open Bioinformatics Journal, Volume: 7 (Suppl-1, M5)*, 2013, pp. 49-62
7. F. Rodik,*Raspoznavanje prometnih znakova neuronskim mrežama* [Završni rad], Sveučilište u Zagrebu, 2009.
8. S. Haykin,*Neural Networks A Comprehensive Foundation*,New Jersey: Prentice Hall International, Inc, 2nd ed., 1999.
9. J. Polañski,Self-organizing neural network for modeling 3D QSAR of colchicinoids. *Acta Biochimica Polonica*,*Volume: 47*, Issue: 1, 2000, pp.37–45.
10. K. Kuča, J. Cabal, D. Jun et al., Strategy For The Development Of New Acetylcholinesterase Reactivators – Antidotes Used For Treatment Of Nerve Agent Poisonings. *Biomed Pap Med Fac Univ Palacky Olomouc Czech Repub., Volume: 149,* Issue: 2,2005, pp. 429–31.
11. Y. Uesawa, K. Mohri, K. Kawase,Quantitative Structure Activity Relationship (QSAR) Analysis of Tumor-specificity of 1,2,3,4-Tetrahydroisoquinoline Derivatives. *Anticancer Research, Volume: 31,* 2011, pp. 4231-4238.
12. B. Shaik, T. Zafar, V. K. Agrawal, Estimation of Anti-HIV Activity of HEPT Analogues Using MLR, ANN, and SVM Techniques. *International Journal of Medicinal Chemistry*, 2013.
13. L. Douali, D. Villemin, D. Cherqaoui, Exploring QSAR of Non-Nucleoside Reverse Transcriptase Inhibitors by Neural Networks: TIBO Derivatives. *Int. J. Mol. Sci., Volume: 5*,2004, pp.48-55.
14. K. Hono'rio, E. F. De Lima, M. G. Quiles et al., Artificial Neural Networks and the Study of the Psychoactivity of Cannabinoid Compounds. *Chem Biol Drug Des*, *Volume: 75*, 2010, pp. 632–640.
15. M. Saracoglu, F. Kandemirli et al., ETM-ANN Approach Application for Thiobenzamide and Quinolizidine Derivatives. *Journal of Biomedicine and Biotechnology*, 2010.
16. M. Torrent, D. Andreu, V. M. Nogue´s, E. Boix, Connecting Peptide Physicochemical and Antimicrobial Properties by a Rational Prediction Model. *PloSONE, 2011,* doi:10.1371/journal.pone.0016968.
17. A. Afantitis, G. Melagraki, H. Sarimveis et al.,A novel simple QSAR model for the prediction of anti-HIV activity using multiple linear regression analysis. *Molecular Diversity*, *Volume: 10*, 2006, pp. 405–414.
18. J. Polañski, A. Bak, R. Gieleciak, T. Magdziarz, Self-organizing Neural Networks for Modeling Robust 3D and 4D QSAR: Application to Dihydrofolate Reductase Inhibitors. *Molecules, Volume 9,* 2004, pp. 1148-1159.
19. F. Zheng, M. J. McConnell, C.-G. Zhan, L. P. Dwoskin, P.A. Crooks, QSAR study on maximal inhibition (Imax) of quaternary ammonium antagonists forS-(−)-nicotine-evoked dopamine release from dopaminergic nerve terminals in rat striatum. *Bioorganic & Medicinal Chemistry, Volume: 17,* Issue 13, 2009, pp. 4477-4485.
20. R. Mueller, E. S. Dawson, C. M. Niswender, M. Butkiewicz, C. R. Hopkins et al., Iterative experimental and virtual high-throughput screening identifies metabotropic glutamate receptor subtype 4 positive allosteric modulators. *J Mol Model, Volume: 18,* Issue 9, 2012, pp. 4437-4446.
21. L. Marsh, Prediction of Ligand Binding Using an Approach Designed to Accommodate Diversity in Protein-Ligand Interactions,*PLoSONE*,2011, doi:10.1371/journal.pone.0023215
22. S. Saaidpour, Prediction of Drug Lipophilicity Using Back Propagation Artificial Neural Network Modeling.*Orient J Chem*, *Volume: 30*, Issue: 2, 2014, pp. 793-802.

Naida Haseljić, PhD Student at the Faculty of Pharmacy, University of Sarajevo, Zmaja od Bosne 8, 71 000 Sarajevo, B&H (phone: 387-61-243-312; e-mail: naida.haseljic@gmail.com).

Metamaterial Absorber Based Biosensor Applications

M. Karaaslan[1], F. Dincer[2], M. Bakir[1], E. Unal[1], K. Delihacioglu[3], Z. Ozer[4], O. Akgol[1] and C. Sabah[5]

[1] Mustafa Kemal University, Department of Electrical and Electronics Engineering, Hatay 31200, Turkey
[2] Mustafa Kemal University, Department of Computer Engineering, Hatay 31200, Turkey
[3] Kilis 7 Aralik University, Department of Electrical and Electronics Engineering, Kilis 79000, Turkey
[4] Mersin University, 1Vocational School of Mersin, Yenisehir, Mersin 33343, Turkey
[5] Middle East Technical University – North. Cyprus Campus, Dept.of Elect.and Elect. Eng.Kalkanli, Guzelyurt, TRNC, Mersin 10, Turkey

Abstract— **In this work, sensor abilities of a metamaterial absorber is investigated and demonstrated. Temperature sensing application is numerically demonstrated in C band frequency regime. This study is important since it has perfect metamaterial absorber and sensor application features together. Sensor application is such a bio sensing application that can be applied to other sensing applications according to sensor layer's contents. This application is related with sensor layer's dielectric constant so if sensor layer is composed of biological tissues, it results with a change in resonance frequency. This change in the resonance frequency can be used to sense material properties accordingly. Numerical results show that absorbance value is greater than 95% in all temperature sensing studies. The proposed perfect MA based sensor variations enable many potential applications in medical or food technologies which will be demonstrated in the paper.**

Keywords— **Metamaterial, Absorber, bio-sensor.**

I. Introduction

Metamaterials (MTMs) are artificially made electromagnetic (EM) materials that consists of metallic array elements have attracted too much attention during past decade by scientists. MTMs show exotic features by manipulating the electromagnetic wave. These exotic features can be used in negative refraction [1, 2], super-lenses [3-5] and absorbers [6-7]. In addition to these featuress, MTM based sensor applications came out in a few years [8-9]. There are different sensor applications as bio sensors [10-12], strain sensors [13], and thin film sensors [14] are one of these sensor applications. Biosensors have many application fields in medicine, physics, environmental and personal safety. Bio sensors can be used for measuring molecular concentrations, investigating the DNA, estimating the pH, etc. These wide range of application area require sensitive, selective, biocompatible designs. Biosensor applications generally make use of biological tissues, which are dipolar materials. These dipolar materials show electronic and atomic polarization and also a polarization arises from the changes in the orientation of dipolar group of atoms. This orientation is affected by temperature, humidity and other environmental parameters which mean that the corresponding dielectric properties are dependent on temperature and other environmental parameters [15]. Curative properties of electromagnetic waves can be investigated by observing the radiated heat from the biological tissues. For this reason, heat sensing of any biological tissue as marrow bone is important to decide electromagnetic absorption rates. In this study, in order to sense the temperature of marrow bone, metamaterial absorber (MA) based design is proposed. There are different studies are realized in order to sense temperature as [8, 9] but this application is based on MA and can be used in C band. Metamaterial absorbers are generally developed to absorb electromagnetic energy in different frequency regimes [16-19]. In this study, it is numerically demonstrated that a MA can be used as a temperature sensor by applying small changes in design. The organization of this study is as follows. In section 2, square-split ring resonator shape is proposed, in section three, numerical results are presented. Finally, summary and conclusions are provided and discussed in section four.

II. Design and Setup

The suggested design MA based on a four gap square resonator-shaped providing high absorption value is designed and fabricated. The designed structure consists of a resonator located at the top layer and a dielectric substrate at the center layer. The bottom layer composes of a metal plate. The top and bottom layers are modeled as copper sheets with electrical conductivity value given as $5.8x10^7$ S/m with 0.035 mm thickness. The selected FR4-dielectric has features of a low cost, efficient, easily accessible and commonly used substrate. Permittivity value of the dielectric is 4.3 and the loss tangent is 0.02. The dimensions of the structure is shown in Fig. 1(a). In addition, Fig. 1(b) presents a picture of the fabricated sample. Also, the numerical simulations of the proposed model are performed by using a commercial 3D full wave solver based on Finite Integration Technique (FIT). In numerical study, the boundary conditions (x-y and z) are defined as periodic and open add space. MA absorber which this study is based on is taken from [19].

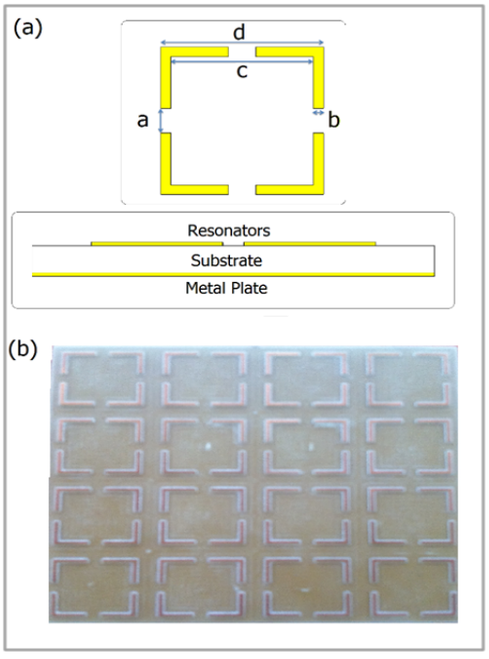

Fig. 1 Designed and fabricated MA based biosensor [19]. (a) Dimensions of the sample (a=4 mm, b=1,5 mm, c=21 mm, d=24 mm), (b) a picture of fabricated structure

III. Numerical and Experimental Results

In order to verify MA operation of the proposed structure in this study, we have performed numerical and experimental and results compared in Fig.2 [19]. As shown in the Fig.2. proposed MA structure shows perfect absorption at 4.28GHz.

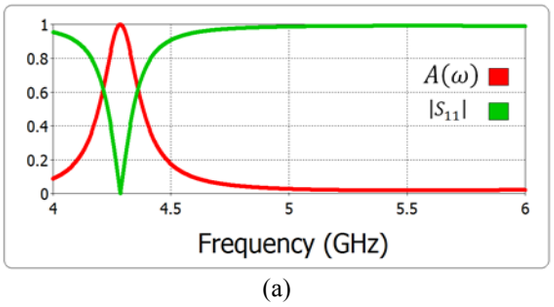

(a)

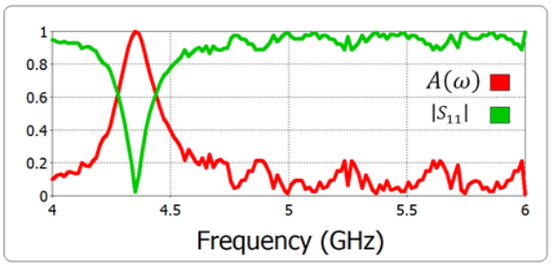

(b)

Fig. 2 Simulated (a) & measured (b) reflection and absorption results of the proposed structure [19]

In order to show the proposed structure can be used as a biosensor, it is necessary to separate metal plate and substrate part and place a sensor layer between them. Sensor layer has the same thickness and dimensions with FR4 substrate. Block diagram of MA based biosensor is given in the Fig.3.

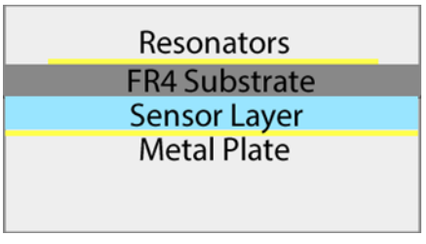

Fig. 3 Block diagram of MA based Bio-Sensor

When sensor layer is composed from tissues, resonance frequency of the overall system changes according to permittivity of the sensor layer. In order to simulate the temperature sensing necessary complex permittivity data is taken from [16]. 5 samples between 30℃ and 80℃ are taken as sample and corresponding permittivity values are entered as an input to sensor layer. Numerical results show that, when temperature of the marrowbone tissue changed, reflection frequency of the proposed MA based biosensor changes according to the temperature of the marrowbone tissue. Reflection and absorption graphics for marrowbone tissue temperature values are given in the Fig.4 and Fig.5. When the temperature of the marrowbone tissue increased from 30℃ to 80℃, reflection frequency of the proposed structure is decreased from 6.75 GHz to 6.505 GHz linearly.

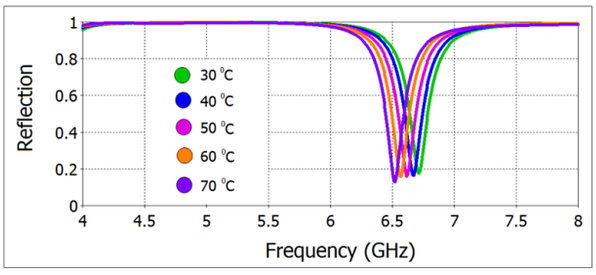

Fig. 4 Simulated reflection results of the proposed structure according to marrowbone tissue temperature

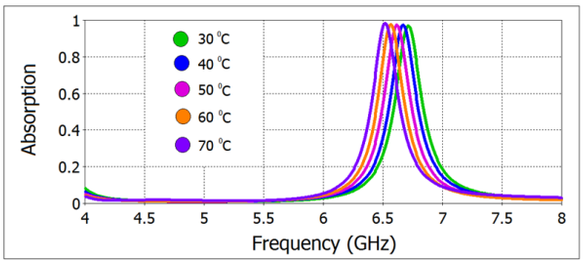

Fig. 5 Simulated absorption results of the proposed structure according to marrowbone tissue temperature

In order to show the absorption, resonance frequency and marrowbone tissue temperature clearly Fig.6 is prepared. Absorption value of the MA based biosensor is stable between 30℃ and 80℃ while the reflection frequency is changing according to the temperature of the marrowbone tissue.

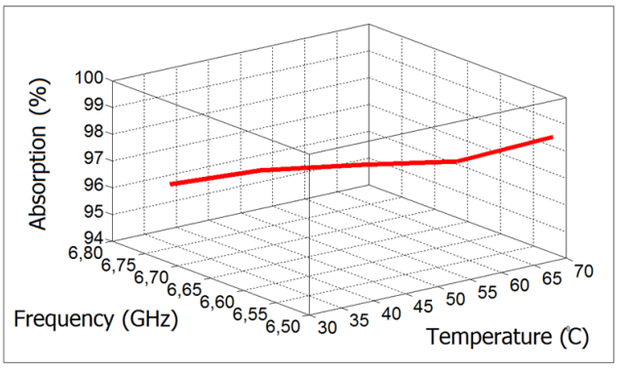

Fig. 6 Marrowbone temperature changing according to the frequency and absorption values

IV. Conclusion

MA based biosensor application is demonstrated numerically and experimentally in this study. Numerical and experimental results showed good agreement with each other. Due to heat absorption effects are important for curative properties of the electromagnetic waves, temperature sensing is taken as sample numerical results show that the MA based biosensor application show linear changes according to the temperature of the marrowbone tissue. Due to complex permittivity value is an input for sensor layer, this study can also be used in other sensing applications such as humidity, density and pressure. Hence, the study gives opportunities to the researches to design novel sensors.

REFERENCES

1. T. W. Ebbesen, H. J. Lezec, H. F. Ghaemi, T. Thio, and P. A. Wolff: "Extraordinary optical transmission through sub-wavelength hole arrays," *Nature Volume*: *391*, 1998, pp. 667-669.
2. J.B. Pendry: "Electromagnetic materials enter the negative age," *Physics World Volume: 14,* Issue: 9, 2001, pp.47-51.
3. J.B. Pendry: "Negative Refraction Makes a Perfect Lens," *Physical Review Letters Volume: 85,* Issue: 18, 2000, pp. 3966–3975.
4. Z. Jacob, L.V. Alekseyev, E, Narimanov: "E. Optical hyperlens: Far-field imaging beyond the diffraction limit," *Opt. Express Volume:14,* 2006, pp. 8247–8256.
5. Z. Liu, H. Lee, Y. Xiong, C. Sun, X. Zhang: "X. Optical hyperlens magnifying sub-diffraction-limitted object," *Science Volume: 315,* 2007, pp.1686–1687.
6. C. Sabah, F. Dincer, M. Karaaslan, E. Unal, O. Akgol: "Polarization-Insensitive FSS based Perfect Metamaterial Absorbers in GHz and THz Frequencies," *Radio Science Volume: 49,* 2014, pp. 306-314.
7. F. Dincer, M. Karaaslan, O. Akgol, C. Sabah: "Design of Polarization and Incident Angle-Independent Perfect Metamaterial Absorber with Interference Theory," *Journal of Electronic Materials Volume:43*, Issue: 11, 2014, pp. 3849-3854.
8. E. Ekmekci, G.T. Sayan, "Multi-functional metamaterial sensor based on a broad-side coupled SRR topology with a multi-layer substrate," Applied Physics A: Materials Science & Processing Volume 110, 2013, pp. 189-197.
9. M. Karaaslan and M. Bakir, "Chiral metamaterial based multifunctional sensor applications," *Progress In Electromagnetics Research Volume 149*, 2014, pp. 55-67.
10. S. Toldo, S. Lampel, S. Stilgenbauer, J. Nickolenko,A. Benner, H.Dohner, T. Cremer, P. Lichter: "Matrix-based comparative genomic hybridization: Bio-chips to screen for genomic imbalances,". *Genes Chromosomes Cancer Volume 20,* 1997, pp. 399–407.
11. X. Michalet, A.N. Kapanidis,T. Laurence, F.Pinaud, S.Doose, M. Pflughoefft, S. Weiss, S: "The power and prospects of fluorescence microscopies and spectroscopies,". *Annu. Rev. Biophys. Biomol. Struct. Volume: 32,* 2003, pp.161–182.
12. S.E.D. Webb, S.K. Roberts, S.R. Needham, C.J. Tynan, D.J. Rolfe, M.D. Winn, D.T. Clarke: "Single-molecule imaging and fluorescence lifetime imaging microscopy show different structures for high and low affinity epidermal growth factor receptors in A431 cells," *Biophys. J. Volume: 94*, 2008, pp. 803–819.
13. R. Melik, E. Unal, N.K. Perkgoz, C. Puttlitz, H.V. Demir, "Metamaterial based telemetric strain sensing in different materials," *Opt. Express Volume: 18,* 2010, pp. 5000–5007.

14. J.F. O'Hara, R. Singh, I. Brener, E. Smirnova, J.G. Han, A.J. Taylor, W.L. Zhang, "Thin-film sensing with planar terahertz metamaterials: Sensitivity and limitations," *Opt. Express Volume:16,* 2008, pp.1786–1795.
15. D. Factorova, "Temperature dependence of biological tissues complex permittivity at microwave frequencies," *Advances in Electrical and Electronic Engineering Volume:* 7, 2008, pp. 354-357.
16. F. Dincer, M. Karaaslan, E. Unal, O. Akgol, E. Demirel, C. Sabah: "Polarization and angle independent perfect metamaterial absorber based on discontinues cross-wire-strips," *Journal of Electromagnetic Waves and Applications Volume: 28,* 2014, pp. 741-751.
17. C. Sabah, F. Dincer, M. Karaaslan, E. Unal, O. Akgol: "Polarization Insensitive FSS based Perfect Metamateriaal Absorbers in GHz and THz Frequencies," *Radio Science Volume 49, 2014, pp. 306-314.*
18. C. Sabah, F. Dincer, M. Karaaslan, E. Unal, O. Akgol, E. Demirel: "Perfect metamaterial absorber with polarization and incident angle independencies based on ring and cross-wire resonators for shielding and a sensor application", *Optics Communications Volume: 322*, 2014, pp. 137-142.
19. F. Dincer, O. Akgol, M. Karaaslan, E. Unal, C. Sabah:"Polarization angle independent perfect metamaterial absorbers for solar cell applications in the microwave, infrared, and visible regime," *Progress In Electromagnetics Research Volume 144,* 2014, pp. 93-101.

Biosensor Application by Using Gammadion Shaped Chiral Metamaterials

M. Karaaslan[1], M. Bakir[1], F. Dincer[2], E. Unal[1], K. Delihacioglu[3], Z. Ozer[4], O. Akgol[1] and C. Sabah[5]

[1] Mustafa Kemal University, Department of Electrical and Electronics Engineering, Hatay 31200, Turkey
[2] Mustafa Kemal University, Department of Computer Engineering, Hatay 31200, Turkey
[3] Kilis 7 Aralik University, Department of Electrical and Electronics Engineering, Kilis 79000, Turkey
[4] Mersin University, Vocational School of Mersin, Yenisehir, Mersin 33343, Turkey
[5] Middle East Technical University – North. Cyprus Campus, Dept.of Elect.and Elect. Eng.Kalkanli, Guzelyurt, TRNC, Mersin 10, Turkey

Abstract— **In this work, sensor abilities of a chiral metamaterial which is based on gammadion shaped resonators is investigated and demonstrated. Moisture content sensing by using gammadion shaped resonators is presented in different frequency bands. Hevea rubber latex is chosen for moisture content sensing. Due to sensor configuration of the structure it is applicable to other sensing applications as temperature and pressure. Simulation studies showed that gammadion shaped chiral metamaterial provides good measurement opportunities in bio sensing. Sensor layer in this biosensing study, creates a suitable approach for sensing biological parameters. When sensor layer is assumed to be composed of related material, it leads to a change in the resonance frequency of the system and which results to shift of the resonance frequency. Numerical results show that gammadion shaped biosensor has nihility function and can be used effectively in bio sensing applications which will be demonstrated in the rest of the paper.**

Keywords— **Metamaterial, Chiral, biosensor, nihility.**

I. Introduction

Metamaterials (MTMs) are such electromagnetic (EM) materials that cannot naturally be found in the nature. MTMs generally consist metallic inclusions on their surface and these metal inclusions are used for different MTM applications in the last decade. MTMs show exotic features by manipulating the electromagnetic wave and these features can be used in negative refraction [1, 2], super lens [3] and absorbers [4-7]. Furthermore new applications are developed for past few years [8-9]. Biosensors [10-12] are one of the new applications of MTMs, biosensors have many application fields in medicine, physics and environmental safety. These sensors can be used for measuring molecular concentrations, investigation of DNA, estimating pH, etc. Due to large number of applications, biosensor must be sensitive, selective, biocompatible and immune to external effects, such as pressure or temperature changes. Moreover, biosensors also must meet general sensor requirements such as low loss factor, measurable signal output and sensitivity. Biological tissues in biosensor applications are dipolar materials which show electronic and atomic polarization in addition to the polarization arises from the changes in the orientation of dipolar group of atoms. Water is one of the example which can be found in biological tissues and which show strong dipolar polarization. Since biological tissues have high percent of water, they show dipolar material properties [13]. In this study as an advantage, gammadion shape chiral metamaterial biosensor study is realized. It is numerically proven that the gammadion shape based chiral metamaterial biosensor which can be used as moisture sensor can be realized together with nihility feature. Chiral nihility is a special kind of chiral medium, which means that the real part of permittivity and permeability are simultaneously zero or refractive index become zero at certain frequency known as nihility frequency [14-16]. Nowadays, chiral nihility can be used in interesting applications such as focusing [17], scattering [18], chiral fibers [19], cloaking [20], fractional solutions [21], photonics [22], and energy transmission [23]. When nihility concept is integrated in to chiral metamaterial sensor technology which is the name and base of this study, chiral nihility based sensor (CNBS) application came outs. In this study to example the humidity sensor application of gammadion shaped chiral metamaterials, Hevea rubber latex is taken as sample. Organization of the study as follows, in section 2 proposed structure is introduced, numerical results are presented in section 3 and conclusions are given at the end of the paper.

II. Design and Numerical Setup of the Unit Cell

Gammadion shaped biosensor unit cell has a sensor layer and two gammadion shaped resonators which are placed in front and in the back of the unit cell, there is 180° difference between front and back side resonators as shown in the Fig.1. Sensor layer is placed between two resonator structures in order to sense moisture content which is also can be accepted as multifunctional sensor due to sensing mechanism. If generic resonance frequency of resonators considered as a RLC circuit, it can be defined as $\frac{1}{\sqrt{LC}}$. Inductance and capacitance parameters of gammadion shaped sensor must include self and mutual terms according to the design of the metamaterial and thickness of substrate [24]. Resonators placed opposite sides of the unit cell to create powerful coupling which can

be used in different physical and biological sensing applications. In this study substrate and metal thickness of resonators are kept fixed to monitor the effect of sensor layer's permittivity ε_s on resonance frequency of the system. Gammadion shaped sensor structures are printed on Roger RT5870 substrate which has dielectric constant of $\varepsilon_m = 2.33$ and loss tangent of $\delta = 0.004$ at 10 GHz, substrate thickness is $d_m = 0.76$. Gammadion shaped resonators are compromised from copper. Copper thickness and conductivity are 0.035mm and $\sigma_{cu} = 58\text{x}10^6$ S/m, respectively. Dimensions of the gammadion shaped sensor structure is given in Fig. 1.a. As it seen from the Fig.1.b, there is 180° difference between front and back side resonators due to strong coupling. Sensor layer as shown in the Fig.1.c is placed between substrates, also its thickness and dielectric constant are defined by the parameters of d_s and ε_s respectively.

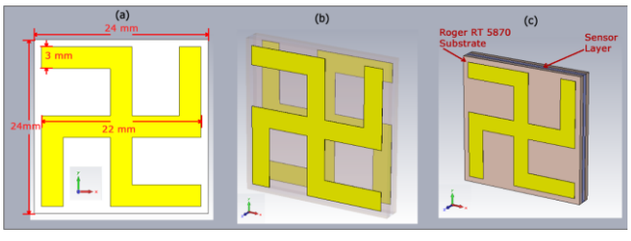

Fig. 1 CNBS Structure, (a) dimensions of the gammadion shaped resonators, (b) front and back side view gammadion shaped resonator, (c) sensor layer placement

III. Numerical Results

Moisture content in Hevea Rubber Latex has been chosen as a sample in this gammadion shape biosensor humidity sensor application. Sensor layer has a thickness of 0.76mm and filled with hevea rubber latex which has different moisture content. Related complex permittivity value is taken from [25]. After obtaining related data and entering correct data as an input to CST microwave studio, variation of reflection coefficient according to different moisture content data is given in Fig.2 and Fig. 3. 5 different moisture contents have been taken as sample. Moisture contents and real permittivity values of Hevea rubber latex are sample moisture contents: $35, 45, 55, 65, 75$ and 85; Real permittivity values are $\varepsilon', 18, 25, 30, 40, 48$ and 55, respectively.

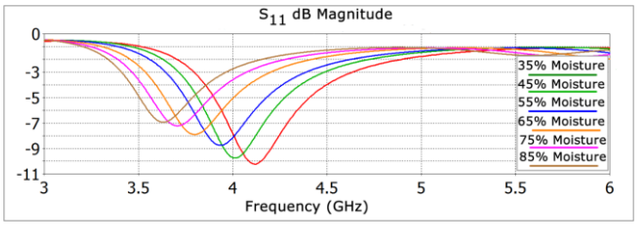

Fig. 2 Reflection coefficient according to moisture content by using CNBS

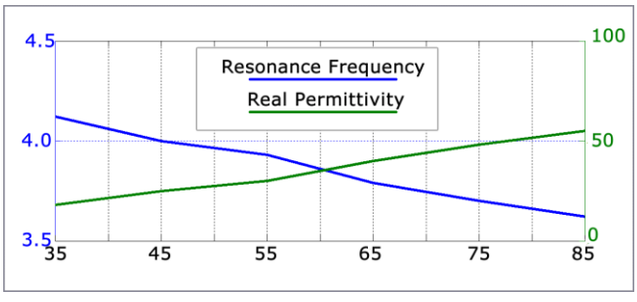

Fig. 3 Resonance Frequency, Real Permittivity and Moisture Content Relation

Resonance Frequency, Real Permittivity and Moisture Content Relation is given in Fig.3. Linear change in both resonance frequency and real permittivity is present every moisture content between 35% and 85% result in 10 Hz change in resonance frequency. While the moisture content increased from 35% to 85%, resonance frequency decreased from 4.122GHz to 3.62GHz and permittivity values increased from 18 to 55.

Chiral nihility property in humidity sensing can be shown in the Fig.4, Fig.5 and Fig.6. 3 moisture content has been taken as sample which are $45\%, 65\%$ and 85% Resonance frequencies at that moisture contents are 4.014, 3.798 and 3.633 GHz, respectively. ε, μ and chirality parameters extracted from formulas which are given in [26]. As shown in the Figs. 4, 5 and 6, chiral nihility can be seen at the resonance frequencies of 4 GHz, 3.75 GHz and 3.60 GHz.

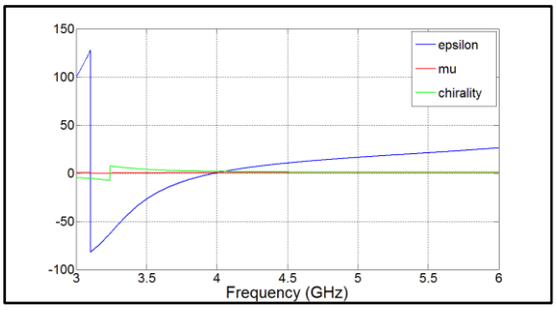

Fig. 4 45% Moisture content permittivity, permeability and chirality graph

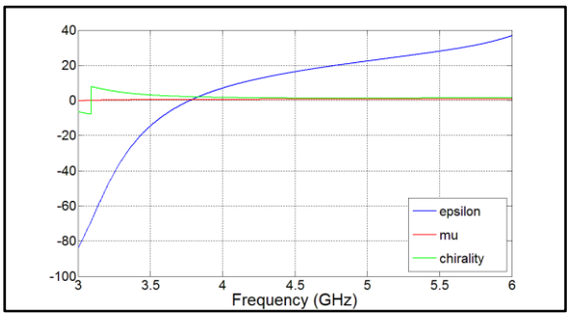

Fig. 5 65% Moisture content permittivity, permeability and chirality graph

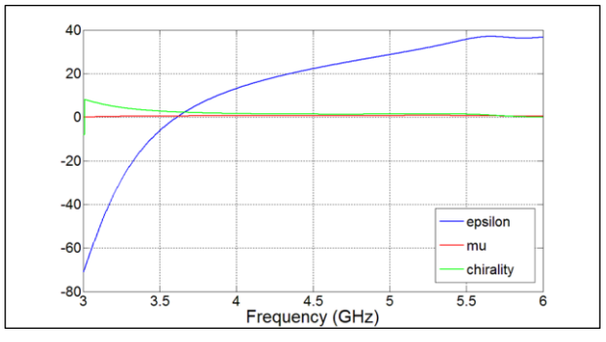

Fig. 6 85% Moisture content permittivity, permeability and chirality graph

The changes of the resonance frequency of overall sensing mechanism can also be described by both equivalent circuit model and the chiral MTM based sensor topology. According to the chiral MTM sensor topology, the increment of the dielectric constant of sensing layer increases the refractive index of the sandwiched layer and thus shifts the wavelength. As a result, the resonance frequency shifts to the upper frequencies. In accordance with equivalent circuit approach, overall capacitance of the circuit is directly proportional with dielectric constant of the sensing layer and the increment of overall capacitance reduces the resonance frequency

IV. Conclusion

Gammadion shaped chiral metamaterial based biosensor application is demonstrated numerically in this study. Due to sensing mechanism of the unit cell, this this sensor can be used not only in moisture content sensing but also temperature, pressure and density sensing which are important parameters for bio sensing. When . ε, μ and chirality parameters retrieved, chiral nihility is came out at the resonance frequencies. Moisture content of Hevea rubber latex is taken as sample and numerical results show that the gammadion shaped chiral metamaterial biosensor shows linear changes according to the moisture content of the samples. As the real permittivity values are such an input of sensor layer, this study gives opportunities to the researches to design novel sensors.

REFERENCES

1. T. W. Ebbesen, H. J. Lezec, H. F. Ghaemi, T. Thio, and P. A. Wolff: "Extraordinary optical transmission through sub-wavelength hole arrays," *Nature Volume*: *391*, 1998, pp. 667-669.
2. J.B. Pendry: "Electromagnetic materials enter the negative age," *Physics World Volume: 14*, Issue: 9, 2001, pp.47-51.
3. J.B. Pendry: "Negative Refraction Makes a Perfect Lens," *Physical Review Letters Volume: 85,* Issue: 18, 2000, pp. 3966–3975.
4. F. Dincer, M. Karaaslan, O. Akgol, C. Sabah: "Design of Polarization and Incident Angle-Independent Perfect Metamaterial Absorber with Interference Theory," *Journal of Electronic Materials Volume:43*, Issue: 11, 2014, pp. 3849-3854.
5. C. Sabah, F. Dincer, M. Karaaslan, E. Unal, O. Akgol: "Polarization-Insensitive FSS based Perfect Metamaterial Absorbers in GHz and THz Frequencies," Radio *Science Volume: 49,* 2014, pp. 306-314.
6. C. Sabah, F. Dincer, M. Karaaslan, E. Unal, O. Akgol, E. Demirel: "Perfect metamaterial absorber with polarization and incident angle independencies based on ring and cross-wire resonators for shielding and a sensor application", *Optics Communications Volume: 322*, 2014, pp. 137-142.
7. N. I. Landy, S. Sajuyigbe, J.J. Mock, D.R. Smith, W. Padilla: "Perfect Metamaterial Absorber," *Phys. Rev. Lett. Volume 100,* 2008, pp. 207402.
8. M. Karaaslan and M. Bakir, "Chiral metamaterial based multifunctional sensor applications," *Progress in Electromagnetics Research Volume 149*, 2014, pp. 55-67.
9. E. Ekmekci, G.T. Sayan, "Multi-functional metamaterial sensor based on a broad-side coupled SRR topology with a multi-layer substrate," *Applied Physics A: Materials Science & Processing Volume 110*, 2013, pp. 189-197.

10. S. Toldo, S. Lampel, S. Stilgenbauer, J. Nickolenko,A. Benner, H.Dohner, T. Cremer, P. Lichter: “Matrix-based comparative genomic hybridization: Bio-chips to screen for genomic imbalances,”. *Genes Chromosomes Cancer Volume 20,* 1997, pp. 399–407.
11. X. Michalet, A.N. Kapanidis,T. Laurence, F.Pinaud, S.Doose, M. Pflughoefft, S. Weiss, S: “The power and prospects of fluorescence microscopies and spectroscopies,”. *Annu. Rev. Biophys. Biomol. Struct. Volume: 32,* 2003, pp.161–182.
12. S.E.D. Webb, S.K. Roberts, S.R. Needham, C.J. Tynan, D.J. Rolfe, M.D. Winn, D.T. Clarke: “Single-molecule imaging and fluorescence lifetime imaging microscopy show different structures for high and low affinity epidermal growth factor receptors in A431 cells,” *Biophys. J. Volume: 94*, 2008, pp. 803–819.
13. D. Factorova, “Temperature dependence of biological tissues complex permittivity at microwave frequencies,” *Advances in Electrical and Electronic Engineering Volume:* 7, 2008, pp. 354-357.
14. A. Lakhtakia, "An electromagnetic trinity from negative permittivity and negative permeability*," Int. J. Inf. and Mil. Wav. Volume. 22,* 2001, pp.1731-1734.
15. S. Tretyakov, I. Nefedov, A. H. Sihvola, S. Maslovki, C. Simovski: "Waves and energy in chiral nihility," *Journal of Electromagnetic Waves and Applications Volume 17*, 2003, pp. 695-706, 2003.
16. M. Baqir, A. Syed, Q. A. Naqvi: "Electromagnetic fields in a circular waveguide containing chiral nihility metamaterial," *Progress In Electromagnetics Research M Volume: 16*, 2011, pp. 85-93.
17. S. Ahmed and Q. A. Naqvi: “Directive EM radiation of a line source in the presence of a coated nihility cylinder,” *J. of Electromagnetic Waves and Applications, Volume: 23*, 2009, pp. 761-771.
18. S. Ahmed and Q. A. Naqvi: “Electromagnetic scattering from a chiral coated nihility cylinder,” *Progress In Electromagnetics Research Letters, PIERL, Volume: 18*, 2010, pp. 41–50.
19. J. Dong, “Exotic characteristics of power propagation in the chiral nihility fiber,” *Progress in Electromagnetics Research, Volume: 99,* 2009, pp. 163–178.
20. X. Cheng, H. Chen, X.-M. Zhang, B. Zhang, B.-I. Wu: "Cloaking a perfectly conducting sphere with rotationally uniaxial nihility media in monostatic radar system," *Progress In Electromagnetics Research, Volume: 100,* 2010, pp. 285-298.
21. Q.A. Naqvi: "Fractional dual solutions in grounded chiral nihility slab and their effect on outside fields," *Journal of Electromagnetic Waves and Applications Volume: 23,* 2009, pp. 773-784.
22. V. R. Tuz, C.-W. Qiu: “Semi-infinite chiral nihility photonics: parametric dependence, wave tunneling and rejection,” *Journal of Electromagnetic Waves and Applications Volume: 103,* 2010, pp. 139-152.
23. C.W. Qiu, N. Burokur, S. Zouhdi, and L. W. Li: "Chiral nihility effects on energy flow in chiral materials," *J. Opt. Soc. Am. A Volume 25*, 2008, pp. 55-63.
24. K. Aydin, I. Bulu, K. Guven, M. Kafesaki, C.M. Soukoulis, E. Ozbay, “Investigation of magnetic resonances for different splitring resonator parameters and designs,” *New J. Phys. Volume 7*, 2005, pp. 168-182.
25. N.Z. Yahaya, Z. Abbas, N.M. Ibrahim, M.H.M. Hafizi: “Permittivity models for determination of moisture content in Hevea Rubber Latex,” *Int J Agric & Biol Eng Volume 7,* 2014, pp. 48－54.
26. F. Dincer, M. Karaaslan, E. Unal, C. Sabah: “Dual-band polarization independent metamaterial absorber based on omega resonator and octa-star strip configuration," *Progress In Electromagnetics Research Volume 141,* 2013, pp. 219-231.

ESTIMATION OF MUCUS CLEARANCE IN PULMONARY AIRWAYS BY MEANS OF A REGRESSION MODEL

Shahriar Shamil Uulu[1], Halil Rıdvan Öz[1*], Ferhat Karaca[2] and Cahit A. Evrensel[3]

[1]Department of Genetics and Bioengineering, Fatih University, 34500 B. Çekmece, Istanbul, Turkey
[2]Department of Civil Engineering, Fatih University, 34500 B. Çekmece, Istanbul, Turkey

[3]Department of Mechanical Engineering, University of Nevada Reno, Reno, NV, USA

[*]Corresponding author e-mail: sshamiluulu@fatih.edu.tr

Abstract- In this study, a multivariate regression analysis was performed on a dataset obtained from experimental tracheal model for mucus clearance in pulmonary airways. Several simulations have been done to verify the validity of the generated regression model. In general, the clearance of mucus in the airways is achieved by the beating action of cilia inside the serous layer which is the primary means of removing inhaled particulates and airway debris from airways in healthy people. In this study, two types of mucus simulants are used in the experimental setup. Clearance distances of a teardrop shape simulant are measured for different velocities, slope angles and surfaces properties. On the obtained data by applying several genuine transformations we developed a multiple regression model that is able to predict clearance up to 86% accuracy. Simulations revealed several important data like direct relation between velocity and clearance and indirect relation between angle and clearance.

Keywords- Mucus Simulant, Tracheal Model, Multivariate Regression Analysis, Linear Model, Simulation.

I. INTRODUCTION

Coughing is necessary for removing inhaled particulates and airway debris from pulmonary airways. There are several studies in the literature for coughing experiments. In some studies, to simulate pulmonary airway, a tygon tube [7], a rigid channel [8], or an endotracheal tube [3-9] were used. Airflow limitation is due to excess mucus and the effectiveness of the mucociliary clearance depends on rheology and the quantity of mucus as well as activity of the cilia indicated by King [11]. Mucus simulants were prepared by cross-linking locust bean gum with sodium tetra borate, 12% to simulate more gel-like mucus with a low V/E (viscosity/elasticity) ratio [1-5]. Aliquots of 3% simulant resemble to normal lung mucus and the stimulant obtained by mixing a higher amount of sodium tetra-borax correlate with diseases such as cystic fibrosis, chronic bronchitis, and asthma [12].

Mucus clearance was investigated mechanically and experimentally (in vitro) for different air velocities, coughing angles and surfaces using different simulants in references before [3-9]. Other references will be explained in the text as appropriate.

In this study, we have performed a multivariate regression analysis on the data set obtained from the tracheal model [4-10] where air flow was controlled by a 3-way solenoid valve between a constant pressure source and the test section, and the duration of flow was 0.2-0.3 seconds. Two different mixtures were used as mucus simulant (MS). During multivariate regression analysis five variables have been used.

II. STATISTICAL TOOLS

In the world of statistics, regression is often used to predict or estimate the future of a given data set. Either linear or logistic regression formula is often used to describe a given data set and thus it helps to predict further values. The formula is selected according to the dataset behavior; scatter diagrams provide a visual technique to display data which show the functional relationship between variables and behavior [13]. In our case the dataset shows linear behavior, as shown in Figure 1 (i.e., for 15 angle, slippery surface and 12% mucus simulant) where clearance increases when velocity increases and data are distributed linearly.

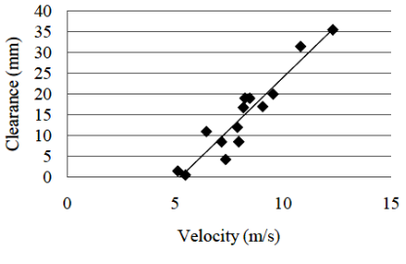

Fig. 1 Scatter diagram between variables

Multivariate regression analysis includes techniques for modeling and analyzing several variables and focuses on the relationship between dependent and one or more independent variables. The general formula for linear regression model is given in equation (1). The proper constant coefficients are obtained when model's squared error is minimal [13]. The x_i are independent variables where they can represent several characteristics of a model for our case see Table 1 and Y is a dependent variable which depends on values of x_i variables, β_i coefficients and c_j constant, thus changes accordingly.

$$Y_i = \beta_1 x_{i1} + \beta_2 x_{i2} + \cdots + \beta_p x_{ip} + c_i = \sum_{i=1}^{k} \beta_i X_{ij} + c_j \quad (1)$$

The format of the paper is as follows; the materials and methods are explained in Section 3, simulation results and discussions are given in Section 4 and the lastly we address the conclusions of the work.

III. MATERIALS AND METHODS

In this section, in-vitro experimental procedure for mucus clearance and multivariate regression analysis procedure configurations for the tracheal model are discussed.

A. Experimental Procedure For In Vitro Mucus Clearance

The experimental tracheal model is shown in Figure 2 [6]. The controlled air flow was supplied with constant pressure towards mucus stimulant resting on a removable flat wall inside a half cylindrical pipe. The angle between the tracheal model and the horizontal was changed during the experiment. Mucus clearance was observed for different angles and air velocities. The setup was composed of the following parts: tracheal model, laminar flow element to prevent turbulent flow, computer, and software which controls air flow, solenoid valve, a close-up high rate imaging system, light source, and a ruler. The stimulant lost its property during long waiting period due to heating of high power light source. That's why the experiments should have been performed rapidly. 1 mm^3 simulant was placed on the tracheal model removable flat wall using a small syringe and allowed settling before sliding it into test section. The air flow was supplied for 0.3 seconds which is approximate coughing duration and the clearance was measured by observing the ruler on the video images and/or also was read directly using the ruler.

The experiments were performed for different angles, different surface properties (dry, adhesive, slippery) and different simulants. The angles are 0, 15, 30, 45, 60 and 75 degrees.

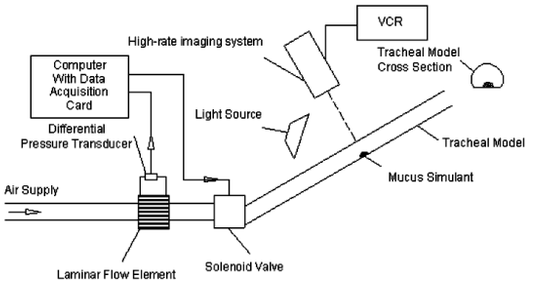

Fig. 2 Experimental Tracheal Model [4-6]

B. Multivariate Regression Analysis Procedure Configurations

While developing the regression model, we have identified one dependent (i.e., clearance) and four independent variables (i.e., mucus simulant – MS, surface – S, velocity – V and CV – transformed variable see Section 3.2.1). Selections were performed according to correlations between dependent and independent variables. Outliers' detection operation which removes the inconsistent data obtained under the same conditions has been performed by checking the residues. For the identification of values for surface and mucus simulants Non-linear Solver Algorithm (i.e., types of algorithms which tend to improve the results in each run, in our case to decrease the squared error [13]) have been used. For our data-set the Non-linear Solver Algorithm showed the best results and fitted our data-set better as compare to other prediction algorithms. The parameters are given in the experimental values part in Table I for details see Section 3. The coefficient values obtained using non-linear solver algorithm is as follows: mucus simulants are 0.6 and 0.2 for 3% and 12% respectively; surfaces are 0.3, 0.6 and 0.9 for slippery, dry and adhesive respectively. To test validity of the regression model several simulations have been performed by using prediction ranges.

Table 1 Variables parameters

	Experimental Values	Prediction Ranges
S	[0.3, 0.6, 0.9]	[0,1]
MS	[0.6, 0.2]	[0,1]
V	[9, 25]	[0, 30]
CV	[9,25]	[0, 30]

C. Transformations on Variables

We have found that when we perform a transformation on variables as stated in the formula "cos(slope in degrees)*Velocity (mm/s)" the correlation increases and gives a positive impact on a linear model due to the physical notation of increasing the effect of force. When slope increases the component of weight of mucus droplet in the direction of motion increases, thus the clearance decreases. Rubin et al. [14] indicated an inverse correlation of cough clearing with the contact angle and adhesiveness of mucus.

4. RESULTS AND DISCUSSION

A. Linear regression model

During multivariate regression analysis, we checked the correlations between dependent and independent variables by observing scatter diagrams and performing detection and omission of outliers. As a result after performing residue analysis on 650 observations the output data set decreased to 480. The equation of a linear model is given in equation [8], for parameters given in Table 1.

$$Clr = 19{,}51 * S - 4{,}00 * MS - 0{,}36 * V + 0{,}74 * \cos(\theta) * V \quad (2)$$

During the tracheal model experiments some of the measurements did not result as expected. At the initial stages the regression analysis showed very low R and R^2. After performing the residual analysis and applying the non-linear solver algorithm, the prediction rate increased substantially as given in Table 2. Simulations showed that clearance decreases with increasing angle. Similarly clearance became larger at higher air velocities (Section 4.2).

Table 2 Statistical parameters

R	0.86
R^2	0.73

B. Model simulations

In this part of our work we explain the results of simulation in order to understand the experimental model and test the regression model. We have observed several important details that are explained in sections below. As stated above mucus shows a very rapid decrease in dynamic viscosity when frequency increases and has less effect on elasticity stated by King and Macklem [12]. In the work of Foster et al. [15] it is stated that increased volume of mucus production and decreased mucociliary clearance may cause accumulation of mucus in the airway tree.

C. Angle with constant velocity values

Simulations in this section have been performed with constant velocity values (i.e., 5, 10, and 15 m/s) and different angles in order to see the effect of two variables on clearance shown in Figure 3. We observed that when angle increases the clearance decreases and at higher velocities the clearance increases. It is also observable that velocity variation has a larger effect at low angles but less effect at larger angles on clearance. It is clear that the relationship between two variables is non-linear.

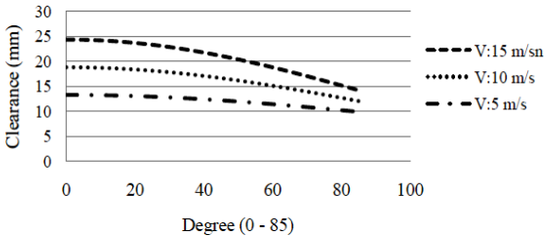

Fig. 3 Angles with constant velocity values

D. Velocity with constant angle degrees

Simulations in this section have been performed with constant angle ranges (i.e., 0, 30, 45, and 60 degrees) and increasing velocity shown in Figure 4. It is also clear that when angle increases the clearance decreases and it is worth mentioning that the relationship between the two variables is linear and higher velocity rates increase the impact of angle variation on clearance.

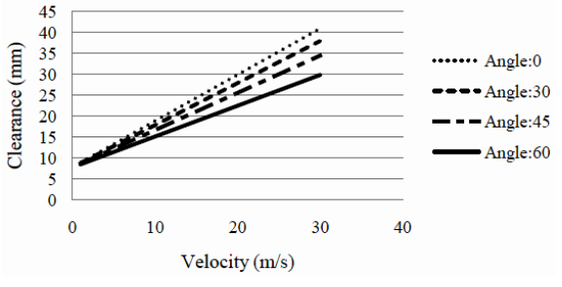

Fig. 4 Velocity with constant angle values

E. Angle with constant mucus simulant parameters

Simulations in this section have been performed with constant mucus simulant values (i.e., 0.25, 0.5, 0.75, and 1.00) and increasing angle shown in Figure 5, for mucus simulant coefficient values see Table I. In order to see that effect of

mucus simulant on clearance, the velocity has been decreased to the lowest value. We have observed that 12% mucus simulant has higher impact on clearance rather than 3% because it is more solid in nature.

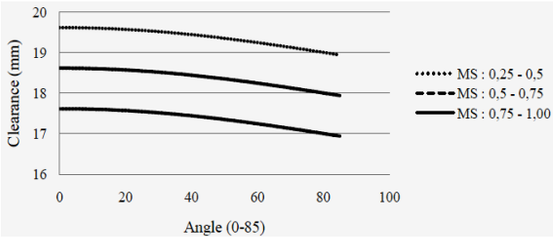

Fig. 5 Angle with constant mucus simulant values

F. Angle with constant surface parameters

Simulations in this section have been performed with constant surface values (i.e., 0.25, 0.5, 0.75, and 1.00) and increasing angle is shown in Figure 6, for surface coefficient values refer Table 1. In order to see the effect of surface on clearance, the velocity has been decreased to the lowest value. We have observed that the clearance increases when surface becomes adhesive, because this type of surface prevents the mucus simulant from going backward and lower clearance for slippery surface, because when the angle increases mucus simulants tend to slide down. King et al. [16] stated that samples with higher elasticity cleared less well. An increased amount of mucus seems to improve clearance stated by Svartengren et al. [17]. From our studies, we observed that generally an adhesive surface has higher impact and slippery surface has lower impact whereas a dry surface is in-between. Because we studied the model generally the error rate is higher for lower angles in this section, in future we shall develop methods that will rectify such problems in more accurately.

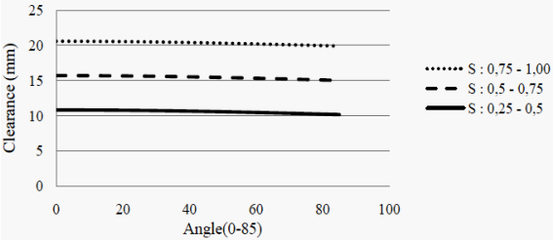

Fig. 6 Angle with constant surface values

V. CONCLUSION

A linear multivariate regression model for mucus clearance in pulmonary airways is generated using experimental data obtained from in-vitro tracheal model tests. The regression model is tested by several simulations for different parameters. Four variables are used in multiple regression analysis (i.e., mucus simulant – MS, surface – S, velocity – V and CV – transformed variable). It is important to state that strong correlations between dependent and independent variables result in better linear model and higher R and R^2 statistical parameters. We have observed that when the angle increases the clearance decreases and with high velocity the clearance increases and 12% mucus simulant has higher impact on clearance rather than 3% due to its solid nature. In addition, we observed that generally the adhesive surface has a higher impact on clearance and the slippery surface has lower impact whereas the dry surface is in between. Simulations revealed several important data like the direct relation between velocity and clearance and indirect relation between angle and clearance.

REFERENCES

1. Xu ZD, Jia DH, Zhang XC, Performance tests and mathematical model considering magnetic saturation for magnetorheological damper, *Journal of Intelligent Matherial Systems and Structures* **23(12)**, 1331-1349, 2012.
2. Guan XC, Guo PF, Modeling of Magnetorheological Dampers Utilizing a General Non-linear Model, *Journal of Intelligent Matherial Systems and Structures* **22(5)**, 435-442, 2011.
3. Öz HR, Karlık B, Evrensel CA, Applications of Artificial Neural Networks Method in Mucus Clearance in Pulmonary Airways, *International Journal of Natural and Engineering Sciences* **3(2)**, 14-16, 2009.
4. Fuchs A, Zhang Q, Elkins J, Gordaninejad F, Evrensel CA, Development and characterization of magnetorheological elastomers, *Journal of Applied Polymer Science* **105(5)**, 2497-2508, 2007.
5. Evrensel CA, Krumpe PE, Hassan AA, Öz HR, Effect of slope and viscoelastic behavior on the clearance of mucus simulant in tracheal models, *Proceedings of 6th Biennial Conference on Engineering Systems Design and Analysis 2002*, Istanbul, TURKEY.
6. Krumpe PE, Öz HR, Evrensel CA, Hassan AA, Why do we sit up to cough? The benefits of vertical posture during cough clearance, *Chest 2001 Annual Meeting,* **120**, 236-237A, 2001, November 4-8,Pennsylvania Convention Center Philadelphia, Pennsylvania, USA.
7. Scherer PW, Burtz L, Fluid mechanics experiments relevant to coughing, *Journal of Biomechanics* **11**, 183-187, 1978.
8. King M, The role of mucus viscoelasticity in cough clearance, *Journal of Biorheology* **6**, 589-597, 1987.
9. Hassan AA, Evrensel CA, Krumpe PE, Interaction of airflow with viscoelastic gel in

endotracheal tubes, *Advances in Bioengineering Journal* **48**, 231-232, 2000.
10. Evrensel CA, Öz, HR, Krumpe PE, Hassan AA, Simulated mucus clearance in horizontal vs. vertically inclined rigid tracheal model, *Proceedings of International Mechanical Engineering Congress and Exposition 2001,* November 11-16, New York, NY, USA.
11. King M, Experimental models for studying mucociliary clearance, *Europian Respiratory Journal* **11**, 222, 1998.
12. King M, Macklem PT, Rheological properties of microliter quantities of normal mucus, *Journal of Applied Physiology: Respiratory Environmental and Exercise Physiology* **42**, 797-802, 1977.
13. Margaret H. Dunham, Data Mining Introductory and Advanced Topics, *Prentice Hall*, ISBN-0-13-088892-3, 2003; pp.54,80.
14. Rubin B.K., Ramirez O., Mellor, J., Cough and Ciliary Clearability of Sputum is Dependent on its Adhesivity and not on Viscoelasticity, *Chest Journal*, **103**, 178S, 1993.
15. Foster, W.M., Langenback, E., Bergofsky, E.H., Measurement of Tracheal and Bronchial Mucus Velocities in Man: Relation to Lung Clearance, *Journal of Applied Physiology,* **48**, 965, 1980.
16. M. King, G. Brock, C. Lundell, Clearance of mucus by simulated cough, *Journal of Applied Physiology* **58**, 1776-1782, 1985.
17. Svartengren K, Philipson K, Svartengren M, Nerbrink O, Camner P, Clearance in smaller airways of inhaled 6-microm particles in subjects with immotile-cilia syndrome, *Journal of Experimental Lung Research,* **21**, 667, 1995.

Comparison of Bioinformatics Web-Tools for Prediction of G-quadruplexes

Fatima Jašarević[1] and Osman Doluca[2]

[1] International Burch University, Sarajevo, Bosnia and Herzegovina
[2] RTA Laboratories, Kocaeli, Turkey

Abstract— **Double stranded is the most common form of DNA. There are other types of DNA topologies that have been gaining interest, such as G-quadruplex. G-quadruplexes are a subject of study because of therapeutic promises they have. Besides the laboratory methods for quadruplex topology and determination of the G-quadruplex structure, the bioinformatics tools are used to predict putative G-quadruplexes. Most of these tools are publicly available on the Internet. In this paper we have investigated online web-tools: QGRS Mapper, nBMST and Pattern Finder. The results showed the comparison between the tools using well-known G-quadruplex forming KIT, MYC and KRAS promoter sequences and KRAS gene sequence as well as *Escherichia coli0157:H7* genome. The results showed that the Web-based tools for G-quadruplex analysis are similar, but with some specific differences. Here we are going to identify these differences and compare their advantages for different applications.**

Keywords— **G-quadruplexes, bioinformatics, Web-based tools, QGRS Mapper, nBMST, Pattern Finder**

I. Introduction

A. G-quadrupexes

For about five decades, it has been known that guanine-rich nucleic acids can self-associate into uncommon structures. These structures were laboratory curiosities until it was found that G-rich sequences have possible functions in a cell, particularly in the telomeres [1].

Structure: G-quadruplexes (GQs) can be formed by one, two or four strands of DNA or RNA. They can appear in different topologies which are dictated by various possible combinations of strand direction and variation in loop size and sequence. Generally, G-quadruplexes are structures with at least two stacked G-tetrads that are held together with loops. [4] A G-tetrad is formed by four guanine bases associated in a planar orientation and stabilized by Hoogsteen interaction with metal ion in the center [2]. G-tetrad are further stabilized in the presence of K+ or Na+ ions. However, they are more stable in the presence of K+ [3, 4].

G-quadruplex structures can be intermolecular (bimolecular and tetramolecular) or intramolecular in nature depending on number of strands they are formed by. [4]

The structure of tetramolecular G-quadruplexes is one of the simplest categories. In this case all strands are parallel to one another and the guanine glycosidic torsion angles are all in the *anti* conformation. Bimolecular quadruplex is formed by association of two strands and have different topological variations. Bimolecular quadruplexes has three different loop types: propeller, lateral and diagonal [1].

A G-quadruplex in a single stranded DNA consists of four runs of guanines and three loops between them. Sizes of both have significant effect on the stability of quadruplex. It becomes less stable if the loop is longer, and more stable if the run of guanines are longer. [5] The loop topologies found in bimolecular quadruplexes are also present in unimolecular quadruplexes [1].

Loops in G-quadruplexes are linkers connect G-strands and support the G-tetrad core in most of the inter-molecular G-quadruplexes and in all of the intra-molecular G-quadruplexes. There are three families of loops: edgewise loops that connect two adjacent guanines, diagonal loops which connect two opposite guanines in the G-quartet and double chain reversal loops run across the G-quadruplex grooves, from one side to another side of G-quadruplex stems. The sequence of loops has influence on the stability of G-quadruplexes. The loop length and loop sequence affect the folding topologies too. Loops are important for biological roles for molecules that bind to G-quadruplexes. The behavior of loops also affects the process of ligands binding to the G-quadruplex [6].

Location: GQs are not randomly distributed but located in specific locations [7]. They can be found at the end of eukaryotic chromosomes [8], in promoter regions, in introns and in untranslated regions [3], as well as in the scaffold of several aptamers which have the ability to bind to biologically relevant proteins and small molecules. Aptamers are oligonucleotides which can bind to their targets with high affinity and specificity because of their three dimensional structure [9]. It is also found in prokaryotes [3].

Structural Variation: G-quadruplex may have different structural features such as molecularity, the size of the loop that connects the strand, the orientation of the strand, core cation and the glycosidic conformation of guanosine residues (*sin/anti*) [3]. The metal cation in the core of the structure stabilizes the structure. The orientation of the strands in the quadruplex can appear in parallel or antiparallel in direction [10]. Several studies showed that the cation have a role in determining the structure of G-quadruplexes, whether

they vill be parallel or antiparallel, tetramolecular or intramolecular [11].

Function: Despite of the studies have been done on GQs in biological systems, their overall function still remain unclear [4]. Although the role of DNA GQs is still under debate, studies on G-quadruplex motifs in the RNA showed clear role in mRNA turnover, translation initiation and repression. Regulated RNA processing is a basic component of gene expression which is central to many biological processes [12].

It is at least known that G-quadruplexes in telomeres have the function of stabilizing the chromosomes [3, 15]. Some studies showed that telomere structural proteins, such as TEBPα and TEBPβ in ciliates and Rap1 in *S.cerevisiae* can promote the formation of GQ DNA *in vitro* without G-quadruplexes, Telomerase functions as a reverse transcriptase and uses its RNA subunits as template to lengthen the G rich of telomere in eukaryotes. Intramolecular antiparallel G quadruplexes formed at telomeres block telomerase activity. On the other hand, intermolecular parallel G4 DNA is permissive for extension by telomerase. Human telomerase is inactive in many somatic cells, but active in most cancer cells and promote lifespan of malignant cells [13].

There are suggestions of potential regulatory roles of G-quadruplex structures in gene regulation because of high concentration of G-quadruplexes potential sequences near the promoter regions. Some bioinformatics studies show that promoters of human oncogene and regulatory genes contain more G-quadruplex motifs than promoters of housekeeping and tumor suppressor genes. The similar situation is with other organisms, such as yeast, plants and bacteria [13]. However, the possible role of G-quadruplexess in promoter region is still not clear. There are hypothesis that they are involved in transcription regulation as repressors [7]. There are experiments which found loop formations in the opposite strand of G4 motifs. These structures may help in keeping DNA template accessible for transcription and G4 in a way that it prevents this loop to anneal to the opposite strand. This could be a role of GQ structures in high transcription levels of certain gene. Some findings based on *in vitro* studies suggest the possible functions of GQ motifs near the promoter: it can inhibit or enhance transcription, and also can bind to the G-quadruplex structure and affect the transcription process [13].

It is found that genes which contain GQs are interfered in control of transcription, translation, structure and stability [3]. Transcription may be altered by G-quadruplex binding proteins in which the role is the formation or unfolding of G-quadruplex structures. For example, myosin D (MyoD) family proteins are transcription factors that bind to E-box on the promoter region of several genes that regulate muscle development. *In vitro* studies, MyoD homodimers bind preferentially to G-quaruplexes which are from the promoter sequences om muscle specific genes. There is a hypothesis that MyoD do not bind to E-box but to the G-quaruplex. The conclusion is that in the case MyoD cannot bind to the Q-quadruplexe, it binds to E-box [13].

Several studies demonstrated that the genetic information required for post-transcriptional control is located mainly in the 5' and 3' untransated regions (UTRs) of mRNA, and may involve the primary sequence and secondary structure of non-protein coding elements [17]. Induction of G-quadruplexes at the UTRs can modulate gene expression at translational level [10].

Therapeutic Promises: Better understanding of the GQs brings higher chances for therapeutic solutions [2]. G-quadruplex structures could be target for several drug designs. Only limited number of G-quadruplexes was resolved by crystallography and NMR [7]. There are evidences of potential therapeutic targets for anticancer therapy. The length and sequence of intertwining loops in GQs direct the stability of quadruplex structure. Beside different conformations quadruplexes can have, the characteristic of all of them is that they have planar quartet structure. This offers a platform for the small organic structures to bind at the top or bottom of the quartet. According to this, ligands can be found with some differences due to the loop lengths [10].

An enzyme responsible for maintenance of telomere, whose hyperactivity is associated with some forms of cancers, inspired the development of molecules that stabilize G-quartet formation. Some of these molecules already prove limiting telomerase activity *in vitro* [11]. Different small molecule ligands with variety of specificity and target regions which bind and stabilize GQ structures are tested in many assays because of the telomeric activity in cancer and role of GQs in it. There is a hope that the ligands which promote the formation of telomeric GQs may inhibit telomerase. The large planar surface of a terminal G-quartet is a common characteristic of all G-quadruplexes. This led to development of small-molecule families which are based on heteroaromatic systems that complement the G-quartet platform. But, this characteristic is not enough for high affinity and most probably is not going to confer selectivity [8, 13, 14].

There are therapeutic potentials of targeting G-quadruplexes in the promoter regions in many genes to regulate the function of these genes. Here we mention some of them: MYC, KIT and KRAS [13].

Transcription factor MYC (or c-MYC) expression is associated with cell proliferation. It can be deregulated by gene amplification, translocation and enhanced transcription as a result of upstream signaling abnormalities. About 80% of solid tumors such as gastrointestinal, ovarian and breast cancer tumors overexpress MYC. This fact leads to interest

of therapeutic target [8, 17]. Since the presence of MYC is crucial for hormone therapy in esterogen-ositive breast cancer, it is not always negative prognostic factor which must be considered before antiMYC therapies [17]. The G-quadruplex structure is a negative regulator of c-MYC. A single base mutation increases c-MYC expression 3-fold. Compounds which stabilize this G-quadruplex structure have the opposite effect: decrease in c-MYC expression [15].

The KIT is proto-oncogene and encodes tyrosine kinase, stimulate cell proliferation, differentiation and survival. Abnormal function and oncogenic cellular transformation can be caused by activating mutation or overexpression in melanocytes, mast cells, myeloid, germ cells and interstitial cells of Cajal lineages. Activation of KIT is the primary pathogenic event in gastrointestinal stromal tumors (GIST) and other tumors where the expression of this gene is increased. KIT protein became main molecular target of focus for GIST therapy. Studies provided evidences that KIT promoter G-quadruplexes can be molecular targets using small molecules [17].

KRAS protein has a role in many signaling pathways and it is important for the pathogenesis of pancreatic carcinoma. The KRAS was pursued as a molecular target for therapeutics but it was also challenging to find the drug at the protein level. Oligonucleotides that imitate one of the G-quadruplexes which were found in the human KRAS promoter were believed to compete for protein binding with the G-quadruplexes in the natural promoter, in a pancreatic nuclear extract. Specific covalently linked polyaromatic stacking units on an application of G-quadruplex-forming oligodeoxynucleotides, where shown to stabilize the G-quadruplexes but also to have a strong antiproliferative effect. There is a common characteristic of all G-quadruplex structures that may be lead to developing a small molecule which bind them. The therapeutic potential of gene promoter G-quadruplexes resulted in very fast increasing number of studies in which small molecules are used as G-quadruplex stabilizers [17].

Methods for Quadruplex Topology and the Determination of the Strucutre: There are many studies which employed methods of biophysical chemistry to assign topology. The mostly used is circular dichroism (CD) which may discriminate between quadruplex topologies of parallel and anti-parallel strand orientation. This rapid method of establishing an overall fold requires very little sample (in μM concentrations). It can examine many different solution conditions and their influence on quadruplex formation. Many sequences that are quadruplex-forming were studied by this technique. Most of initial sequences studies (mostly telomeric) were in one of two characteristic spectral forms: parallel and anti-parallel. As more quadruplex-forming sequence are examined, beside telomeric sequences, topologies may not conform to those that are observed with telomeric quadruplexes. Some disadvantages are that multiple species cannot be identified in CD spectra and non-telomeric loop sequence may confuse the CD spectra in unexpected ways [1].

X-ray crystallography and high-field NMR spectroscopy give the possibility to get topological assignment and atomic-level structure. G-quadruplex structure is determined by NMR when sequence form kinetically stable species in solution. This can be avoided by the use of modified or mutated sequence which is based on the original G-rich sequence and that form only a single species in solution [1].

Computational approaches to study G-quadruplexes give the opportunity to detailed analysis of genes, especially in humans [7]. There are different algorithm rules that can be used to see the possible formation of G-quadruplexes [18]. Some of the tools were available on the internet, but are canceled and some of them can still be used.

G-quadruplex Competition Tools: Bioinformatic approaches play an important role in identifying putative G-quadruplex sequences within genomes. Bioinformatics approaches to the identification of G-quadruplex sequences focus on intramolecular G4 structures. These methods are quite useful because they have successfully predicted sequences that proved to form G4 structures in vitro [19].

There are three Web-based bioinforamtics tools for the prediction of G-quadruplexes that are analysed in this paper. Those are QGRS Mapper [12], nBMST [20] and Pattern Finder [21].

The goal of this paper is to compare these available tools. There are different sets of parameters for stems and loops on each tool. Taking them into consideration, we chose well-known G-quadruplex forming nucleotide sequences and tested using these tools. We compared the results to identify differences and which of them is most suitable for the finding of putative G-quadruplexes.

II. RESULTS

Table 1 Comparison of parameter options from different tools

Bioinformatics tools	Parameters: Loop size	Stem size
QGRS Mapper	1-7	3-6
nBMST	1-7 (in the algorithm)	Minimum 3 (in the algorithm)
Pattern Finder	1-7	3-5

Table 2 Results of putative G-quadrupex sequences using: QGRS Mapper, nMBST and Pattern Finder. Parameters used for the comparison are: QGRS Mapper: Max length 41, Min G-group 3, Loop size 1-7; nBMST: Stem size min 3, loop size 1-7, Pattern Finder: Stem size 3-5, loop size 1-7.

Bioinformatics tools	Positive (+) or negative (-) strand	Numeber of putative G-quadruplexes in different sequences				
		KIT Promoter	*MYC* Promoter	*KRAS* Promoter	*KRAS* Gene	*E.Coli O157:H7* genome
QGRS Mapper	+	2 (4 overlaps)	0	0	2 (85 overlaps)	22 (161 overlaps)
	-	0	1 (79 overlaps)	2 (22 overlaps)	error	error
nBMST	+	2	0	0	1	25
	-	0	1	2	6	22
Pattern Finder	+	2	0	0	13	error
	-	error	10	1	error	error

*The results shown from different tools in the table look different but actually they are not. Different numbers in result represent the same sequences, but the way the tools work effects on the number of G-qudruplexes in the results. That is the reason why the results do not look the same.

Each bioinformatics web-based tool for the prediction of putative G-quadruplex sequence has parameters that determine loop and stem of the G-quadruplex. According to those parameters tools recognize the wanted sequence (Table 1). In the case o QGRS Mapper and Pattern Finder, we have the option to set these parameters, but in nBMST the parameters are fixed in the algorithm. For that reason we have used the pre-set algorithms of nBMST for the other two.

We chose well-known G-quadruplex forming nucleotide sequences: KIT promoter, MYC promoter, KRAS promoter and for the study with a longer sequence we used KRAS gene and Escherichia Coli O157:H7 (Table 2).

Unfortunately, the Pattern Finder website failed after our first test with KRAS and MYC genes and hasn't been fixed since then, best to our knowledge. For this reason, rest of the sequences could not be tested using this tool. In cases of promoters, both nBMST and QGRS mapper successfully detected G-quadruplexes. However, when it comes to KRAS gene and *E. coli* genome there is discrepancy. In the positive strand of KRAS gene while QGRS manages to find two separate putative sequences, nBMST combines and finds them as one putative sequence. We were unable to search KRAS gene and *E.coli* genome in QGRS again for negative strand due to server error. In MYC promoter region Patttern Finder found more G-quadrulexes than in the other two tools. The reason for this is that the other tools recognize sequence with several G repeats in one run as one putative G-quadruplex while Pattern Finder looks for more possible starts of the G-quadruplex inside the G-repeats.

For *E.coli* genome positive strand, nBMST manages to find 3 extra G-quadruplexes than QGRS. In both cases, same putative sequences are detected however, the number of predicted G-quadruplexes differ depending on which four G-runs are selected. QGRS has advantage of finding all potential putative sequences as overlaps, and lists separately.

III. Discussion

The results confirm that the tools for G-quadruplex analysis available on the internet are basically similar, but with some specific differences. It is important to note that each tool is made for unimolecular GQs. Each consider stem to be the same number while the number of loops vary in determining in GQs. Each of them considers parameters that are the same or very close to it (GxNy1GxNy2GxNy3Gx). Each of them gives the option to put wanted sequence and to search for putative G-quadruplex sequence. Each tool in the results gives the information about the length of GQ sequence, beginning and the end of it. The parameters that represents the loop and stem size can be modified in testing to find a desired kind of G-quadruplex (length of loops and number of Gs in the stem) in QGRS Mapper and Pattern Finder. Unfortunately sometimes these webtools may be available due to server error, so it is always beneficial to have a standalone program.

In nBMST parameters are fixed in the algorithm and putative sequences cannot be searched with different parameters. This enables QGRS and Pattern Finder users to search for more specific G-quadruplexes. This is especially useful when looking for highly stable G-quadruplexes that contain long G-runs. For example, in longer sequences, such as *E. coli* sequence or *KRAS* gene there is a higher number of possibilities to have overlaps inside one putative G-quadruplex sequences than in other tools. While nBMST gives 22 results for E. coli genome in positive strand, QGRS Mapper gives 161 overlaps; or while nBMST shows seven overlaps, QGRS Mapper gives results 85 for overlaps. Also, in MYC promoter region QGRS Mapper gives precise results for all possible overlaps, while nBMST shows only one G-quadruplex.

On the other hand nBMST has other advantages in comparison. nBMST gives the results for both given sequence and its reverse complement, while the other tools do not. In those cases, we need to find the reverse complement before testing the sequence. From this aspect, the nBMST is much better and gives the simple way to find putative GQs in the sequence and in its reverse, when working with double

stranded DNA. nBMST can analyze bigger sequences such as E. coli genome. Max length of sequence file can be 20MB. Also, nBMST offers the option to download data.

Pattern Finder represents the number of G-quadruplex sequences in a way that it counts each possible option that this sequence could start inside the region of the sequence that gives repeats of G repeats. Also, the nBMST calculates the number of possible GQ sequences in the same way, but with a little bit less precision. However, QGRS Mapper gives the results in a different way. First, it gives in the results the number of regions where at least four G repeats are present. In the overlaps it shows possibilities of the putative GQ sequences, where it starts and the number of these possibilities. For example, if QGRS Mapper showed that MYC promoter sequence has only one putative G-quadruplex, the tool in the same time gives the result for the overlaps which is 79. Among these 79 overlaps there are sequences that have the same beginning and the end but the difference is that some guanines inside are once considered as part of stem, and in the other cases other guanines. The QGRS Mapper is very practical if we need to know the number of places on the sequence where the G-repeats occur instead of getting the huge number of GQ sequences that represents the overlapping while the number of occurrence of at least G repeats is a few. In the comparison with other two tools, QGRS Mapper has scoring system.

IV. Conclusions

It is important to know the mechanism of each tool used as a bioinformatics predictor for G-quadruplexes and that is the reason why this study is important. If we know the logic on which each of them works we can easily decide which of the tools to use for particular purposes. Also, it is important to know the quality of the all programs available now so to know how to make some new improvements.

These analyses were possible because of the availability of the tools that some scientists made and the papers that explained them clearly. However, this study differs from the previous works because here we used all programs available publicly and tested them with particular sequences and got new results. Besides the results we have gotten in this study and conclusion we have made about the programs, they could be also analyses in a different ways. For example, someone can take one of the tools and try to improve it by changing the algorithm.

This work had some limitations. Unfortunately Pattern Finder had gone offline soon after start of this study. Moreover, QGRS mapper occasionally failed when working with large sequences. Even though, these tools that were available on the Internet and used recently in different studies were currently unavailable, they are nicely described in the scientific papers. We did not give the new algorithm so to test it and see new possible type of outcomes. Also, many tools used for the same purpose are in the private possession, sometimes mentioned in some studies as a method for G-quadruplex analysis but not available publicly. That is why we cannot consider the tools on the Internet as a newest version. There are other scientists that work on the creation of new tools for G-guadruplexes.

Tools for G-quadruplex analysis available publicly have a very important role in helping biologists to test sequences and make possible assumptions on making drug designs for G-quadruplex targeting. In order to results get as good as possible, the best option is to use each of these tools and to get the advantages that each of them offers.

REFERENCES

1. S. Burge, G. N. Parkinson, P. Hazel, A. K. Todd and S. Neidle, Survey and summary, Quadruplex DNA: sequence, topology and structure. *Nucleis acids Research* , 2006, Vol. 34, No. 19
2. N. Borbone, J. Amato, G. Olivero, V. D'Atri, V. Gaelica, E. De Pauw, G. Piccalli and L. Mayol, d(CGGTGGT) forms an octameric parallel G-quadruplex via stacking of unusual G(:C):G(:C):G(:C):G(:C) octads, *Nucleic Acids Research*, Vol. 39, No. 17, 2011, pp. 7848–7857
3. M. A. Mullen, K. J. Olson, P. Dallaire, F. Major, S. M. Assamann and P. C. Bevilcqua, RNA G-Quadruplexes in the model plant species Arabidopsis thaliana: prevalence and possible function rules, *Nucleic Acid Research*, 2010, doi:10.1093/nar/gkq809
4. A. Arora, M. Dutkiewicz, V. Scaria, M. Hariharan, S. Maiti and Jens Kurreck, Inhibition of translation in living eucariotic cells by an RNA G-quadruplex motifs, *RNA* 14(7), 2008, 1290-1296
5. F. N. Memon, A. M. Owen, O. Sanchez-Graillet, G. J. G. Upton and A. P. Harrison, Identifying the impact of G-quadruplexes on Affymetrix 3' arrays using cloud computing, *Journal of Integrative Bioinformatics*, 2010, doi: 10.2390/biecoll-jib-2010-111.
6. H. Zhu, S. Xiao, H. Liang Structural Dynamics of Human Telomeric G-Quadruplex Loops Studied by Molecular Dynamics Simulations, *PLoS ONE*, 2013, doi:10.1371/journal.pone.0071380
7. F. Fogolari, H. Haridas, A. Corazza, P. Viglino, D. Cora, M. Caselle, G. Esposito ad L. E. Xodo, Molecular models for intrastrand DNA G-quadruplexes, *BMC Structural Biology* , 2009, doi: 10.1186/1472-6807-9-64.
8. Nancy Maizels, Lucas T. Gray, The G4 Genome, *PLOS Genetics*, Volume 9, Issue 4, 2013
9. K.-M. Song, S. Lee and C. Ban Aptamers and their Biological applications, *Sensors*, 2(11), 2012, doi:3390/s120100612
10. L. H. Hurley, R. T. Wheelhouse, D. Sun, S. M. Kerwin, M. Salazar, O. Y.. Fedoroft, F. X. Han, . Han, E. Izbicka, D. D. V. Hoft, G-quadruplexes as targets for drug design, *Pharmacology and Therapeutics* 85, 2000, pp. 141-158
11. P. Schultze, N. V. Hud, F. W. Smith and J. Feigon, The effect of sodium, potassium and ammonium ions on the conformation of the dimeric quadruplex formed by the Oxytricha nova telomere repeat oligonucleotide d(G4T4G4), Nucleic Acids Research Vol. 27, No. 15, 1999

12. O. Kikin, L. D'Antoni and P. Bagga, QGRS Mapper: a web-based server for prediction G-quadrupleses in nucleotide sequence, Nucleic Acids Research, Vol. 34, 2006
13. M. L. Bochman, K. Paeschke and V. A.Zakian, DNA secondary structures: stability and function of quadruplex structures, Nat Rev Genet, 13(11), 2012, pp. 770-780
14. J. L. Huppert, A. Bugaut, S. Kumari and S. Balasubramanian, G-quadruplexes: the beginning and end of UTRs, 6260–6268 *Nucleic Acids Research* Vol. 36, No. 19, 2008, doi:10.1093/nar/gkn511
15. A. Siddiqui-Jain, C. L. rand, D. J. Bearss and L. H. Hurley, Direct evidence for a G-quadruplex in promoter region and its targeting with small molecule to repress *c-MYC* transcription, *PNAS*, Vol. 9, No. 18., 2002, pp. 11593-11598
16. S. Neidle, Human telomeric G-quadruplex: The urrent status of telomeric G-quadruplexes as therapeuti targets in human cancer, *FEBS Journal 277*, 2009, pp. 1118-1125
17. Shankra Balasubramanian, Laurence H. Hurley and Stephen Naidle Targeting G-quadruplexes in gene promoters: a novel anticancer strategy?, *Nat Rev Genet*, 10(4), 2002, 261-275
18. H. M. Wong, O. Stegle, S. Rofgers and J. L. Huppert , A toolbox for predicting G-quadruplex formation and stability, *Journal of Nucleic Acids*, Volume 2010, Article ID 564946, 6 pages, 2010
19. Cao K, Ryvkin P, Johnson FB. Computational detection and analysis of sequences with duplex-derived interstrand G-quadruplex forming potential, *Methods* 57(1):3-10. 2012, doi: 10.1016/j.ymeth.2012.05.002.
20. R. Z. Cer, D. E. Donohue, U. S. Mudunuri, N. A. Temiz, M. A. Loss, N. J. Starner, G. N. Halusa, N. Volfovsky, M. Yi, B. T. Luke, A. Bacolla, J. R. Collin and R. M. Stephens, Non-B DB v2.0: a database of predicted non-B DNA-forming motifs and its associated tools, *Nucleic Acids Research*, 2013, Vol. 41, Database issue Published online 3 November 2012 doi:10.1093/nar/gks955
21. V. K. Yadav, J. K. Abraham, P. Mani, Ra. Kulshrestha and S. Chowdhury, QuadBase: genome-wide database of G4 DNA—occurrence and conservation in human, chimpanzee, mouse and rat promoters and 146 microbes, *Nucleic Acids Research*, Vol. 36, 2007, pp. 381–385

A virtual environment to test and validate model based insulin infusion therapies

Dinka Smajlagić[1] and Pasquale Palumbo[2]

[1] Faculty of Biomedical Engineering, University of Technology, Gußhausstraße 27-29, A-1040 Vienna, Austria;
[2]Istituto di Analisi dei Sistemi ed Informatica "A.Ruberti", Consiglio Nazionale delle Ricerche (IASI-CNR), BioMatLab – UCSC – Largo A. Gemelli 8, 00168 Rome, Italy;

Abstract— **In the last decades many closed-loop control algorithms have been published, mainly devoted to control Type 1 diabetic patients, who definitely lack the endogenous insulin release. Recently a novel model-based approach has been developed to investigate the artificial pancreas for Type 2 diabetic patients who, differently from Type 1, do have a pancreatic insulin release, though it reveals to be not sufficient.**

This note applies the aforementioned algorithm and tests it on a virtual environment that accounts for the many uncertainties a real artificial pancreas is forced to cope with. Numerical results show the robustness of the model-based control law.

Keywords— **Time-delay systems, non-linear observer, feedback control law, artificial pancreas.**

I. Introduction

Diabetes mellitus is a group of metabolic diseases, characterized by hyperglycemia, condition in which glucose level is above normal in blood plasma, over a prolonged period, resulting from defects in insulin secretion, insulin action, or both. The two main types of diabetes are type 1 and type 2. In one category (Type 1 diabetes), there is an absolute deficiency of insulin secretion, these patients require exogenous insulin administration to survive. In the other category, the cause is a combination of resistance to insulin action and inadequate compensatory insulin secretory response. These individuals have therefore insulin resistance and usually have relative (rather than absolute) insulin deficiency, in the face of increased levels of circulating insulin. This note investigates closed-loop control scheme for Type 2 diabetic patients. Insulin is supposed to be delivered intravenously.

The chosen control strategy suitably exploits a mathematical model of the glucose-insulin system, since the regulator design makes use of the model. See [3,4] and references therein for a comprehensive review of modeling the glucose-insulin system as well as for model-based (and model less) approaches for the artificial pancreas. The chosen model is a discrete-delay differential equation (DDE) model, which is able to properly account for the endogenous pancreatic release, not negligible for Type 2 diabetes.

The novelty of the present contribution is the building of a virtual environment onto test and validate the theoretical methodology in spite of the unavoidable uncertainties affective real-time devices.

II. The DDE model-based control law

The DDE model adopted to design the control law consists of a single discrete-delay differential equation system where *G(t)*, [mM], is plasma glycemia and *I(t)*, [pM], plasma insulinemia. See [1] and references therein for the details as well as the meaning of the model parameters:

$$\frac{dG(t)}{dt} = -K_{xgi}G(t)I(t) + \frac{T_{gh}}{V_G}, \quad t \geq 0,$$

$$\frac{dI(t)}{dt} = -K_{xi}I(t) + \frac{T_{iGmax}}{V_I} f\left(G(t-\tau_g)\right) + u(t), \tag{1}$$

with initial conditions:

$$G(\tau) = G_0(\tau),\ I(\tau) = I_0(\tau),\ \tau \in [-\tau_g, 0], \tag{2}$$

u(t), [pM/min], is the exogenous intra-venous insulin delivery rate, i.e., the control input;

$G_0(\tau)$, $I_0(\tau)$ is the pair of initial conditions, corresponding to the plasma glucose/insulin concentrations before the control input *u(t)* is applied. For instance, they can be assumed equal to the constant basal levels *(Gb*, *Ib)*;

The nonlinear function $f(\cdot)$ models the pancreatic Insulin Delivery Rate as:

$$f(G) = \frac{(\frac{G}{G^*})^\gamma}{1+(\frac{G}{G^*})^\gamma}; \tag{3}$$

The control law proposed in (2):

$$u(t) = \frac{S(G(t),I(t),G(t-\tau_g)) - v(t)}{K_{xgi}G(t)}, \quad t \geq 0, \tag{4}$$

consisted of a feedback from the state of the system (i.e. glycemia and insulinemia at the actual and at the retarded state, see [1] for the details on the nonlinear function *S*) where

$$v(t) = \ddot{G}_{ref}(t) + Re(t), \qquad R \in \mathbb{R}^{1x2}$$

with

$$e(t) = \begin{bmatrix} e_1(t) \\ e_2(t) \end{bmatrix} = Z(t) - Z_{ref}(t)$$

and

$$Z(t) = \begin{bmatrix} z_1(t) \\ z_2(t) \end{bmatrix} = \begin{bmatrix} G(t) \\ -K_{xgi}G(t)I(t) + \frac{T_{gh}}{V_G} \end{bmatrix}, Z_{ref}(t) = \begin{bmatrix} G_{ref}(t) \\ \dot{G}_{ref}(t) \end{bmatrix}$$

$G_{ref}(t)$ is the desired glucose reference trajectory. It has been proven in [2] that the control gain R can be designed such that the closed loop error $e(t)$ exponentially converges to zero. Unfortunately, the control algorithm would require both glucose and insulin measurements, whilst it is known that real-time plasma insulin measurements are cumbersome to obtain, more expensive and less reliable than glucose measurements. Such a drawback has been overcome in [1] by suitably exploiting an observer for nonlinear time-delay systems. The observer algorithm provides the estimates for the insulin measurements and allows to design the feedback control law based on only glucose measurements.

Below follow a set of 100 simulations carried out on a set of rather homogeneous virtual patients, whose basal levels are randomly distributed with a 10% coefficient of variation (see [1] for the setting of the other model parameters as well as for the shape of the desired glucose profile to be tracked and for the control parameters). Simulations have run on Simulink. On the other hand, the same control law is applied, in order to test its robustness in spite of different model parameter settings. Fig.1 and Fig.2 refer to plasma glycemia and insulinemia. It worth notice that, in spite of a high basal glycemia, it is reduced down to a safe level within the first three hours of treatment. Fig.3 refers to the applied control law.

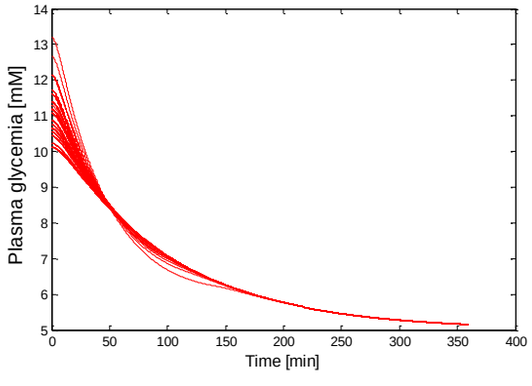

Fig. 1 - Plasma glycemia

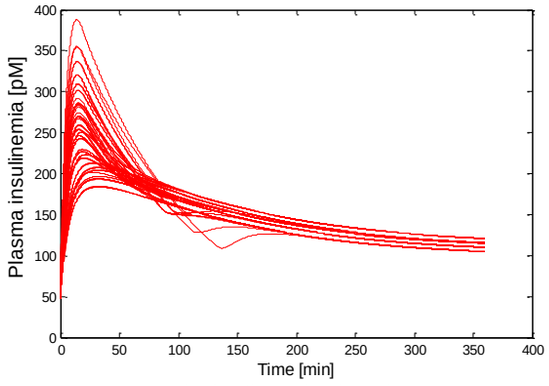

Fig. 2 - Plasma insulinemia

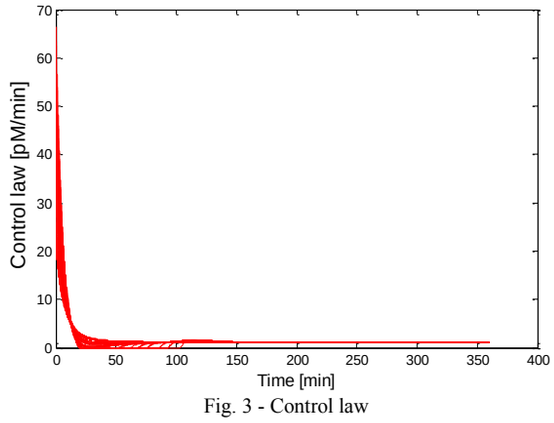

Fig. 3 - Control law

III. CONCLUSIONS

The control problem of tracking a desired plasma glucose evolution by means of insulin administration has been investigated, and a virtual environment is proposed to validate the control law on a population of rather homogeneous virtual patients.

REFERENCES

1. P. Palumbo, P. Pepe, S. Panunzi, A. De Gaetano, Time-delay model-based control of the glucose–insulin system, by means of a state observer, Eur. J.Control 6 (2012) 591–606.
2. P. Palumbo, P. Pepe, S. Panunzi, A. De Gaetano, *Robust closed loop control of plasma glycemia: A discrete-delay model approach*, AIMS Journals, 2009.
3. F. Chee, T. Fernando, *Closed Loop Control of Blood Glucose*, Springer-Verlag Berlin Heidelberg, 2007
4. C. Cobelli,, C. Dalla Man, M. G. Pedersen, A. Bertoldo, G. Toffolo, Advancing our understanding of the glucose system via modeling: A perspective, IEEE Trans. Biomed. Eng. Vol 61, 5 (2014) 1577-92

Dinka Smajlagić is with the Faculty of Biomedical Engineering, University of Technology, Gußhausstraße 27-29, A-1040 Vienna, Austria (phone: +436507439060; e-mail: dinka.smajlagic@mathmods.eu

Mogućnosti određivanja fokus kožne distance pomoću kamere s ciljem verifikacije tačnosti pozicioniranja pacijenata u radioterapijskom tretmanu

Semir Fazlić[1], Hasan Osmić[2], Jakub Osmić[3]

[1] UKC TUZLA/Služba za medicinsku fiziku i zaštitu od zračenja, Tuzla, BiH
[2]UKC TUZLA/Klinika za OHR, Odjel Radioterapije, Tuzla, BiH
[3]UNIVERZITET U TUZLI/Fakultet elektrotehnike, Tuzla, BiH

Abstrakt— **U radu je izvršen pregled mogućnosti određivanja fokus kožne distance reda veličine milimetra, korištenjem kamere kao i mogućnosti primjene fokus kožne distance u verifikaciji tačnosti pozicioniranja pacijenata kod radioterpijskih tretmana. Osim toga u radu je predložen jednostavan metod za određivanje fokus kožne distance koristeći fotografije projektovanog svjetlosnog polja na koži pacijenta i vrijednosti fokus kožne distance koja se dobija iz sistema za planiranje. Fokus kožna distanca je veličina koja pokazuje udaljenost između tačke fokusa linearnog elektronskog akceleratora i kože pacijenta. Svaki tretmantski plan je isplaniran u sistemu za planiranje, koji na osnovu snimaka kompjuterske tomografije rekonstruiše virtuelnog 3D pacijenta. Kao izlazni podatak sa sistema za planiranje dobija se i fokus kožna distanca. Zajedno sa radiografskim snimkama anatomskih struktura pacijenta koje se nalaze u zračnom polju, fokus kožna distanaca služi za verifikaciju pozicije definitivnog izocentra u prostoru, a koji se nalazi u samom pacijentu. Skala fokus kožne distance je centimetarska, a projektuje se kao svjetlosni pokazivač na površini kože pacijenta. Očitana vrijednost fokus kožne distance treba da odgovara dobijenoj vrijednosti iz sistema za planiranje.**

Ključne riječi— **Fokus kožna distanca, pozicioniranje pacijenta, izocentar.**

I. Uvod

U radu je izvršen pregled mogućnosti određivanja fokus kožne distance korištenjem kamere kao i mogućnosti primjene fokus kožne distance u verifikaciji tačnosti pozicioniranja pacijenata kod radioterpijskih tretmana. Problem pozicioniranja pacijenta se svodi na precizan transfer planirane radioterapijske tehnike na pacijenta. To znači da se pacijent postavlja u istu poziciju kao i prilikom kompjuterske tomografije [1-3]. Absorbovana doza ima kvadratnu zavisnost od promjene u udaljenosti od izvora zračenja. Objavljeni su mnogi radovi na temu pomjeranja prilikom pozicioniranja pacijenta i ovisnost asorbovane doze od relativnog odstupanja od planiranog izocentra [4-10].

Fokus kožna distanca je veličina koja pokazuje udaljenost između tačke fokusa linearnog elektronskog akceleratora i kože pacijenta, ili između izvora i kože pacijenta za slučaj Kobalt tretmanske jedinice. Svaki tretmantski plan je isplaniran u sistemu za planiranje, koji na osnovu snimaka kompjuterske tomografije rekonstruiše virtuelnog 3D pacijenta. Kao izlazni podatak sa sistema za planiranje dobija se i fokus kožna distanca. Zajedno sa radiografskim snimkama anatomskih struktura pacijenta koje se nalaze u zračnom polju, fokus kožna distanaca služi za verifikaciju pozicije definitivnog izocentra u prostoru, a koji se nalazi u samom pacijentu. Skala fokus kožne distance se projektuje kao svjetlosni pokazivač na površini kože pacijenta. Očitana vrijednost fokus kožne distance treba da odgovara dobijenoj vrijednosti iz sistema za planiranje. Problem kod preciznog pozicioniranja pacijenta je što je projektovana skala fokus kožne distance (FKD) reda veličine centimetra (Fig. 1), a vrijednost fokus kožne distance dobijene sa sistema za planiranje je reda veličine milimetra.

Cilj ovog rada je da pokaže mogućnost određivanja vrijednosti fokus kožne distance reda veličine milimetra.

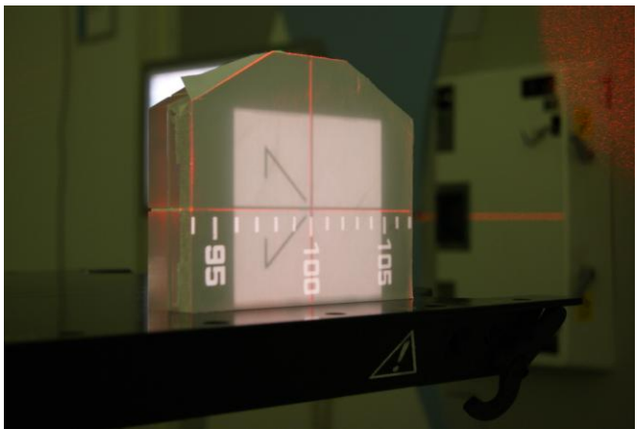

Fig. 1 Skala FKD

II. METODI

U radu je prezentiran jednostavan metod za određivanje fokus kožne distance koristeći fotografije projektovanog svjetlosnog polja na koži pacijenta. Verifikacija dobijenog rezultata se vrši pomoću vrijednosti fokus kožne distance, dobijene iz sistema za planiranje. Metod je testiran na linearnom elektronskom akceleratoru Elekta Synergy Platform. Pomoću dvije fotografije, jedne poznatog polja 10 cm x 10 cm u ravni izocentra i druge projekcije svjetlosnog polja na koži pacijenta analizirana je mogućnost preciznog određivanja fokus kožne distance. Za analizu preciznog određivanja fokus kožne distance, u MATLAB programskom paketu realizirana je funkcija koja na osnovu transformacije prve fotografije analizira drugu fotografiju te upoređuje sa podacima iz sistema za planiranje. Za fizičku korekciju pozicije izocentra koristi se mogućnost pomjeranja stola linearnog elektronskog akceleratora Elekta Precise Table u sve tri dimenzije. Fotografije su napravljene sa Sony α 230 DSLR kamerom 10.1 mega pixela. Za simulaciju pacijenta je korišten fantom-lutka koja se inače koristi za obuku davanja umjetnog disanja, da bi testna situacija bila što bliža realnoj situaciji. Fantom je skeniran na Philips Briliance kompjuterskoj tomografiji koja se koristi na odjelu radioterapije za simulaciju pacijenata. Radioterapijski plan je urađen na CMS XiO sistemu za planiranje, gdje je određen definitivni izocentar te je na osnovu rekonstruisanog 3D virtuelnog pacijenta dobijena fokus kožna distanca. Predloženi metod se bazira na triangulaciji optičke ravni kamere i pozicije projekcije končanice na površinu pacijenta. Sličan način određivanja distance je proučavan u sistemima koji se sastoje od kamere i lasera [11, 12]. Projekcija končanice obilježava centralnu osu glave akceleratora. Dobijeni rezultat verificira se sa slikom iz sistema za planiranje. Ako je poznata udaljenost između kamere i fokusa, te fokusa linearnog elektronskog akceleratora i izocentra moguće je kalibrisati sistem tako da mjeri fokus kožnu distancu (Fig. 2). Sa slike se vidi da je

$$tg\alpha = \frac{d}{X} \tag{1}$$

te da je

$$tg(\alpha - \beta) = \frac{d_1}{X} \tag{2}$$

pri čemu je: udaljenost između kamere i fokusa linearnog elektronskog akceleratora X, d je udaljenost između fokusa linearnog akceleratora i pozicije izocentra, d_1 udaljenost između fokusa linearnog akceleratora i nove pozicije projekcije končanice na površinu fantoma. Da bi se broj piksela sa fotografije mogao povezati sa centimetrima za mjerenje distance potrebno je napraviti fotografiju poznatog polja u poziciji izocentra.

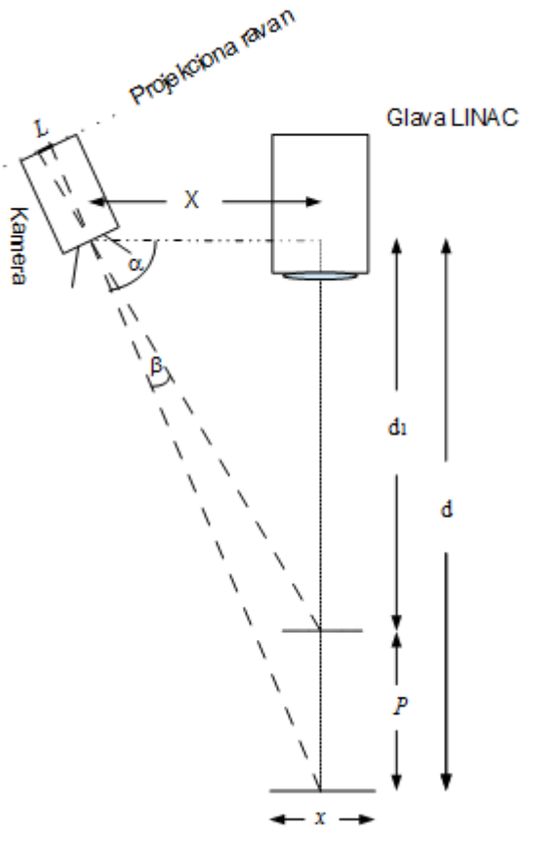

Fig. 2 Eksperimentalna postavka

Matematička povezanost tačke u prostoru i njene projekcije u ravni slike je objašnjena tačkastim modelom kamere. Kamera je predstavljena kao tačka bez korištenja leće za fokusiranje svjetlosti. Ovaj model kamere se može koristiti kao aproksimacija prvog reda mapiranja 3D scene u 2D sliku ne ulazeći u efekte koji se u realnosti javljaju zbog prisustva leće. Pouzdanost ovakvog modela kamere zavisi od kvaliteta kamere [13].

$$\frac{P}{p} = \frac{L}{f} \tag{3}$$

pri čemu je P visina predmeta, p udaljenost predmeta, L visina lika i f fokalna dužina kamere.

U predloženom metodu kombinacijom dvije fotografije, kalibracione koja je slikana u poziciji izocentra sa projekcijom poznatog polja i fotografije koja se koristi za određivanje fokus kožne distance, dobija se formula za izračun nove fokus kožne distance d_1.

$$d_1 = X * \frac{\frac{d}{X} - \frac{L}{f}}{1 + \frac{d}{X} * \frac{L}{f}} \tag{4}$$

III. REZULTATI

Fokus linearnog elektronskog akceleratora je doveden u poziciju da je u istoj ravni sa kamerom. Izmjerena je udaljenost između kamere i fokusa linearnog elektronskog akceleratora *X*. Na stolu je postavljen ravni predmet na koji se u ravni izocentra projektuje polje poznatih dimenzija 10 cm x 10 cm, na fokus kožnoj distanci od 100 cm *d*. Kamera je postavljena u mod koji ne dozvoljava korekciju vibracija, fotografije se uzimaju sa tajmerom za odgođeno fotografisanje. Prva fotografija je projekcija poznatog polja na ravnu plohu u ravni izocentra i ona se koristi kao kalibraciona fotografija. Zatim se na sto u poziciju izocentra postavi fantom koji je prethodno isplaniran na sistemu za planiranje. Fantom ima oblik ljudske glave. Iz iste pozicije kamere uzimaju se fotografije projekcije polja na fantom sa uvedenim relativnim pomjeranjem u odnosu na poziciju izocentra. Relativna pomjeranja u odnosu na izocentar se kreću od -5 cm do +5 cm sa korakom od 1 cm do 1 mm. Dobijene fotografije se učitaju u funkciju realiziranu u MATLAB programskom paketu da bi se dobila vrijednost fokus kožne distance. Rezultati su prikazani u Tabeli 1.

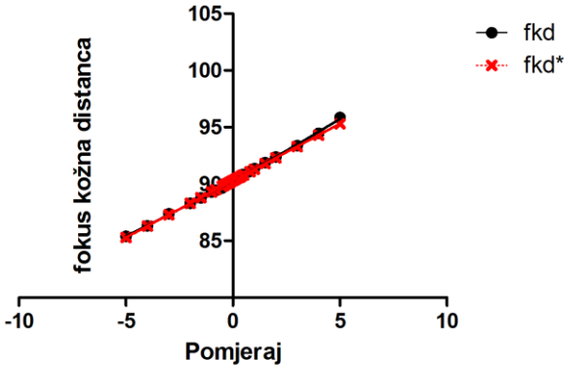

Fig. 3 Mjerena i prava vrijednost FKD

U Tabeli 1. su prikazane vrijednosti fokus kožne distance fkd određene pomoću kamere. Upoređene su sa stvarnim vrijednostima fkd* te su izračunate greške pri određivanju fokus kožne distance novom metodom. Nađena je vrijednost medijana i standardne devijacije apsolutne greške Δ. Sl.3. prikazuje mjerene i stvarne vrijednosti fokus kožne distance u intervalu pomjeraja D.

Tabela 1.

D cm	fkd* cm	fkd cm	Δ cm	Greška %
-5	85.3	85.40441	0.104408	0.122401
-4	86.3	86.33276	0.032759	0.037959
-3	87.3	87.37781	0.077815	0.089135
-2	88.3	88.30422	0.004218	0.004777
-1.5	88.8	88.79045	0.00955	0.010755
-1	89.3	89.30765	0.00765	0.008566
-0.8	89.5	89.44126	0.058735	0.065626
-0.5	89.8	89.65414	0.145856	0.162423
-0.4	89.9	89.85733	0.042671	0.047465
-0.3	90	89.97085	0.02915	0.032389
-0.2	90.1	90.13055	0.030555	0.033912
-0.1	90.2	90.11912	0.080883	0.08967
0	90.3	90.29117	0.008829	0.009777
0.1	90.4	90.47586	0.075859	0.083915
0.2	90.5	90.53382	0.033822	0.037372
0.3	90.6	90.5919	0.008096	0.008936
0.4	90.7	90.8137	0.113705	0.125363
0.5	90.8	90.84888	0.048884	0.053837
0.8	91.1	91.1082	0.008203	0.009005
1	91.3	91.36989	0.069893	0.076553
1.5	91.8	91.87618	0.076182	0.082987
2	92.3	92.37909	0.079089	0.085687
3	93.3	93.3859	0.085902	0.09207
4	94.3	94.46775	0.167747	0.177886
5	95.3	95.86621	0.566209	0.594134
		STDEV	0.110649	
		MEDIAN	0.058735	
		MAX	0.566209	
		MIN	0.004218	

IV. ZAKLJUČAK

U radu je pokazano da je moguće odrediti fokus kožnu distancu reda veličine milimetra. Što predstavlja poboljšanje verifikacije izocentra prilikom pozicioniranja pacijenta, jer je moguće uporediti određenu fokus kožnu distancu sa

onom koja se dobije sa sistema za planiranje radioterapijskog sistema. Iz eksperimentalnih podataka zaključuje se da je metoda pouzdana i sigurna pogotovo u području oko stvarne vrijednosti fokus kožne distance. Metod je testiran na linearnom elektronskom akceleratoru Elekta Synergy Platform. Pomoću dvije fotografije, jedne poznatog polja u ravni izocentra i druge projekcije svjetlosnog polja na koži pacijenta. Analizirana je mogućnost preciznog određivanja fokus kožne distance. Za analizu preciznog određivanja fokus kožne distance, u MATLAB programskom paketu realizirana je funkcija koja na osnovu transformacije prve fotografije analizira drugu fotografiju te upoređuje sa podacima iz sistema za planiranje. Za fizičku korekciju pozicije izocentra koristi se mogućnost pomjeranja stola linearnog elektronskog akceleratora Elekta Precise Table u sve tri dimenzije.

Zbog dobre rezolucije današnjih CCD kamera dobija se vrijednost fokus kožne distance reda veličine milimetra.

Uz tačno određene dvije ortogonalne fokus kožne distance moguće je pozicioniranje pacijenta tj. određivanje definitivnog izocentra u prostoru.

Budući rad će se bazirati na implementaciji sistema za praćenje pozicioniranja pacijenta uživo na osnovama metode predstavljene u ovom radu.

REFERENCE

1. Khan, F.M., *The Physics of Radiation Therapy*. 2010: Wolters Kluwer Health.
2. Schlegel, W.C., T. Bortfeld, and A.L. Grosu, *New Technologies in Radiation Oncology*. 2006: Springer.
3. Webb, S., *The Physics of Three Dimensional Radiation Therapy: Conformal Radiotherapy, Radiosurgery and Treatment Planning*. 1993: CRC Press.
4. Marosevic, G., et al., *Inter-application displacement of brachytherapy dose received by the bladder and rectum of the patients with inoperable cervical cancer.* Radiol Oncol, 2014. **48**(2): p. 203-9.
5. Allgower, C.E., et al., *Experiences with an application of industrial robotics for accurate patient positioning in proton radiotherapy.* Int J Med Robot, 2007. **3**: p. 72-81.
6. Brahme, A., P. Nyman, and B. Skatt, *4D laser camera for accurate patient positioning, collision avoidance, image fusion and adaptive approaches during diagnostic and therapeutic procedures.* Med Phys, 2008. **35**(5): p. 1670-81.
7. Fukuda, A., *[Measurements of TMR, Absorbed Dose using Long SSD TBI Dosimetry and Calculation Accuracy of Treatment Planning System].* Igaku Butsuri, 2009. **29**(2): p. 23-8.
8. Gaisberger, C., et al., *Three-dimensional surface scanning for accurate patient positioning and monitoring during breast cancer radiotherapy.* Strahlenther Onkol, 2013. **189**(10): p. 887-93.
9. Kadiri, L., A. Poynter, and P. Waldock, *An external marker for accurate patient positioning in radiotherapy CT scanning.* Radiother Oncol, 1998. **48**(3): p. 343-4.
10. Olofsen-van Acht, M., et al., *Reduction of irradiated small bowel volume and accurate patient positioning by use of a bellyboard device in pelvic radiotherapy of gynecological cancer patients.* Radiother Oncol, 2001. **59**(1): p. 87-93.
11. Ming-Chih, L., W. Wei-Yen, and C. Chun-Yen, *Image-based distance and area measuring systems.* Sensors Journal, IEEE, 2006. **6**(2): p. 495-503.
12. Ferreira Barreto, S.V., R. Eskinazi Sant'Anna, and M.A.F. Feitosa. *A method for image processing and distance measuring based on laser distance triangulation*. in *Electronics, Circuits, and Systems (ICECS),* 2013. *IEEE 20th International Conference on*.
13. *Pinhole camera model*. Available from: http://en.wikipedia.org/wiki/Pinhole_camera_model

Semir Fazlić, Služba za medicinsku fiziku i zaštitu od zračenja, Univerzitetski Klinički Centar Tuzla, Trnovac bb, 75000 Tuzla, BiH (tel:387-61-227-157; e-mail: fazlicsema@yahoo.com).

Fractal Analysis of Digital Mammograms

E. Đedović[1], A. Gazibegović-Busuladžić[1] and A. Beganović[1,2]

[1]Faculty of Science, Department of Physics, Sarajevo, Bosnia and Herzegovina
[2]Clinical Center University of Sarajevo, Sarajevo, Bosnia and Herzegovina

Abstract— **It has been shown that fractal analysis is useful in image processing, texture analyses and texture image segmentation. It is important to clearly detect edges of breast masses, and precisely locate individual microcalcification in mammograms. We present practical help in that area by fractal analysis, using the concept of fractional Brownian motion. It can be shown that there is a correlation between specific quantitative result of such analysis (Hurst coefficient) and the type of breast mass or tumor.**

Keywords— **digital mammograms, image segmentation, fractals, fractional Brownian motion, Hurst coefficient .**

Introduction

Mammography is one of the main imaging techniques for breast cancer. However, confirmation of malignancy of a tumor mass registered on mammogram often relies on biopsy. It is important to correctly detect the edges of breast masses in order to classify them and successfully treat the cancer.

There are attempts to establish computer analysis of digital mammograms that would help physicians to correctly determine the edges of the breast masses and to classify them, and possibly reduce the need for biopsies. Fractal analysis of digital medical images are widely used for this purposes. Box counting method, ruler method, fractional Brownian motion method are some of them. In this paper we are analysing digital mammograms applying fractional Brownian motion method to determine fractal dimension of specific regions, and so called Sobel method to segment individual microcalcifications and precisely determine the edges of microcalcification grupations. We are going to conduct this kind of analysis within different specified regions of interest (ROI-s). We intend to explore the correlation of obtained value of Hurst parameter and type of the analyzed tumor.

The base for this kind of medical image processing lies in the self-similar structure of human tissue. Self-similarity is the basic property of fractal object [1]. Fractal dimension of ROI-s is the measure of the roughness of digital image in the specified region and can be helpful in determination of concerning tumor type [2]. It is necessary to recognize ROI that includes suspicious objects that differs from surrounding tissue background in order to reduce time for computer analysis. It is possible to use MATLAB code that includes some predefined subroutines for adequately preparing and image processing in order to acquire proper image segmentation [3].

Metodology

Sobel method for edge detection

Edge detection technique uses the abrupt intensity changes between the pixels of an image. The edge consists of the pixels that lie on the boundary between two regions. The magnitude of the gradient, i.e. first derivative, is used to detect an edge. The first-order derivatives in an image can be computed using the Gradient operator. It is convenient to use Sobel method to calculate x and y gradient component. Pixel at position (x,y) is going to be considered as one at the edge if gradient intensity calculated for that position is greater than some predefined value. We are going to use modified Sobel method that modifies that predefined value according to the roughness of the digital image. The MATLAB code used for the edge detection is given in the appendix.

Fractional Brownian function

Function $\mathbf{I}(\vec{\mathbf{r}})$ is considered as fractional Brownian function with Hurst coefficient H when cumulative distribution function $F(z)$ is defined as:

$$\mathbf{F(z)} = \mathbf{Pr}\left(\frac{\mathbf{I}(\vec{\mathbf{r}}+\Delta\vec{\mathbf{r}})-\mathbf{I}(\vec{\mathbf{r}})}{|\Delta\vec{\mathbf{r}}|^{\mathbf{H}}} < z\right),\ z \in R. \qquad (1)$$

Fractal dimension D for digital images with self-similar structure is obtained as $D = 3 - H$.

One need to calculate intensity difference for several distances $|\Delta\vec{\mathbf{r}}|$ to obtain multiscale intensity difference vector MIDV. Hurst coefficient can obtained from linear regression of MIDV on $|\Delta\vec{\mathbf{r}}|$ within log-log scale [4].

Morphological operators

Morphological processing of digital image implies changes of dimensions of specific objects on the image to obtain their segmentation and shape description. The basic morphological operations used in the paper are dilation and erosion. In digital morphology, a small pattern or shape, known as structuring element, probes the image. For the dilation operation, the area around a pixel is set as the structuring element and the original object is allowed to grow larger. Erosion is an operation on the image in which the pixels matching the structuring element are deleted.

Digital mammograms we are going to analyze are grey scale images. Intensity level function $I(x,y)$ of the pixel at the position (x,y) carries the information about the tissue structure. Contrast enhancement is performed in the way that original value of intensity level function $I(x,y)$ is replaced with $I_{out}(x,y)$ on the final image histogram, so that it approximately matches some predefined histogram.

RESULTS

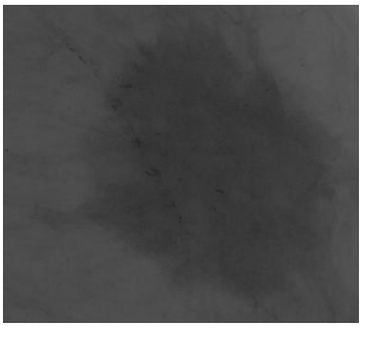

Fig. 1 ROI-I1 that contains dense mass with microcalcifications.

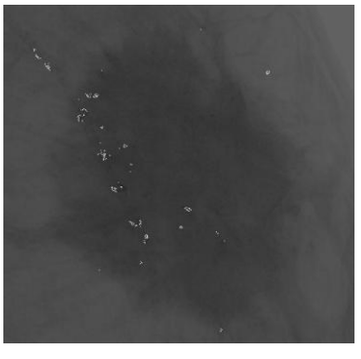

Fig. 2 ROI-I1 with segmented microcalcifications obtained by modified Sobel method with Hurst coefficient for presented ROI.

On the figures Fig. 1, and Fig. 2 specific region of interest from digital mammogram I1 is presented before and after the segmentation. The edges of the microcalcificates are clearly visible after segmentation by modified Sobel method with Hurst coefficient for the ROI. This coefficient is taken as the measure of roughness of the image.

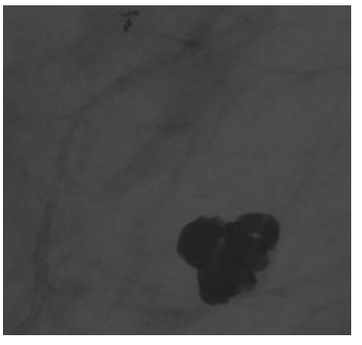

Fig. 3 ROI-I2 that contains grouped microcalcifications.

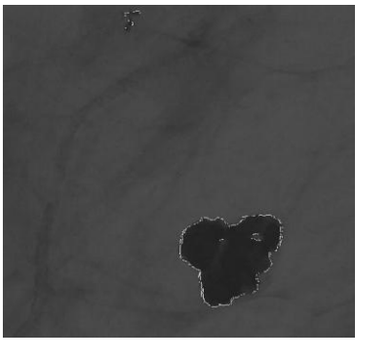

Fig. 4 ROI-I2 with grouped microcalcifications segmented by modified Sobel method with Hurst coefficient for presented ROI .

Figures Fig. 3 and Fig. 4 presents ROI of digital image I2 that contains grouped microcalcifications before and after image processing of segmentation by modified Sobel method respectively. Calculated value of Hurst coefficient for presented ROI of digital image I1 is 0.2002, and for presented ROI of digital image I2 is 0.2463. Value of Hurst coefficient depends on selected ROI, and especially whether it is calculated for entire rectangular ROI or for the region near the edge of suspicious object. The results of modified Sobel method should depend on the choice of the region for Hurst coefficient calculation, and we wanted to further investigate influence of this choice to the edge detection. On the Fig. 5 segmented microcalcifications for ROI-I3 are obtained with Sobel method modified by Hurst coefficient calculated for entire rectangular ROI, while on the Fig. 6 microcalcifications are segmented with Sobel method in which intensity gradient is compared to combination of Hurst coefficients calculated for entire rectangular ROI and for the narrow region around suspicious area.

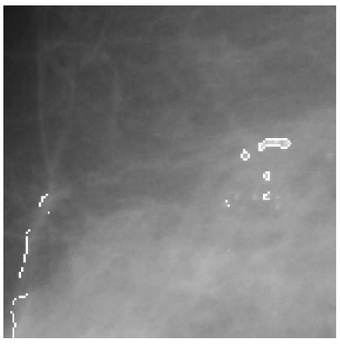

Fig. 5 ROI-I3 with segmented microcalcifications obtained by modified Sobel method with Hurst coefficient for presented rectangular ROI.

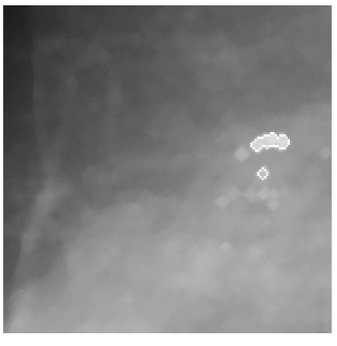

Fig. 6 ROI-I3 with segmented microcalcifications obtained by modified Sobel method with combinated Hurst coefficient.

CONCLUSIONS

Modified Sobelov method of segmentation is tested on different digital mammograms. Using the Hurst coefficient for determination of pixel intensity gradient that corresponds to the edge of microcalcifications, image segmentation quality and edge determination precision is increased. Hurst coefficient is considered as the measure of the roughness of the image, and its calculated value depends on the size of rectangular area around suspicious mass. That is why Hurst coefficient calculated for rectangular ROI may not be precise and sufficient parameter to distinguish between benign and malignant masses. There is more information needed for sufficiently reliable conclusion on the type of tumor. The difference between Hurst coefficient for entire rectangular ROI, and for more narrow region around suspicious may provide additional information that can help to estimate if concerned tumor is benign or malignant. In the case of segmented microcalcifications, determination of the corresponding edges depends largely on the parameter used for Sobel method. For precise determination of segmented microcalcifications edges, suitable parameter should be carefully chosen. Underestimation or overestimation of that parameter leads to different image segmentation.

APPENDIX

```
se = strel('disk',5);
se1 = strel('disk',3);
Jd = imdilate(I,se); figure, imshow(Jd);
Je = imerode(Jd,se1); figure, imshow(Je);
[j,t] = edge(imadjust(I),'sobel');
T = H(1,1)*t;
BWs = edge(Je,'sobel',T);
BWs1 = edge(Je,'sobel',t*0.5);
se2 = strel('line',1,90);
se3 = strel('line',1,0);
se4 = strel('disk',3);
BWs = imdilate(BWs,[se3,se2]);
BWs1 = imdilate(BWs1,[se3,se2]);
BWdfill = imfill(BWs, 'holes');
BWdfill1 = imfill(BWs1, 'holes');
BWoutlineH = bwperim(BWdfill);
BWoutlineS = bwperim(BWdfill1);
Segout1 = I;
Segout2 = I;
Segout1(BWoutlineH) = 255;
Segout2(BWoutlineS) = 255;
figure, imshow(Segout1, 'InitialMagnification', 200),
title('outlined original imageH');
```

REFERENCES

1. Pentland A. Fractal-based description of natural scenes. *IEEE Trans Pattern Anal Mach Intell* 1984;6(6):661– 74.
2. DR Chen, RF Chang, CJ Chen, MF Ho, SJ Kuo,ST Chen, SJ Hung, WK Moon: Classification of breast ultrasound images using fractal feature. *ELSEVIER Journal of Clinical Imaging* 29 (2005) 235–245.
3. Rafael C. Gonzalez, Richard E. Woods: *Digital Image Processing*, Second Edition. Prentice Hall (2009).
4. Chen CC, Daponte JS, Fox MD. Fractal feature analysis and classification in medical imaging. *IEEE Trans Med Imag* 8(2) (1989):133– 42.

Heart rate variability in assessment of autonomic nervous system function in preoperative period

Omerbegović M[1], Ferhatović M.[2]

[1] University Clinical Centre Sarajevo, Clinic of Anesthesia, Resuscitation and ICU, Sarajevo, Bosnia and Herzegovina
[2] University Clinical Centre Sarajevo, Clinic of Infectious diseases, Sarajevo, Bosnia and Herzegovina

Abstract

Integrity of autonomic nervous system function has been known as an essential condition for maintaining homeorhesis and dynamic stability during perioperative period. Heart rate variability which describes alterations of the length of consecutive heart cycles has been proposed as clinically important in prognostication and monitoring in patients with different cardiac disease and patients with diabetes mellitus. Assessment of heart rate variability in preoperative evaluation could be of great interest in clinical anesthesia since perioperative period could present different demanding conditions for the patients who undergo elective surgical procedures with increased risk of cardiac events despite scrupulous technical and procedural preparations. Monitoring of baseline heart rate variability as a measure of autonomic nervous system function or dysfunction could be very important for predicting any possible hemodynamic instability and tailoring of the preoperative evaluation and preparation for surgical and anesthesia procedures and follow up during the periprocedural period. Some linear and nonlinear parameters of heart rate variability in preoperative period in patients scheduled for elective surgery with different comorbid states are presented in this paper.

Key words: heart rate variability, autonomic nervous system, perioperative period

INTRODUCTION

Perioperative period characterize complex physiological reaction to stress conditions. Appropriate autonomic nervous system function is of great importance for overcoming all physiological alterations that may happen during and after surgery and anesthesia. As for present level of perioperative assessment and monitoring there is no routine evaluation of the physiology of the autonomic nervous system and no recommended tests for such assessment. Monitoring of heart rate variability could be a valuable tool for evaluation of baseline autonomic nervous system tone. The process of acquisition of the data and analysis of the different parameters are shown in the Figure 1. Since Consensus conference in 1996 standards of measurements and physiological correlates for different parameters of heart rate variability have been established (1). Linear measures consist of time-domain parameters and frequency-domain parameters.

In nonlinear analysis of heart rate variability, based on nonlinear mathematics, the focus of researchers is on attempt to delineate the complexity of the R-R interval time series(2). Poincaré plot as a visual presentation of time series of RR intervals has been proposed for quantifying of the parameters of heart rate variability(3). Quite common linear measures of heart rate variability are listed in Table 1 (1). Some nonlinear measures of heart rate variability are listed in Table 2.

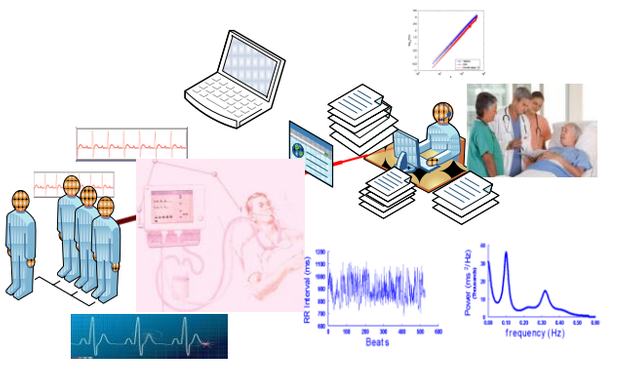

Figure 1.Process of obtaining data and analysis of the ECG recordings for calculation of different parameters of heart rate variability

Alterations of the autonomic nervous system tone predispose patients to wide variations of hemodynamic parameters which could be imperiling for the general well condition during perioperative period. In the patients who are diagnosed with coronary artery disease and diabetes mellitus it has been recommended that monitoring of heart rate variability could be of clinical interest (1,3,4).

In the most severe condition of coronary artery disease, after myocardial infarction, there is a sudden drop of all parameters of heart rate variability. This finding is so consistent that heart rate variability had been used as a prognostic marker for predicting sudden death and convalescence after myocardial infarction (5). In the clinical scenario of chronic coronary artery disease there have been consistent finding of lower heart rate variability in different measured parameters (6,7). Depressed heart rate variability in the patients with arterial hypertension could be also a component of explanation of cardiovascular morbidity in patients with controlled arterial hypertension in perioperative period(8). Alterations

of different linear and nonlinear measures of heart rate variability have been investigated in patients with different forms of cardiomyopathy with aim of finding the most appropriate prognostic parameters for follow up and long-term prognosis(9).

Table 1.Linear measures of HRV in Time-domain analysis (modified from „Heart rate variability: standards of measurement, physiogical interpretation and clinical use“Circulation 1996)

TIME-DOMAIN PARAMETERS
SDNN
Standard deviation of all NN intervals (ms)
SDANN
Standard deviation of the averages of NN intervals in all 5-minute segments of the recording (ms)
RMSSD
Square root of the mean of the sum of the squares of differences between adjacent NN intervals (ms)
NN50 count
Number of pairs of adjacent NN intervals differing by more than 50 ms in the entire recording

Table 2.Linear measures of HRV in Frequency–domain analysis (modified from „Heart rate variability: standards of measurement, physiogical interpretation and clinical use“Circulation 1996)

FREQUENCY- DOMAIN PARAMETERS		
VLF	Power of VLF range	=< 0,04Hz
LF	Power in LF range	0,04-0,15Hz
HF	Power in HF range	0,15-0,4 Hz
LF/HF	Ratio LF(ms²)/ HF(ms²)	

Table 3. Some nonlinear measures of heart rate variability

NONLINEAR MEASURES OF HEART RATE VARIABILITY
Fractal measures
Entropy measures
Symbolic dynamic measures
Poincaré plot

Cardiovascular autonomic neuropathy , quite serious complication of the dysfunction of glucose metabolism in diabetes mellitus may result in haemodynamic instability what is emphasized in the perioperaive period. Assessment of heart rate variability could be of great importance in unraveling this complication in subjects with diabetes mellitus(10). It is estimated that cardiovascular morbidity is highly increased in patients with diabetes in regard to patients who do not glucose metabolism disorder. Chronic renal disease has been accompanied with higher sympathetic tone and autonomic dysfunction. Recent data from a large cohort study unraveled that many risk factors for renal and cardiovascular pathological conditions were associated with lower heart rate variability and that linear some parameters of heart rate variability could be independent risk factor in patients with chronic renal disease (11).

There are also numerous clinical investigations of the possible importance of monitoring heart rate variability in the patients in the perioperative period with focus on management and maintenance of the hemodynamic stability which is the most important parameter for maintenance of the stabile recovery and convalescence (12).

In this paper short term heart rate variability was analysed in consecutive patients with different comorbid states who were scheduled for elective surgery.

PATIENTS AND METHODS

Thirty six consecutive patients scheduled for elective surgery were included in observational trial. Electrocardiogram was recorded in preinduction period in patients who were scheduled for elective surgery with different comorbid states of ASA physical status 2 category, that included : 1)arterial hypertension (n=15), 2)diabetes mellitus controlled by peroral drugs (n=12) , 3)stable coronary artery disease (n=9). Recording was performed in the supine position, during normal spontaneous breathing, in the calm environment with appropriate environmental temperature; patients were advised to stop consuming coffee and products with nicotine in previous period. Patients were under different medication therapy, most of them continued taking therapy unless contraindicated according to the anesthesiology protocol. After recording short-term segments of electrocardiograms (5 minutes), analysis was performed by means of software packages for heart rate analysis (HrvFreq version 4.0, ©2006 and Kubios HRV version 2.1,2012). Linear parameters in time domain (mean RR, mean HR, SDNN) and parameters in frequency domain (Log TP, Log LF, LogHF, LF/HF) and parameters of Poincaré plot (SD1,SD2) were analysed (shown in the Table 4).

Table 4.Summary statistics for demographic data and heart rate variability parameters for the group of individuals with different disease conditions

	Age	BMI	Mean_HR	Mean_RR	SDNN	LOG TP	LOG LF	LOG HF	SD1	SD2	LF_HF
N	36	36	36	36	36	36	36	36	36	36	36
Mean	58,722	23,550	81,059	755,775	44,231	3,017	2,360	2,238	28,894	52,158	2,143
95% CI	56,580 - 60,865	23,125 - 23,975	78,168 - 83,950	728,622 - 782,928	38,014 - 50,447	2,871 - 3,162	2,165 - 2,555	2,029 - 2,446	21,452 - 36,337	45,077 - 59,239	1,436 - 2,849
Variance	40,0921	1,5791	73,0052	6440,2351	337,5999	0,1857	0,3322	0,3787	483,8514	437,9756	4,3610
SD	6,3318	1,2566	8,5443	80,2511	18,3739	0,4309	0,5763	0,6154	21,9966	20,9279	2,0883
Median	59,000	23,500	81,300	746,700	42,900	3,079	2,310	2,096	21,700	51,550	1,845
95% CI	56,000 - 62,000	23,100 - 24,300	76,495 - 85,634	707,000 - 790,309	37,038 - 52,475	2,756 - 3,265	2,127 - 2,849	1,901 - 2,487	16,466 - 27,736	39,613 - 59,909	1,073 - 2,351
Minimum	43,000	20,100	66,600	624,400	16,600	2,121	1,079	1,114	6,100	19,700	0,0530
Maximum	68,000	25,700	96,200	913,700	99,100	3,856	3,208	3,714	101,700	101,400	9,100
10 - 90 P	49,400 - 67,000	22,100 - 25,100	68,130 - 93,991	642,150 - 885,740	24,560 - 60,530	2,418 - 3,492	1,582 - 3,106	1,614 - 3,104	11,920 - 57,440	24,530 - 80,800	0,307 - 4,374

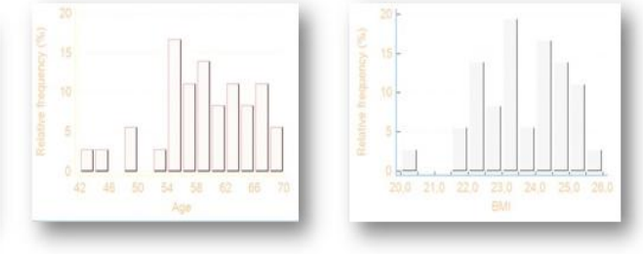

Figure 2. Demografic data -relative distribution in regard to gender, age and BMI

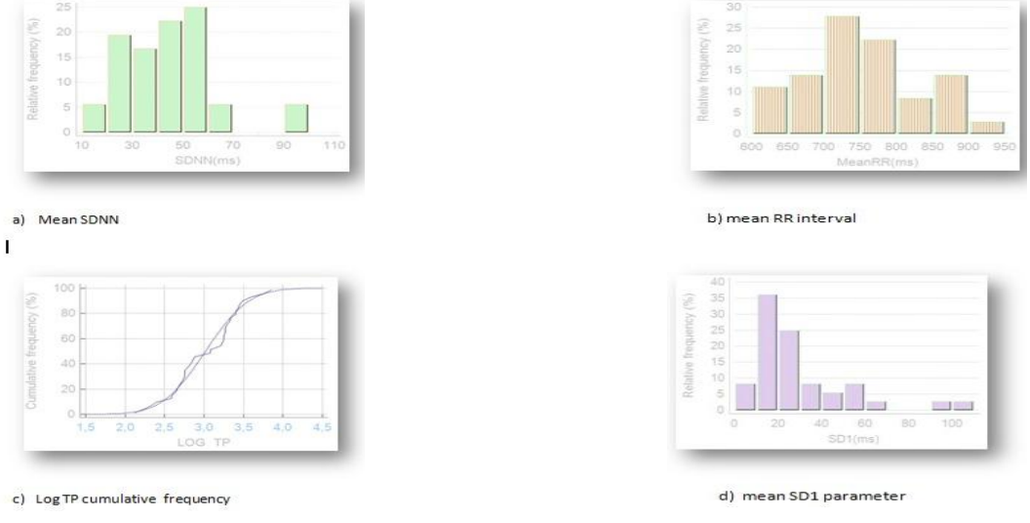

a) Mean SDNN

b) mean RR interval

c) Log TP cumulative frequency

d) mean SD1 parameter

Figure3. Distribution of different parameters of heart rate variability: a)mean SDNN, b)mean RR interval , c)LOG TP cumulative frequency distribution, d) mean SD1 parameter of Poincaré plot

RESULTS

Statistical analysis was performed by statistical software MedCalc ®Version 14.8.1. Diversity of the clinical conditions of the patients and different medications that were used on regular bases limited statistical analysis to only descriptive statistics. Results of descriptive statistics are shown in Table 4 and in the Figures 2 and 3. Parameters of frequency domain analysis were logarithmically transformed for the skewness of the variable distribution.

DISCUSSION

Numerous papers of clinical investigation of heart rate variability deal with the changes of this parameter during perioperative period with special interest on possible changes of sympathovagal balance and possible effects of different anesthetic agents on this parameter. Most findings that were published could not give decisive conclusions on the possible significant effects of specific anesthetic agents unless the fact that parameters of heart rate variability are mostly altered during surgery and general anesthesia and are rapidly returned to preoperative values after conclusion of surgery.

Preoperative assessment of the autonomic nervous system tone could be of great interest for clinicians and researchers as many patients may have some form of autonomic nervous system dysfunction while that condition could not be clearly recognized. Such patients are prone to more emphasized hemodynamic variations.

Hemodynamic variations throughout perioperative period could be quite unpredictable in patients who develop cardiac autonomic neuropathy, a complication of diabetes mellitus which is not routinely searched for in subjects who suffer from diabetes mellitus. While resting tachycardia and postural hypotension are indicative of developed condition of CAN altered heart rate variability has been shown as an early sign of cardiac diabetic autonomic neuropathy. Although Keyl C. and coworkers did not find relationship between hemodynamic changes and cardiovascular autonomic dysfunction (13), this relationship has been confirmed in later papers (14,15,16).

Keet SW. and coworkers have shown high agreement of heart rate variability with most autonomic function tests, and Knüttgen D. et al. have shown relationship between heart rate variability and blood pressure variations in the patients with diabetes mellitus who underwent ophtalmosurgical procedures (14,15). Huang CJ et al. followed haemodynamic parameters in patients with diabetes mellitus and nondiabetic patients who underwent elective surgery and found that monitoring of heart rate variability could be sensitive for predicting haemodynamic instability in patients who did not have clinical signs of cardiac autonomic neuropathy (16).

Heart rate variability has been used as a predictor of risk of cardiac ischemia in patients who underwent general anesthesia. Hanss R. and coworkers investigated if heart rate variability was predictive of hemodynamic instability in high risk patients according to Revised Cardiac Risk Index score of 3 who were planned for elective surgery and they found that patients who had lower values of total power of the spectrum of heart rate variability had also greater variations of hemodynamic parameters (17). Filipović M. and coworkers investigated the possible predictors of long-term outcome in patients with documented or suspected coronary artery disease after major noncardiac surgery and found that heart rate variability could be an independent predictor of cardiac morbidity in patients undergoing major noncardiac surgery(18).

Laitio T. and coworkers investigated ECG recordings in thirty-two patients scheduled for surgical repair of a traumatic hip fracture and have implicated that preoperative increase in randomness of heart rate variability could be predictive for postoperative, silent prolonged myocardial ischemia(19).

The main limitation of our paper is the small number of patients that were enrolled what had limited analysis of the data to descriptive statistics only. Nevertheless, the aim of this paper was to emphasize the importance of monitoring of autonomic nervous system function in the patients scheduled for elective surgical procedures. At present there is a shift of thinking of the anesthesiologists on the issue of autonomic nervous system (ANS) dysfunction as a possible part of preoperative examination in everyday clinical practice, but routine monitoring of the parameters of ANS function is still unavailable.

The most obvious changes of heart rate variability are shown in patients after recent myocardial infarction, patients with coronary disease, patients with cardiomyopathy and patients with diabetes mellitus. There are also other populations of individuals who suffer from neurological, endocrine, renal and psychiatric disorders who could have alterations of heart rate variability and different clinical conditions during perioperative period.

Conclusion

Monitoring of heart rate variability in perioperative period could be very important in preoperative assessment of functional status of autonomic nervous system, what could be of great benefit and prognostic value in patients who had already had autonomic nervous dysfunction as a consequence of cardiovascular and endocrine diseases, but there should be possibility of monitoring of this pa-

rameter in the different larger groups of individuals of similar demographic characteristic throughout longer periods in order to evaluate baseline values and follow the changes and alterations in different clinical end environmental situations.

References :

1.Task Force of The European Society of Cardiolgy and the North American Society of Pacing and Electrophy-siology. Heart rate variability: standards of measurement, physiological interpretation and clinical use. Circulation 1996; 93: 1043-65.

2. Goldberger AL, Amaral LA, Hausdorff JM, Ivanov P, Peng CK, et al. Fractal dynamics in physiology: alterations with disease and aging. Proc Natl Acad Sci. 2002; 99 (1):2466–2472.

3. Rezek IA, Roberts SA: Stochastic complexity measures for physiological signal analysis. IEEE T-BME, 1998;45(9): 1186–91

4. Vinik AI, Ziegler D. Diabetic Cardiovascular Autonomic Neuropathy Circulation 2007;115:387-397

5. Camm AJ,Pratt CM,Schwartz PJ,Al-Khalidi HR,Spyt MJ, Holroyde MJ et al. Mortality in patients after recent myocardial infarction: a randomized, placebo- controlled trial of azimilide using heart rate variability for risk stratification(ALIVE - Azimilide post Infarct surVival Evaluation Trial). Circulation 2004;109:990-996

6. Wennerblom B, Lurje L, Tygesen H, Vahisalo R, Hjalmarson Ă. Patients with uncomplicated coronary artery disease have reduced haert rate variability mainly affecting vagal tone.Heart 2000;83:290-294

7. Laitio T, Jalonen J, Kuusela T, Scheinin H. The role of heart rate variability in risk stratification for adverse postoperative cardiac events. Anesth Analg 2007;105(6):1548-60

8. Lucini D, Mela GS, Malliani AP, Pagani M. Impairment in cardiac autonomic regulations preceding arterial hypertension in humans.Circulation 2002;106:2673-2679

9. Krstačić G,Parati G,Gamberger D,Castiglioni P, Krstačić A, Steiner R. Heart rate vaiability and nonlinear dynamic analysis in patients with stress-induced cardiomyopathy. Med Biol Eng Comput 2012 ;50 (10):1037-46

10. Ziegler D, Zentai CP, Perz S, Rathmann W, Haastert B, Döring A, Meisinger C.KORA Study Group. Prediction of mortality using measures of cardiac autonomic dysfunction in the diabetic and nondiabetic population: the MONICA /KORA Augsburg Cohort Study. Diabetes Care 2008; 31: 556– 561

11. Chandra P, Sands RL, Gillespie BW, Levin NW, Kotanko P, Kiser M, Finkelstein F, Hinderliter A, Pop-Busui R, Rajagopalan S, Saran R: Predictors of heart rate variability and its prognostic significance in chronic kidney disease. Nephrol Dial Transplant 2012;27:700-709

12.Galletly DC, Corfiatis T,Westenberg AM, Robinson BJ. Heart rate periodicities during induction of propofol-nitrous oxide-isoflurane anaesthesia.Br J Anaesth 1992;68(4):360-4

13.Keyl C, Lemberger P, Palitzsch KD, Hochmuth K, Liebold A, Hobbhahn J. Cardiovascular autonomic dysfunction and hemodynamic response to anesthetic induction in patients with coronary artery disease and diabetes mellitus.Anesth Analg. 1999 May;88(5):985-91.

14.Keet SW, Bulte CS, Sivanathan A, Verhees L, Allaart CP, Boer C, Bouwman RA.Cardiovascular autonomic function testing under non-standardised and standardised conditions in cardiovascular patients with type-2 diabetes mellitus. Anaesthesia. 2014;69(5):476-83

15.Knüttgen D, Trojan S, Weber M, Wolf M, Wappler F. Pre-operative measurement of heart rate variability in diabetics: a method to estimate blood pressure stability during anaesthesia induction. Anaesthesist. 2005 May;54(5):442-9.

16.Huang CJ, Kuok CH, Kuo TBJ, Hsu YW, Tsai PS. Preoperative measurement of heart rate variability predicts hypotension during general anesthesia. Acta Anaesthesiol Scand 2006; 50: 542—548

17.Hanss R, Renner J, Ilies C, Moikow L, Buell O, Steinfath M, Scholz J, Bein B. Does heart rate variability predict hypotension and bradiycardia after induction of general anaesthesia in high risk cardiovascular patients? Anaesthesia. 2008 Feb;63(2):129-35.

18. Filipovic M, Jeger R, Probst C, Girard T, Pfisterer M, Gürke L, Skarvan K, Seeberger MD. Heart rate variability and cardiac troponin I are incremental and independent predictors of one-year all-cause mortality after major noncardiac surgery in patients at risk of coronary artery disease. J Am Coll Cardiol. 2003;42(10):1767-1776.

19. Laitio TT, Huikuri HV, Makikallio TH, Jalonen J, Kentala ES, Hekenius H. The breakdown of fractal heart dynamics predicts prolonged postoperative myocardial ischaemia. Anesth Analg 2004; 98:1239-44

Corresponding author:
Meldijana Omerbegović,
University Clinical Centre Sarajevo, Bolnička 25, Sarajevo, 71000(phone:387-33-297-576;e-mail: institutnir@kcus.ba

Adjustment of quantification of catecholamines and their metabolites in biological samples using the Shimadzu LCSOL SINGLE-LC EN HPLC system with electrochemical detection

S. Ibragic[1] and E. Sofic[1,2]

[1] University of Sarajevo, Faculty of Science, Zmaja od Bosne 33-35, 71000 Sarajevo, Bosnia and Herzegovina
[2]University of Sarajevo, Faculty of Pharmacy, Zmaja od Bosne 8, 71000 Sarajevo, Bosnia and Herzegovina

Abstract— **BACKGROUND: Catecholamines are a group of biogenic amines, present in low concentrations in human physiological fluids, yet involved in the regulation of numerous physiological processes (neurotransmitters and hormones). They are sensitive to oxidative degradation and their determination in complex biological matrices was a challenge in the development of highly sensitive bio-analytical techniques that enable precise quantification. OBJECTIVE: To adjust the method of quantification [1] of adrenaline (A), noradrenaline (NA), dopamine (DA), 5-hydroxyindoleacetic acid (5-HIAA) and homovanillic acid (HVA) in biological samples using the Shimadzu LCSOL SINGLE-LC EN HPLC system that allows a maximum injection volume of 20 µl. The system was coupled to the BAS liquid chromatography CC-5E LC-4C Amperometric Detector with a glassy carbon working electrode and Ag/AgCl reference electrode. METHODS: Catecholamines from human serum and cerebrospinal fluid (CSF) were adsorbed on alumina, eluted with only 40 µl perchloric acid and 20 µl sample injected into the HPLC-ED system. The mobile phase, delivered at the flow rate of 1 ml/min, consisted of 23.0 g citric acid monohydrate, 11.5 g sodium hydroxyde, 27.2 g sodium acetate, 4.2 ml of 100% acetic acid and water up to 1 l. Then, 300 ml of that solution was diluted with 600 ml water and used as a mobile phase. The stationary phase was the BDS Hypersil C18, 250 x 4.6 column, the potential was 0.70 V. Dihydroxybenzylamine (DHBA) was used as an internal standard. The metabolites were determined in CSF, which was diluted and centrifuged. The mobile phase had a flow rate of 1 ml/min and consisted of 372 mg EDTA, 0.1 M sodium acetate, 50 % methanol (63.3 ml), 7.9 ml glacial acetic acid and filled with water to 1 l. A BDS Hypersil C18, 250 x 4.6 column was used and the potential was 0.75 V. RESULTS AND CONCLUSIONS: The utilisation of the described method enabled a precise quantification of catecholamines and their metabolites that are present in the pg/ml and ng/ml range, respectively. The development of electrochemical detectors has led to quantitative and qualitative analyses of electroactive substances. Such analyses are fundamental for diagnostic purposes, clinical and pharmacological research.**

Keywords— **biogenic amines, serum, cerebrospinal fluid, HPLC-ED**

I. Introduction

Catecholamines belong to the class of biogenic amines. As neurotransmitters and hormones, they are responsible for the regulation of a wide range of physiological processes and conditions such as cognitive processes, mood states, blood pressure and body temperature. Aberrations of concentrations of catecholamines and their metabolites reflect the activity of the sympatho-adrenal system and can indicate pathological conditions. Therefore, developing sensitive analytical methods for their quantification in physiological fluids is of clinical interest. In the present work, a previously established method [1] has been adjusted to determine catecholamines and their metabolites by adsorbing them on alumina, eluting with 40 µl perchloric acid and injecting only 20 µl of that eluent. A similar HPLC-ED method has been employed to determine 5-hydroxyindoleacetic acid (5-HIAA) and homovanillic acid (HVA) in 10 µl cerebrospinal fluid diluted with 10 µl perchloric acid.

II. Materials and methods

A. Quantification of catecholamines in human serum and cerebrospinal fluid

Chemicals. Noradrenaline-L-bitartrate hydrate min. 99 % was purchased from Aldrich; 3,4-dihydroxybenzylamine hydrobromide 98 % and disodium ethylenediaminetetraacetate (EDTA) dihydrate min. 94 % from Sigma, o-phosphoric acid p.a., ≥ 85 % and water Chromasolv® plus for HPLC from Sigma Aldrich, hydrochloric acid p.a., 37 % and sodium hydroxyde p.a. from Panreac. Tris(hydroxymethyl)-aminomethane, perchloric acid p.a. 60 %, acetic anhydride p.a. 100 %, aluminium oxide 90 active (activity stage I) for column chromatography 0.063-0.200 mm, citric acid monohydrate, p.a. and sodium acetate anhydrous p.a. were purchased from Merck.

Sample preparation. Blood samples were centrifuged at 3000 rpm for 10 min at 20 °C. Samples of the cerebrospinal fluid were directly used for the analysis, without centrifugation, according to the procedure below.

Preparation of standard solutions. Stock standard solutions for noradrenaline (NA), adrenaline (A), dihydroxybenzylamine (DHBA) and dopamine (DA) had the concentration of 10 mg free base / 10 ml solvent (*o*-H_3PO_4). The stock solutions were diluted 1:100 (v), the obtained solution (v) was further diluted 1:100 (vv), and the (vv) solution was diluted 1:10 (vvv). The concentration of the (vvv) diluted solution was 10 ng/ml.

Working solutions. The TRIS-HCl buffer solution was prepared by dissolving 30.27 g Tris – HCl in 250 ml water and adding 5 g EDTA. The pH was adjusted to 8.6 using 25% HCl. For the procedure it was also necessary to prepare 0.4 M $HClO_4$, 0.1 M $HClO_4$ and 0.1 M HCl.
The mobile phase was prepared by mixing 23.0 g citric acid monohydrate, 11.5 g sodium hydroxyde, 27.2 g sodium acetate, 4.2 ml of 100% acetic acid and filling with water up to 1 l. Then, 300 ml of that solution was diluted with 600 ml water, filtrated, degassed and used as a mobile phase.

Alumina activation. Aluminium oxide was added into 200 ml 1M HCl, the suspension was stirred in a fridge over night and then washed out with water (HPLC grade) until it became neutral. In the following 12-18 hours the alumina was dried at 220 °C and stored in a desiccator.

Instrumentation. Quantification of catecholamines was performed using the Shimadzu LCSOL SINGLE-LC EN HPLC system that allows a maximum injection volume of 20 µl. The system was coupled to the BAS liquid chromatography CC-5E LC-4C amperometric detector with a glassy carbon working electrode and Ag/AgCl reference electrode. The stationary phase was the BDS Hypersil C18, 250 x 4.6 column, the potential was set at 0.70 V. The mobile phase was delivered by an isocratic pump LC-20AT at the flow rate of 1 ml/min.

Procedure. Eppendorf tubes were placed on ice and into each tube 50 µl DHBA (vvv dilution) was transferred. Then, 1 ml sample, ca. 25 mg Al_2O_3 and 450 µl TRIS-HCl buffer (with EDTA) pH=8.66. was added. The tube contents were vortex-mixed for a short time and then put on a shaker for 15 minutes. The tubes were put into a centrifuge, at 12000 rpm and the upper layer was aspirated and discarded. Next, 1 ml in water diluted TRIS-HCl buffer (1:100) was added into the tubes which were then put on vortex, centrifuged again for 1 min and the supernatant was removed. The alumina was washed twice with diluted TRIS-HCl buffer, centrifuged for three minutes and the supernatant was discarded. The catecholamines adsorbed on alumina were eluted with only 40 µl perchloric acid and 20 µl of the eluent injected into the HPLC-ED system. Standards of catecholamines were prepared by transferring 50 µl DHBA (dilution vvv), 50 µl standard (dilution vvv), 900 µl 0.1 M $HClO_4$ and ca. 25 mg Al_2O_3 into tubes kept on ice. Then, 450 µl TRIS-HCl (with EDTA) was added and steps followed as for the samples procedure.

B. Quantification of 5-HIAA and HVA in cerebrospinal fluid

Chemicals. Perchloric acid p.a. 60 %, sodium acetate anhydrous p.a. and methanol LiChrosolv were purchased from Merck. Disodium ethylenediaminetetraacetate (EDTA) dihydrate was purchased from Sigma, 5-hydroxyindoleacetic acid 99 % and homovanillic acid 98% were purchased from Aldrich. Water HPLC grade and glacial acetic acid 99.8% were purchased from Panreac.

Sample preparation. Cerebrospinal fluid samples were stored at -80°C until analysis. The CSF was diluted with 0.2M $HClO_4$ (1:1), centrifuged at 15000 rpm for 30 min at 4°C. The supernatant was transferred into clean Eppendorf tubes, centrifuged at 15000 rpm for 10 min at 4°C and 20 µl of the supernatant was injected into the HPLC-ED system.

Preparation of standard solutions. Stock standard solutions for 5-HIAA and HVA were prepared by dissolving 10.0 mg pure substance in 10.0 ml 0.2 M $HClO_4$. The stock solutions were diluted 1:100 (v), the obtained solution (v) was further diluted 1:100 (vv). Then, 50 µl of the (vv) solution was transferred into a tube and 1950 µl 0.2 M $HClO_4$ was added to obtain the concentration of 250 ng/ml.

Working solutions. The mobile phase consisted of 372 mg EDTA, 0.1 M sodium acetate, 50 % methanol (63.3 ml), 7.9 ml glacial acetic acid and filled with water to 1 l.

Instrumentation. Quantification of analytes was performed using the HPLC-ED described for the quantification of catecholamines. The potential was set at 0.75 V. The mobile phase was delivered by an isocratic pump LC-20AT at the flow rate of 1 ml/min.

III. RESULTS

The catecholamines were isolated from 1 ml biological sample by adsorption onto alumina and were then desorbed by elution with only 40 µl perchloric acid. Dihydroxybenzilamine was used as the internal standard. Figure 1 shows a typical chromatogram of standard solutions each containing 200 pg noradrenaline, adrenaline, dihydroxybenzylamine and dopamine in 20 µl injection volume. The separation of catecholamines from CSF and serum samples is shown in figure 2 and 3, respectively.

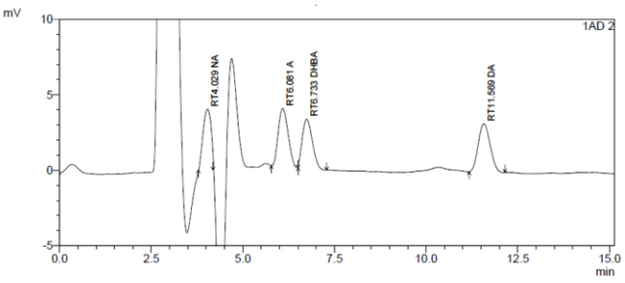

Fig. 1 Typical chromatogram of standard solutions for noradrenaline, adrenaline, dihydroxybenzylamine and dopamine (each 200 pg / 20 µl)

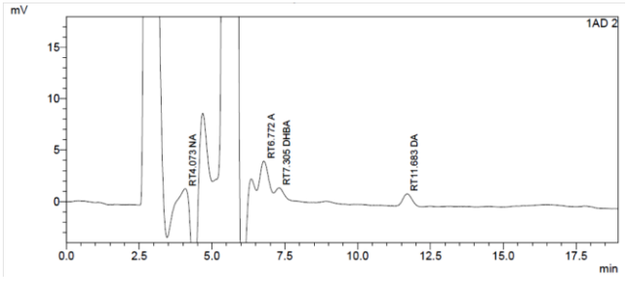

Fig. 2 Separation of catecholamines from cerebrospinal fluid; injection volume: 20 µl of the perchloric acid eluent

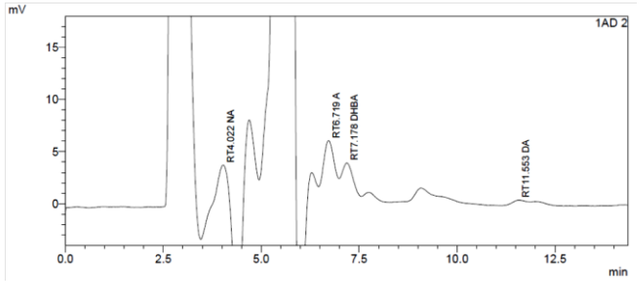

Fig. 3 Separation of catecholamines from serum; injection volume: 20 µl of the perchloric acid eluent

The quantification of 5-HIAA and HVA in 10 µl CSF diluted with 10 µl perchloric acid, was performed according to the chromatogram shown in figure 4.

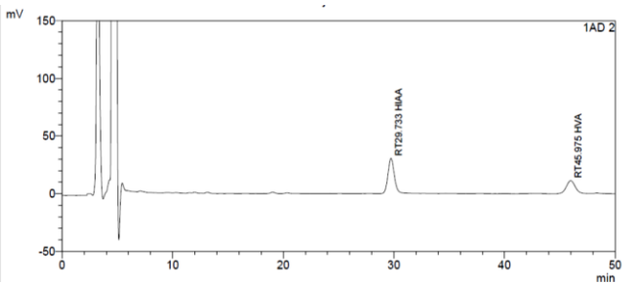

Fig. 4 Separation of 5-HIAA and HVA in diluted cerebrospinal fluid; injection volume 20 µl.

IV. Discussion

Catecholamines are derived from L-tyrosine and contain a catechol nucleus and an amine group. Referent values for serum and plasma concentrations of noradrenaline, adrenaline and dopamine are in the low concentration range of 100 - 650 pg/ml, 5 - 100 pg/ml and 5 - 80 pg/ml, respectively. Compared to serum, in the cerebrospinal fluid noradrenaline and adrenaline are present in even lower concentrations (30 - 350 pg/ml and 5 - 80 pg/ml, respectively), whereas only dopamine has a higher concentration in the range between 5 - 110 pg/ml. The concentration of the metabolites 5-HIAA and HVA is expressed in the ng/ml range (13 - 35 ng/ml and 15 - 40 ng/ml, respectively) [2]. Despite being present is such low concentrations, biogenic amines are involved in the regulation of numerous phyisiological processes. Catecholamine concentrations can rise due to postural changes, physical and emotional stress, hypovolemia, hypoglycemia and intake of specific drugs. Serotonin is an indolamine synthesized from tryptophan. In patients with neuroectodermal tumors serotonin levels are elevated in plasma and platelets, whereas 5-HIAA levels are elevated in urin. Levels of catecholamines, serotonin and their metabolites are used in the diagnosis of several diseases including heart diseases, phaeochromocitoma, carcinoid syndrom and neurological disorders. Consequently, there is a need for reliable, simple and very sensitive analytical methods that enable their accurate quantification. Apart from the low concentrations, the determination of catecholamines is challenging in a way that they are sensitive to oxidative degradation and that biological samples are very complex matrices. Earlier procedures utilizing radioenzymatic and immunological assays, gas chromatography or fluorimetry have generally been superseded by highly sensitive and selective chromatographic methods utilizing electrochemical or fluorimetric detection [3]. Radioenzymatic analytical methods, though sensitive and specific, are laborious, require radiolabelled reagents, and cannot differentiate the three individual catecholamines

without an additional thin-layer chromatography step [4]. Our aim was to determine biogenic amines present in physiological fluids by adjusting a previously established HPLC-ED method [1]. Catecholamines were extracted by alumina and separated by reversed phase HPLC coupled to the BAS liquid chromatography CC-5E LC-4C amperometric detector with a glassy carbon working electrode and Ag/AgCl reference electrode. The blood sample was centrifuged prior the analyses but the CSF sample was used directly for the analytical procedure. The separation was controlled and corrected with the internal standard DHBA. The modifications include the elution of catecholamines with 40 µl perchloric acid instead of 100 µl as given in the original procedure, and injecting only 20 µl from that volume into the HPLC-ED system. Electrochemical detectors are highly sensitive and enable the quantification of 1 pg/ml and the detection of molecules that can be oxidized at potentials reaching 1.2 V [5]. The analysis had a short run time, all catecholamines were separated within 15 min. The same HPLC-ED system enabled the determination of 5-HIAA and HVA by using only 10 µl CSF diluted with 10 µl perchloric acid. For this analysis, a different mobile phase and a slightly higher potential (0.75 V) was used. The total run time was 50 minutes.

V. Conclusions

The adjustment of a previously established HPLC-ED method [1] is reflected in eluting the adsorbed catecholamines from 1 ml serum and CSF with only 40 µl perchloric acid and injecting only 20 µl of the eluent, as that is the maximum injection volume of the Shimadzu LCSOL SINGLE-LC EN HPLC system. Such an adjustment resulted with a successful separation and quantification of catecholamines. Furthermore, metabolites 5-HIAA and HVA were also determined in 20 µl (1:1) diluted CSF using HPLC-ED. Offering very high sensitivity, electrochemical detectors are often coupled to HPLC systems and widely used in routine measurements of catecholamines, their metabolites and other electroactive biomolecules. Compared to other methods, HPLC-ED is cost effective, fast and very sensitive and as such also potentially important in both research and clinical settings.

References

1. E. Sofic, Untersuchungen von biogenen Aminen, Metaboliten, Ascorbinsäure und Glutathion mittels HPLC-ECD und deren Verhalten in ausgewählten Lebensmittel und im Organismus von Tier und Mensch. Doctoral dissertation, 1986, The Vienna University of Technology, Austria, pp. 26 - 32.
2. E. Sofic, Metabolic turnover of biogenic amines in physiological fluids: diagnostic significances. *Turk J Biochem*, Volume: 32, Issue: 3, 2007, pp. 120 - 9.
3. R.T. Peaston, Weinkove C (2004) Measurement of catecholamines and their metabolites. *Ann Clin Biochem* 41(Pt 1):17-38.
4. D. D. Koch, G. L. Polzin, Effect of Sample Preparation and Liquid Chromatography Column Choice on Selectivity and Precision of Plasma Catecholamines Determination. *J Chromatogr*, Volume: 386, 1987, pp. 19–24.
5. B. Straus , A. Stavljenic-Rukavina, F. Plavsic et al. Analitičke tehnike u kliničkom laboratoriju. Medicinska naklada, Zagreb, 1997, p 254.

S. Ibragic is with the University of Sarajevo, Faculty of Science, Zmaja od Bosne 33 - 35, 71000 Sarajevo, Bosnia and Herzegovina (phone: +38733 279 905; email: saidetun@yahoo.com)

A polymer-based, optical biosensor chip for detection of microbial leucine aminopetidase (LAP) activity and its potential as a novel, medical diagnostic test

Nadira Ibrišimović- Mehmedinović[1], Mirza Ibrišimović[2], Aldina Kesić[1]

[1]Department of Chemistry, Faculty of Science, University of Tuzla,

Univerzitetska 4, 75000 Tuzla, Bosnia and Herzegovina

Contact e-mail: nadira.ibrisimovic@untz.ba

[2]Medical School Faculty-Sarajevo School of Science and Technology,

Hrasnièka cesta 3a, 71 000 Sarajevo, Bosnia and Herzegovina

Contact e-mail: mirza.ibrisimovic@ssst.edu.ba

***Abstract*— The test methods commonly used for detection of microorganisms are often demanding, expensive, time-consuming or not fast enough to start with a therapy at early phase of infection. Leucine aminopeptidase (LAP) enzyme is produced by various microbes, including hospital bacteria of *Pseudomonas* and *Enterobacter* genus. The aim of this study was to demonstrate the ability of a thin-layer, polymer-based biosensor chip for detection of heat activated bacterial LAP, within a few hours. The biosensor setup is described in one of our previous studies consisting of a thin-metal layer called inconnel, which is covered by polymer layer that can be degraded by lytic enzymes such as LAP. A reduction of polymer thickness, caused by degrading action of the LAP enzyme, is manifested as a colour change of the sensor's surface that is visually detectable. We also investigated bacterial LAP activity in correlation with a total bacterial count. This fast, inexpensive biosensor technology shows a great potential for becoming a quantitative method for detection of bacterial infections in a real-time. Here tested biosensor chip could reduce time between microbial detection and patient's drug treatment, or prevent unnecessary antibiotic treatments before bacterial infection was confirmed.**

Keywords— **Biosensor chip, polymer, leucine aminopeptidase, microbial detection, quantitative test**

I. INTRODUCTION

Many patients in hospitals who have been connected to respiratory machines for longer period of time, or have required urinary and intravenous catheters, are often exposed to microbial infections. Serious bacterial infections can be caused by *Pseudomonas aeruginosa* [3], *Enterobacteriaceae*, *Acinetobacter*, *Staphylococcus aureus* or by some other pathogenic bacteria that are becoming more and more resistant to variety of antibiotics [4]. Microbial testing of patients is normally done when the first symptoms of bacterial infection occur, and is often expensive, demanding and time consuming. For the immunodeficient patients, such as patients undergoing a solid organ or stem cell transplantation, mentioned bacterial infections can be a cause for increased mortality [5]. Based on that, a novel and faster methods for detection of microbial infections are required. In our study we are presenting a polymer-based biosensor chip able to detect bacterial leucine aminopeptidase (LAP) enzyme, whose activity is triggered by heat. Bacteria exhibit several aminopeptidase activities which may be localised in the cytoplasm, on membranes, associated with the cell envelope or secreted into the extracellular media [11]. The setup of here evaluated biosensor is already described in some our previous work [1][2], and consists of two layers: a) a thin-metal layer called inconnel and b) a polymer layer that is degraded due to microbial enzymatic activity. The sensing element of biosensors usually responds to the substances that are mostly biological in their nature, such as enzymes, antibodies or nucleic acids. Biosensors are devices with incorporated biological element as a main part of their matrix that is connected to a transducer. A transducer converts those chemical or physical changes into a signal that can be measured in a real-time [6][9]. A polymer-based biosensor that was tested during our work is able to respond to bacterial LAP activity, displaying a signal via colour change that can be visible with a naked eye [1]. Many of today's biosensors have found their application in medicine, pharmaceutical and food industry, environmental monitoring, defence and security [7]. Currently, the most dominant biosensors are electrochemical biosensors which are used for metabolite monitoring [7]. However, the optical biosensors are the next most commonly used transducers,

with several preferred detection principles such as simple light absorption, refractive index, fluorescence or bio/chemiluminescence [8][10].

II. Materials and Methods

A. Liquid media for bacterial growth and enzyme secretion- LM medium

Liquid media can be used for not only to help bacterial growth but also to stimulate bacterial enzyme production. For example, some of them such as LM-Medium, that we used during here presented study, contains phosphate in form of Na_2HPO_4 x $2H_2O$.

Phosphate is an important inducer and activator of lipolytic enzymes such as aminopeptidase and phospholipase.

B. Solid media for detection of microbial enzymatic activity- Tributyrin agar base

Tributyrin agar base (Acila Sarl) is a solid culture medium for testing the lipolytic capacity of microorganisms. Tributyrin is a very good lipid source for detection of lipolytic microorganisms because some microorganisms, which are able to hydrolyze tributyrin, will not hydrolyze other triglycerides or fats containing longer fatty chains.

C. Determination of leucine aminopeptidase activity- generation of calibration line

In order to determine the enzymatic activity of investigated bacteria (*Pseudomonas* and *Enterobacter*), an enzymatic assay of leucine aminopeptidase (LAP) was performed. The activity of the exopeptidase LAP, that selectively releases N-terminal amino acid residues from polypeptides and proteins, was examined at pH of 7.2. 2 ml of freshly prepared 1.66 mM L-leucine p-nitroanilide solution (Sigma Aldrich) served as a substrate.

Since the temperature plays very important role in activation of the enzyme, the enzyme dilutions were incubated for 15 minutes at 37°C. A calibration line was generated by means of increasing LAP activities (Fig. 2). Therefore a stock of LAP with a specific activity of 10 U/mg was prepared. The used LAP dilutions were in the range of 10 to 1000 mU/ mg. The reagents which have been used are:

a. 60 mM Phosphate Buffer, pH 7.2 at 37 °C (Prepare 100 ml in deionized water using potassium phosphate, monobasic, anhydrous. Adjust to pH 7.2 at 37 °C with 1 M KOH.)
b. 1.66 mM L-Leucine p-Nitroanilide Solution (L-Leu_NA)
(Prepare 30 ml in Reagent a using L-leucine p-nitroanilide hydrochloride. Prepare fresh!)
c. 10 mM TrisHCl Buffer with 1 mM $MgCl_2$, pH 8.0 at 37 °C (Activation Buffer)
(Prepare 20 ml deionized water using Trizma Base. Adjust to pH 8.0 at 37 °C with 1 M HCl and then add $MgCl_2$ x $6H_2O$).
d. Leucine Aminopeptidase Enzyme Solution, Non-Activated (Enz-Non Act)
(Immediately before use, prepare a solution containing 0.3 unit/ml of leucine aminopeptidase in cold deionized water).
e. Leucine Aminopeptidase Enzyme Solution, Acivated (Enz-Act); (Immediately before use, prepare a solution containing 0.1 U/ml of leucine aminopeptidase in cold Reagent c. Incubate at 37 °C for 15 minutes to activate.

D. LAP activity in test sample

To determine the role of LAP activity of *Pseudomonas* and *Enterobacter* bacteria in LM medium, the samples were first spinned down (2 minutes at 1000 rpm), and only the supernatant was used for the measurements.

E. Biosensor setup

For the biosensor setup, as has been previously described [1][2], the biomimetic polymer solution of PLGA [poly(lactic-coglycolic acid)] is directly transferred onto the Inconnel layer via Gravure Printing. The polymer solution has to be applied onto the printing plate, after which the impression roller can be run over the plate resulting in a defined layer with the desired thickness over the mirror layer. Between printing procedures, the plate, impression roller and doctor blade have to be cleaned thoroughly with 2-butanol and trichloromethan.

F. Biosensor sensitivity test

In order to test the biosensor´s potential for changing its colour in contact with bacterial enzymes, it was exposed to bacterial mixture of *Pseudomonas* and *Enterobacter* bacteria, with different bacterial counts (10^6 CFU/mm^3 and 10^8 CFU/mm^3). As a positive control, a commercial lipolytic enzyme such as aminopeptidase was used. The Ringer solution (pH 7.0) served as a negative control. About 2 µl of the sample were pipetted onto the biosensor surface and incubated in a humid chamber for 6 hours at 37 °C.

After this incubation time, the biosensor was washed with double-distilled water and then dried under an intensive air-stream.

III. Results and Discussion

A. Quantitative detection of bacterial lipolytic activity

Bacteria of *Pseudomonas* and *Enterobacter* genus were examined for exogenous lipolytic activity by using tributyrin agar base. Optimal culture parameters including different incubation temperatures (4°C, 30°C and 37°C), which could influence bacterial growth and production of lipolytic enzymes such as leucine aminopeptidase, were also investigated. Here tested bacteria showed the highest enzymatic activity in bacterial count of 10^6 CFU/mm^3 and 10^8 CFU/mm^3, after 24 hours at 37 °C. Evidences of the lipolytic enzyme activity were observed as a dark circle forming around the growing bacterial colonies (Fig. 1).

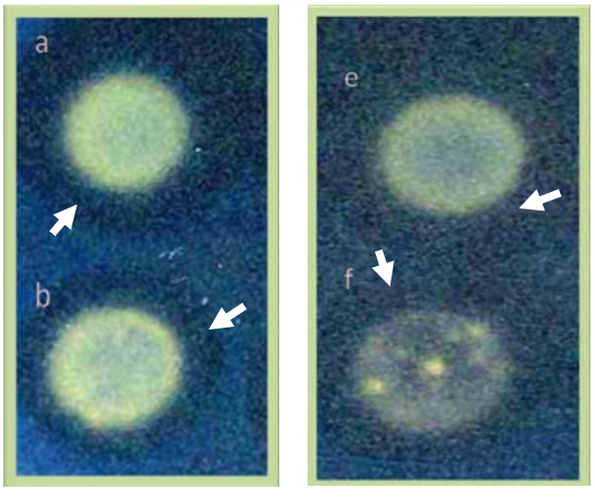

Figure 1. Lipolytic enzyme activity for *Pseudomonas* (a: 10^8 CFU/mm^3 and b: 10^6 CFU/mm^3) and *Enterobacter* (c: 10^8 CFU/mm^3 and d: 10^6 CFU/mm^3) by using tributyrin agar base as a nutrient medium. Incubation at 37°C for 24 hours.

A high enzymatic activity has also been seen at 30°C after 24 hours of incubation. However, the first signs of enzymatic activity for the bacteria incubated at 4°C could not be detected before 72 hours.

B. Determination of leucine aminopeptidase (LAP) activity

Aminopeptidase enzymes are type of exopeptidases which cleave free N-terminus of polypeptides and proteins in order to release a single amino acid residue such as L-leucine [11][12]. Generation of the calibration line was performed with a stock of leucine aminopeptidase (10 U/mg). Dilutions of enzyme solutions were made in reagent C (Materials and Methods).

The following activities of the leucine aminopeptidase were included for the activated enzyme and calibration line generation: 10, 25, 50, 60, 75, 100, 200, 300, 400, 500, 600, 700, 800, 900, 1000 mU/mg. The values of the measured absorption ranged from 0.001 up to 0.589 (Fig. 2).

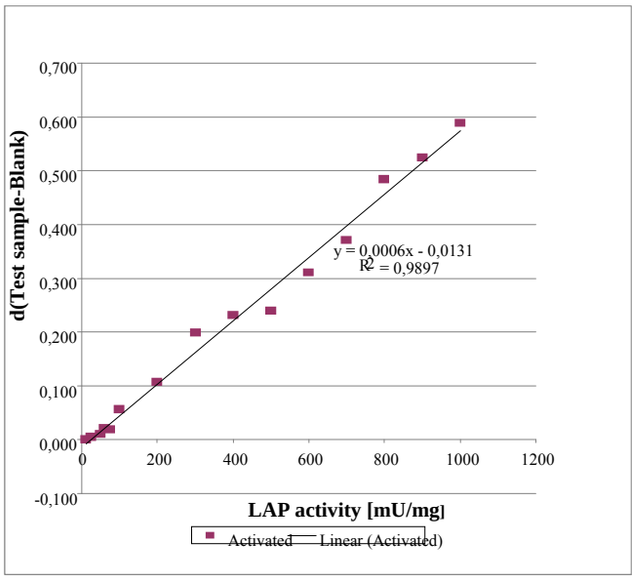

Figure 2. Heat-activated leucine aminopeptidase (LAP)- Calibration line.

C. LAP activity in correlation with bacterial growth

The LAP activity was measured for *Pseudomonas* and *Enterobacter* bacteria grown in LM medium. The samples that have been analysed are taken within the range of the *log* phase. As shown in Fig. 3, *Pseudomonas* exhibited the highest LAP activity of 35.17 mU, after 7 hours of incubation at 37°C, in bacterial count of 1.6 x 10^7 CFU/mm^3. In contrast to *Pseudomonas*, the *Enterobacter* showed a very high LAP activity after 14 hours of incubation at 37°C, even the total bacterial count was not so high, counting 1.5 x 10^5 CFU/mm^3.

The highest LAP yield was determined after 16 hours of incubation (Fig. 4). However, the LAP activity after 15 hours of incubation at 37°C was significantly lower as one hour before. This high level of LAP activity could be observed even the total bacterial count was much higher, counting 1 x 10^8 CFU/mm^3.

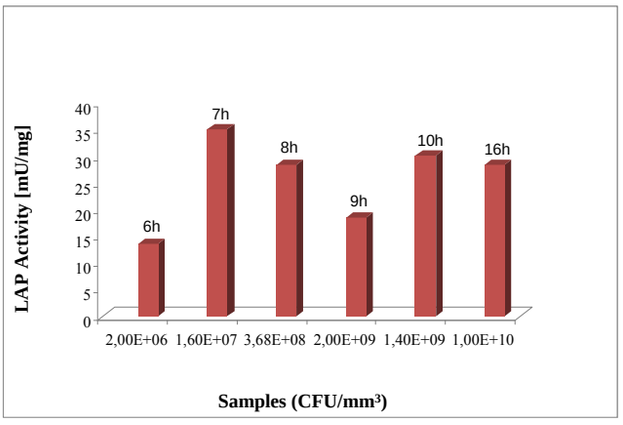

Figure 3. LAP activity of *Pseudomonas* in *log* phase in LM medium.

These finding suggest that even with high total bacterial count, the LAP activity does not have to increase compulsorily.

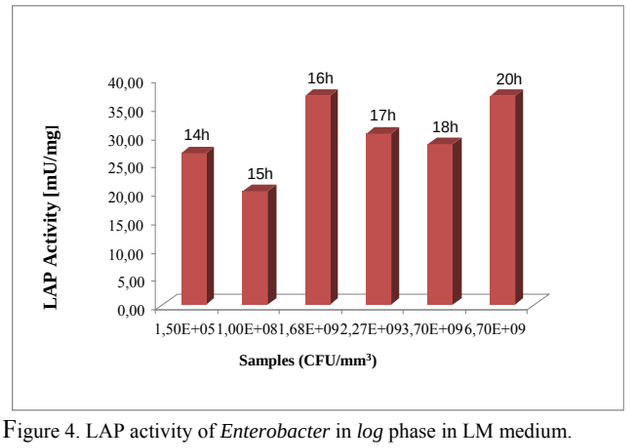

Figure 4. LAP activity of *Enterobacter* in *log* phase in LM medium.

D. Degradation of the biosensor´s polymer layer

The biosensor setup according to [1] and [2], with PLGA [poly(lactic-coglycolic acid)] polymer layer was tested on bacterial enzymatic activity and its ability to show the signal in contact with microbial lipolytic enzymes such as leucine aminopeptidase (LAP). As it was shown during this study in experiments with *Pseudomonas* and *Enterobacter*, the LAP is one of the major bacterial secreting enzymes. After bacteria have adaptated to polymer senor surface, they begin to excrete enzymes which cause degradation of the polymer layer and evince the signal via colour change, which can be visible even with the naked eye (Fig. 5). The strong signal was observed for both bacterial samples in a different total bacterial count (Fig. 5, a and b). The positive control with the commercial lipolytic enzyme, also displayed a strong signal as it was expected (Fig. 5, c). The spot on the sensor where the Ringer´s solution was pipetted as the negative control (Fig. 5, d), did not show colour change of the biosensor.

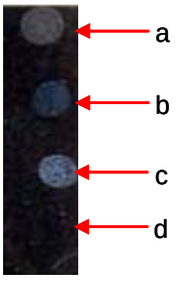

Figure 5. Biosensor sensitivity test. a: bacteria in LM medium (10^8 CFU/mm^3), b: bacteria in LM medium (10^6 CFU/mm^3), c: positive control, d: negative control.

IV. Conclusions

The aim of this study was to investigate amount of lipolytic enzymes such as leucine aminopeptidase (LAP) and the ability of described biosensor technology [1] [2] to show a colour change as microbial detection signal.

We first investigated the presence and thereafter the amount of secreted LAP in bacteria of *Pseudomonas* and *Enterobacter* genus, in correlation with their total bacterial counts. The highest amount of the excreted enzymes could be observed in the *log* phase of bacterial growth. Interestingly, the highest LAP yield was not always detectable by highest bacterial counts, and very high amounts of LAP could be found even at lower bacterial counts. However, since there is enough enzyme to be detected by the biosensor at lower bacterial counts, this technology has a great potential to be very helpful in detection of early bacterial infections in patients or beginning of some product deterioration. The biosensor changes its colour after only few hours of incubation with bacteria and exhibits nicely visible signal. This biosensor chip displays great advantage over conventional microbiological test methods, which are reversible and not able to provide information on the microbial status very fast.

V. References

1. N. Ibrišimović, M. Ibrišimovć, M. Barth, U. Bohrn, "Biomimetic PLGA sensor: proof of principle and application"; *Chemical Monthly*, 141:125-130, 2010.

2. F. Pittner, N. Ibrišimović, M. Ibrišimovć, M. Barth, Patent: "Device comprising a polymer layer and a reflecting layer"; U 7145/ DB, 2009.
3. Zhi-Gang Xu, Yu Gao, Jing-Guo He, Wei-Feng Xu, Mei Jiang, and Huan-Sheng Jin, "Effects of azithromycin on *Pseudomonas* aeruginosa isolates from catheter-associated urinary tract infection; *Exp Ther Med.* Feb 2015; 9(2): 569–572., doi: 10.3892/etm.2014.2120.
4. J. Haaber, C. Friberg, M. McCreary, R. Lin,S.N. Cohen, H. Ingmer, "Reversible Antibiotic Tolerance Induced in Staphylococcus aureus by Concurrent Drug Exposure"; *MBio*. 2015 Jan 13;6(1). pii: e02268-14. doi: 10.1128/mBio.02268-14.
5. T. Hara, A. Soyama, M. Takatsuki, M. Hidaka, I. Carpenterr, A. Kinoshita, T. Adachi, A. Kitasato, T. Kuroki , S. Eguchi, "The impact of treated bacterial infections within one month before living donor liver transplantation in adults", *Ann Transplant.* 2014 Dec 23;19:674-9, doi: 10.12659/AOT.892095.
6. D.R. Th´venot, K. Toth, R.A. Durst, G.S. Wilson, "Electrochemical biosensors: recommended definitions and classification"; *Pure and Applied Chemistry*. 1999. Vol. 71, No. 12, pp. 2333-2348.
7. A. P. F. Turner, "Biosensors: sense and sensibility"; *Chem. Soc. Rev.*, 2013, **42**, 3184.
8. K. S. Alva, C. G. Roger, S. Gudial, US Patent #6863800: „Electrochemical biosensor strip for analysis of liquid samples", 2002.
9. G. S. Wilson, R. Gifford, "Biosensors for real-time in vivo measurments"; *Biosensors and Bioelectronics*, Vol. 20, pp. 2388-2403, 2005.
10. G. Gauglitz, "Direct optical sensors: principles and selected applications", *Anal. Bioanal. Chem*., 2005, 381: 141-155.
11. T. Gonzales, J. Robert-Baudouy, "Bacterial aminopeptidases: properties and functions"; *FEMS Microbiol Rev*., 1996 Jul.; 18(4): 319-44.
12. M. B. Rao, A. M. Tanksale, M. S. Ghatge and V. V. Desphande. "Molecular and Biotechnological Aspects of Microbial Proteases". *Microbiology and Molecular Biology Reviews*., 1998 Sept.; 1092-2172, p.597-635.

Evaluation of factors that influence the occurrence of early hypothyroidism following radioactive iodine treatment in thyrotoxicosis

Mirna Džubur[1], Elma Kučukalić – Selimović[2], Mirela Dzubur-Aganovic[3], Azra Bahtić[1], Edin Begić[1], Semir Hrvo[1]

[1]Medical faculty, University of Sarajevo, Sarajevo, Bosnia and Herzegovina
[2]Department of Nuclear medicine, Clinical Center University of Sarajevo, Bosnia and Herzegovina

Abstract—Introduction: **Factors that could determine the patient's response following radioactive iodine (I-131) treatment in thyrotoxicosis are the type of disease, elevated thyroid autoantibodies, duration of the disease, previous use of anti-thyroid drugs (ATDs) or a partial thyroidectomy, I-131 dose, thyroid gland volume and hormone levels.**

Aim: **The aim of this study was to evaluate the patient's response to radioiodine treatment (RAI), determine the correlation between prognostic factors and occurrence of hypothyroidism one year following the treatment and defining the possibility of predicting the outcome of RAI treatment.**

Material and methods: **The medical records of 120 patients treated with I-131 from January 2004 to September 2014, were retrospectively analyzed. Factors were analyzed a day before and one year after RAI treatment. Results: 83% of patients were female. The mean age was 55,5 years old (31-81 years, SD-10,66). 15,8% of patients had positive thyroid autoantibodies (Graves disease), and 84,2% had negative thyroid autoantibodies (diffuse thyroid autonomy- 23,7%, uninodular toxic goiter- 43,5%, multinodular toxic goiter- 32,8%). 75% of patients were treated with ATDs, while 15% were thyroidectomized. Hypothyroidism was found in 36 (30%) patients (Graves disease-57,88% (RR-2,34, p<0,05), other diseases-22,5%). Hypothyroidism was found in 45,8% of patients with diffuse thyroid autonomy, 5% with uninodular and 30,3% with multinodular toxic goiter. Persistent thyrotoxicosis was found in 4 patients. The thyroid gland volume was ultrasonographically measured and hypothyroidism was found in 28% of patients with the volume <25 ml, in 30% with volume 25-35 ml, and in 28,5% with patients with volume >35ml (Pearson coefficient r-0,51, p<0,05). Patients treated with I-131> 20 mCi, hypothyroidism was found in 66,6% of patients (RR-2,29, p<0,05). There is no statistically significant correlation between the duration of thyrotoxicosis and the occurrence of hypothyroidism (p>0,05).**

Conclusion: **RAI treatment is a powerful therapeutic modality in selected patients with thyrotoxicosis. Hypothyroidism following RAI treatment is very common and it can often be expected in patients who received high I-131 doses, who have high titers of thyroid autoantibodies, who were previously treated with ATDs or underwent partial thyroidectomy.**

Keywords— **radioactive iodine, hypothyroidism, thyrotoxicosis, risk factors**

I. Introduction

Hyperthyroidism is a condition that is characterized by increased synthesis of excessive amounts of free thyroid hormones- T3 (triiodothyronine) and T4 (tetraiodothyronine or tiroxin). These two hormones in the blood are controlled by the hypothalamic-pituitary feedback system. Releasing hormones of the hypothalamus stimulate the pituitary gland and synthesizes TSH hormone. The main aim of TSH is to regulate the levels of T3 and T4 in the blood. T4 is the metabolic product of T3, which explains why in physiological conditions, his level is higher than the level of T3.

The most common cause of hyperthyroidism is Graves' disease, followed by solitary and multinodular adenomas of the thyroid gland. Symptoms of hyperthyroidism are: palpitations, arrhythmia (irregular heart beat), sweating, tremor (shaking hands), thinning skin, diarrhea, weight loss despite increased appetite, nervousness, anxiety, irritability, difficulty of sleeping, and many more. Hyperthyroidism changes the entire metabolic status. It is also proven that increased levels of thyroid hormones lead to faster blood coagulation. This condition can be treated with anti-thyroid drugs (ATD), surgical removal (partial and total thyroidectomy), and radioactive iodine (I-131).

I-131 has been used for treatment of thyrotoxicosis for more than 60 years. Iodine-131 (I131, radioiodine) is an important radioisotope of iodine discovered by Glenn Seaborgand and John Livingood in 1938 at the University of California, Berkeley. Radioactive iodine uptake by the thyroid is not distinguishable from ordinary iodine, thus radioactive iodine is trapped in thyroid cells (1). After being taken up by thyroid cells, beta-emissions bring about the destruction of the iodine trapping-cells and those in close proximity (2). Around ten different isotopes of iodine have been used in medicine.

I-123 (I123) is the isotope most frequently used for scintigraphic imaging of thyroid structure and function. I-131 has a half-life of 6–8 days and emits beta particles and gamma rays. Radioactive iodine use for thyroid ablation was introduced in the 1940's at the Massachusetts Institute of Technology and Massachusetts General Hospital (3). Because of the intrinsic advantages a longer half-life iso-

tope, 131I quickly became the favored iodine isotope for treating thyroid cancer and hyperthyroidism (1).

The goal for I-131 therapy in thyrotoxicosis is to bring patients into a euthyroid state. Medical treatment by ATD is generally associated with a high relapse rate, risk of side effects including hepatic failure and bone marrow suppression, and low compliance associated with prolonged ATD therapy. Several studies reported that after ATD medications are discontinued, 35-60% of patients may experience relapse (4). Therefore, definitive therapy is favored as the first-line treatment in several countries. Thyroidectomy is associated with very high cure rates and a small risk of hypoparathyroidism and recurrent laryngeal nerve damage. Disadvantages of this method are surgical complications and hospitalization cost.(6)

Due to its very high cure rate, there is a tendency to administer I-131 as first therapeutic modality. Radioactive iodine treats hyperthyroidism by destroying parts of the gland. Unlike anti-thyroid medications, radioactive iodine is a permanent and more reliable cure for hyperthyroidism. Approximately 90% of patients need only one dose before they are cured of their hyperthyroidism. Cure rates are higher in patients treated with larger than smaller amounts of I-131.

The most common side effect of I-131 therapy is hypothyroidism. The radioactive iodine often kills an excessive amount of thyroid cells, leaving the thyroid unable to produce enough hormones. The development of hypothyroidism following I-131 treatment has long been recognized as a problem. However, hypothyroidism is much easier to treat on a long-term basis than hyperthyroidism. Hypothyroidism is treated with a life-long thyroid hormone replacement therapy, which is a safe, reliable and cost-effective treatment. Nevertheless, it is still very important to identify patients who are at greater risk of developing hypothyroidism following I-131 treatment. (7)

Many dosage schedules of RAI, ranging from arbitrary deliberate ablation (8) to elaborately calculated doses based on the size of the thyroid gland, uptake of radioiodine or the turnover

of radioiodine (8, 9), have been used with little consensus about the most appropriate dosage regimen. Whilst it is possible to deliver a relatively accurate radiation dose to the thyroid gland, the biological response of the gland remains unpredictable (10).

Radioiodine therapy's success is influenced by the thyroid gland size and by circulating levels of thyroid autoantibodies. Patients with very large glands and high thyroid autoantibodies levels have lower responses to I-131 therapy than patients with smaller glands (14). Because of poor response rates with very large glands, thyroidectomy should be considered for individuals with glands greater than 80 gm. But, if I-131 is used in this setting, patients should be counseled that the risk of needing an additional dose, would be higher than for patients with a smaller gland. Furthermore, surgical removal of very large glands will be associated with greater risk than removal of a smaller gland. (15)

Likewise, factors that could determine the patient's response following radioactive iodine (I-131) treatment in thyrotoxicosis are presence of thyroid autoantibodies (11), type of disease (12), duration of the disease, previous use of anti-thyroid drugs (ATDs) (13) or a partial thyroidectomy, I-131 dose, thyroid gland volume and hormone levels.

Consequently, in this study we evaluated the patient's response to radioiodine treatment and determined the correlation between prognostic factors and occurrence of hypothyroidism one year following the treatment. Also, we made an attempt to define the possibility of predicting the outcome of RAI treatment.

II. Materials and methods

This study was conducted at the Department of Nuclear medicine at the Clinical Center University of Sarajevo. The medical records of 120 patients treated with I-131 from the period of January 2004 to September 2014, were retrospectively analyzed. The diagnosis of hyperthyroidism was based on clinical features, suppressed thyrotropin (TSH) levels and increased total thyroxine (T4), free T4 or free triiodothyronine (T3). Euthyroidism was defined as FT4 and FT3 within the normal range; hyperthyroidism was defined as increased FT4 and/or FT3 in addition to a decreased TSH level; permanent hypothyroidism was defined as a decreased FT4 and an elevated TSH level. The I-131 therapy was dosed according to a simplified algorithm taking only the thyroid volume into account. According to several studies (8, 16) on I-131 therapy in hyperthyroid diseases, the use of calculated doses does not carry any advantages compared with fixed doses. All patients received doses between 10 and 25 mCi. The average dose was 13 mCi. Collected information contained age, gender, type of disease (hyperthyroidism), presence or absence of thyroid autoantibodies, ATD treatment prior to I-131 therapy (given or not given), partial thyreidectomy prior to I-131 therapy, length of disease prior to treatment, thyroid gland volume (measured by ultrasound), hormone levels (elevated or in normal range) and I-131 dose. All 120 patients were included in the study.

Patients were classified in four groups depending on the type of benign thyroid disease they had: Graves' disease, diffuse thyroid autonomy, unifocal thyroid autonomy and multifocal thyroid autonomy. Same factors were analyzed a day before and one year after RAI treatment.

Following I-131 treatment, the outcome was classified as persistent thyrotoxicosis, euthyroidism or hypothyroidism, based on the functional status of the thyroid. Thyroid status was evaluated again one year after the therapy. Persistent thyrotoxicosis was diagnosed if free T4 or T3 remained elevated. Euthyroidism was diagnosed if patients remained euthyroid while off all treatment for one year. Hypothyroidism was diagnosed if TSH was elevated and serum T4 or T3 was below the normal reference range. Thyroid hormone replacement therapy started after hypothyroidism was confirmed. Patients who received ATD prior to I-131 treatment have been instructed to stop medication 7 days before the treatment.

Statistical analysis was performed using "SPSS statistics v.21". Values are shown as means ± standard deviation (SD). A P-value of less than 0.05 was considered to indicate a statistically significant difference.

III. Results

83% of patients were female. The mean age was 55, 5 years (31-81 years, SD-10,66). 19 (15,8%) patients had positive thyroid autoantibodies (Graves' disease), and 101 (84,2%) had negative thyroid autoantibodies (diffuse thyroid autonomy- 23,7%, unifocal thyroid autonomy 43,5%, multifocal thyroid autonomy- 32,8%). 75% of patients were treated with ATDs, while 15% were thyroidectomized before application of radioactive iodine.

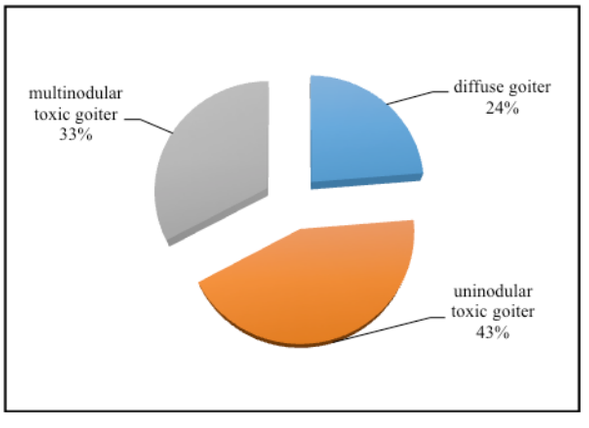

Fig.1. Patients with negative thyroid autoantibodies

Hypothyroidism was found in 36 (30%) patients. 11 (57,88%, RR-2,34, p<0,05) of them had Graves' disease, the other 25 patients (22,5%) had negative thyroid autoantibodies. Hypothyroidism was found in 45,8% of patients with diffuse thyroid autonomy, 5% with unifocal and 30,3% with multifocal thyroid autonomy.

Persistent thyrotoxicosis was found in 4 patients out of which 2 were with multifocal thyroid autonomy and 2 with diffuse thyroid autonomy. These patients were retreated with another dose of I-131.

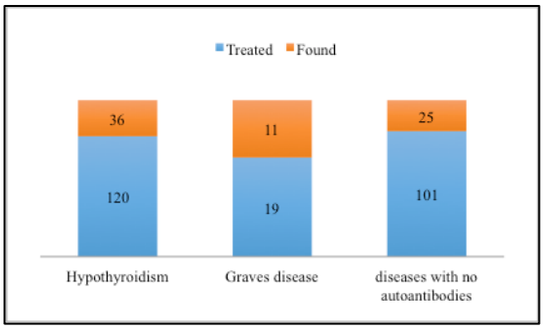

Fig.2.Found hypothyroidism in Graves disease and diseases with no autoantibodies

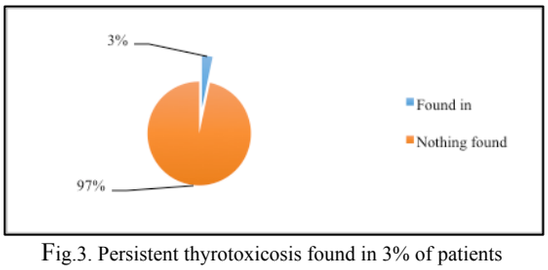

Fig.3. Persistent thyrotoxicosis found in 3% of patients

The thyroid gland volume was ultrasonographically measured and hypothyroidism was found in 28% of patients with the volume <25 ml, in 30% with volume 25-35 ml, and in 28,5% with patients with volume >35ml (Pearson coefficient r-0,51, p<0,05).

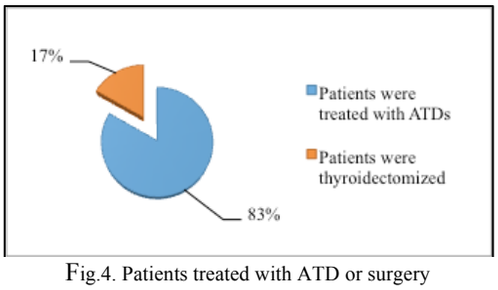

Fig.4. Patients treated with ATD or surgery

There is a statistically significant correlation between presence of TSH autoantibodies (Graves' disease) and the occurrence of hypothyroidism, as well as between the volume of the thyroid gland before and after the treatment with I-131.

In patients treated with I-131> 20 mCi, hypothyroidism was found in 66,6% (RR-2,29, p<0,05). There is a statistically significant correlation between I-131 dose > 20 mCi and the occurrence of hypothyroidism (RR- 2,29, p<0,05). There is no statistically significant correlation between the duration of thyrotoxicosis and the occurrence of hypothyroidism (p>0,05).

The correlation between the thyroid gland volume and the occurrence of hypothyroidism one year following I-131 treatment is statistically weak (r= -0,09).

IV. Discussion

Our study provides information on the independent prognostic significance of the several known risk factors influencing the outcome of radioactive iodine treatment. The cumulative incidence of hypothyroidism during the period of January 2004 to September 2014 was 30%. Graves's disease, high doses of I-131, high titers of thyroid autoantibodies, pretreatment with ATDs and partial thyroidectomy were identified as significant risk factors with different prognostic values. The risk of developing hypothyroidism, therefore, depends of the number of risk factors and their individual predictive value prior to RAI. The risk of developing hypothyroidism after treatment with radioactive iodine is 2 (almost 3) times greater in patients with Graves' disease. The risk increases linearly as the number of risk factors increases. One advantage of the objective estimates for the probability of developing hypothyroidism is that they help in understanding the relative influences of specific prognostic risk factors. Although studies have reported antithyroid drug treatment (17, 18, 19), goiter size (20) and dose of RAI (21, 22) as contributors to the development of hypothyroidism, few studies have emphasized the contribution of thyroid antibodies on the outcome following RAI (20). Our study emphasizes the degree to which both Graves' disease and the presence of thyroid antibodies contribute to influencing the outcome following RAI and suggests that these two are the strongest predictors of developing hypothyroidism following RAI.

Our results can help and contribute identifying patients who have an increased risk of developing hypothyroidism. These kind of patients require a smaller dose of I-131 than those with a lower number of risk factors who have a reduced chance of developing hypothyroidism and may benefit with a larger dose of I-131.

In our series of patients, hypothyroidism was found in half of the of patients with diffuse thyroid autonomy, the third with multifocal thyroid autonomy and only in 5% with unifocal thyroid autonomy.

Evidence suggests that anti-thyroid treatment before radioactive iodine leads to a reduction of early-onset hypothyroidism (17, 23) and an increased rate of single dose RAI treatment failure (23). These studies suggest a radioprotective effect of anti-thyroid drugs. In our study, we showed that anti-thyroid drugs and a prior thyroidectomy are in a strongly correlation with the occurrence of hypothyroidism after RAI, so we cannot agree with these results. These two therapeutic approaches may have caused decreasing of the T3 and T4, so the effect of radioactive iodine is added to the prior and causes a stronger hypothyroid effect.

There remains controversy about the effect of thyroid antibodies on the outcome following RAI treatment (17, 24). Since RAI treatment triggers a humoral and possible cell-mediated autoimmune response within thyroid gland, it is quite likely that the co-existing thyroiditis represented by the presence of autoantibodies (25) contributes to the progressive development of hypothyroidism. Our study supports this concept and demonstrates the prognostic significance of the presence of thyroid autoantibodies on the development of hypothyroidism following I-131 treatment.

The ideal dose of RAI that would render euthyroid, avoiding a high incidence of hypothyroidism and single-dose RAI treatment failure rate, remains elusive. It can be argued that ablative RAI therapy may be preferable in treating patients with Graves' disease, as the single dose RAI treatment failure is reported to be higher in patients treated with low or calculated RAI doses, whereas the incidence of hypothyroidism is similar in the long-term (17, 26).

The duration of the thyroid disease does not effect the occurrence of hypothyroidism in our patients.

Other predictive values and risk factors such as antithyroid drugs, prior thyreoidectomy, high levels of autoantibodies can contribute to predict hypothyroidism after RAI. We suggest that clinicians and nuclear medicine departments use this model and probability estimates to predict the risk of developing hypothyroidism and to calculate the dose of RAI depending on the presence or absence of one or more of these risk factors. Future studies may be able to demonstrate a method to calculate an ideal dose of radioactive iodine that can secure euthyroid condition to the patient.

V. Conclusions

RAI treatment is a powerful therapeutic modality in selected patients with thyrotoxicosis. Hypothyroidism following RAI treatment is very common. In accordance with our results, factors that significantly influence the occurrence of hypothyroidism one year following I-131 treatment are: I-131 dose (>20mCi), elevated thyroid autoantibodies, previ-

ous ATD treatment and surgical removal of a part of the gland. Thyroid gland volume did not significantly influence the occurrence of hypothyroidism; neither did the duration of the disease prior to I-131 treatment.

Therefore, hypothyroidism following radioiodine treatment can often be expected in patients who received high doses of I-131, have high titers of thyroid autoantibodies and were previously treated with ATDs or underwent partial thyroidectomy.

REFERENCES

1. Goolden AW & Stewart JS. Long-term results from graded low dose radioactive iodine therapy for thyrotoxicosis. Clinical Endocrinology 1986 24 217–222.
2. Williams ED: Biological effects of radiation on the thyroid. In The Thyroid. Edited by Braverman LE, Utiger RD. Philadelphia: J.B. Lippincott Co; 1986:421–436
3. Chapman EM: History of the discovery and early use of radioactive iodine. JAMA 1983, 250:2042–2044.
4. Kaguelidou F, Alberti C, Castanet M, Guitteny MA, Czernichow P, Léger J; French Childhood Graves' Disease Study Group. Predictors of autoimmune hyperthyroidism relapse in children after discontinuation of antithyroid drug treatment. J ClinEndocrinolMetab 2008;93:3817-3826. Epub 2008 Jul 15
5. Radioactive Iodine for Thyrotoxicosis in Childhood and Adolescence: Treatment and Outcomes 2013 95:97 NamwongpromSirianong. UnachakKevalee. Dejkhamron Prapai. Ua-apisitwongSupoj.EkmahachaiMolrudee
6. Erem C, Kandemir N, Hacihasanoglu A, Ersöz HO, Ukinc K, Kocak M. Radioiodine treatment of hyperthyroidism: prognostic factors affecting outcome. Endocrine. 2004 Oct;25(1):55-60.
7. N. R. Peden, I. R. Hart. The early development of transient and permanent hypothyroidism following radioiodine therapy for hyperthyroid Graves' disease. Can Med Assoc J. 1984 May 1; 130(9): 1141–1144.
8. Jarløv AE, Hegedu¨s L, Kristensen LO, Nygaard B & Hansen JM. Is calculation of the dose in radioiodine therapy of hyperthyroidism worth while? Clinical Endocrinology 1995 43 325–329.
9. Franklyn JA, Daykin J, Drolc Z, Farmer M & Sheppard MC. Longterm follow-up of treatment of thyrotoxicosis by three different methods. Clinical Endocrinology 1991 34 71–76. 8
10. Ahmad AM, Ahmad M, Young ET. Objective estimates of the probability of developing hypothyroidism following radioactive iodine treatment of thyrotoxicosis.Eur J Endocrinol. 2002 Jun;146(6):767-75.
11. Lundell G & Holm LE. Hypothyroidism following 131I therapy for hyperthyroidism in relation to immunologic parameters. ActaRadiologica. Oncology 1980 19 449–454.
12. Franklyn JA, Daykin J, Holder R & Sheppard MC. Radioiodine therapy compared in patients with toxic nodular or Graves' hyperthyroidism. Quarterly Journal of Medicine 1995 88 175–180.
13. Sabri O, Zimny M, Schulz G, Schreckenberger M, Reinartz P, Willmes K et al. Success rate of radioiodine therapy in Graves' disease: the influence of thyrostatic medication. Journal of Clinical Endocrinology and Metabolism 1999 84 1229–1233.
14. Peters H, Fischer C, Bogner U, Reiners C, Schleusener H: Treatment of Graves' hyperthyroidism with radioiodine: results of a prospective randomized study. Thyroid 1997, 7:247–251.
15. Rivkees SA. Pediatric Graves' disease: management in the post-propylthiouracil Era.Int J PediatrEndocrinol. 2014;2014(1):10. doi: 10.1186/1687-9856-2014-10. Epub 2014 Jun 16.
16. Leslie WD, Ward L, Salamon EA, Ludwig S, Rowe RC & Cowden EA. A randomized comparison of radioiodine doses in Graves' hyperthyroidism. Journal of Clinical Endocrinology and Metabolism 2003 88 978–983.
17. Sridama V, McCormick M, Kaplan EL, Fauchet R &DeGroot LJ. Long-term follow-up study of compensated low-dose 131I therapy for Graves' disease. New England Journal of Medicine 1984 311426 – 432.
18. Koroscil TM. Thionamides alter the efficacy of radioiodine treat- ment in patients with Graves' disease. Southern Medical Journal. 1995 88 831 – 836.
19. Sabri O, Zimny M, Schulz G, Schreckenberger M, Reinartz P, Willmes K et al. Success rate of radioiodine therapy in Graves' disease: the influence of thyrostatic medication. Journal of Clinical Endocrinology and Metabolism 1999 84 1229 – 1233.
20. Marcocci C, Gianchecchi D, Masini I, Golia F, Ceccarelli C, Bracci E et al. A reappraisal of the role of methimazole and other factors on the efficacy and outcome of radioiodine therapy of Graves' hyperthyroidism. Journal ofEndocrinological Investigation 199013 513 – 520.
21. Franklyn JA, Daykin J, Drolc Z, Farmer M & Sheppard MC. Long- term follow-up of treatment of thyrotoxicosis by three different methods. Clinical Endocrinology 1991 34 71 – 76.
22. Allahabadia A, Daykin J, Sheppard MC, Gough SC & Franklyn JA. Radioiodine treatment of hyperthyroidism – prognostic factors for outcome. Journal of Clinical Endocrinology and Metabolism 2001 86 3611 – 3617.
23. Reynolds LR &Kotchen TA. Antithyroid drugs and radioactive iodine. Fifteen years' experience with Graves' disease. Archives of Internal Medicine 1979 139 651 – 653.
24. Latapie JL, Lefort G, Commenges M, Roger P, Riviere LJ & Mauriac L. The utilization of small repeated doses of iodine 131 in the treatment of Graves' disease. Results. Annalesd'Endocrinologie 1980 41 601 – 605.
25. Doniach D. Humoral and genetic aspects of thyroid autoimmun- ity. Clinical Endocrinology and Metabolism 1975 4 267.
26. Watson AB, Brownlie BE, Frampton CM, Turner JG & Rogers TG. Outcome following standardized 185 MBq dose 131I therapy forGraves' disease. Clinical Endocrinology 1988 28 487 – 496

Mirna Džubur, Medical faculty, University of Sarajevo, Čekaluša 90, 71 000Sarajevo, BiH (phone: 387-61-276-212; e-mail: mirna.dzubur@gmail.com)

Nanoparticles as bioactive nanocarriers for cancer therapy

E. Vranić[1*], O. Rahić[1], J. Hadžiabdić[1], A. Elezović[1], D. Bošković[2]

[1] Department of Pharmaceutical Technology, Faculty of Pharmacy, University of Sarajevo, Zmaja od Bosne 8, 71 000 Sarajevo, Bosnia and Herzegovina
[2] Department of Automatic Control and Electronics, Faculty of Electrical Engineering, University of Sarajevo, Zmaja od Bosne bb, 71 000 Sarajevo, Bosnia and Herzegovina

Abstract- **Nanotechnology is widely seen as a great potential to bring benefits to many areas of research and applications. Areas that are covered include nanoscale phenomena and processes, nanomaterials, nanosacale devices, instrumentation research, and standards for nanotechnology as well.**

Currently used nanoparticles demonstrate a variety of properties, such as: longevity in the blood and maintenance in the body, allowing for their accumulation in pathological areas with compromised vasculature; specific targeting to certain disease sites due to various targeting ligands attached to the nanocarrier surface; enhanced intracellular penetration with the help of surface – attached cell – penetrating molecules; contrast properties due to carrier loading with various contrast materials allowing for direct carrier visualization *in vivo*; stimuli – sensitivity allowing for drug release from the carriers under certain conditions.

Pharmaceutical nanocarriers could be used as the part of drug delivery systems and for therapeutic/ diagnostic / imaging purposes. Methods for nanoparticle manufacturing are: spray drying, aerosol flow reactor, mechanical methods (milling, homogenization under high pressure), precipitation techniques, techniques using supercritical fluids, methods for emulsion preparing and freezing (lyophilization).

If nanoparticles are used as drug nanocarriers, biophisycal characteristics of the drug and biological aspects that enable targeting of destructed or hurt tissues and organs have to be known. The principles of passive and active targeting of nanosized carriers to inflamed and cancerous tissues with increased vascular permeability, over-expression of specific epitopes, and cellular uptake of these systems are very important. The reduction or prevention of side effects can also be achieved by controlled release.

Development of nanotechnology in the future enables new opportunities for pharmaceutical technology, pointing out the way of producing particles of active and auxiliary compounds with more and more decreased dimensions. The progress is multidisciplinary process, combining methods used in medicine, engineering, materials studying, information technologies and physics.

Keywords— **Nanoparticles, Nanocarriers, Cancer, Therapy**

I. Introduction

Nanoparticle delivery system is a system in which nanocarriers are used to encapsulate bioactive compounds and deliver these compounds to either enhance their absorption in the gastrointestinal tract by active endocytosis or improve bioactivity in body circulation by specific targeting [1, 2, 3].

Nanotechnology, which is a multidisciplinary science involving chemistry, biochemistry, physics, and materials science, has found uses in a wide spectrum of medicine-related applications. These include nanoparticle-based imaging, drug delivery, biosensoring, and hyperthermia, and in the past decade, a number of these nanoparticle-based techniques have been translated into clinical applications [4]. Materials exhibit unique physical and biochemical properties when their dimensions are reduced to between several to hundreds of nanometers. By taking advantage of these unique characteristics, nanodevices can be developed that can sense and monitor biological events with unprecedented efficiency and sensitivity. When coupled to the targeting ligands, one "smart" nanoprobes can be produced that can interact with a biological system and sense changes on the molecular level. This can take place *in vivo*, where nanoprobes are systematically administrated, accumulated in tumors through ligand–biomarker interaction, and send out signals for sensitive diagnostic imaging. The nanoprobes are also useful to *in vitro* diagnosis and analysis of biological samples such as saliva, blood, and urine. Both applications are invaluable and hold great promise in revolutionizing cancer management [4, 5].

II. Neoplastic tissues compartments

Neoplastic tissues may be divided into three subcompartments: vascular, interstitial and cellular [6]. The vascularization of tumors is heterogeneous, showing regions of necrosis or hemorrhages as well as regions which are densely vascularized in order to sustain an adequate supply of nutrients and oxygen for rapid tumor growth (angiogenesis) [7]. Tumor blood vessels present several abnormalities in comparison with normal physiological vessels, often including a relatively high proportion of proliferating endothelial cells, an increased tortuosity, a deficiency in pericytes and an aberrant basement membrane formation [8,9]. The resulting enhanced permeability of tumor vasculature is thought to be regulated by various mediators, such as vascular endothelium growth factor

(VEGF), bradykinin, nitric oxide, prostaglandins and matrix metalloproteinases [10].

Macromolecular transport pathways across tumor vessels have been shown to occur via open gaps (interendothelial junctions and transendothelial channels), vesicular vacuolar organelles (VVO) and fenestrations [11]. It remains, however, controversial as to which pathways are predominantly responsible for tumor hyperpermeability and macromolecular transvascular transport [12]. Regardless of the transport mechanism, the pore cutoff size of several tumor models has been reported ranging between 380 and 780 nm [12,13]. *In vivo* fluorescence microscopy has even permitted direct measurement of the extravasation of sterically stabilized liposomes into solid tumor tissue (neuroblastome C-1300), suggesting that the cutoff size of the pores lies around 400 nm [14]. The tumor interstitial compartment is predominantly composed of a collagen and elastic fiber network [6]. Interdispersed within this cross-linked structure are the interstitial fluid and macromolecular constituents (hyaluronate and proteoglycans), which form a hydrophilic gel [6]. The interstitium, unlike most normal tissues, is also characterized by a high interstitial pressure leading to an outward convective interstitial fluid flow, as well as the absence of an anatomically well-defined functioning lymphatic network [6,7]. Hence, the transport of an anticancer drug in the interstitium will be governed by physiological (i.e. pressure) and physicochemical (i.e. composition, structure, charge) properties of the interstitium and by the physicochemical properties of the molecule (size, configuration, charge, hydrophobicity) itself [6]. Thus, to deliver therapeutic agents to tumor cells *in vivo*, the following problems must be solved: (i) drug resistance at the tumor level due to physiological barriers (non cellular based mechanisms), (ii) drug resistance at the cellular level (cellular mechanisms), and (iii) distribution, biotransformation and clearance of anticancer drugs in the body.

In chemotherapy, clinical drug resistance may be defined either as a lack of tumor size reduction or as the occurrence of clinical relapse after an initial positive response to anti-tumor treatment [15]. First, non-cellular drug resistance mechanisms could be due to poorly vascularized tumor regions which can effectively reduce drug access to the tumor and thus protect cancerous cells from cytotoxicity.

The acidic environment in tumors can also confer a resistance mechanism against basic drugs. These compounds would be ionized, preventing their diffusion across cellular membrane. High interstitial pressure and low microvascular pressure may also retard or impede extravasation of molecules [16]. Then, the resistance of tumors to therapeutic intervention may be due to cellular mechanisms, which are categorized in term of alterations in the biochemistry of malignant cells. They comprise altered activity of specific enzyme systems (for example topoisomerase activity), altered apoptosis regulation, or transport based mechanisms, like P-glycoprotein efflux system, responsible for the multi-drug resistance (MDR), or the multi-drug resistance associated protein (MRP) [15,16].

Finally, anticancer drugs generally feature large volumes of distribution. As cancer fighting drugs are toxic to both tumor and normal cells, the efficacy of chemotherapy is often limited by important side-effects [16].

A strategy could be to associate antitumor drugs with nanoparticles, with the aim to overcome non-cellular and cellular based mechanisms of resistance and to increase selectivity of drugs towards cancer cells while reducing their toxicity towards normal tissues [16] .

III. NANOPARTICLES AND CANCER TARGETING

Nanoparticles can be used as probes in *in vivo* imaging, biosensing, and immunostaining because nanoparticle-based probes offer many advantages in tumor targeting. First of all, they deliver high sensitivity. Many nanoscale materials show unique magnetic, optical, or acoustic properties and they can be further imparted with other types of imaging functionalities to result in probes with multimodal abilities. Secondly, their size is appropriate. Most nanoparticles have a size that is above the threshold of renal clearance (<7 nm) allowing them to remain in circulation for a relatively long time before reaching the desired targets. On the other hand, nanoparticles are also small enough to penetrate many biological barriers such as endothelial barriers, cell membranes, or even nuclear envelopes to efficiently interact with biological systems on the molecular level. Thirdly, they are multivalent. Multiple targeting ligands can be tethered onto one nanoparticle surface. This leads to a larger rate of receptor binding and smaller rate of dissociation, both contributing to higher tumor uptake and longer retention time, the so-called multivalency effect. Moreover, it is possible to impart more than one type of targeting ligand. Recent studies have confirmed improved tumor cell selectivity from such a dually targeting targeted approach. Fourthly, they offer combined therapy and diagnosis. In addition to imaging functionalities, therapeutics can be loaded onto nanoplatforms. The resulting nanoparticles, so-called nano-theranostics, have both imaging and therapeutic capabilities. Nanotheranostics are appealing for potentially allowing therapy response to be monitored in real-time by imaging methods, an emerging concept in modern personalized medicine [5].

IV. NANOMATERIALS FOR CANCER THERAPY

The most commonly analysed nanomaterials for cancer therapy are polymers, inorganic nanoparticles such as gold, iron oxide and mesoporous silica, and carbon based materials such as carbon nanotubes or graphene. Polymer nanoparticles have been researched extensively for drug delivery applications and have well characterized synthesis methods including solvent evaporation, nanoprecipitation, emulsion polymerization, and controlled/living radical polymerizations [17]. Both degradable and non-degradable nanoparticles have been investigated for cancer therapies, with the most commonly employed polymeric material being poly(lactic acid-co-glycolic acid) (PLGA) due to relatively non-toxic degradation products and FDA approval. Gold and iron oxide nanoparticles have been of great interest because of their ability to be remotely heated by IR light and magnetic fields respectively [17]. Mesoporous silica based nanotherapeutics have increased in popularity because of the ability to tailor surface functionality and load drugs into pores [17]. Carbon based materials such as carbon nanotubes and graphene have also emerged as promising candidates for cancer therapy due to high surface area and ability to be used in photothermal therapies [17].

V. TECHNOLOGICAL PERSPECTIVES FOR CANCER TREATMENT

In recent years it has become more and more obvious that the development of new therapies *per se* is not enough to verify progress in drug therapy. Experimental figures obtained *in vitro* are very often followed by unacceptable results *in vivo*. A hopeful strategy to overcome this problem includes the development of suitable drug carrier systems. The key advantage is that the *in vivo* fate of the drug is no longer mainly determined by the characteristics of the drug, but by the carrier system, which must permit a localized and controlled drug release [18].

VI. NANOCARRIERS

Colloidal carriers have attracted increasing attention during recent years. They are vesicular or particulate forms of nanometer size, required for effective carriage of loaded drug to the target. Investigational approaches include nanoparticles, nanoemulsions, nanosuspensions, liposomes, micelles, vesicles, soluble polymer–drug conjugates, and liquid crystal dispersions. The existence of diverse colloidal carrier systems raises the question as to which of them might be the most suitable for the desired purpose. Aspects to consider include drug loading capacity, possibility of drug targeting, *in vivo* target of the carrier (interaction with the biological surrounding, degradation rate, accumulation in organs), toxicity, scaling up production, storage stability and, of course, overall costs of the process [19].

Polymers and polymeric nanoparticles. Polymers from natural and synthetic sources have been used for carrying purposes [20]. These systems in the submicron dimensions comprise nanospheres, polymeric nanocapsules, polymersomes, dendrimers and water soluble polymer–drug conjugates. The main benefit of these systems is the wealth of chemical modifications. Nonetheless, problems of polymer based nanoparticles (NPs) arise from its toxicity, residual organic solvents (from the production process) and the scaling up for industrial production. Additionally, polymer hydrolysis during storage has to be taken in account and lyophilization is often required to prevent polymer degradation [19].

Liposomes. Liposomes are globular vesicles composed of one or more phospholipid bilayers. Hydrophilic substances are solubilized in the inner aqueous core and lipophilic drugs may be incorporated into the lipid bilayers [21]. Drug release, biodistribution and *in vivo* stability depend on particle size, surface hydrophobicity, charge and membrane fluidity [21]. It is possible to avoid liposomes' fast reticuloendothelial uptake through the incorporation of natural compounds (as gangliosides), by the use of chemically modified polyethylene glycols (PEGs) or by the incorporation of specific antibodies.

Nanosuspensions and nanoemulsions. Nanosuspensions are colloidal particles composed of only a drug and an emulsifier. Nanoemulsions (composed of oil-in-water (O/W) or water-in-oil (W/O)) are lipid droplets with a drug and an emulsifier. Fatty oils or middle chain triglycerides are used for the lipid phase, which amounts to typically 10–20% of the emulsion. Systems based on nanosuspensions/ nanoemlusions are employed as drug carriers for lipophilic drugs and several formulations are commercialized so far. In fact, compared with solubilization based formulations of the same drug, a decrease of side effects was found using these systems [21].

Lipid nanoparticles. Lipid nanoparticles are pioneering carrier systems technologically developed as an alternative to traditional vehicles such as polymeric nanoparticle, liposomes and emulsions. These traditional vehicles revealed relevant advantages such as site-specific targeting and modified release of the active pharmaceutical substance. Nonetheless, no irrelevant problems arose, such as cytotoxicity of the polymers and a complex scaling up process [22]. A lipid nanoparticle is described as a solid lipophilic matrix in which active substances can be incorporated. Dimensions are mostly between 150 and 300 nm, but smaller sizes, as <100 nm, or larger sizes, up to 1000 nm, can be obtained

and employed for special needs [23]. They can be derived from oil-in water nanoemulsions, where the liquid lipid of the oil droplets is replaced by a solid lipid, i.e. solid at body temperature. Therefore, lipid nanoparticles remain solid after administration. This means that they may provide a matrix for modified release of the active substances. At the same time, chemically labile active molecules can be protected by the matrix [23].

Carbon-based nanoparticles. Carbon-based materials like graphite, fullerenes, diamond, nanowires, nanotubes, nanoribbons and graphene have been used for various applications in optoelectronics, tissue and biomedical engineering, sensors, medical implants and medical devices. Nanowires are a nanostructure characterized by cylindrical cross-sections of less than 100 nm but can be hundreds of microns long, and includes the well-described carbon nanotubes. Several studies have been performed with carbon nanotubes (long carbon tubes that can be single or multi-walled and have the ability to act as biopersistent fibers [24]) but also with fullerenes (1-nm scale carbon spheres of 60 carbon atoms) [24].

Magnetic nanoparticles. The potential of magnetic nanoparticles in nanotechnology has been strongly discussed. Magnetic/metallic nanoparticles are small, which may be valuable for aspects of cell targeting [25]. Crystal symmetry breaking at the surface has profound ramifications. For example, in metallic compounds, the surface atoms oxidize rapidly, forming oxides that are typically ferromagnetic or antiferromagnetic [25]. Two features play an important role for the *in vivo* uses: size and surface functionality. Particles with diameters of 10–40 nm including ultra-small magnetic nanoparticles are important for prolonged blood circulation. Biomedical applications *in vivo* may be separated in therapeutic (hyperthermia and drug-targeting) and diagnostic applications (Magnetic Resonance Imaging (MRI)) [25].

Gold nanoparticles. Gold nanoparticles are being studied for a long time. Although common oxidation states of gold include +1 and +3, gold nanoparticles exist in a nonoxidized state (Au [0]) [26]. For clinical use, they are being studied as carriers for delivery of drugs, imaging molecules, genes and for the development of novel cancer therapy products [26]. These nanoparticles possess several characteristics that are useful for cancer therapy. Besides being small, they can penetrate through the body, accumulating in tumors. In addition, gold nanoparticles exhibit single physicochemical properties, as surface plasmon resonance (SPR) and the ability to bind amine and thiol groups, tolerating surface modification [26].

Modular nanotransporters. Modular nanotransporter is a modular polypeptide that may contain four moieties: an internalizable ligand, an endosomolytic module, a nuclear localization sequence (NLS) and a carrier domain [27]. The first MNT module ligand has two functions: specific acknowledgment of a cancer target cell and penetration via receptor-mediated endocytosis. The endosomolytic module makes it possible to leave the endocytotic pathway before getting into lysosomes, in order to have time for contact with importins. Therefore, this second module is able to make defects in membranes only at the pH of endosomes. The third module (NLS) permits delivery into the cell nucleus, recognizing importins located in the hyaloplasm. Last but not least, the fourth module acts as a carrier for joining the transported drug. Depending on the type of ligand, MNT for different target cells may be produced [27].

Redox-active nanoparticles. The employment of cerium oxide nanoparticles is a novel and encouraging approach, as those particles *per se* appear to demonstrate an antineoplastic effect via their oxygen chemical reactivity. These nanoparticles of spherical shape have unique antioxidant capacity due to alternating Ce (+3) and Ce (+4) oxidation states and crystal defects (defects in the crystal framework due to the presence of Ce (+3) play an important role in tuning the redox activity of cerium oxide nanoparticles) [28].

They were found to be effective against pathologies linked to chronic oxidative stress and inflammation. Cerium oxide nanoparticles are well tolerated, which makes these particles suitable for nanobiology and regenerative medicine [28]. Therefore, the effect of those nanoparticles was investigated [29], *in vitro* and *in vivo*. Interestingly, concentrations of cerium oxide nanoparticles (polymer-coated) being innocuous for stromal cells showed a cytotoxic, proapoptotic, and anti-invasive capacity on melanoma [29].

Quantum dots (QDs). Recently, nanocrystal semiconductor QDs have attracted the attention of many scientific groups owing to their potential for use in the management and treatment of cancer. QDs provide a nanoscale scaffold for designing multifunctional NPs with both imaging and therapeutic functions. The surface of QDs may be modified to improve specificity, sensitivity, solubility, and visualization of the target tissue. However, due to their composition of heavy metals and a few reports of cytotoxicity, QDs have been the subject of toxicological analysis and several groups have reported that the release of toxic metals might be limited with surface coatings, such as PEG or micelle encapsulation [30].

VII. Conclusions

Nanoparticle-based treatments for cancer therapy represent a promising strategy to enhance therapeutic outcomes by reducing off-target side effects compared to intrave-

nously administered chemotherapeutics. With respect to the design of these systems, nanomateials with a size on the order of 100–200 nm of various morphologies are popular because of their ability to escape renal, hepatic, and lymphatic clearance.

With the prominence of drug-resistant cancers, there is an increasing need to design therapeutic agents with the ability to sensitize or synergistically target cancerous cells over healthy cells to effectively reduce off-target effects. Furthermore, in the case of metastatic cancers, delivery of nanoparticles rationally designed to overcome the characteristic physiological barriers associated with the affected organ will be most effective. Finally, clinical impact of nanotechnology for cancer treatment will strongly benefit from customized nanoparticle-based therapies that are designed to overcome diverse physiological contexts of varying disease states.

REFERENCES

1. R. H., Müller, K., Mäder, S. Gohla. Solid lipid nanoparticles (SLN) for controlled drug delivery - a review of the state of the art. European *Journal of Pharmaceutics and Biopharmaceutics*, *Volume:* 50, 2000, pp 161-177.
2. A. des Rieux, V. Fievez, M. Garinot, Y.-J Schneider, V. Préat, V. Nanoparticles as potential oral delivery systems of proteins and vaccines: a mechanistic approach. *Journal of Controlled Release*, *Volume:* 116, 2006, pp 1-27.
3. Z. Li, H. Jiang, C. Xu, L. Gu. A review: Using nanoparticles to enhance absorption bioavailability of phenolic phytochemicals. *Food Hydrocolloids, Volume: 43*, 2015, pp 153-164
4. M. Ferrari, Cancer nanotechnology: opportunities and challenges. *Nature Reviews. Cancer, Volume: 5,* 2005, pp 161–171
5. H Chen, Z Zhen, T Todd, PK Chu, J. Xie. Nanoparticles for improving cancer diagnosis. *Materials Science and Engineering R, Volume:* 74, 2013, pp 35–69
6. R.K. Jain, Transport of molecules in the tumor interstitium: a review, *Cancer Research*, *Volume:* 47, 1987, pp 3039–3051.
7. R.K. Jain, Delivery of molecular medicine to solid tumors: lessons from in vivo imaging of gene expression and function, *Journal of Controlled Release, Volume:* 74, 2001, pp 7–25.
8. L.W. Seymour. Passive tumor targeting of soluble macromolecules and drug conjugates, *Critical Reviews in Therapeutic Drug Carrier Systems*, *Volume:* 9, 1992, pp 135–187.
9. D. Baban, L.W. Seymour. Control of tumor vascular permeability, *Advanced Drug Delivery Reviews, Volume:* 34, 1998, pp 109–119.
10. H. Maeda. The enhanced permeability and retention (EPR) effect in tumor vasculature: the key role of tumor-selectivemacromolecular drug targeting, *Advances in Enzyme Regulation, Volume:* 41, 2001, pp 189–207.
11. S.K. Hobbs, W.L. Monsky, F. Yuan, W.G. Roberts, L. Griffith, V.P. Torchilin, R.K. Jain, Regulation of transport pathways in tumor vessels: role of tumor type and microenvironment, *Proceedings of the National Academy of Sciences of the United States of America*, *Volume:* 95, 1998, pp 4607–4612.
12. F. Yuan, M. Dellian, D. Fukumura, M. Leuning, D.D. Berk, V.P. Yorchilin, R.K. Jain, Vascular permeability in a human tumor xenograft: molecular size dependence and cutoff size, *Cancer Research, Volume:* 55, 1995, pp 3752–3756.
13. S. Unezaki, K. Maruyama, J.-I. Hosoda, I. Nagae, Y. Koyanagi, M. Nakata, O. Ishida, M. Iwatsuru, S. Tsuchiya, Direct measurement of the extravasation of polyethyleneglycol-coated liposomes into solid tumor tissue by in vivo fluorescence microscopy, *International Journal of Pharmaceutics, Volume:* 144, 1996, pp 11–17.
14. M. Links, R. Brown, Clinical relevance of the molecular mechanisms of resistance to anti-cancer drugs, *Expert Reviews in Molecular Medicine*, *Volume:* 1, 1999, pp 1–21.
15. R. Krishna, L.D. Mayer, Multidrug resistance (MDR) in cancer-mechanisms, reversal using modulators of MDR and the role of MDR modulators in influencing the pharmacokinetics of anticancer drugs, *European Journal of Cancer, Volume:* 11, 2000, pp 265–283.
16. I. Brigger, C. Dubernet, P. Couvreur. Nanoparticles in cancer therapy and diagnosis, *Advanced Drug Delivery Reviews, Volume:* 64, 2012, pp 24–36
17. M.C.F. Simões, J.J.S. Sousa, A.A.C.C. Pais. Skin cancer and new treatment perspectives: A review. *Cancer Letters*, *Volume:* 357, 2015, pp 8-42.
18. W. Mehnert, K. Mäder. Solid lipid nanoparticles: production, characterization and applications, *Advanced Drug Delivery Reviews, Volume*: 47, 2001, pp 165-196.
19. D.K. Thukral, S. Dumoga, A.K.Mishra Solid lipid nanoparticles: promising therapeutic nanocarriers for drug delivery. *Current Drug Delivery, Volume* 11, 2014, pp 771-791.
20. Y. Hoshino, H. Koide, K. Furuya, W.W. Haberaecker 3rd, S.H. Lee, T. Kodama, et al., The rational design of a synthetic polymer nanoparticle that neutralizes a toxic peptide in vivo, *Proceedings of the National Academy of Sciences of the United States of America*, *Volume:*109, 2012, pp 33–38
21. R. Parhi, P. Suresh, Preparation and characterization of solid lipid nanoparticles-a review, *Current Drug Discovery Technologies, Volume:* 9, 2012, pp 2–16
22. C. Puglia, F. Bonina, Lipid nanoparticles as novel delivery systems for cosmetics and dermal pharmaceuticals, *Expert Opinion on Drug Delivery, Volume:* 9, 2012, pp 429–441
23. R.H. Muller, R. Shegokar, C.M. Keck, 20 years of lipid nanoparticles (SLN and NLC): present state of development and industrial applications, *Current Drug Discovery Technologies, Volume:* 8, 2011, pp 207–227
24. W.H. De Jong, P.J. Borm, Drug delivery and nanoparticles: applications and hazards, *International Journal of Nanomedicine, Volume:* 3, 2008, pp 133–149.
25. A. Akbarzadeh, M. Samiei, S. Davaran, Magnetic nanoparticles: preparation, physical properties, and applications in biomedicine, *Nanoscale Research Letters, Volume:* 7, 2012, pp 1-13
26. S. Jain, D.G. Hirst, J.M. O'Sullivan, Gold nanoparticles as novel agents for cancer therapy, *British Journal of Radiology, Volume*: 85, 2012, 101–113
27. T.A. Slastnikova, A.A. Rosenkranz, P.V. Gulak, R.M. Schiffelers, T.N. Lupanova, Y.V. Khramtsov, et al., Modular nanotransporters: a multipurpose in vivo working platform for targeted drug delivery, *International Journal of Nanomedicine, Volume*: 7, 2012, pp 467-482
28. S. Das, J.M. Dowding, K.E. Klump, J.F. McGinnis,W. Self, S. Seal, Cerium oxide nanoparticles: applications and prospects in nanomedicine, *Nanomedicine , Volume:* 8 , 2013, pp1483–1508
29. L. Alili, M. Sack, C. von Montfort, S. Giri, S. Das, K.S. Carroll, et al., Downregulation of tumor growth and invasion by redox-active nanoparticles, *Antioxidants & Redox Signaling, Volume*: 19, 2013, pp 765–778
30. I.A. Siddiqui, V.M. Adhami, J.C. Chamcheu, H. Mukhtar, Impact of nanotechnology in cancer: emphasis on nanochemoprevention. *International Journal of Nanomedicine. Volume*: 7, 2012, pp 591–605

E. Vranic, Department of Pharmaceutical Technology, Faculty of Pharmacy, University of Sarajevo, Zmaja od Bosne 8, 71 000 Sarajevo, Bosnia and Herzegovina (phone: 387-33-586-176; e-mail: evranic@yahoo.com).

Promising tissue engineering approaches using biodegradable poly(D,L-lactic-co-glycolic acid) scaffolds

D. Grizić[1], E. Vranić[2] and A. Lamprecht[1,3]

[1]Laboratory of Pharmaceutical Technology and Biopharmaceutics, Pharmaceutical Institute, University of Bonn, Gerhard-Domagk-Str. 3, 53121 Bonn, Germany
[2]Department of Pharmaceutical Technology, Faculty of Pharmacy, University of Sarajevo, Zmaja od Bosne 8, 71 000 Sarajevo, Bosnia and Herzegovina
[3]Laboratory of Pharmaceutical Engineering, University of Franche-Comté, Place Saint Jacques, 25030 Besançon, France

Abstract— **Tissue engineering has emerged as a promising alternative approach to tissue transplantation. In this approach, a temporary scaffold is needed to serve as an adhesive substrate for the implanted cells or growth factors of interest. The capability of providing good cell adhesion and extracellular matrix deposition, allowing the unhindered transport of all necessary factors which play a vital role for the cells is crucial. In this sense, biodegradable polymeric scaffolds show promising properties, due to their biocompatibility, biodegradability and mechanical properties. Poly(D,L-lactide-co-glycolide) is currently one of the mostly used copolymers for biomedical applications. It exhibits all properties which are needed for scaffolds to be used in regenerative tissue engineering: biodegradability, controlled release of bioactive factors (release of proteins locally at slow rates), wide spectrum of technological formulation possibilities and more.**

Keywords— **Tissue engineering, Regenerative medicine, PLGA, Biodegradable scaffolds, Polymeric microparticle scaffolds.**

I. Introduction

The interests in biodegradable polymeric biomaterials for biomedical engineering and regenerative medicine use have increased dramatically during the past years. Biomaterials are, according to the definition proposed at the Consensus Conference of the European Society for Biomaterials, Chester, England in March 1986 "any substance, other than a drug, or combination of substances, synthetic or natural in origin, which can be used for any period of time, as a whole or as a part of a system which treats, augments, or replaces any tissue, organ, or function of the body" [1]. The term regenerative medicine stands as a broad term for both, tissue engineering leading to tissue substitutes and the possibility to induce tissue/organ regeneration. The knowledge which revolves around these two possibilities is tightly connected to the biological processes which occur in these tissues/organs [2]. One of the major death causes in intensive care is at present the organ failure, where the transplantation of organs serves as the only treatment for these patients. In this context, tissue engineering offers a great potential towards the development of an alternative therapy to transplantation [3]. It aims to solve the problem of shortage of donor tissues and organs associated with transplantation, by using in vitro engineered implantable tissues/organ scaffolds, which resemble as closely as possible the natural ones. These implants can further generate natural tissue and the components of the scaffold will, due to their biodegradability, be degraded in the body.

II. Tissue engineering and scaffolds

The major principle of tissue engineering includes the design and development of functional three-dimensional tissues by culturing cells on biodegradable 3D supports (scaffolds). In contrast to permanent implants, tissue-engineered polymeric scaffolds can be temporary implants used to facilitate the tissue repair and regeneration process [2]. These scaffolds must be capable of providing good cell adhesion and extracellular matrix deposition, allowing the unhindered transport of all necessary factors which play a vital role for the cells, in terms of their survival, proliferation and differentiation. This is very important due to the fact that the scaffolds serve as a microclimate to the host cells, which should mimic the properties of the tissue where these cells are found [4]. The geometrical representation of the used scaffolds should represent the physiological features of the targeted tissue or organ. The ideal premise would be that the degradation rate of the scaffold should correspond to the rate of new tissue formation. Since this can be a huge individual feature of every patient, this drawback still persists. This degradation rate can be influenced by many factors, such as the properties of the matrix substances (the molecular weight, crystallinity, glass transition temperature, porosity, pH etc.), but also by the in vivo environmental factors (enzymatic activities, microenvironmental pH etc.) [5].

III. Current approaches

Currently, a promising approach of tissue engineering is the use of grafted cells, which could be helpful strategies to repair injured organs. However, improvement of cell survival after transplantation is crucial. In this manner, growth, differentiation and migration factor-based tissue engineering strategies became powerful tools in regenerative medicine [6], [7]. Factors like nerve growth factor (NGF), transforming growth factor-beta 3 (TGF-β3) and neurotropin-3 (NT3) may lead to better cell survival and to a better integration of the used grafts [8]. All these strategies, combined with biomedical scaffolds, can provide physical support, help cell integration and support the proliferation and differentiation of cells. Furthermore, current approaches combine cell-free scaffolds with bioactive factors that recruit the patient's own cells for subsequent in situ repair [9]. It is essential to control the temporal concentration of these factors, while maintaining their stability and availability for a prolonged period of time, which in turn suggests the use of appropriate delivery devices. The sensitive structure of these factors still remains a technological challenge of delivery. To overcome these difficulties, biodegradable polymeric scaffolds which offer controlled and sustained release after administration can protect the growth factors [6], [10].

IV. Biodegradable polymeric scaffolds

Biodegradable polymeric biomaterials have the major advantage that they do not elicit permanent chronic foreign body reactions, due to the fact that they are gradually absorbed by the human body and do not leave residues in the implantation sites [5]. Compared to metal or ceramic biomaterials, polymeric biomaterials used as scaffold matrices have many advantages (deformity into various shapes, biodegradability, economical aspects etc.). Commercially most significant biodegradable polymeric biomaterials are originating from linear aliphatic polyesters like polyglycolide and polylactide [5]. This class of biodegradable polymeric biomaterials is also the one most studied for their physicochemical and biological properties. Polylactic (PLA), polyglycolic (PLGA) and poly(lactic-co-glycolic) (PLGA) acids are biodegradable polyesters belonging to the group of poly-α-hydroxy acids. All of these polymers degrade by nonspecific hydrolysis of their ester bonds, which results in a decrease in the polymer molecular weight [11].

V. PLGA, a promising tool for tissue engineering

PLGA is the co-polymer of glycolic and lactic acid, synthesized by means of random ring-opening co-polymerization of lactide and glycolide. Poly(D,L-lactide-co-glycolide), a Food and Drug Administration (FDA) approved synthetic polymer [12], is currently one of the mostly used copolymers of this group for biomedical applications [5]. It exhibits all properties, which are needed for scaffolds to be used in regenerative tissue engineering: biodegradability, mechanical stability, controlled release of bioactive factors (release of proteins locally at slow rates), wide spectrum of technological formulation possibilities etc. [13]. However, the hydrophobic character of PLGA scaffolds is the primary limitation of their use, leading to sub-optimal adhesion and growth of cells on its surface [14], which can be improved by incorporation of different hydrophilic substances [15]. In particular, biodegradable poly(D,L-lactide–co-glycolide) (PLGA) scaffolds have already facilitated distinct advances in growth factor delivery for numerous tissue engineering applications. PLGA has the ability to be used for the fabrication of different forms of scaffolds, such as fibres [15], foams [4], membranes [16], porous scaffolds [17], hybrid sponges [18] etc. The production of PLGA scaffolds relies on different technique, such as solvent casting/particulate leaching technique, phase separation, emulsion freeze-drying, gas foaming, electro spinning and 3D printing [19], [4], [17], differing mostly due to the needed scaffold shape. Currently, the formulation of PLGA microparticulate implantable scaffolds show promising characteristics, regarding the encapsulation of sensitive substances, as well as having optimal scaffold properties. The study of *Andreas et al.* showed that the encapsulation of insulin, which acts as a growth factor for cartilage tissue, in polymeric PLGA microparticle scaffolds stimulates the formation of cartilage considerably in chondrocytes (leading to an increased secretion of proteoglycans and collagen type II) [6]. The incorporation of hydrophilic excipients to the PLGA scaffold matrix offten leads to better scaffold properties. This was underlined in the study of *Tran et al.*, which used the incorporation of hydrophilic polyoxyethylene into the PLGA chains, leading to a continuous release profile of the encapsulated lysozyme from the prepared microparticles. The cell adherence was satisfactory, concluding that the PLGA segments on the microparticle surface provided the optimal places for fibronectin attachment, leading to a good cell adherence [20]. This approach of raising the hydrophilicity of PLGA scaffolds was also confirmed by *Qodratnama et al.* [9]. PLGA nanofiber scaffolds for tend-on-bone were successfully formulated by *Kolluru et al.*, demonstrated outstanding strain-hardening behaviour and ductility when stretched uniaxially, even in the presence of surface mineralization [21].

VI. Conclusions

Tissue engineering offers a great potential towards the development of an alternative therapy to transplantation. The development of new and safe biomaterials, as well as the development of new formulation technologies, will eventually lead to a wide abundance of these materials in tissue engineering. Currently, polymeric biodegradable biomaterials are used and fabricated into various shapes, possessing the properties of being carriers of both cells and growth factors. Due to the promising properties, such as biocompatibility, biodegradability and mechanical stability, poly(D,L-lactic-co-glycolic acid) scaffolds gained much attention. As a conclusion it can be stated that biodegradable poly(D,L-lactic-co-glycolic acid) scaffolds present promising materials for diverse tissue engineering approaches.

REFERENCES

1. D.F. Williams. Definitions in biomaterials: *proceedings of a consensus conference of the European society for biomaterials*, Chester, England, March 3-5 1986
2. R. Lanza R. Langer, J. Vacanti. *Principles of tissue engineering*, USA Elsevier Academic Press; Third Edition, 2007.
3. G. Chen, T. Ushida, T. Tateishi. Scaffold design for tissue engineering. *Macromolecular bioscience, Volume: 2*, Issues 2, 2002, pp 67-77
4. S.C. Baker, G. Rohman, J. Southgate, N.R. Cameron. The relationship between the mechanical properties and cell behaviour on PLGA and PCL scaffolds for bladder tissue engineering. *Biomaterials, Volume: 30*, 2009, pp 1321-1328
5. J. D. Bronzino, R. P. Donald. *Tissue Engineering and Artificial Organs*. In: The Biomedical Engineering Handbook, Editor: J. D. Bronzino, Third Edition, Volume 3, USA CRC Press, 2006
6. K. Andreas, R. Zehbe, M. Kazubek, K. Grzeschik, N. Sternberg, H. Bäumler, H. Schubert, M. Sittinger, J. Ringe. Biodegradable insulin-loaded PLGA microspheres fabricated by three different emulsification techniques: Investigation for cartilage tissue engineering. *Acta Biomaterialia,* Volume: 7, 2011, pp 1485-1495
7. L. Nie, G. Zhang, R. Hou, R. Xu, Y. Li, J. Fu. Controllable promotion of chontrocyte adhesion and growth on PVA hydrogels by controlled release of TGF-β1 from porous PLGA microspheres. *Colloids and Surfaces B: Biointerfaces, Volume: 125,* 2015, pp 51-57
8. J.E. Samorezov, E. Alsberg. Spatial regulation of controlled bioactive factor delivery for bone tissue engineering, 2015, *In press*
9. R. Qodratnama, L.P. Perino, H.C. Cox, O. Qutachi, L.J. White. Formulations for modulation of protein release from large-size PLGA microparticles for tissue engineering. *Materials Science and Engineering C, Volume: 47*, 2015, pp 230-236
10. H. Nojehdehian, F. Moztarzadeh, H. Baharvand, H. Nazarian, M. Tahriri. Preparation and surface characterization of poly-L-lysine-coated PLGA microsphere scaffolds containing retinoic acid for nerve tissue engineering: In vitro study. *Colloids and Surfaces B: Biointerfaces, Volume: 73*, 2009, pp 23-29
11. M. Vert, S.M. Li, G. Spenlehauer, P. Guerin. Bioresorbability and biocompatibility of aliphatic polyesters. *Journal of Material Science: Materials in Medicine, Volume: 3,* 1992, pp 432-446
12. R.A. Jain, C.T. Rhodes, A.M. Railkar, A.W. Malick, N.H. Shah. Controlled release of drugs from injectable in situ formed biodegradable PLGA microspheres: effect of various formulation variables. *European Journal of Pharmaceutics and Biopharmaceutics, Volume: 50,* 2000, pp 257-262
13. A. Dogan, S. Demirci, Y. Bayir, Z. Halici, E. Karakus, A. Aydin et al. Boron containing poly-(lactide-co-glycolide) (PLGA) scaffolds for bone tissue engineering. *Material Science and Engineering C, Volume: 44*, 2014, pp 246-253
14. H. Shearer, M.J. Ellis, S.P. Perera, J.B. Chaudhuri. Effects of common sterilization methods on the structure and properties of poly(D,L lactic-co-glycolic acid) scaffolds. *Tissue Engineering, Volume: 12,* Issues: 10, 2006, pp 2717-2727
15. M. Thomas, A. Arora, D.S. Katti. Surface hydrophilicity of PLGA fibers governs in vitro mineralization and osteogenic differentiation. *Materials Science and Engineering: C, Volume: 45,* 2014, pp 320-332
16. H. Suhaimi, S. Wang, T. Thornton, D.B. Das. On glucose diffusivity of tissue engineering membranes and scaffolds. *Chemical Engineering Science, Volume: 126*, 2015, pp 244-256
17. J.J. Lee, S.G. Lee, J.C. Park, Y.I. Yang, J.K. Kim. Investigation on biodegradable PLGA scaffold with various pore size structure for skin tissue engineering. *Current Applied Physics, Volume: 7*, 2007, pp 37-40
18. T. Sato, G. Chen, T. Ushida, T. Ishii, N. Ochiai, T. Tateishi. Tissue-engineered cartilage by in vivo culturing of chondrocytes in PLGA-collagen hybrid sponge. *Materials Science and Engineering: C, Volume: 17*, Issue: 1, 2011, pp 83-89
19. S.H. Oh, S.G. Kang, J.H. Lee. Degradation behaviour of hydrophilized PLGA scaffolds prepared by melt-molding particulate-leaching method: Comparison with control hydrophobic one. *Journal of Materials Science-Materials in Medicine, Volume: 17*, Issue: 2, 2006, pp 131-137
20. V.T. Tran, J.P. Karam, X. Garric, J. Coudane, J.P. Benoit, C.N. Montero-Menei, M.C. Venier-Julienne. Protein-loaded PLGA-PEG-PLGA microspheres: A tool for cell therapy. *European Journal of Pharmaceutical Sciences, Volume: 45,* Issue: 1-2, 2012, pp 128-137
21. P. Kolluru, J. Lipner, W. Liu, Y. Xia, S. Thomopoulos, G.M. Genin, I. Chasiotis. Strong and though mineralized PLGA nanofibres for tendon-to-bone scaffolds. *Acta Biomaterialia, Volume: 9,* 2013, pp 9442-9450

D. Grizić, Laboratory of Pharmaceutical Technology and Biopharmaceutics, Pharmaceutical Institute, University of Bonn, Gerhard-Domagk-Str. 3, 53121 Bonn, Germany (phone: +49 1577 0353579; E-Mail: daris.grizic@uni-bonn.de)

Human skin substitutes

E. Vranić[1], D. Grizić[2], and A. Lamprecht[2,3]

[1] Department of Pharmaceutical Technology, Faculty of Pharmacy, University of Sarajevo, Zmaja od Bosne 8, 71 000 Sarajevo, Bosnia and Herzegovina

[2] Laboratory of Pharmaceutical Technology and Biopharmaceutics, Pharmaceutical Institute, University of Bonn, Gerhard-Domagk-Str. 3, 53121 Bonn, Germany

[3]Laboratory of Pharmaceutical Engineering, University of Franche-Comté, Place Saint Jacques, 25030 Besançon, France

Abstract— **To be useful in a clinical setting, the primary goal for any skin substitute is restoration of skin barrier, normally a function of the epidermis, which helps to minimize protein and fluid loss and prevent infection temporary wound coverage or partial skin replacement. Currently, limitations of bioengineered skin substitutes, compared with native skin grafts, include: reduced rates of engraftment, increased microbial contamination, mechanical fragility, increased time to healing, increased requirement for re-grafting, and very high cost. These complications may increase, rather than decrease, the risks to patients and delay recovery. Therefore, the use of skin substitutes may be suitable as an adjunctive therapy in cases without other alternatives, such as very large burns or chronic wounds that have failed to respond to conventional treatments.**

Skin replacements should promote permanent engraftment without the need for re-grafting; allow rapid healing to replace both dermal and epidermal layers; be ready to use when needed; achieve acceptable functional and cosmetic outcome; and be free from risk of disease transmission and immunological reaction. Tissue engineered skin refers to a material made up of cells, extracellular matrix or combination of both.

Technological advances in the production of biomaterials and the culture of skin cells have permitted the production of bioengineered skin substitutes. These have provided improved therapeutic options for patients suffering from acute or chronic wounds, and offer the promise of new treatments for inherited cutaneous diseases.

Keywords— **Skin substitutes, Wounds, Compostion, Stability, Biodegradability**

I. Introduction

Burn injuries are among the most complex and harmful physical injuries to evaluate and manage. In addition to pain and distress, a large burn will leave the patient with visible physical scars and invisible psychological sequelae. Currently, autograft is the best replacement for lost skin. However, in clinical practice this is not always possible, particularly in large total body surface area burns, as there is often an insufficient amount of skin for autografting available at the time of burn excision, or the physiological condition of the patient precludes the harvesting of skin. Allografts and xenografts can be used to provide temporary wound coverage, but there are issues with graft rejection, availability, and the possibility of disease transfer [1, 2].

The timely restoration of skin protective functions is the key to the successful treatment of patients with various degrees of damaged skin. Conventionally, autologous split or full-thickness skin graft have been recognised as the best definitive burn wound coverage, but it is constrained by the limited available sources, especially in major burns. Donor site morbidities in term of additional wounds and scarring are also of concern of the autograft application. Skin substitutes are required in the acutely burned patients as well as in those requiring extensive post burn reconstructions [3].

The gold standard for burn wound treatment and repair where necessary has been, and remains, the patients' own skin, either as split-thickness autograft or full thickness transferred or transplanted to close the wounded area [4]. The ideal skin substitute should have properties comparable to those of human skin. Accordingly, the question of why substitutes should be considered is highly relevant. To date, no substitute or replacement for the patients' own skin has been prepared that approaches the qualities that autogenous material possesses.

II. Skin substitutes

Skin substitutes are a heterogeneous group of biological and/or synthetic elements that enable the temporary or permanent occlusion of wounds. Although dermal substitutes can vary from skin xenografts or allografts to a combination of autologous keratinocytes over the dermal matrix, their common objective is to achieve the greatest possible similarity with the patient's skin [5, 6].

There will be different objectives for substitute use in the different depths of burns under treatment. It could not be

expect to use the same substitute for the same objectives in superficial wounds and full-thickness wounds. Perhaps the answer to the selection of individual substitutes for specific cases will be found by considering some general functions that different substitutes will offer and that can be used to best effect in reaching the clinical objectives of treating the wounds under consideration [7].

Several skin substitutes are currently available for a variety of applications, which enables the choice of a suitable substitute for each clinical application [8].

III. Composition of Skin Substitutes

There are various ways to classify skin substitutes. A classification was proposed based on composition as follows [8]:

Class I: Temporary impervious dressing materials

a) single layer materials

- ◊ naturally occurring or biological dressing substitute, e.g. amniotic membrane, potato peel
- ◊ synthetic dressing substitute, e.g. synthetic polymer sheet, polymer foam or spray

b) bi-layered tissue engineered materials

Class II: Single layer durable skin substitutes

a) *Epidermal substitutes*, e.g. cultured epithelial autograft (CEA),

b) *Dermal substuitutes* such as*:*

- ◊ bovine collagen sheet,
- ◊ porcine collagen sheet,
- ◊ bovine dermal matrix,
- ◊ human dermal matrix.

Class III: Composite skin substitutes

a) *Skin graft*

- ◊ Allograft
- ◊ Xenograft

b) *Tissue engineered skin*

- ◊ Dermal regeneration template,
- ◊ Acellular biocomposite dressing.

IV. Features of the Ideal Skin Substitute

The optimal skin substitute will provide for immediate replacement of both the lost dermis and epidermis, with permanent wound coverage [9]. Other features of the ideal skin substitute should have the following features [10]:

(A) Protection of the wound from infection and loss of fluid;

(B) Providing a stable and biodegradable template for the synthesis of neodermal tissue;

C) Either hosting or enabling the influx of cells that will function as dermal cells, producing dermal tissue rather than scar tissue;

(D) Allowing ease of handling and resist tear forces.

V. Stability and Biodegradability of Skin Substitutes

Stability, biodegradation and immunocompatibility are key issues for design and function of a skin substitute [8].

The material should preferably represent a temporary replacement of the lost dermal tissue, and provide an adequate environment for the formation of new and functional dermal tissue. Although optimal degradation time of a scaffold is unknown, general statements on the time the scaffold must remain in the wound environment can be made [8].

If stability of substitute materials is too low (disintegration within days), the template function of the substitute will not be fulfilled. In humans, the proliferation/ migration phase of the wound healing process will generally take up to three weeks. During at least this period, the dermal substitute should provide a temporary three-dimensional structure to allow ingrowth of blood vessels, fibroblasts and coverage by epithelial cells. Stability of biomaterials can generally be increased by physical and/ or chemical crosslinking of the material [11,12]. Care should be taken in application of such methods, since the crosslinking agents may seriously affect wound healing, e.g. by toxicity due to remnants of crosslinking agents or induction of a foreign body response. Biodegradation should preferably take place after this period, and by such a process that no massive foreign body reaction is induced. This would increase the inflammatory response, which is usually already high especially in burn wounds, and which is associated with profound scarring. Furthermore, the skin substitute should be composed of immunocompatible material, to avoid immunoreactive processes [8].

VI. Regulatory Status

Depending on the purpose of the product and how it functions, skin substitutes are regulated by the FDA premarket approval (PMA) process, 510(k) premarket notification process, or the FDA regulations for banked human tissue [13].

Products that are classified by the FDA as an interactive wound and burn dressing are approved under the PMA process as a class III, high-risk device and require clinical data to support their claims for use. These devices may be used as a long-term skin substitute or a temporary synthetic

skin substitute. They actively promote healing by interacting directly or indirectly with the body tissues [13].

VII. Conclusions

New advances in the production of biomaterials and the culture of skin cells have permitted the production of bioengineered skin substitutes. These have provided improved therapeutic options for patients suffering from acute or chronic wounds, and offer the promise of new treatments. These improvements will lead to enhanced performance of engineered skin grafts and greater clinical efficacy as well.

REFERENCES

1. D Eisenbud, NF Huang, S Luke, M Silberklang. Skin substitutes and wound healing: current status and challenges. *Wounds*, *Volume: 16*, Issue 1, 2004, pp 2-17
2. C. Pham, J. Greenwood, H. Cleland, P. Woodruff, G. Maddern. Bioengineered skin substitutes for the management of burns: A systematic review, *Burns, Volume:* 33, 2007, pp 946– 957
3. AS Halim , TL Khoo, SJ Mohd Yussof . Biologic and synthetic skin substitutes: An overview, *Indian Journal of Plastic Surgery* , *Volume:* 43(Suppl), 2010, pp S23-S28.
4. RG Tompkins, JF. Burke *Alternative wound coverings*. In: DN Herndon, editor. Total burn care. Philadelphia, Saunders; 1996, p. 164
5. JT Shores, A Gabriel, S Gupta. Skin substitutes and alternatives: a review. *Advanced Skin Wound Care*. *Volume:* 20(9 Pt 1), 2007, pp. 493-508.
6. AO Paggiaro, C Isaac, G Bariani, M Mathor, MR Herson, MC Ferreira. Construção de equivalente dermo-epidérmico in vitro. *Revista Brasileira de Cirurgia Plástica Volume:* 22, Issue 3, 2007, pp 153-157.
7. PG Shakespeare. The role of skin substitutes burn injuries. *Clinics in Dermatology, Volume*: 23, 2005, pp 413-418
8. P. Kumar Classification of skin substitutes. *Burns, Volume:* 34, 2008, pp 148–149.
9. RL Sheridan, C Moreno. Skin substitutes in burns. *Burns, Volume:* 27, 2001, p 92.
10. JT Shores, A Gabriel, S Gupta. Skin substitutes and alternatives: a review. *Adv Skin Wound Care*, *Volume:* 20, 2007, pp 493–508.
11. M McKegney, I Taggart, MH Grant. The influence of crosslinking agents and diamines on the pore size, morphology and the biological stability of collagen sponges and their effect on cell penetration through the sponge matrix. *Journal of Materials Science: Materials in Medicine*, *Volume:* 12, 2001, pp 833–844.
12. C Nishi, N Nakajima, Y Ikada. In vitro evaluation of cytotoxicity of diepoxy compounds used for biomaterial modification. *J Biomedical Materials Research, Volume:* 29, 1995, pp 829-834.
13. UCare Clinical & Quality Management. Bioengineered skin substitutes. Policy Number: 2013M0011A, 2014

E. Vranić, Department of Pharmaceutical Technology, Faculty of Pharmacy, University of Sarajevo, Zmaja od Bosne 8, 71 000 Sarajevo, Bosnia and Herzegovina (phone: 387-33-586-176; e-mail: evranic@yahoo.com).

Determination of gender and age specific differences in total iron levels in human serum using a spectrophotometric method

I. Tahirovic[1], A. Boloban[1], S. Ibragic[1], H. Dzudzevic-Cancar[2], J. Toromanovic[3], O. Lepara[4], A. Ajanovic[5], M. Dizdar[1]
[1] Faculty of Science, Department of Chemistry, University of Sarajevo, Zmaja od Bosne 35, 71000 Sarajevo, Bosnia and Herzegovina
[2]Faculty of Pharmacy, Department of Chemistry, University of Sarajevo, Zmaja od Bosne 8, 71000 Sarajevo, Bosnia and Herzegovina
[3]University of Bihać, School of Medical Studies, Žegarska aleja bb, 77000 Bihać, Bosnia and Herzegovina
[4]Department of Physiology, School of Medicine, University of Sarajevo, Čekaluša 90, 71000 Sarajevo, Bosnia and Herzegovina
[5]University of Sarajevo, Veterinary Faculty in Sarajevo, Zmaja od Bosne 90, 71000 Sarajevo, Bosnia and Herzegovina

Abstract - **Despite being present in trace amounts, iron is required for a number of complex metabolic processes that are indispensable to human life. As a part of the haemoglobin molecule, it has a fundamental role in the transportation of oxygen. It is required for haematopoiesis, production of enzymes, proper functioning of the immune system and other essential metabolic reactions. The aim of this study was to determine the total iron content in human serum samples of 500 individuals classified into groups based on gender and age. For that purpose we used a spectrophotometric method and the Iron Flex reagent. The method is based on measuring the absorbance of the blue coloured Fe(II)-feren complex at 600 nm. The obtained results are in line with expectations. The serum iron concentrations (SICs) for men were in the interval 11.52-25.30 µmol/l, whereas the range for women was lower, 9.00-20.16 µmol/l. In the age groups 20-40 years (y.), 40-60 y. and >60 y., women had significantly lower levels of serum iron than men. Also, SICs in postmenopausal women (age >60 y.) were statistically significantly lower than SICs of younger women (age ≤20 y.), and SICs in pre-/postmenopausal women (age 40-60 y.) were statistically significantly lower than those in younger women. Statistic analysis performed by Student's t test and by one way ANOVA shows significantly differences between the serum iron levels in the groups of interest.**

Keywords – **serum iron, spectrophotometric method, feren complex**

1. INTRODUCTION

Iron is involved in a wide range of metabolic processes, however it cannot be synthesized in the human body and sufficient daily amounts must be obtained from food. It is being recycled which is an important step in its rationalization. The daily intake must be in accordance with physiological requirements, for children that is 10-15 mg/day, for adolescents and men 5-10 mg/day and for women 14-28 mg/day. Ascorbic, lactic and citric acid as well as gastric acid and meat elevate the absorption of iron, whereas other factors such as dietary fibres, calcium, phosphor and polyphenols decrease its absorption.

Most of the iron in the body is present in the erythrocytes as haemoglobin (60-70%), ca. 20-30% is stored in the reticuloendothelial system, 3-5% in myoglobin and the rest is incorporated in different enzymes such as the catalase, peroxydase and cytochrome. Haemoglobin is composed of four units, each containing one heme group and one protein chain. The four iron atoms can be fully loaded with oxygen thus facilitating its transport from the lungs via the blood vessels to all cells throughout the body. After unloading the oxygen, haemoglobin via α-amino group of N-terminal ends of every globin chain binds carbon dioxide, which is then transported back to the lungs from where it gets exhaled. The link between oxygen and iron is strengthened by the multiple effects of their metabolism. An example that depicts that is genetic anemia where the deficiency of metabolic oxygen increases the iron absorption even in cases of normal or excessive iron levels [1].

Myoglobin and cytochromes, further oxygen storage proteins, contain one heme unit and one globin chain. Cytochromes act as electron carriers supporting the energy production within the cell and are not capable of reversible loading and unloading of oxygen. Cell growth and differentiation, DNA synthesis, signal controlling in some neurotransmitters, the proper functioning of the immune system are further physiological processes where iron play a valuable role.

In the liver, spleen and bone marrow, iron is reversibly stored as ferritin and hemosiderin, whereas transferrin is a protein responsible for its transport between different compartments in the body. It is the amount of transferrin in blood that determines the total iron binding capacity (TIBC). Normally, only one part of the serum transferrin is bound to iron, while the other part is free and related to the unsaturated iron binding capacity.

The normal reference range of serum iron for men is 14-27 µmol/l, whereas for women that range is 10-15% lower and varies between 12,5-25 µmol/l. Iron deficiency is estimated to impact more than 1.6 billion individuals worldwide, affecting child, maternal, and perinatal mortality [2]. In general, the main causes for iron deficiency are increased iron requirements, inadequate iron absorption and insufficient intake. Numerous physiologic states require additional iron supplies. Worldwide, the highest prevalence

of iron deficiency is found in infants, children, adolescents, and women of childbearing age, especially pregnant women. Currently, there is no consensus regarding the optimum iron supplementation during pregnancy. The conclusion of a recent study that included Mediterranian women with iron stores close to deficit was that daily doses of iron between 60 and 100 mg appear to be the most beneficial for the health of mother and child [3]. Another study suggests that high iron intake during pregnancy increases the risk of gestational diabetes mellitus (GDM) especially in women who are not anaemic in early pregnancy and who are at increased risk of GDM [4].

Newborns and babies have bigger iron needs than children and those may not be covered at all times. During the first two months of life, haemoglobin concentration falls because of the improved oxygen situation in the newborn infant compared with the intrauterine foetus, which is why iron is redistributed to iron stores. Premature and low birth-weight infants needs are in a less favourable situation and have even higher iron requirements. Acute or chronic blood loss such as during menstrual bleeding, malign diseases, hemorrhagic ulcers or blood donations can lead to iron deficiency which must be compensated either by iron supplementation or by increasing the dietary intake of iron. Anemia is one of the most frequent complications in many diseases, ulcerative colitis being one of them [5]. Blood donation is associated with decreased iron stores in blood donors which may affect the development of physiological functions and overall health. Previous studies reported a wide variation in the prevalence of iron deficiency in the population of blood donors (1% to 62%). A recent study however obtained iron deficiency prevalence in blood donors over higher risk groups like children, being higher in female and repetitive donors [6].

Particular emphasis on improving the bio-availability of the dietary iron is especially welcome. It should be noted that iron from meat and fish is absorbed twice as fast as from plants. The amount of iron that can be absorbed from food depends on all nutrients that are taken in during a meal. Vitamin C increases the absorption of iron, while polyphenols and calcium present in coffee, tea and dairy products decrease it. Symptoms of iron deficiency include tiredness, pale skin, insomnia, the syndrome of restless legs, impaired intellectual function, slow cognitive and social development during childhood, breathlessness, loss of appetite and frequent infections.

2. MATERIALS AND METHODS

A. Materials

IRON Flex reagent cartridge Cat. No. DF85, IRON Calibrator Cat. No. DC85, Quality Control Materials.

B. Samples

Human serum samples of 500 individuals from the town of Konjic and the nearby areas, classified into groups according to gender (213 male, 287 female) and age (≤20, 20-40, 40-60, and >60 years). Preparation of samples: between 8 a.m. - 10 a.m. blood samples were collected by venipuncture. It should be noted that serum iron levels have a circadian rhythm. The lowest serum iron concentrations are observed at 8 a.m., and the highest at 2 p.m. [7]. Blood stored in sterile test tubes was centrifuged (Eppendorf centrifuge) in order to obtain serum. Ready serum is put into the instrument Dimension RxL Max by Siemens.

C. Methods

The principle of this method is as follows:

$$Fe^{3+} - transferrin \rightarrow Fe^{3+} + transferrin$$

$$2Fe^{3+} + ascorbic\ acid \rightarrow 2Fe^{2+} + dehydroascorbic\ acid + 2H^{+}$$

$$Fe^{2+} + 3Feren \rightarrow Fe^{2+} - Feren\ complex\ (absorbance\ at\ 600\ nm)$$

Fe^{2+} creates a blue coloured complex with the disodium salt of the 5,5'-(3-(2-pyridyl)-1,2,4-triazine-5,6-diyl)-bis-2-furansulfonic acid, which is named Feren.

IRON Flex reagent cartridge is stable until the date of expiry at the temperature of 2-8 °C. The working temperature of the instrument is 37 °C; with two wavelengths: 600 and 700 nm. Taking the sample, dosing the reagents, mixing, separation and printing the results is all completed automatically by the instrument Dimension system. Results are also being automatically converted into concentration values expressed in µmol/l and printed out.

3. RESULTS AND DISCUSSION

In accordance with previous literature findings and studies, our results indicate that men have higher serum iron levels than women (18.41±6.89 µmol/l in comparison to 14.58±5.58 µmol/l, $p^{***}<0,001$; Student's t test) (Table 1):

Table 1 Mean serum iron concentrations in men and women

Gender	Number of samples	Mean serum iron concentration (μmol/l ± SD)
Male	213	18.41 ± 6.89
Female	287	14.58 ± 5.58***

*** - $p < 0.001$, Student's t test.

The mean iron concentration of all 500 human serum samples is 16.26±6.51 μmol/l within the interval 9.74-22.77 μmol/l. The serum iron concentration for men was in the range between 11.52 μmol/l and 25.30 μmol/l, whereas the range for women was lower, between 9.00 μmol/l and 20.16 μmol/l.

Mean serum iron concentrations in men and women aged 20-40, 40-60, and >60 years (y.) are presented in Table 2:

Table 2. Mean serum iron concentrations in men and women (age 20-40, 40-60, and >60 y.)

Gender	Age (y.)	Number of samples	Mean serum iron concentration (μmol/l ± SD)
Male	20-40	65	19.00 ± 6.50
Female		98	15.02 ± 5.67**
Male	40-60	76	18.63 ± 6.88
Female		96	14.02 ± 4.83***
Male	>60	48	18.52 ± 7.36
Female		53	13.24 ± 5.64**

** - significantly lower than iron level of male group ($p<0.01$, one way ANOVA).

*** - significantly lower than iron level of male group ($p<0.001$, one way ANOVA).

Also, the results showed that serum iron concentrations in postmenopausal women (age >60 y.) were statistically significantly lower in comparison to those of younger women (age ≤20 y., interval 2-20 y., mean 12.35±6.93 y.) (Table 3). In the same Table, it is presented that serum iron concentrations in pre-/postmenopausal women (age 40-60 y.) were statistically significantly lower than in younger women:

Table 3. Mean serum iron concentrations in younger (≤20 y.), postmenopausal (>60 y.), and pre-/postmenopausal (40-60 y.) women

Gender/(Age, y.)	Number of samples	Mean serum iron concentration (μmol/l ± SD)
Female (≤20)	40	16.60 ± 6.04
Female (>60)	53	13.24 ± 5.64**
Female (40-60)	96	14.02 ± 4.83*

** - significantly lower than iron levels of younger women ($p<0.01$, one way ANOVA).

* - significantly lower than iron level of younger women ($p<0.05$, one way ANOVA).

The results also showed that serum iron concentrations in adolescent male group (age 20-40 y.) were statistically significantly higher in comparison to those of the younger males (age 2-20 y., mean 12.21±6.43 y.) (Table 4):

Table 4. Mean serum iron concentrations in different age groups of men

Gender/(Age, y.)	Number of samples	Mean serum iron concentration (μmol/l ± SD)
Male (≤20)	24	15.87 ± 6.84
Male (20-40)	65	19.00 ± 6.50*

* - significantly higher than iron level of younger group of men ($p<0.05$, one way ANOVA).

The reference range for serum iron measured by the same method on the instrument Dimension RxL Max is: 9-30.4 μmol/l for women and 11.6-31.3 μmol/l for men. There are numerous factors that influence the reference range and can be classified into three main groups: genetic, endogenous and exogenous.

In praxis, iron deficiency is more common than increased serum iron levels. While interpreting the serum iron concentration, it is important to take into account all the factors that could influence the results. Patients who are taking oral iron supplements should analyse their iron serum levels 10 days after completing the therapy. The period for intravenous iron supplements is shorter and lasts three days, while intramuscular supplements demand a period of a month to pass in order to acquire reliable results [8]. The subjects included in this research were informed about these statements, and the specimens collected required a period of time after iron therapy. Women during the menstrual cycle were excluded from the study. Recent studies have shown potentially harmful effects of intravenous iron supplements taken with vitamin C. During the therapy, vitamin C reduces Fe^{3+} into Fe^{2+}, a form which can generate free radicals and oxidative stress [9].

Apart from menstruation, women also lose iron during both pregnancy and lactation. During pregnancy the blood volume increases, which is why both mother and foetus have additional iron needs. Iron deficiency often affects old people due to their decreased production of hydrochloric acid, which takes part in the conversion of Fe^{2+} into Fe^{3+}. Surgeries and hemorrhagic injuries can lead to the state of anaemia. Various diseases and inadequate iron absorption can be further reasons for iron deficiency. In contrast, serum iron levels can be increased by the acetylsalicylic acid, chloramphenicol, oral contraceptives, multivitamins and chemotherapeutic agents. The serum iron concentration depends on several factors including the iron absorption from the intestines, its storage in the intestines, liver, spleen and bone marrow, the degradation and synthesis of haemoglobin.

IV. CONCLUSIONS

The human serum iron concentrations of analysed individuals from the town of Konjic and the nearby areas are within the reference interval by the same method on the instrument Dimension RxL Max by Siemens.

The serum iron levels of the male individuals is close to the reference interval, while the serum iron levels of female individuals is within that reference interval.

Men have higher serum iron levels than women and there is a statistically significant difference between the mean serum iron levels in the groups of interest (20-40, 40-60, and >60 y.).

Also, the serum iron concentrations in postmenopausal (>60 y.) and pre-/postmenopausal (40-60 y.) women were statistically significantly lower in comparison to those of younger (≤20 y.) women.

The results also showed that serum iron concentrations in adolescent male group (20-40 y.) were statistically significantly higher in comparison to those of the younger males (2-20 y.).

REFERENCES

1. C. F. M. Gaudin, C. J. Grigg, L. A. Arrieta, M.E.P. Murphy, Unique Heme-Iron Coordination by the Hemoglobin Receptor IsdB of Staphylococcus aureus, *Biochem*, Volume: 50, Issue: 24, 2011, pp. 5443-5452.
2. K. A. Grimm, K. M. Sullivan, D. Alasfoor, I. Parvanta, A. J. Suleiman, M. Kaur, F. O. Al-Hatmi, L. J. Ruth, Iron-fortified wheat flour and iron deficiency among women. *Food Nutr Bull*, Volume: 33, Issue: 3, 2012, pp 180-185.
3. B. Ribot, N. Aranda, M. Giralt, M. Romeu, A. Balaguer, V Arija, Effect of different doses of iron supplementation during pregnancy on maternal and infant health, *Ann Hematol*, Volume: 92, Issue: 2, 2012, pp. 221-229.
4. A. Helin, T Kinnunen. I., J. Raitanen, S. Ahonen, S. M. Virtanen, R. Luoto, Iron intake, haemoglobin and risk of gestational diabetes: a prospective cohort study. *BMJ Open*, Volume: 2, Issue: 5, 2012.
5. E. Krzesiek, A. Flis, B. Iwańczak, Frequency of anemia in ulcerative colitis in children. *Pol Merkur Lekarski Volume*: 33, Issue: 195, 2012, pp 138-142.
6. C. Y. Mantilla-Gutiérrez, J. A. Cardona-Arias, Iron deficiency prevalence in blood donors: a systematic review, 2001-2011. *Rev Esp Salud Publica*, Volume: 86, Issue: 4, 2012, pp 357-369
7. B. Straus, A. Stavljenic-Rukavina, F. Plavsic, Analitičke tehnike u kliničkom laboratoriju, Zagreb Medicinska naklada, 1997, at: URL: <http://www.healthbosnia.com/dijagnostika/biohemija/krv.htm > (accessed: March, 2012)
8. F. Cetinic, E. Suljevic, Metodološko uputstvo u biohemijsko-laboratorijskoj dijagnostici, Sarajevo, 1991, at: URL: <http://www.healthbosnia.com/dijagnostika/biohemija/krv.htm > (accessed: March, 2012)
9. D. Cakaric, Primjena cikličke voltametrije u određivanju antioksidativne aktivnosti bioloških uzoraka, Zagreb, 2009, at: URL: <www. bib.irb.hr/datoteka> (accessed: April, 2012)

Dr. Sc. Ismet Tahirović, Associate Professor
University of Sarajevo, Faculty of Science, Department of Chemistry
Zmaja od Bosne 35, 71 000 Sarajevo
Bosnia and Herzegovina
Phone: ++387 33 279 905; ++387 61 836 001
Fax: ++387 33 649-359;
E-mail: itah@pmf.unsa.ba
ismet_tahirovic@yahoo.com

PRACTICES THE DIFFERENT CELLS TYPES LIKE TARGET GENOTOXIC ENDPOINT IN MICRONUCLEUS ASSEY

Velickova, N., Milev, M., Nedeljkovik, B., Gorgieva, P.

Faculty of medical science

University "Goce Delcev" – Stip R.Macedonia

Apstract:

Introduction: The toxicological relevance of the micronucleus (MN) assey is well defined: it is a multi-target genotoxic endpoint, assessing not only clastogenic and aneugenic events but also some epigenetic effects, which is simple to score, accurate, applicable in different cell types. Scoring of micronuclei can be performed relatively easily and on different cell types relevant for human biomonitoring: lymphocytes, fibroblasts and exfoliated epithelial cells. Aims of the study: To indicate the importance of the application of micronucleus test as standardized cytogenetic method as an important biomarker in detecting the impact of ionizing radiation on the entire genetic material in occupationally exposed health care workers. Matherial and methods: The study include health professionals who are directly and on daily basses exposed to ionizing radiation as physical agents and a control group that represents young and healthy population that is not exposed to any physical and chemical agents. Results. The major advantage of lymphocytes is that they are primary cells, easy to culture in suspension. The choice between whole blood and isolated lymphocytes depends upon the question addressed. The most important differences among the protocols are the hypotonic treatment (critical in particular for image analysis), fixation of the cells (dependent on laboratory preferences) and the final slide preparation. Conclusion: In recent years the in vitro micronucleus test has become an attractive tool for genotoxicity testing because of its simplicity of scoring and wide applicability in different cell types but the lymphocytes are the most reperesentative cells for this kind of research.

Keywords: cells cultures, lymphocytes, micronucleus, genotoxicology, radiation

Introduction: The in vitro micronucleus assay is a genotoxicity test for the detection of micronuclei (MN) in the cytoplasm of interphase cells. Micronuclei may originate from acentric chromosome fragments (i.e. lacking a centromere), or whole chromosomes that are unable to migrate to the poles during the anaphase stage of cell division. The assay detects the activity of clastogenic and aneugenic chemicals (Kirsch-Volders, M. (1997), Parry, J.M. and Sors, A. (1993), in cells that have undergone cell division during or after exposure to the test substance. The addition of cytoB prior to the targeted mitosis allows for the identification and selective analysis of micronucleus frequency in cells that have completed one mitosis because such cells are binucleate (Fenech, M. and Morley, A.A. (1985), Kirsch-Volders and all.(2000). The toxicological relevance of the micronucleus (MN) assey is well defined: it is a multi-target genotoxic endpoint, assessing not only clastogenic and aneugenic events but also some epigenetic effects, which is simple to score, accurate, applicable in different cell types. In addition, it is predictive for cancer, amenable for automation and allows good extrapolation for potential limits of exposure or thresholds and it is easily measured in experimental both *in vitro* and *in vivo* systems. Furthermore, the importance of adequate design of protocols is highlighted and new developments. We address future research perspectives including the possibility of a combined primary 3D human skin and primary human whole blood culture system, and the need for adaptation of the in vitro MN assays to assess the genotoxic potential of new materials, in particular nanomaterials. So many studies indicate that the use of cell lines can be recommended, it should be underlined that most of the cell lines are deficient in p53 or apoptosis controlling genes that lead to higher frequencies of MN and is thought to lead to positive results that are not confirmed in vivo in some cases. In contrast, for mechanistic studies, the use of cell lines can be very useful. The OECD guideline is not restricted to synchronised cells since it aims at maximising the probability of detecting an aneugen or clastogen acting at any stage of the cell cycle; therefore, a sufficient number of cells should be treated with the test substance during all the phases of their cell cycle (Volders and all., 2011). Scoring of micronuclei can be performed relatively easily and on different cell types relevant for human biomonitoring: lymphocytes, fibroblasts and exfoliated epithelial cells, without extra in vitro cultivation step. MN observed in exfoliated cells are not induced when the cells are at the epithelial surface, but when they are in the basal layer. An ex vivo/ in vitro analysis of lymphocytes in the presence of cytochalasin-B (added 44 hours after the start of cultivation), an inhibitor of actins, allows to distinguish easily between mononucleated cells which did not divide and binucleated cells which completed nuclear division during in vitro culture. Indeed, in these conditions the frequencies of mononucleated cells provide an indication of the

material in occupationally exposed health care workers. The micronucleus test (MNT) determines the frequency of the radiation induced micronuclei (MN) in peripheral blood lymphocytes, which could serve as an indicator of intrinsic cell radiosensitivity. After mutagen attack, MN in interphase cells are formed by mitotic loss of acentric fragments or chromosomes which are not incorporated in the daughter cell nuclei (Fenech, M. and Neville, S. (1992).

Matherial and methods: The study include health professionals who are directly and on daily basses exposed to ionizing radiation as physical agents and a control group that represents young and healthy population that is not exposed to any physical and chemical agents. By applying the micronucleus test, quantitative and qualitative analysis are performed on binuclear lymphocytes and micronucleus as reliable indicators of possible chromosomal damage in the cells. For the scoring of micronuclei the following criteria were adopted from Fenech et all, (2003): the diameter of the MN should be less than one-third of the main nucleus, MN should be separated from or marginally overlap with main nucleus as long as there is clear identification of the nuclear boundary, MN should have similar staining as the main nucleus. Whole blood treated with an anti-coagulant (e.g. heparin), or separated lymphocytes, are cultured at 37°C in the presence of a mitogen e.g. phytohaemagglutinin (PHA) prior to exposure to the test substance and cytoB.

Results. The number of micronucleus in the control group is in the normal reference values. The major advantage of lymphocytes is that they are primary cells, easy to culture in suspension. The choice between whole blood and isolated lymphocytes depends upon the question addressed. The most important differences among the protocols are the hypotonic treatment (critical in particular for image analysis), fixation of the cells (dependent on laboratory preferences) and the final slide preparation. These different parameters significantly influence cell density and cytoplasm preservation. A detailed protocol for isolated lymphocyte and whole blood culture MN assays was recently published and included detailed scoring criteria validated and recommended by protocol.

Conclusion: In recent years the in vitro micronucleus test has become an attractive tool for genotoxicity testing because of its simplicity of scoring and wide applicability in different cell types. Because of its reliability and easy performance, MN asseys could be a promising method for evaluating normal tissue morbidity in cancer patients during radiotherapy with results yielded in less than 2 weeks.

material in occupationally exposed health care workers. The micronucleus test (MNT) determines the frequency of the radiation induced micronuclei (MN) in peripheral blood lymphocytes, which could serve as an indicator of intrinsic cell radiosensitivity. After mutagen attack, MN in interphase cells are formed by mitotic loss of acentric fragments or chromosomes which are not incorporated in the daughter cell nuclei (Fenech, M. and Neville, S. (1992).

Matherial and methods: The study include health professionals who are directly and on daily basses exposed to ionizing radiation as physical agents and a control group that represents young and healthy population that is not exposed to any physical and chemical agents. By applying the micronucleus test, quantitative and qualitative analysis are performed on binuclear lymphocytes and micronucleus as reliable indicators of possible chromosomal damage in the cells. For the scoring of micronuclei the following criteria were adopted from Fenech et all, (2003): the diameter of the MN should be less than one-third of the main nucleus, MN should be separated from or marginally overlap with main nucleus as long as there is clear identification of the nuclear boundary, MN should have similar staining as the main nucleus. Whole blood treated with an anti-coagulant (e.g. heparin), or separated lymphocytes, are cultured at 37°C in the presence of a mitogen e.g. phytohaemagglutinin (PHA) prior to exposure to the test substance and cytoB.

Results. The number of micronucleus in the control group is in the normal reference values. The major advantage of lymphocytes is that they are primary cells, easy to culture in suspension. The choice between whole blood and isolated lymphocytes depends upon the question addressed. The most important differences among the protocols are the hypotonic treatment (critical in particular for image analysis), fixation of the cells (dependent on laboratory preferences) and the final slide preparation. These different parameters significantly influence cell density and cytoplasm preservation. A detailed protocol for isolated lymphocyte and whole blood culture MN assays was recently published and included detailed scoring criteria validated and recommended by protocol.

Conclusion: In recent years the in vitro micronucleus test has become an attractive tool for genotoxicity testing because of its simplicity of scoring and wide applicability in different cell types. Because of its reliability and easy performance, MN asseys could be a promising method for evaluating normal tissue morbidity in cancer patients during radiotherapy with results yielded in less than 2 weeks.

Refferences:

1. Biete, A., Valduvieco, I., Rovirosa, A., Farrus, B., Casas, F., and Conill, C. Whole abdominal radiotherapy in ovarian cancer. *Rep Prac Oncol Radiother*. 2010; 15: 27–30

2. Elyan, S.A. et al. The intrinsic radiosensitivity of normal and tumor cells. *Int J Radiat Biol*. 1998; 73: 409–413

3. Fenech, M. and Morley, A.A. (1985), Solutions to the kinetic problem in the micronucleus assay, Cytobios., 43, 233-246.

4. Fenech, M. and Neville, S. (1992): Conversion of excision-repairable DNA lesions to micronuclei one cell cycle in human lymphocytes. *Environ Mol Mutagen*. 1992; 19: 27–36

5. Kirsch-Volders, M. (1997), Towards a validation of the micronucleus test. Mutation Res., 392, 1-4. (2) Parry, J.M. and Sors, A. (1993), The detection and assessment of the aneugenic potential of environmental chemicals: the European Community aneuploidy project, Mutation Res., 287, 3-15.

6. Kirsch-Volders, M., Sofuni, T., Aardema, M., Albertini, S., Eastmond, D., Fenech, M., Ishidate, M. Jr, Lorge, E., Norppa, H., Surralles, J., von der Hude, W. and Wakata, A. **(2000), Report** from the In Vitro Micronucleus Assay Working Group, Environ. Mol. Mutagen., 35, 167-172.

7. Micheline Kirsch-Volders, Ilse Decordier, Azeddine Elhajouji1, Gina Plas,Marilyn J. Aardema2 and Michael Fenech (2011):Mutagenesis vol. 26 no. 1 pp. 177–184, 2011 doi:10.1093/mutage/geq068 REVIEW In vitro genotoxicity testing using the micronucleus assay in cell lines, human lymphocytes and 3D human skin models

8. RefBurnet, N.G., Nyman, J., Turesson, I., Wurm, R., Yarnold, J.R., and Peacock, J.H. The relationship between cellular radiation sensitivity and tissue response may provide the basis for individualizing radiotherapy schedules. *Radiother Oncol*. 1994; 33: 228–238

9. Peacock, J., Ashton, A., Bliss, J. et al. Cellular radiosensitivity and complication risk after curative radiotherapy. *Radiother Oncol*. 2000; 55: 173–178

10. West, C.M., Davidson, S.E., Elyan, S.A. et al. Lymphocyte radiosensitivity is a significant prognostic factor for morbidity in carcinoma of the cervix. *Int J Radiat Oncol Biol Phys*. 2001; 51: 10–15

Nevenka Velickova is the First author, Facukty of medical science, University Goce Delcev – Stip, R. Macedonia, Krste Misirkov, 10 a, Stip, R.Macedonia (phone: 032550436, nevenka.velickova@ugd.edu.mk)

Localization and 2D imaging of ST elevation myocardial infarction using software differentiation

Vildana Huskić [1], Almir Vardo[2], Edin Begić[1], Emina Hrvat[1], Lejla Gurbeta[2], Mirna Džubur[1], Almir Badnjević[3], Armin Dajić[2] Azra Kadić[1]

[1] Faculty of Medicine, University of Sarajevo, BiH
[2] Faculty of Electrical Engineering, University of Sarajevo, BiH
[3] Verlab, Sarajevo, BiH

Abstract—**The key diagnostic procedure in patients with suspected acute coronary syndrome is recording of a standard 12-lead electrocardiogram (ECG) with a device that detects and records the heart's electrical activity (electrocardiograph). Localization of myocardial infarction and its developmental stages are indicated by: T wave, ST-segment and QRS complex (Q wave). T-wave inversion shows the zone of reduced blood supply (ischemia), ST segment (elevation or depression) points at the ischemic injury- lesion, and a deep Q wave indicates a developed infarction. Using these characteristics, a software application is developed. The application aim is to enable effective monitoring of patients with urgent acute conditions as well as timely therapeutic effect. The software application is developed in VisualStudio2010 and it provides a practical and clear user interface. It also detects changes related to the QRS complexes, P and T waves (using Wavelet transformation and various filters for eliminating noise), and it displays the location of myocardial infarction in a 2D view of the heart.**

Keywords— **Acute myocardial infarction, ST-elevation, software application, 2D.**

I. Introduction

Cardiovascular diseases are one of the most important health challenges in the world. Acute myocardial infarction, is one of the manifestations of ischemic heart disease, with stable/unstable angina pectoris, ischemic cardiomyopathy and sudden cardiac death caused by ischemia. Myocardial infarction represents a major cause of death and disability worldwide. (1) The first clinical descriptions of myocardial infarction are only around 100 years old. In 1959 was set up the first working group by the World Health Organization (WHO) to define the disease ~~–a~~cute myocardial infarction (AMI)" in order to study disease prevalence. Later WHO described AMI as a combination of: typical symptoms, enzyme rise and a typical ECG pattern. ECG was still mainly based diagnosis. In that definition of IM implied that any necrosis in the context of myocardial ischemia can be characterized as IM. (2)

The heart, like any other muscle in the body, constantly requires its own supply of nutrient and oxygen, which is delivered by two large, branching coronary arteries. If one of these arteries or branches becomes blocked suddenly, arises „cardiac ischemia". This occlusion is most commonly due to rupture of a vulnerable atherosclerotic plaque. If the flow is completely broken or severely reduced more than a few minutes, part of the heart muscle dies. This is a heart attack, otherwise known as a myocardial infarction. (3)

Initial care of the patient with suspected acute MI should include the early and simultaneous achievement of four goals: confirmation of the diagnosis clinical history, biomarker measurement (like creatine kinase-MB (CK-MB) fraction and the troponin levels); ECG confirmation (which is the most important tool in the initial evaluation and triage of patients with suspected myocardial infarction-confirmatory of the diagnosis in approximately 80% of cases); relief of ischemic pain and assessment of the hemodynamic state and correction of abnormalities that may be present. (4)

The electrocardiogram (ECG) is the most common non-invasive method of monitoring cardiac activity and a diagnostic tool that is routinely used to assess the electrical and muscular functions of the heart.

The heart is a two stage electrical pump and electrodes placed on the skin can measure the heart's electrical activity. The ECG machine that records this electrical activity is called an electrocardiograph; while the obtained printed view of these recordings is called an electrocardiogram. The electrocardiograph can measure the rate and rhythm of the heartbeat, as well as provide indirect evidence of blood flow to the heart muscle.(5)

The ECG waves are recorded on special graph paper that is divided into 1 mm^2 grid-like boxes. The ECG paper speed is ordinarily 25mm/sec. As a result, each 1 mm (small) horizontal box corresponds to 0.04 second (40 ms), with heavier lines forming larger boxes that include five small boxes and hence represent 0.20 sec (200 ms) intervals. Each large box is therefore only 0.10 sec and each small box is only 0.02 sec. In addition, the heart rate appears to be one-half of what is recorded at 25 mm/sec paper speed, and all of the ECG intervals are twice as long as normal. (6)

Vertically, the ECG graph measures the height (amplitude) of a given wave or deflection, as 10 mm (10 small

boxes) equals 1 mV with standard calibration. On occasion, particularly when the waveforms are small, double standard is used (20 mm equals 1 mV). When the wave forms are very large, half standard may be used (5 mm equals 1 mV). Paper speed and voltage are usually printed on the bottom of the ECG.(7) A standardized system has been developed for the electrode placement for a routine ECG. Ten electrodes are needed to produce 12 electrical views of the heart. An electrode lead, or patch, is placed on each arm and leg and six are placed across the chest wall (precordial leads). The signals received from each electrode are recorded.

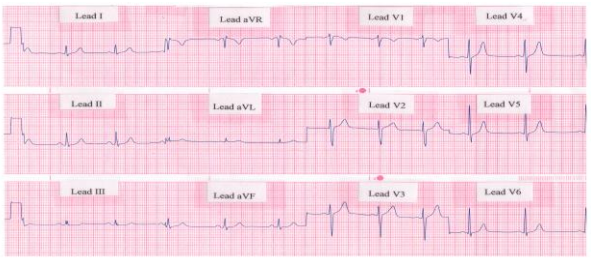

Fig. 1 Rhythm strip showing a normal 12-lead ECG

Electrode leads on the chest wall are able to detect electrical impulses that are generated by the heart. Multiple leads provide many electrical views of the heart. By interpreting the tracing, the physician can learn about the heart rate and rhythm as well as blood flow to the ventricles (indirectly). A 12 lead ECG is obtained from the information collated from 10 electrode cables. Using a central reference point, the ECG machine is able to calculate the required information to produce 12 different electrical views of the heart. (8) This is achieved by two different methods: Three bipolar leads I, II & III using 1 positive & 1 negative lead.

Three unipolar leads (augmented leads & chest leads) using 1 positive electrode and calculating a notional central reference point (central terminal) within the heart. (aVR, aVL, aVF). Six precordial leads (V1, V2, V3, V4, V5, V6)

Table 1: ECG Manifestations of Acute Myocardial Ischemia

ST elevation	New ST elevation at the J-point in two contiguous leads with the cut-off points: ≥0.2 mV in men or ≥0.15 mV in women in leads V2–V3 and/or ≥0.1 mV in other leads
ST depression and T-wave changes	New horizontal or down-sloping ST depression ≥0.05 mV in two contiguous leads; and/or T inversion ≥0.1 mV in two contiguous leads with prominent R-wave or R/S ratio >1

Almost all transmural myocardial infarctions (defined as trasmural if they are extended through more than 50% of the thickness of the muscle wall) affect at least a part of the left ventricle and interventricular septum. Nearly 15-30% of myocardial infarctions that affect the posterior wall or the posterior wall and the septum are spanning over the wall of the right ventricle. However, isolated infarctions of the right ventricle are seen in only 1-3% of patients. Even in transmural infarctions, there is a narrow edge (-0,1mm) of live,subendocardially located myocardium, which is preserved because it gets oxygen and nutrients through diffusion from the ventricular lumen.

The posterior descending artery is formed from the right coronary artery in 90% of people. In those people, we can say that the right artery is dominant and here the following distribution of myocardial infarction is seen:

- Left anterior interventricular branch of left coronary artery (40-50%)- infarction affects the anterior wall of the left ventricle, anterior and apical area of the heart,
- Right coronary artery (30-40%)- infarction affects the posterior area of the left ventricle and septum, and sometimes the free wall of the right ventricle,
- Left circumflex branch of left coronary artery (15-20%)- infarction affects the lateral wall of the left ventricle, except the apex of the heart. (9)

As a result of normal vascularization of the heart, in case of left main coronary artery obstruction, the most difficult form of myocardial infarction occurs. Acute myocardial infarction due to left main coronary artery occlusion remains catastrophic and mostly fatal due to severe cardiogenic shock and arrhythmia. (10)

II. Materials and Methods

A. Materials

While creating this study, an ECG signal in digital form (The PTB Diagnostic ECG Database) was used, and as such, entered into a software solution. (11) Wavelet transformation for every ECG signal has been made in order to detect abnormalities, especially myocardial ischemia.

During the research, ECG examples of all types and subtypes of myocardial infarctions were used, regardless of gender and age of patients.

B. Methods

In order to detect myocardial ischemia and other irregularities in the ECG signal and to present them graphically, continuous (CWT) and fast wavelet transform are used. The algorithm works in two phases: QRS detection followed by localization of P and T wave.

ECG signal has variety of different frequency components. High frequencies are usually due to noise that is indispensable component of every real ECG signal. To reinforce QRS signal and to separate low-frequency P and T wave and high-frequency noise CWT transformation at 12Hz and inverse wavelet-transform is applied. CWT spectrum is further filtered with FWT transformation with the use of interpolation filters to delete frequency contents below 30Hz. Noise is eliminated from the rest of signal frequency spectrum by using thresholds and MINIMAX estimation. The reconstructed ECG contains only peaks with nonzero values on positions of the QRS complex. PQ junction point and J point are located by obtained peak limits.

After detection of the QRS complex, the intervals between them are processed in order to detect the P and T waves. Frequency CWT can be adjusted in the range of 1.5 to 4 Hz, along with the duration of the segment in order to better adapt to different morphologies of the QT interval. It allows adaptation to specific forms of T wave. An analogous procedure is applied to search for P waves to the PQ interval. CWT frequency spectrum of detection P wave is varied in the range 4-9Hz. (14)

Information of the number of channels, number of samples, sampling frequency, number of bits AD converter, WMV (units per millivolt), the duration of the signal, high signal value, minimum and maximum values of the signal, the number of beats (which corresponds to the total number of detected QRS complex, processing time, found the number of annotations and the mean value of BPM (beats per minute) are obtained. These information are used to detect irregularities in ECG signal. Myocardial ischemia is detected using its characteristic: ST elevation. Obtained information are presented graphically through developed user interface.

Table2: Leads indicating wall

Leads	Wall (AIM)	Possible artery
II, III, aVF	Inferior	RCA
V1, V2	Septal	LAD
V2-V4	Anterior	LAD
I, V5, V6, aVL	Lateral	Circumflex
V1, V2, (ST depression)	Posterior	RCA or CX
V1, RV4	Right Ventricle	RCA or CX

III. Results

In results we present case of patient with diagnosed acute anterior myocardial infarction with characteristic changes (ST elevation) on ECG.

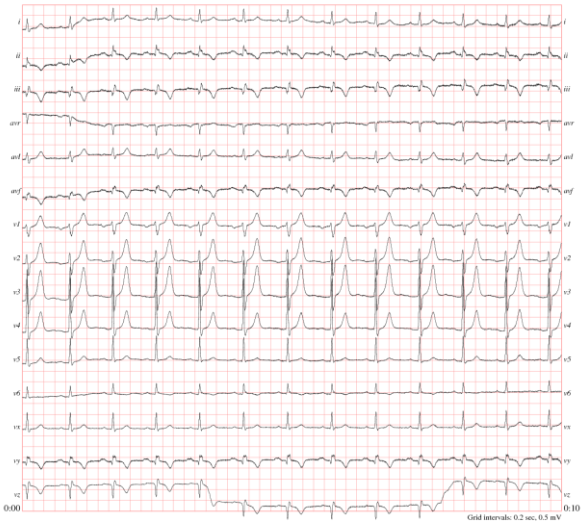

Fig. 2. ECG (anterior AIM)

After initiating program and entering certain leads, we get Fig 3. (lead V_1) and Fig. 4 (lead V_4) with specific picture showing heart in specific state. In left upper corner, there are presented all characteristics of signal that is analyzed. On the top menu, there can be set number of leads and all values related to that signal.

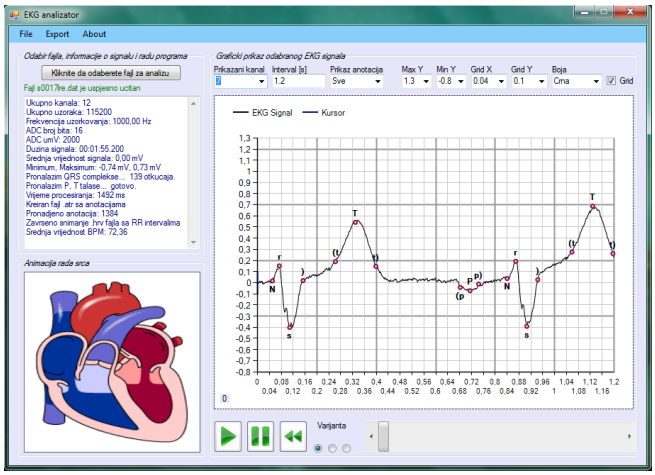

Fig. 3. Lead V_1

Fig. 4. Lead V_4

After clicking the Play button, animation starts and in right lower corner, there is showed animation of the hearts' activity what is accompanied by moving the cursor on graph.

When the program detects that it is a ECG with myocardial infarction, it is going to show picture like Fig 5. The program gives a warning that it is a myocardial infarction, and shows localization of its occurrence.

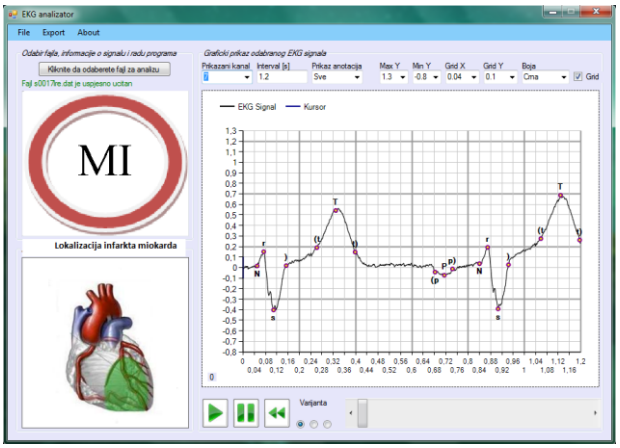

Fig. 5. Localization of AIM detected by application

IV. Discussion

Noninvasive imaging plays many roles in patients with known or suspected myocardial infarction, but this section concerns only its role in the diagnosis and characterization of infarction. The underlying rationale is that regional myocardial hypoperfusion and ischeamia lead to a cascade of events including myocardial dysfunction, cell death, and healing by fibrosis. Important imaging parameters are therefore perfusion, myocyte viability, myocardial thickness, thickening, and motion, and the effects of fibrosis on the kinetics of radiolabelled and paramagnetic contrast agents.

ECG is the most important non-invasive method of the diagnostic ECG protocol. In the diagnostic approach to a patient with acute pain in the chest, ECG divides the patients into those with an ST elevation and those without it. A high T wave on an ECG is a very early sign of myocardial infarction and the result of it is localization of hyperkalemia. Quickly following the high T wave, an ST elevation occurs as a result of the impaired electrical activity in the myocardium.

Also, in every diagnostic procedure there are some pitfalls that can influence on accuracy of diagnose. Common ECG pitfalls in diagnosing Myocardial infarction are:

-False positives: benign early repolarisation, pulmonary embolism, Brugada syndrome, peri/myocarditis, LBBB, Subarachnoid haemorrhage, Metabolic disturbances such as hyperkalaemia, Failure to recognize normal limits for J-point displacement, Lead transposition or use of modified Mason–Likar configuration, Cholecystitis (13)

-False negatives: Prior myocardial infarction with Q-waves and/or persistent ST elevation, Paced rhythm, LBBB.

ECG is extremely necessary for the localization of myocardial infarction. Assessment of necrosis localization, gives a lot of information about the further treatment of the patient, as well as the outcome. Involvement of coronary arteries, which supply the necrotic part, gives the doctor the ability to predict complications after myocardial infarction. The basis of treatment of myocardial infarction is reperfusion therapy (medication reperfusion with fibrinolytics, mechanical reperfusion-primary PCI and surgical reperfusion), which should start as soon as possible in patients with acute angina pain that lasts longer than 20 minutes and ST elevation $\geq$ 1 mm in two or more bipolar leads, or ST elevation in two or more precordial leads of the same region, or a new onset left bundle branch block. (12)

The success of reperfusion therapy is assessed on the basis of resolution of ST elevation (an indirect indicator of regression of ischemia) as well as the early large increase of

enzymes, which will be a reflection of the normalization of the flow through the coronary circulation.

Early complications of myocardial infarction are arrhythmias and conduction disturbances, heart medication chamber until cardiogenic shock and mechanical complications such as rupture of the left ventricular wall, interventricular septum rupture and dysfunction or rupture of papillary muscle.

The software solution, shown in this paper, is to help the doctor in the diagnosis of myocardial infarction, to show to the doctor a clear picture about the localization of infarction and to guide interventional cardiologists about the possibility of its localization, at the end to guide them in the cardiac catheterization. Early detection of infarction and treatment as soon as possible, but according to the given guidelines, improves prognosis and therapeutic efficacy of treatment.

The software solution needs to continue its development, and to take into account the variability of vascularization of the heart, and to complete with other diagnostic methods.

Commonly used imaging techniques in acute and chronic infarction are echocardiography, radionuclide ventriculography, myocardial perfusion scintigraphy (MPS), and magnetic resonance imaging (MRI). Positron emission tomography (PET) and X-ray computed tomography (CT) are less common. There is considerable overlap in their capabilities, but only the radionuclide techniques provide a direct assessment of myocardial viability because of the properties of the tracers used. Other techniques provide indirect assessments of myocardial viability, such as myocardial function from echocardiography or myocardial fibrosis from MRI.(13)

V. Conclusions

The correct analysis of the ECG requires knowledge, thoroughness and experience of doctors. It is essential in the evaluation of ECG to know the patient's age, gender, medications you take, blood pressure, and diagnosis. ECG is evaluated according to the established order and rules, that are already given.ECG is the most important noninvasive method of diagnosis of acute myocardial infarction, and because of that is irreplaceable, not only in primary, but also in other levels of the health system. Early diagnosis of myocardial infarction reduces the mortality of the same, and promotes the application of the therapy and improves the outcome for the patient. The software solution can certainly be of great help in the diagnosis of myocardial infarction localization, and it is an excellent solution in the learning process of students and other medical workers, on the issue, the most current topics of modern medicine- acute myocardial infarction.

REFERENCES

1. AhmadiA, KhaledifarA, SajjadiH, Soori H Relationship between risk factors and in-hospital mortality due to myocardial infarction by educational level: a national prospective study in Iran. [Online]. 2014. Available on: http://www.equityhealthj.com/content/13/1/116.
2. Thygesen K, Alpert J. S, Jaffe S.A, Simoons M. L, Chaitman B. R, White H. D, Treća univerzalna definicija infarkta miokarda. European Heart Journal (2012) 33, 2551-2567.
3. WebMD[Online]. 2014. Heart Attacks and Heart Disease. Available on:http://www.webmd.com/heart-disease/guide/heart-disease-heart-attacks
4. Reeder S.G, Kennedy H.L, Criteria for the diagnosis of acute myocardial infarction[Online]. Available on: http://www.uptodate.com/contents/criteria-for-the-diagnosis-of-acute-myocardial-infarction
5. Emedicinehealth (Online). 2014. Electrocardiogram. Available on:http://www.emedicinehealth.com/electrocardiogram_ecg/article_em.htm
6. Fundamentals of Electrocardiography Interpretation. Daniel E Becker, DDS. AnesthProg. 2006 Summer; 53(2): 53–64.
7. ECG tutorial: Basic principles of ECG analysis. Jordan M Prutkin (Online). Available on: http://www.uptodate.com/contents/ecg-tutorial-basic-principles-of-ecg-analysis
8. Libelli Medici. Elektrokardiografija u praksi.Lj. Baric. Volumen V. Zagreb 1976. Pliva
9. Kummar V., Abbas A., Fausto N., Mitchell N.R. Robinsove osnove patologije, 8 izdanje, DATA STATUS, Beograd, 2010.
10. Shigemitsu O1, Hadama T, Miyamoto S, Anai H, Sako H, Iwata E. Acute myocardial infarction due to left main coronary artery occlusion. Therapeutic strategy. Jpn J Thorac Cardiovasc Surg. 2002 Apr;50(4):146-51
11. Goldberger AL, Amaral LAN, Glass L, Hausdorff JM, Ivanov PCh, Mark RG, Mietus JE, Moody GB, Peng C-K, Stanley HE. PhysioBank, PhysioToolkit, and PhysioNet: Components of a New Research Resource for Complex Physiologic Signals. Circulation 101(23):e215-e220 [Circulation Electronic Pages; http://circ.ahajournals.org/cgi/content/full/101/23/e215]; 2000 (June 13).
12. Vrhovac B, JakšićB. ,Reiner Ž., Vucelić B. Interna medicina. Naklada Ljevak, Zagreb 2008.
13. Kristian Thygesen; Joseph S. Alpert; Harvey D. White; on behalf of the Joint ESC/ACCF/AHA/WHF Task Force for the Redefinition of Myocardial Infarction, Volume 50, Issue 22, November 2007.
14. Chesnokov Yuriy, *ECG Annotation C++ Library, http://www.codeproject.com/Articles/20995/ECG-Annotation-C-Library, Oct 2007.*

Vildana Huskić, Medicinski fakultet, Univerzitet u Sarajevu, Čekaluša 90, 71 000 Sarajevo, BiH (phone: 387-61-815-863; e-mail: wildana_huskic@hotmail.com)

Serum nitric oxide levels in patients with acute myocardial infarction with ST elevation (STEMI)

A.Badnjević[1], P.Kovačević[2], A.Badnjević[3], L.Gurbeta[3]

[1] Canton Hospital, Zenica, Bosnia and Herzegovina
[2] University hospital Banja Luka, Bosnia and Herzegovina
[3] Verlab Ltd Sarajevo, Medical Device Verification Laboratory, Sarajevo, Bosnia and Herzegovina

Abstract — **Reduced activity of nitric oxide (NO) is one of the first and most important signs of endothelial dysfunction and it is a common feature of many atherosclerosis risk factors. Many studies have shown that the values of NO in patients with acute myocardial infarction are reduced, which is not in accordance with the results of this research. The study included 80 patients, of which 40 patients with acute myocardial infarction with ST elevation (STEMI) who were treated in the Coronary Care Unit of the Department for Internal Diseases of Cantonal Hospital in Zenica in the period from 01 January 2014 to 01 June 2014. The control group consisted of 40 healthy subjects. All study subjects were evaluated for serum nitric oxide by Griess method. The results of this study show that the mean serum levels of NO in patients with STEMI were 26.7 qmol/l (26,7 +/- 12,9), while the mean serum NO concentrations of healthy population were 4.8 qmol/l. Statistical analysis of the obtained data shows that there is a statistically significant difference between the groups (p <0.05). The conclusion of the study is that patients with STEMI with associated risk factors such as hypertension, diabetes, hyperlipidemia, cigarette smoking, have significantly higher serum levels of NO in relation to the value of NO in healthy individuals.**

Keywords— **nitric oxide, STEMI**

I. Introduction

Nitric oxide (NO) is a product of the endothelium and plays an important role in the regulation of vascular tone of blood vessels, especially in the coronary circulation. Reduced activity of NO is one of the first and most important signs of endothelial dysfunction that is a common feature of many risk factors for atherosclerosis, such as aging, hyperlipidemia, diabetes and hypertension, which results in the formation of one of the forms of acute coronary syndrome. Lack of NO contributes to the weakening of vascular relaxation, platelet aggregation, stimulates proliferation of smooth muscle cells of blood vessels and the adhesion of leukocytes to the endothelium. Today, endothelial dysfunction can be considered as a manifestation of systemic syndrome that defines the cardiovascular morbidity and mortality. [1][2][3] The most common form of acute coronary syndrome is a myocardial infarction with ST segment elevation. According to the guidelines of the European Cardiac Society: stenocardia accompanied by J-point elevation in two or more consecutive leads of 2 or more mV in V1, V2 and/or V3, or 1 mV or more in other leads meets with the diagnostic criteria of STEMI. [4] The aim of the study was to determine the serum levels of NO in patients with STEMI infarction and to compare the obtained values with the values from subjects in the control group.

II. RESEARCH

A. Patients and Methods

The research was designed as a prospective study and it includes the period from 01 January 2014 to 01 June 2014. The study included 80 patients, of which 40 patients with acute myocardial infarction with ST segment elevation who were treated in the Coronary Care Unit of the Service of Internal Medicine of Cantonal Hospital in Zenica (study group) and 40 healthy individuals (control group). The diagnosis of STEMI was set on the basis of: medical history, ECG registrations and laboratory testing for troponin I in serum, echocardiographic findings, and enzymatic analysis (determination of nitric oxide using Griess method). Results were analyzed using standard statistical method (Student t test), and displayed in text and graphs. p values <0.05 were considered statistically significant. In addition, anthropological parameters (age and sex) of all subjects were examined. The results are shown textually and graphically.

B. Results

The study included 80 patients who were divided into two groups (STEMI and control groups). The group consisted of 40 patients with acute myocardial infarction with ST segment elevation; 31 men and 9 women. The mean age of the STEMI group was 62.7 +/- 10.8. The control group consisted of 40 healthy individuals, mean age 50.5 ± 40.8. The mean concentration of NO3 / NO2 levels in STEMI patients was 26.66 mmol/l. Table 1 shows the basic charac-

teristics (laboratory findings and history of the patient's current risk factors) of studied groups.

Table 1. Basic characteristics (laboratory findings and history of the patient's current risk factors) of studied groups.

Parameters	Study group
Age (years)	62,7 +/-10,8
Hypertension (%)	70,0
Diabetes mellitus (%)	22,5
Smoking (%)	45,0
Nitric oxide (qmol/l)	26,7 +/-12,9
Cholesterol (mmol/l)	5,67 +/-1,30
Triglycerides (mmol/l)	2,06 +/- 1,11
HDL-cholesterol (mmol/l)	0,93 +/- 0,31
LDL-cholesterol (mmol/l)	3,74 +/- 1,11

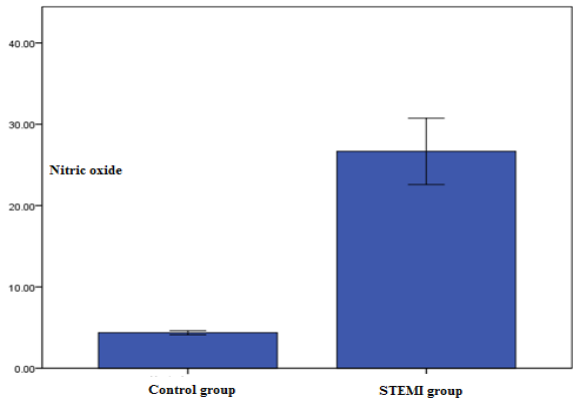

Fig1. Serum concentrations of nitric oxide in patients with myocardial infarction with ST segment elevation (study group) compared to the control, healthy group of subjects

Serum concentrations of nitric oxide in patients with myocardial infarction with ST segment elevation (study group) compared to the control, healthy group of subjects is given in Fig1. Using statistical test, Student's t test, it was found that there is a statistically significant difference between the values of serum NO in healthy individuals compared to patients from the STEMI group ($p < 0.05$).

Comparison between mean values of nitric oxide concentration in the serum of patients with acute myocardial infarction with ST-segment elevation in relation to gender is given in Fig2. Using statistical test, Student's t-test, it was found that there was no statistically significant difference between the values of serum NO in patients with STEMI in relation to gender ($p > 0.05$).

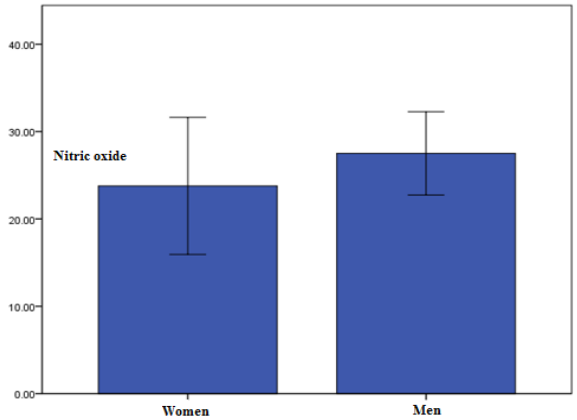

Fig2. Comparison between mean values of nitric oxide concentration in the serum of patients with acute myocardial infarction with ST-segment elevation in relation to gender

III. Conclusions

The results of statistical analysis of the mean values of serum NO in the STEMI group of patients compared to healthy individuals group show that there is a significantly higher value of NO in the STEMI group compared to healthy individuals. Similar results have been found by other authors such as Node et al. and Akiyama et al. [5][6]. A possible explanation for this is the fact that the induction of myocardial ischemia during exercise testing increases the production of nitric oxide in the myocardium of patients with effort angina pectoris. In their research, the production of nitric oxide and lactate are correlated, it is likely that the increased NO synthesis during stress tests causes myocardial ischemia. It is believed that the cardio myocytes and endothelial cells are potential sources of NO in ischemic heart, but it is not known which type of cell is the main site of production of NO. [5] Serum values of NO are not statistically significantly changing with regard to the affected area of myocardial infarction. Values of NO can identify patient's long-term risk of death or warning sign of reinfarction in those patients who have acute myocardial infarction with ST-segment elevation. [7] Through their studies some authors have found that serum levels of nitric oxide significantly higher in patients with STEMI compared to healthy individuals, particularly in patients with coronary heart disease, diabetes, hyperlipidemia and hypertension. [8][9][10] Đorđević et al found that the serum levels of NO were significantly elevated in patients with STEMI who suffered cardiac death during the follow-up. They also found increased levels of NO in patients with repeated myocardial infarction. Their results show that serum levels of NO in patients with stable angina pectoris, if they are regularly monitored over time by a doctor, may indicate

instability of the atherosclerotic plaque [11]. The research of Caimi et al. and Akarasereenont et al. show significantly higher serum concentrations of NOx in patients with coronary artery disease compared to the control, healthy group of subjects, which is explained by the existence of prolonged inflammation of the coronary endothelial cells of blood vessels and the significant impact of the simultaneous presence of several risk factors for cardiovascular disease. [12][13]

In conclusion, this study points out that patients with STEMI produce a higher concentration of NO compared to healthy individuals. The likely cause is the unstable atherosclerotic plaque that leads to critical ischemia.

REFERENCES

1. Davignon J, Ganz P. Role of endothelial dysfunction in atherosclerosis. Circulation, 2004; 109(23): III27-32.
2. Matsubara TT, Ishibashi TH, Ozaki K, Mezaki T, et al. Association between coronary endothelial dysfunction and local inflammation of atherosclerotic coronary arteries. Mol Cell Biochem, 2003; 249: 67-73.
3. Chen SM, Tsai TH, Hang CL, et al. Endothelial dysfunction in young patients with acute ST elevation myocardial infarction. Heart Vessels, 2011; 26(1): 2-9.
4. Hamm CW, Bassand JP, Agewall S, Bax j and other members of the European Society of Cardiology. ESC Guidelines for the management of acute coronary syndromes in patients presenting without persistent ST segment elevation. European Heart Journal (2011) 32, 2999–3054.
5. Node K, Kitakaze M, Sato H, Koretsune Y et al. Increased release of nitric oxide in ischemic hearts after exercise in patients with effort angina. J Am Coll Cardiol 1998; 32(1): 63-68.
6. Akiyama K, Kimura A, Suzuki H, Takeyama Y, et al. Production of oxidative products of nitric oxide in infarcted human heart. J Amer Coll Cardiol 1998; 32(2): 373-379.
7. Marwan SM Al-Nimer, Alhusseiny AH. Significant alteration of nitrogen species in acutemyocardial infarction does not releate to the site of infarction. Eur J Gen Med 2014;11(1): 10-14.
8. Higashino H, Tabuchi M, Yamagata S, Kurita T, Miya H, Mukai H, Miya Y. Serum nitric oxide metabolite levels in groups of patients with various diseases in comparison of healthy control subjects. J Med Sci 2010; 10(1): 1-11.
9. Toda N, Tanabe S, Nakanishi S. Nitric oxide-mediated coronary flow regulation in patients with coronary artery disease: recent advances. Int J angiol 2011; 20(3): 121-134.
10. Feng Q, Lu X, Jones DL, Shen J, Arnold O. Increased inducible nitric oxide synthase expression contributes to myocardial dysfunction and higher mortality after myocardial infarction in mice. Circulation 2001; 104: 700-704.
11. Đorđević VB, Stojanović I, Ćosić V, Zvezdanović L, Deljanin-Ilić M, et al. Serum neopterin, nitric oxide, inducible nitric oxide synthase and tumor necrosis factor- alpha levels in patients with ischemic heart disease. Clin Chem Lab Med 2008; 46(8): 1149-55.
12. Caimi G, Montana M, Calandrino V, Caruso M, Carollo C, Catania A, Lo Presti R. Nitric oxide metabolites (nitrite and nitrate) in young patients with recent acute myocardial infarction. Clin Haemorheol Microcirc 2008; 40(2): 157-63.
13. Akarasereenont P, Nuamchit T, Thaworn A, Leowattana W, Chotewuttakorn S, Khunawat P. Serum nitric oxide levels in patients with coronary artery disease. J Med Assoc Thai 2001; 84(3): S730-9.

Alma Badnjević is with Canton hospital, Zenica, B&H (phone: 387-35-259-600; e-mail: office@untz.ba).